

Special Publication SJ2002-SP4

**Photosynthetically Active Radiation, Water Quality, and
Submerged Aquatic Vegetation in Indian River Lagoon**

Final Report for Contract No. 93W199

**Prepared for
St. Johns River Water Management District
P.O. Box 1429
Palatka, FL 32178-1429**

**By
M. Dennis Hanisak**

**Marine Botany Department
Harbor Branch Oceanographic Institution
5600 US 1 North
Fort Pierce, FL 34966**



HBOI Contribution #1467

December 2001

The contents of this report are produced as received from the contractor. The opinions, findings, and conclusions are not necessarily those of the St. Johns River Management District, nor does mention of company names or products constitute endorsement by the St. Johns River Management District.

The citation for this document is:

Hanisak, M.D. 2001. Photosynthetically Active Radiation, Water Quality, and Submerged Aquatic Vegetation in Indian River Lagoon. Final Report for Contract No. 93W199. St. Johns River Water Management District, Palatka, Florida. 502 pp.

Photosynthetically Active Radiation, Water Quality, and Submerged Aquatic Vegetation in Indian River Lagoon

Executive Summary

Overview of the Study (Chapter 1)

Submerged aquatic vegetation (SAV; i.e., seagrasses and benthic macroalgae) is a critical component of Indian River Lagoon (IRL), playing important roles in biological productivity and species diversity. This study determined the relationship of SAV in the lagoon to water quality, submarine PAR (Photosynthetically Active Radiation), and underwater light attenuation (K). Stations within IRL were established for continuous monitoring of PAR, as well as for measurements of water quality, SAV epiphytes, productivity, and grazers. These stations represented a range of PAR, water quality, and SAV conditions and included both healthy and stressed seagrass beds. From north to south, these stations were: BR ("Banana River"), MB ("Melbourne"), TC ("Turkey Creek"), SN ("Sebastian-North"), SS ("Sebastian-South"), VB ("Vero Beach"), and LP ("Link Port").

At each station, arrays of PAR sensors were deployed and maintained for 2 years (November 1993–November 1995). Continuous PAR measurements were integrated and recorded every 15 minutes and the amount of light attenuation in the water column calculated. Water quality parameters relevant to light attenuation and/or growth of SAV and algae were measured weekly. SAV, epiphyte load on seagrass blades, and productivity of SAV and epiphytes were measured seasonally. SAV parameters measured were species composition, above- and below-ground biomass, shoot density, percent cover, canopy height, and abundance of macroalgae. Data were analyzed to address relationships between PAR, light attenuation, seagrass, epiphytes, and water quality. Recommendations were made on the monitoring and management of SAV and water quality in the lagoon.

PAR Monitoring (Chapter 2)

Highly significant seasonal differences in PAR and K were found at all stations. PAR reaching the seagrass canopy was maximal in spring (March–May) followed in order by summer (June–August), winter (December–February), and fall (September–November). K was maximal in the fall and minimal in spring.

There were significant differences in both PAR and K among stations. Mean K was lowest (0.85/m) at BR and highest (2.58/m) at SN. The reverse pattern was observed for PAR. Although the same patterns among stations occurred in both years, there were significant interannual differences.

The frequency of measurements required to characterize PAR and K at a site in IRL is dependent upon location and the desired levels of accuracy and precision. While in most cases, differentiation among stations continues to improve all the way up to continuous monitoring, reasonably good estimates of PAR and K ($\pm 10\%$ accuracy) at any particular site can be made by sampling every 2 weeks. At all stations, an accuracy of $\pm 20\%$ required sampling every month for PAR or every 2 months for K.

Water Quality Monitoring (Chapter 3)

There was a high frequency of correlation among the water quality parameters measured. In particular, salinity was strongly negatively correlated with water color, total nitrogen, total dissolved phosphorus, silicate, and chlorophyll *a*, but was strongly positively correlated to suspended solids. Salinity was strongly influenced by freshwater runoff.

Salinity patterns were variable among stations. At one extreme, BR had a relatively stable salinity throughout the first year of the study (90% of the salinity values were in the range of 26 to 32 ppt). A pronounced decline was associated with the passage of Tropical Storm Gordon in November 1995. The lack of recovery to Year 1 salinity levels during Year 2 was probably due to the long residence time of water in that portion of IRL. Variability in salinity was greatest at the Sebastian stations because of their proximity to large inputs of freshwater from the Sebastian River as well as inputs of high-salinity water through Sebastian Inlet. LP had the highest average salinity among stations.

Patterns of color were variable among stations. At BR and MB, color was relatively stable and low. At TC, color was elevated during the wet season. Variability in color was greatest at SN and SS. Color was generally low at VB and LP, with increased levels observed during the later part of the wet season. Increased water color was related to reduced salinity associated with freshwater inputs.

Turbidity was elevated during periods of high winds associated with winter cold fronts and a tropical storm. BR and MB were significantly less turbid than the other stations. Patterns of suspended solids were similar to those of turbidity, with most of the suspended solids being inorganic.

Mean nitrogen concentrations decreased and phosphorus concentrations increased along a north-south gradient. IRL appears to be generally nitrogen-limited, but not consistently throughout. Phosphorus limitation may, at times, play an important role in limiting algal growth. Higher silicate levels were associated with freshwater inputs.

SAV (Chapter 4)

The most common seasonal pattern for seagrass cover, shoot density, and biomass was August maximum and November minimum. Interannual differences in seagrass parameters were significant, with a considerable decline at most stations during 1995. The decline at BR was precipitous; *Halodule wrightii* began to recover later in the year, but there was no indication of recovery by *Syringodium filiforme*, and *Halophila engelmannii* was not found for the remainder of the study. This decline appears to be related to sharply reduced salinities associated with high rainfall.

Halodule wrightii was the predominant seagrass overall and the only seagrass species present at all stations. Cover was highest at BR, SN, and SS. Shoot density and all 3 biomass parameters were always highest at BR, followed by SN and SS.

Syringodium filiforme was a major component of the seagrass community at BR and LP, and present in small amounts at VB and SS. There was a precipitous decline in this species at BR during 1995. During 1994, all SAV parameters were significantly higher at BR than at LP, but during 1995, this pattern was completely reversed, due to a decline in this species at BR.

Correlation analyses indicated that shoot density was highly correlated with above-ground biomass, below-ground biomass, and total biomass for each of the major seagrass species.

The macroalgal community at these stations was almost exclusively unattached, "drift" algae; 65% of the total belonged to the red algal genus *Gracilaria*. Macroalgal abundance increased along the north-south gradient of stations.

Epiphytes (Chapter 5)

For all species combined, epiphytic chlorophyll averaged over 50 mg chl *a*/shoot. Epiphytic chlorophyll exceeded 0.3 g chl *a*/g epiphyte dry weight and exceeded 1.3 g chl *a*/g shoot dry weight. Epiphyte:shoot dry weight ratios were over 9.

Halodule wrightii had the highest epiphyte:shoot dry weight ratio, followed in order by *Syringodium filiforme*, *Thalassia testudinum*, and *Halophila engelmannii*.

Epiphytic chlorophyll values were similar for all stations, except MB, which had significantly lower values. Epiphyte:shoot dry weight ratios were higher at MB, SS, and SN, where *H. wrightii* was dominant, than at BR, VB, and LP, which had mixed seagrass communities.

Epiphyte seasonality within stations was more significant than differences in epiphyte loads among stations. Epiphyte loads were maximal in August and November.

Primary Productivity (Chapter 6)

The primary productivity rate for all seagrass species (grand mean) was 9.48 mg C g dry weight⁻¹ h⁻¹. There were no significant differences in productivity among the major species of seagrass (*Halodule wrightii*, *Syringodium filiforme*, and *Thalassia testudinum*), but the productivity of *Halophila engelmannii* was significantly lower. The primary productivity rate for epiphytes on all seagrass species (grand mean) was 13.42 mg C g dry weight⁻¹ h⁻¹, a value 42% greater than that of seagrass.

Overall, the primary productivity of seagrass and epiphytes was much greater (ca. 15-30 times) than that of phytoplankton and benthic microalgae. Mean areal productivity (g C m⁻² h⁻¹) for all incubations was 0.76 for seagrass, 1.01 for epiphytes, 0.03 for phytoplankton, and 0.05 for benthic microalgae. Thus, seagrasses and their epiphytes accounted for 96% of the carbon fixed (41% and 55%, for seagrass and epiphytes, respectively).

The lack of pattern in carbon fixation among stations suggests that primary productivity, as measured in this study, has limited value as an index of SAV conditions.

Relationships of Light Attenuation, Water Quality, and SAV (Chapter 7)

Multiple regression analysis of K and water quality parameters indicated that, for the complete data set, turbidity was the first significant factor to enter the model, followed by color, inorganic suspended solids, salinity, and total suspended solids. Multiple regression analyses of water quality parameters and K showed station-specific differences, which demonstrate the need for a segment-by-segment approach to water quality management in IRL.

For the full data set, there were significant correlations and regressions between PAR and seagrass above-ground biomass and between K and both seagrass cover and seagrass above-ground biomass. There were only a few significant site-specific relationships found between seagrass abundance or epiphyte load with PAR and K. For the full data set, seagrass cover was significantly correlated with salinity, total phosphorus, and silicate. Seagrass above-ground biomass was significantly correlated with temperature, salinity, and silicate. The relationships with temperature and salinity were all positive, while those with phosphorus and silicate were negative. The only water quality parameter significantly related to epiphyte load was silicate.

Ancillary Information on Epiphyte Grazers, Nutrient-Epiphyte Interactions, and PAR Attenuation Due to Epiphytes (Chapter 8)

Measurements of grazing epifauna support the hypothesis that decreased grazing pressure can increase epiphyte loads and reduce seagrass biomass, as well as the hypothesis that increased seagrass biomass can increase the amount of grazing epifauna and reduced epiphyte loads. "Healthy seagrass" may thus be either a cause or an effect of the grazer-epiphyte relationship. Grazers may be more important than nutrients in mediating seagrass-epiphyte interactions in IRL.

Management Recommendations (Chapter 9)

SAV Monitoring

The high degree of correlation among seagrass parameters suggests that rapid assessment techniques for determining seagrass status and changes through time, such as the District's current monitoring of permanent transects, merit continued study. The sampling frequency (twice per year) of the District's current monitoring network of transects is appropriate to assess long-term changes in IRL.

The lack of pattern in carbon fixation by seagrasses among stations suggests that there is limited value in that parameter as an index of seagrass conditions. Other seagrass parameters (percent cover, biomass, growth rates) are much more likely to be effective biological integrators of environmental conditions in an IRL monitoring program.

PAR Monitoring

Continuous monitoring of underwater PAR is not required to adequately characterize underwater PAR or K in IRL. While in most cases, differentiation among stations continues to improve all the way up to continuous monitoring, reasonably good estimates of PAR and K ($\pm 10\%$ accuracy) at any particular site can be made by sampling every 2 weeks. At all stations, an accuracy of $\pm 20\%$ required sampling every month for PAR or every 2 months for K.

If both measurements of PAR and K are desired, it is recommended that the standard procedure of making measurements between the hours of 1000 to 1400 be followed. If K alone is of interest, there is a broader period of time each day when measurements can be made. This period is somewhat site- and season-specific; without site-specific information, it is recommended that K measurements be made between the hours of 0900 to 1500.

Partitioning of water quality factors associated with light attenuation can be used to direct management actions. Light attenuation coefficients (K) are more useful than PAR measurements in addressing water quality effects on underwater light availability. The strategy of managing seagrass by addressing water quality problems that elevate K appears sound.

Water Quality Monitoring

Turbidity is the most significant attenuator of light in IRL. Measurement of turbidity, which can be made quickly in field monitoring efforts, may serve as a good proxy of suspended solids in IRL. Reducing the input of suspended solids into IRL may be the single most effective management action to increase water clarity, and, thus, enhance seagrass in the lagoon.

The relative and absolute roles of nitrogen and phosphorus as factors limiting algal growth in IRL merit study.

Relationships among water quality parameters and their relationships with extinction coefficients derived in the current study could be broadly applied to the IRL water quality database and be used in development and verification of water quality models.

Emphasis on water quality-light attenuation relationships should be the focus of near-term management and modeling efforts, with impacts on seagrass simulated by models and verified by *in situ* measurements.

Turbidity and color are water quality parameters that are important to light attenuation and that can be quickly measured in field monitoring efforts. Rapid assessment of light and water quality, perhaps in relationship to the District's extensive monitoring network of seagrass transects, would provide a fairly simply obtained, yet meaningful, synoptic evaluation of a large area of the lagoon.

Integrated water column sampling should provide an adequate characterization of water quality at any site in the lagoon.

The northern lagoon may merit additional study as to ecological function in what are relatively pristine conditions in IRL, with limited anthropogenic impacts. Water quality conditions in that portion of the lagoon system may be eventual targets for lagoon managers to achieve for most of IRL.

Acknowledgments

The support provided by the St. Johns River Water Management District for this project (Contract No. 93W199) is gratefully acknowledged. I thank Lori Morris and Bob Virmstein of the District for providing input into the work plan and the selection of stations, collecting and making available seagrass transect cover data, reviewing drafts of this report, and being very patient during the entire report process.

I also thank: Dan Miller and Patrick Monaghan (HBOI), who were the chief assistants for the field work and who did some of the sample processing; Bida Chen (HBOI), who processed most of the field samples, conducted data entry for portions of the study, and produced most of the figures; and Paul Zimba, formerly of the University of Florida, who was responsible for conducting the productivity measurements, analyzing the epiphyte collections, and providing rough drafts of the epiphyte and productivity chapters. All nutrient, chlorophyll, and suspended solids samples were analyzed by the Water Chemistry Lab at the University of Florida's Department of Fisheries and Aquatic Sciences.

Photosynthetically Active Radiation, Water Quality, and Submerged Aquatic Vegetation in Indian River Lagoon

Table of Contents

Chapter 1: Overview of the Study	1.1
1.1 Background	1.1
1.2 Objectives	1.2
1.3 Overview of Work Plan	1.3
1.4 Table	1.5
1.5 Figure	1.6
Chapter 2: PAR Monitoring	2.1
2.1 Introduction	2.1
2.2 Description of Tasks.....	2.1
2.3 Methods	2.1
2.3.1 Station Selection	2.1
2.3.2 PAR Monitoring	2.3
2.3.3 Data Analysis	2.6
2.4 Results	2.7
2.4.1 Initial Analyses: Sensor Fouling	2.8
2.4.2 Diel Patterns	2.9
2.4.3 Effects of Fouling	2.10
2.4.4 Differences among Stations and Years	2.10
2.4.5 Seasonal Differences	2.11
2.4.6 Monthly Differences	2.11
2.4.7 Effects of Sampling Frequency on Estimates of PAR and K	2.11
2.4.8 Comparison of Different Sensor Types	2.12
2.5 Discussion	2.13
2.6 Summary	2.16
2.7 Tables	2.19
2.8 Figures	2.24
Chapter 3: Water Quality	3.1
3.1 Introduction	3.1
3.2 Task Description	3.1
3.3 Methods	3.1
3.4 Results	3.3
3.4.1 Water Quality Measurements: Weekly Integrated Samples	3.3
3.4.2 Water Quality Measurements: Stratified Sampling	3.7
3.4.3 Cluster Analyses of Stations	3.8
3.4.4 Correlation Matrix of Water Quality Parameters	3.8
3.4.5 Regression Analyses of Water Quality Parameters	3.9

Table of Contents (Continued)

3.4.6 Effects of Sampling Frequency on Estimates of Water Quality Parameters	3.11
3.5 Discussion	3.13
3.6 Summary	3.18
3.7 Tables	3.23
3.8 Figures	3.29
Chapter 4: SAV	4.1
4.1 Introduction	4.1
4.2 Task Description	4.2
4.3 Methods	4.2
4.4 Results	4.4
4.4.1 Seagrass Overview	4.4
4.4.2 Station Overview	4.5
4.4.3 Transect Differences in SAV	4.7
4.4.4 Seasonality of SAV	4.9
4.4.5 Comparisons of SAV among Stations and among Years	4.14
4.4.6 Correlation and Regression Analyses of SAV Parameters	4.17
4.5 Discussion	4.17
4.6 Summary	4.21
4.7 Tables	4.25
4.8 Figures	4.35
Chapter 5: Epiphytes	5.1
5.1 Introduction	5.1
5.2 Task Description	5.1
5.3 Methods	5.1
5.4 Results	5.3
5.4.1 Overview	5.3
5.4.2 Seagrass Species-Specific Patterns in Epiphyte Parameters	5.3
5.4.3 Differences in Epiphyte Loads among Transects	5.4
5.4.4 Seasonality of Epiphytes	5.4
5.4.5 Differences in Epiphyte Loads among Stations	5.4
5.5 Discussion	5.5
5.6 Summary	5.7
5.7 Tables.....	5.9
5.8 Figures	5.12
Chapter 6: Primary Productivity	6.1
6.1 Introduction	6.1
6.2 Task Description	6.1

Table of Contents (Continued)

6.3	Methods	6.1
6.4	Results	6.3
6.4.1	Comparison of Productivity among Seagrass Species	6.3
6.4.2	Comparison of Productivity among Seasons	6.3
6.4.3	Comparison of Productivity between Transects	6.4
6.4.4	Comparison of Productivity among Stations	6.4
6.4.5	Comparison of Primary Productivity of Seagrass, Epiphytes, Phytoplankton, and Benthic Microalgae	6.4
6.5	Discussion	6.5
6.6	Summary	6.6
6.7	Figures	6.8
Chapter 7: Relationships of Light Attenuation, Water Quality, and SAV		7.1
7.1	Introduction	7.1
7.2	Task Description	7.1
7.3	Methods	7.1
7.4	Results	7.2
7.4.1	Correlation Analyses of Underwater PAR and K with Water Quality Parameters	7.3
7.4.2	Linear Regression Analyses of K with Water Quality Parameters	7.5
7.4.3	Multiple Regression Analyses of Underwater PAR and K with Water Quality Parameters	7.7
7.4.4	Relationships of Seagrass Abundance and Epiphyte Load with Underwater PAR and K	7.8
7.4.5	Relationships of Seagrass Abundance and Epiphyte Load with Water Quality Parameters	7.9
7.5	Discussion	7.10
7.6	Summary	7.12
7.7	Tables	7.15
7.8	Figures	7.24
Chapter 8: Ancillary Information on Epiphyte Grazers, Nutrient-Epiphyte Interactions and Par Attenuation Due to Epiphytes		8.1
8.1	Introduction	8.1
8.2	Task Description	8.1
8.3	Methods	8.1
8.4	Results	8.2
8.4.1	Abundance of Epiphyte Grazers	8.3
8.4.2	Regression Analyses: Grazers, Epiphytes, and SAV Interactions	8.4
8.4.3	Nutrient-Epiphyte-Seagrass Interactions	8.4

Table of Contents (Continued)

8.4.4 Attenuation of PAR by Epiphytes	8.6
8.5 Discussion	8.7
8.6 Summary	8.9
8.7 Figures	8.13
Chapter 9: Management Recommendations	9.1
9.1 Background	9.1
9.2 Task Description	9.1
9.3 Recommendations	9.1
9.3.1 Seagrass Monitoring	9.2
9.3.2 PAR Monitoring	9.3
9.3.3 Water Quality Monitoring	9.4
Chapter 10: Literature Cited	10.1

List of Tables

Table 1.1	Frequency of sampling and other activities associated with this study	1.5
Table 2.1	Number of data points, by station, for various analyses performed on PAR and K	2.19
Table 2.2	Scenarios for analysis of sampling frequency of PAR and K	2.20
Table 2.3	Means by station for K, calculated from data collected during the hours of 1000-1400, within 48 hours of cleaning sensors	2.21
Table 2.4	Relationship of sampling frequency with the ability to statistically determine site-specific differences for PAR and K	2.22
Table 2.5	Comparison of attenuation coefficients calculated from cosine and spherical sensors at BR and LP	2.23
Table 3.1	Scenarios for analysis of water quality sampling frequency	3.23
Table 3.2	Correlation matrix of temperature, salinity, color, turbidity, total suspended solids, inorganic suspended solids, organic suspended solids, total nitrogen, total dissolved nitrogen, total phosphorus, total dissolved phosphorus, total silicate, and chlorophyll <i>a</i>	3.24
Table 3.3	Stepwise multiple regression models for chlorophyll <i>a</i> as a function of total nitrogen, total phosphorus, and total silicate	3.25
Table 3.4	Minimal sampling frequency to achieve mean values within the range of $\pm 10\%$ and $\pm 20\%$ of the weekly means for water quality parameters	3.26
Table 3.5	Relationship of sampling frequency with the ability to statistically determine site-specific differences for water quality parameters	3.27
Table 4.1	Dates of quarterly SAV samplings	4.25
Table 4.2	Mean depth of seagrass beds and depth, distance from shore, and species present at the "deep edge" at IRL stations during the quarterly SAV samplings	4.26
Table 4.3	<i>Halodule wrightii</i> . Correlation matrix of shoot density, above-ground, below-ground, and total biomass, cover, and canopy height	4.29

List of Tables (Continued)

Table 4.4	<i>Syringodium filiforme</i> . Correlation matrix of shoot density, above-ground, below-ground, and total biomass, cover, and canopy height	4.30
Table 4.5	<i>Thalassia testudinum</i> . Correlation matrix of shoot density, above-ground, below-ground, and total biomass, cover, and canopy height	4.31
Table 4.6	<i>Halodule wrightii</i> . Stepwise multiple regression models for above-ground, below-ground, and total biomass, as a function of shoot density, cover, and canopy height	4.32
Table 4.7	<i>Syringodium filiforme</i> . Stepwise multiple regression models for above-ground, below-ground, and total biomass, as a function of shoot density, cover, and canopy height	4.33
Table 4.8	<i>Thalassia testudinum</i> . Stepwise multiple regression models for above-ground, below-ground, and total biomass, as a function of shoot density, cover, and canopy height	4.34
Table 5.1	Correlation matrix of shoot dry weight, epiphyte dry weight, and epiphytic chlorophyll/shoot	5.9
Table 5.2	Correlation matrix of shoot dry weight, epiphyte dry weight, and epiphytic chlorophyll/shoot, for each seagrass species	5.10
Table 5.3	<i>Halodule wrightii</i> . Groupings of months sampled resulting from Tukey range test following ANOVA for epiphytic chlorophyll/shoot dry weight	5.11
Table 7.1	Correlation coefficients of underwater PAR with temperature, salinity, color, turbidity, total suspended solids, inorganic suspended solids, organic suspended solids, total nitrogen, total dissolved nitrogen, total phosphorus, total dissolved phosphorus, total silicate, and chlorophyll <i>a</i> , for all stations, and by station	7.15
Table 7.2	Correlation coefficients of K with temperature, salinity, color, turbidity, total suspended solids, inorganic suspended solids, organic suspended solids, total nitrogen, total dissolved nitrogen, total phosphorus, total dissolved phosphorus, total silicate, and chlorophyll <i>a</i> , for all stations, and by station	7.16

List of Tables (Continued)

Table 7.3	Stepwise multiple regression models for underwater PAR with temperature, salinity, color, turbidity, total suspended solids, inorganic suspended solids, organic suspended solids, total nitrogen, total dissolved nitrogen, total phosphorus, total dissolved phosphorus, total silicate, and chlorophyll <i>a</i> , for all stations, and by station	7.17
Table 7.4	Stepwise multiple regression models for K with temperature, salinity, color, turbidity, total suspended solids, inorganic suspended solids, organic suspended solids, total nitrogen, dissolved nitrogen, total phosphorus, dissolved phosphorus, total silicate, and chlorophyll <i>a</i> , for all stations, and by station	7.18
Table 7.5	Correlation coefficients of seagrass cover, seagrass above-ground biomass, and epiphyte loads with underwater PAR for all stations, and by station	7.19
Table 7.6	Correlation coefficients of seagrass cover, seagrass above-ground biomass, and epiphyte loads with K for all stations, and by station	7.20
Table 7.7	Correlation coefficients of seagrass cover with temperature, salinity, color, turbidity, total suspended solids, inorganic suspended solids, organic suspended solids, total nitrogen, dissolved nitrogen, total phosphorus, dissolved phosphorus, total silicate, and chlorophyll <i>a</i> , for all stations, and by station	7.21
Table 7.8	Correlation coefficients of seagrass above-ground biomass with temperature, salinity, color, turbidity, total suspended solids, inorganic suspended solids, organic suspended solids, total nitrogen, dissolved nitrogen, total phosphorus, dissolved phosphorus, total silicate, and chlorophyll <i>a</i> , for all stations, and by station	7.22
Table 7.9	Correlation coefficients of epiphyte load with temperature, salinity, color, turbidity, total suspended solids, inorganic suspended solids, organic suspended solids, total nitrogen, dissolved nitrogen, total phosphorus, dissolved phosphorus, total silicate, and chlorophyll <i>a</i> , for all stations, and by station	7.23

List of Figures

Fig. 1.1	Location of stations sampled in this study within Indian River Lagoon	1.6
Fig. 2.1	PAR measured by the C0, S1, and S2 sensors, and K, before and after sensor cleaning, at BR, from November 30, 1993 to November 30, 1995	2.24
Fig. 2.2	PAR measured by the C0, S1, and S2 sensors, and K, before and after sensor cleaning, at MB, from November 30, 1993 to November 30, 1995	2.25
Fig. 2.3	PAR measured by the C0, S1, and S2 sensors, and K, before and after sensor cleaning, at TC, from December 1, 1994 to November 30, 1995	2.26
Fig. 2.4	PAR measured by the C0, S1, and S2 sensors, and K, before and after sensor cleaning, at SN, from November 30, 1993 to November 30, 1995	2.27
Fig. 2.5	PAR measured by the C0, S1, and S2 sensors, and K, before and after sensor cleaning, at SS, from November 30, 1993 to November 30, 1995	2.28
Fig. 2.6	PAR measured by the C0, S1, and S2 sensors, and K, before and after sensor cleaning, at VB, from November 30, 1993 to November 30, 1994	2.29
Fig. 2.7	PAR measured by the C0, S1, and S2 sensors, and K, before and after sensor cleaning, at LP, from November 30, 1993 to November 30, 1995	2.30
Fig. 2.8	PAR measured by the C0, S1, and S2 sensors, and K, at 1200 noon, at BR, from November 30, 1993 to November 30, 1995	2.31
Fig. 2.9	PAR measured by the C0, S1, and S2 sensors, and K, at 1200 noon, at MB, from November 30, 1993 to November 30, 1995	2.32
Fig. 2.10	PAR measured by the C0, S1, and S2 sensors, and K, at 1200 noon, at TC, from December 1, 1994 to November 30, 1995	2.33
Fig. 2.11	PAR measured by the C0, S1, and S2 sensors, and K, at 1200 noon, at SN, from November 30, 1993 to November 30, 1995	2.34
Fig. 2.12	PAR measured by the C0, S1, and S2 sensors, and K, at 1200 noon, at SS, from November 30, 1993 to November 30, 1995	2.35
Fig. 2.13	PAR measured by the C0, S1, and S2 sensors, and K, at 1200 noon, at VB, from November 30, 1993 to November 30, 1994	2.36

List of Figures (Continued)

Fig. 2.14 PAR measured by the C0, S1, and S2 sensors, and K, at 1200 noon, at LP, from November 30, 1993 to November 30, 1995	2.37
Fig. 2.15 Effect of time since sensor cleaning on K, based on 1200 noon data, at BR, from November 30, 1993 to November 30, 1995	2.38
Fig. 2.16 Effect of time since sensor cleaning on K, based on 1200 noon data, at MB, from November 30, 1993 to November 30, 1995	2.39
Fig. 2.17 Effect of time since sensor cleaning on K, based on 1200 noon data, at TC, from December 1, 1994 to November 30, 1995	2.40
Fig. 2.18 Effect of time since sensor cleaning on K, based on 1200 noon data, at SN, from November 30, 1993 to November 30, 1995	2.41
Fig. 2.19 Effect of time since sensor cleaning on K, based on 1200 noon data, at SS, from November 30, 1993 to November 30, 1995	2.42
Fig. 2.20 Effect of time since sensor cleaning on K, based on 1200 noon data, at VB, from November 30, 1993 to November 30, 1994	2.43
Fig. 2.21 Effect of time since sensor cleaning on K, based on 1200 noon data, at LP, from November 30, 1993 to November 30, 1995	2.44
Fig. 2.22 Examples of raw data for PAR measured by the C0 sensor over the course of the photoperiod	2.45
Fig. 2.23 Examples of raw data for PAR measured by the S1 sensor over the course of the photoperiod	2.46
Fig. 2.24 Examples of raw data for PAR measured by the S2 sensor over the course of the photoperiod	2.47
Fig. 2.25 Examples of K calculated from the S1 and S2 sensors over the course of the photoperiod	2.48
Fig. 2.26 Diel patterns in PAR measured by the C0, S1, and S2 sensors, and K, at BR, from November 30, 1993 to November 30, 1995	2.49
Fig. 2.27 Diel patterns in PAR measured by the C0, S1, and S2 sensors, and K, at MB, from November 30, 1993 to November 30, 1995	2.50

List of Figures (Continued)

- Fig. 2.28 Diel patterns in PAR measured by the C0, S1, and S2 sensors, and K, at TC, from December 1, 1994 to November 30, 1995 2.51
- Fig. 2.29 Diel patterns in PAR measured by the C0, S1, and S2 sensors, and K, at SN, from November 30, 1993 to November 30, 1995 2.52
- Fig. 2.30 Diel patterns in PAR measured by the C0, S1, and S2 sensors, and K, at SS, from November 30, 1993 to November 30, 1995 2.53
- Fig. 2.31 Diel patterns in PAR measured by the C0, S1, and S2 sensors, and K, at VB, from November 30, 1993 to November 30, 1994 2.54
- Fig. 2.32 Diel patterns in PAR measured by the C0, S1, and S2 sensors, and K, at LP, from November 30, 1993 to November 30, 1995 2.55
- Fig. 2.33 PAR measured by the C0, S1, and S2 sensors, and K, within 3 days after cleaning of sensors, and by day since sensor cleaning, at BR, from November 30, 1993 to November 30, 1995 2.56
- Fig. 2.34 PAR measured by the C0, S1, and S2 sensors, and K, within 3 days after cleaning of sensors, and by day since sensor cleaning, at MB, from November 30, 1993 to November 30, 1995 2.57
- Fig. 2.35 PAR measured by the C0, S1, and S2 sensors, and K, within 3 days after cleaning of sensors, and by day since sensor cleaning, at TC, from December 1, 1994 to November 30, 1995 2.58
- Fig. 2.36 PAR measured by the C0, S1, and S2 sensors, and K, within 3 days after cleaning of sensors, and by day since sensor cleaning, at SN, from November 30, 1993 to November 30, 1995 2.59
- Fig. 2.37 PAR measured by the C0, S1, and S2 sensors, and K, within 3 days after cleaning of sensors, and by day since sensor cleaning, at SS, from November 30, 1993 to November 30, 1995 2.60
- Fig. 2.38 PAR measured by the C0, S1, and S2 sensors, and K, within 3 days after cleaning of sensors, and by day since sensor cleaning, at VB, from November 30, 1993 to November 30, 1994 2.61

List of Figures (Continued)

- Fig. 2.39 PAR measured by the C0, S1, and S2 sensors, and K, within 3 days after cleaning of sensors, and by day since sensor cleaning, at LP, from November 30, 1993 to November 30, 1995 2.62
- Fig. 2.40 Mean PAR measured by the C0, S1, and S2 sensors, and K, for all data between the hours of 1000-1400, within 48 hours after sensor cleaning, for all stations, for the entire study and by year 2.63
- Fig. 2.41 Seasonal means for PAR measured by the C0 sensor, between 1000-1400, within 48 hours after sensor cleaning, at all stations 2.64
- Fig. 2.42 Seasonal means for PAR measured by the S1 sensor, between 1000-1400, within 48 hours after sensor cleaning, at all stations 2.65
- Fig. 2.43 Seasonal means for PAR measured by the S2 sensor, between 1000-1400, within 48 hours after sensor cleaning, at all stations 2.66
- Fig. 2.44 Seasonal means for K, between 1000-1400, within 48 hours after sensor cleaning, at all stations 2.67
- Fig. 2.45 Monthly means for PAR measured by the C0 sensor, between 1000-1400, within 48 hours after sensor cleaning, at all stations, for the entire study 2.68
- Fig. 2.46 Monthly means for PAR measured by the S1 sensor, between 1000-1400, within 48 hours after sensor cleaning, at all stations, for the entire study 2.69
- Fig. 2.47 Monthly means for PAR measured by the S2 sensor, between 1000-1400, within 48 hours after sensor cleaning, at all stations, for the entire study 2.70
- Fig. 2.48 Monthly means for K, between 1000-1400, within 48 hours after sensor cleaning, at all stations, for the entire study 2.71
- Fig. 2.49 Station means for PAR measured by the C0 sensor as a function of sampling frequency 2.72
- Fig. 2.50 Station means for PAR measured by the S1 sensor as a function of sampling frequency 2.73
- Fig. 2.51 Station means for PAR measured by the S2 sensor as a function of sampling frequency 2.74

List of Figures (Continued)

Fig. 2.52	Station means for K as a function of sampling frequency	2.75
Fig. 2.53	PAR measured by the C1, S1, C2, S2, C3, and S3 sensors, before and after sensor cleaning, at BR, from November 30, 1993 to November 30, 1995	2.76
Fig. 2.54	K, before and after sensor cleaning, at BR, from November 30, 1993 to November 30, 1995	2.77
Fig. 2.55	PAR measured by the C1, S1, C2, S2, C3, and S3 sensors, before and after sensor cleaning, at LP, from November 30, 1993 to November 30, 1995	2.78
Fig. 2.56	K, before and after sensor cleaning, at LP, from November 30, 1993 to November 30, 1995	2.79
Fig. 2.57	PAR measured by the C1, S1, C2, S2, C3, and S3 sensors, at 1200 noon, at BR, from November 30, 1993 to November 30, 1995	2.80
Fig. 2.58	K at 1200 noon, at BR, from November 30, 1993 to November 30, 1995	2.81
Fig. 2.59	PAR measured by the C1, S1, C2, S2, C3, and S3 sensors, at 1200 noon, at LP, from November 30, 1993 to November 30, 1995	2.82
Fig. 2.60	K at 1200 noon, at LP, from November 30, 1993 to November 30, 1995 ...	2.83
Fig. 2.61	Diel patterns in PAR measured by the C1, S1, C1, S2, C3, and S3 sensors, at BR, from November 30, 1993 to November 30, 1995	2.84
Fig. 2.62	Diel patterns in K, at BR, from November 30, 1993 to November 30, 1995	2.85
Fig. 2.63	Diel patterns in PAR measured by the C1, S1, C1, S2, C3, and S3 sensors, at LP, from November 30, 1993 to November 30, 1995	2.86
Fig. 2.64	Diel patterns in K, at LP, from November 30, 1993 to November 30, 1995	2.87
Fig. 2.65	PAR measured by the C1, S1, C1, S2, C3, and S3 sensors, within 3 days after cleaning of sensors, and by day since sensor cleaning, at BR, from November 30, 1993 to November 30, 1995	2.88

List of Figures (Continued)

- Fig. 2.66 K, within 3 days after sensor cleaning, and by day since sensor cleaning, at BR, from November 30, 1993 to November 30, 1995 2.89
- Fig. 2.67 PAR measured by the C1, S1, C1, S2, C3, and S3 sensors, within 3 days after cleaning of sensors, and by day since sensor cleaning, at LP, from November 30, 1993 to November 30, 1995 2.90
- Fig. 2.68 K, within 3 days after cleaning of sensors, and by day since sensor cleaning at LP, from November 30, 1993 to November 30, 1995 2.91
- Fig. 2.69 Mean PAR measured by the C1, S1, C2, S2, C3 and S3 sensors, K, and the ratio of K calculated from cosine sensors to that from spherical sensors, for all data at BR between the hours of 1000-1400, within 48 hours after cleaning of sensors from November 30, 1993 to November 30, 1995 2.92
- Fig. 2.70 Mean PAR measured by the C1, S1, C2, S2, C3 and S3 sensors, K, and the ratio of K calculated from cosine sensors to that from spherical sensors, for all data at LP between the hours of 1000-1400, within 48 hours after cleaning of sensors from November 30, 1993 to November 30, 1995 2.93
- Fig. 2.71 Seasonal means of PAR measured at BR by the C1, S1, C2, S2, C3, and S3 sensors, between the hours of 1000-1400, within 48 hours after sensor cleaning 2.94
- Fig. 2.72 Seasonal means of K, at BR, between the hours of 1000-1400, within 48 hours after sensor cleaning 2.95
- Fig. 2.73 Seasonal means of PAR measured at LP by the C1, S1, C2, S2, C3, and S3 sensors, between the hours of 1000-1400, within 48 hours after sensor cleaning 2.96
- Fig. 2.74 Seasonal means of K, at LP, between the hours of 1000-1400, within 48 hours after sensor cleaning 2.97
- Fig. 2.75 Monthly means of PAR measured at BR by the C1, S1, C2, S2, C3, and S3 sensors, between the hours of 1000-1400, within 48 hours after sensor cleaning 2.98
- Fig. 2.76 Monthly means of K, at BR, between the hours of 1000-1400, within 48 hours after sensor cleaning 2.99

List of Figures (Continued)

Fig. 2.77 Monthly means of PAR measured at LP by the C1, S1, C2, S2, C3, and S3 sensors, between the hours of 1000-1400, within 48 hours after sensor cleaning	2.100
Fig. 2.78 Monthly means of K, at LP, between the hours of 1000-1400, within 48 hours after sensor cleaning	2.101
Fig. 3.1 Temperature of weekly integrated water column samples at IRL stations	3.29
Fig. 3.2 Station means for temperature and salinity of weekly integrated water column samples	3.30
Fig. 3.3 Interannual variation in temperature and salinity based on station means of weekly integrated water column samples	3.31
Fig. 3.4 Salinity of weekly integrated water column samples at IRL stations	3.32
Fig. 3.5 Color of weekly integrated water column samples at IRL stations	3.33
Fig. 3.6 Station means for color of weekly integrated water column samples	3.34
Fig. 3.7 Interannual variation in color based on station means of weekly integrated water column samples	3.35
Fig. 3.8 Turbidity of weekly integrated water column samples at IRL stations	3.36
Fig. 3.9 Station means for turbidity and total, inorganic, and organic suspended solids of weekly integrated water column samples	3.37
Fig. 3.10 Interannual variation in turbidity and total, inorganic, and organic suspended solids based on station means of weekly integrated water column samples	3.38
Fig. 3.11 Total, inorganic, and organic suspended solids of weekly integrated water column samples at IRL stations	3.39
Fig. 3.12 Total and total dissolved nitrogen concentrations of weekly integrated water column samples at IRL stations	3.40
Fig. 3.13 Station means for nutrient concentrations of weekly integrated water column samples: total and total dissolved nitrogen, total and total dissolved phosphorus, and total silicate	3.41

List of Figures (Continued)

Fig 3.14	Interannual variation in nutrient concentrations based on station means of weekly integrated water column samples: total and total dissolved nitrogen, total and total dissolved phosphorus, and total silicate	3.42
Fig. 3.15	Total and total dissolved phosphorus concentration of weekly integrated water column samples at IRL stations	3.43
Fig. 3.16	Total silicate concentration of weekly integrated water column samples at IRL stations	3.44
Fig. 3.17	Chlorophyll <i>a</i> concentration of weekly integrated water column samples at IRL stations	3.45
Fig. 3.18	Station means for chlorophyll <i>a</i> concentration of weekly integrated water column samples	3.46
Fig. 3.19	Interannual variation in chlorophyll <i>a</i> concentration based on station means of weekly integrated water column samples	3.47
Fig. 3.20	Temperature and salinity of weekly surface and bottom water samples at SN and SS	3.48
Fig. 3.21	Color and turbidity of weekly surface and bottom water samples at SN and SS	3.49
Fig. 3.22	Total, inorganic, and organic suspended solids of weekly surface and bottom water samples at SN and SS	3.50
Fig. 3.23	Total and total dissolved nitrogen of weekly surface and bottom water samples at SN and SS	3.51
Fig. 3.24	Total and total dissolved phosphorus of weekly surface and bottom water samples at SN and SS	3.52
Fig. 3.25	Total silicate and chlorophyll <i>a</i> of weekly surface and bottom water samples at SN and SS	3.53
Fig. 3.26	Means for temperature, salinity, and color of weekly stratified water column samples at SN and SS	3.54

List of Figures (Continued)

Fig. 3.27 Means for turbidity and total, inorganic, and organic suspended solids of weekly stratified water column samples at SN and SS	3.55
Fig. 3.28 Means for nutrient concentrations of weekly stratified water column samples at SN and SS: total and total dissolved nitrogen, total and total dissolved phosphorus, and total silicate	3.56
Fig. 3.29 Means for chlorophyll a concentration of weekly stratified water column samples at SN and SS	3.57
Fig. 3.30 Cluster analysis of IRL stations, based on weekly integrated water quality measurements (Years 1 and 2)	3.58
Fig. 3.31 Cluster analysis of IRL stations, based on weekly integrated water quality measurements (Year 1)	3.59
Fig. 3.32 Cluster analysis of IRL stations, based on weekly integrated water quality measurements (Year 2)	3.60
Fig. 3.33 Linear regression analysis of water color vs. salinity for the complete data set (all stations)	3.61
Fig. 3.34 Linear regression analysis of water color vs. salinity for each station	3.62
Fig. 3.35 Linear regression analyses of total and total dissolved nitrogen vs. salinity for the complete data set (all stations)	3.63
Fig. 3.36 Linear regression analysis of total nitrogen vs. salinity for each station	3.64
Fig. 3.37 Linear regression analysis of total dissolved nitrogen vs. salinity for each station	3.65
Fig. 3.38 Linear regression analyses of total and total dissolved phosphorus vs. salinity for the complete data set (all stations)	3.66
Fig. 3.39 Linear regression analysis of total phosphorus vs. salinity for each station	3.67
Fig. 3.40 Linear regression analysis of total dissolved phosphorus vs. salinity for each station	3.68

List of Figures (Continued)

Fig. 3.41	Linear regression analysis of total silicate vs. salinity for the complete data set (all stations)	3.69
Fig. 3.42	Linear regression analysis of total silicate vs. salinity for each station	3.70
Fig. 3.43	Linear regression analysis of chlorophyll <i>a</i> vs. salinity for the complete data set (all stations)	3.71
Fig. 3.44	Linear regression analysis of chlorophyll <i>a</i> vs. salinity for each station	3.72
Fig. 3.45	Linear regression analyses of turbidity vs. total, inorganic, and organic suspended solids for the complete data set (all stations)	3.73
Fig. 3.46	Linear regression analysis of turbidity vs. total suspended solids for each station	3.74
Fig. 3.47	Linear regression analysis of turbidity vs. inorganic suspended solids for each station	3.75
Fig. 3.48	Linear regression analysis of turbidity vs. organic suspended solids for each station	3.76
Fig. 3.49	Linear regression analysis of turbidity vs. chlorophyll <i>a</i> for the complete data set (all stations)	3.77
Fig. 3.50	Linear regression analysis of turbidity vs. chlorophyll <i>a</i> for each station	3.78
Fig. 3.51	Linear regression analyses of chlorophyll <i>a</i> vs. total and total dissolved nitrogen for the complete data set (all stations)	3.79
Fig. 3.52	Linear regression analysis of chlorophyll <i>a</i> vs. total nitrogen for each station	3.80
Fig. 3.53	Linear regression analysis of chlorophyll <i>a</i> vs. total dissolved nitrogen for each station	3.81
Fig. 3.54	Linear regression analyses of chlorophyll <i>a</i> vs. total and total dissolved phosphorus for the complete data set (all stations)	3.82
Fig. 3.55	Linear regression analysis of chlorophyll <i>a</i> vs. total phosphorus for each station	3.83

List of Figures (Continued)

Fig. 3.56	Linear regression analysis of chlorophyll <i>a</i> vs. total dissolved phosphorus for each station	3.84
Fig. 3.57	Linear regression analyses of chlorophyll <i>a</i> vs. total silicate for the complete data set (all stations)	3.85
Fig. 3.58	Linear regression analysis of chlorophyll <i>a</i> vs. total silicate for each station	3.86
Fig. 3.59	Station means for temperature as a function of sampling frequency	3.87
Fig. 3.60	Station means for salinity as a function of sampling frequency	3.88
Fig. 3.61	Station means for color as a function of sampling frequency	3.89
Fig. 3.62	Station means for turbidity as a function of sampling frequency	3.90
Fig. 3.63	Station means for total suspended solids as a function of sampling frequency	3.91
Fig. 3.64	Station means for inorganic suspended solids as a function of sampling frequency	3.92
Fig. 3.65	Station means for organic suspended solids as a function of sampling frequency	3.93
Fig. 3.66	Station means for total nitrogen as a function of sampling frequency	3.94
Fig. 3.67	Station means for total dissolved nitrogen as a function of sampling frequency	3.95
Fig. 3.68	Station means for total phosphorus as a function of sampling frequency	3.96
Fig. 3.69	Station means for total dissolved phosphorus as a function of sampling frequency	3.97
Fig. 3.70	Station means for total silicate as a function of sampling frequency	3.98
Fig. 3.71	Station means for chlorophyll <i>a</i> as a function of sampling frequency	3.99

List of Figures (Continued)

- Fig. 4.1 Grand means for cover, canopy height, shoot density, and above-ground, below-ground, and total biomass by species, and all species of seagrass, for the entire study 4.35
- Fig. 4.2 Seagrass cover, by species and season, vs. depth and distance from shore at BR 4.36
- Fig. 4.3 Seagrass cover, by species and season, vs. depth and distance from shore at MB 4.37
- Fig. 4.4 Seagrass cover, by species and season, vs. depth and distance from shore at TC 4.38
- Fig. 4.5 Seagrass cover, by species and season, vs. depth and distance from shore at SN 4.39
- Fig. 4.6 Seagrass cover, by species and season, vs. depth and distance from shore at SS 4.40
- Fig. 4.7 Seagrass cover, by species and season, vs. depth and distance from shore at VB 4.41
- Fig. 4.8 Seagrass cover, by species and season, vs. depth and distance from shore at LP 4.42
- Fig. 4.9 Station means for cover and canopy height of *Halodule wrightii*, *Halophila engelmannii*, *Syringodium filiforme*, and *Thalassia testudinum*, for the entire study 4.43
- Fig. 4.10 Station means for shoot density and above-ground, below-ground, and total biomass of the seagrass community, by season and transect 4.44
- Fig. 4.11 Station means for cover, canopy height, shoot density, and above-ground, below-ground, and total biomass of *Halodule wrightii*, by season and transect 4.45
- Fig. 4.12 Station means for cover, canopy height, shoot density, and above-ground, below-ground, and total biomass of *Syringodium filiforme*, by season and transect 4.46

List of Figures (Continued)

Fig. 4.13 Station means for cover, canopy height, shoot density, and above-ground, below-ground, and total biomass of <i>Thalassia testudinum</i> , by season and transect	4.47
Fig. 4.14 Station means for cover, canopy height, shoot density, and above-ground, below-ground, and total biomass of <i>Halophila engelmannii</i> , by season and transect	4.48
Fig. 4.15 Station means for cover and biomass of all macroalgae and biomass of <i>Gracilaria</i> spp., by season and transect	4.49
Fig. 4.16 Shoot density of the seagrass community, by station, transect, and season	4.50
Fig. 4.17 Above-ground biomass of the seagrass community, by station, transect, and season	4.51
Fig. 4.18 Below-ground biomass of the seagrass community, by station, transect, and season	4.52
Fig. 4.19 Total biomass of the seagrass community, by station, transect, and season	4.53
Fig. 4.20 Shoot density of <i>Halodule wrightii</i> , by station, transect, and season	4.54
Fig. 4.21 Above-ground biomass of <i>Halodule wrightii</i> , by station, transect, and season	4.55
Fig. 4.22 Below-ground biomass of <i>Halodule wrightii</i> , by station, transect, and season	4.56
Fig. 4.23 Total biomass of <i>Halodule wrightii</i> , by station, transect, and season	4.57
Fig. 4.24 Shoot density of <i>Syringodium filiforme</i> , by station, transect, and season	4.58
Fig. 4.25 Above-ground biomass of <i>Syringodium filiforme</i> , by station, transect, and season	4.59
Fig. 4.26 Below-ground biomass of <i>Syringodium filiforme</i> , by station, transect, and season	4.60

List of Figures (Continued)

- Fig. 4.27 Total biomass of *Syringodium filiforme*, by station, transect, and season ... 4.61
- Fig. 4.28 Shoot density of *Thalassia testudinum*, by station, transect, and season ... 4.62
- Fig. 4.29 Above-ground biomass of *Thalassia testudinum*, by station, transect, and season 4.63
- Fig. 4.30 Below-ground biomass of *Thalassia testudinum*, by station, transect, and season 4.64
- Fig. 4.31 Total biomass of *Thalassia testudinum*, by station, transect, and season ... 4.65
- Fig. 4.32 Shoot density of *Halophila engelmannii*, by station, transect, and season .. 4.66
- Fig. 4.33 Above-ground biomass of *Halophila engelmannii*, by station, transect, and season 4.67
- Fig. 4.34 Below-ground biomass of *Halophila engelmannii*, by station, transect, and season 4.68
- Fig. 4.35 Total biomass of *Halophila engelmannii*, by station, transect, and season 4.69
- Fig. 4.36 Total biomass of all macroalgae, by station, transect, and season 4.70
- Fig. 4.37 Total biomass of *Gracilaria* spp., by station, transect, and season 4.71
- Fig. 4.38 Shoot density and above-ground, below-ground, and total biomass of the seagrass community, by station and season 4.72
- Fig. 4.39 Cover, canopy height, shoot density, and above-ground, below-ground, and total biomass of *Halodule wrightii*, by station and season 4.73
- Fig. 4.40 Cover, canopy height, shoot density, and above-ground, below-ground, and total biomass of *Syringodium filiforme*, by station and season 4.74
- Fig. 4.41 Cover, canopy height, shoot density, and above-ground, below-ground, and total biomass of *Thalassia testudinum*, by station and season 4.75
- Fig. 4.42 Cover, canopy height, shoot density, and above-ground, below-ground, and total biomass of *Halophila engelmannii*, by station and season 4.76

List of Figures (Continued)

- Fig. 4.43 Cover and biomass of all macroalgae and biomass of *Gracilaria* spp., by station and season4.77
- Fig. 4.44 Interannual variation in shoot density and above-ground, below-ground, and total biomass of the seagrass community based on station means for Transects 1 and 2 4.78
- Fig. 4.45 Interannual variation in cover, canopy height, shoot density, above-ground, below-ground, and total biomass of *Halodule wrightii* based on station means for Transects 1 and 2 4.79
- Fig. 4.46 Interannual variation in cover, canopy height, shoot density, above-ground, below-ground, and total biomass of *Syringodium filiforme* based on station means for Transects 1 and 2 4.80
- Fig. 4.47 Interannual variation in cover, canopy height, shoot density, above-ground, below-ground, and total biomass of *Thalassia testudinum* based on station means for Transects 1 and 2 4.81
- Fig. 4.48 Interannual variation in cover, canopy height, shoot density, above-ground, below-ground, and total biomass of *Halophila engelmannii* based on station means for Transects 1 and 2 4.82
- Fig. 4.49 Interannual variation in cover and biomass of all macroalgae and biomass of *Gracilaria* spp. based on station means for Transects 1 and 2 4.83
- Fig. 4.50 Linear regressions of above-ground, below-ground, and total biomass vs. shoot density of *Halodule wrightii*, based on seasonal station means 4.84
- Fig. 4.51 Linear regressions of above-ground, below-ground, and total biomass vs. shoot density of *Syringodium filiforme*, based on seasonal station means 4.85
- Fig. 4.52 Linear regressions of above-ground, below-ground, and total biomass vs. shoot density of *Thalassia testudinum*, based on seasonal station means 4.86
- Fig. 4.53 Linear regressions of shoot density, above-ground, below-ground, and total biomass vs. cover of *Halodule wrightii*, based on seasonal station means 4.87
- Fig. 4.54 Linear regressions of shoot density, above-ground, below-ground, and total biomass vs. cover of *Syringodium filiforme*, based on seasonal station means 4.88

List of Figures (Continued)

- Fig. 4.55 Linear regressions of shoot density, above-ground, below-ground, and total biomass vs. cover of *Thalassia testudinum*, based on seasonal station means 4.89
- Fig. 4.56 Linear regressions of shoot density, above-ground, below-ground, and total biomass vs. canopy height of *Halodule wrightii*, based on seasonal station means 4.90
- Fig. 4.57 Linear regressions of shoot density, above-ground, below-ground, and total biomass vs. canopy height of *Syringodium filiforme*, based on seasonal station means 4.91
- Fig. 4.58 Linear regressions of shoot density, above-ground, below-ground, and total biomass vs. canopy height of *Thalassia testudinum*, based on seasonal station means 4.92
- Fig. 5.1 Epiphytic chlorophyll *a* on a per seagrass shoot basis by station, transect, and season for all seagrass species combined 5.12
- Fig. 5.2 Epiphytic chlorophyll *a* normalized to epiphyte dry weight by station, transect, and season for all seagrass species combined 5.13
- Fig. 5.3 Epiphytic chlorophyll *a* normalized to seagrass shoot dry weight by station, transect, and season for all seagrass species combined 5.14
- Fig. 5.4 Epiphyte:seagrass shoot dry weight ratio by station, transect, and season for all seagrass species combined 5.15
- Fig. 5.5 Epiphytic chlorophyll *a* on a per seagrass shoot basis and epiphytic chlorophyll *a* normalized to epiphyte dry weight, by seagrass species and for all species combined, for the entire study 5.16
- Fig. 5.6 Epiphytic chlorophyll *a* normalized to seagrass shoot dry weight and epiphyte:seagrass shoot dry weight ratio, by seagrass species and for all species combined, for the entire study 5.17
- Fig. 5.7 Epiphytic chlorophyll *a* normalized to seagrass shoot dry weight by species, station, and transect 5.18
- Fig. 5.8 Epiphyte:shoot dry weight ratios by species, station, and transect 5.19

List of Figures (Continued)

Fig. 5.9 Epiphytic chlorophyll <i>a</i> normalized to seagrass shoot dry weight by species, station, and season	5.20
Fig. 5.10 Epiphyte:shoot dry weight ratios by species, station, and season	5.21
Fig. 5.11 Epiphytic chlorophyll <i>a</i> normalized to seagrass shoot dry weight and epiphyte:seagrass shoot dry weight ratio by station, for all species combined, for the entire study	5.22
Fig. 5.12 Epiphytic chlorophyll <i>a</i> normalized to seagrass shoot dry weight and epiphyte:seagrass shoot dry weight ratio by station, for each seagrass species	5.23
Fig. 6.1 Seagrass and epiphyte productivity and ratio of epiphyte:seagrass productivity by species and for all species combined	6.8
Fig. 6.2 Seagrass productivity, by month, station, and seagrass species, for the “mid-bed” Transect 2	6.9
Fig. 6.3 Seagrass productivity, by month, station, and seagrass species, for the “deep-edge” Transect 3	6.10
Fig. 6.4 Epiphyte productivity, by month, station, and seagrass species, for the “mid-bed” Transect 2	6.11
Fig. 6.5 Epiphyte productivity, by month, station, and seagrass species, for the “deep-edge” Transect 3	6.12
Fig. 6.6 Ratio of epiphyte:seagrass productivity, by month, station, and seagrass species, for the “mid-bed” Transect 2	6.13
Fig. 6.7 Ratio of epiphyte:seagrass productivity, by month, station, and seagrass species, for the “deep-edge” Transect 3	6.14
Fig. 6.8 Seagrass productivity by month, station, and transect for <i>Halodule wrightii</i>	6.15
Fig. 6.9 Seagrass productivity by month, station, and transect for <i>Syringodium filiforme</i>	6.16
Fig. 6.10 Epiphyte productivity by month, station, and transect for <i>Halodule wrightii</i>	6.17

List of Figures (Continued)

Fig. 6.11 Epiphyte productivity by month, station, and transect for <i>Syringodium filiforme</i>	6.18
Fig. 6.12 Ratio of epiphyte:seagrass productivity by month, station, and transect for <i>Halodule wrightii</i>	6.19
Fig. 6.13 Ratio of epiphyte:seagrass productivity by month, station, and transect for <i>Syringodium filiforme</i>	6.20
Fig. 6.14 Areal seagrass productivity by species and for all species combined	6.21
Fig. 6.15 Areal productivity of seagrass by species, epiphytes, phytoplankton, and benthic microalgae, by station, for the “mid-bed” Transect 2	6.22
Fig. 6.16 Areal productivity of seagrass, by station and seagrass species, for the “mid-bed” Transect 2	6.23
Fig. 6.17 Areal productivity of epiphytes, by station and seagrass species, for the “mid-bed” Transect 2	6.24
Fig. 7.1 Linear regression analysis of K vs. underwater PAR based on weekly water quality sampling at IRL monitoring stations (all stations combined)	7.24
Fig. 7.2 Linear regression analysis of K vs. underwater PAR based on weekly water quality sampling at each IRL monitoring station	7.25
Fig. 7.3 Linear regression analysis of underwater PAR vs. temperature based on weekly water quality sampling at IRL monitoring stations (all stations combined)	7.26
Fig. 7.4 Linear regression analysis of underwater PAR vs. temperature based on weekly water quality sampling at each IRL monitoring station	7.27
Fig. 7.5 Linear regression analysis of underwater PAR vs. salinity based on weekly water quality sampling at IRL monitoring stations (all stations combined)	7.28
Fig. 7.6 Linear regression analysis of underwater PAR vs. salinity based on weekly water quality sampling at each IRL monitoring station	7.29
Fig. 7.7 Linear regression analysis of underwater PAR vs. color based on weekly water quality sampling at IRL monitoring stations (all stations combined)	7.30

List of Figures (Continued)

- Fig. 7.8 Linear regression analysis of underwater PAR vs. color based on weekly water quality sampling at each IRL monitoring station 7.31
- Fig. 7.9 Linear regression analysis of underwater PAR vs. turbidity based on weekly water quality sampling at IRL monitoring stations (all stations combined) 7.32
- Fig. 7.10 Linear regression analysis of underwater PAR vs. turbidity based on weekly water quality sampling at each IRL monitoring station 7.33
- Fig. 7.11 Linear regression analysis of underwater PAR vs. total, inorganic, and organic suspended solids based on weekly water quality sampling at IRL monitoring stations (all stations combined) 7.34
- Fig. 7.12 Linear regression analysis of underwater PAR vs. total suspended solids based on weekly water quality sampling at each IRL monitoring station 7.35
- Fig. 7.13 Linear regression analysis of underwater PAR vs. inorganic suspended solids based on weekly water quality sampling at each IRL monitoring station 7.36
- Fig. 7.14 Linear regression analysis of underwater PAR vs. organic suspended solids based on weekly water quality sampling at each IRL monitoring station 7.37
- Fig. 7.15 Linear regression analysis of underwater PAR vs. total nitrogen and total dissolved nitrogen based on weekly water quality sampling at IRL monitoring stations (all stations combined) 7.38
- Fig. 7.16 Linear regression analysis of underwater PAR vs. total nitrogen based on weekly water quality sampling at each IRL monitoring station 7.39
- Fig. 7.17 Linear regression analysis of underwater PAR vs. total dissolved nitrogen based on weekly water quality sampling at IRL monitoring stations for each station 7.40
- Fig. 7.18 Linear regression analysis of underwater PAR vs. total phosphorus and total dissolved phosphorus based on weekly water quality sampling at IRL monitoring stations (all stations combined) 7.41
- Fig. 7.19 Linear regression analysis of underwater PAR vs. total phosphorus based on weekly water quality sampling at each IRL monitoring station 7.42

List of Figures (Continued)

Fig. 7.20	Linear regression analysis of underwater PAR vs. total dissolved phosphorus based on weekly water quality sampling at each IRL monitoring station	7.43
Fig. 7.21	Linear regression analysis of underwater PAR vs. total silicate based on weekly water quality sampling at IRL monitoring stations (all stations combined)	7.44
Fig. 7.22	Linear regression analysis of underwater PAR vs. total silicate based on weekly water quality sampling at each IRL monitoring station	7.45
Fig. 7.23	Linear regression analysis of underwater PAR vs. chlorophyll <i>a</i> based on weekly water quality sampling at IRL monitoring stations (all stations combined) ..	7.46
Fig. 7.24	Linear regression analysis of underwater PAR vs. chlorophyll <i>a</i> based on weekly water quality sampling at each IRL monitoring station	7.47
Fig. 7.25	Linear regression analysis of K vs. temperature based on weekly water quality sampling at IRL monitoring stations (all stations combined)	7.48
Fig. 7.26	Linear regression analysis of K vs. temperature based on weekly water quality sampling at each IRL monitoring station	7.49
Fig. 7.27	Linear regression analysis of K vs. salinity based on weekly water quality sampling at IRL monitoring stations (all stations combined)	7.50
Fig. 7.28	Linear regression analysis of K vs. salinity based on weekly water quality sampling at each IRL monitoring station	7.51
Fig. 7.29	Linear regression analysis of K vs. color based on weekly water quality sampling at IRL monitoring stations (all stations combined)	7.52
Fig. 7.30	Linear regression analysis of K vs. color based on weekly water quality sampling at each IRL monitoring station	7.53
Fig. 7.31	Linear regression analysis of K vs. turbidity based on weekly water quality sampling at IRL monitoring stations (all stations combined)	7.54
Fig. 7.32	Linear regression analysis of K vs. turbidity based on weekly water quality sampling at each IRL monitoring station	7.55

List of Figures (Continued)

- Fig. 7.33 Linear regression analysis of K vs. total, inorganic, and inorganic suspended solids based on weekly water quality sampling at IRL monitoring stations (all stations combined) 7.56
- Fig. 7.34 Linear regression analysis of K vs. total suspended solids based on weekly water quality sampling at each IRL monitoring station 7.57
- Fig. 7.35 Linear regression analysis of K vs. inorganic suspended solids based on weekly water quality sampling at each IRL monitoring station 7.58
- Fig. 7.36 Linear regression analysis of K vs. organic suspended solids based on weekly water quality sampling at each IRL monitoring station 7.59
- Fig. 7.37 Linear regression analysis of K vs. total nitrogen and total dissolved nitrogen based on weekly water quality sampling at IRL monitoring stations (all stations combined) 7.60
- Fig. 7.38 Linear regression analysis of K vs. total nitrogen based on weekly water quality sampling at each IRL monitoring station 7.61
- Fig. 7.39 Linear regression analysis of K vs. total dissolved nitrogen based on weekly water quality sampling at each IRL monitoring station 7.62
- Fig. 7.40 Linear regression analysis of K vs. total phosphorus and total dissolved phosphorus based on weekly water quality sampling at IRL monitoring stations (all stations combined) 7.63
- Fig. 7.41 Linear regression analysis of K vs. total phosphorus based on weekly water quality sampling at each IRL monitoring station 7.64
- Fig. 7.42 Linear regression analysis of K vs. total dissolved phosphorus based on weekly water quality sampling at each IRL monitoring station 7.65
- Fig. 7.43 Linear regression analysis of K vs. total silicate based on weekly water quality sampling at IRL monitoring stations (all stations combined) 7.66
- Fig. 7.44 Linear regression analysis of K vs. total silicate based on weekly water quality sampling at each IRL monitoring station 7.67
- Fig. 7.45 Linear regression analysis of K vs. chlorophyll *a* based on weekly water quality sampling at IRL monitoring stations (all stations combined) 7.68

List of Figures (Continued)

Fig. 7.46 Linear regression analysis of K vs. chlorophyll a based on weekly water quality sampling at each IRL monitoring station 7.69

Fig. 7.47 Linear regression analysis of seagrass cover vs. underwater PAR and K based on quarterly sampling of seagrass and quarterly means for PAR and K at IRL monitoring stations (all stations combined) 7.70

Fig. 7.48 Linear regression analysis of above-ground seagrass biomass vs. underwater PAR and K based on quarterly sampling of seagrass and quarterly means for PAR and K at IRL monitoring stations (all stations combined) 7.71

Fig. 7.49 Linear regression analysis of epiphyte load vs. underwater PAR and K based on quarterly sampling of epiphyte loads and quarterly means for PAR and K at IRL monitoring stations (all stations combined) 7.72

Fig. 7.50 Linear regression analysis of seagrass cover vs. underwater PAR and K based on quarterly sampling of seagrass and quarterly means for PAR and K at SS 7.73

Fig. 7.51 Linear regression analysis of above-ground seagrass biomass vs. underwater PAR and K based on quarterly sampling of seagrass and quarterly means for PAR and K at LP 7.74

Fig. 7.52 Linear regression analysis of above-ground seagrass biomass vs. temperature based on quarterly sampling of seagrass and quarterly means for temperature at IRL monitoring stations (all stations combined) 7.75

Fig. 7.53 Linear regression analysis of seagrass cover vs. total phosphorus based on quarterly sampling of seagrass and quarterly means for total phosphorus at IRL monitoring stations (all stations combined) 7.76

Fig. 7.54 Linear regression analysis of seagrass cover and above-ground seagrass biomass vs. salinity based on quarterly sampling of seagrass and quarterly means for salinity at IRL monitoring stations (all stations combined) 7.77

Fig. 7.55 Linear regression analysis of seagrass cover and above-ground seagrass biomass vs. total silicate based on quarterly sampling of seagrass and quarterly means for total silicate at IRL monitoring stations (all stations combined) 7.78

Fig. 7.56 Linear regression analysis of epiphyte load vs. total silicate based on quarterly sampling of epiphyte loads and quarterly means for total silicate at IRL monitoring stations (all stations combined) 7.79

List of Figures (Continued)

- Fig. 7.57 Linear regression analysis of seagrass cover vs. temperature based on quarterly sampling of seagrass and quarterly means for temperature at SS and LP 7.80
- Fig. 7.58 Linear regression analysis of seagrass cover vs. total silicate based on quarterly sampling of seagrass and quarterly means for total silicate at BR 7.81
- Fig. 7.59 Linear regression analysis of seagrass cover and above-ground seagrass biomass vs. chlorophyll *a* based on quarterly sampling of seagrass and quarterly means for chlorophyll *a* at SS 7.82
- Fig. 7.60 Linear regression analysis of above-ground seagrass biomass vs. temperature based on quarterly sampling of seagrass and quarterly means for temperature at SS 7.83
- Fig. 7.61 Linear regression analysis of above-ground seagrass biomass vs. salinity based on quarterly sampling of seagrass and quarterly means for salinity at BR ... 7.84
- Fig. 7.62 Linear regression analysis of above-ground seagrass biomass vs. turbidity based on quarterly sampling of seagrass and quarterly means for turbidity at TC 7.85
- Fig. 7.63 Linear regression analysis of epiphyte load vs. salinity, color, and chlorophyll *a* based on quarterly sampling of epiphyte loads and quarterly means for salinity, color and chlorophyll *a* at MB 7.86
- Fig. 8.1 Abundance of grazing epifauna, by taxonomic groups for the entire study and for individual years 8.13
- Fig. 8.2 Abundance of grazing epifauna, by station for the entire study and for individual years 8.14
- Fig. 8.3 Abundance of grazing epifauna, by station and taxonomic groups for the entire study and for individual years 8.15
- Fig. 8.4 Abundance of grazing epifauna, by station and season for the entire study and for individual years 8.16
- Fig. 8.5 Abundance of grazing epifauna, by station, transect, and season for the entire study and for individual years 8.17

List of Figures (Continued)

Fig. 8.6 Linear regression analysis of epiphyte load vs. abundance of grazing epifauna, based on station means 8.18

Fig. 8.7 Linear regression analysis of abundance of grazing epifauna vs. above-ground seagrass biomass based on station means 8.19

Fig. 8.8 Linear regression analysis of above-ground seagrass biomass vs. epiphyte load based on station means 8.20

Chapter 1: Overview of the Study

1.1 Background

The ecological importance of Submerged Aquatic Vegetation (SAV) in estuaries and coastal zones throughout the world is well established (e.g., Wood et al. 1969, Thayer et al. 1984, Larkum et al. 1989). These highly productive plants provide critical habitat and food for many organisms within coastal and estuarine waters (e.g., Lubbers et al. 1990, Pohle et al. 1991) and are important in nutrient cycling and water movement in the system (e.g., Powell and Schaffner 1991). SAV has major impacts on other biotic resources, including fisheries, with considerable economic significance (e.g., Gilmore 1987, Livingston 1987, Durako et al. 1988). The realization that healthy SAV is required for the ecological functioning and the economical viability of estuarine and coastal ecosystems has triggered significant interest in a better understanding and management of this resource.

Major declines in SAV have been documented from a variety of estuarine habitats, including the Chesapeake Bay (Orth and Moore 1983, Twilley et al. 1985), Tampa Bay (Whaley 1990), and Florida Bay (Tomasko 1992, Moncreiff et al. 1992). SAV declines have been attributed to several factors: increased nutrient loadings (Orth and Moore 1983, Whaley 1990), selective light attenuation (Congdon and McComb 1979, Tomasko 1992), or decreased seed germination resulting from low salinity (Caye et al. 1992).

A high priority for the management of the Indian River Lagoon (IRL) is attaining and maintaining a functioning macrophyte-based ecosystem (IRLNEP 1993; Steward et al. 1994). The lagoon, located along over 150 miles of the east-central coast of Florida, has the highest biodiversity of any estuarine system in the continental United States (e.g., Gilmore et al. 1983; dedicated issue of *Bulletin of Marine Science*, July 1995). This richness is attributed both to its geographical location, where the warm temperate and tropical flora and fauna overlap, and to its diverse and complex macrophyte-defined habitats, which include seagrass beds, salt marshes, mangrove forests, and macroalgal communities. SAV is a critical component of the lagoon, playing an important role in biological productivity and species diversity. Within IRL, there are approximately 100,000 acres of seagrass; all seven species of Florida/Caribbean seagrasses are present (Dawes et al. 1995). The predominant species are *Halodule wrightii* (shoal grass) and *Syringodium filiforme* (manatee grass), with lesser amounts of *Thalassia testudinum* (turtle grass; its northern limit is near Sebastian Inlet), *Ruppia maritima*, and 3 species of *Halophila*.

Since the 1950's, the areal extent of SAV within IRL has been dramatically reduced, with estimated losses as high as 100% in certain areas (Haddad 1985). This

decline in SAV coverage has been largely attributed to adverse water quality conditions (i.e., increased nutrients and suspended solids), and the resulting reduction in water clarity. The SAV issue is perhaps best stated as follows (IRLNEP 1993, p. 36): "Seagrass meadows within the Indian River Lagoon are an extremely important component in the ecosystem and are directly linked to the fisheries production within the lagoon and offshore waters. There is evidence that these meadows are declining because of decreased water quality, but there has been no attempt to scientifically identify the processes which are causing these declines."

Water clarity and the availability of light determine seagrass productivity and abundance and the maximal depth to which different species will grow (Dennison 1987, Zieman 1987). For plants, light is best measured as Photosynthetically Active Radiation (PAR), that part of the electromagnetic spectrum which can be used for photosynthesis. Various aspects of water quality can affect the relationship of seagrass and PAR. For example, increased nutrient inputs may indirectly limit seagrasses by stimulating epiphyte growth on seagrass leaves. Excessive epiphytes may cause lower shoot densities, lower leaf area, and lower overall biomass of seagrasses by reducing the amount of light the leaves receive.

This generalized model (i.e., that the health of the seagrass resource is primarily a function of *in situ* PAR and nutrient conditions) is readily applicable to IRL. A first step in determining causes of seagrass decline in the lagoon and in establishing environmental conditions under which seagrass habitat can expand is understanding the interactions of PAR, nutrients and other water quality parameters, and the abundance and productivity of seagrasses and their epiphytes. These interactions are complex because of the large amount of spatial and temporal variability in both the seagrass itself and in PAR and water quality parameters. Decreased water clarity and elevated nutrients occur on various time scales – some in short pulses (hours to days) and others over longer time periods (weeks to months). Incident PAR varies within the course of a day, from day-to-day, and among seasons. Although the general factors contributing to PAR attenuation in estuaries and lagoons are well known, specific causes vary from site to site. Site-specific studies, on a frequent sampling interval, are needed to discern naturally occurring events from unnatural threats to the health of seagrass.

1.2 Objectives

While there is evidence that the health of SAV within IRL has declined because of decreased water quality, there is not a clear understanding of how this decline is related to differences in manageable water quality parameters. This study addresses the problem of SAV loss by determining the relationship of SAV status in the lagoon to water quality, epiphytes, and, in particular, to submarine PAR. This study is a site-specific one

conducted at sites representing a range of PAR and water quality conditions. Results of this study are intended to be a mechanism to assist decision-making in regards to managing the SAV and water quality within IRL.

The objectives of this study are:

- (1) To establish and maintain PAR-monitoring stations at selected stations in IRL that represent a wide range of light, SAV, and water quality conditions;
- (2) To monitor the temporal and spatial variability of PAR and the amount of light attenuation due to the water column at these stations on a continuous basis for 2 years;
- (3) To measure major water quality parameters at these stations weekly for 2 years;
- (4) To quantify the SAV resource at these stations quarterly for 2 years;
- (5) To quantify the epiphyte load on seagrass blades at these stations quarterly for one year;
- (6) To quantify the productivity of seagrass and seagrass epiphytes at these stations quarterly for one year;
- (7) To analyze the resulting data to address the relationships between PAR, light attenuation, seagrass, epiphytes, and water quality;
- (8) To provide or obtain data relevant, but ancillary, to the other tasks, specifically on the relative abundance of epiphyte grazers, nutrient-epiphyte interactions, and PAR attenuation due to epiphytes; and
- (9) To provide information from this study in a form that will be useful in making decisions relevant to the management of SAV and water quality in IRL.

1.3 Overview of Work Plan

The work plan was based on two important assumed relationships: (1) light is the primary factor determining seagrass distribution in IRL, and (2) water clarity is the primary factor determining the amount of light available to seagrass. But in addition: (3) water clarity is determined by several physical, chemical, and biological factors, and (4) to manage for SAV, the relationships between PAR, seagrass, epiphytes, and measurable water quality parameters need to be determined.

Photosynthetically Active Radiation, Water Quality, and Submerged Aquatic Vegetation in IRL

Stations within IRL (Fig. 1.1) were established for continuous monitoring of PAR (Chapter 2), as well as for measurements of water quality (Chapter 3), SAV (Chapter 4), epiphytes (Chapter 5), productivity (Chapter 6), and grazers (Chapter 8). During the selection of these stations, it was believed that they would represent a range of PAR, water quality, and SAV conditions (see Chapter 2 for the rationale of station selection). These stations included both healthy seagrass areas and stressed seagrass beds. Two stations were located near Sebastian River as this portion of IRL is potentially subjected to significant impact in PAR associated with freshwater influences.

Arrays of PAR sensors were deployed and maintained at each station (see Table 1.1 for details on the overall sampling schedule). During the year, continuous PAR measurements were integrated and recorded every 15 minutes and the amount of light attenuation in the water column calculated. Important water quality parameters relevant to light attenuation and/or growth of SAV and algae (i.e., temperature; salinity; water color; turbidity; inorganic, organic, and total suspended solids; total and dissolved nitrogen; total and dissolved phosphorus; total silicate; chlorophyll *a*) were measured weekly. SAV, epiphyte load on seagrass blades, and productivity of SAV and epiphytes were quantified quarterly. The SAV parameters measured were those expected to respond to changes in PAR and nutrients: species composition, above- and below-ground biomass, shoot density, percent cover, canopy height, and abundance of macroalgae.

The resulting data were analyzed to address relationships between PAR, light attenuation, seagrass, epiphytes, and water quality (Chapter 7). Ancillary information was obtained on other aspects of the PAR-SAV-water quality issue, including the relative abundance of epiphyte grazers, experimental manipulations of PAR and nutrient enrichments on the survival and productivity of seagrass, and estimates of light attenuation due to epiphytes (Chapter 8). Recommendations are made on appropriate sampling schedules for measuring PAR, water quality, and SAV in the lagoon (Chapter 9).

Table 1.1 Frequency of sampling and other activities associated with this study. Additional details are provided in the appropriate chapter of this report.

Sampling/ Activity	Frequency and Duration	Chapter
PAR Monitoring	Continuously for 2 years	2
Download PAR Dataloggers	Weekly for 2 years	2
Clean PAR Sensors	Twice per week for 2 years	2
Water Quality	Weekly for 2 years	3
SAV	Quarterly for 2 years	4
Epiphytes	Quarterly for 1 year	5
Primary Productivity	Quarterly for 1 year	6
Grazers	Quarterly for 2 years	8

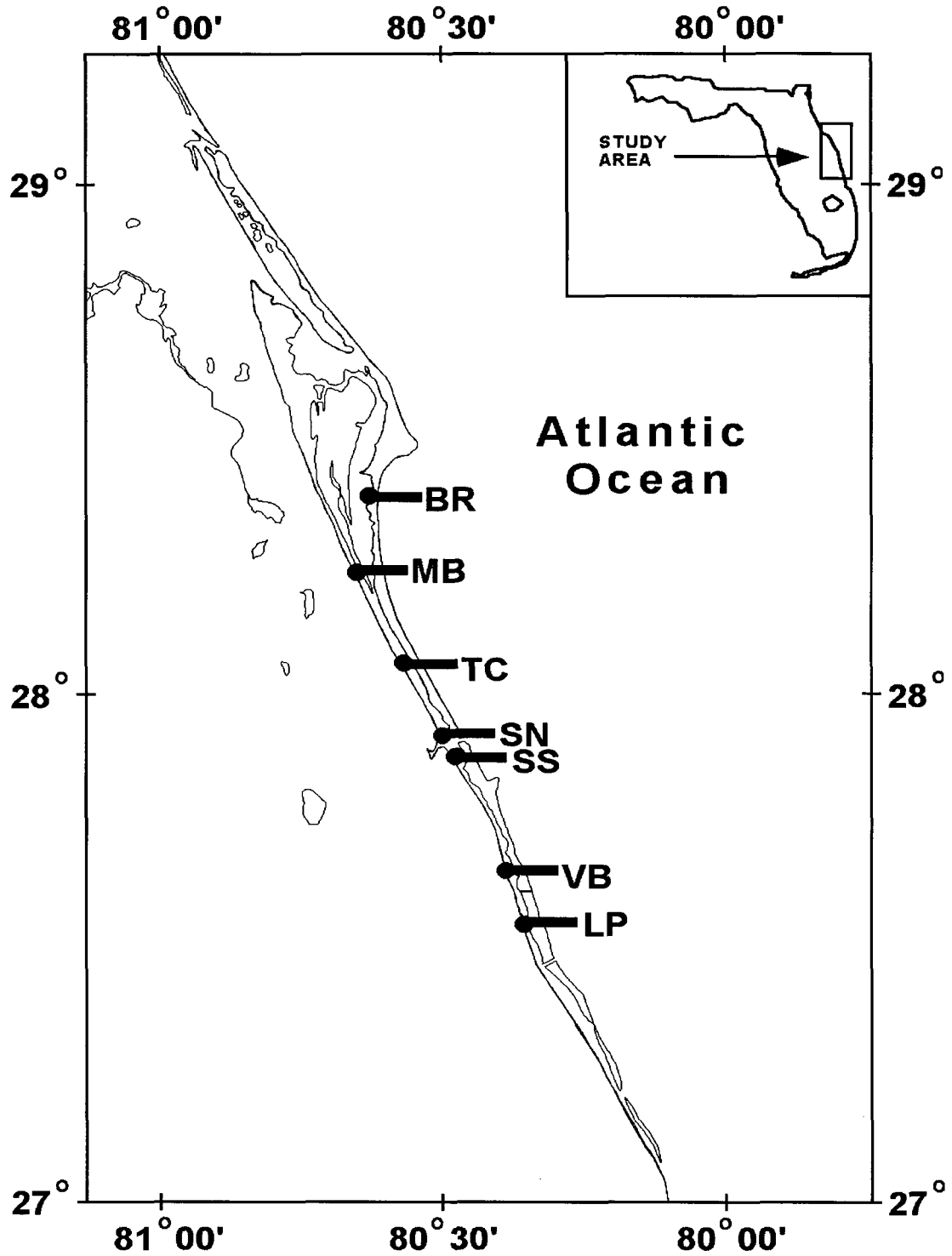


Fig. 1.1 Location of stations sampled in this study within Indian River Lagoon. See Chapter 2 for additional details.

Chapter 2: PAR Monitoring

2.1 Introduction

Seagrasses have a high light requirement, relative to other aquatic plants. Water clarity and light availability determine seagrass productivity and abundance and the maximal depth to which different seagrass species will grow, or indeed, if they will grow at all. Incident light and its attenuation within the water column vary within the course of a day, from day to day, and among seasons. Although the general factors contributing to light attenuation in estuaries and lagoons are well known, specific causes vary from site to site.

For plants, light is best measured as Photosynthetically Active Radiation (PAR), that part of the electromagnetic spectrum which can be used for photosynthesis. The purpose of monitoring PAR in this study was to determine site-specific differences in PAR and in underwater light attenuation (K) at various sites in IRL; there are few such data available. The stations selected for this monitoring represent a range of light, water quality, and SAV conditions and include both healthy and stressed seagrass beds. Two stations were located near Sebastian River, as this portion of IRL is potentially subjected to significant impacts on PAR associated with freshwater influences. At two other stations, comparisons were made of PAR and K measured by two types (spherical and cosine) of underwater sensors.

2.2 Description of Tasks

Task 1: To establish and maintain PAR-monitoring stations at selected stations in IRL that represent a wide range of light, SAV, and water quality conditions.

Task 2: To monitor the temporal and spatial variability of PAR and the amount of light attenuation due to the water column at these stations on a continuous basis for 2 years.

2.3 Methods

2.3.1 Station Selection

Following several weeks of reconnaissance of potential sites in IRL, and by mutual consent with the District, 6 stations were established for continuous monitoring of PAR and less frequent measurements of water quality, SAV, epiphytes, productivity, and grazers (see Chapters 3 through 8). One station (VB) sampled during Year 1 was

Photosynthetically Active Radiation, Water Quality, and Submerged Aquatic Vegetation in IRL

replaced for Year 2 monitoring by another station (TC) due to the loss of access to the dock housing the datalogger at the former site. Thus, 5 stations were continuously monitored for 2 years, and 2 stations were monitored for 1 year each.

Important criteria for station selection were species composition and condition of SAV, security of the PAR-monitoring equipment, and ease of installation and maintenance of the equipment. All stations either were already part of the District's lagoon-wide seagrass monitoring program at the start of this study, or were added to that program, concurrent with this study. The 7 stations (Fig. 1.1) were:

BR ("Banana River"; 28° 30.34' N, 80° 35.30' W) - This station was located in northern Banana River, which, along with the northern region of IRL proper and southern Mosquito Lagoon, are generally considered to be the least impacted, most natural areas of the IRL system. Additional assets of this station were a well-developed, multi-species seagrass bed (primarily consisting of *Halodule wrightii* and *Syringodium filiforme*, with small quantities of *Halophila englemannii*), existence of historical data and other ongoing environmental monitoring by Dynamac, Inc. (formerly Bionetics, Inc.), a well-defined "deep end" of the seagrass bed, and a high degree of security for locating additional sensors for the cosine vs. spherical sensor comparison.

MB ("Melbourne"; 28° 09.00' N, 80° 38.11' W) - This station was located north of Eau Galle Causeway on the western shore of IRL, within a section of IRL in the Melbourne area of Brevard County that has been almost completely devoid of seagrasses since at least 1980. This station was selected to represent an area of stunted, sparse seagrass (the only species present was *H. wrightii*) and potentially poor water quality.

TC ("Turkey Creek"; 28° 01.89' N, 80° 34.55' W) - This station, monitored only during Year 2, was located south of Melbourne and south of Turkey Creek. Like MB, TC was in an area of sparse seagrass (the only species present was *H. wrightii*) and potentially poor water quality. This station was added because of the loss of the VB station and the District's interest in the Turkey Creek area.

SN ("Sebastian-North"; 27° 51.81' N, 80° 29.53' W)

SS ("Sebastian-South"; 27° 50.98' N, 80° 29.21' W) - These two stations were located on the western shore of IRL, near the mouth of the Sebastian River, a colored, nutrient-rich, freshwater system. Seagrass at these stations consisted of nearly monospecific beds of *H. wrightii*, with traces of *S. filiforme* and *Halophila* spp. During the reconnaissance, the individual seagrass plants at the southern station appeared to be more robust than those at the northern station. The colored, nutrient-rich freshwater flows predominately north out of the mouth of the river.

VB ("Vero Beach"; 27° 34.52' N, 80° 21.51' W) - This station, located near the southern end of Vero Beach, on the western shore of IRL, was sampled only during

Year 1. This site, along with the next station (LP), were selected because they both were in lush, multi-species seagrass beds, consisting of *H. wrightii*, *S. filiforme*, and *Thalassia testudinum*, more typical of southern IRL.

The PAR monitoring array at this station had to be re-located 100 m further north in July 1994 because of a problem with the property owner. PAR data from the replacement site (OR = Oslo Road) were combined with the VB station; measurement of water quality parameters continued at VB throughout Year 1, as well as at OR when the PAR instrumentation was on line at that site; measurements of SAV, epiphytes, productivity, and grazers continued to be made at the original VB site during the course of the year.

Collection of PAR data at OR was limited by shallow water during the late summer months; by mutual consent with the District, the PAR monitoring array was removed when the water level was too shallow to keep the sensors submerged. It appears that a similar problem would have also occurred at the original sensor site; a considerable amount of seagrass at both sites from the shore to the sensors was exposed in late summer, with mortality of above-ground biomass.

No PAR measurements were made at this station in Year 2.

LP ("Link Port"; 27° 32.10' N, 80° 20.86' W) - This station was located at a site that probably has the greatest history of sampling anywhere in IRL, because of its proximity to Harbor Branch Oceanographic Institution. In addition to its extensive seagrass bed, this site had considerable security for the additional PAR-monitoring equipment used in the comparison of sensor types conducted at this station.

Collectively these stations encompassed considerable variability in SAV and water quality parameters within IRL. BR was representative of conditions in the northern IRL; VB and LP were more representative of conditions in the southern IRL. Those 3 stations all had high-biomass seagrass beds. MB, and to a lesser extent, TC had a stunted seagrass population. The 2 Sebastian stations facilitated the monitoring of the immediate impacts of freshwater inputs. Four stations (MB, TC, SN, SS) had single-species (*H. wrightii*) beds; 3 stations (BR, VB, LP) had multiple species. *H. wrightii* was present at all stations.

2.3.2 PAR Monitoring

Arrays of PAR sensors were deployed and maintained at each station over the period of November 30, 1993 to November 30, 1995. The equipment for measuring, recording, and downloading PAR data was purchased and provided by SJRWMD/ IRLNEP. There were 3 types of Li-Cor quantum sensors used:

- (1) Deck "cosine" or " 2π " sensors (LI-190SA Quantum Sensors) - These flat sensors measure incident vector irradiance in the air.
- (2) Underwater "cosine" or " 2π " sensors (LI-192SA Underwater Quantum Sensors) - These flat, underwater sensors measure sub-surface vector irradiance. They may also be used in the air, with the appropriate calibration correction.
- (3) Underwater "spherical" or " 4π " sensors (LI-193SA Spherical Underwater Quantum Sensors) - These spherical underwater sensors measure sub-surface scalar irradiance. They may also be used in the air, with the appropriate calibration correction.

All sensors measured PAR in the 400 to 700 nm wavelength band, in units of micromoles per square meter per second ($\mu\text{mol m}^{-2} \text{s}^{-1}$). Prior to deployment, all sensors were cross-calibrated to determine the existence of any irregularities and were found to be well within Li-Cor's specifications of $\pm 5\%$ (within any one type of sensor). Data collected by the sensors were stored in Li-Cor LI-1000 DataLoggers.

Typically, the PAR array at each station consisted of a datalogger with a deck cosine sensor (labeled "C0"), a deck spherical sensor (using the "air" calibration; labeled "S0"), and 2 submersed spherical sensors (using the "water" calibration; labeled "S1" and "S2" for the shallower and deeper sensors, respectively). Because of the number of dataloggers available, SN did not have deck sensors because of its proximity to SS which had the more secure location of the 2 stations. The underwater cables were enclosed in PVC pipe and securely anchored to the bottom. The dataloggers were securely fastened on posts on land or on docks. The spherical sensors measured PAR at 2 depths in the water column: mid-depth (S1 sensor) and just above the seagrass canopy (S2 sensor). Differences in depths of the underwater sensors at each station were determined when the water was calm.

Additional sensors were deployed at BR and LP for a comparison of cosine vs. spherical sensors. Those stations offered the existence of historic data gathered with cosine sensors, the greatest amount of security for the additional instrumentation, and the greatest depth gradient (at BR). Pairs of sensors (cosine vs. spherical) were deployed at the same locations (i.e., "C1" and "S1" were mid-depth and "C2" and "S2" were just above the seagrass canopy) as the other stations and also at a site further offshore (using the 100-m cables). The deep pair of sensors ("C3" and "S3") at BR was at the deep end of the vegetation, readily discernible at this station. At LP, the 100-m cables were used to establish a station in a *Syringodium* bed, in contrast to the multi-species bed that was within reach of the 30-m cables.

PAR measurements were made every 5 seconds continuously and recorded as mean values every 15 minutes for all sensors during the entire photoperiod for 2 years. All dataloggers were synchronized to Eastern Standard Time. Additional HBOI dataloggers permitted a system of switching out dataloggers each week as well as

Photosynthetically Active Radiation, Water Quality, and Submerged Aquatic Vegetation in IRL

downloading data, checking/replacing batteries, and maintaining dataloggers under more environmentally friendly laboratory conditions. Weekly downloading also ensured that HBOI met the requirement that the maximal loss of data permitted was 10 days following discovery of a malfunction or loss. Batteries were changed as needed (low battery warnings provided adequate lead time for changing batteries, given the frequency of downloading).

Because of the rapid fouling of sensors, all submersed sensors were manually cleaned twice weekly, a frequency initially based on previous experience in IRL (M.D. Hanisak, unpublished). Dataloggers were switched out on the same day that water quality sampling occurred. The times of sensor cleaning, switching dataloggers, and other maintenance activities were recorded. Any problems with sensors or dataloggers were corrected during the twice-weekly trips, or, if additional equipment was needed, well within the 10 days specified by the contract.

Limitations/Problems

The instrumentation and cable available put some constraints on this study. The most significant constraint affecting station locations was the length of cable available. Relying mostly on 30-m lengths of cable limited the number of locations where sensors could be deployed "mid-bed". Also, the attempt to deploy the cosine vs. spherical sensor comparison at the "deep edge" of the beds was only successful at one station (BR) because all of the other stations (except MB, which was not an appropriate station for the comparison because of its small seagrass population) would have required much more than the available 100-m cables (e.g., LP would have required 500 m of cable).

Problems with the sensors included physical damage/loss, usually at night, probably as a result of boating or fishing activities (not vandalism). 6 significant impacts (2 each at TC and SS, 1 each at SN and LP) occurred. In addition, 3 sensors spontaneously failed (1 underwater sensor at MB, 2 deck sensors at SS).

Sensor drift of the underwater sensors was a problem initially identified by comparing the readings of the deployed sensors with a newly calibrated one. This problem was addressed by rotating sensors back to Li-Cor for calibration much earlier than Li-Cor's recommendation of calibration every 2 years and incorporating a correction for the measured drift (see Section 2.3.3).

Limited loss of data occurred due to unexplained datalogger shut downs (according to Li-Cor, the units sometimes stopped logging for no apparent reason, i.e., the batteries are good). These problems were quite sporadic, but more frequent during periods of high humidity and rainfall. By weekly monitoring of each unit's battery power, data loss due to "low battery" was avoided. New batteries typically provided 6-

8 weeks of data collection before needing to be replaced. Factors that influenced battery performance included the number of sensors logging, the amount of memory available on the datalogger, and temperature.

The most annoying problem with the PAR-monitoring instrumentation was intermittent data loss due to problems associated with the BNC connectors and terminal blocks which connected additional sensors (beyond the first 2) to the dataloggers. These problems were identified as a result of observing negative PAR readings. Usually, the problems were temporary (less than an hour to a few hours) and were associated with high humidity or heavy rains. Most of the problems disappeared when the BNC connectors were replaced or the terminal blocks were brought back to the lab for a thorough cleaning in distilled water and subsequently redeployed. However, some terminal blocks failed completely, apparently due to small amounts of corrosion. New terminal blocks, treated with silicon spray, experienced much less frequent problems.

Dataloggers were removed for 3 or 4 days in November 1994 from 3 stations (BR, SS, OR) where they appeared to be at risk due to high water and flooding caused by the passage of Tropical Storm Gordon. This storm caused no damage to the underwater PAR-monitoring arrays or the dataloggers left on station.

2.3.3 Data Analyses

Data sets were assembled for each station by combining the appropriate individual weekly data files. Any lines of data with missing values for any of the underwater sensors were omitted (i.e., if one of those sensors did not have a valid reading, then light attenuation could not be calculated). Typically, such missing values occurred near the beginning and end of the photoperiod, or as a result of negative readings due to terminal block problems (previously discussed). Also, anomalous data that could be removed because of direct field observations, primarily limited to drift algae obstruction of one or more sensors at 2 stations (VB and LP), were also removed at this time. Data were loaded into an Excel spreadsheet. Corrections for sensor drift were applied to the raw data by assuming a linear drift during the period of deployment (Li-Cor, personal communication). Vertical attenuation coefficients (K) were calculated from the standard equation (Kenworthy and Haurert 1991):

$$K = -\ln(I_z/I_o) / z$$

where K = vertical attenuation coefficient

I_z = PAR at the deeper sensor ($\mu\text{mol m}^{-2} \text{s}^{-1}$)

I_o = PAR at the shallower sensor ($\mu\text{mol m}^{-2} \text{s}^{-1}$)

z = difference between the depths of the 2 sensors (meters)

Data recorded during periods of station maintenance (e.g., changing out of dataloggers or sensors, cleaning of sensors) were not included in the statistical analyses. Although plotted in the initial presentation of results, K values that were either obviously too low ($k \leq 0$) or too high ($k > 8$) were removed from later statistical analyses. These extreme values were caused by a number of problems including differential or heavy fouling of the sensors, drift algal accumulations obstructing sensors, and, often, the first and last readings during the photoperiod when sun angle was extreme and relatively rapid changes in PAR occurred. One consequence of this data editing was to reduce impacts of sensor fouling on the data, an issue that will be addressed in detail (see Sections 2.4.1 and 2.4.3). An evaluation of how sensor fouling altered PAR readings was made by comparing immediate pre- and post-cleaning readings for each sensor. Additional data reduction occurred after considering diel patterns (see Section 2.4.2) and fouling of sensors (see Section 2.4.3) in greater detail. These reductions in the data sets are summarized in Table 2.1.

In addition to presenting some raw data graphically, data are presented as means \pm standard errors (SE). Statistical analyses were performed with SAS statistical software (SAS Institute 1988). Student's paired t-test of PAR and K before and after sensor cleanings determined if fouling of the sensors was significant. Otherwise, statistical significance among means was tested with analysis of variance (ANOVA). When ANOVA indicated the existence of significant differences, the Tukey-Kramer test (T-K) determined which means were significantly different ($P \leq 0.05$).

Data sets for the 5 stations sampled during both years of the study were analyzed to determine the effect of sampling frequency on the accuracy and precision of means of PAR and K. Accuracy is "the closeness of a measured or computed value to its true value"; precision is "the closeness of repeated measurements of the same quantity" (Sokal and Rohlf 1981). Seven sampling scenarios, with frequencies ranging from continuous to quarterly sampling efforts (Table 2.2), were compared. "True values" were assumed to be the means of each parameter measured during continuous sampling (i.e., the most intensive effort). Means and standard errors for each parameter were calculated for each sampling scenario, for each station. Estimates were made of the sampling frequency needed to obtain means within 10% and 20% of the "true" values (i.e., estimates of the sampling effort required for certain degrees of "accuracy"). In addition, for each sampling scenario, station means for PAR and K were compared with ANOVA and Tukey-Kramer tests.

2.4 Results

The presentation of results begins with the initial analyses performed on the complete data sets for each station and addresses the effects of sensor fouling on

measurements of underwater PAR and K (Section 2.4.1). Because of the observed degree of sensor fouling, only data collected within the first 3 days following sensor cleanings were used in the next analysis on diel patterns (Section 2.4.2). The resulting diel patterns led to a further reduction of the data set to include only data collected between 1000 and 1400 hours. These data are re-examined for the effects of sensor fouling (Section 2.4.3); at some stations there was an effect on PAR and/or K by the third day after sensors were cleaned. Thus, for the remaining, but most important analyses, only data collected between the hours of 1000 and 1400, and within the first 48 hours after sensor cleanings, are used. These analyses include: differences among stations and years (Section 2.4.4), seasonal patterns (Section 2.4.5), and monthly patterns (Section 2.4.6). The analysis of the effects of sampling frequency on estimates of PAR and K is presented with the purpose of making recommendations on the frequency of future PAR sampling in IRL (Section 2.4.7). Lastly, measurements of PAR and K made with cosine sensors at 2 stations (BR and LP) are compared with those made with spherical sensors at the same stations (Section 2.4.8). Those comparisons follow the same progression of analyses previously presented for the spherical sensors (i.e., Sections 2.4.1-2.4.6).

2.4.1 Initial Analyses: Sensor Fouling

Sensor fouling was a major contributor to anomalously high or low K values (e.g., Figs. 2.1-2.7); extremely high K values were often the result of higher fouling of the deeper (S2) sensor, while low, "impossible" K values (i.e., $K < 0$) resulted when the shallower (S1) sensor was much more fouled than the deeper sensor (thus, the deeper sensor was recording higher PAR values). Comparisons of PAR before and after sensor cleanings were made for all stations (Figs. 2.1-2.7). Significant differences (Paired t-test: $P < 0.05$) in underwater PAR before and after cleanings were found at 4 stations (BR, MB, TC, and SN), but not at SS, VB, and LP. K was somewhat less sensitive to fouling: a significant difference (Paired t-test: $P < 0.05$) in K before and after sensor cleanings was found at 3 stations (MB, TC, and LP).

The degree to which PAR or K varied as a result of fouling was variable throughout the year at each station, and even at each sensor. Of the stations sampled during both years, the fouling effect was greatest at MB (Fig. 2.2). At that station, fouling significantly reduced PAR measured by the 2 underwater sensors (Paired t-test: $P < 0.05$), more so for the shallower S1 sensor. With the exception of winter 1995 (December 1994-February 1995), S1 values recorded immediately before and after sensor cleanings were always significantly different (Paired t-test: $P < 0.05$; on average, a 30% reduction in PAR due to fouling). The S2 sensor was less impacted by fouling; values recorded immediately before and after sensor cleanings were significantly different (Paired t-test: $P < 0.05$; on average, a 33% reduction in PAR due to fouling) in 5 of the 8 quarters of sampling [differences were not significant in both

winters (December-February) and in spring 1994 (March-May)]. At MB, K, before and after sensor cleanings, was significantly different (Paired t-test: $P < 0.05$; on average, a 27% increase in K due to fouling) during winter 1994, both summers (June-August), and fall 1995 (September-November). At the 2 other stations where fouling significantly impacted K, K was significantly different at TC throughout the entire year, except fall, and, in contrast, only significantly different at LP during both falls.

These initial analyses suggested that it would be necessary to consider sensor fouling before making temporal and spatial comparisons of PAR and K. To eliminate any potential diel effect masking or interfering with fouling effects, the next analysis used all data points collected at 1200 noon (Figs. 2.8-2.14). These data were subdivided based on the amount of time since the last cleaning (Figs. 2.15-Fig. 2.21). There was not always a consistent pattern in the data; generally, increasing variability in K occurred with time. The 1200 noon plots (Figs. 2.8-2.14) also serve to show day-to-day variations for the data sets; K at BR (Fig. 2.8) was generally much less variable than at the other stations.

2.4.2 Diel Patterns

In addition to the overlying diel and seasonal rhythms in PAR that are driven primarily by solar angle and elevation, local meteorological conditions could cause rapid changes in PAR within a given photoperiod (Figs. 2.22-2.24). K (Fig. 2.25) tended to change less abruptly than PAR did. Commonly, K was elevated at the beginning and end of the photoperiod, due to the sharp angle of the sun. But there were also days when K continually changed during the photoperiod (e.g., BR951104 in Fig. 2.25).

Because the initial analysis indicated that sensor fouling could significantly effect PAR, and, to a lesser extent, K, only data collected within 3 days (72 hours) of sensor cleanings were used to determine the overall diel pattern of PAR and K (Figs. 2.26-2.32). All stations had a bell-shaped curve, peaking mid-day, for PAR. Attenuation coefficients varied relatively little during most of the day, being minimal mid-day and usually increasing at the beginning and end of the photoperiod. This U-shaped pattern was more obvious at BR (Fig. 2.26), MB (Fig. 2.27), and VB (Fig. 2.31). SN (Fig. 2.29) had an unusual pattern of K slowly increasing during the day. ANOVA indicated highly significant ($P = 0.0001$) diel variations in K for all stations. Tukey-Kramer analyses indicated that K was statistically equal ($P > 0.05$) over most of the day: 0900 to 1700 for BR (Fig. 2.26), 0800 to 1500 for MB (Fig. 2.27) and SN (Fig. 2.29), 0600 to 1800 for SS (Fig. 2.30), 0700 to 1700 for VB (Fig. 2.31), and 0800 to 1800 for TC (Fig. 2.28) and LP (Fig. 2.32).

While there were highly significant seasonal and monthly differences in the absolute values of PAR and K (see Sections 2.4.5 and 2.4.6) at each station, the diel patterns in PAR and K were consistent throughout seasons and months of the study: maximal PAR mid-day and relatively little variation in K during the photoperiod, with the exception of the beginning and end of the day.

Although the emphasis of data analysis was on K, more so than on PAR, because of the link of K to water quality parameters (see Chapter 7), and given the diel patterns observed in PAR, further analyses were limited to data collected between the hours of 1000 and 1400 (i.e., the range of peak daily PAR and that portion of the photoperiod frequently recommended for measurement of underwater light). Given the large amount of data collected, this portion of the data set provided more than adequate samples for these analyses (Table 2.1).

2.4.3 Effects of Fouling

Using only data collected between the hours of 1000 and 1400 for both years of the study, the effects of fouling on PAR and K were once again analyzed (Figs. 2.33-2.39). ANOVA indicated no significant differences ($P > 0.05$) in PAR among the first 3 days after sensor cleanings only at 2 stations (BR and LP); significant decreases ($P < 0.05$) occurred over the 3 days at all other stations. ANOVA indicated no significant differences in K among the first 3 days after sensor cleanings at 3 stations (BR, VB, and LP); at the other stations, significant increases occurred by Day 3. If one wishes to use a criterion for fouling to be a maximal decline in PAR or a maximal change in K of 10% of Day 1 values, that criterion was met at all stations for the first 2 days of readings, but not for Day 3 values. For example, over the 3-day period, K increased at MB from 1.70 to 1.91 and from 1.88 to 2.19 at TC. Because most of the stations had substantial (>10%) fouling impacts on PAR or K during the third day, it was decided that further spatial and temporal analyses would use only data collected within 2 days (48 hours) of sensor cleanings, during the daily window of the hours of 1000-1400.

2.4.4 Differences among Stations and Years

Comparisons of all stations over both years of the study (Fig. 2.40, Table 2.3), using only data collected between the hours of 1000 to 1400, during the first 48 hours following the cleaning of sensors, indicated significant differences (ANOVA: $P = 0.0001$) in both PAR and K among stations. K was lowest at BR, highest at SN, and intermediate at the other stations. The reverse pattern was observed for PAR reaching the seagrass canopy (i.e., the S2 sensor).

Although the same patterns among stations occurred in both years of sampling, there were significant interannual differences (ANOVA: $P = 0.0001$) at the 5 stations sampled during both years. K was higher in Year 2 at BR, MB, and LP, but higher in Year 1 at SN and SS. The interannual pattern in the amount of underwater PAR reaching the seagrass canopy (i.e., the S2 sensor) at the individual stations was essentially the inverse of that observed for K. Underwater PAR was higher during Year 1 at BR, MB, and LP, but higher during Year 2 at SN. The interannual difference in the amount of underwater PAR reaching the seagrass canopy was not significant between years at SS.

2.4.5 Seasonal Differences

Highly significant (ANOVA: $P = 0.0001$) seasonal differences in PAR and K were found at all stations (Figs. 2.41-2.44). For both years, underwater PAR (Figs. 2.42-2.43) was maximal in spring followed in order by summer, winter, and fall, with the following exceptions: (1) PAR at both BR sensors was statistically equal (T-K: $P > 0.05$) in spring and summer of Year 1, (2) PAR at the S2 sensor at LP was statistically equal (T-K: $P > 0.05$) in spring and summer of Year 1, and (3) PAR at both LP sensors were statistically equal (T-K: $P > 0.05$) in winter and fall of Year 2. The seasonal pattern of K (Fig. 2.44) was considerably more variable. In general, K was usually maximal in fall and minimal in spring.

2.4.6 Monthly Differences

Monthly means for PAR and K (Figs. 2.45-2.48) were calculated for each station and provided additional temporal resolution beyond seasonal analyses. Peak underwater PAR (Figs. 2.46-2.47) usually occurred in April/May, with some stations having an additional peak in July in Year 1. Minimal PAR usually occurred in October/November, but PAR was generally low from September to December or January. The lowest K was typically found in May. K increased at all stations over the summer and fall, usually being highest during the period of July through November. The increase in K was greater, and began earlier, at SN and TC than at the other stations, in Years 1 and 2, respectively. K was low at BR in both years, with the notable exceptions of December 1994-January 1995 and August-November 1995.

2.4.7 Effects of Sampling Frequency on Estimates of PAR and K

Both precision and accuracy of the means of PAR and K improved as sampling frequency increased from quarterly to continuous sampling (Figs. 2.49-2.52). There were no significant differences (ANOVA: $P > 0.05$) among the means of underwater

PAR or K as a function of sampling frequency at any station; this observation was due to the large amount of variability that occurred in low-sampling frequency scenarios. To achieve $\pm 20\%$ accuracy at all stations required at least monthly sampling for PAR (Figs. 2.49-2.51), but only sampling every 2 months for K (Fig. 2.52). To achieve $\pm 10\%$ accuracy required sampling at least every 2 weeks for both PAR and K (Figs. 2.51).

While the previous analysis focused on accurate estimates of means, it also showed that increased sampling effort increased precision (i.e., variability around the means was reduced). The effect of improved precision was more important when comparison of sites, rather than estimates of PAR and/or K at a single site, is desired. ANOVA and Tukey-Kramer analyses demonstrated that increased precision resulted in enhanced ability to distinguish PAR and K among stations (Table 2.4). The ability to determine site-specific differences increased as sampling effort intensified from quarterly to continuous sampling; PAR for the S1 sensor was the only parameter which did not continue to improve with continuous sampling (i.e., for the S1 sensor, no further improvement in the ability to discriminate differences among sites occurred when sampling increased from daily to continuous sampling). Thus, the advantage of frequent PAR sampling was primarily to increase the ability to measure differences among sites than to determine PAR and K characteristics at individual sites.

2.4.8 Comparison of Different Sensor Types

The same type of analyses conducted for spherical sensors in the main portion of the study was also performed for cosine sensors deployed at BR and LP, with the primary intent of comparing sensor types.

Fouling of the 2 types of sensors, and the associated problems with PAR measurements, were different at the 2 stations (Figs. 2.53-2.56). At BR, fouling significantly (Paired t-test: $P < 0.05$) reduced PAR measured at all sensors of both types (Fig. 2.53). Overall, K measured before and after sensor cleanings (Fig. 2.54) was also significantly different with one exception, K_{S1-S2} , where the difference was almost significant (Paired t-test: $P = 0.06$). K measured from cosine sensors was more adversely affected by sensor fouling than that from spherical sensors. In contrast, at LP, fouling did not significantly (Paired t-test: $P > 0.05$) reduce PAR measured for either sensor type (Fig. 2.55), but K from spherical sensors was slightly more adversely affected. The only overall significant difference (Paired t-test: $P < 0.05$) in K measured before and after sensor cleanings (Fig. 2.56) was for K_{S1-S2} . This difference was due to measurements made in fall (September-November) of both years. Deployment of sensors in deeper water (the C3 and S3 sensors at BR) greatly reduced the variability of K (Fig. 2.54).

Comparison of the 1200 (noon) raw data sets for the 2 sensor types (Figs. 2.57-2.60) indicated similar patterns, but different absolute values, for both PAR (Figs. 2.57, 2.59) and K (Figs. 2.58, 2.60). As noted above, considerable reduction in variability was achieved when one of the sensors, regardless of sensor type, was deployed in deeper water (the C3 and S3 sensors at BR; Fig. 2.58).

Diel patterns were similar for the 2 sensor types (Figs. 2.61-2.64), although cosine sensors had flatter bell-shaped curves than spherical ones (Figs. 2.61, 2.63). K calculated from either type was usually more variable at the beginning and end of the day (Fig 2.62, Fig. 2.64). Cosine sensors had a broader window of time when K was equivalent to noon readings (e.g., 0700 to 1800 for K_{C1-C2} vs. 0900 to 1700 for K_{S1-S2} at BR, 0600 to 1800 for K_{C1-C2} vs. 0800 to 1800 for K_{S1-S2} at LP).

In the analysis of the 1000-1400 hours data set, cosine sensors were found to be much more affected by fouling than spherical ones (Fig. 2.65-2.68). At BR, there was no difference (ANOVA: $P > 0.05$) in K over the 3-day period for spherical sensors, but there was a significant increase (ANOVA: $P = 0.0001$; Tukey-Kramer: $P < 0.05$) in K among each of the 3 days for cosine sensors (Fig. 2.66). At LP, there was no difference (ANOVA: $P > 0.05$) in K over the 3-day period from spherical sensors, but a significantly higher K (Tukey-Kramer: $P < 0.05$) during Day 3 than the previous 2 days from cosine sensors (Fig 2.68).

Calculation of the ratio of K from cosine:spherical sensors (Figs. 2.69-2.70, Table 2.5) over the entire study indicated that cosine sensors had a K 20% and 24% higher at BR and LP, respectively, than spherical sensors. At BR, this ratio was lower (12%) when all sensors were in shallow water than when one of the sensor pairs was in deep water (23 and 26%). Additional temporal resolution (seasonal: Figs. 2.71-2.74; monthly: Figs. 2.75-2.78) demonstrated similar patterns of PAR and K for the 2 sensor types.

2.5 Discussion

There are few readily accessible PAR data sets from IRL (Kenworthy 1993), and none have employed continuous monitoring of PAR as was done in this study. This site-specific study determined significant differences in K among stations, with K minimal at BR, maximal at SN, and intermediate at the other stations. Several potential attenuators of light were quantified during the weekly water quality measurements made concurrently with the PAR monitoring, including color, turbidity, suspended solids, and chlorophyll (Chapter 3); all four parameters were lowest at BR. In contrast, water quality at SN, which had the highest light attenuation, was heavily impacted by freshwater and had elevated water color and turbidity levels.

Highly significant seasonal differences in PAR and K were found at all stations. Underwater PAR was maximal in spring followed in order by summer, winter, and fall; this pattern may directly influence seasonal patterns of seagrass biomass (Chapter 4) and productivity (Chapter 6). Both water quality and K were less variable at BR than at the other stations. The sharp seasonal increase in K at SN was consistent with the onset of the wet season in both years. At all stations, in both years, K increased during the wet season, suggesting that freshwater impacts on K (hence, seagrass) in IRL is an important management issue to address. The relationship of water quality parameters and K is analyzed and addressed in greater detail in Chapter 7.

Temporal variability also was readily apparent within individual days (diel variation) and from day to day (daily variation). While the diel curves of PAR were “textbook” in appearance, the relative insensitivity of K to diel fluctuations was surprising. This latter finding suggests that if K, but not PAR, is the parameter of interest, then monitoring of K need not be limited to the traditional “10 to 2” window.

While many factors contributed to short-term variability in measurements of K, much of it appears to be due to the shallow deployment of the sensors, which was necessitated because of the shallowness of the “mid-bed” locations. The higher variability of shallower sensors is probably due to higher wave action and more fouling of the sensors. If there is to be any significant continuous monitoring of PAR in the future, it might be appropriate to locate the instrumentation in deeper areas of seagrass beds (e.g., near the “deep edge”), rather than mid-bed.

Traditionally, underwater PAR has usually been measured with cosine sensors; however, the current trend (Morris and Tomasko 1993) is to favor spherical sensors as they better measure PAR available to plants for photosynthesis. *In situ* comparisons of the 2 sensor types in IRL indicated that cosine sensors routinely measured a K 20-24% higher than what was obtained with spherical ones. This difference is similar to what others have measured (Moore and Goodman 1993), but was somewhat site-specific. It is highly likely that, at a given site, historical cosine-derived measurements could be reasonably converted to values comparable to what would be obtained with spherical sensors.

Cosine sensors were more rapidly fouled than spherical sensors, thus more likely to alter measurements of both PAR and K. Often cosine sensors were observed to have collected what appeared to be re-suspended sediments, which were less likely to be collected by spherical sensors. Although cosine sensors did provide the same temporal (diel, monthly, and seasonal) patterns of PAR and K as spherical sensors, spherical sensors are recommended over cosine ones for all future monitoring that focuses on SAV/PAR relationships in IRL because spherical sensors measure all of the photons available for photosynthesis by seagrass and other primary producers and because PAR and K are less quickly altered as a result of sensor fouling.

The concept of continuous PAR monitoring has merit: it is technically feasible to collect a rather large data set at multiple sites, which may be needed to characterize a dynamic, spatially and temporally heterogeneous environment such as IRL. Data can be collected year-round, regardless of weather and holidays. Data can be obtained during phytoplankton blooms, storm events, major freshwater discharges, etc. without trying to schedule sampling of such stochastic events in advance. However, continuous monitoring also has considerable disadvantages, including the need for regular (in IRL, twice weekly) cleaning of sensors and maintenance of dataloggers. The magnitude of sensor drift and the problems with terminal blocks suggest that the instrumentation is not yet as hardy as is desirable for longer-term monitoring in the humid Florida environment. Other issues such as the uncertain movements of drift algae (a problem relatively localized in time and space in this study) and the potential physical loss/vandalism of monitoring equipment (a problem that was much less than what was anticipated at the start of this study) are also constraints to continuous monitoring. Lastly, in many cases, the resulting, enormous data sets (at least using the 15-minute intervals required for this study) are not required to adequately categorize PAR and K.

How often PAR and K should be measured in future studies depends greatly on their purpose and location in IRL. Based on the different amounts of station-specific variability in PAR and K measurements, the frequency of sampling required to characterize a site in IRL is dependent upon location. For example, with the same level of sampling effort, more precise and accurate estimates of PAR and K can be made at BR, which has much more stable underwater light attenuation, than at SS, where clearly the factors that control light attenuation are much more dynamic. Characterizing a station for PAR and K can be done with less measurements than what is required to compare stations. Reasonably good estimates of PAR and K at any particular site can be made with sampling every 2 weeks; in most cases, differentiation among stations continues to improve all the way up to continuous sampling. Yet the considerable constraints and commitments required for continuous monitoring may seldom be worth the additional level of precision that is obtained. In most cases, it will probably be better to put limited financial resources into other management needs (e.g., more intensive water quality monitoring) than into continuous monitoring of PAR.

Before more PAR monitoring programs in IRL are implemented, it might be wise to consider to what extent K is manageable. It must be recognized that although PAR is the primary factor that determines the productivity and survival of seagrass, PAR is not something that managers can directly manage. What is needed is a better understanding of how differences in PAR are related to differences in water quality parameters which can be managed or regulated; partitioning of factors associated with PAR reduction could be used to direct management actions. There is encouraging

evidence that management action in Tampa Bay, a system rather similar to IRL, has resulted in improved water quality and led to improvements in water clarity and an increase in seagrass cover (D. Tomasko, personal communication). The starting point for justifying similar management action in IRL is the analysis of the PAR-water quality relationships in this study (Chapter 7) and ongoing efforts to develop a water quality model by the District.

2.6 Summary

PAR monitoring was conducted at selected stations in IRL continuously for 2 years to determine site-specific differences in PAR and in underwater light attenuation (K). The stations selected for this monitoring represent a range of light, water quality, and SAV conditions and include both healthy and stressed seagrass beds. Two stations were located near Sebastian River, as this portion of IRL is potentially subjected to significant impacts on PAR associated with freshwater influences. At 2 other stations, comparisons of PAR and K were made between 2 types (spherical and cosine) of underwater sensors. Initial data analyses indicated that, even with twice a week cleaning of sensors, fouling of the sensors had significant impacts on PAR and/or K measurements by the third day at most stations. Also, there was considerable diel variation in PAR and, to a much lesser extent, K. Thus, the major spatial and temporal analyses used only data collected within 2 days (48 hours) of sensor cleanings, during the daily window of the hours of 1000-1400.

The major results of this study were:

- (1) Comparison of all stations over both years of the study indicated significant differences in both PAR and K among stations. K was lowest at BR, highest at SN, and intermediate at the other stations. The reverse pattern was observed for PAR reaching the seagrass canopy.
- (2) Although the same patterns among stations occurred in both years of sampling, there were significant interannual differences at each station sampled during both years. K was higher in Year 2 at BR, MB, and LP, but higher in Year 1 at SN and SS. The interannual pattern in the amount of underwater PAR reaching the seagrass canopy at the individual stations was essentially the inverse of that observed for K. Underwater PAR was higher in Year 1 at BR, MB, and LP, but higher in Year 2 at SN.
- (3) Highly significant seasonal differences in PAR and K were found at all stations. PAR reaching the seagrass canopy was maximal in spring followed in order by summer, winter, and fall. The seasonal pattern of K was more variable, but K was usually maximal in fall and minimal in spring.

- (4) Peak underwater PAR reaching the seagrass canopy usually occurred in April/ May, with some stations having an additional peak in July during Year 1. Minimal PAR usually occurred in October/November, but PAR was generally low from September to December or January. The lowest K was typically found in May. K increased at all stations over the summer and fall, usually being highest from July through November. The increase in K was greater, and began earlier, at SN and TC than at the other stations, in Years 1 and 2, respectively. K was low at BR in both years, with the notable exceptions of December 1994-January 1995 and August-November 1995.
- (5) While absolute values of PAR and K changed throughout the year, diel patterns in PAR and K were consistent throughout seasons and months of the study: strong diel patterns in underwater PAR, characterized by a bell-shaped curve, peaking mid-day, and a relatively constant K throughout most of the photoperiod, usually increasing at the beginning and end of the photoperiod.
- (6) Deployment of sensors at a greater depth substantially reduced the variability of K estimates during continuous monitoring. The higher variability of shallower sensors is believed to be due to higher wave action and more fouling of the sensors.
- (7) *In situ* comparisons of the 2 sensor types in IRL indicated that cosine sensors routinely measured a K 20-24% higher than what was obtained with spherical ones. This relationship was somewhat site-specific. At a given site, cosine-derived measurements could be reasonably converted to values comparable to what would be obtained with spherical sensors. Cosine sensors do not measure all PAR available for seagrass, as do spherical sensors, but do provide similar temporal (diel, monthly, and seasonal) patterns of PAR and K. Spherical sensors are recommended for future monitoring that focuses on SAV/PAR relationships in IRL because they measure all of the photons available for photosynthesis by seagrass and other primary producers.
- (8) The frequency of measurements required to characterize PAR and K at a site in IRL is dependent upon location and the desired levels of accuracy and precision. The amount of sampling required to characterize a station is less than what is needed to detect differences among stations. While in most cases, differentiation among stations continues to improve all the way up to continuous monitoring, reasonably good estimates of PAR and K ($\pm 10\%$ accuracy) at any particular site can be made by sampling every 2 weeks.
- (9) While continuous monitoring of PAR has the advantages of providing a large data set for detailed analysis of underwater PAR and estimates of K, there are

significant disadvantages, including the need for regular (twice weekly) cleaning of sensors and maintenance of dataloggers. Fouling of the sensors significantly impacted measurement of PAR and K within 2 or 3 days after sensors were cleaned at most sites.

- (10) Continuous monitoring may be desirable for some efforts (e.g., site-specific model development and verification), but the considerable added expense, constraints, and commitments required for continuous monitoring may seldom be worth the additional level of precision that is obtained. In most cases, it will probably be better to put limited financial resources into other management needs (e.g., more intensive water quality monitoring) than continuous monitoring of PAR.

Table 2.1 Number of data points, by station, for various analyses performed on PAR and K. See p. 2.8 for details.

Analysis [Text Section]	Year	Station						
		BR	MB	TC	SN	SS	VB	LP
Total (full rows) [2.3.3]	1	14,224	17,906	—	16,827	15,841	12,680	14,670
	2	14,865	16,576	15,738	17,118	17,275	—	14,858
	1&2	29,089	34,482	15,738	33,945	33,116	12,680	29,528
After cleaning & maintenance [2.3.3]	1	14,061	17,540	—	16,667	15,685	12,572	14,440
	2	14,699	16,422	15,571	16,947	17,132	—	14,745
	1&2	28,760	33,962	15,571	33,614	32,817	12,572	29,185
Removal of rows with $K \leq 0$, $K > 8$ [2.4.1]	1	12,192	16,157	—	15,631	12,349	10,828	13,124
	2	13,181	15,385	13,908	14,932	15,806	—	13,886
	1&2	25,373	31,542	13,908	30,563	28,155	10,828	27,010
10:00-14:00, within 72 h of cleaning [2.4.2]	1	4,183	4,521	—	4,432	4,045	3,293	4,214
	2	4,255	4,551	4,384	4,495	4,625	—	4,489
	1&2	8,438	9,072	4,384	8,927	8,670	3,293	8,703
10:00-14:00, within 48 h of cleaning [2.4.3]	1	2,988	3,290	—	3,142	2,899	2,340	2,990
	2	2,927	3,109	3,006	3,133	3,235	—	3,124
	1&2	5,915	6,399	3,006	6,275	6,134	2,340	6,114

Table 2.2 Scenarios for analysis of sampling frequency of PAR and K. Data in these analyses were obtained from continuous monitoring of PAR and K (November 30, 1993-November 30, 1995). Analyses were restricted to the 5 stations which were sampled for the entire 2-year period.

Sampling Frequency	Number of Samples/Year	Samples Used from this Study
Continuous	2,899-3,235	All measurements made between the hours of 1000-1400, within 48 h of sensor cleanings; see Table 2.1 for details relating to sample range
Daily	365	One randomly selected sample per day, from the above continuous sampling data set
Weekly	52	One sample per week from the above daily data set, at approximate seven day intervals
Biweekly	26	Samples from alternate weeks of the above weekly data set
Monthly	12	One sample per month (closest sample to mid-month from the above biweekly data set)
Bimonthly	6	Subset of monthly samples (even-numbered months)
Quarterly	4	Subset of monthly samples (January, April, July, October)

Table 2.3 Means (\pm SE) by station for K, calculated from data collected during the hours of 1000-1400, within 48 hours of cleaning sensors.

Station	Years	n	Mean	\pm SE
BR	1	2,998	0.78	0.01
	2	2,927	1.01	0.02
	1 & 2	5,915	0.89	0.01
MB	1	3,290	1.60	0.02
	2	3,109	1.95	0.02
	1 & 2	6,399	1.77	0.01
TC	1	—	—	—
	2	3,006	1.97	0.02
	1 & 2	3,006	1.97	0.02
SN	1	3,142	3.08	0.02
	2	3,133	2.07	0.02
	1 & 2	6,275	2.58	0.02
SS	1	2,899	1.65	0.02
	2	3,235	1.56	0.02
	1 & 2	6,134	1.60	0.01
VB	1	2,340	1.56	0.02
	2	—	—	—
	1 & 2	2,340	1.56	0.02
LP	1	2,990	1.71	0.02
	2	3,124	2.00	0.02
	1 & 2	6,114	1.86	0.01

Table 2.4 Relationship of sampling frequency with the ability to statistically determine site-specific differences for PAR and K. Data in this analysis were from the continuous PAR monitoring for all stations which were sampled for the entire 2 years of this study; see Table 2.1 for details on how data for each sampling frequency were derived. Codes for sampling frequency are: Q = quarterly, BM = bimonthly, M = monthly, BW = biweekly, W = weekly, D = daily, C = continuous. For each line, P = probability of any significant difference among stations based on ANOVA; stations with identical letters are not significantly different (Tukey-Kramer: $P > 0.05$).

Parameter	Frequency	P	BR	MB	SN	SS	LP
PAR (C0)	Q	0.21	a	a	a	a	a
	BM	0.63	a	a	a	a	a
	M	0.74	a	a	a	a	a
	BW	0.37	a	a	a	a	a
	W	0.30	a	a	a	a	a
	D	0.0001	b	a	a	a	a
	C	0.0001	c	a	b	b	b
PAR (S1)	Q	0.03	a	a	a	a	a
	BM	0.04	a	ab	b	ab	ab
	M	0.0003	a	ab	c	bc	bc
	BW	0.0001	a	ab	c	bc	c
	W	0.0001	a	a	c	b	bc
	D	0.0001	a	a	d	b	c
	C	0.0001	a	a	d	b	c
PAR (S2)	Q	0.02	a	ab	ab	ab	b
	BM	0.01	a	ab	b	ab	b
	M	0.0001	a	ab	c	bc	bc
	BW	0.0001	a	ab	d	bc	cd
	W	0.0001	a	ab	c	b	c
	D	0.0001	a	b	c	b	c
	C	0.0001	a	b	e	c	d
K	Q	0.14	a	a	a	a	a
	BM	0.001	b	ab	a	b	ab
	M	0.0001	b	ab	b	b	b
	BW	0.0001	c	b	a	bc	b
	W	0.0001	c	b	a	b	b
	D	0.0001	d	bc	a	c	b
	C	0.0001	e	c	a	d	b

Table 2.5 Comparison of attenuation coefficients calculated from cosine (C) and spherical (S) sensors at BR and LP. C1 = mid-depth cosine sensor, S1 = mid-depth spherical sensor, C2 = cosine sensor deployed above seagrass canopy, S2 = spherical sensor deployed above seagrass canopy, C3 = deep cosine sensor, S3 = deep spherical sensor. K_{C1-C2} is calculated from C1 and C2 sensors, K_{S1-S2} from S1 and S2 sensors, K_{C1-C3} from C1 and C3 sensors, K_{S1-S3} from S1 and S3 sensors, K_{C2-C3} from C2 and C3 sensors, K_{S2-S3} from S2 and S3 sensors.

Station	Years	Attenuation Coefficients						Ratio Cosine/Spherical Sensor			
		K_{C1-C2}	K_{S1-S2}	K_{C1-C3}	K_{S1-S3}	K_{C2-C3}	K_{S2-S3}	K_{C1-C2} / K_{S1-S2}	K_{C1-C3} / K_{S1-S3}	K_{C2-C3} / K_{S2-S3}	Mean
BR	1	0.93	0.78	0.80	0.64	0.80	0.64	1.19	1.25	1.25	1.23
	2	1.09	1.01	1.03	0.83	1.04	0.81	1.08	1.24	1.28	1.20
	1&2	1.00	0.89	0.91	0.74	0.92	0.73	1.12	1.23	1.26	1.20
LP	1	2.07	1.71	2.12	1.72	—	—	1.21	1.23	—	1.22
	2	2.50	2.00	2.16	1.70	—	—	1.25	1.27	—	1.26
	1&2	2.29	1.86	2.14	1.71	—	—	1.23	1.25	—	1.24

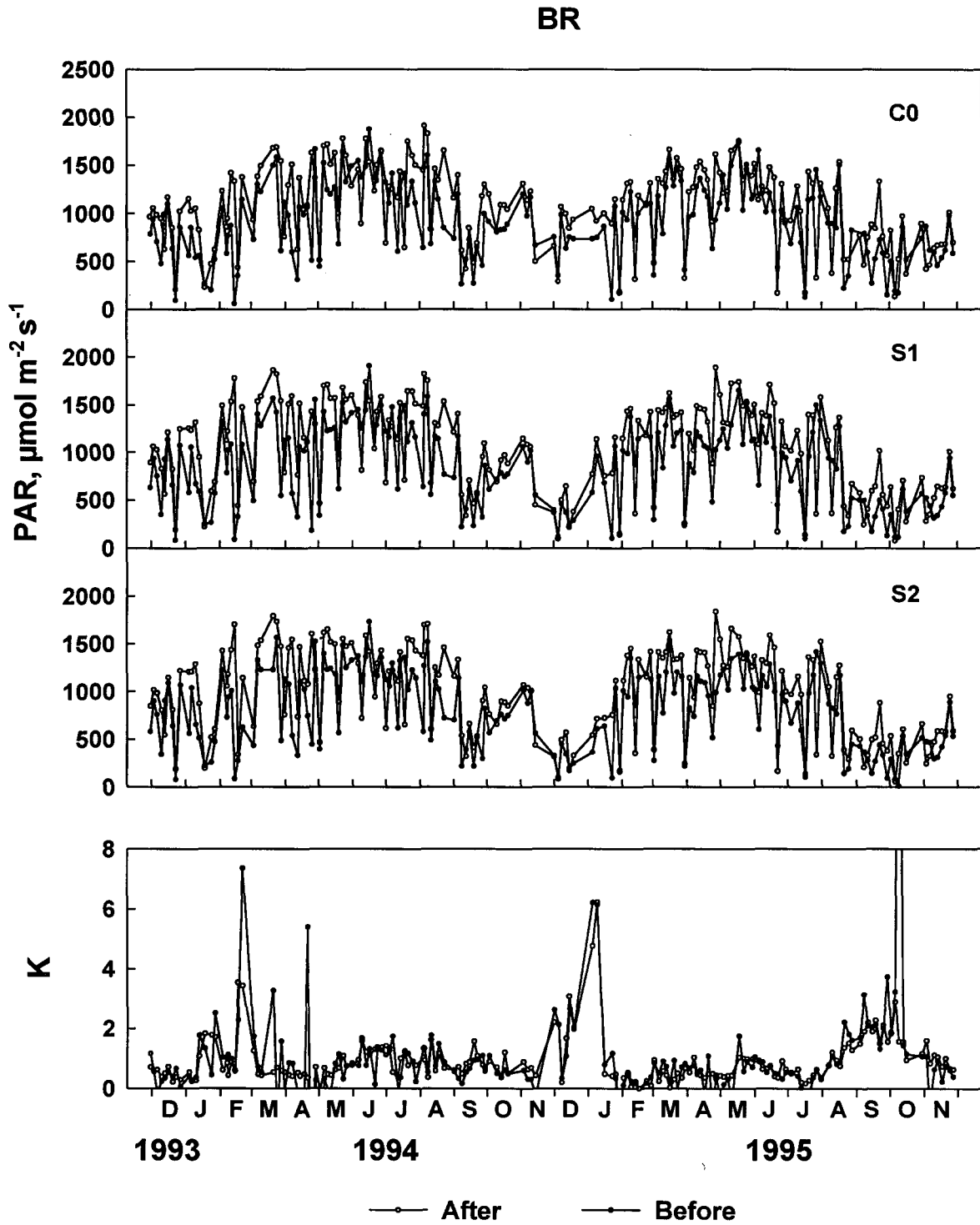


Fig. 2.1 PAR measured by the C0, S1, and S2 sensors, and K, before and after sensor cleaning, at BR, from November 30, 1993 to November 30, 1995.

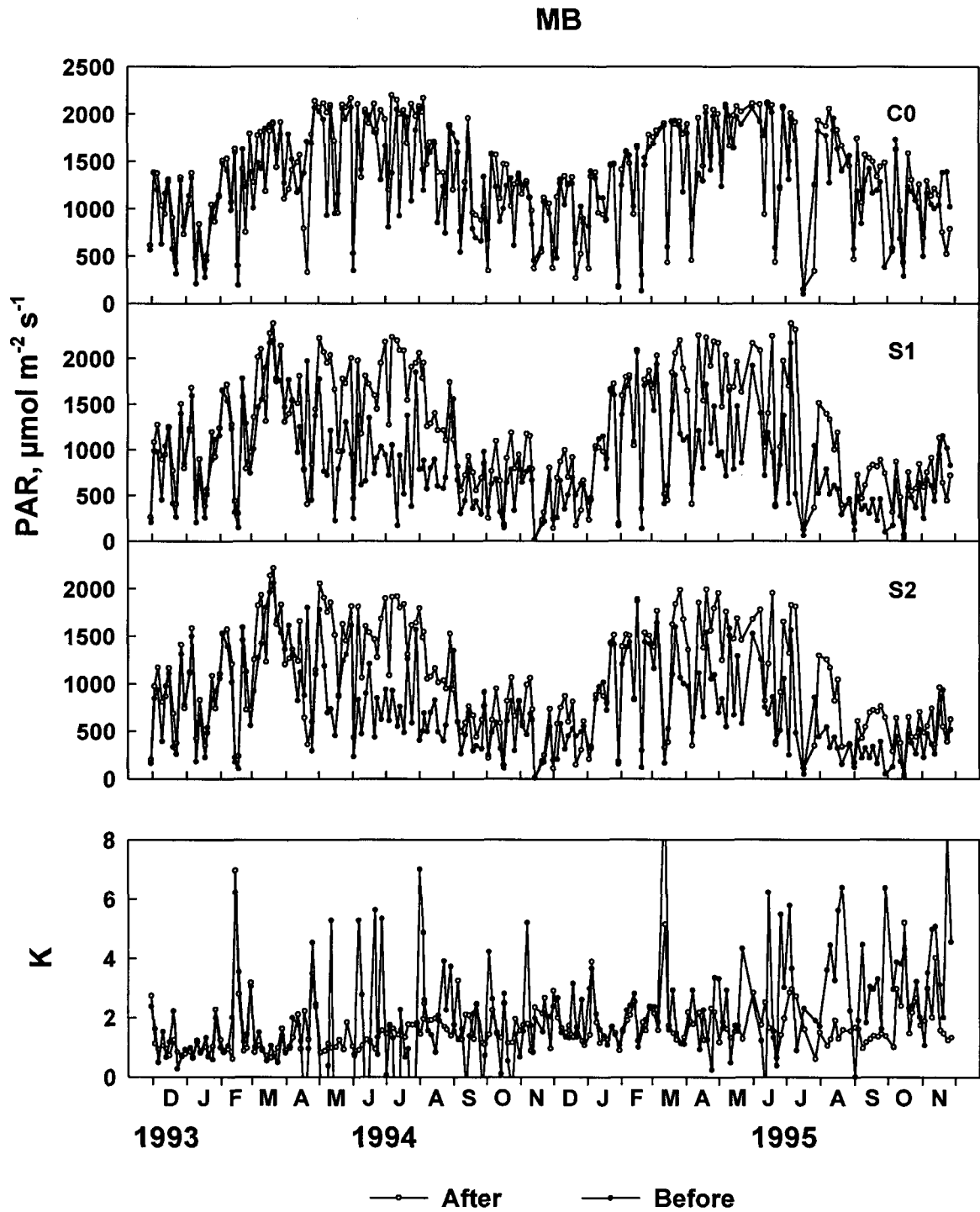


Fig. 2.2 PAR measured by the C0, S1, and S2 sensors, and K, before and after sensor cleaning, at MB, from November 30, 1993 to November 30, 1995.

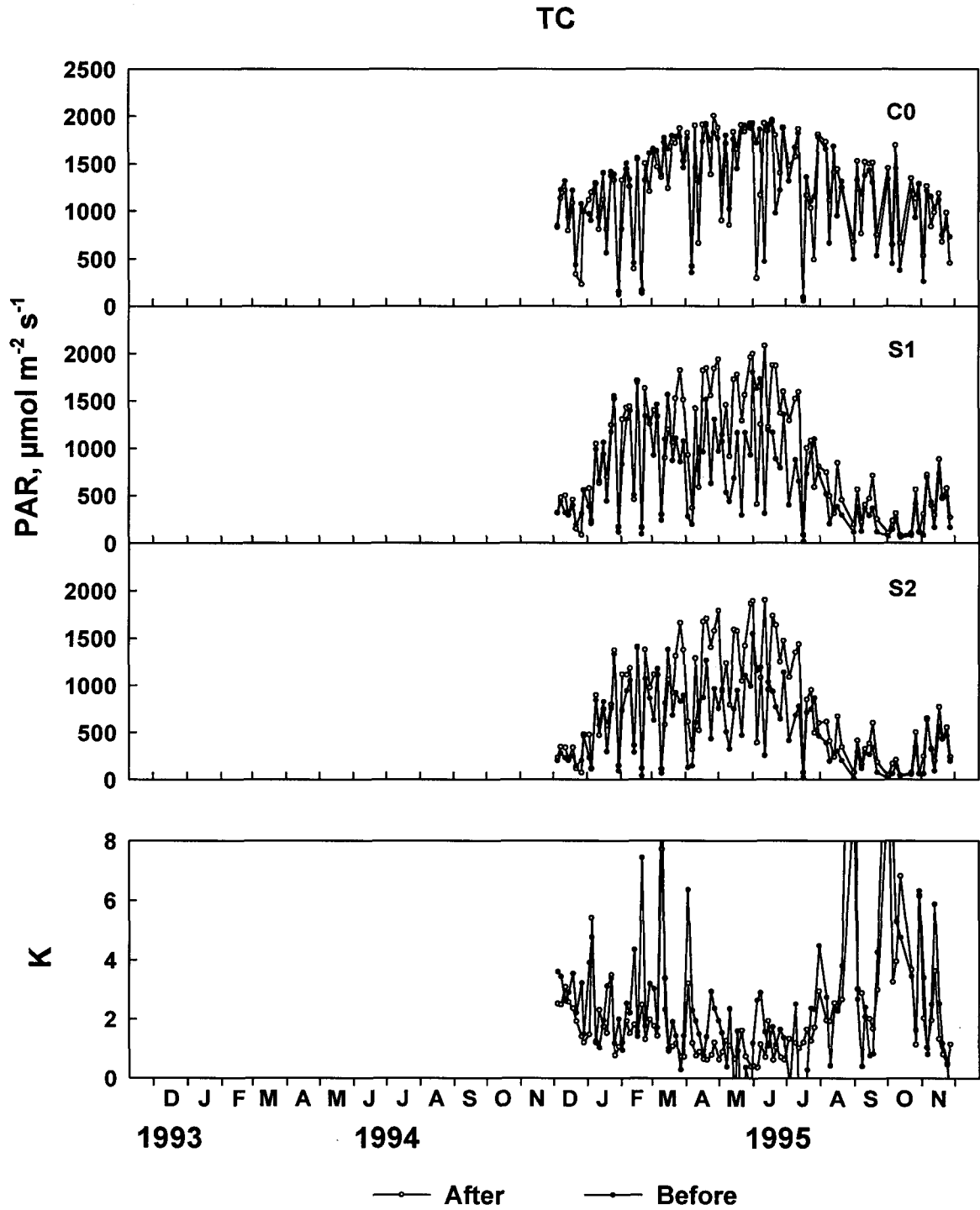


Fig. 2.3 PAR measured by the C0, S1, and S2 sensors, and K, before and after sensor cleaning, at TC, from December 1, 1994 to November 30, 1995.

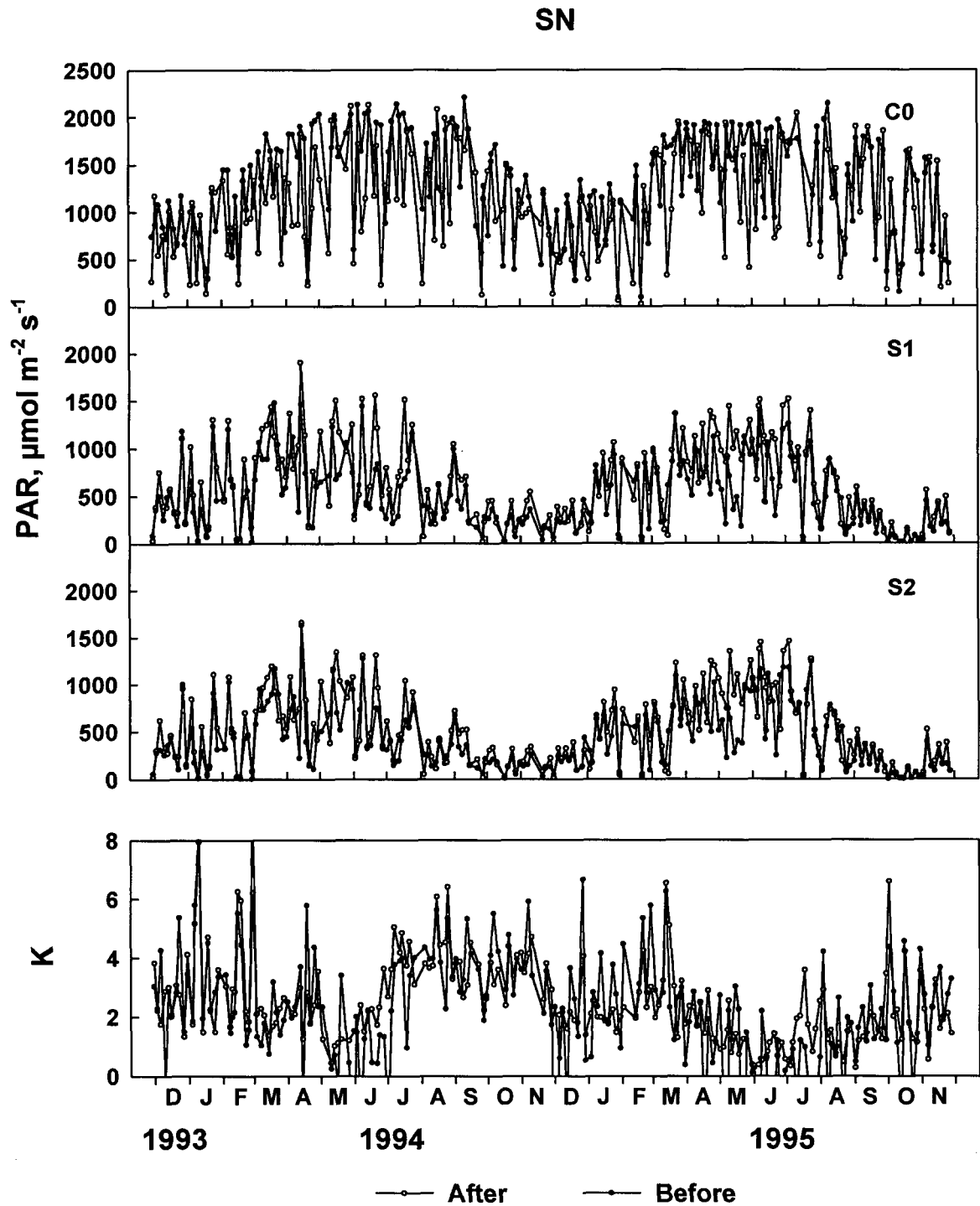


Fig. 2.4 PAR measured by the C0, S1, and S2 sensors, and K, before and after sensor cleaning, at SN, from November 30, 1993 to November 30, 1995.

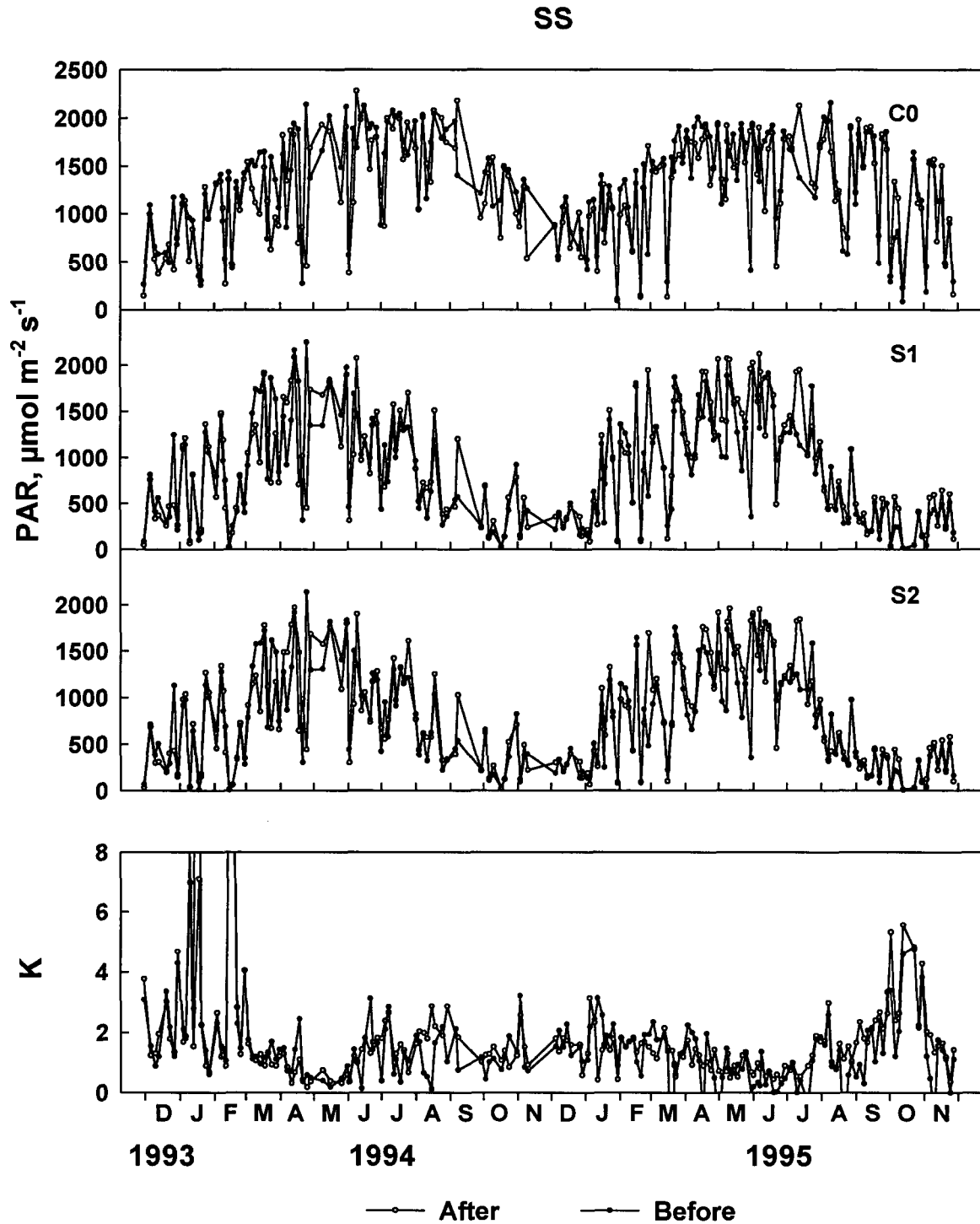


Fig. 2.5 PAR measured by the C0, S1, and S2 sensors, and K, before and after sensor cleaning, at SS, from November 30, 1993 to November 30, 1995.

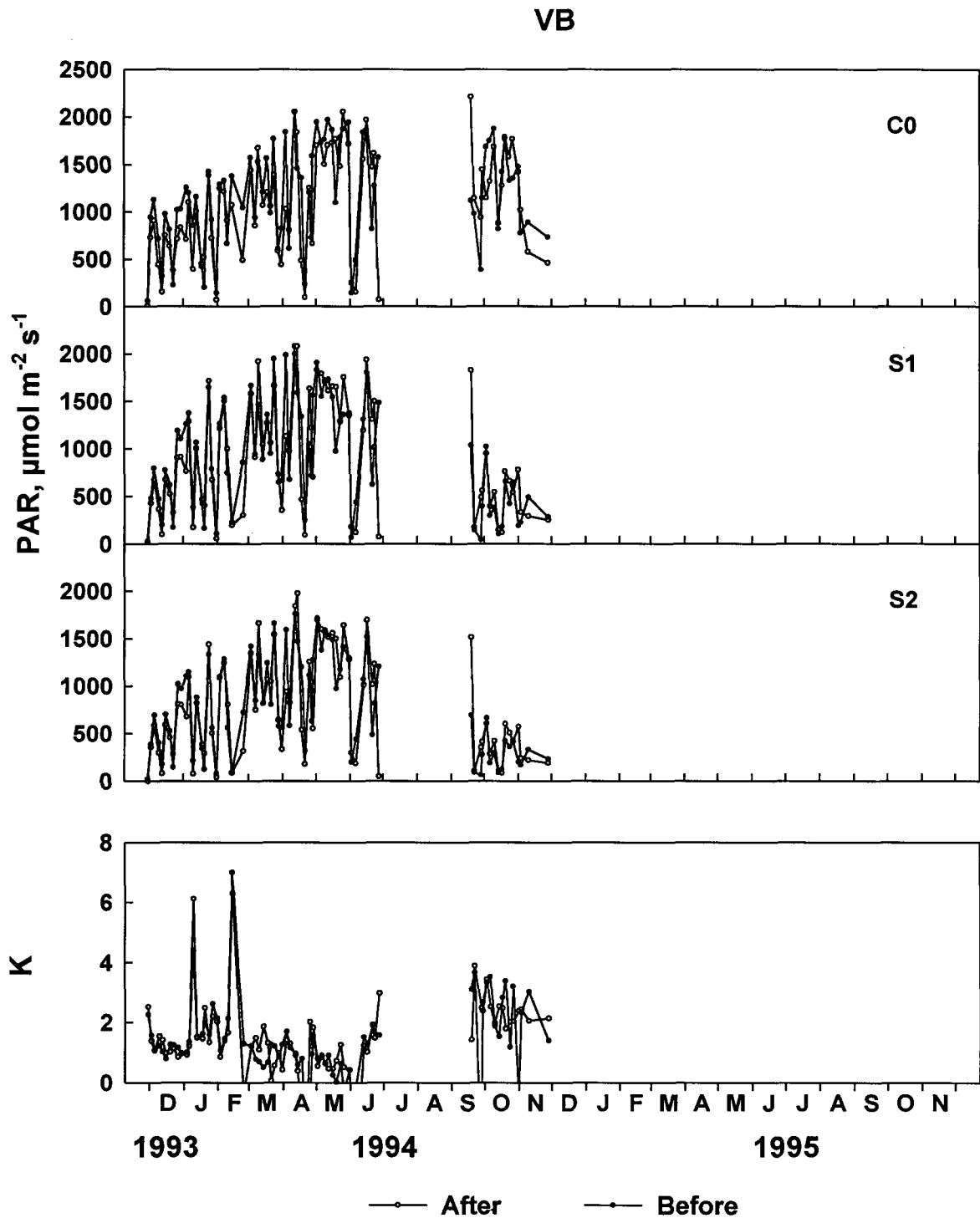


Fig. 2.6 PAR measured by the C0, S1, and S2 sensors, and K, before and after sensor cleaning, at VB, from November 30, 1993 to November 30, 1994.

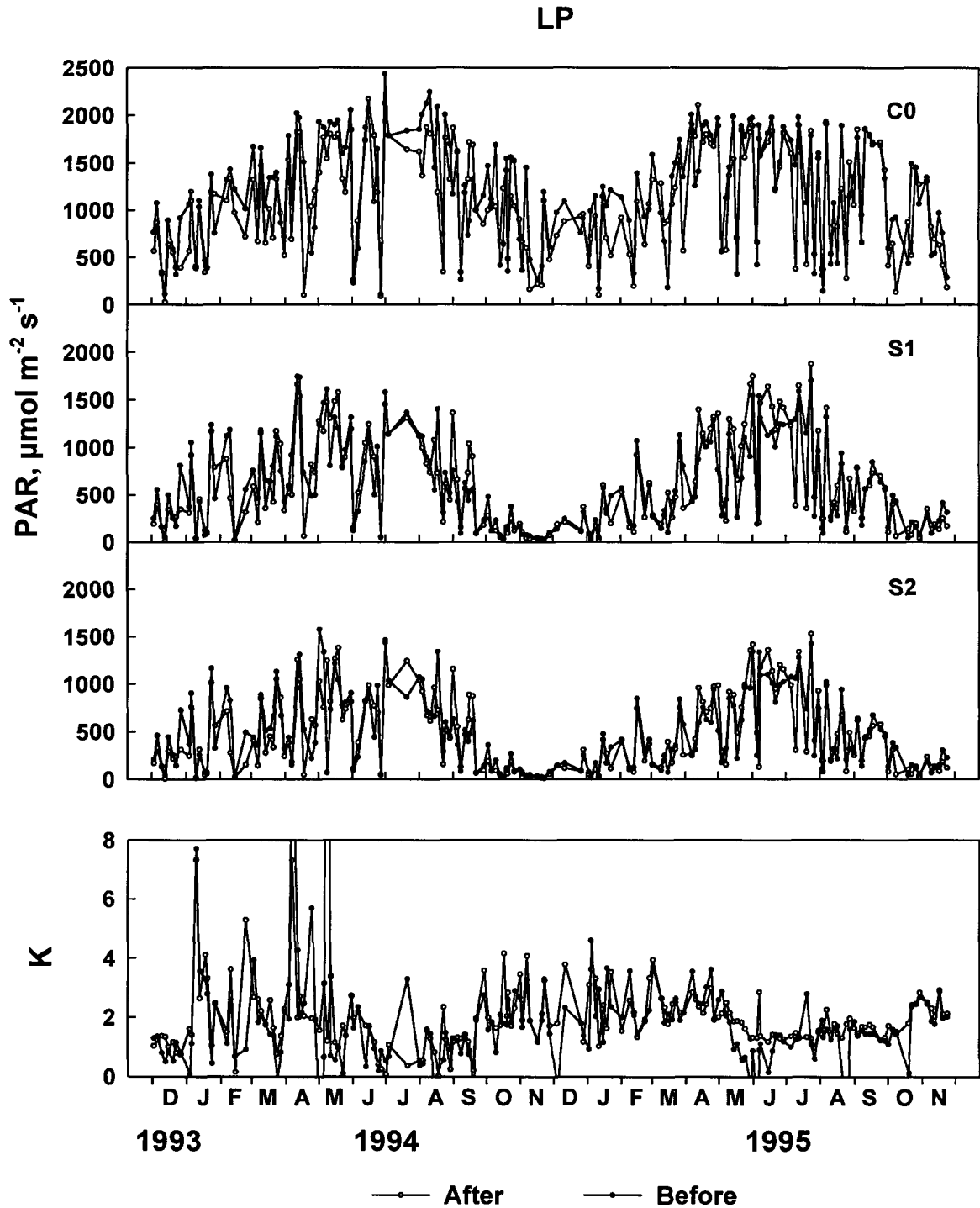


Fig. 2.7 PAR measured by the C0, S1, and S2 sensors, and K, before and after sensor cleaning, at LP, from November 30, 1993 to November 30, 1995.

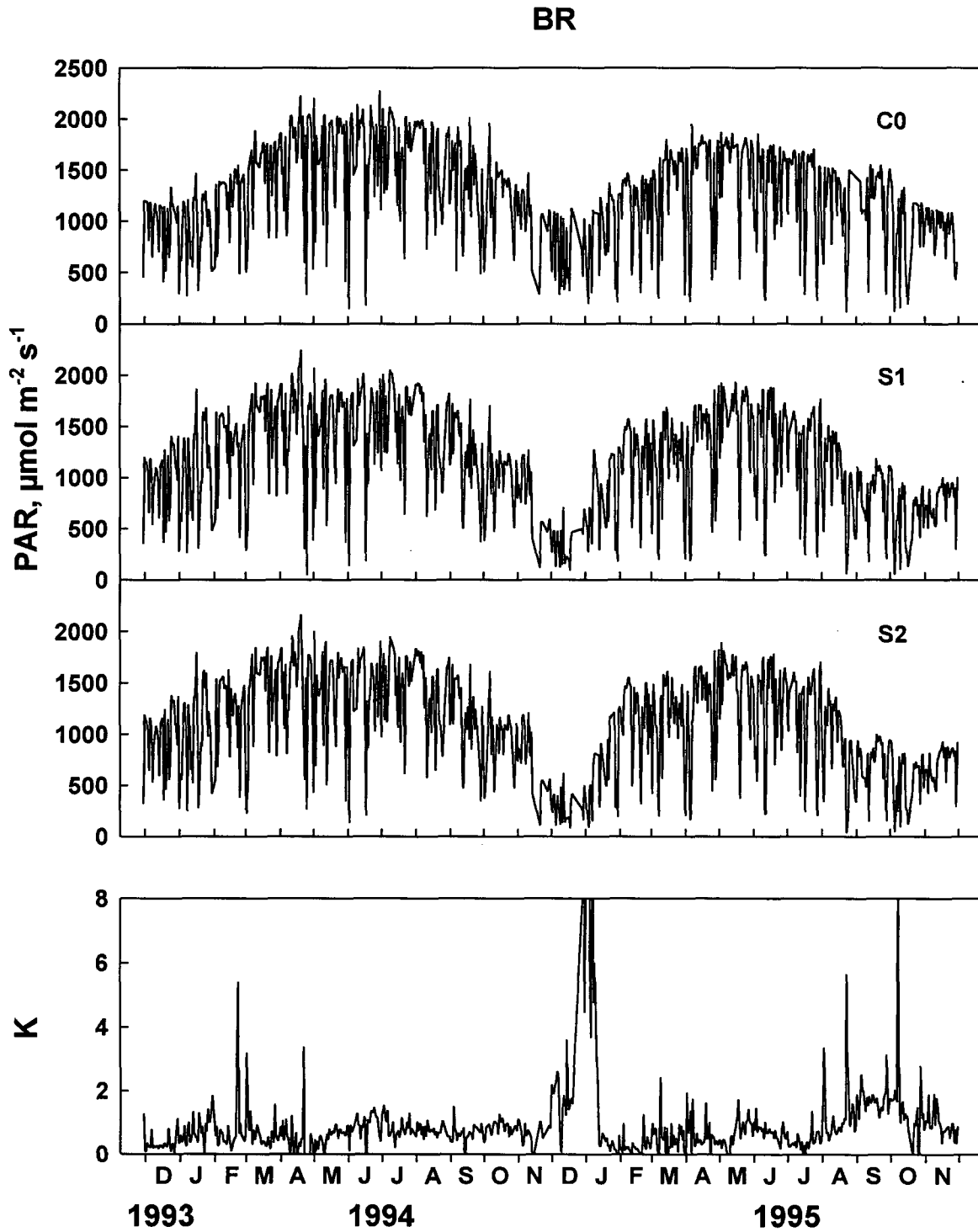


Fig. 2.8 PAR measured by the C0, S1, and S2 sensors, and K, at 1200 noon, at BR, from November 30, 1993 to November 30, 1995.

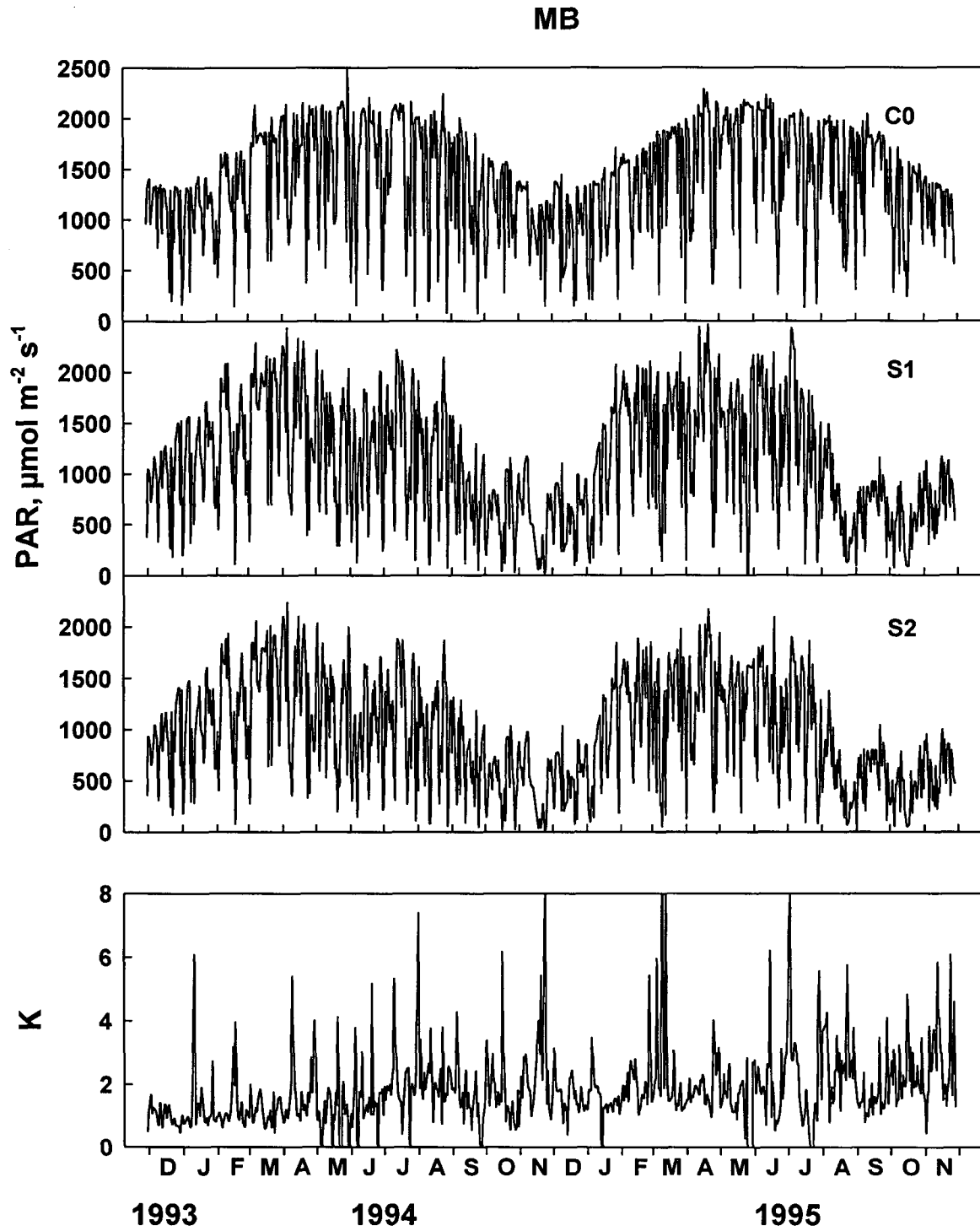


Fig. 2.9 PAR measured by the C0, S1, and S2 sensors, and K, at 1200 noon, at MB, from November 30, 1993 to November 30, 1995.

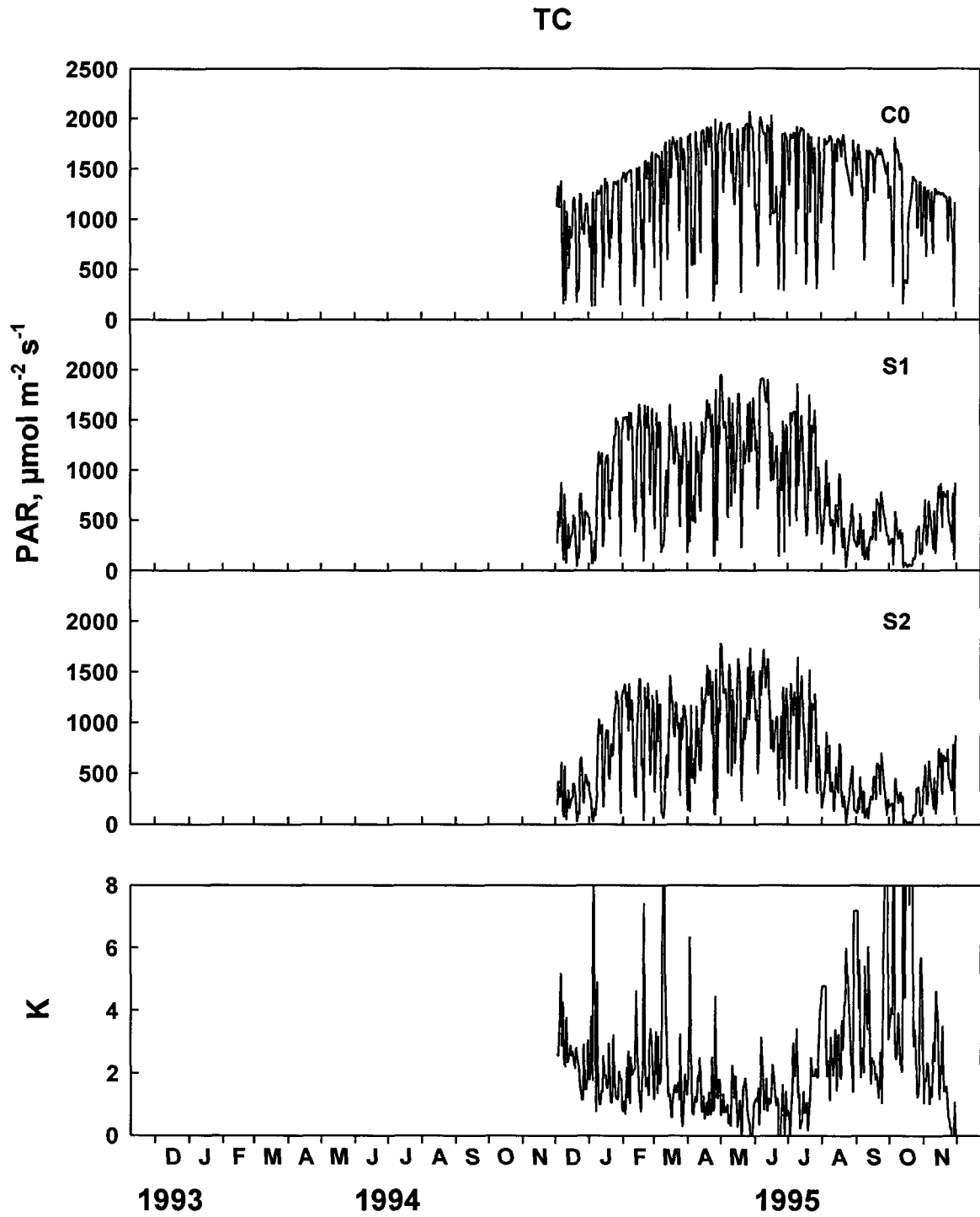


Fig. 2.10 PAR measured by the C0, S1, and S2 sensors, and K, at 1200 noon, at TC, from December 1, 1994 to November 30, 1995.

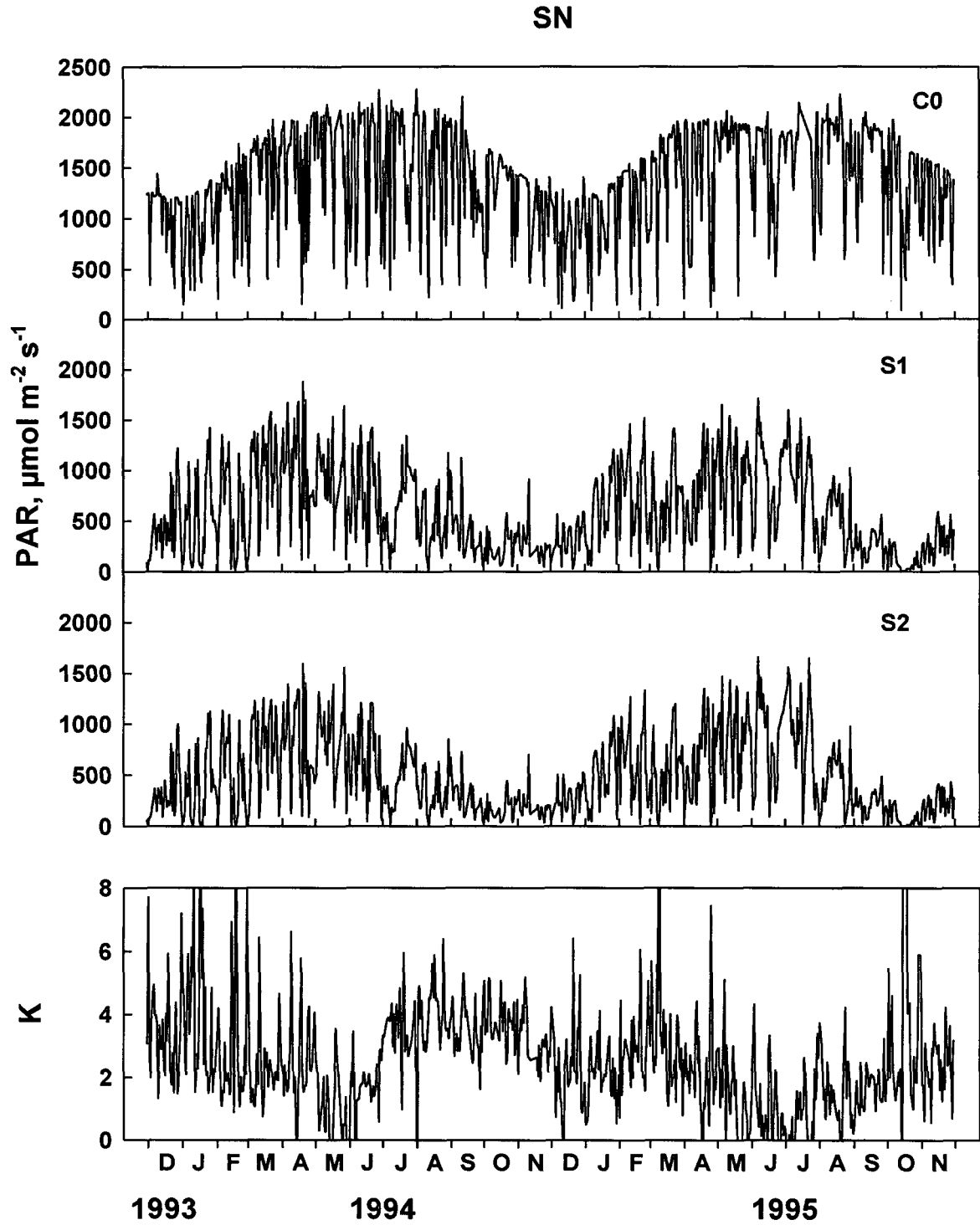


Fig. 2.11 PAR measured by the C0, S1, and S2 sensors, and K, at 1200 noon, at SN, from November 30, 1993 to November 30, 1995.

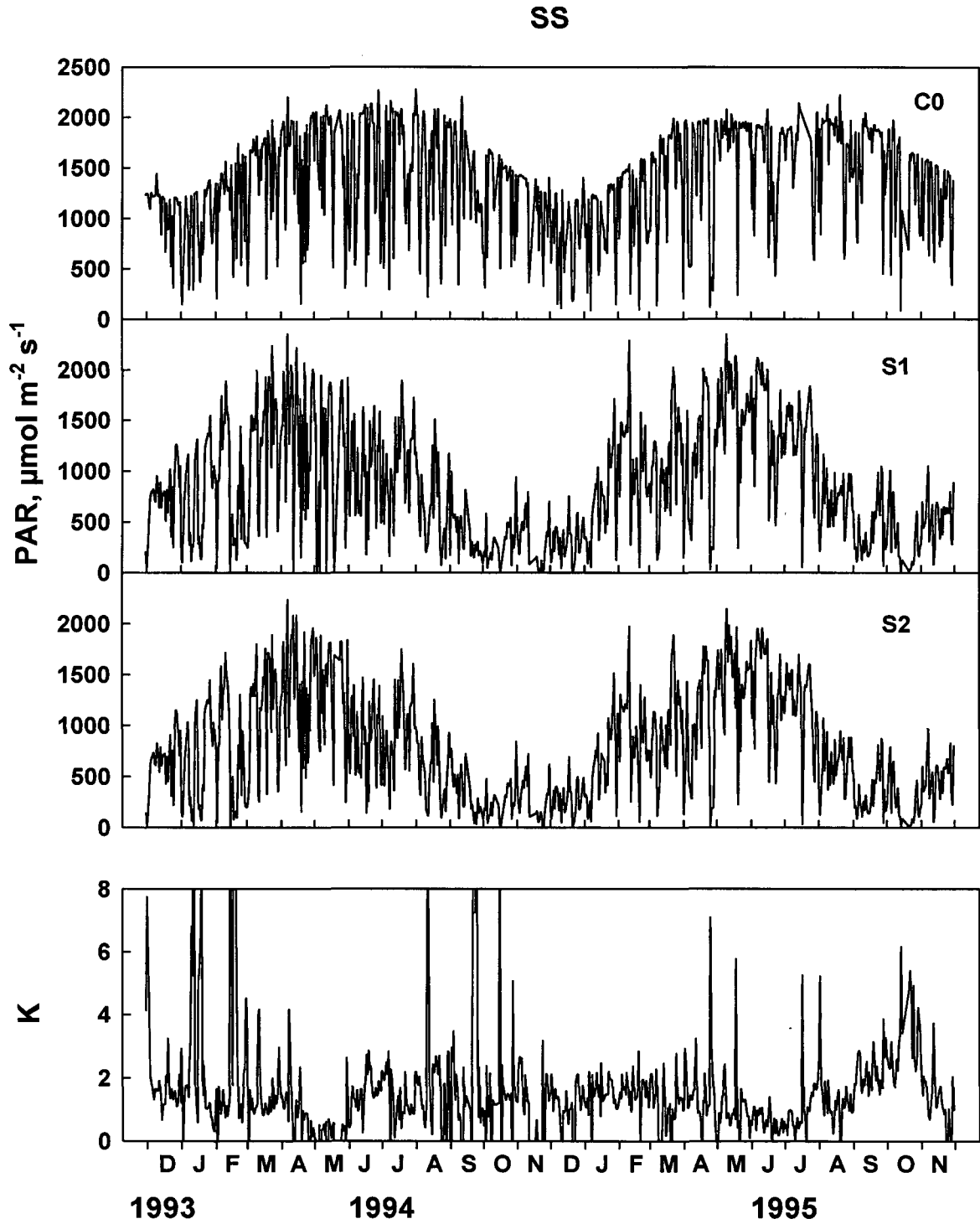


Fig. 2.12 PAR measured by the C0, S1, and S2 sensors, and K, at 1200 noon, at SS, from November 30, 1993 to November 30, 1995.

VB

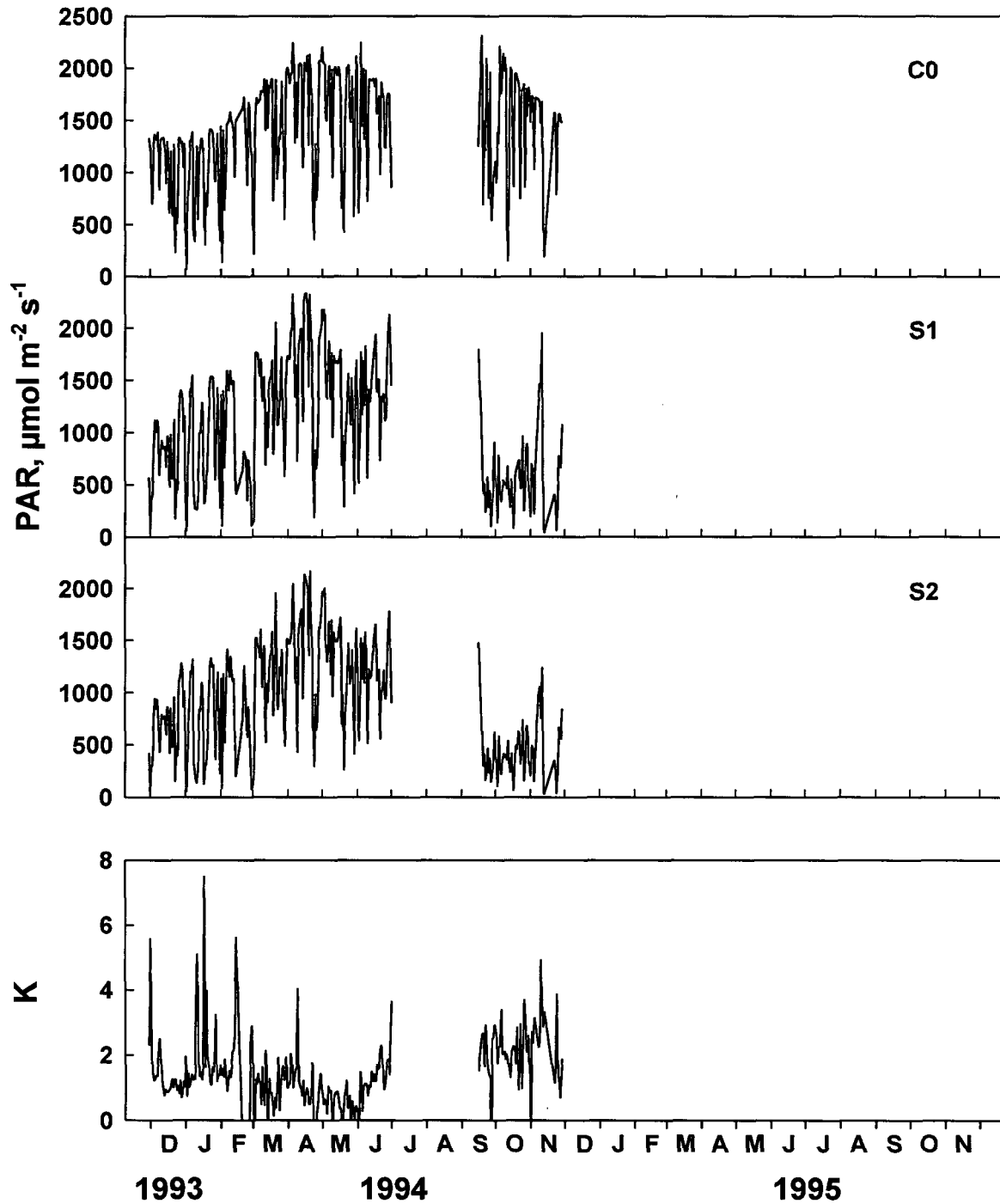


Fig. 2.13 PAR measured by the C0, S1, and S2 sensors, and K, at 1200 noon, at VB, from November 30, 1993 to November 30, 1994.

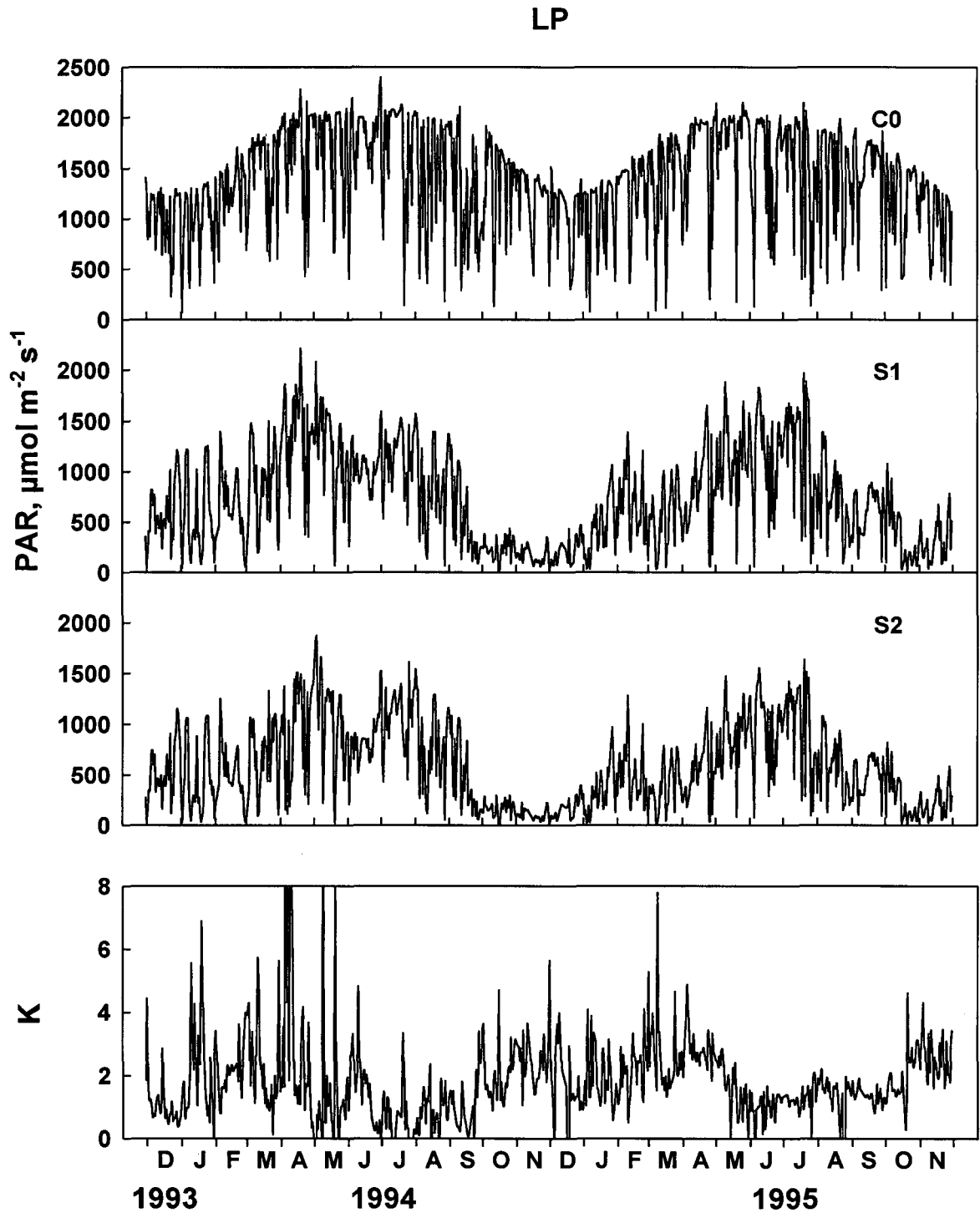


Fig. 2.14 PAR measured by the C0, S1, and S2 sensors, and K, at 1200 noon, at LP, from November 30, 1993 to November 30, 1995.

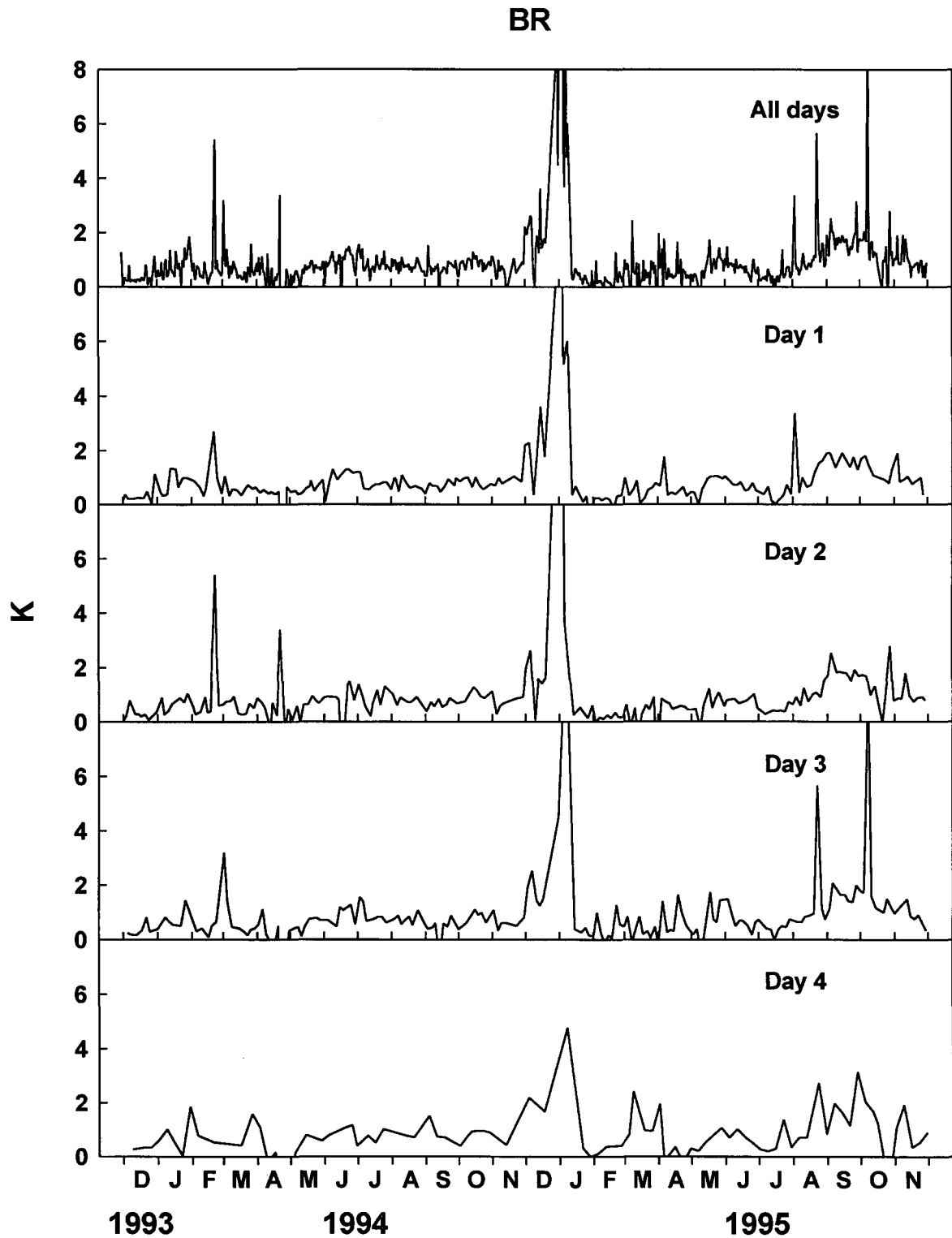


Fig. 2.15 Effect of time since sensor cleaning on K, based on 1200 noon data, at BR, from November 30, 1993 to November 30, 1995. Day 1 = 0-24 hours after cleaning, Day 2 = 24-48 hours, Day 3 = 48-72 hours, Day 4 = 72-96 hours.

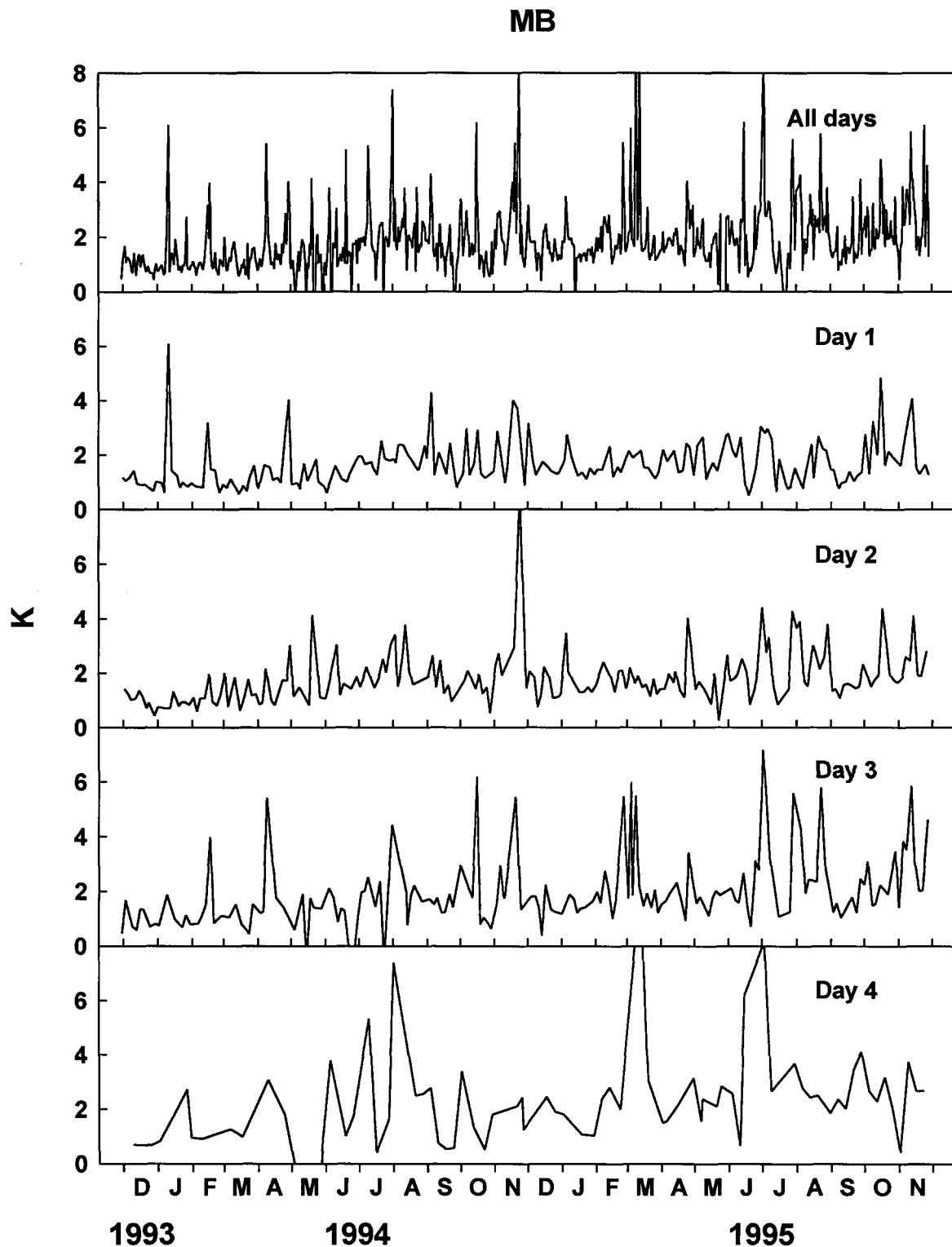


Fig. 2.16 Effect of time since sensor cleaning on K, based on 1200 noon data, at MB, from November 30, 1993 to November 30, 1995. Day 1 = 0-24 hours after cleaning, Day 2 = 24-48 hours, Day 3 = 48-72 hours, Day 4 = 72-96 hours.

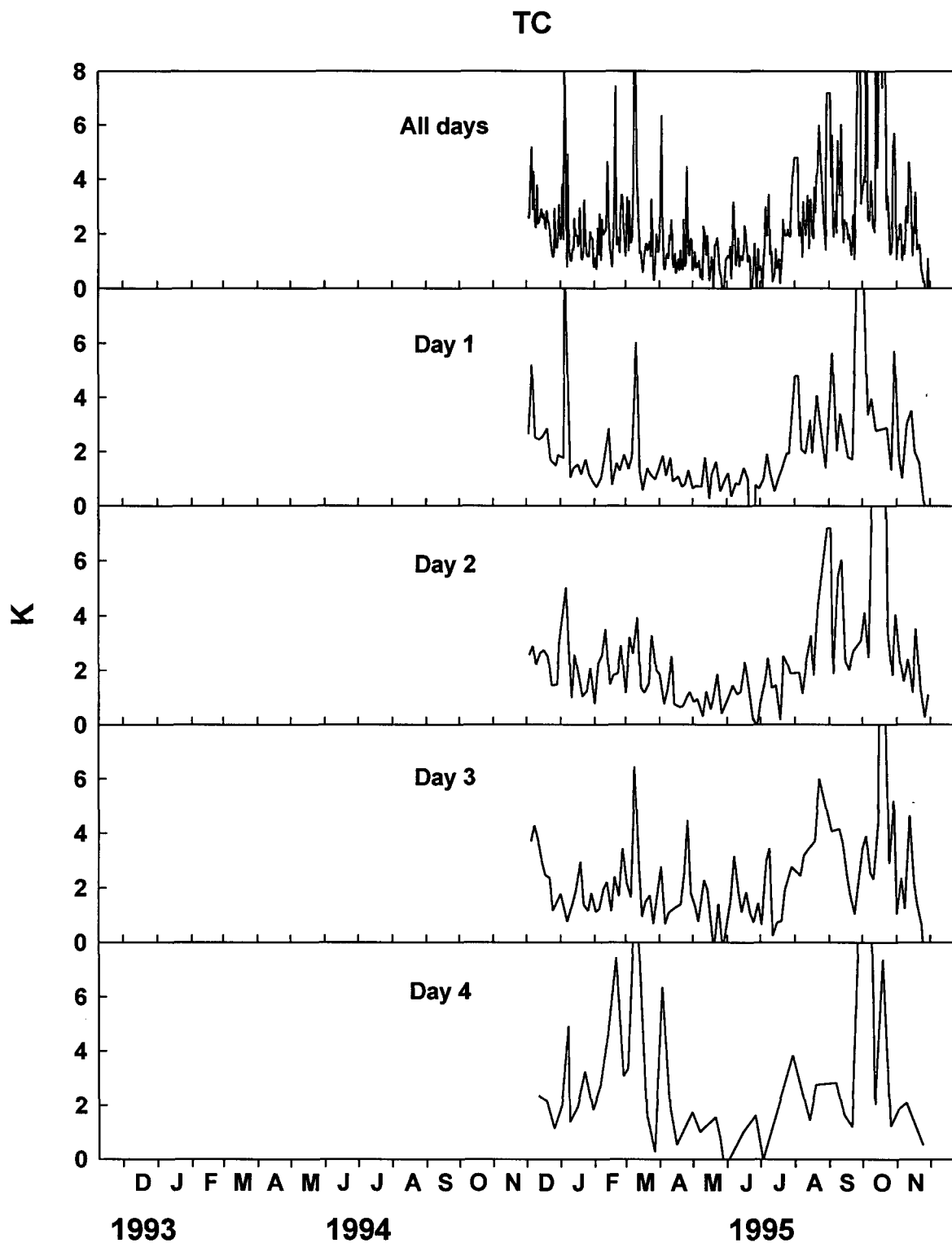


Fig. 2.17 Effect of time since sensor cleaning on K, based on 1200 noon data, at TC, from December 1, 1994 to November 30, 1995. Day 1 = 0-24 hours after cleaning, Day 2 = 24-48 hours, Day 3 = 48-72 hours, Day 4 = 72-96 hours.

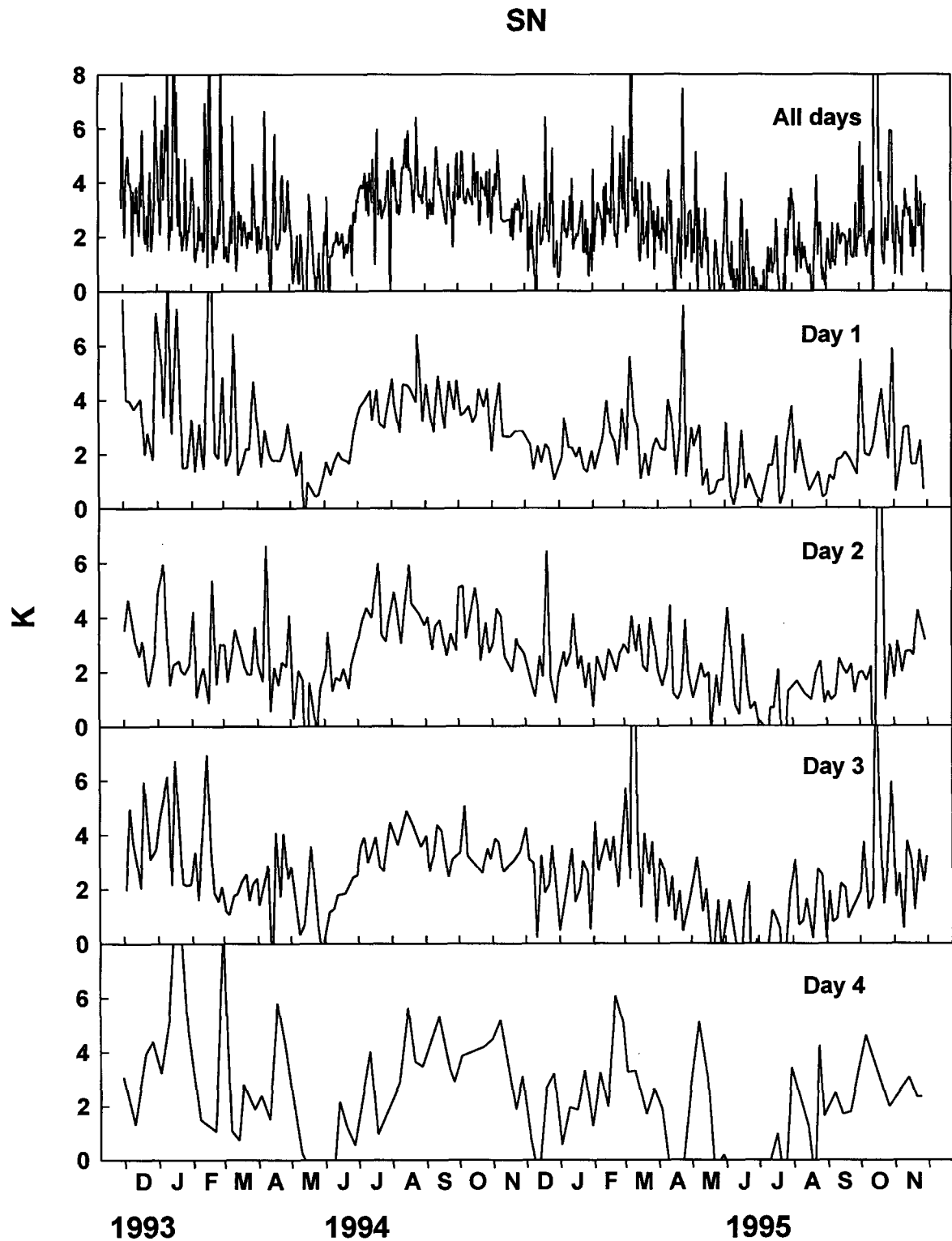


Fig. 2.18 Effect of time since sensor cleaning on K, based on 1200 noon data, at SN, from November 30, 1993 to November 30, 1995. Day 1 = 0-24 hours after cleaning, Day 2 = 24-48 hours, Day 3 = 48-72 hours, Day 4 = 72-96 hours.

SS

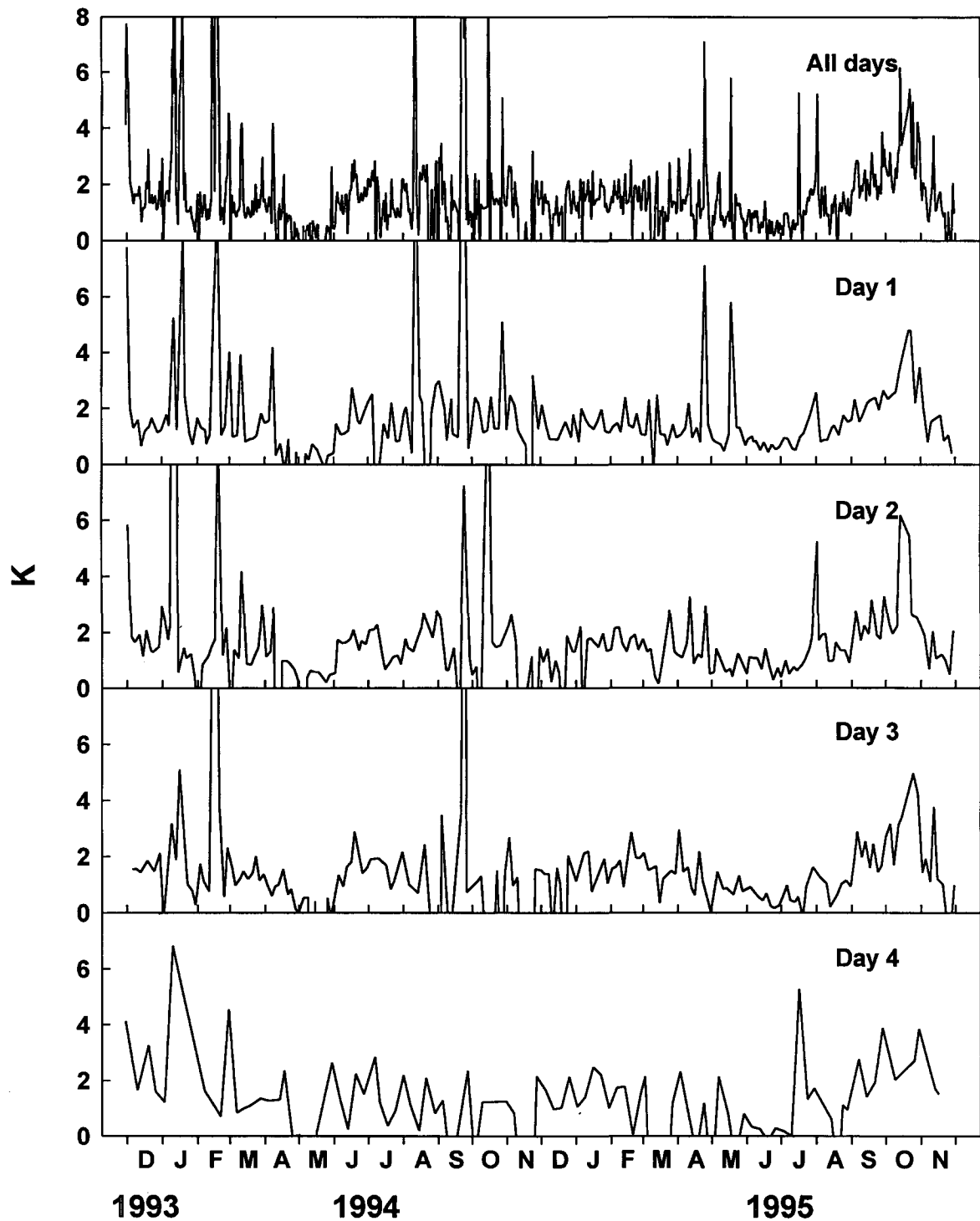


Fig. 2.19 Effect of time since sensor cleaning on K, based on 1200 noon data, at SS, from November 30, 1993 to November 30, 1995. Day 1 = 0-24 hours after cleaning, Day 2 = 24-48 hours, Day 3 = 48-72 hours, Day 4 = 72-96 hours.

VB

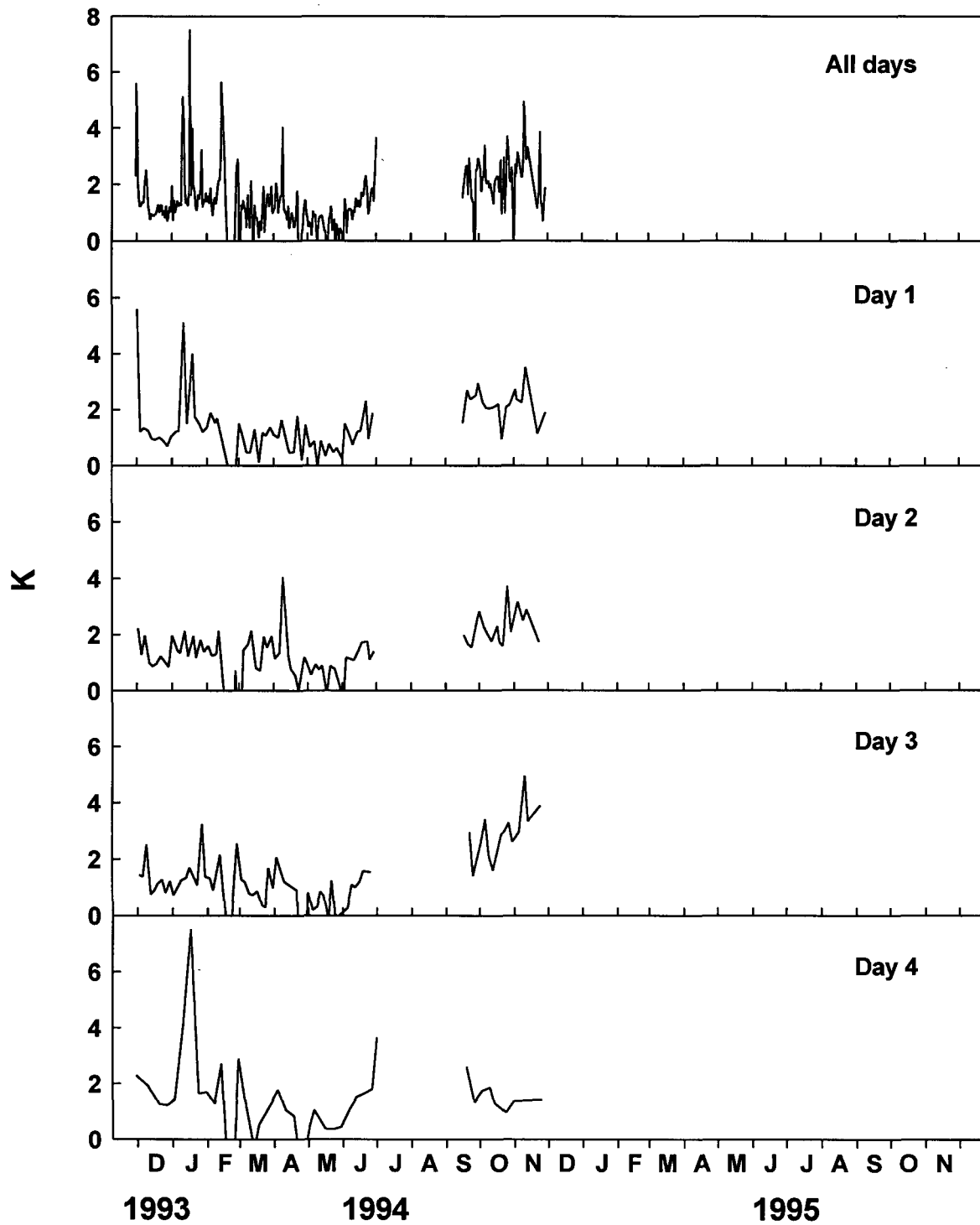


Fig. 2.20 Effect of time since sensor cleaning on K, based on 1200 noon data, at VB, from November 30, 1993 to November 30, 1994. Day 1 = 0-24 hours after cleaning, Day 2 = 24-48 hours, Day 3 = 48-72 hours, Day 4 = 72-96 hours.

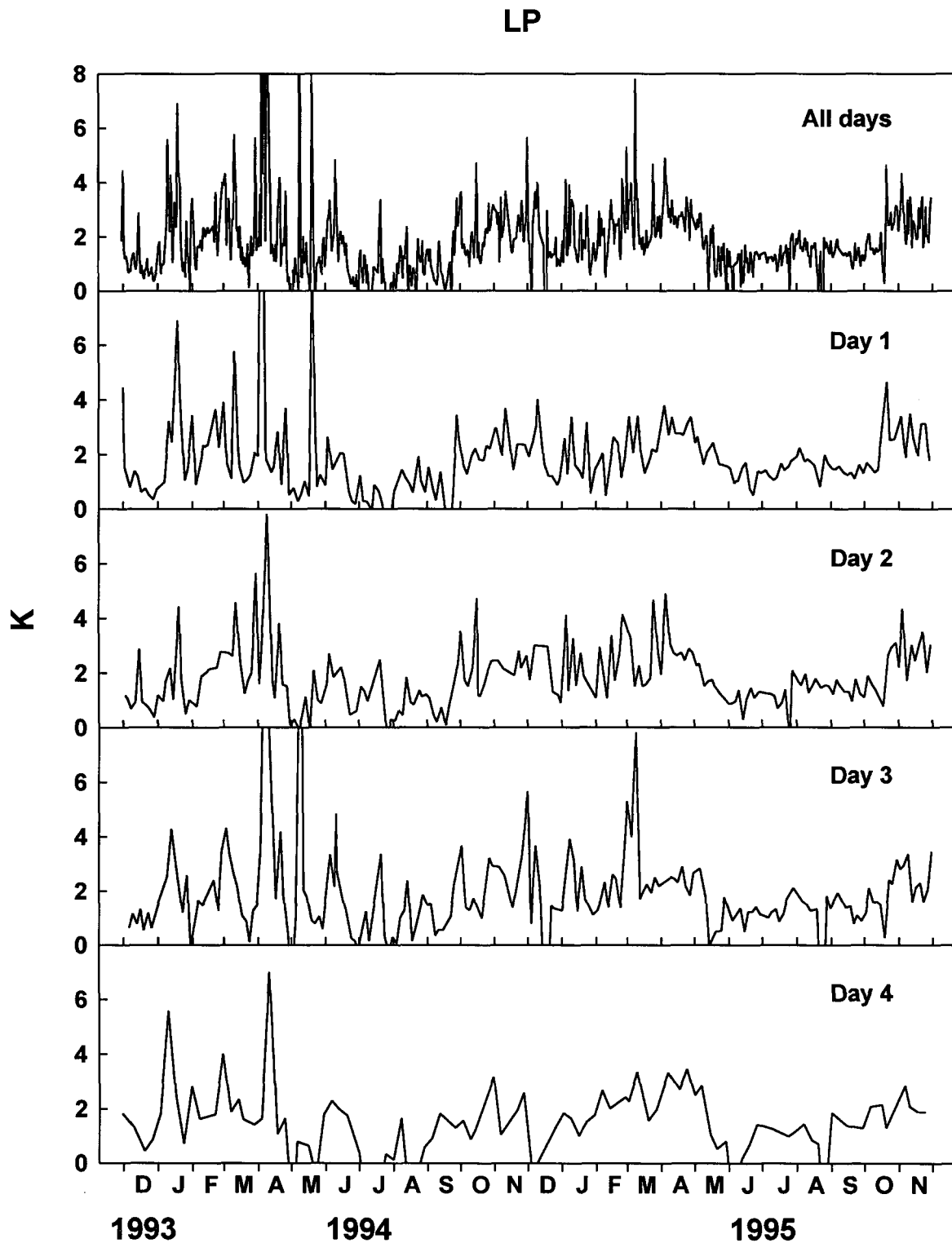


Fig. 2.21 Effect of time since sensor cleaning on K, based on 1200 noon data, at LP, from November 30, 1993 to November 30, 1995. Day 1 = 0-24 hours after cleaning, Day 2 = 24-48 hours, Day 3 = 48-72 hours, Day 4 = 72-96 hours.

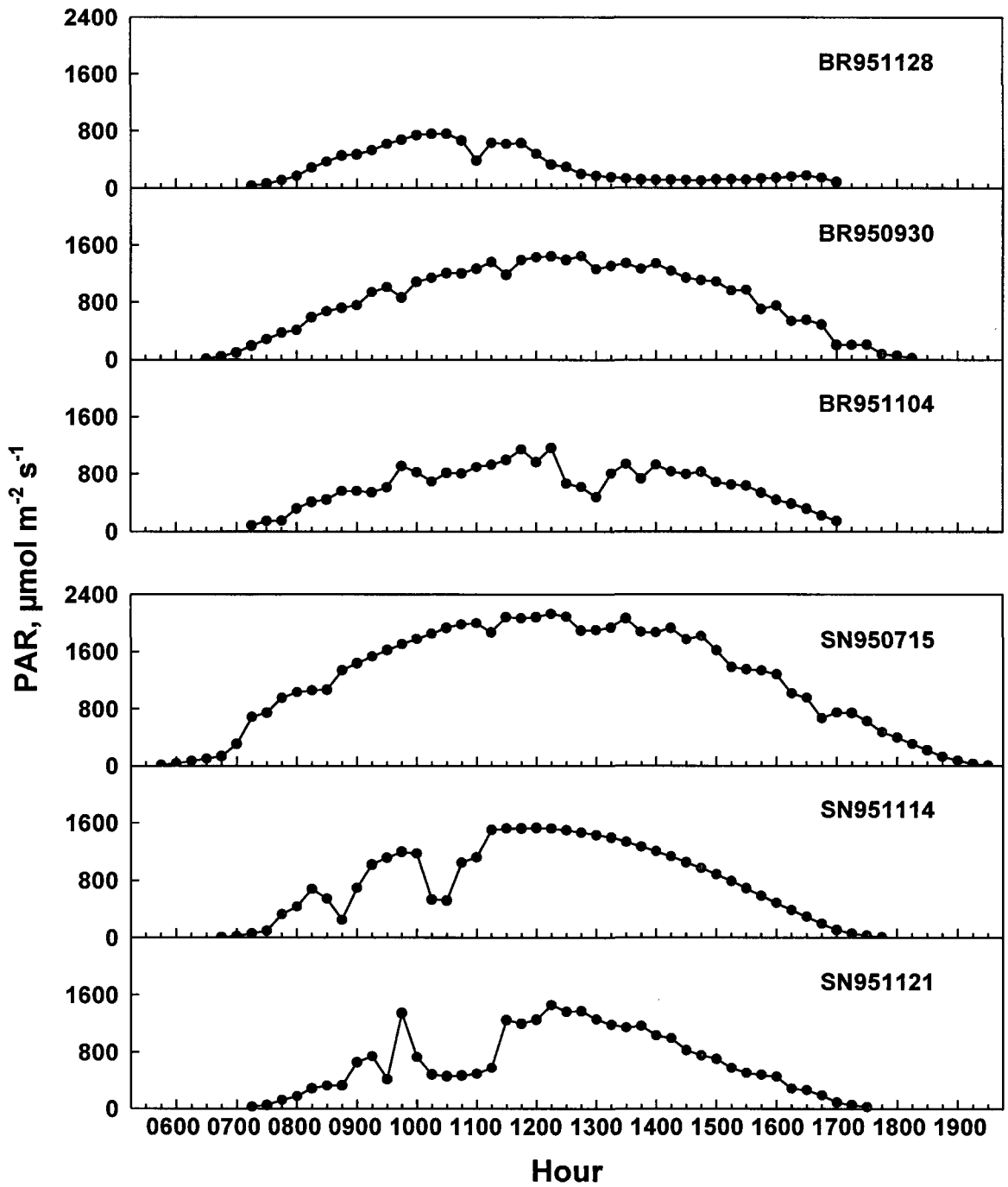


Fig. 2.22 Examples of raw data for PAR measured by the C0 sensor over the course of the photoperiod. PAR was measured every 5 seconds and recorded as mean values every 15 minutes.

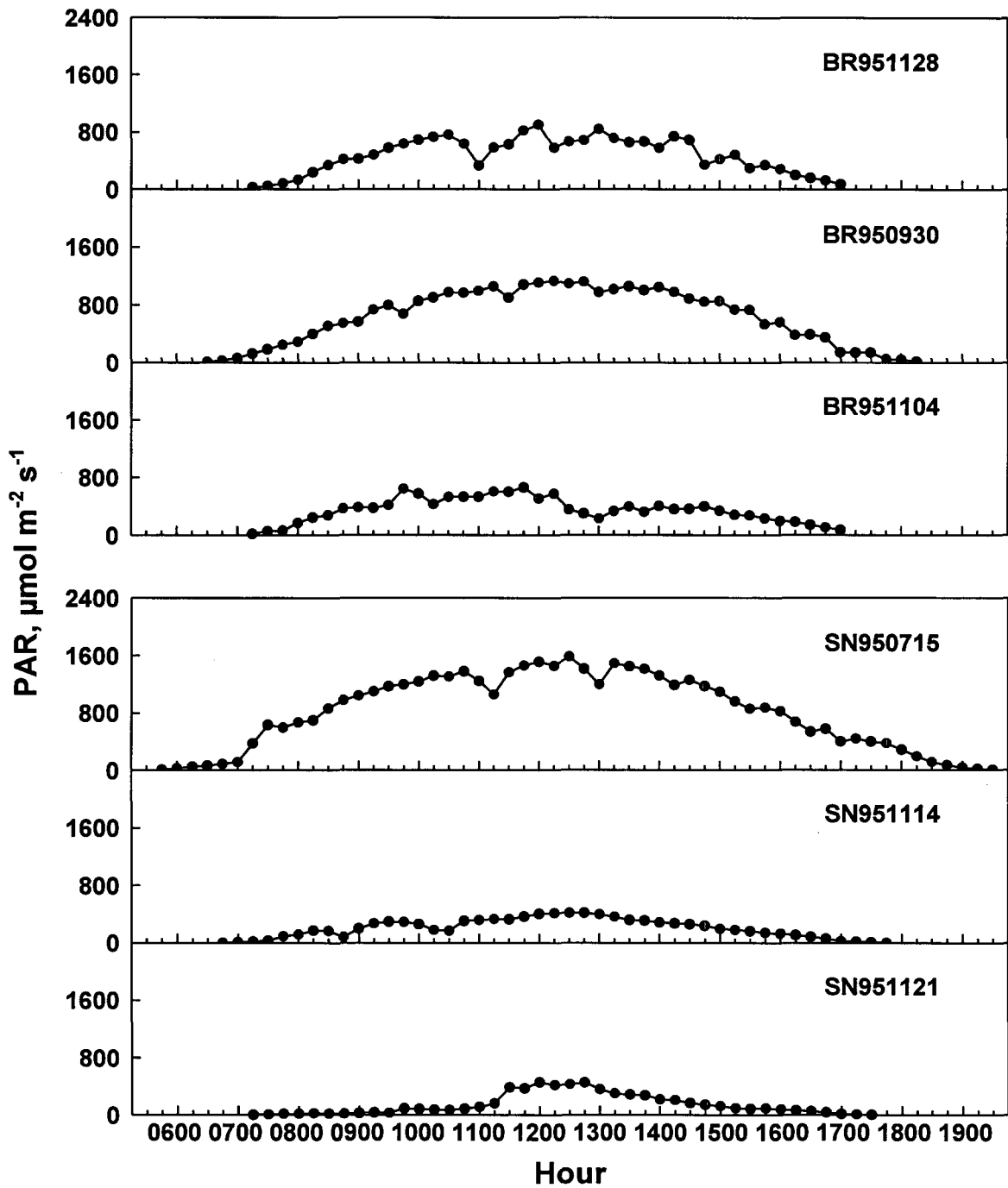


Fig. 2.23 Examples of raw data for PAR measured by the S1 sensor over the course of the photoperiod. PAR was measured every 5 seconds and recorded as mean values every 15 minutes.

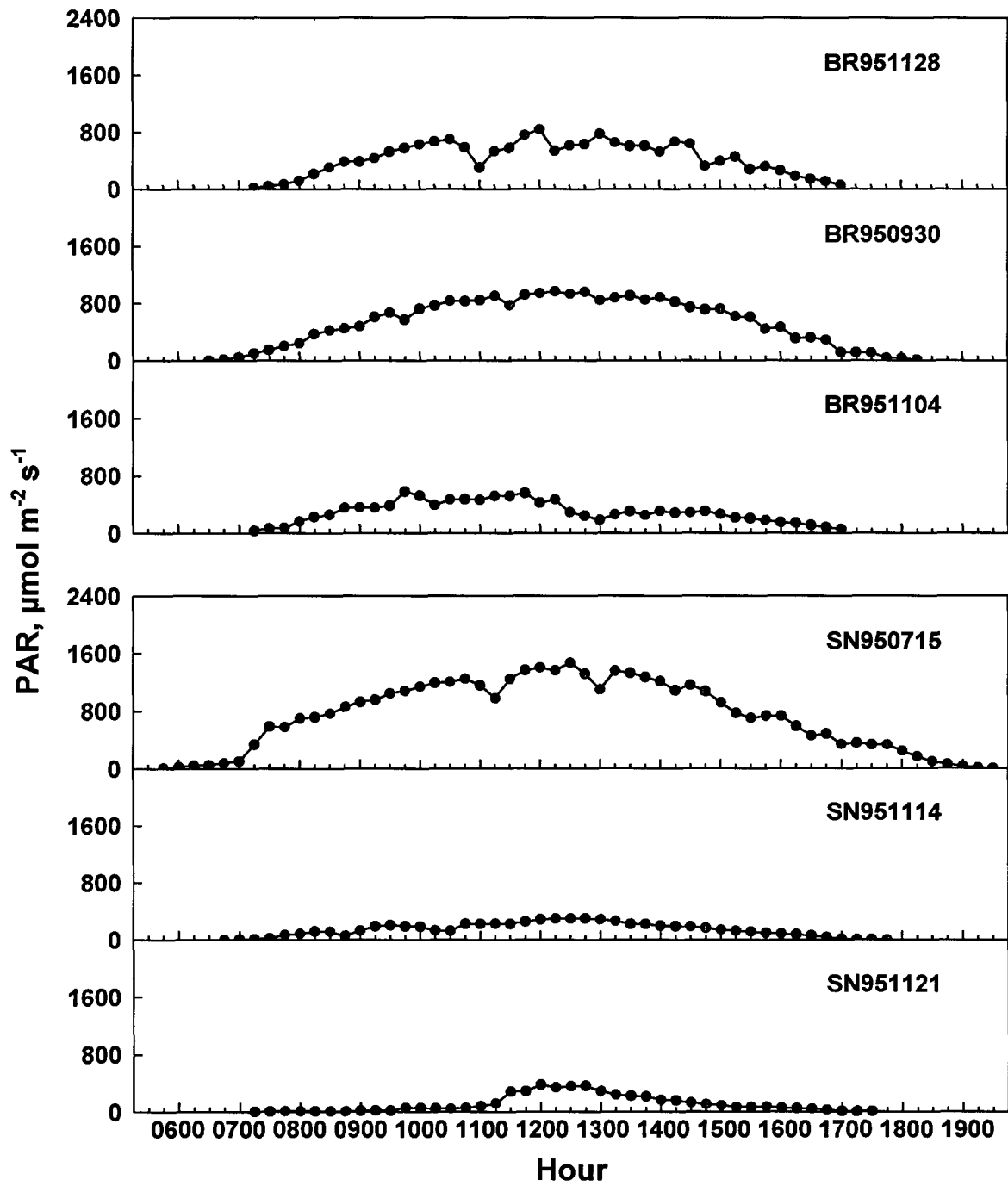


Fig. 2.24 Examples of raw data for PAR measured by the S2 sensor over the course of the photoperiod. PAR was measured every 5 seconds and recorded as mean values every 15 minutes.

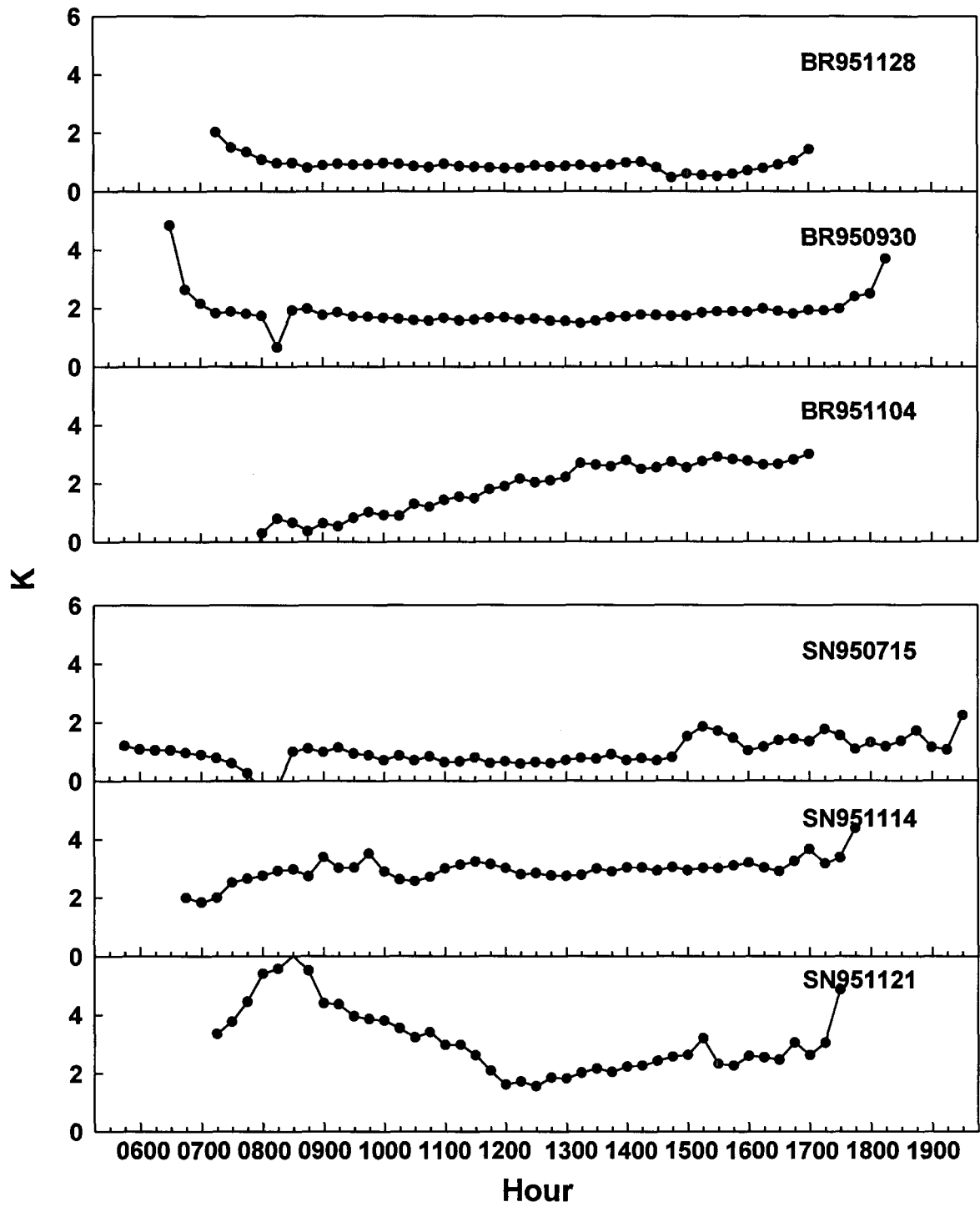


Fig. 2.25 Examples of K calculated from the S1 and S2 sensors over the course of the photoperiod. K was calculated from the mean PAR values from the S1 and S2 sensors, every 15 minutes.

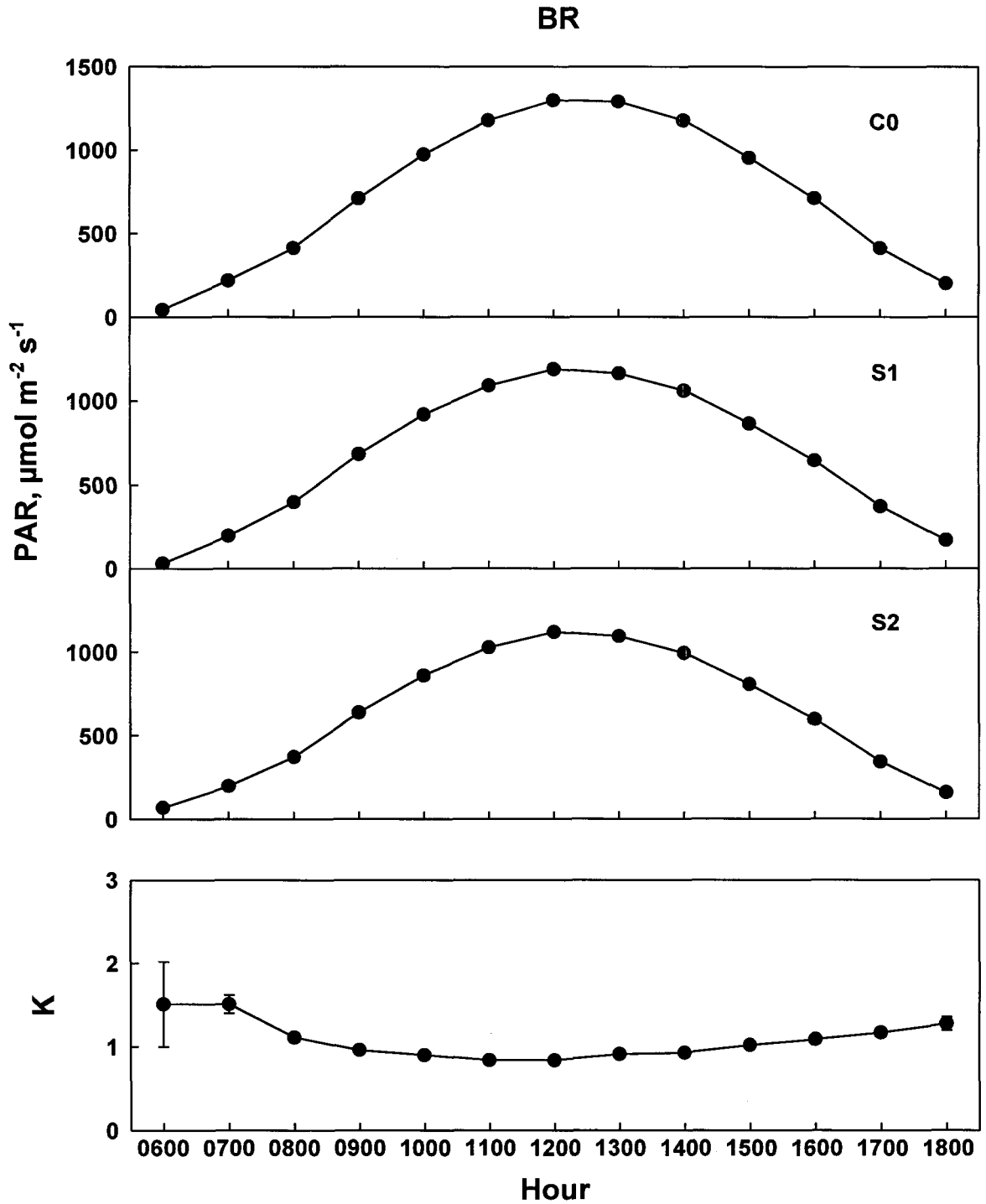


Fig. 2.26 Diel patterns in PAR measured by the C0, S1, and S2 sensors, and K, at BR, from November 30, 1993 to November 30, 1995. Data are hourly means (\pm SE) for the entire study.

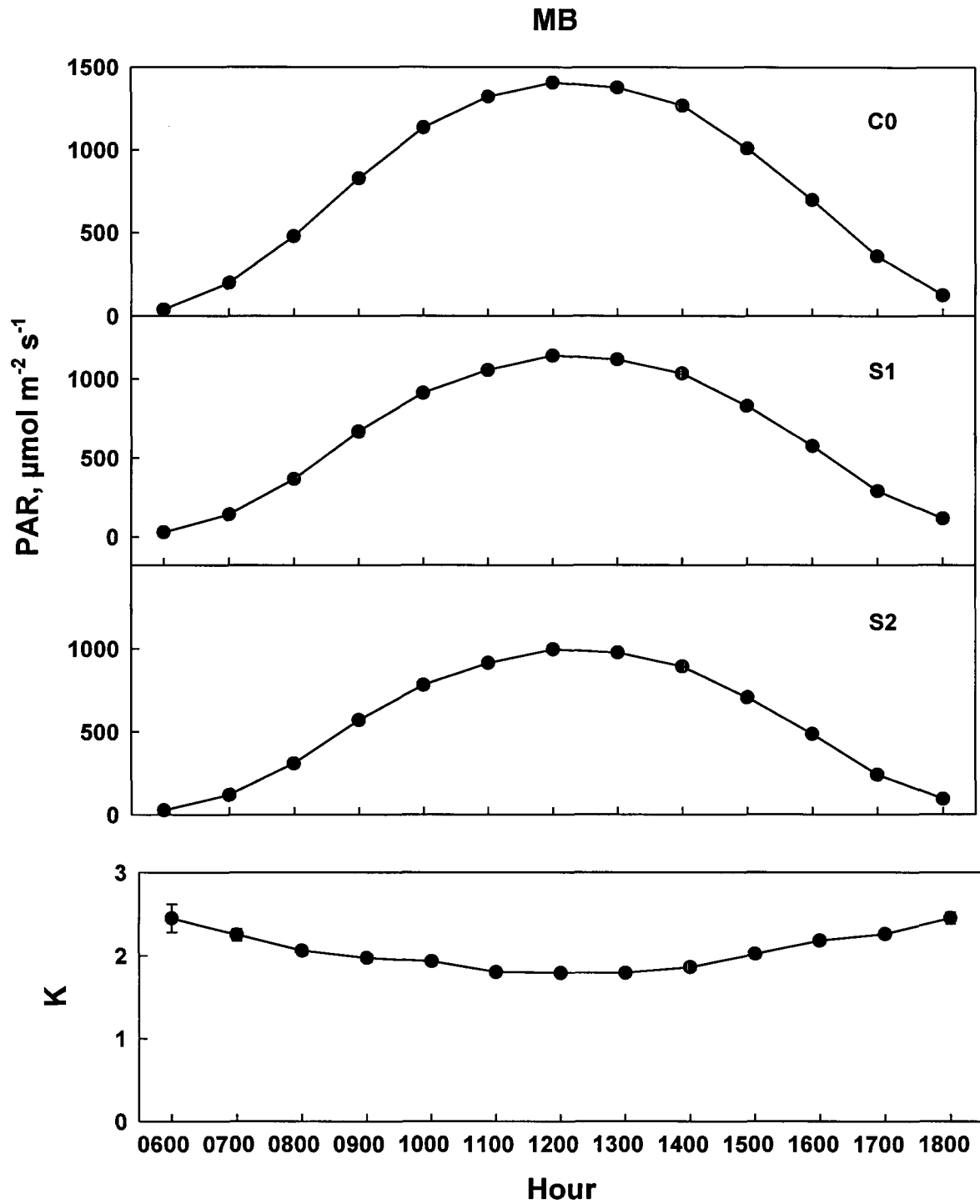


Fig. 2.27 Diel patterns in PAR measured by the C0, S1, and S2 sensors, and K, at MB, from November 30, 1993 to November 30, 1995. Data are hourly means (\pm SE) for the entire study.

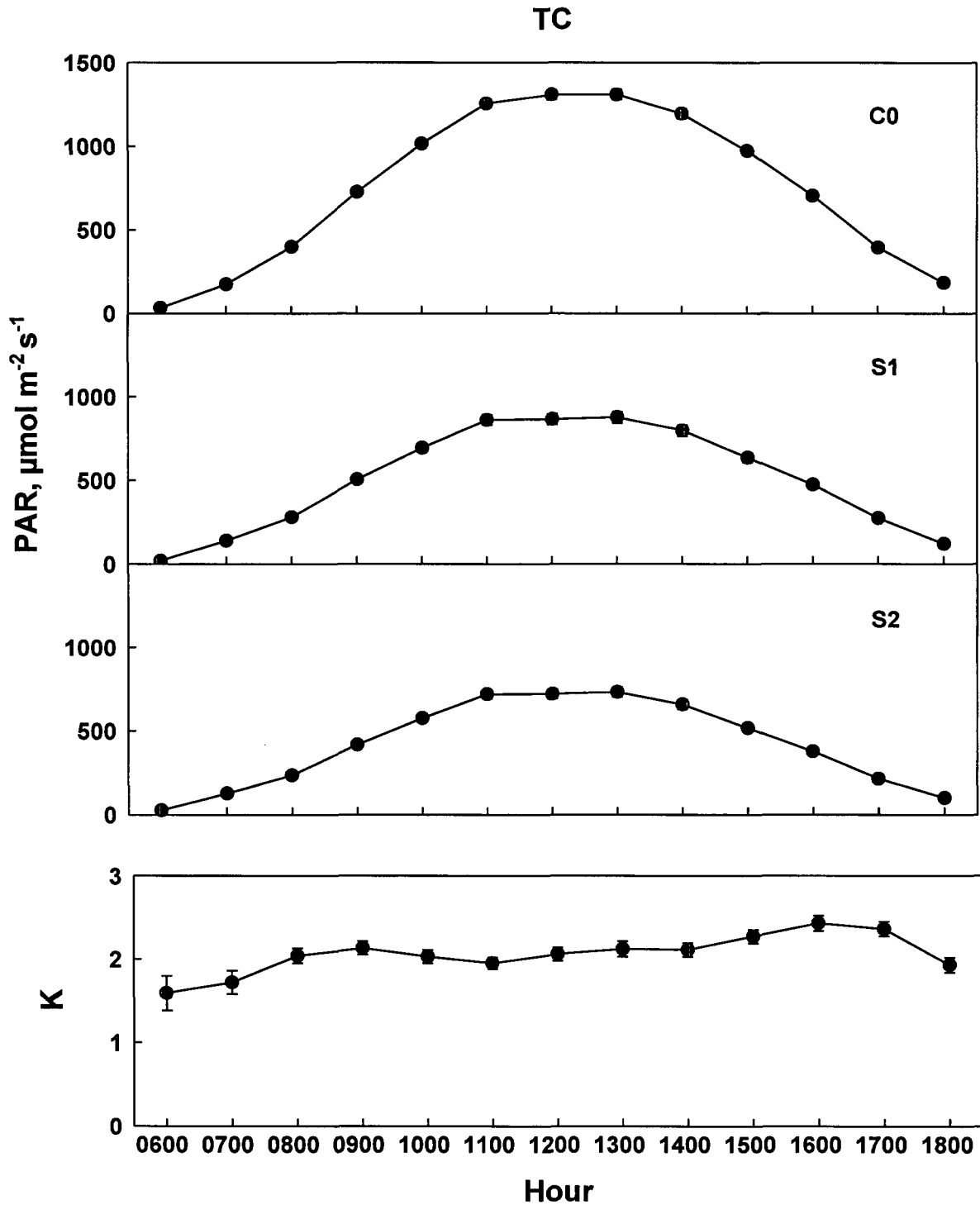


Fig. 2.28 Diel patterns in PAR measured by the C0, S1, and S2 sensors, and K, at TC, from December 1, 1994 to November 30, 1995. Data are hourly means (\pm SE) for the entire study.

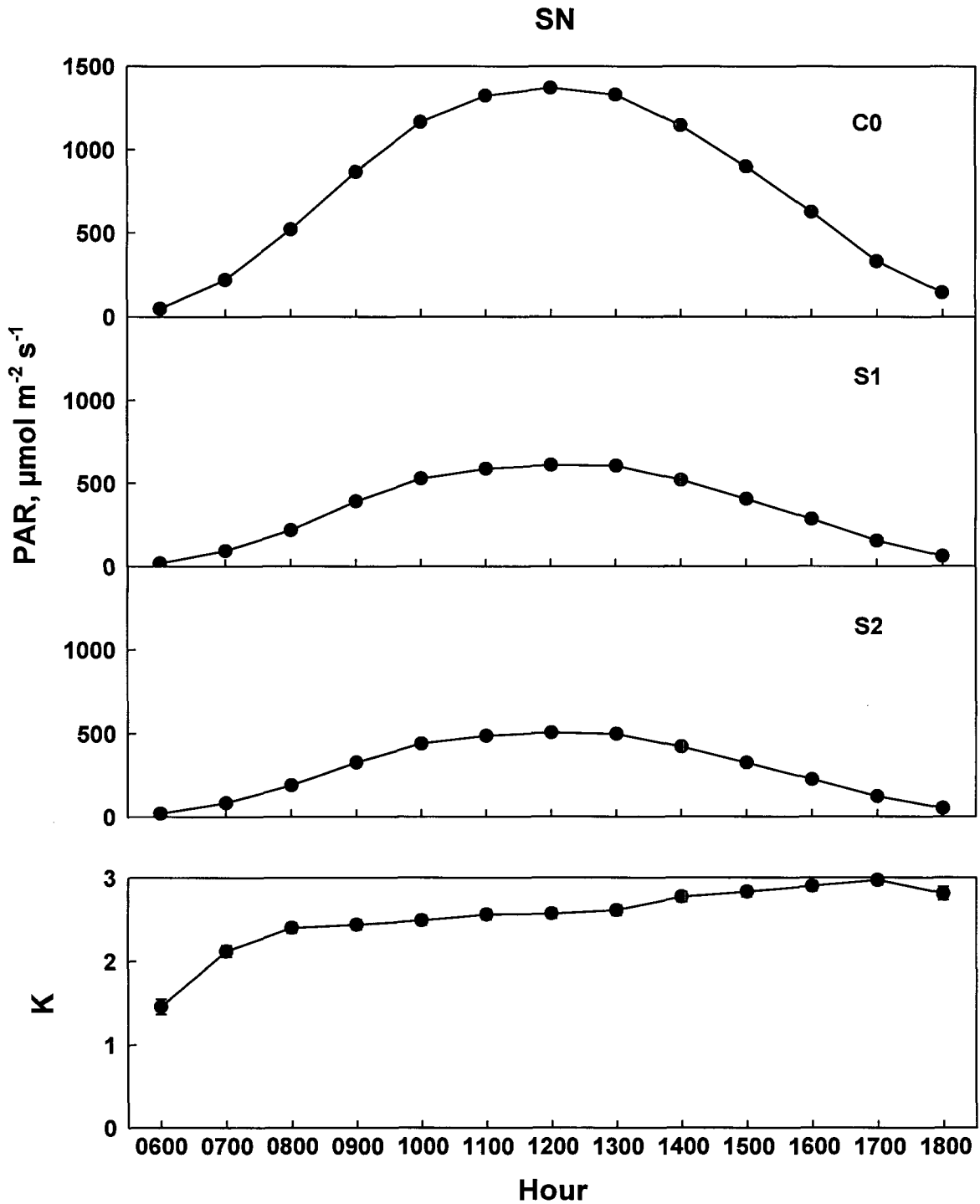


Fig. 2.29 Diel patterns in PAR measured by the C0, S1, and S2 sensors, and K, at SN, from November 30, 1993 to November 30, 1995. Data are hourly means (\pm SE) for the entire study.

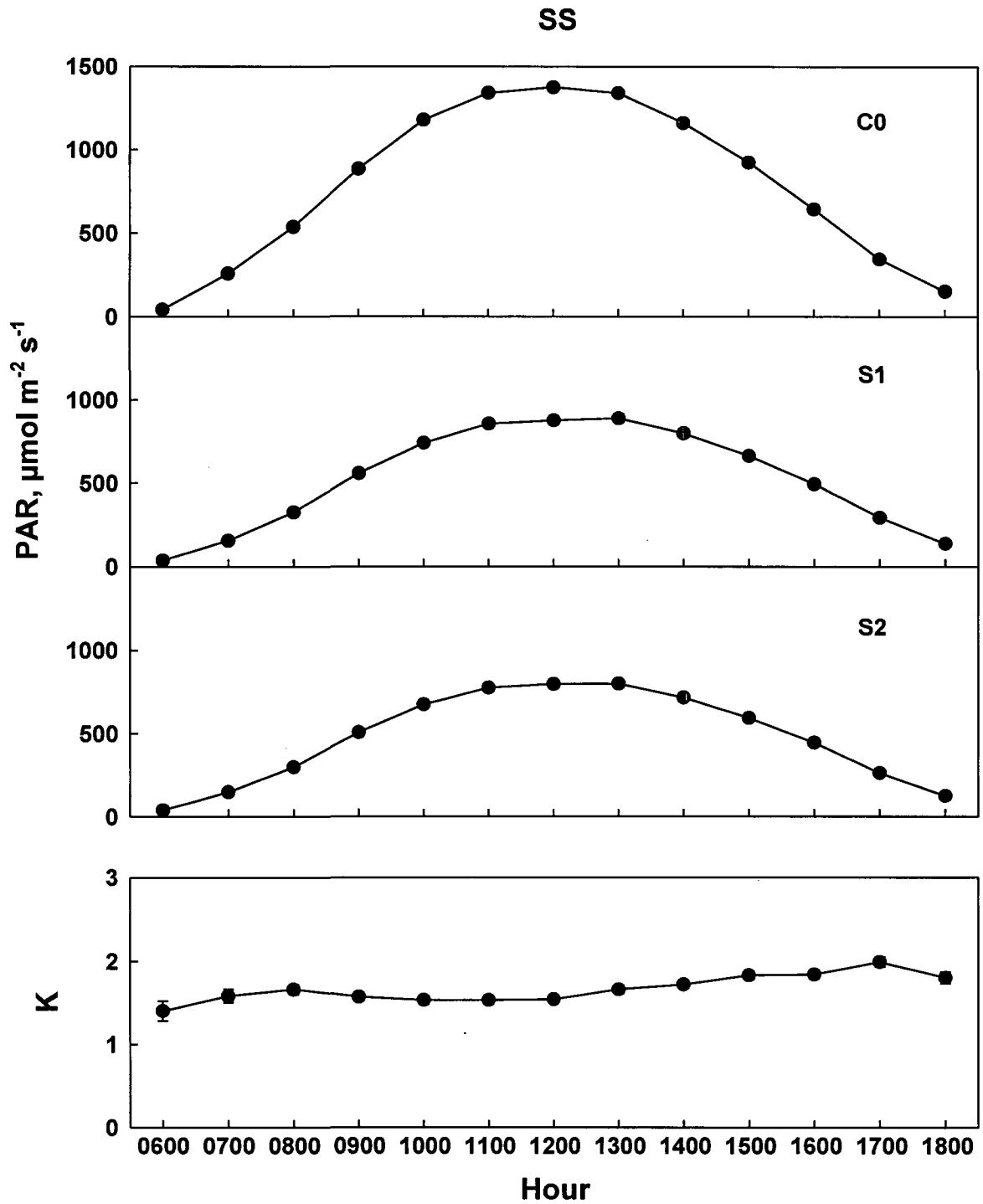


Fig. 2.30 Diel patterns in PAR measured by the C0, S1, and S2 sensors, and K, at SS, from November 30, 1993 to November 30, 1995. Data are hourly means (\pm SE) for the entire study.

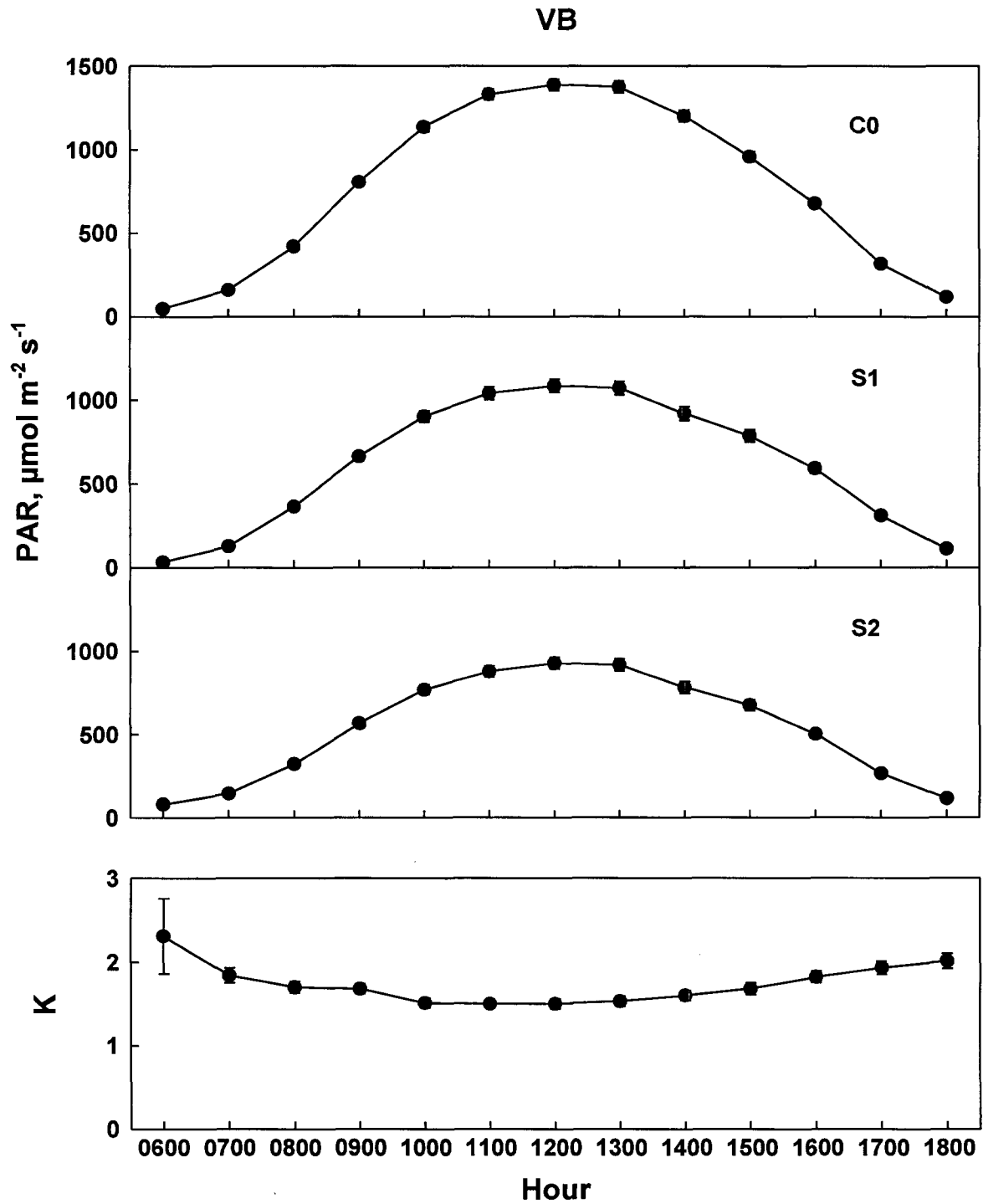


Fig. 2.31 Diel patterns in PAR measured by the C0, S1, and S2 sensors, and K, at VB, from November 30, 1993 to November 30, 1994. Data are hourly means (\pm SE) for the entire study.

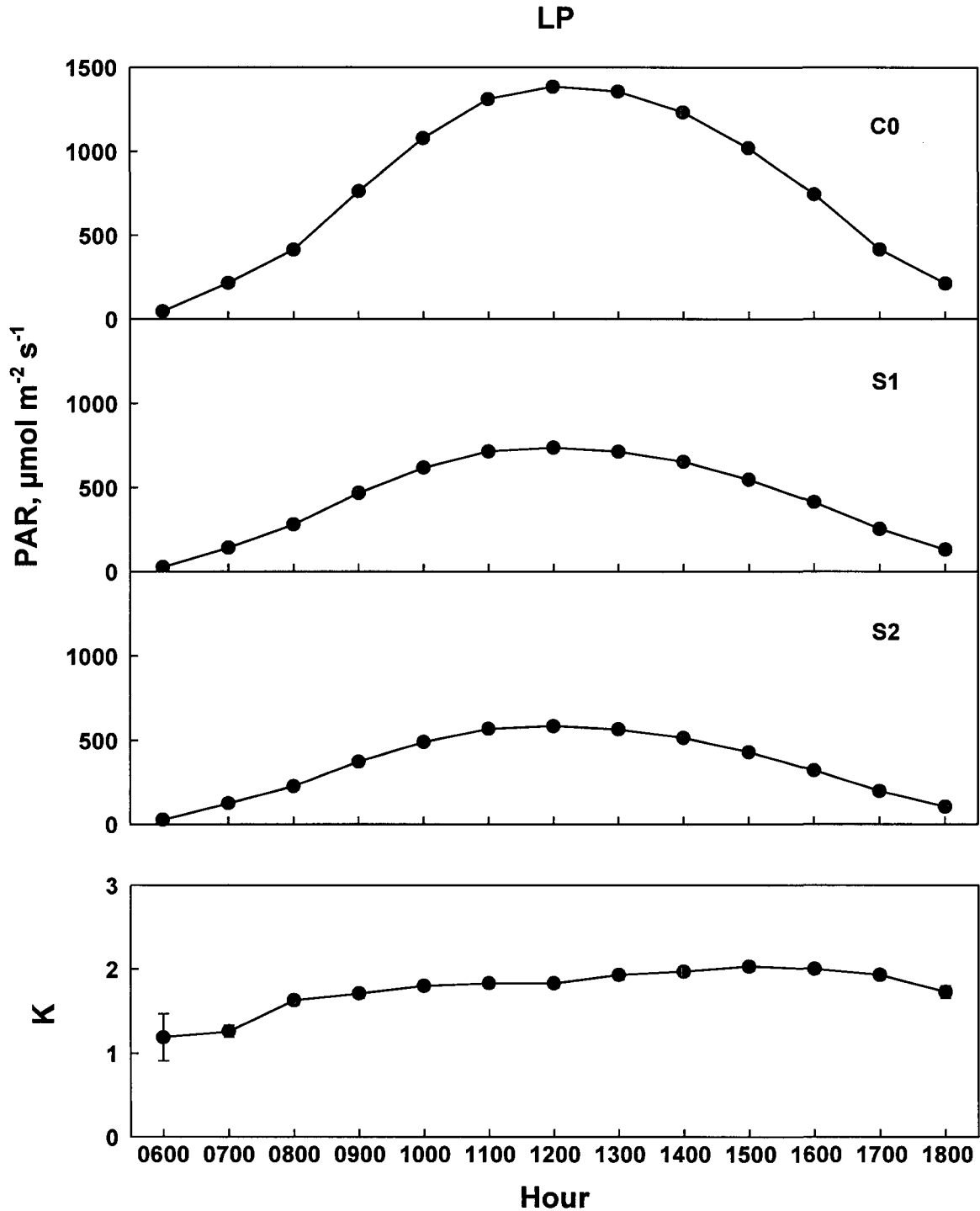


Fig. 2.32 Diel patterns in PAR measured by the C0, S1, and S2 sensors, and K, at LP, from November 30, 1993 to November 30, 1995. Data are hourly means (\pm SE) for the entire study.

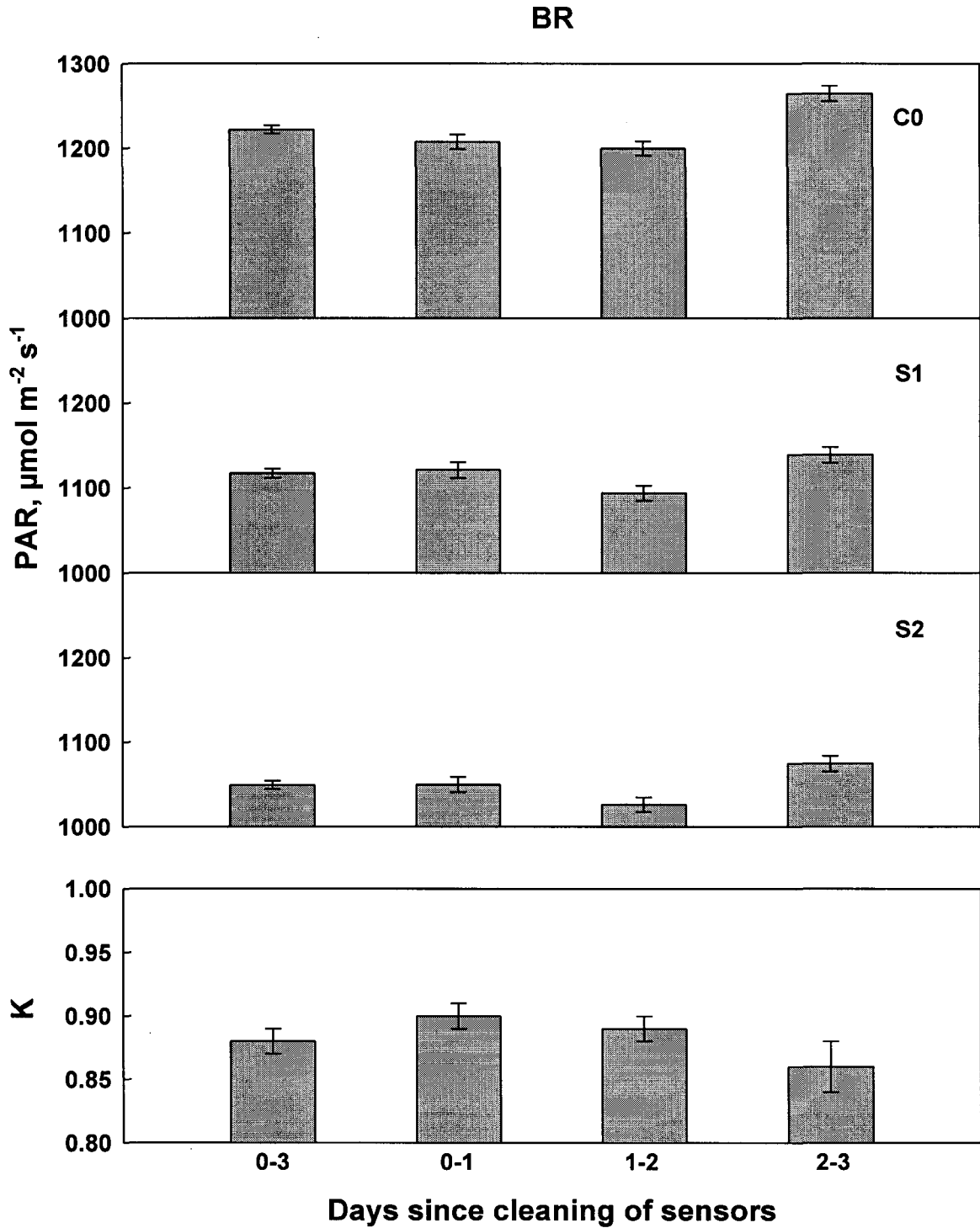


Fig. 2.33 PAR measured by the C0, S1, and S2 sensors, and K, within 3 days (72 hours) after cleaning of sensors, and by day since sensor cleaning, at BR, from November 30, 1993 to November 30, 1995. Data are means (\pm SE).

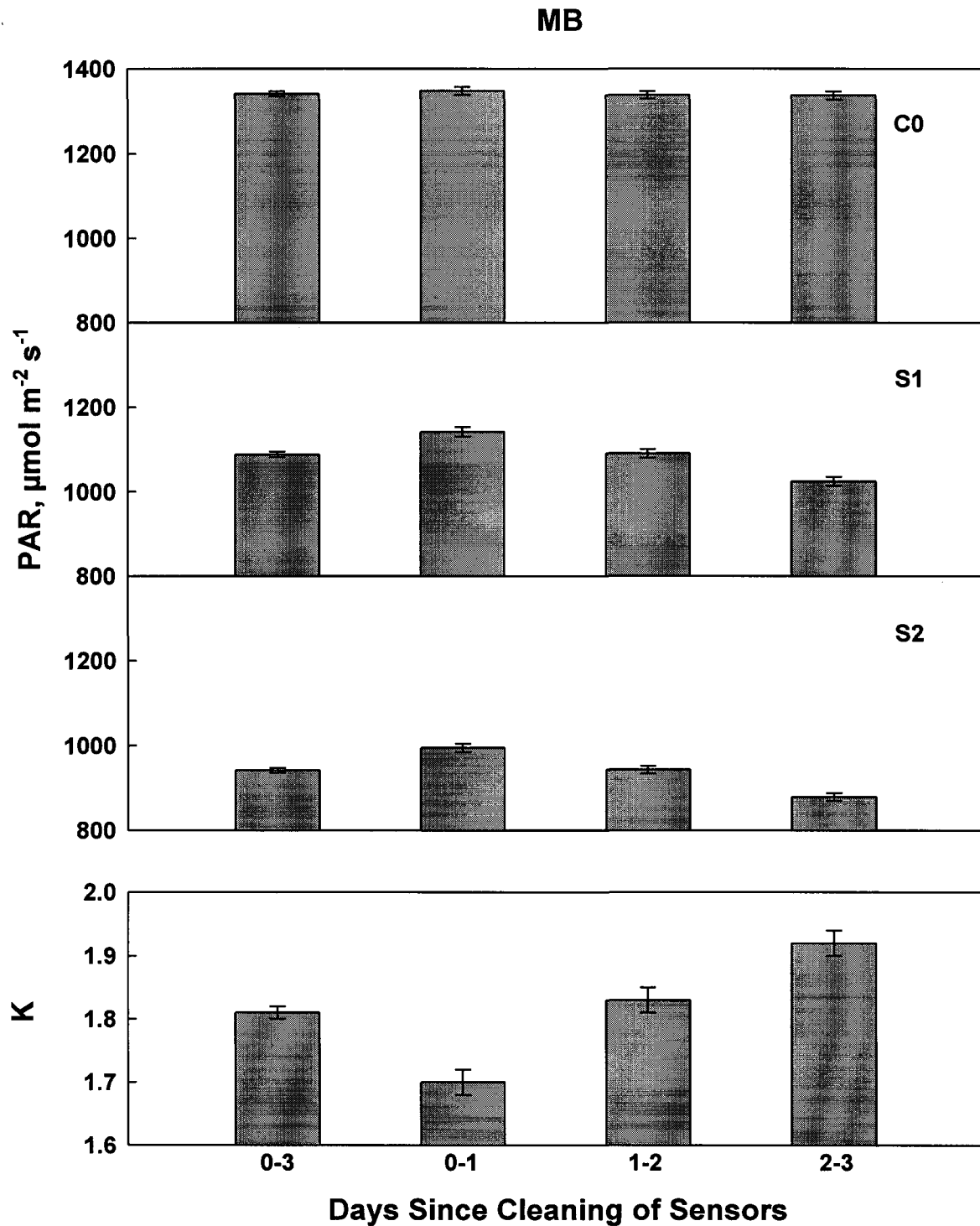


Fig. 2.34 PAR measured by the C0, S1, and S2 sensors, and K, within 3 days (72 hours) after cleaning of sensors, and by day since sensor cleaning, at MB, from November 30, 1993 to November 30, 1995. Data are means (\pm SE).

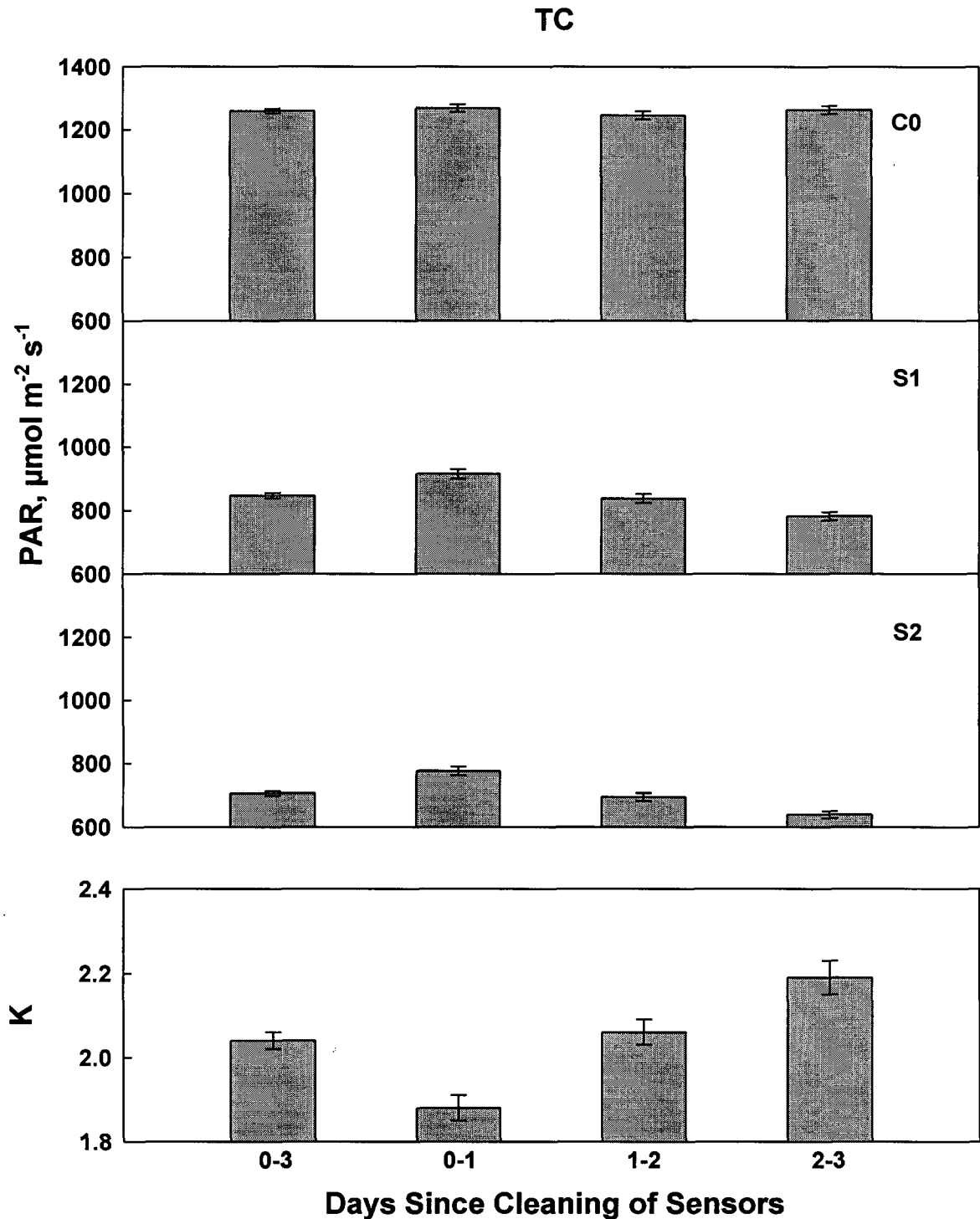


Fig. 2.35 PAR measured by the C0, S1, and S2 sensors, and K, within 3 days (72 hours) after cleaning of sensors, and by day since sensor cleaning, at TC, from December 1, 1994 to November 30, 1995. Data are means (\pm SE).

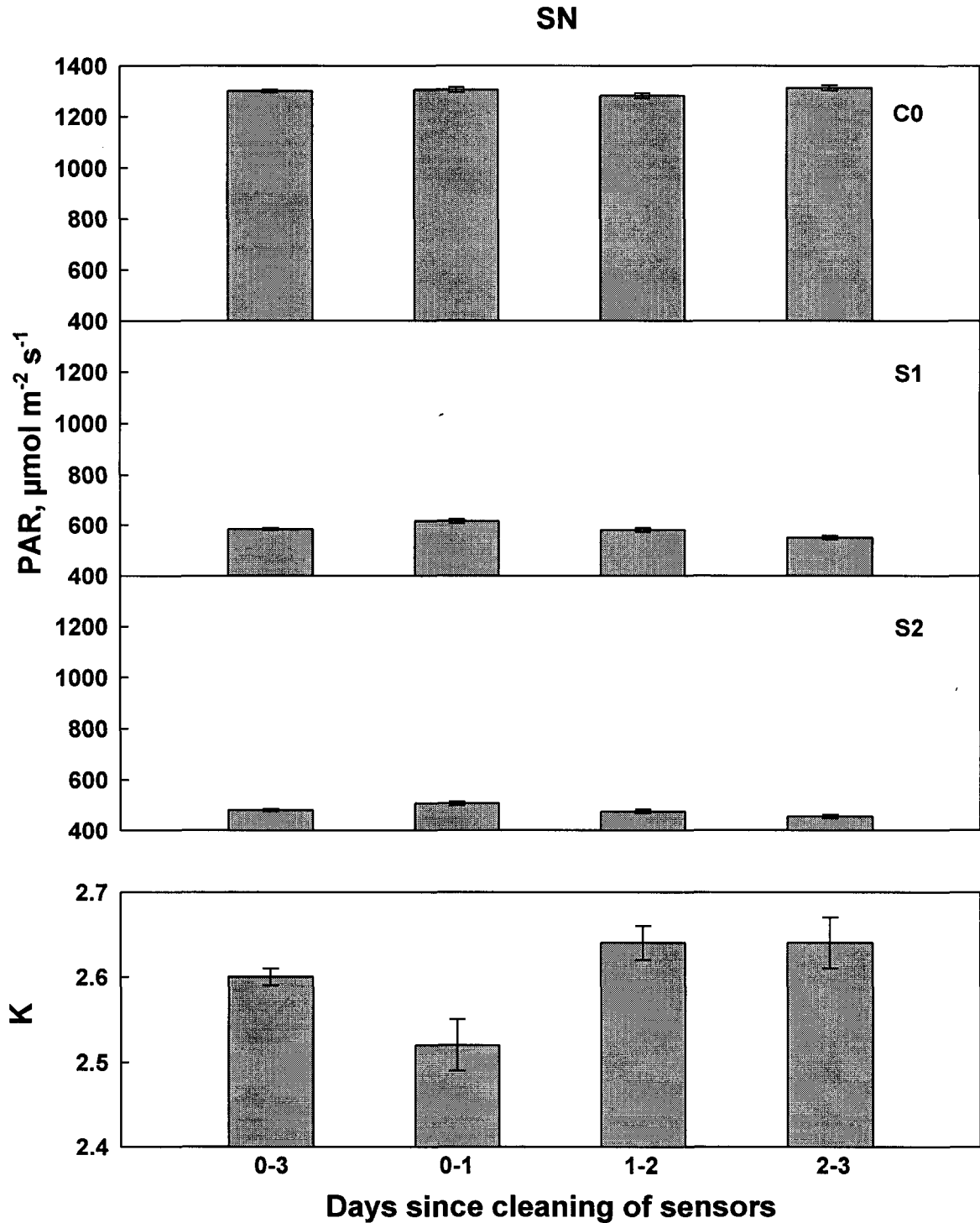


Fig. 2.36 PAR measured by the C0, S1, and S2 sensors, and K, within 3 days (72 hours) after cleaning of sensors, and by day since sensor cleaning, at SN, from November 30, 1993 to November 30, 1995. Data are means (\pm SE).

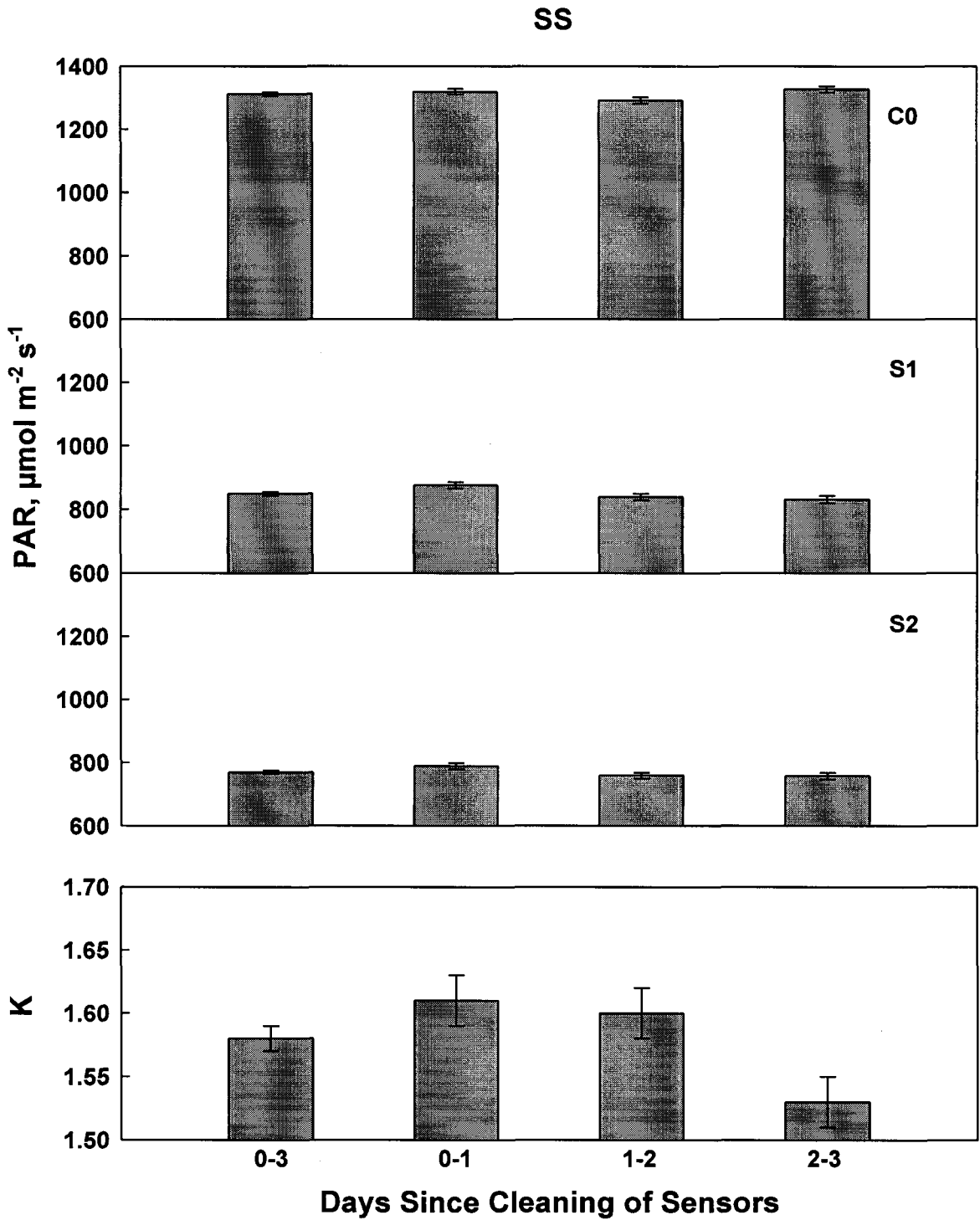


Fig. 2.37 PAR measured by the C0, S1, and S2 sensors, and K, within 3 days (72 hours) after cleaning of sensors, and by day since sensor cleaning, at SS, from November 30, 1993 to November 30, 1995. Data are means (\pm SE).

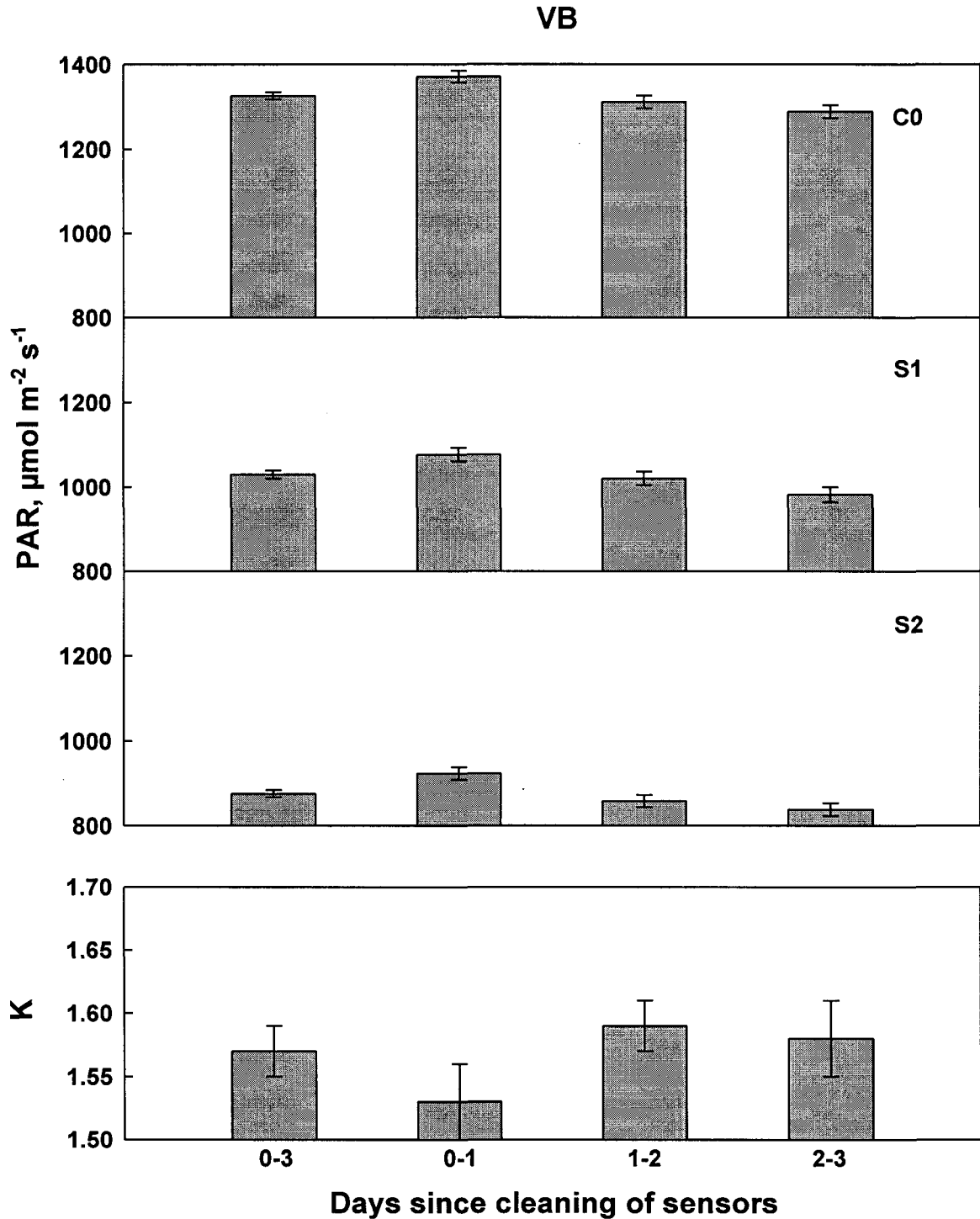


Fig. 2.38 PAR measured by the C0, S1, and S2 sensors, and K, within 3 days (72 hours) after cleaning of sensors, and by day since sensor cleaning, at VB, from November 30, 1993 to November 30, 1994. Data are means (\pm SE).

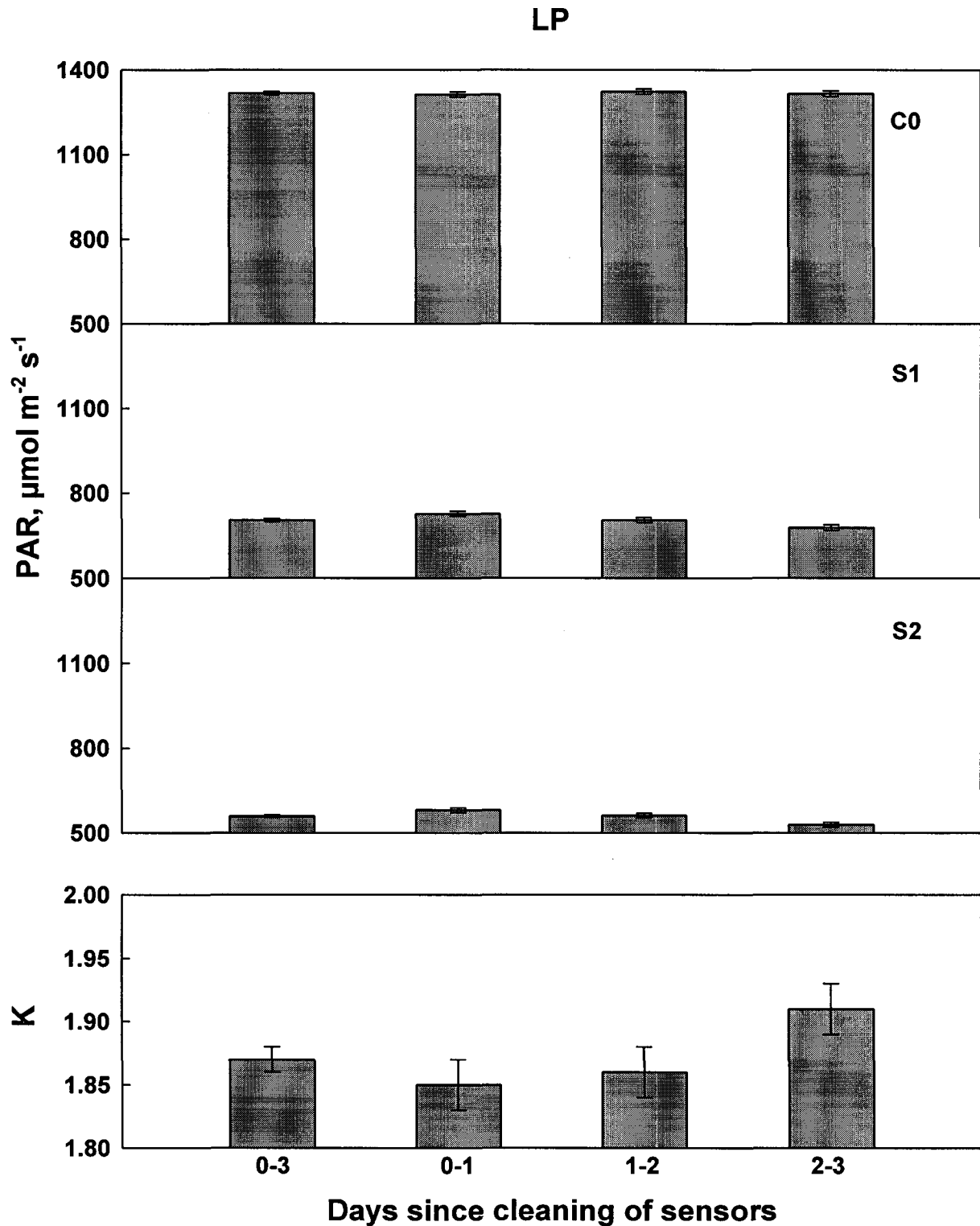


Fig. 2.39 PAR measured by the C0, S1, and S2 sensors, and K, within 3 days (72 hours) after cleaning of sensors, and by day since sensor cleaning, at LP, from November 30, 1993 to November 30, 1995. Data are means (\pm SE).

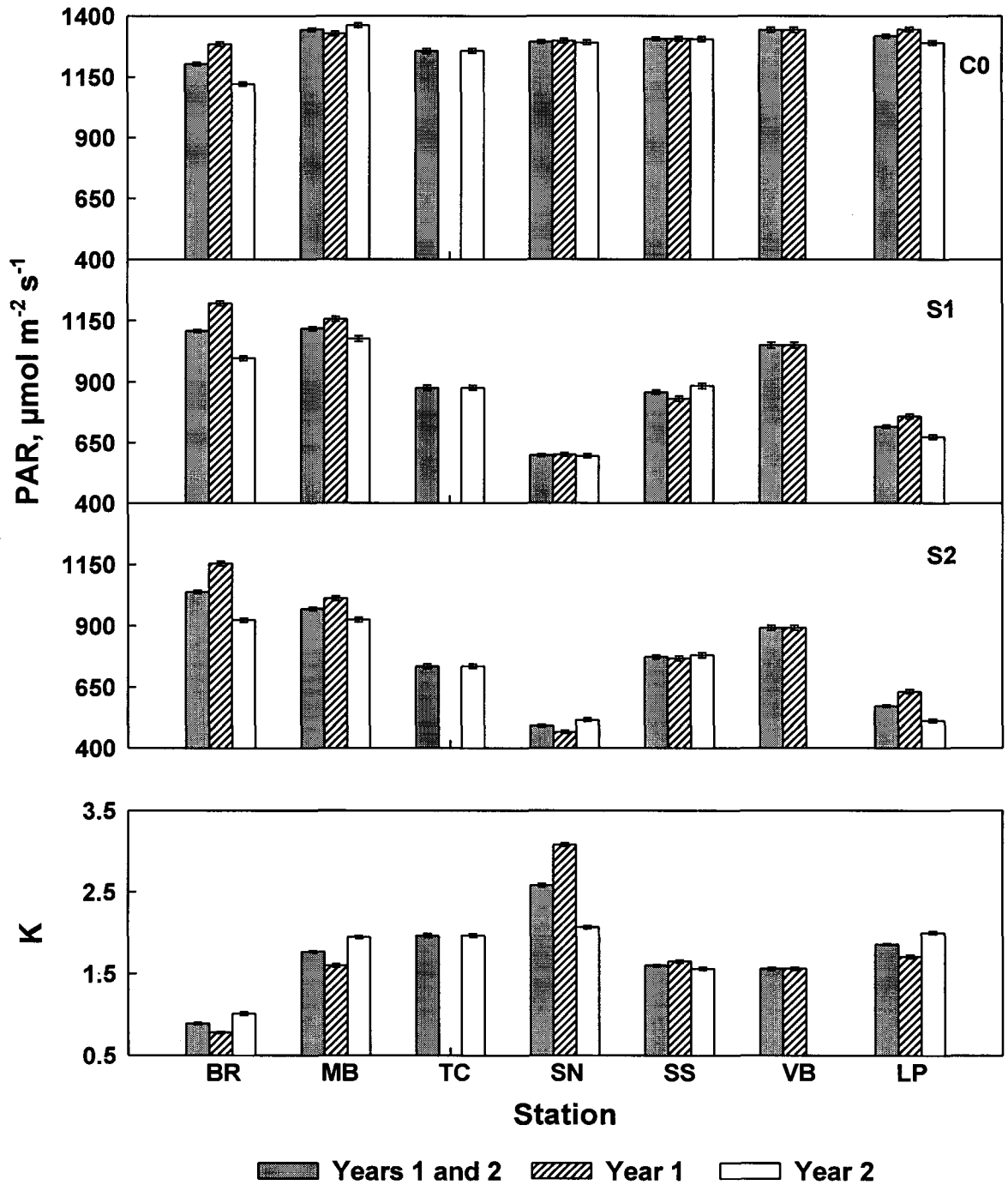


Fig. 2.40 Mean PAR measured by the C0, S1, and S2 sensors, and K, for all data between the hours of 1000-1400, within 48 hours after sensor cleaning, for all stations, for the entire study and by year. Data are means (\pm SE).

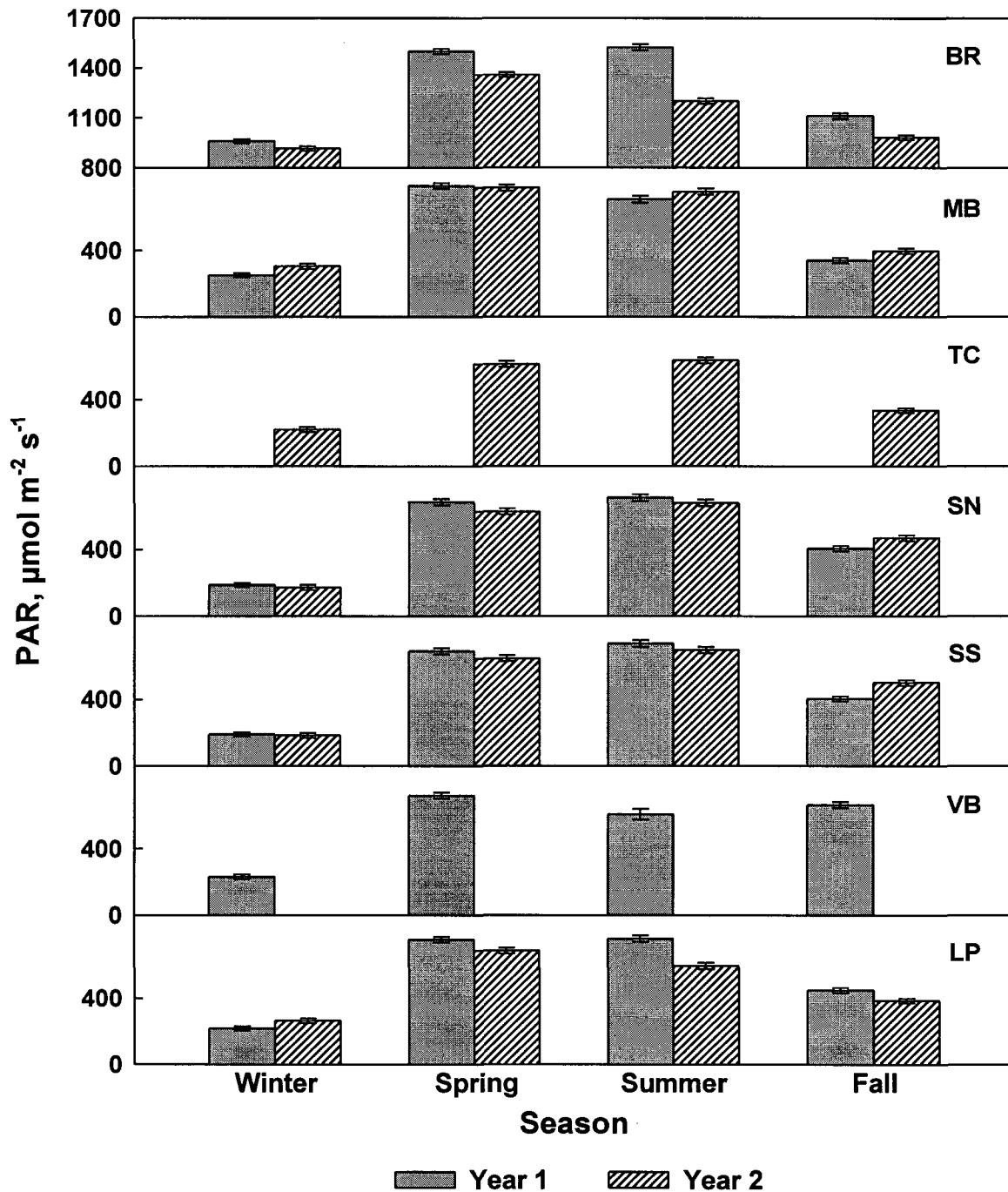


Fig. 2.41 Seasonal means (\pm SE) for PAR measured by the C0 sensor, between 1000-1400, within 48 hours after sensor cleaning, at all stations. Winter = December to February; Spring = March to May; Summer = June to August; Fall = September to November.

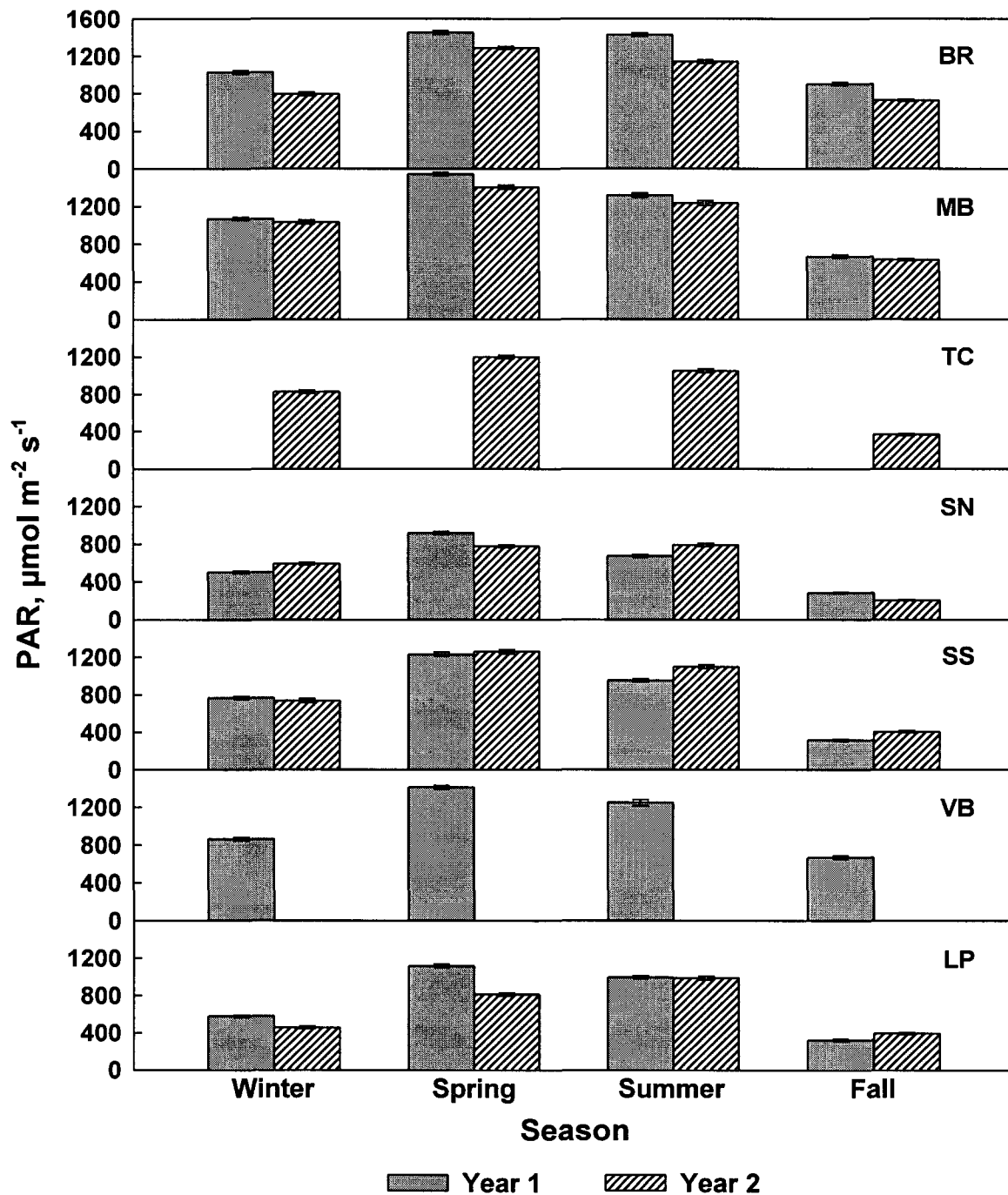


Fig. 2.42 Seasonal means (\pm SE) for PAR measured by the S1 sensor, between 1000-1400, within 48 hours after sensor cleaning, at all stations. Winter = December to February; Spring = March to May; Summer = June to August; Fall = September to November.

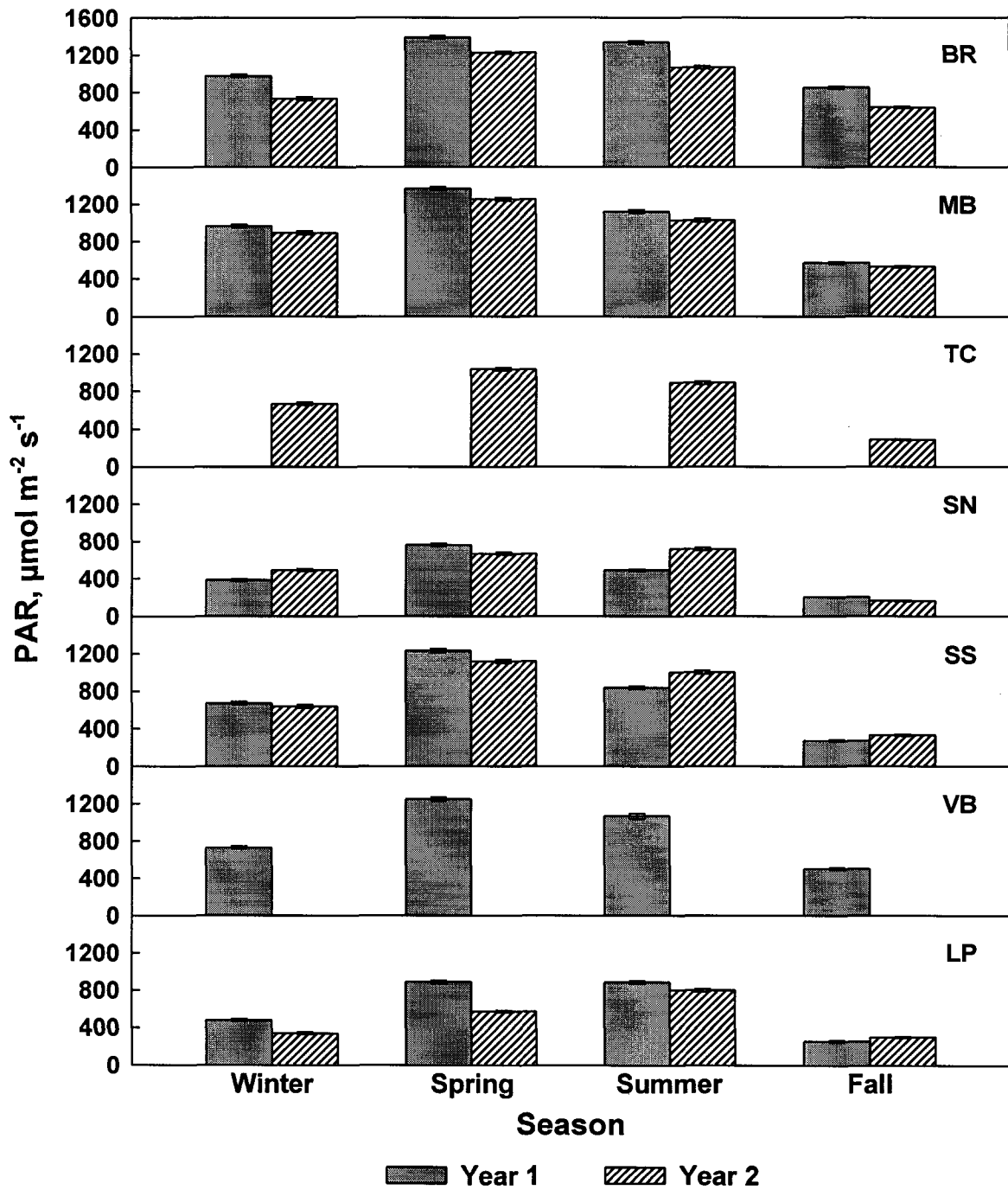


Fig. 2.43 Seasonal means (\pm SE) for PAR measured by the S2 sensor, between 1000-1400, within 48 hours after sensor cleaning, at all stations. Winter = December to February; Spring = March to May; Summer = June to August; Fall = September to November.

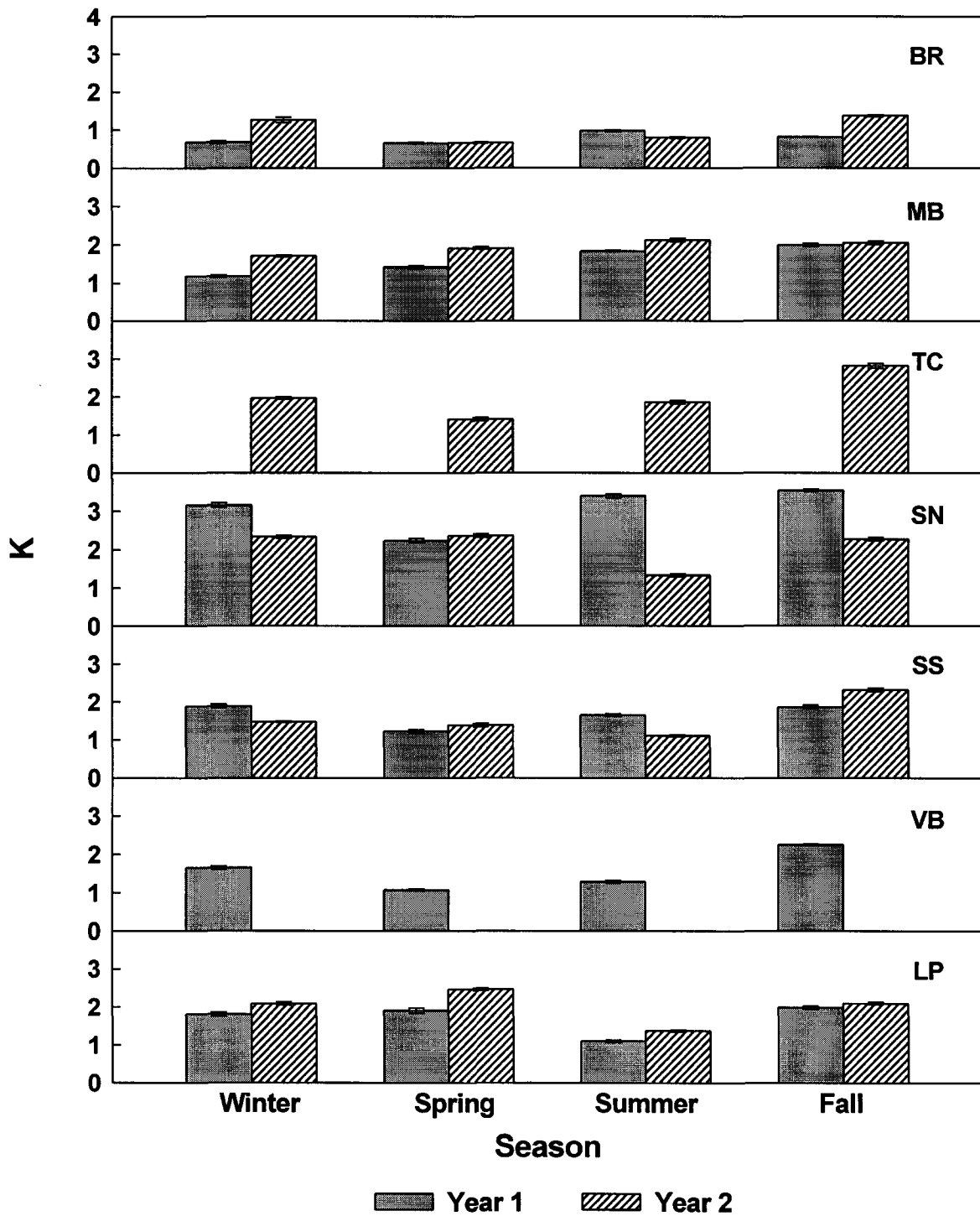


Fig. 2.44 Seasonal means (\pm SE) for K, between 1000-1400, within 48 hours after sensor cleaning, at all stations. Winter = December to February; Spring = March to May; Summer = June to August; Fall = September to November.

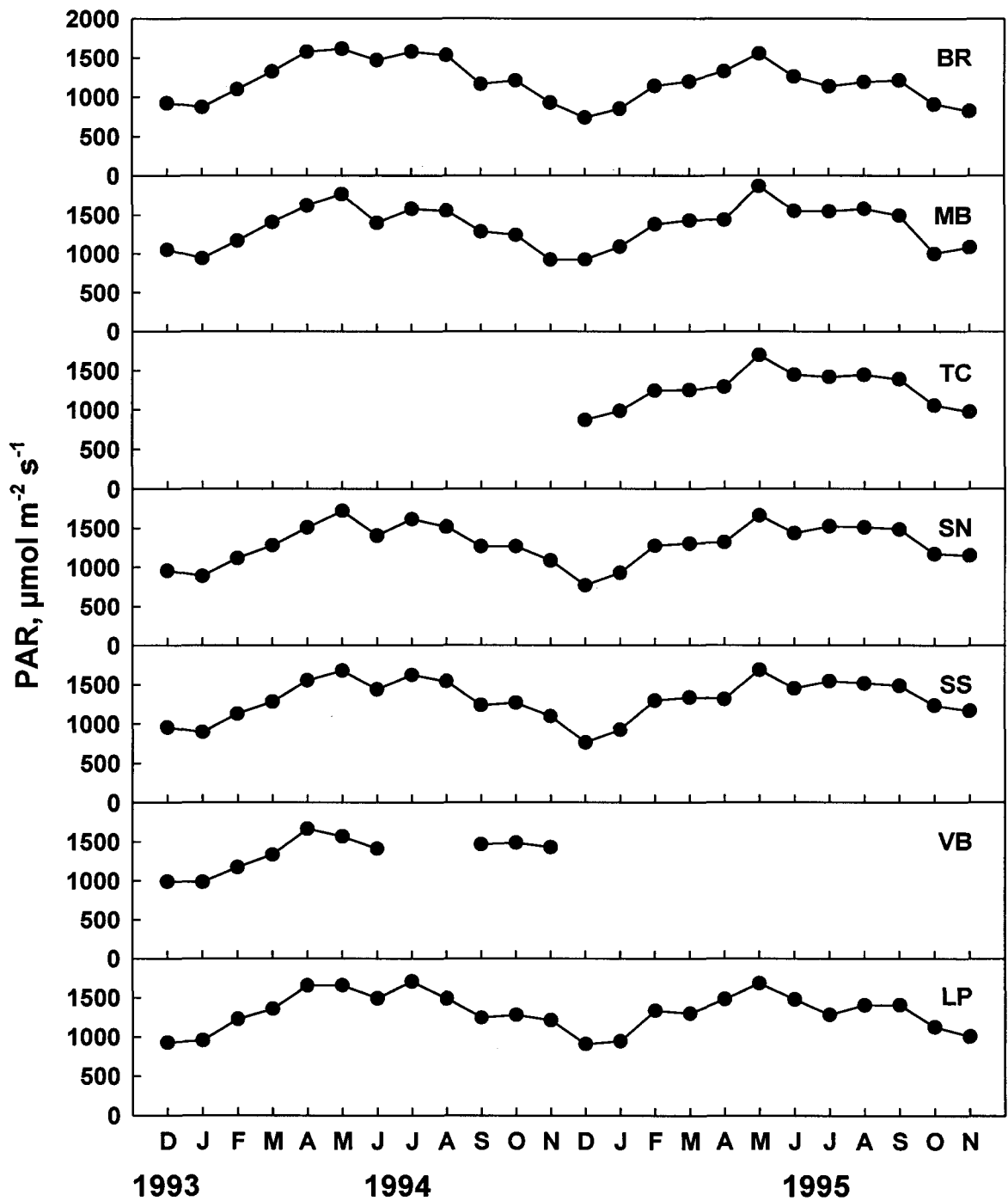


Fig. 2.45 Monthly means (\pm SE) for PAR measured by the C0 sensor, between 1000-1400, within 48 hours after sensor cleaning, at all stations, for the entire study.

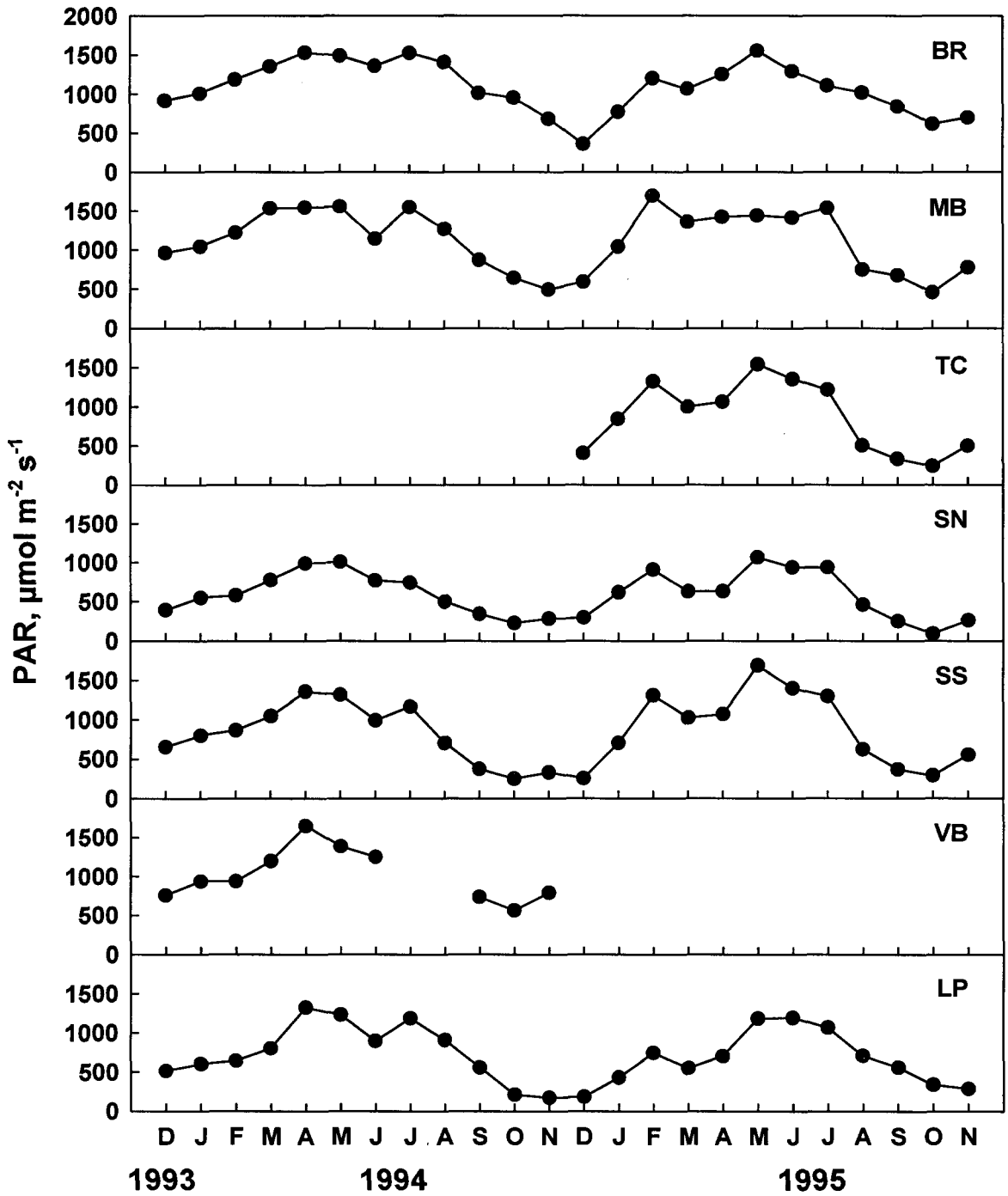


Fig. 2.46 Monthly means (\pm SE) for PAR measured by the S1 sensor, between 1000-1400, within 48 hours after sensor cleaning, at all stations, for the entire study.

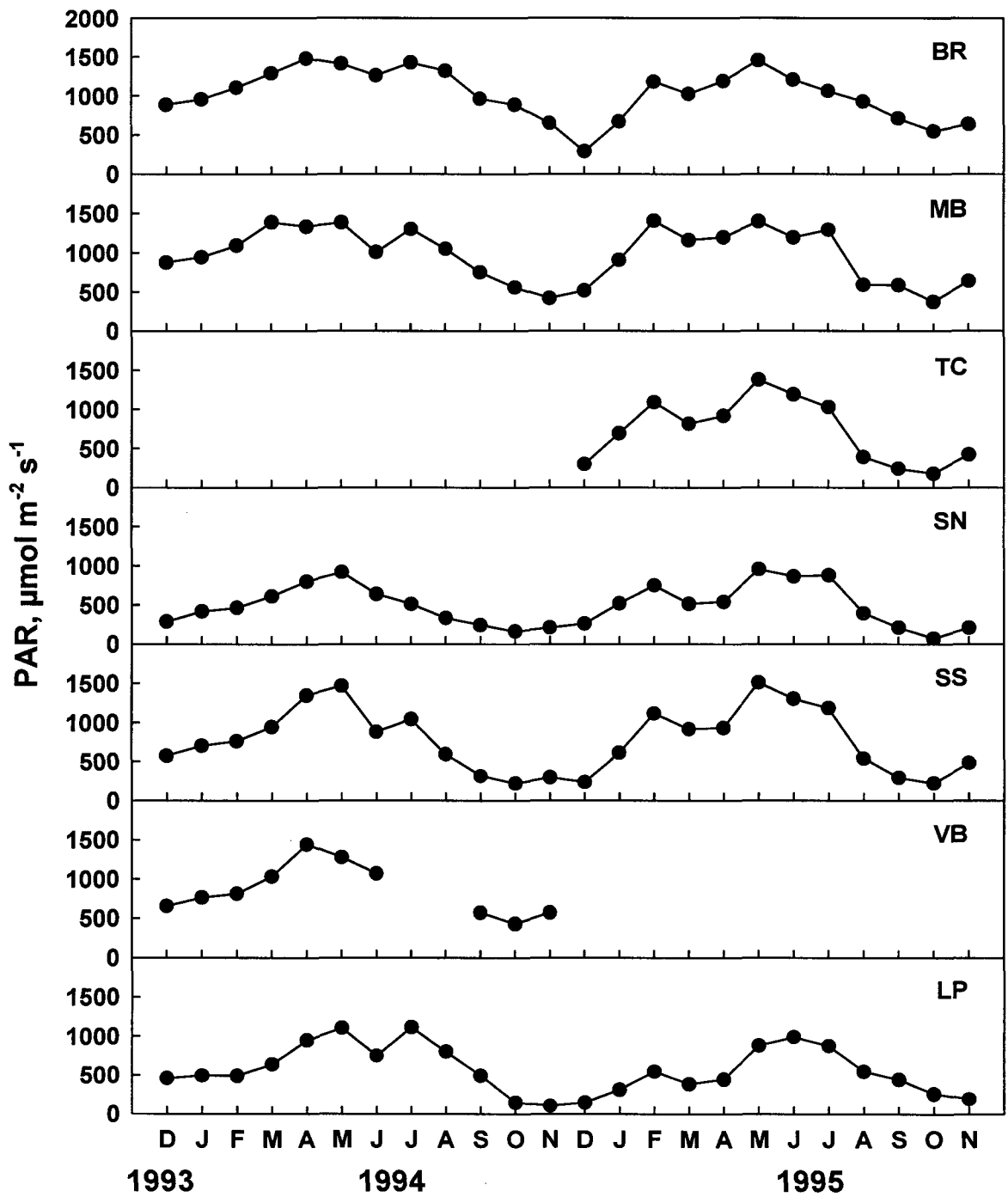


Fig. 2.47 Monthly means (\pm SE) for PAR measured by the S2 sensor, between 1000-1400, within 48 hours after sensor cleaning, at all stations, for the entire study.

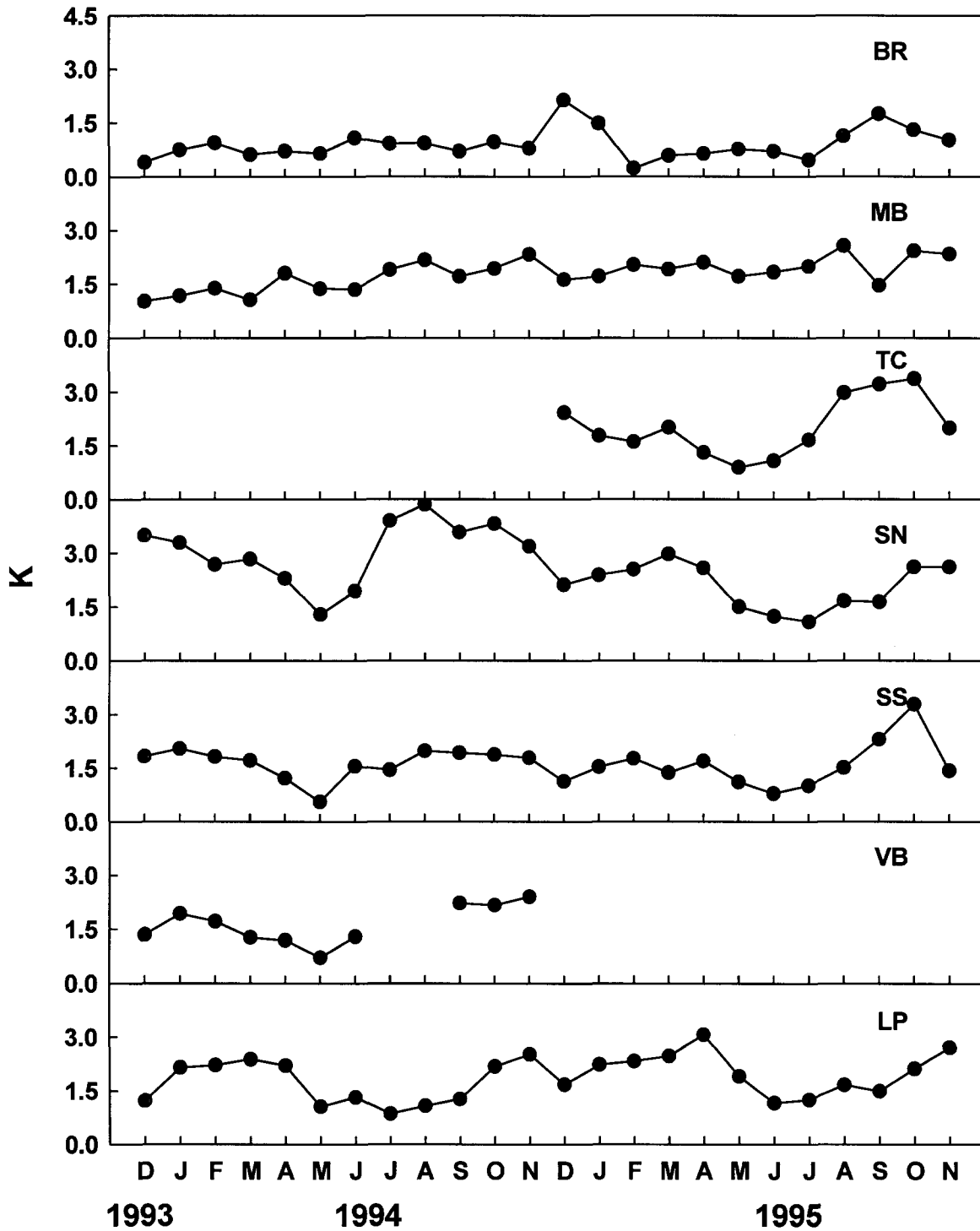


Fig. 2.48 Monthly means (\pm SE) for K, between 1000-1400, within 48 hours after sensor cleaning, at all stations, for the entire study.

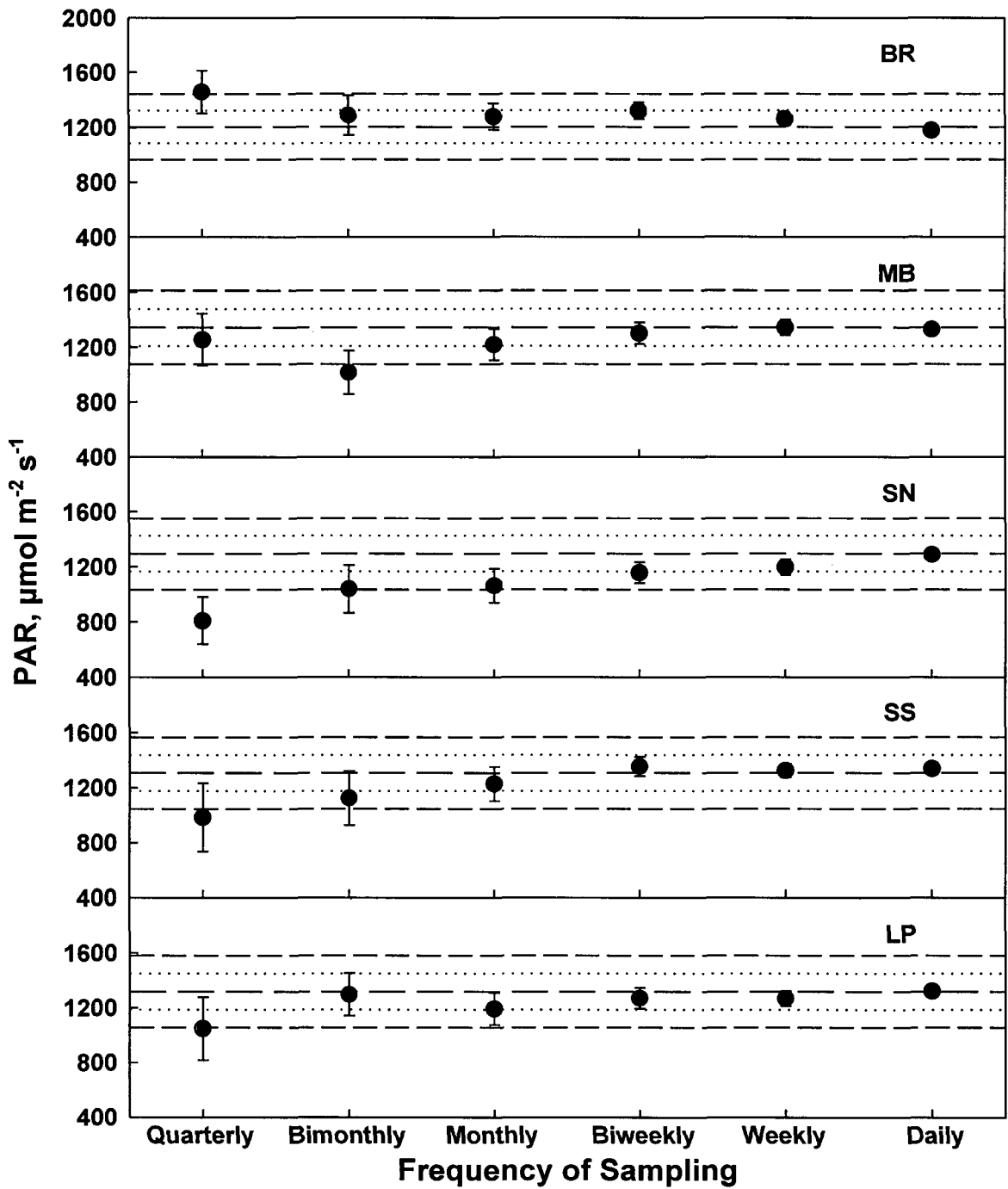


Fig. 2.49 Station means (\pm SE) for PAR measured by the C0 sensor as a function of sampling frequency. The center line indicates the mean value from continuous sampling; the dotted and outer broken lines indicate values that are $\pm 10\%$ and $\pm 20\%$, respectively, of the station means for continuous sampling.

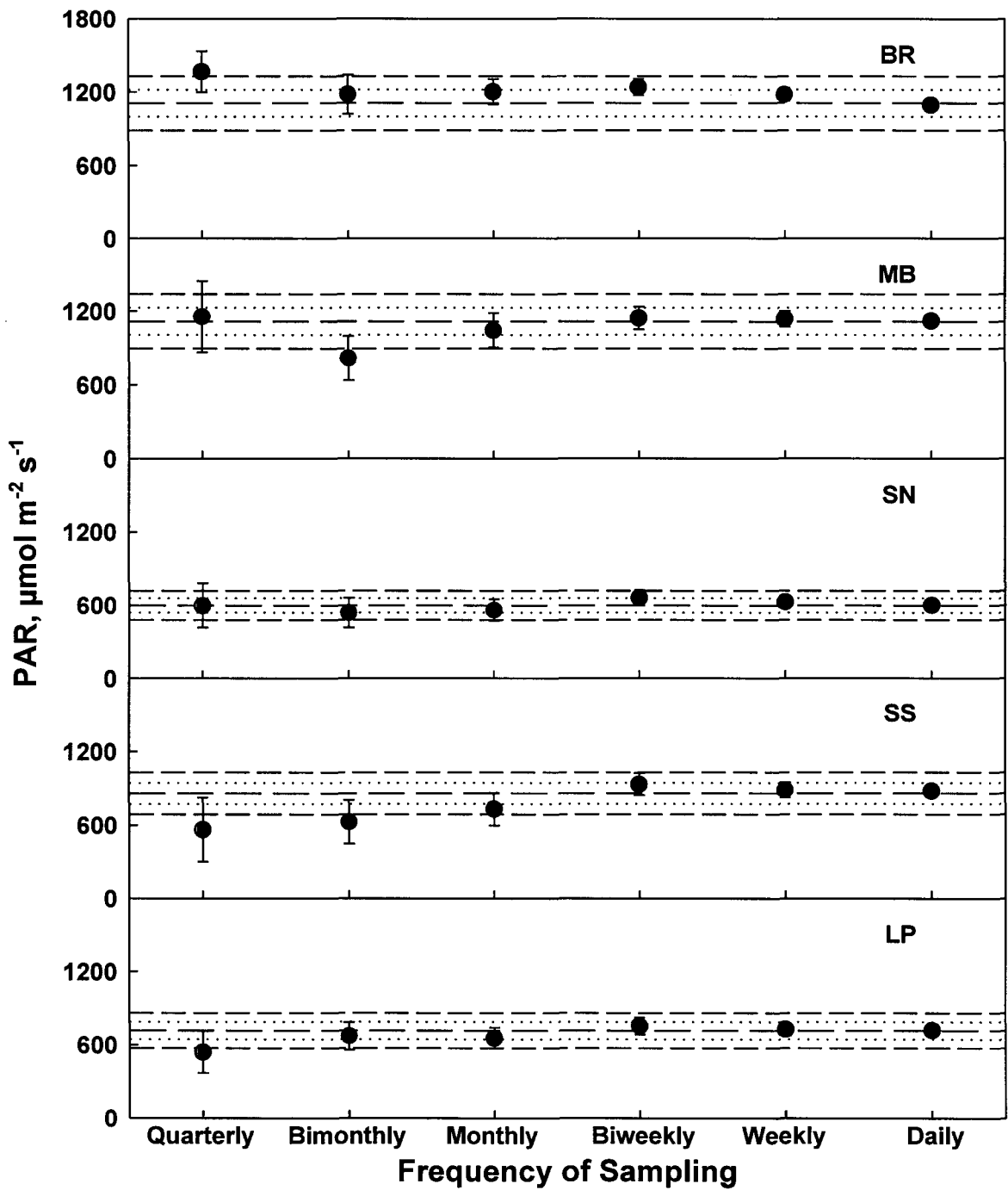


Fig. 2.50 Station means (\pm SE) for PAR measured by the S1 sensor as a function of sampling frequency. The center line indicates the mean value from continuous sampling; the dotted and outer broken lines indicate values that are $\pm 10\%$ and $\pm 20\%$, respectively, of the station means for continuous sampling.

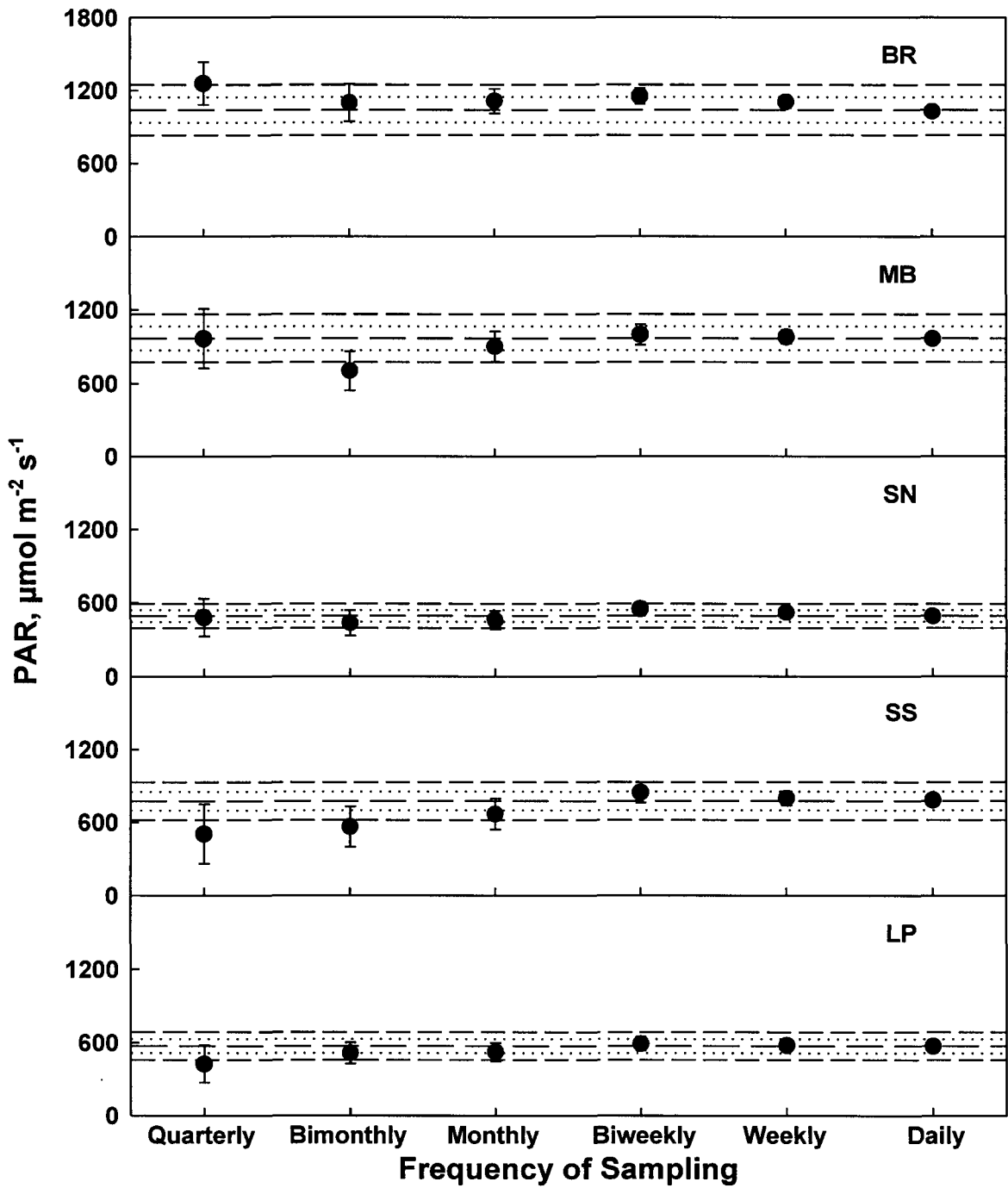


Fig. 2.51 Station means ($\pm\text{SE}$) for PAR measured by the S2 sensor as a function of sampling frequency. The center line indicates the mean value from continuous sampling; the dotted and outer broken lines indicate values that are $\pm 10\%$ and $\pm 20\%$, respectively, of the station means for continuous sampling.

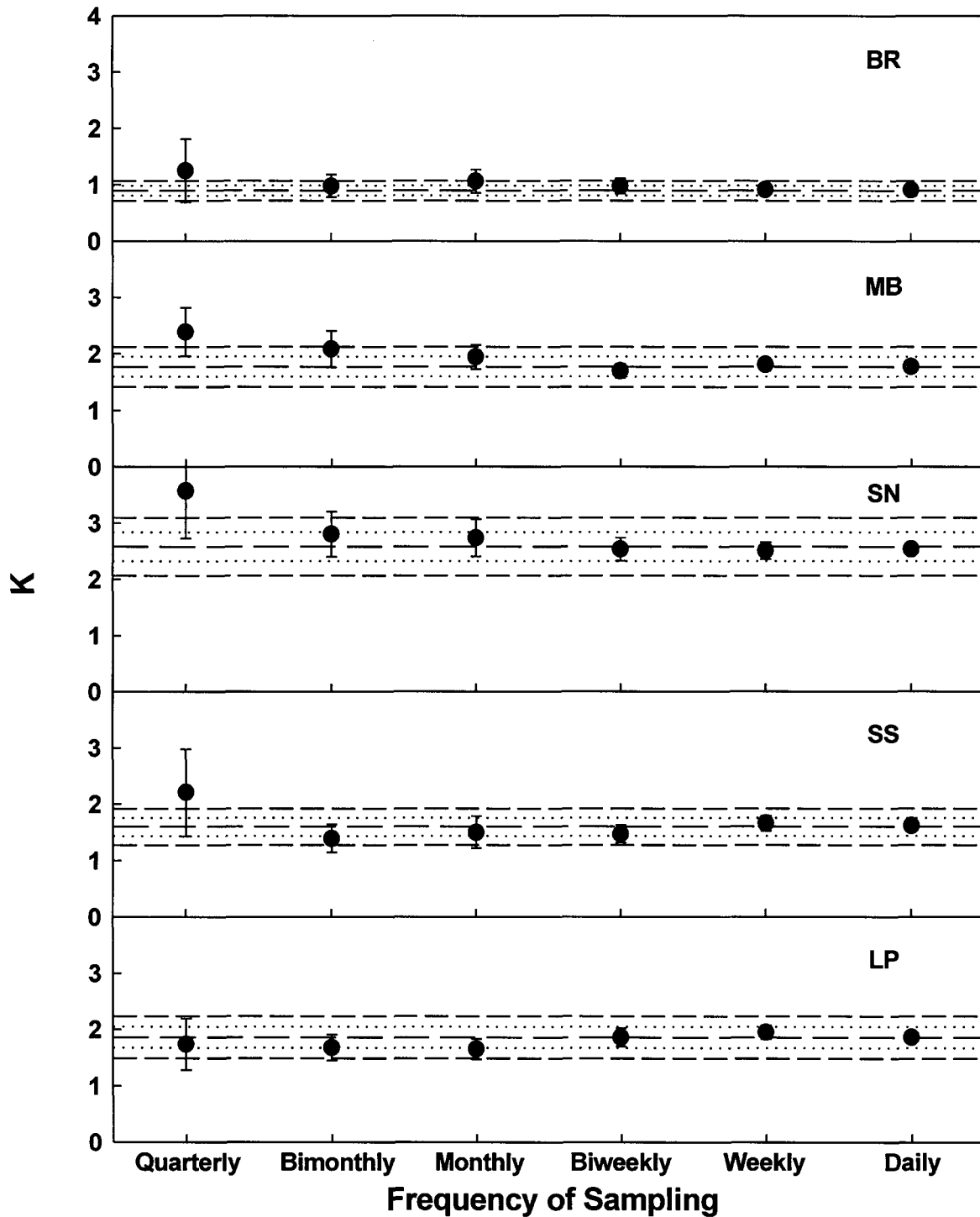


Fig. 2.52 Station means (\pm SE) for K as a function of sampling frequency. The center line indicates the mean value from continuous sampling; the dotted and outer broken lines indicate values that are $\pm 10\%$ and $\pm 20\%$, respectively, of the station means for continuous sampling.

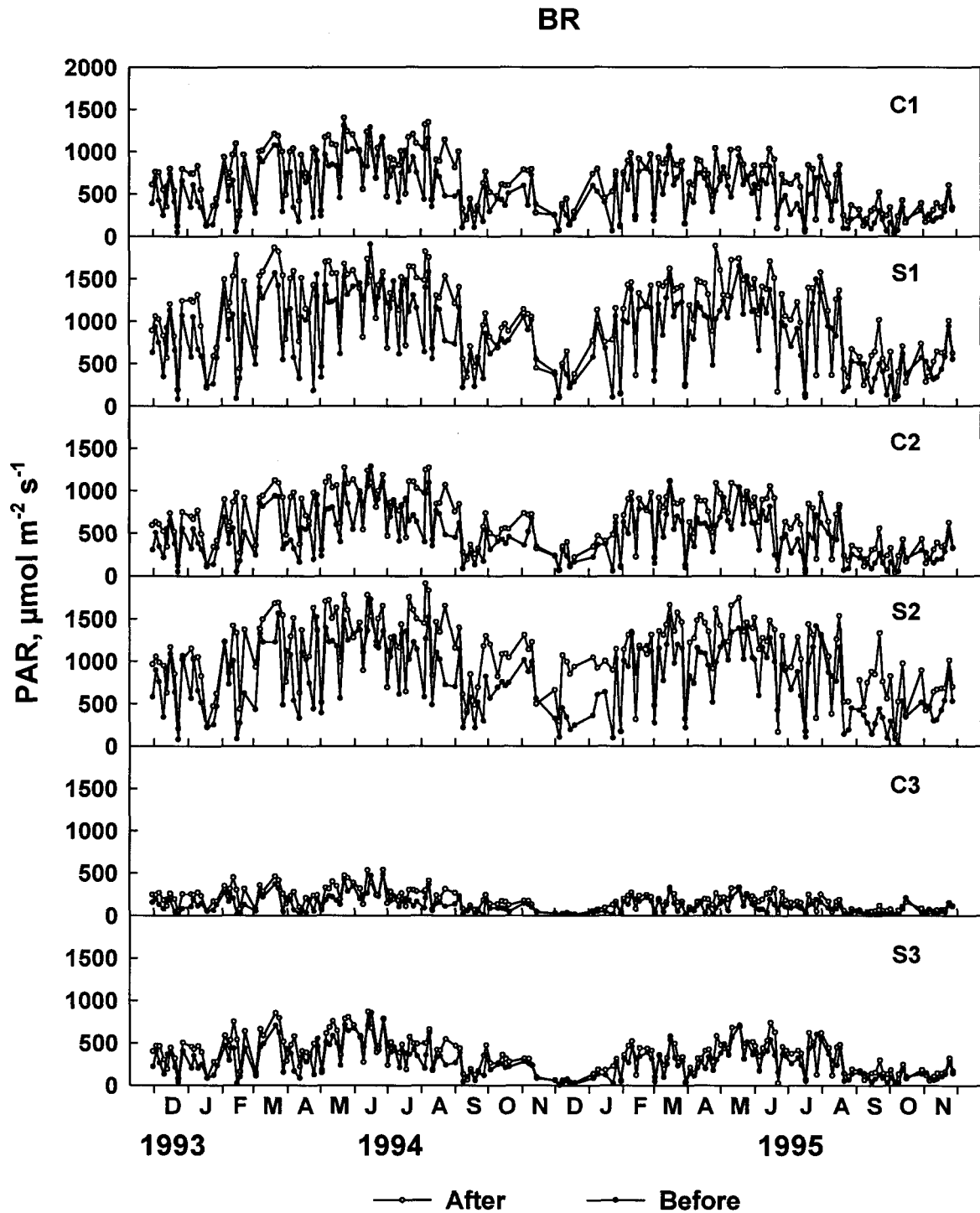


Fig. 2.53 PAR measured by the C1, S1, C2, S2, C3, and S3 sensors, before and after sensor cleaning, at BR, from November 30, 1993 to November 30, 1995. C1 = mid-depth cosine sensor, S1 = mid-depth spherical sensor, C2 = cosine sensor deployed above seagrass canopy, S2 = spherical sensor deployed above seagrass canopy, C3 = deep cosine sensor, S3 = deep spherical sensor.

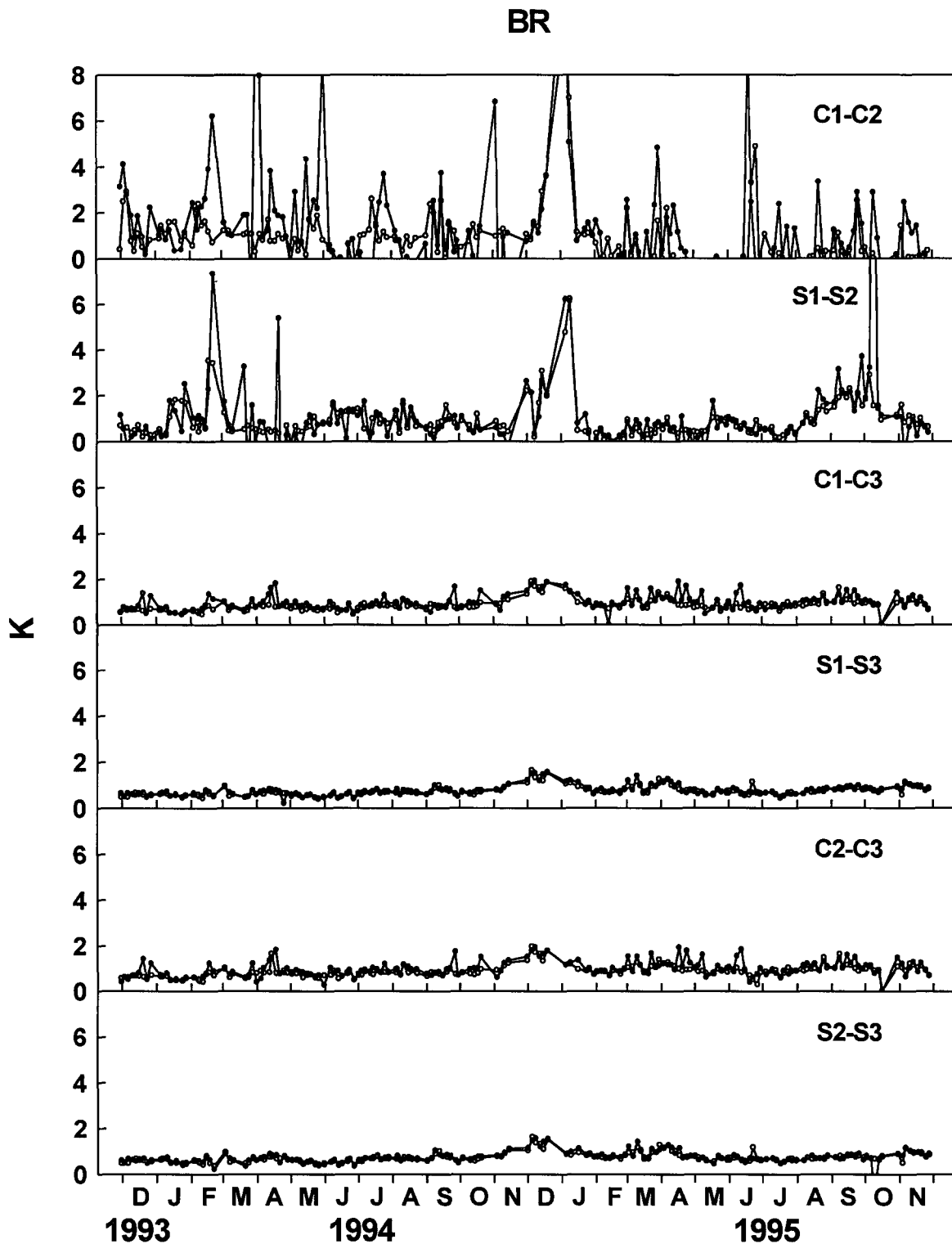


Fig. 2.54 K , before and after sensor cleaning, at BR, from November 30, 1993 to November 30, 1995. K_{C1-C2} is calculated from C1 and C2 sensors, K_{S1-S2} from S1 and S2 sensors, K_{C1-C3} from C1 and C3 sensors, K_{S1-S3} from S1 and S3 sensors, K_{C2-C3} from C2 and C3 sensors, K_{S2-S3} from S2 and S3 sensors.

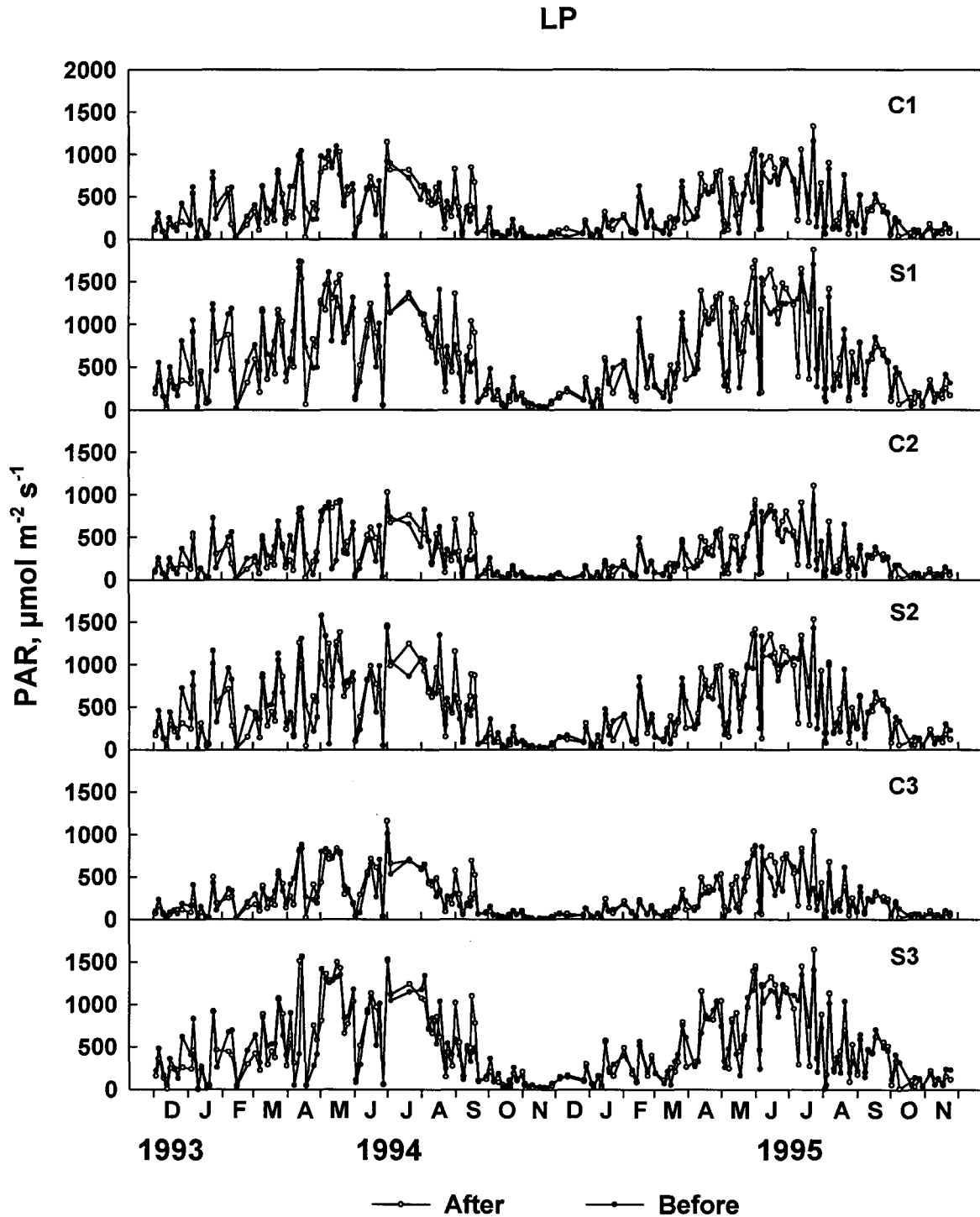


Fig. 2.55 PAR measured by the C1, S1, C2, S2, C3, and S3 sensors, before and after sensor cleaning, at LP, from November 30, 1993 to November 30, 1995. C1 = mid-depth cosine sensor, S1 = mid-depth spherical sensor, C2 = cosine sensor deployed above seagrass canopy, S2 = spherical sensor deployed above seagrass canopy, C3 = deep cosine sensor, S3 = deep spherical sensor.

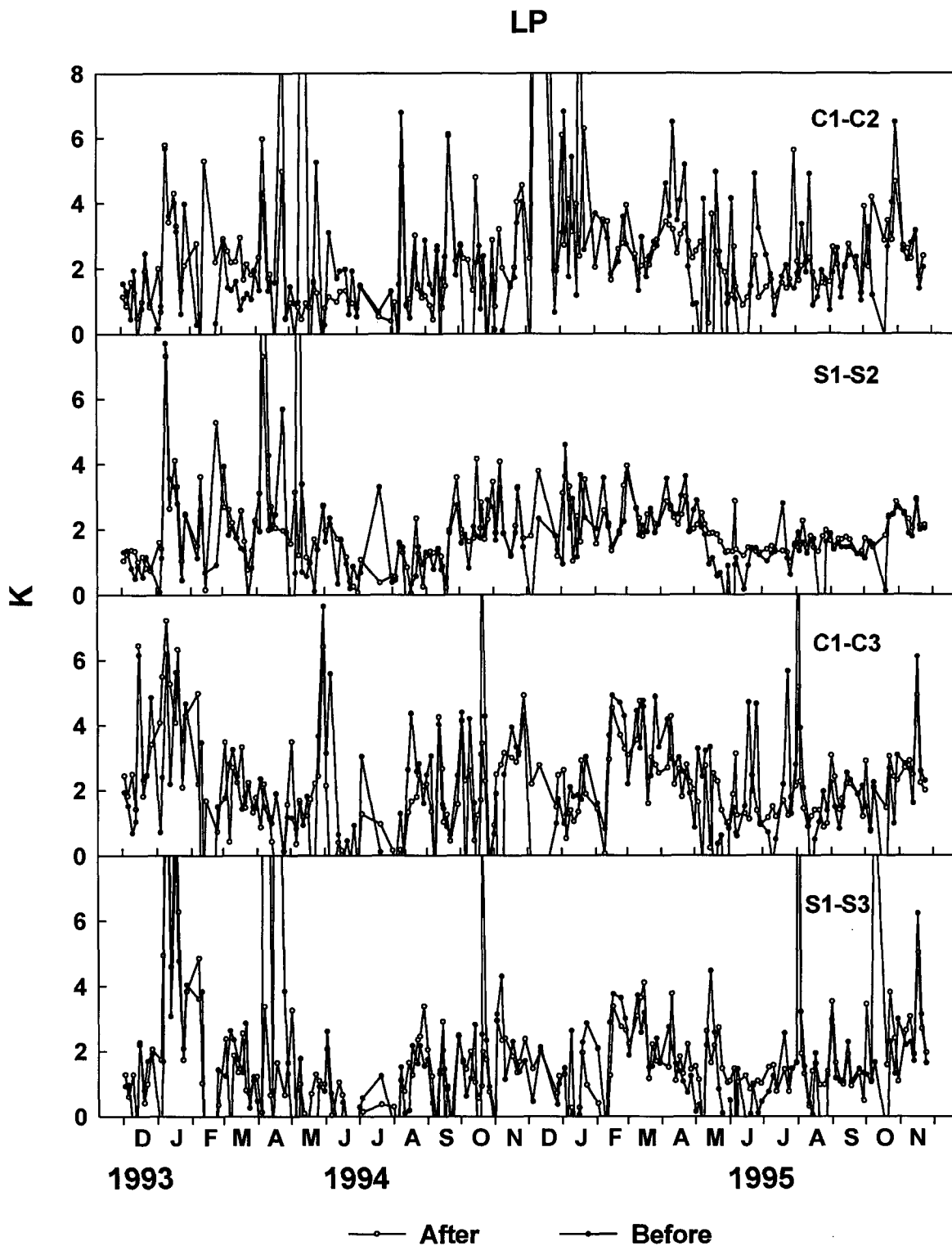


Fig. 2.56 K , before and after sensor cleaning, at LP, from November 30, 1993 to November 30, 1995. K_{C1-C2} is calculated from C1 and C2 sensors, K_{S1-S2} from S1 and S2 sensors, K_{C1-C3} from C1 and C3 sensors, K_{S1-S3} from S1 and S3 sensors.

BR

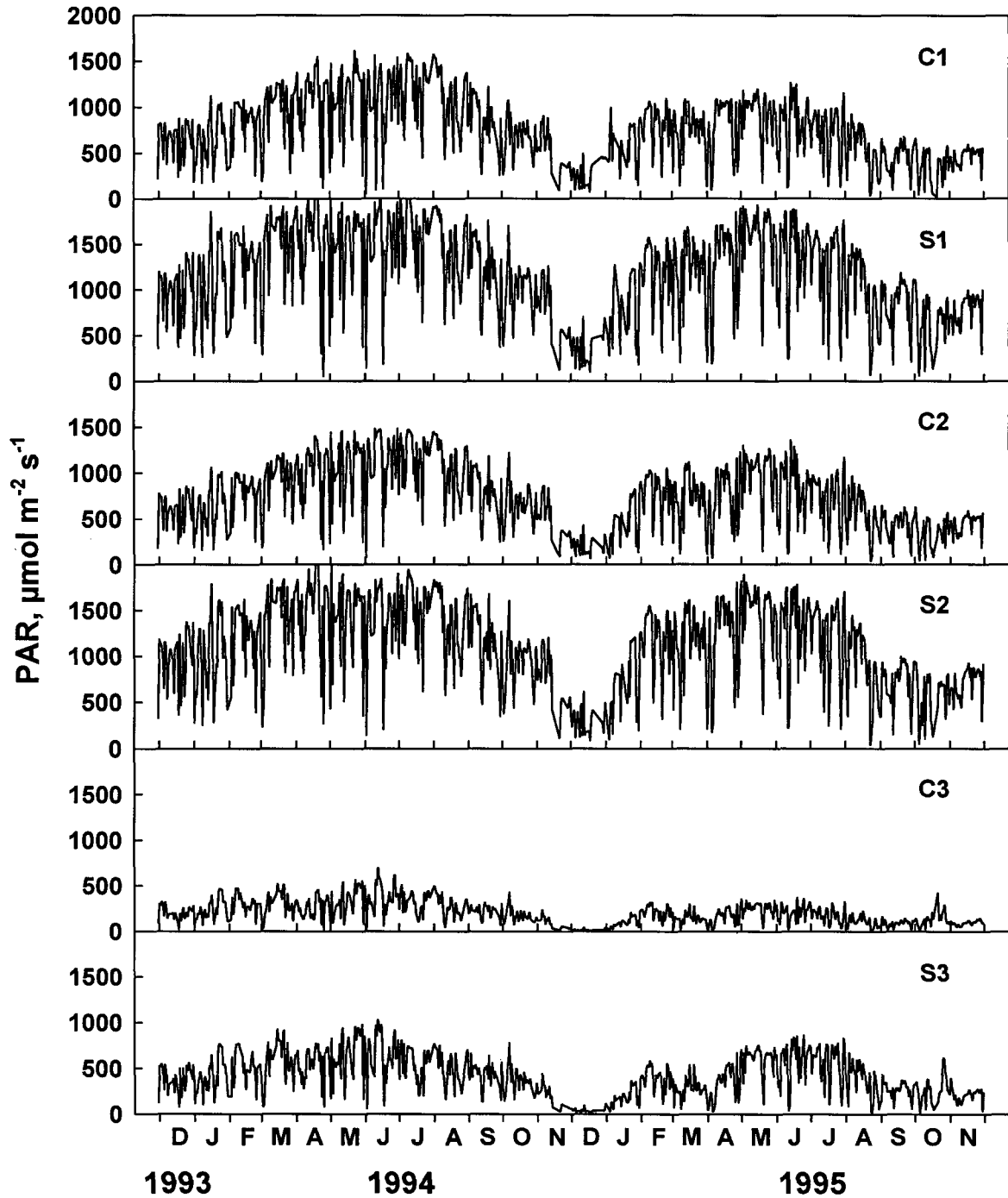


Fig. 2.57 PAR measured by the C1, S1, C2, S2, C3, and S3 sensors, at 1200 noon, at BR, from November 30, 1993 to November 30, 1995. C1 = mid-depth cosine sensor, S1 = mid-depth spherical sensor, C2 = cosine sensor deployed above seagrass canopy, S2 = spherical sensor deployed above seagrass canopy, C3 = deep cosine sensor, S3 = deep spherical sensor.

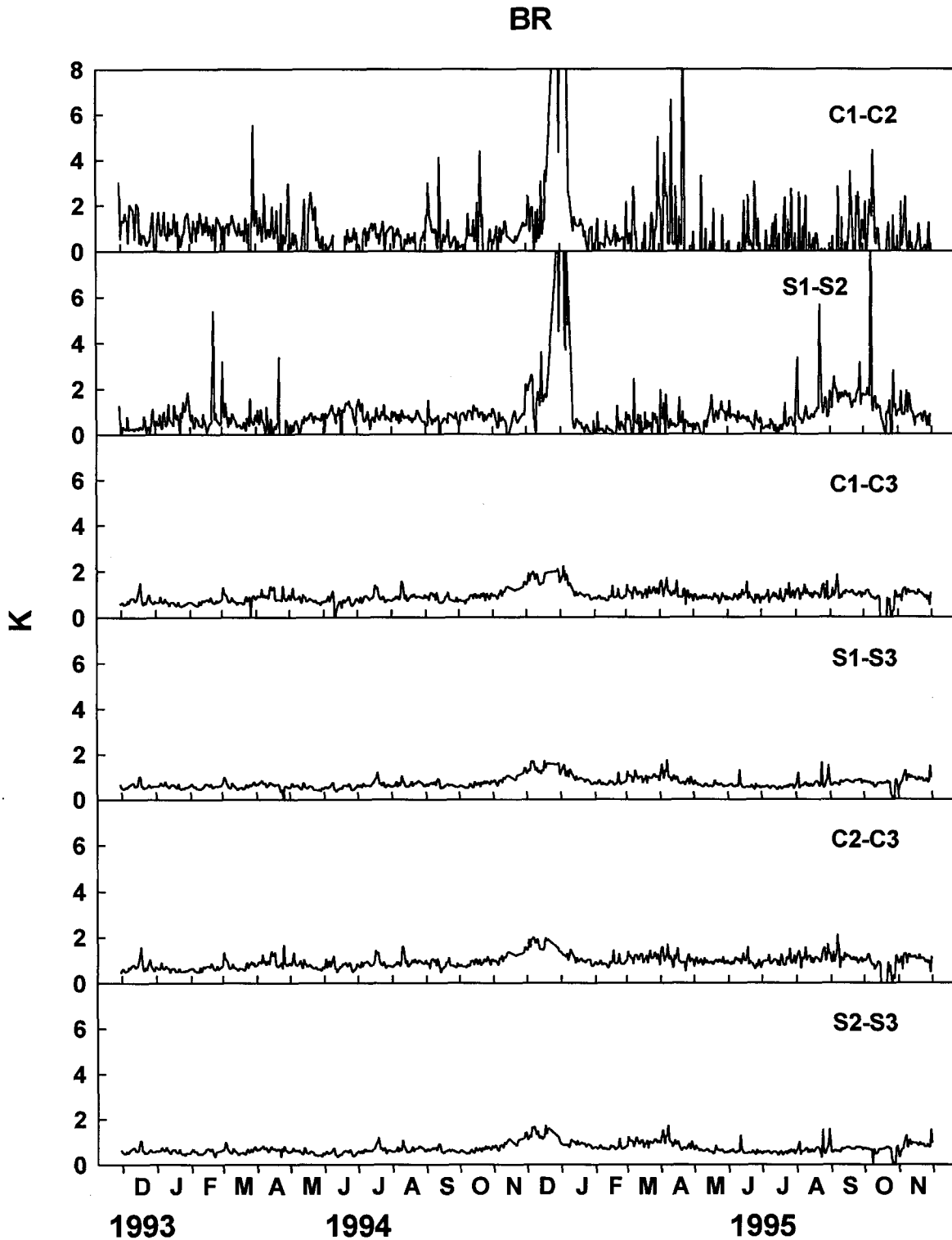


Fig. 2.58 K at 1200 noon, at BR, from November 30, 1993 to November 30, 1995. K_{C1-C2} is calculated from C1 and C2 sensors, K_{S1-S2} from S1 and S2 sensors, K_{C1-C3} from C1 and C3 sensors, K_{S1-S3} from S1 and S3 sensors, K_{C2-C3} from C2 and C3 sensors, K_{S2-S3} from S2 and S3 sensors.

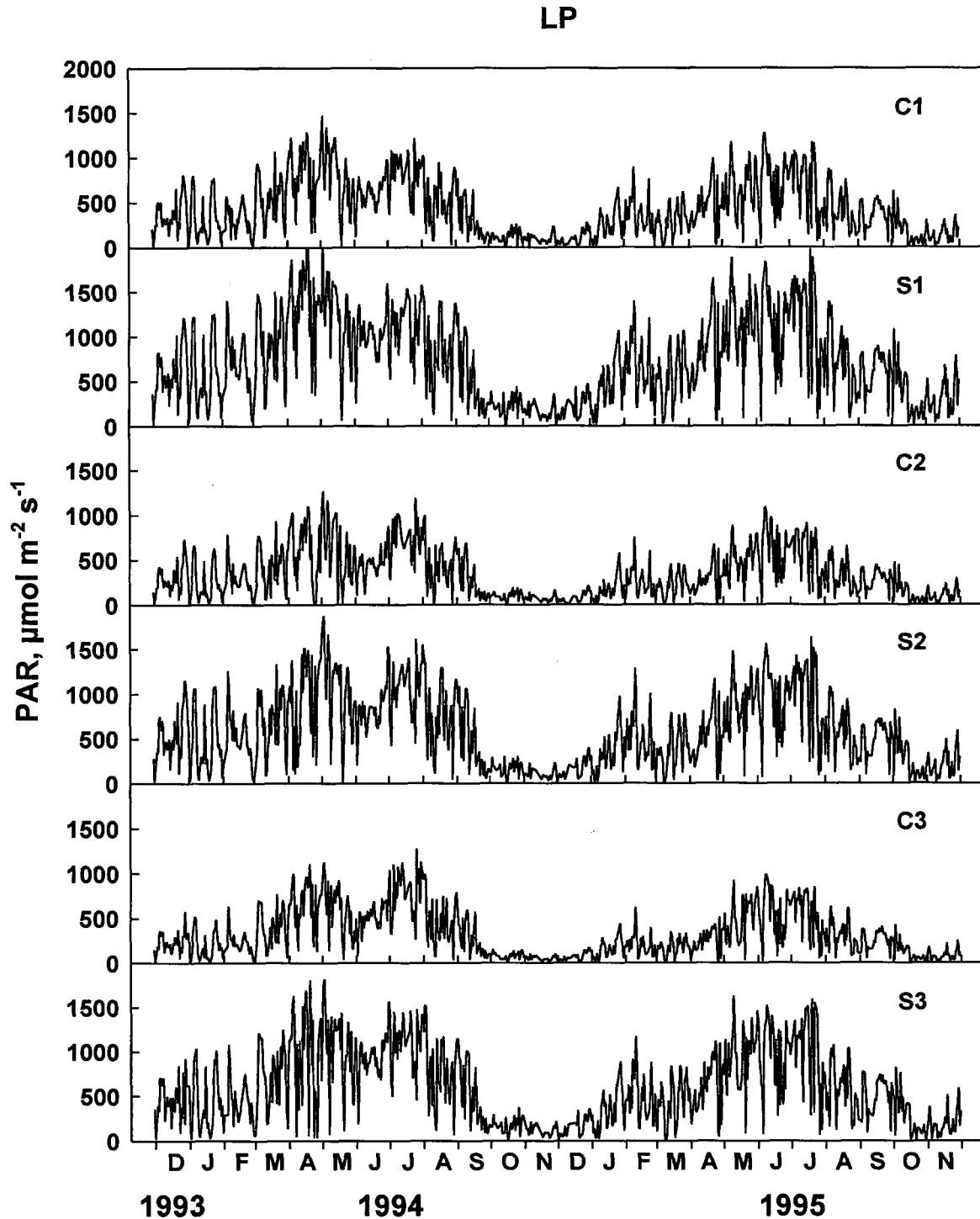


Fig. 2.59 PAR measured by the C1, S1, C2, S2, C3, and S3 sensors, at 1200 noon, at LP, from November 30, 1993 to November 30, 1995. C1 = mid-depth cosine sensor, S1 = mid-depth spherical sensor, C2 = cosine sensor deployed above seagrass canopy, S2 = spherical sensor deployed above seagrass canopy, C3 = deep cosine sensor, S3 = deep spherical sensor.

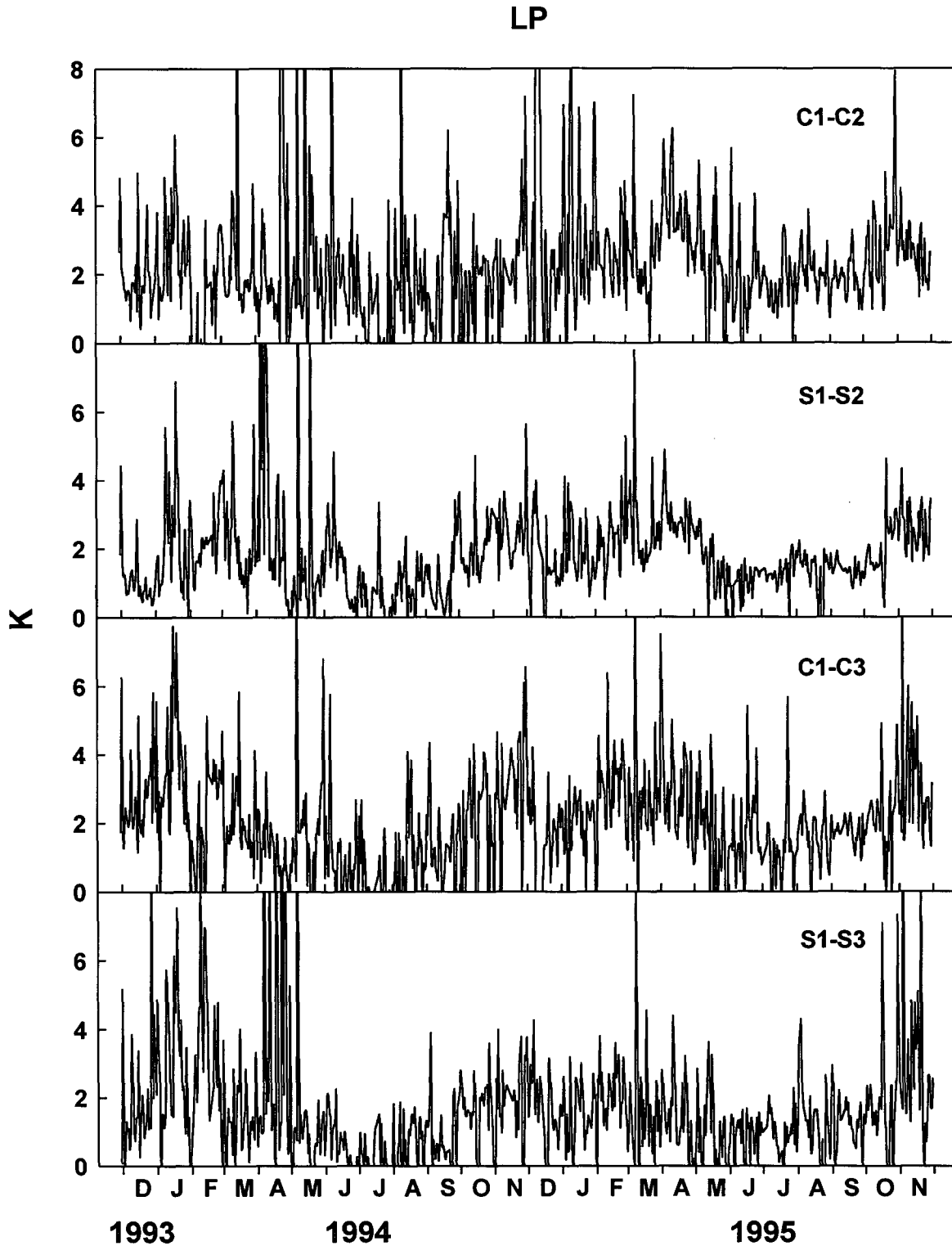


Fig. 2.60 K at 1200 noon, at LP, from November 30, 1993 to November 30, 1995. K_{C1-C2} is calculated from C1 and C2 sensors, K_{S1-S2} from S1 and S2 sensors, K_{C1-C3} from C1 and C3 sensors, K_{S1-S3} from S1 and S3 sensors.

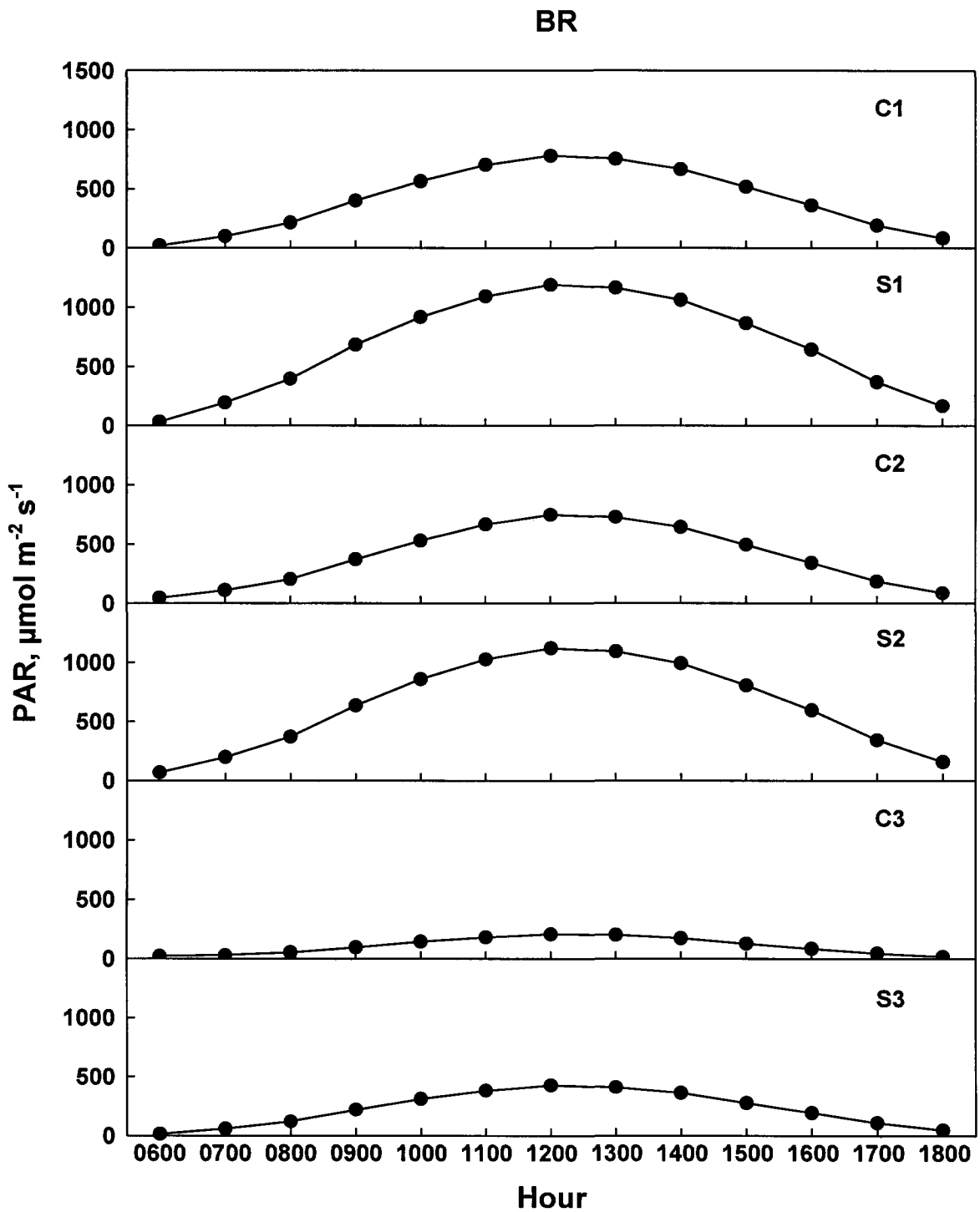


Fig. 2.61 Diel patterns in PAR measured by the C1, S1, C1, S2, C3, and S3 sensors, at BR, from November 30, 1993 to November 30, 1995. Data are hourly means (\pm SE) for the entire study.

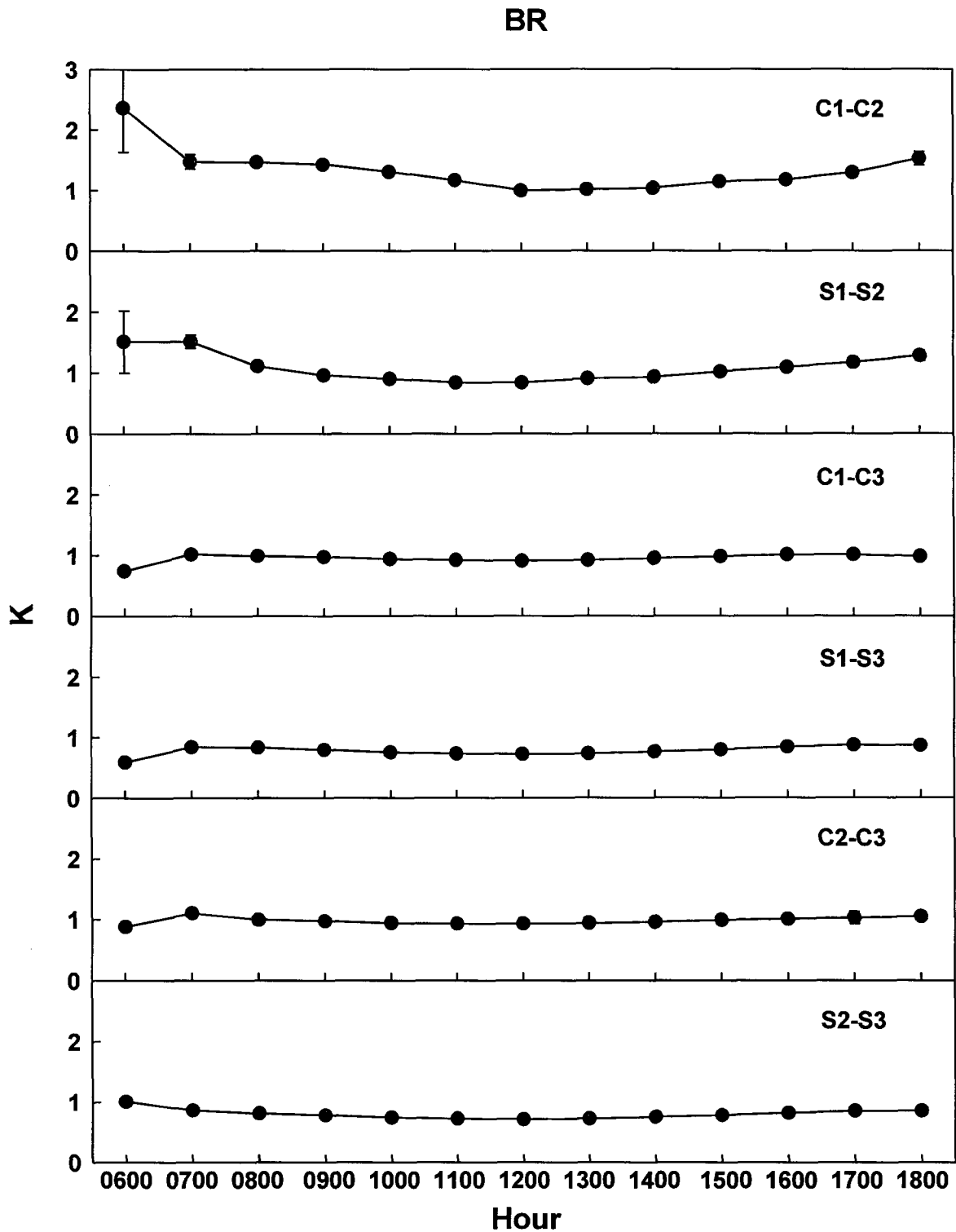


Fig. 2.62 Diel patterns in K, at BR, from November 30, 1993 to November 30, 1995. Data are hourly means (\pm SE). K_{C1-C2} is calculated from C1 and C2 sensors, K_{S1-S2} from S1 and S2 sensors, K_{C1-C3} from C1 and C3 sensors, K_{S1-S3} from S1 and S3 sensors, K_{C2-C3} from C2 and C3 sensors, K_{S2-S3} from S2 and S3 sensors.

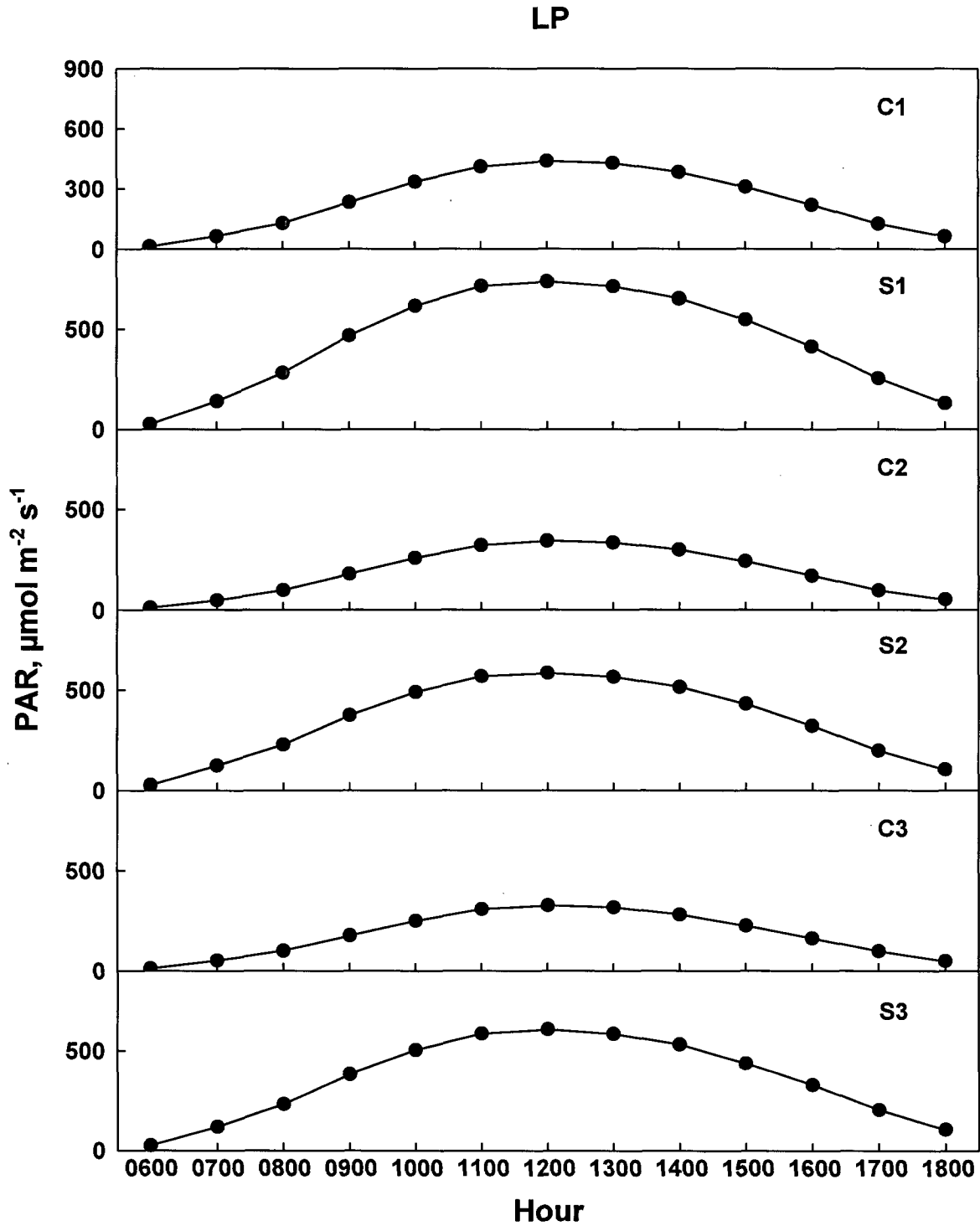


Fig. 2.63 Diel patterns in PAR measured by the C1, S1, C1, S2, C3, and S3 sensors, at LP, from November 30, 1993 to November 30, 1995. Data are hourly means (\pm SE) for the entire study.

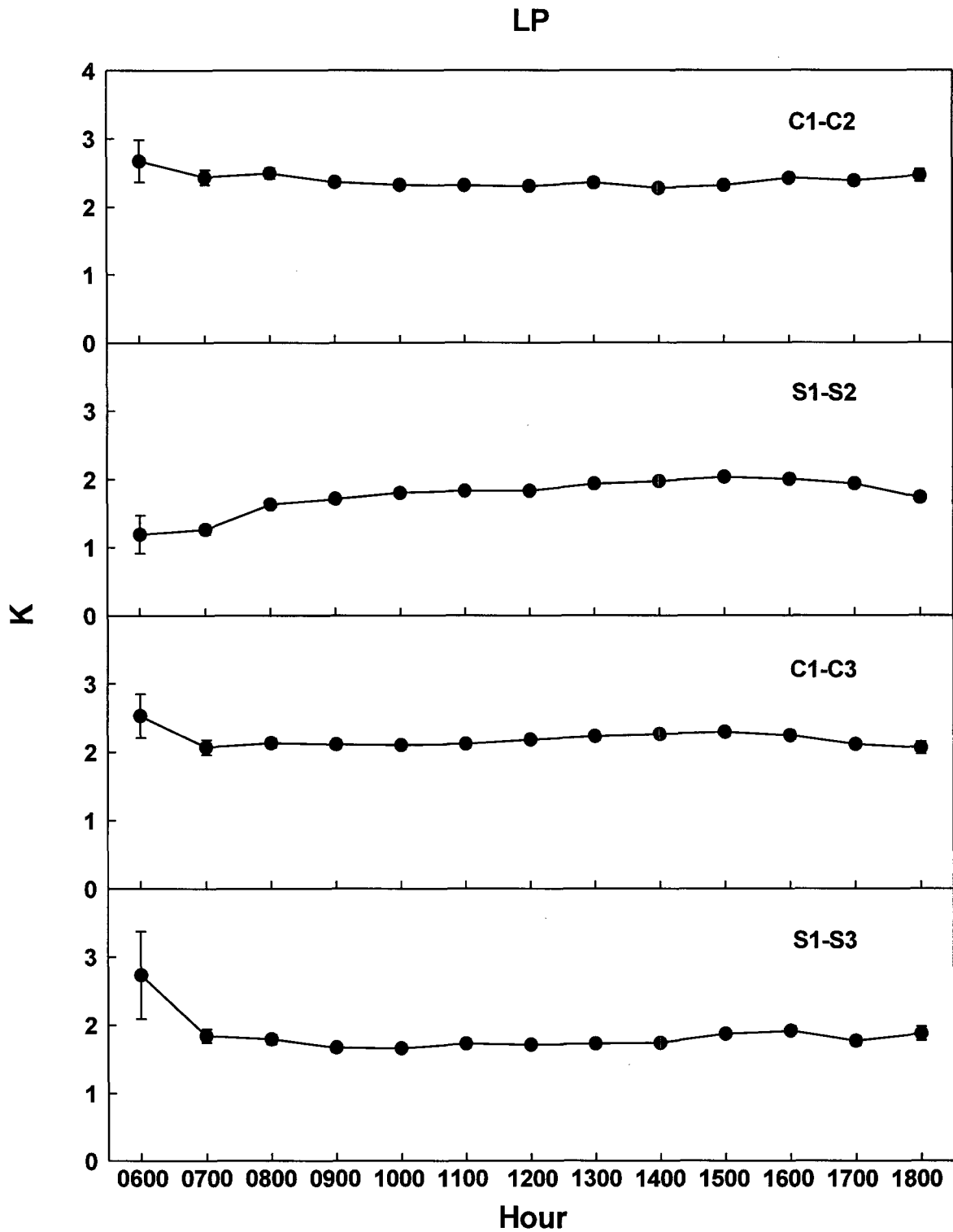


Fig. 2.64 Diel patterns in K, at LP, from November 30, 1993 to November 30, 1995. Data are hourly means (\pm SE). K_{C1-C2} is calculated from C1 and C2 sensors, K_{S1-S2} from S1 and S2 sensors, K_{C1-C3} from C1 and C3 sensors, K_{S1-S3} from S1 and S3 sensors.

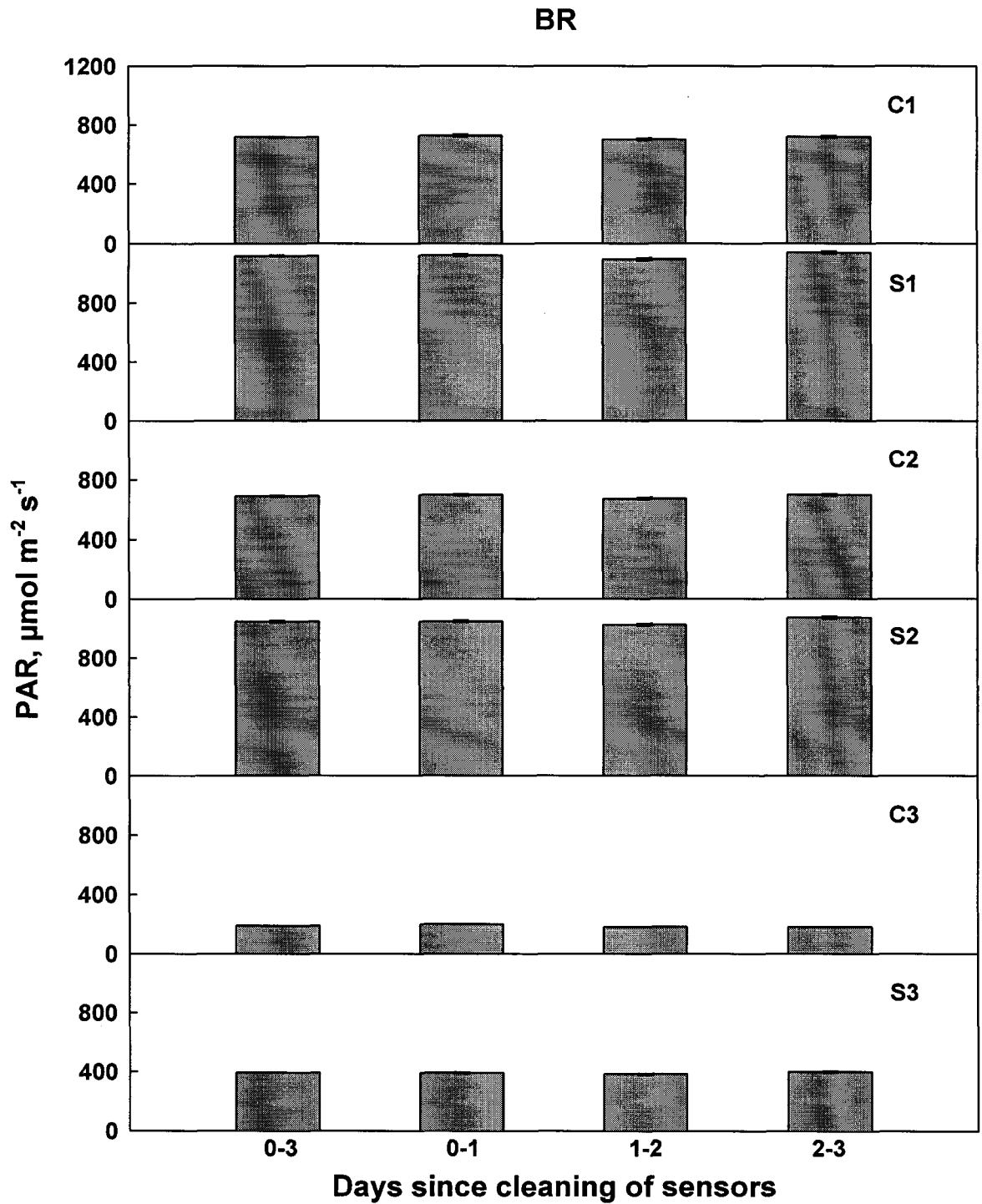


Fig. 2.65 PAR measured by the C1, S1, C1, S2, C3, and S3 sensors, within 3 days (72 hours) after cleaning of sensors, and by day since sensor cleaning, at BR, from November 30, 1993 to November 30, 1995. Data are means (\pm SE).

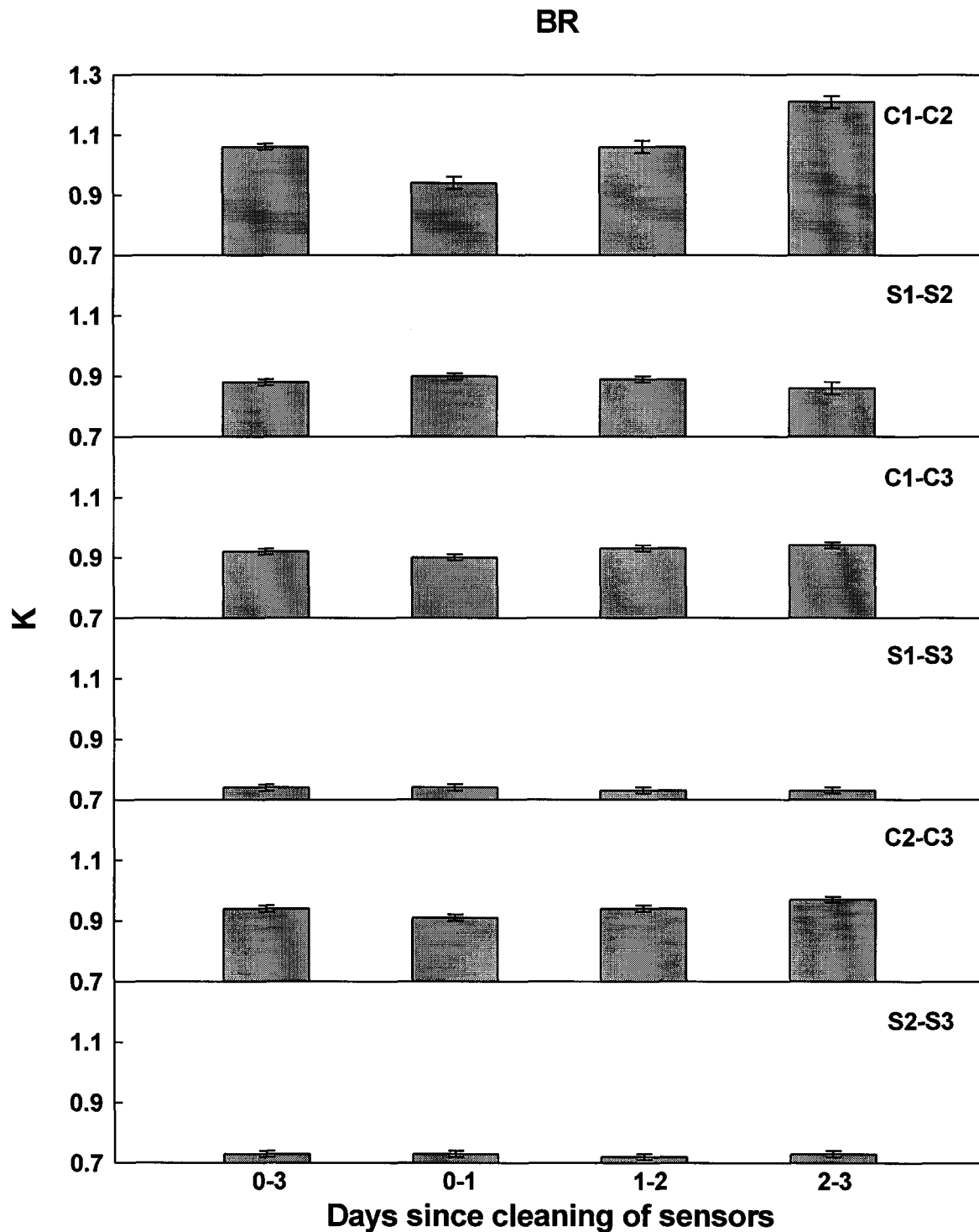


Fig. 2.66 K, within 3 days (72 hours) after sensor cleaning, and by day since sensor cleaning, at BR, from November 30, 1993 to November 30, 1995. Data are means (\pm SE). K_{C1-C2} is calculated from C1 and C2 sensors, K_{S1-S2} from S1 and S2 sensors, K_{C1-C3} from C1 and C3 sensors, K_{S1-S3} from S1 and S3 sensors, K_{C2-C3} from C2 and C3 sensors, K_{S2-S3} from S2 and S3 sensors.

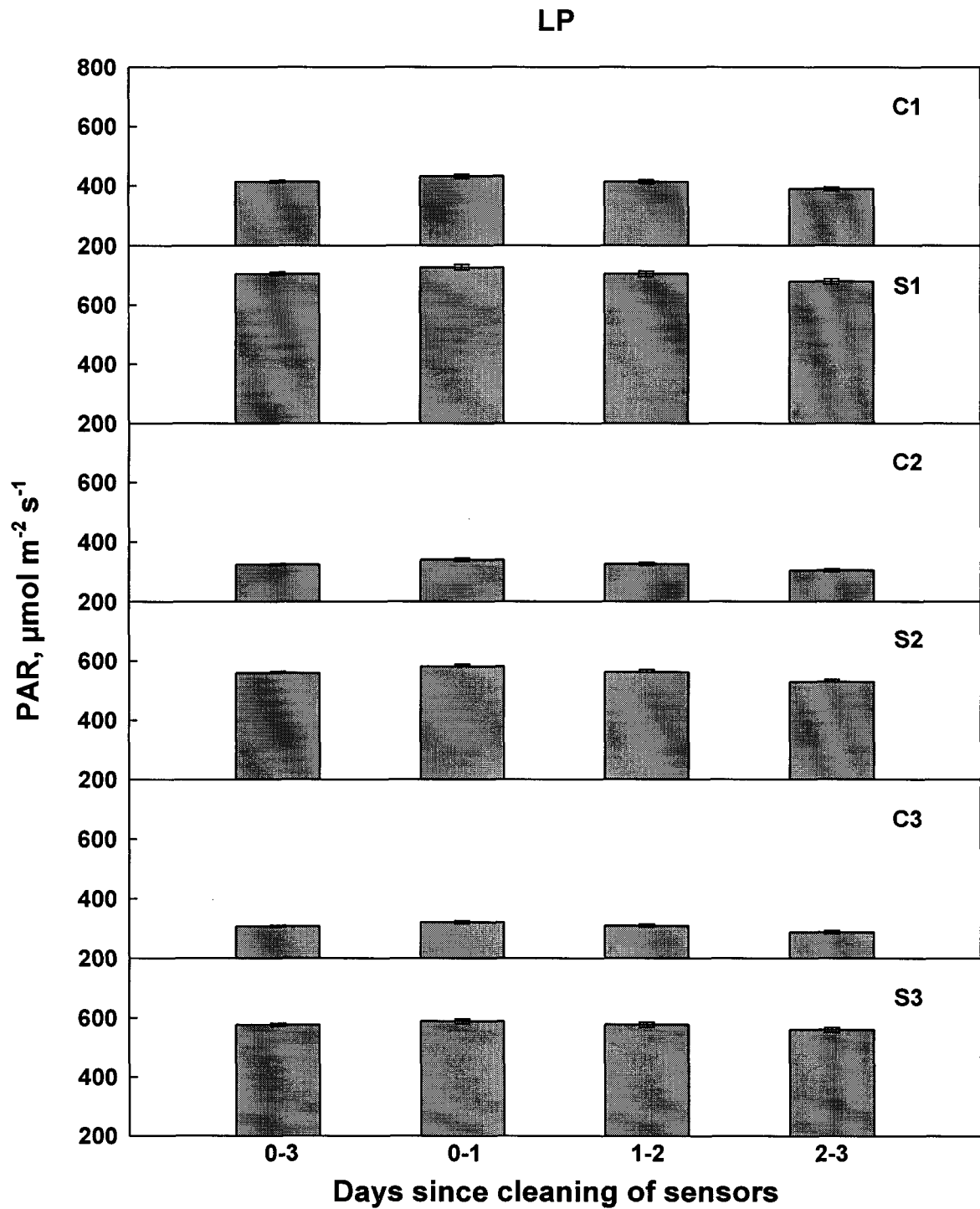


Fig. 2.67 PAR measured by the C1, S1, C1, S2, C3, and S3 sensors, within 3 days (72 hours) after cleaning of sensors, and by day since sensor cleaning, at LP, from November 30, 1993 to November 30, 1995. Data are means (\pm SE).

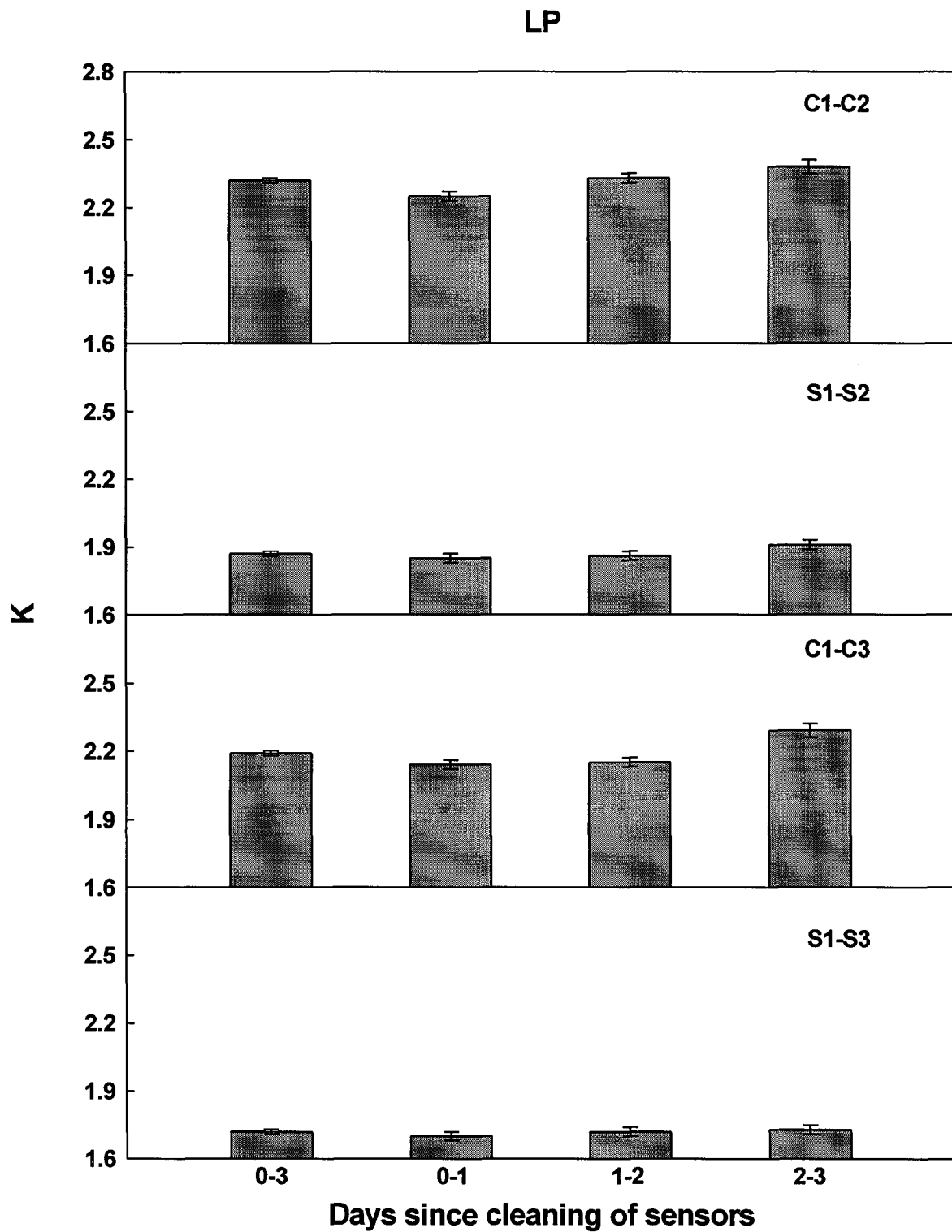


Fig. 2.68 K, within 3 days (72 hours) after cleaning of sensors, and by day since sensor cleaning at LP, from November 30, 1993 to November 30, 1995. Data are means (\pm SE). K_{C1-C2} is calculated from C1 and C2 sensors, K_{S1-S2} from S1 and S2 sensors, K_{C1-C3} from C1 and C3 sensors, K_{S1-S3} from S1 and S3 sensors.

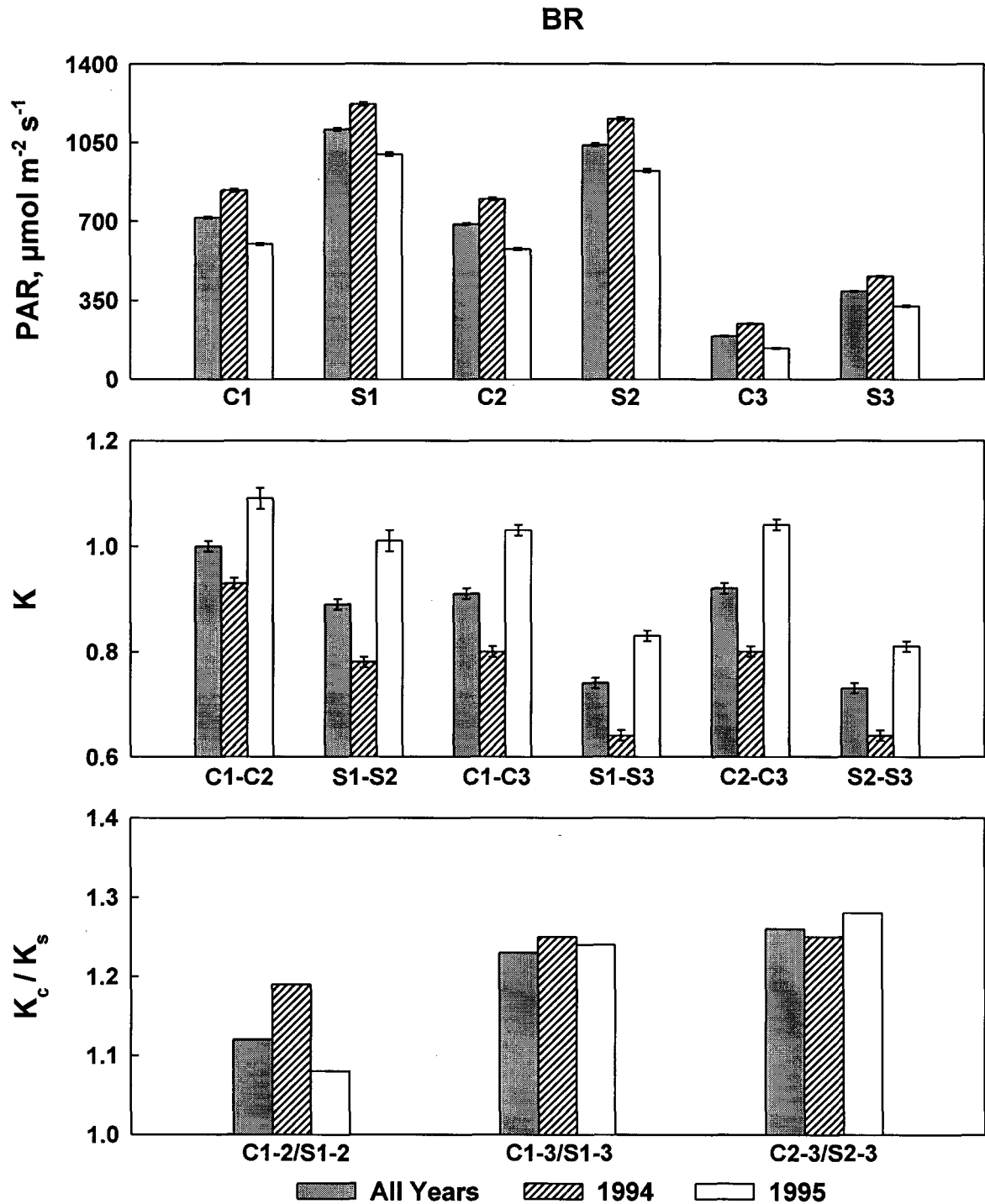


Fig. 2.69 Mean PAR (\pm SE) measured by the C1, S1, C2, S2, C3 and S3 sensors, K, and the ratio of K calculated from cosine sensors to that from spherical sensors (K_c/K_s), for all data at BR between the hours of 1000-1400, within 48 hours after cleaning of sensors from November 30, 1993 to November 30, 1995.

LP

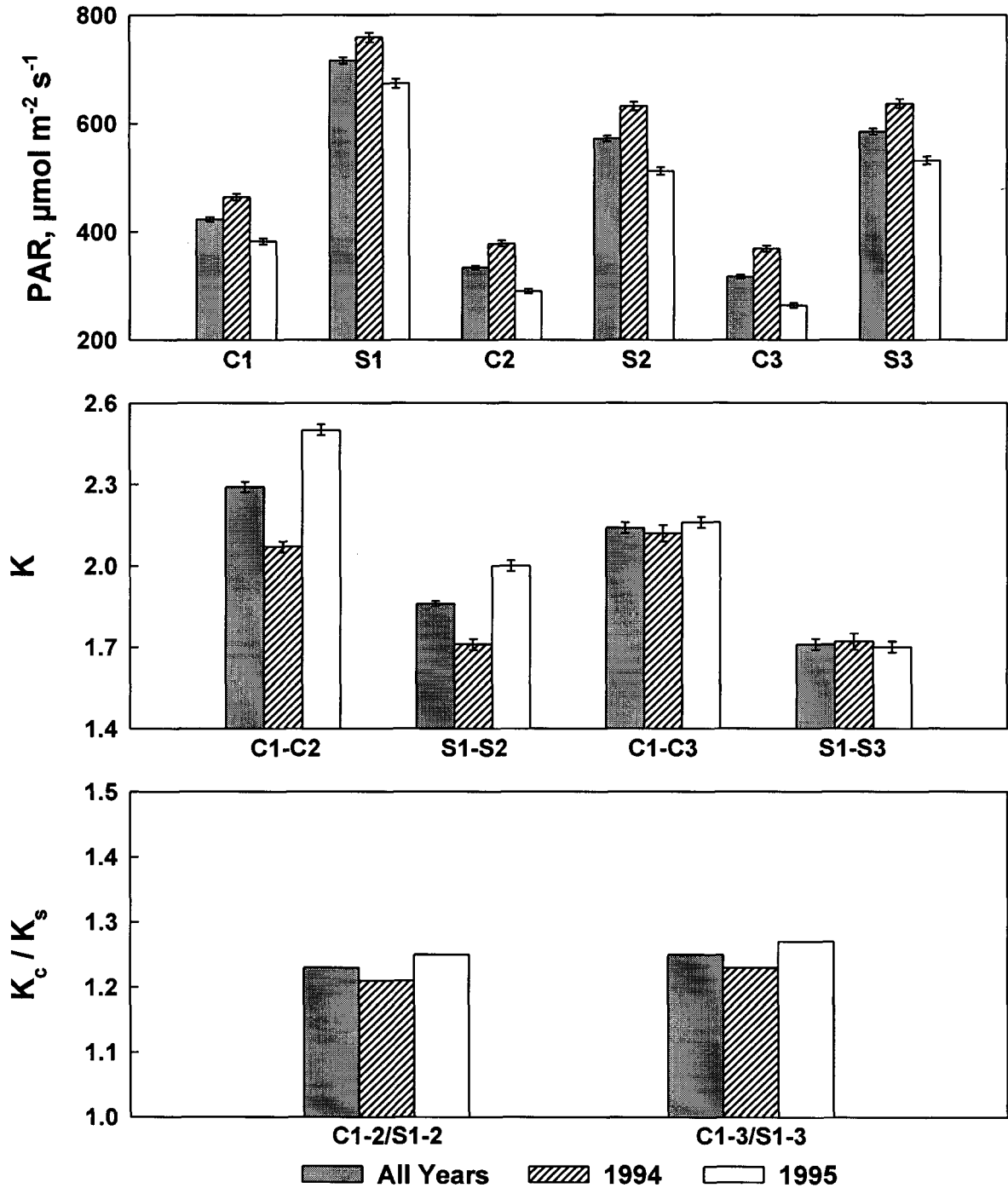


Fig. 2.70 Mean PAR (\pm SE) measured by the C1, S1, C2, S2, C3 and S3 sensors, K, and the ratio of K calculated from cosine sensors to that from spherical sensors (K_c/K_s), for all data at LP between the hours of 1000-1400, within 48 hours after cleaning of sensors from November 30, 1993 to November 30, 1995.

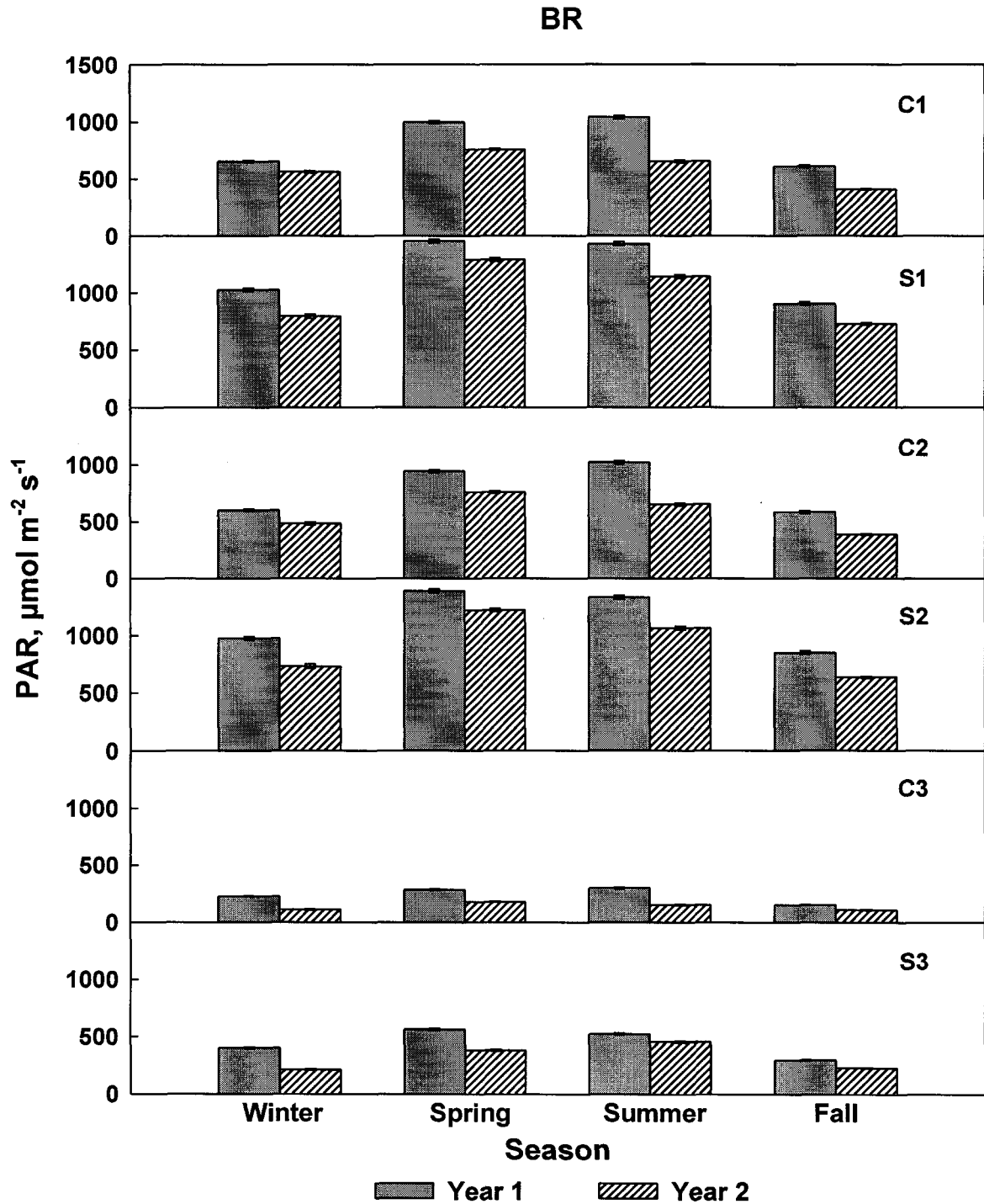


Fig. 2.71 Seasonal means (\pm SE) of PAR measured at BR by the C1, S1, C2, S2, C3, and S3 sensors, between the hours of 1000-1400, within 48 hours after sensor cleaning. Winter = December-February; Spring = March-May; Summer = June-August; Fall = September-November.

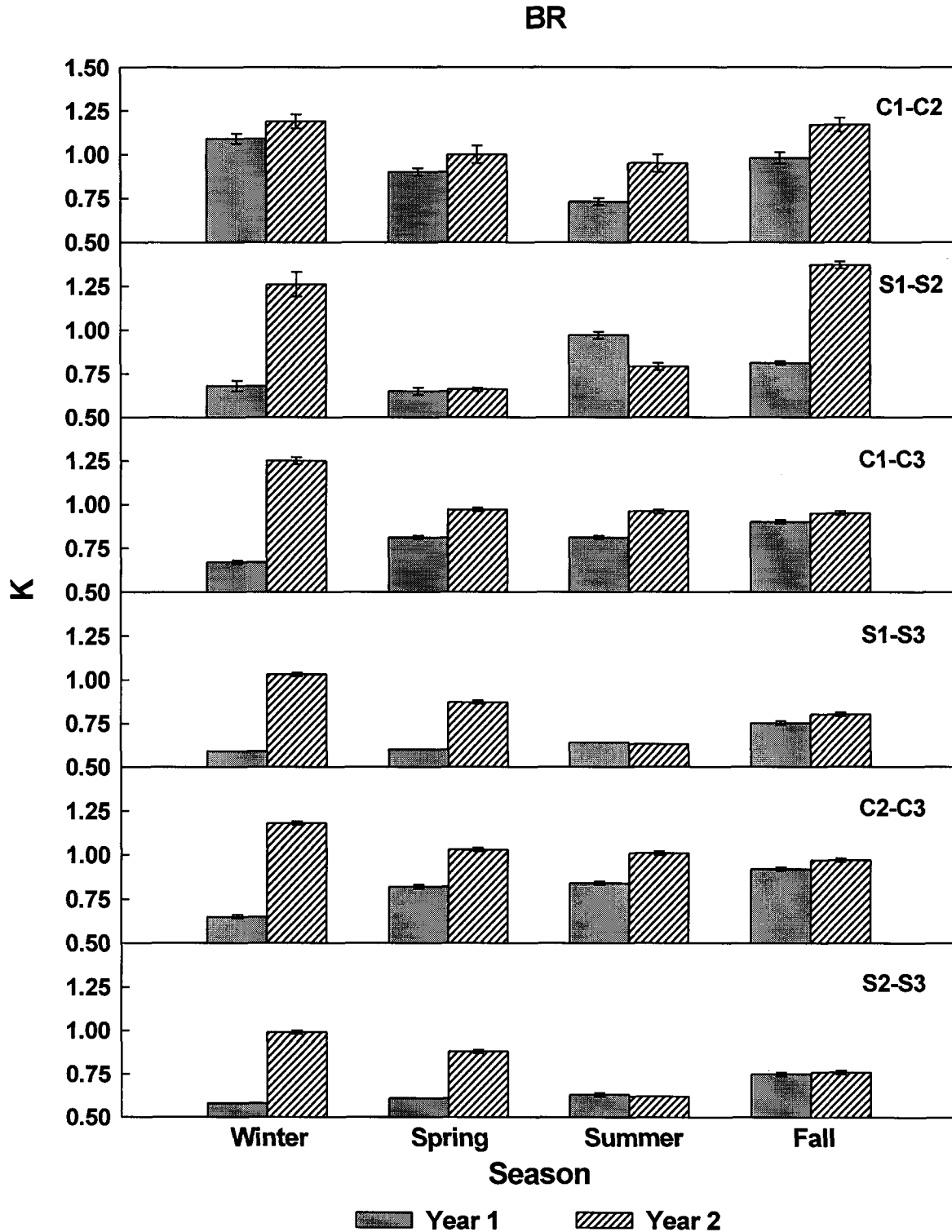


Fig. 2.72 Seasonal means (\pm SE) of K, at BR, between the hours of 1000-1400, within 48 hours after sensor cleaning. K_{C1-C2} is calculated from C1 and C2 sensors, K_{S1-S2} from S1 and S2 sensors, K_{C1-C3} from C1 and C3 sensors, K_{S1-S3} from S1 and S3 sensors, K_{C2-C3} from C2 and C3 sensors, K_{S2-S3} from S2 and S3 sensors.

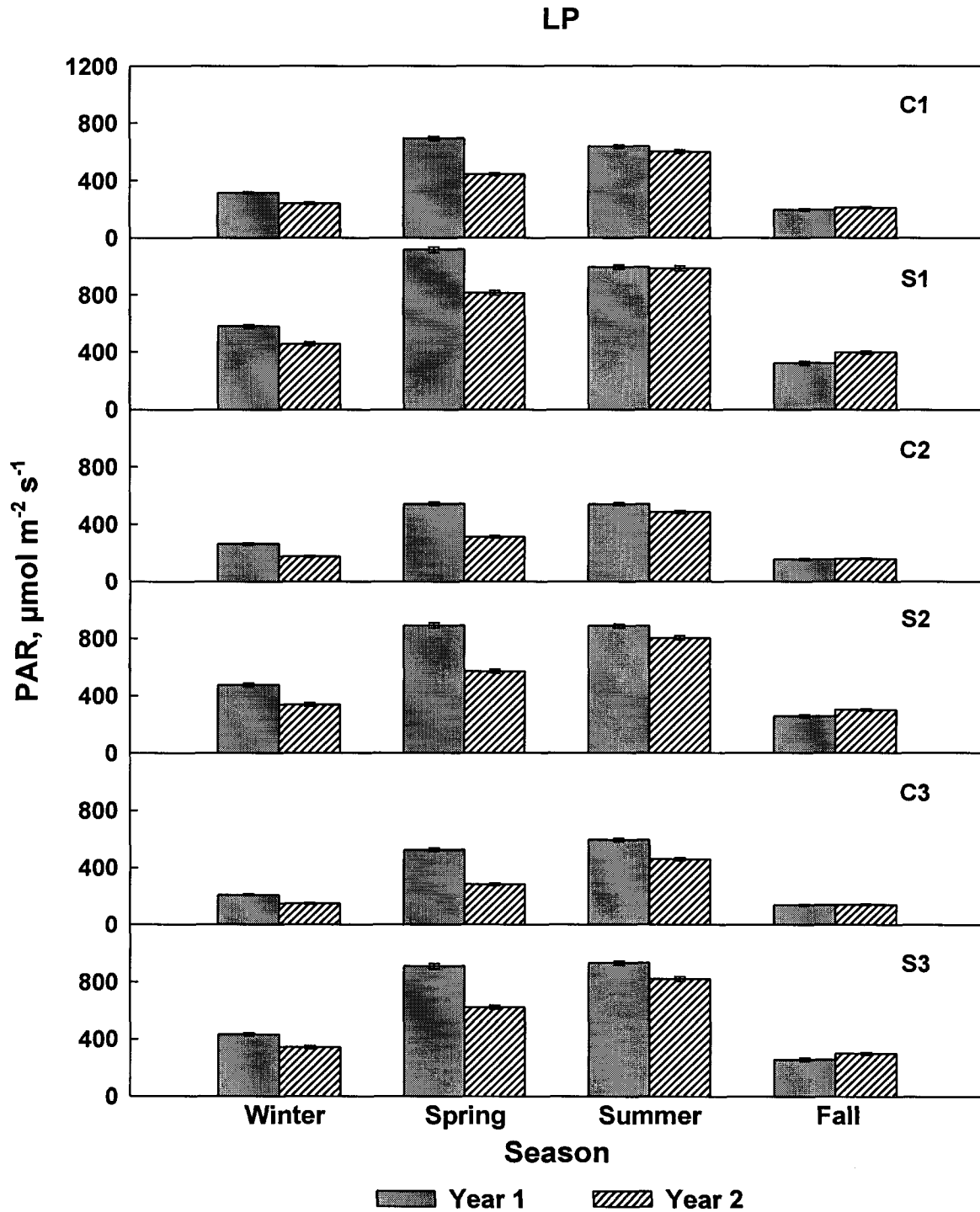


Fig. 2.73 Seasonal means (\pm SE) of PAR measured at LP by the C1, S1, C2, S2, C3, and S3 sensors, between the hours of 1000-1400, within 48 hours after sensor cleaning. Winter = December-February; Spring = March-May; Summer = June-August; Fall = September-November.

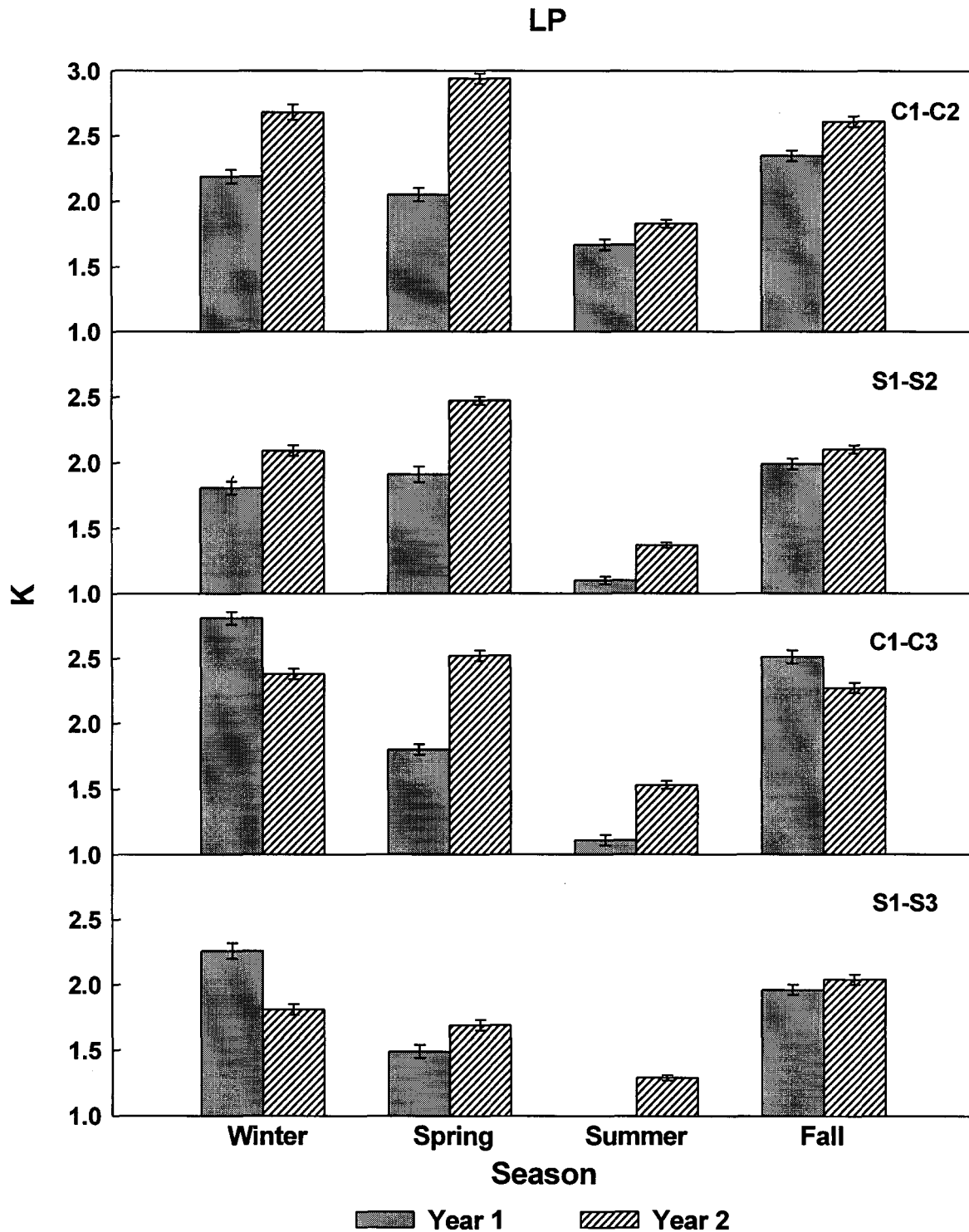


Fig. 2.74 Seasonal means (\pm SE) of K, at LP, between the hours of 1000-1400, within 48 hours after sensor cleaning. K_{C1-C2} is calculated from C1 and C2 sensors, K_{S1-S2} from S1 and S2 sensors, K_{C1-C3} from C1 and C3 sensors, K_{S1-S3} from S1 and S3 sensors. Winter = December-February; Spring = March-May; Summer = June-August; Fall = September-November.

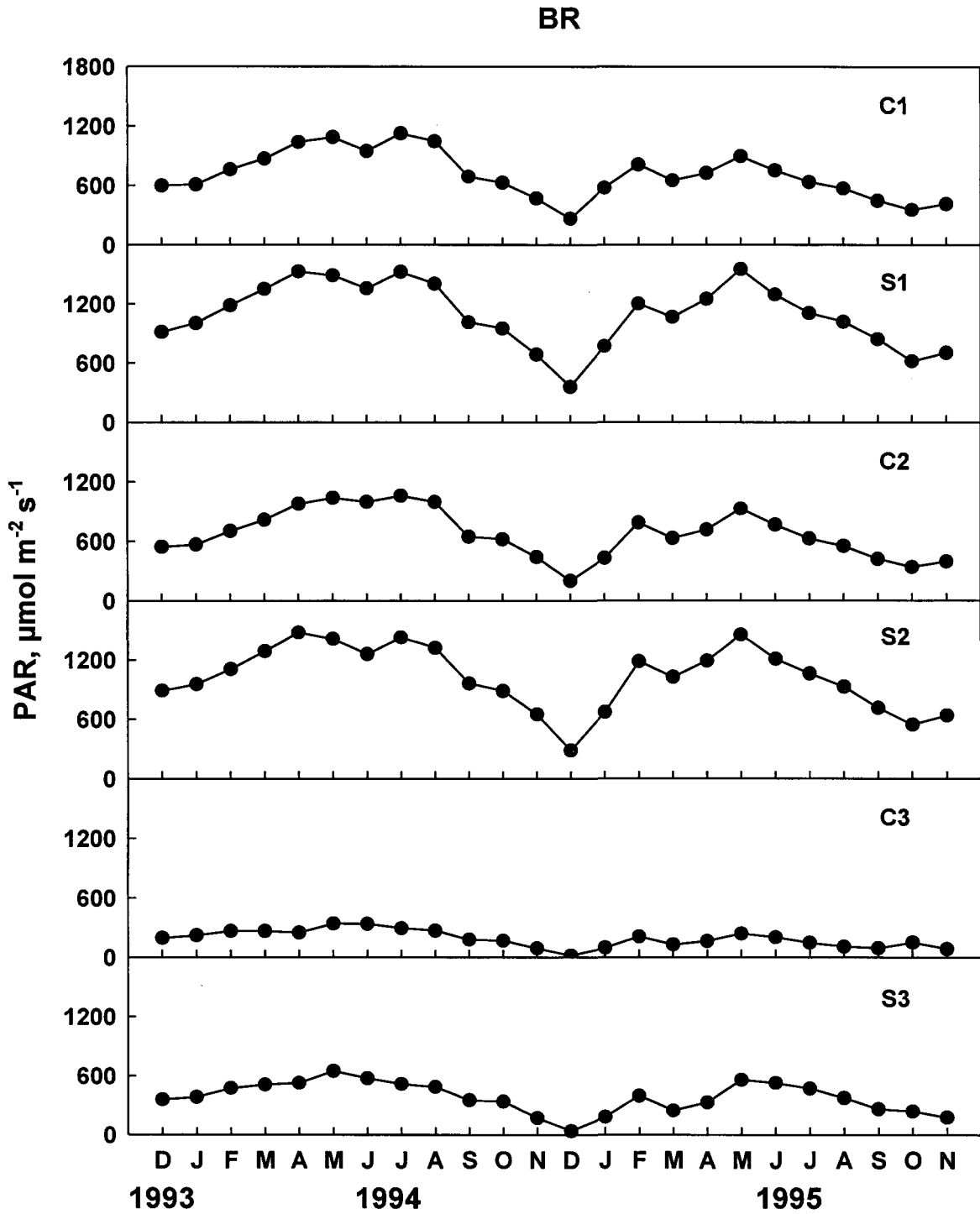


Fig. 2.75 Monthly means (\pm SE) of PAR measured at BR by the C1, S1, C2, S2, C3, and S3 sensors, between the hours of 1000-1400, within 48 hours after sensor cleaning.

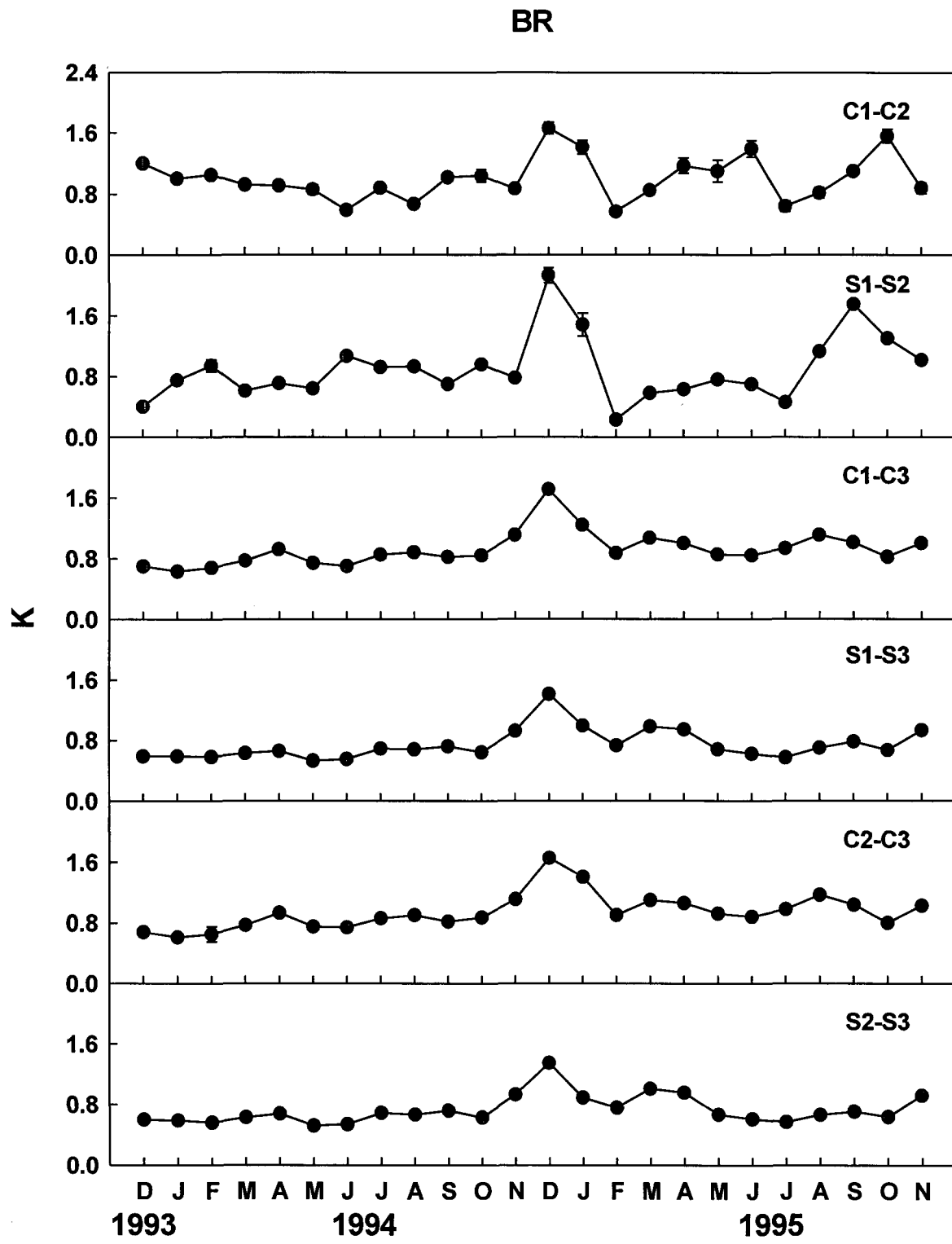


Fig. 2.76 Monthly means (\pm SE) of K, at BR, between the hours of 1000-1400, within 48 hours after sensor cleaning. K_{C1-C2} is calculated from C1 and C2 sensors, K_{S1-S2} from S1 and S2 sensors, K_{C1-C3} from C1 and C3 sensors, K_{S1-S3} from S1 and S3 sensors, K_{C2-C3} from C2 and C3 sensors, K_{S2-S3} from S2 and S3 sensors.

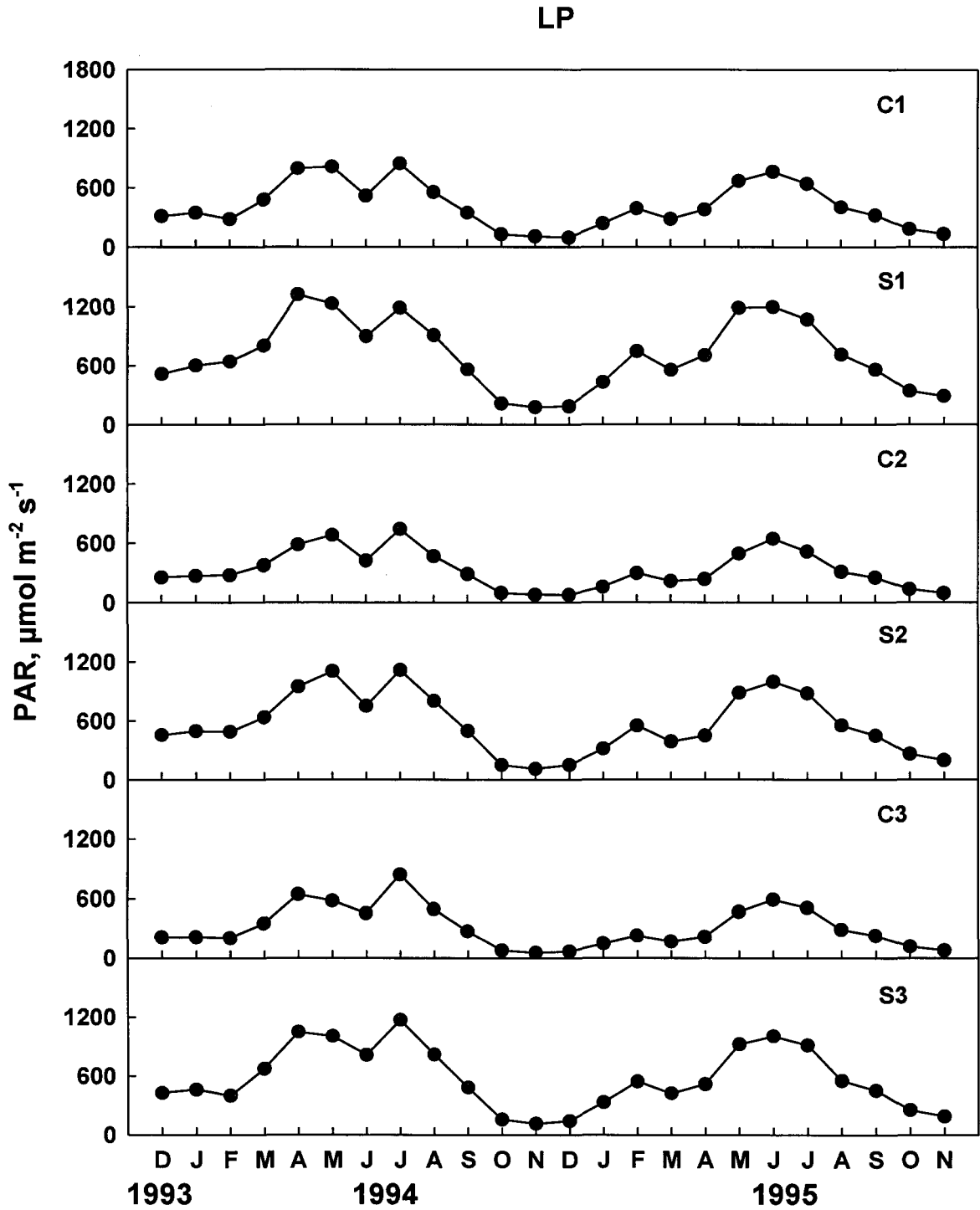


Fig. 2.77 Monthly means (\pm SE) of PAR measured at LP by the C1, S1, C2, S2, C3, and S3 sensors, between the hours of 1000-1400, within 48 hours after sensor cleaning.

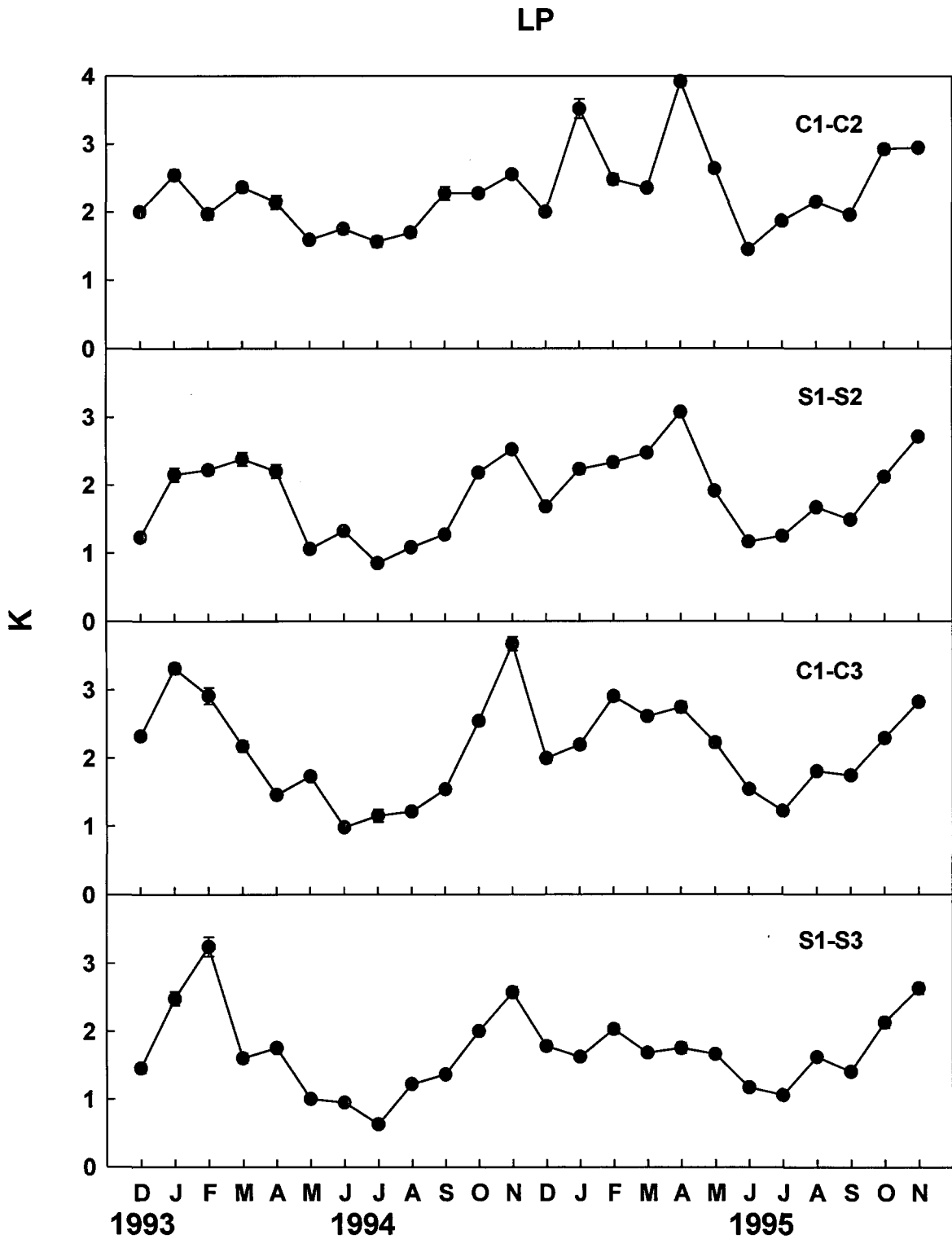


Fig. 2.78 Monthly means (\pm SE) of K, at LP, between the hours of 1000-1400, within 48 hours after sensor cleaning. K_{C1-C2} is calculated from C1 and C2 sensors, K_{S1-S2} from S1 and S2 sensors, K_{C1-C3} from C1 and C3 sensors, K_{S1-S3} from S1 and S3 sensors.

Chapter 3: Water Quality

3.1 Introduction

Although underwater light is the primary factor that determines the productivity and survival of seagrass, light is not something that managers can directly manage. Ambient light levels are strongly influenced by various water quality parameters. Loss of seagrass in Indian River Lagoon has largely been attributed to adverse water quality conditions (i.e., increased nutrients and suspended solids) and the resulting reduction in water clarity. While there is evidence that seagrass is declining because of decreased water quality, there has been no attempt to scientifically identify the processes which are causing these declines (IRLNEP 1993). What is needed is a better understanding of how differences in underwater light are related to differences in water quality parameters which can be managed or regulated; partitioning of factors associated with PAR reduction could be used to direct management actions. Ultimately, protection of seagrass habitat will need to be translated into water quality "standards" or targets.

The purpose of the water quality sampling conducted in this study was to determine site-specific differences in water quality at various sites in IRL and to relate those water quality parameters to underwater light attenuation. This chapter focuses on presenting water quality data from the various stations and the interrelationships among various water quality parameters. Relationships between water quality and underwater light attenuation are presented in Chapter 7.

3.2 Task Description

Task 3: To measure major water quality parameters at selected stations in Indian River Lagoon weekly for 2 years.

3.3 Methods

Water quality sampling was conducted near the mid-bed PAR sensors at the IRL stations (see Chapter 1 for station locations) weekly for 2 years. Temperature and salinity were measured at mid-depth with a HYDROLAB Surveyor II or a Horiba U-10 Water Quality Checker calibrated prior to use. Integrated water column samples were taken for color; turbidity; total, inorganic, and organic suspended solids; total and dissolved nitrogen; total and dissolved phosphorus; total silicate; and chlorophyll *a*.

Integrated water samples were collected with a 5-cm (diameter) PVC pipe that was placed vertically through the water column, but kept 10 cm off bottom to avoid disturbing sediments and contaminating the water column sample. The emergent end of the PVC pipe was stoppered and water was collected into a clean bucket by releasing the stopper. Sub-samples from the bucket were poured into acid-washed plastic bottles and transported to the lab on ice. In addition, at the Sebastian stations, SN and SS, 2 additional samples (surface = top 10 cm, and bottom = 10 cm off bottom) were taken as well as the integrated samples because of the occasional existence of a stratified water column at those stations.

Upon return to the lab, color and turbidity measurements were made. Color (as Pt units, mg/L) was measured with the method of Cuthbert and del Giorgio (1992). Turbidity (as NTU) was measured with a Hach DRT-15C turbidimeter. Standard methods were employed for the other water quality analyses (as mg/L, except chlorophyll *a*, which was expressed as $\mu\text{g/L}$): total, inorganic (fixed), and organic (volatile) suspended solids (APHA 1985); total (= particulate and dissolved) and dissolved (= organic and inorganic) nitrogen; total and dissolved phosphorus; total silicate (EPA 1979); and chlorophyll *a* (Jeffrey and Humphrey 1975). Nutrient samples were frozen, with dissolved nutrient samples first filtered through Gelman Type A/E glass fiber filters. Chlorophyll *a* samples were frozen on their filters. Suspended solids were dried on filters and stored in a desiccator. All nutrient, chlorophyll *a*, and suspended solids samples were analyzed by the University of Florida's Department of Fisheries and Aquatic Sciences.

Data are presented as weekly measurements of each water quality parameter for each station as well as station means \pm standard error (SE). Statistical analyses were performed with SAS statistical software (SAS Institute 1988). Statistical significance among stations was tested with analysis of variance (ANOVA). When ANOVA indicated the existence of significant differences, the Tukey-Kramer test (T-K) determined which means were significantly different ($P \leq 0.05$). A multi-parameter cluster analysis of stations was performed to determine the degree of similarity among stations based on the annual means for the various water quality parameters. In the cluster analysis, all possible pairs of stations were compared by the Euclidean distance coefficient. Correlation and linear regression analyses (Sokal and Rohlf 1981) determined the relationships of water quality parameters for the integrated samples at each station and for the complete data set (all stations combined). Stepwise multiple regression (Sokal and Rohlf 1981) determined the relationship of chlorophyll *a* (dependent variable) with nutrients (total nitrogen, total phosphorus, and total silicate). The minimal level of statistical significance for all regression analyses was $P \leq 0.05$.

Data sets for the five stations sampled during both years of the study were analyzed to determine the effect of sampling frequency on the accuracy and precision of means of the various water quality parameters. Accuracy is "the closeness of a

measured or computed value to its true value”; precision is “the closeness of repeated measurements of the same quantity” (Sokal and Rohlf 1981). Five hypothetical sampling scenarios, with frequencies ranging from weekly to quarterly sampling (Table 3.1), were compared. “True values” were assumed to be the means of each parameter measured during weekly sampling (i.e., the most intensive effort). Means and standard errors for each parameter were calculated for each sampling scenario, for each station. Estimates were made of the sampling frequency needed to obtain means within 10% and 20% of the “true” values (i.e., estimates of the sampling effort required for certain degrees of “accuracy”). In addition, for each sampling scenario, station means for each water quality parameter were compared with ANOVA and T-K tests.

3.4 Results

The presentation of results begins with patterns of each water quality parameter for the weekly integrated samples, including graphic presentation of each parameter through time at each station and comparison of station means (Section 3.4.1). Next, the results of the stratified weekly sampling conducted at the Sebastian stations are presented (Section 3.4.2). The cluster analysis indicates the relationship of the stations based on their water quality data (Section 3.4.3). Correlation analysis (Section 3.4.4) and regression analyses (Section 3.4.5) define the relationship of the water quality parameters, both for the complete data set (all stations) and for each station. Lastly, the analysis of the effects of sampling frequency on estimates of water quality parameters are presented (Section 3.4.6) with the purpose of making recommendations on the frequency of future water quality sampling in IRL.

3.4.1 Water Quality Measurements: Weekly Integrated Samples

Temperature

Temperature had a predictable seasonal pattern of December minima and July-August maxima (Fig. 3.1). Within IRL, there was a north-south temperature gradient (Fig. 3.2). BR, the northernmost station, was significantly cooler (by 1.7-2.4°C; T-K: $P < 0.05$) than the five southernmost stations, with MB intermediate. There were no significant interannual differences in temperatures at any of the five stations sampled in both years of the study (Fig. 3.3).

Salinity

Unlike temperature, there was considerable variability in salinity patterns among stations (Fig. 3.4) and significant interannual variability at some stations (Fig.

3.3). BR was characterized (Fig. 3.4) by a relatively stable salinity throughout the first year of the study (90% of the salinity values were in the range of 26 to 32 ppt). A pronounced decline was associated with the passage of Tropical Storm Gordon in November 1994. Salinity levels after that event never returned to the levels previously observed. Salinities during 1995 had little week-to-week variability and remained low (90% of the salinity values were in the range of 13.5 to 19.8 ppt).

The seasonal pattern in salinity at MB was similar to that at BR, but the decline began earlier (Fig. 3.4). The salinity pattern at TC, sampled only in Year 2, was similar to that of MB in the dry season, but salinity declined much more in the wet season. Variability in salinity was greatest at SN and SS because of their proximity to large inputs of freshwater from the Sebastian River as well as inputs of high-salinity water through Sebastian Inlet. The lowest salinity of the study (1.8 ppt) was recorded at SN (October 1995). Interannual variability in salinity at SN and SS was not significant (Fig. 3.3). The seasonal patterns at VB and LP (Fig. 3.4) were similar to each other and intermediate between the other stations: salinity was relatively high during most of the year, but declined substantially from August to October (Year 2) or November (Year 1). The highest salinity of the study (37 ppt) was recorded at LP (May 1995). Acutely low salinities were evident at the three stations (TC, SN, and SS) closest to point sources of freshwater inputs; there were 22 salinity measurements below 10 ppt during the study: 9 each at SS and TC, and 4 at SN.

In Year 1, mean salinity (Fig. 3.3) was significantly higher (T-K: $P < 0.05$) at the two endpoints (BR and LP) than at the other four stations. In Year 2, while salinity remained high at LP, salinity at BR was significantly depressed (ANOVA: $P = 0.0001$; a mean of 17.3 ppt in Year 2 vs. 28.6 ppt in Year 1, a 40% decline). The only other significant interannual difference occurred at MB (ANOVA: $P = 0.0001$; a mean of 15.6 ppt in Year 2 vs. 23.4 ppt in Year 1, a 33% decline). In Year 2, salinities at BR, MB, and TC (17.3, 15.6, and 15.1 ppt, respectively) were statistically equivalent (T-K: $P > 0.05$).

Color

There was considerable variability in the patterns of color among stations (Fig. 3.5). At BR and MB, color was relatively stable and low, although higher in Year 2 than in Year 1. At TC, color was elevated during the wet season. Variability in color was greatest at SN and SS, with large increases during the wet season indicative of strong freshwater influence from the nearby Sebastian River. Color was generally low at VB and LP, with increased levels observed during the later part of the wet season.

The differences in color among stations were significant (T-K: $P < 0.05$), with BR, MB, and LP significantly lower than TC, SN, and SS, and VB intermediate between the other two groupings of stations (Fig. 3.6).

Photosynthetically Active Radiation, Water Quality, and Submerged Aquatic Vegetation in IRL

The only significant interannual differences (ANOVA: $P = 0.0001$) in color were at the two northernmost stations, BR and MB (Fig. 3.7); color (Pt units) increased from 8.71 to 11.71 mg/L at BR (a 34% increase) and from 10.24 to 14.25 mg/L at MB (a 39% increase) between Years 1 and 2.

Turbidity

In contrast to color which had a seasonal pattern associated with wet vs. dry season, turbidity (Fig. 3.8) was elevated during periods of high winds: winter cold fronts (January through March) and Tropical Storm Gordon in November 1994; minor peaks were associated with localized wind events. However, the passage of Hurricane Erin (August 1995) did not result in substantial increases in turbidity as was the case with Gordon the previous year.

Overall, BR and MB were significantly less turbid (T-K: $P < 0.05$) than TC, SN, VB, and LP; SS was intermediate between the two groupings of stations (Fig. 3.9).

Interannual variability (Fig. 3.10) was not significant, except at BR, where turbidity was significantly higher (ANOVA: $P = 0.001$) in Year 2 (mean = 4.3 NTU) than in Year 1 (mean = 3.1 NTU), an increase of 39%.

Suspended Solids

The seasonal patterns of suspended solids (Fig. 3.11) were similar to those of turbidity, with most of the suspended solids being inorganic. As with other parameters, the variability in suspended solids at BR was less than that at the other stations.

Mean total suspended solids (TSS) were significantly greater (T-K: $P < 0.05$) at LP than at BR, MB, TC, and SS; SN and VB were intermediate between the two groupings of stations (Fig. 3.9). Mean inorganic suspended solids (ISS) were significantly greater (T-K: $P < 0.05$) at SN, VB, and LP than at BR, MB, and TC; SS was intermediate between the two groupings of stations. Mean organic suspended solids (OSS) were significantly greater (T-K: $P < 0.05$) at TC and LP than at the other 5 stations.

The interannual variability in TSS (ANOVA: $P = 0.003$) was significant at BR (Fig. 3.10), increasing from 49.1 to 56.6 mg/L from Year 1 to Year 2, due to the significant increase (ANOVA: $P = 0.0001$) in OSS from 16.0 to 25.2 mg/L. The only other significant interannual difference for suspended solids was for ISS at MB, where ISS declined from 40.6 to 33.7 mg/L (ANOVA: $P = 0.02$).

Nitrogen

Both total (TN) and total dissolved nitrogen (TDN) had relatively limited seasonality (Fig. 3.12), with more variability during the wet season.

The means of both forms of nitrogen were highest at BR, intermediate at MB and TC, and lowest at the four remaining stations (Fig. 3.13). In all cases, most of the total nitrogen was in the dissolved form.

Declines in both forms of nitrogen in Year 2 were significant (ANOVA; $P < 0.05$) at BR, MB, and SN, as was the decline in TN at SS (Fig. 3.14).

Phosphorus

Seasonal and spatial differences were more evident for phosphorus than for nitrogen (Fig. 3.15). At BR, the northernmost station, phosphorus concentrations were low throughout the year, with highest levels present during the wet season. At the remaining stations, phosphorus levels were higher than at BR, with periods of higher concentrations primarily in the wet season, but with some significant pulses in winter.

VB had significantly higher, and BR had significantly lower, mean phosphorus levels than the other stations (Fig. 3.13). About half of the total phosphorus was in the dissolved form.

The only significant interannual variation in either form of phosphorus was for total phosphorus (TP) at BR and total dissolved phosphorus (TDP) at LP (Fig. 3.14); in both cases, phosphorus concentration was higher in Year 2.

Silicate

The seasonal and spatial patterns of total silicate (Fig. 3.16) were different than nitrogen and phosphorus. At the most northern station, BR, silicate was low throughout Year 1 and had no evidence of seasonality, but was more elevated in Year 2. Silicate concentration was higher at MB than at BR and much more so during the wet season. Silicate patterns were similar at TC to MB during the wet season, but more elevated in the dry season. At SN and SS, silicate concentrations were considerably variable, but elevated, during the year. The patterns at VB and LP were intermediate among the other stations with higher levels generally present during late summer and fall (September-November).

Overall, the mean silicate concentration was lowest at BR and LP, highest at TC, and intermediate at the other four stations (Fig. 3.13).

The only significant interannual variability in silicate was at BR (2.49 mg/L in Year 2 vs. 0.84 mg/L in Year 1, nearly a three-fold increase; ANOVA: $P = 0.0001$) and LP (3.50 mg/L in Year 2 vs. 2.19 mg/L in Year 1, a 59% increase; ANOVA: $P = 0.001$).

Chlorophyll *a*

There were considerable temporal and spatial variations in chlorophyll *a* levels (Fig. 3.17). Chlorophyll *a* was typically low at BR, but a phytoplankton bloom in December 1994 had the highest chlorophyll *a* values (about 80 $\mu\text{g/L}$) for any station during the study. Seasonal patterns were more variable at the other stations, with a tendency to higher concentrations during the wet season.

Mean chlorophyll *a* values (Fig. 3.18) were lower for BR, SS, and MB than for VB, TC, and LP (T-K: $P < 0.05$). Among stations that were sampled both years, significant station differences occurred in Year 1 (ANOVA: $P = 0.0001$), but there were no significant station differences (ANOVA: $P > 0.05$) in Year 2 (Fig. 3.19).

The only significant interannual variability in chlorophyll *a* (Fig. 3.19) was found at BR, where chlorophyll *a* concentration increased 2.4 fold (from 6.3 to 15.2 $\mu\text{g/L}$; ANOVA: $P = 0.001$), and at MB, where chlorophyll *a* concentration increased by 45% (from 12.6 to 18.3 $\mu\text{g/L}$; ANOVA: $P = 0.01$).

3.4.2 Water Quality Measurements: Stratified Sampling

Stratified water column sampling at the Sebastian stations indicated occasional, sharp differences in water quality between surface and bottom layers (Figs. 3.20-3.25). These differences were usually related to a sharp halocline that occurred primarily in the wet season (Fig. 3.20) because of freshwater inputs from the nearby Sebastian River and high-salinity inputs through Sebastian Inlet. There was seldom a thermal gradient with depth. Overall, the surface water was fresher, more colored than the bottom layer (Fig. 3.26). The bottom layer tended to have higher turbidity and higher levels of suspended solids, primarily due to an increase in inorganic solids (Fig. 3.27). There was a tendency for lower TN and silicate in the bottom layer, but very little difference in TP (Fig. 3.28). Chlorophyll *a* tended to be higher in the bottom layer than in the surface layer (Fig. 3.29).

Because of the large amount of variability throughout the year, there were no significant differences (ANOVA: $P > 0.05$; all data were used) between surface, bottom, and integrated means for the various water quality parameters at either station. Thus, integrated water column samples provided good estimates of water quality parameters even at locations where water column stratification occurred.

When the data from both stations were pooled, significant differences (ANOVA: $P < 0.05$) between surface and bottom strata were found for several parameters: salinity, turbidity, TSS, ISS, and chlorophyll *a* were all lower, and color was higher, at the surface.

3.4.3 Cluster Analysis of Stations

The overall relationships of the stations were determined by cluster analysis performed on means for the various water quality parameters (Fig. 3.30). This analysis demonstrated that the Sebastian stations were most similar, with TC and MB subsequently joining the Sebastian cluster; VB and LP formed a separate initial cluster which then combined with the MB-TC-SN-SS cluster; the last station to be added (i.e., the most dissimilar station) was BR. This clustering was consistent with the relative geographical location of the stations.

Separate cluster analyses for Year 1 (Fig. 3.31) and Year 2 (Fig. 3.32) yielded similar results to the analysis of the two-year data set. The minor differences were: (1) in Year 1 (Fig. 3.31), LP did not form an initial cluster with VB, and (2) in Year 2 (Fig. 3.32), MB and TC formed a distinct cluster before joining with SN-SS-LP.

3.4.4 Correlation Matrix of Water Quality Parameters

Correlation analyses for the entire data set revealed a high frequency of correlation among the various water quality parameters (all stations; Table 3.2). For the 13 water quality parameters under consideration, there was a significant ($P < 0.05$) correlation among 62 of the 78 possible combinations of factors. Because of the large number of samples in the study, many of these significant relationships had a low correlation coefficient (e.g., salinity and temperature, $r = 0.095$, $P = 0.02$) and will not be considered in detail because they contribute little to understanding this complex water quality data set. However, 27 combinations of the water quality parameters had a correlation coefficient above 0.3 and a $P \leq 0.0001$; these correlations will be examined further in this section and will be the basis for the station-specific presentation in the following section.

Highly significant correlations included a number of obvious relationships in which one factor was a subset of another (e.g., TSS, ISS, and OSS; TN and TDN; TP and TDP). Otherwise, the highest correlations were found between turbidity and TSS ($r = 0.769$), ISS ($r = 0.739$), and OSS ($r = 0.675$). Salinity was strongly negatively correlated with color ($r = -0.582$), TN ($r = -0.341$), TDP ($r = -0.318$), silicate ($r = -0.495$), and chlorophyll *a* ($r = -0.334$). In contrast, both TSS ($r = 0.344$) and ISS ($r = 0.377$) were strongly positively related to salinity. In addition to suspended solids, turbidity

was strongly correlated to both TP ($r = 0.500$) and chlorophyll *a* ($r = 0.511$). In addition to salinity, color was strongly, but positively, correlated to TP ($r = 0.408$), TDP ($r = 0.510$), and silicate (0.376). In addition to color and turbidity, TP was highly correlated with TSS ($r = 0.311$) and OSS ($r = 0.365$). OSS was also strongly correlated ($r = 0.357$, $P = 0.0001$) with chlorophyll *a*.

In regards to correlations among the three nutrients measured: the correlation between nitrogen and phosphorus was not significant for either total or dissolved forms. There were significant correlations between silicate and both TP ($r = 0.357$, $P = 0.0001$) and TDP ($r = 0.410$, $P = 0.0001$). The correlations between TN or TDN and silicate were not significant. Chlorophyll *a* was strongly correlated with phosphorus ($r = 0.524$ for TP, 0.242 for TDP; $P = 0.0001$) and silicate ($r = 0.220$, $P = 0.0001$), but weakly correlated with TN ($r = 0.080$, $P = 0.05$) and not significantly correlated to TDN.

3.4.5 Regression Analyses of Water Quality Parameters

Linear regressions of the relationships between various combinations of water quality parameters were conducted on the complete water quality data set (all stations) as well as on a station-specific basis. Linear regression models of the more significant relationships are presented graphically (Figs. 3.33-3.58). The order of presentation is: relationships of salinity with water color, nutrients, and chlorophyll *a*; relationships of turbidity with suspended solids and chlorophyll *a*; and relationships of chlorophyll *a* with nutrients.

Salinity and Water Color

The relationship between water color and salinity was highly significant for the complete data set (all stations; Fig. 3.33). This relationship was significant at all stations (Fig. 3.34), but the slopes and R^2 values for BR and MB were less than those at VB and LP and much less than those at TC, SN, and SS.

Salinity and Nutrients

The regression models for both total and dissolved nitrogen vs. salinity were highly significant for the complete data set (all stations; Fig. 3.35), but the regressions had relatively low R^2 values (0.116 and 0.088 for TN and TDN, respectively). There was no significant relationship at BR, MB, and TC for TN (Fig. 3.36) and at MB and TC for TDN (Fig. 3.37). The strongest regression models (highest R^2 values) for TN were at SS, SN, and LP, all of which had similar slopes (Fig. 3.36). The strongest regression models for TDN were at SS, VB, and SN, all of which had similar slopes (Fig. 3.37).

Regression models for TP and TDP vs. salinity for the complete data set (all stations; Fig. 3.38) were highly significant ($p = 0.0001$), but they had relatively low R^2 values (0.066 and 0.101 for TP and TDP, respectively). There was no significant relationship at MB and TC with TP (Fig. 3.39) or TDP (Fig. 3.40). The strongest regression models (highest R^2 values) with TP were at SS, VB, and LP, all of which had similar slopes (Fig. 3.39). The strongest regression models with TDP were at SS, LP, VB, and SN, all of which had similar slopes (Fig. 3.40).

The regression of silicate vs. salinity was highly significant for the complete data set (all stations; Fig. 3.41) and for each station except TC (Fig. 3.42). The strongest (highest R^2 values) models were at VB, LP, and SS. The slope of the silicate-salinity relationship was variable among stations, being lowest at BR and highest at VB.

Salinity and Chlorophyll *a*

The regression model of chlorophyll *a* vs. salinity was significant for the complete data set (all stations, Fig. 3.43), but only accounted for 11% of the variance. While this relationship was significant at each station (Fig. 3.44), R^2 values were between 0.103 to 0.210 for all stations, except LP ($R^2 = 0.331$). The slope of the chlorophyll *a*-salinity regression was greater at VB and LP than at the other stations.

Turbidity and Suspended Solids

The regression models for turbidity vs. TSS, ISS, and OSS were highly significant ($p = 0.0001$) for the complete data set (all stations; Fig. 3.45), as well as for each station (Figs. 3.46-3.48), with the exception of turbidity vs. ISS at BR where the relationship was not significant. The strongest regression model ($R^2 = 0.808$) and highest slope for turbidity vs. TSS were at VB; the weakest model ($R^2 = 0.169$) and smallest slope were at BR (Fig. 3.46). Regressions for the other stations had R^2 values in the range of 0.478 to 0.649 and similar slopes. The slope of turbidity vs. OSS (Fig. 3.48) was always higher than that of turbidity vs. ISS (Fig. 3.47).

Turbidity and Chlorophyll *a*

The regression model for turbidity vs. chlorophyll *a* was highly significant for the complete data set (all stations; Fig. 3.49), as well as for the individual stations (Fig. 3.50). Among the stations, the strongest regression model ($R^2 = 0.584$) was at BR, followed by TC, SN, and SS. The slopes for the turbidity vs. chlorophyll *a* models were greatest at TC, SN, and SS, and least at BR.

Chlorophyll *a* and Nutrients

The regression model of chlorophyll *a* with TN for the complete data set (all stations; Fig. 3.51) was significant ($P = 0.05$), but the model had a very low R^2 (0.006). Among individual stations (Fig. 3.52), this relationship was significant at SN, SS, LP; the strongest regression model ($R^2 = 0.251$) was at SN. The slope of these significant relationships was variable among stations.

The regression model of chlorophyll *a* with TDN for the complete data set (all stations; Fig. 3.51) was not significant. However, there was a significant relationship between chlorophyll *a* and TDN at three stations (SN, SS, LP; Fig. 3.53), but the amount of variance explained by these models was low (R^2 ranged between 0.067 and 0.145). Among the three stations where chlorophyll *a* was significantly related to both TN and TDN (SN, SS, LP), the models with TN were always stronger (higher R^2 values) than those with TDN (Figs. 3.52-3.53).

In contrast to nitrogen, regression models of chlorophyll *a* with TP or TDP were both significant for the complete data set (all stations; Fig. 3.54); the regression model was stronger (higher R^2 value) for TP than for TDP. The chlorophyll *a*-TP relationship was significant at all stations (Fig. 3.55), although only the LP model had an R^2 value > 0.3 . The chlorophyll *a*-TDP relationship was significant at three stations (BR, MB, LP; Fig. 3.56), but with low R^2 values (range = 0.052 to 0.076).

The regression model of chlorophyll *a* with silicate was highly significant ($P = 0.0001$) for the complete data set (all stations; Fig. 3.57), but the R^2 value was low (0.048). The chlorophyll *a*-silicate relationship was significant at all stations but BR and TC (Fig. 3.58); the amount of variance explained by the models was relatively low ($R^2 = 0.040$ to 0.130).

Step-wise multiple regression analysis of chlorophyll *a* with TP, TN, and total silicate indicated that, for the complete data set (all stations, Table 3.3), TP was the first significant factor to enter into the model, followed by TN. For the individual stations, TP was usually the first and only factor to enter into the model (Table 3.3). At SN, the first significant factor to enter into the model was TN, followed by TP. At TC, the first significant factor to enter into the model was TP, followed by silicate.

3.4.6 Effects of Sampling Frequency on Estimates of Water Quality Parameters

Both precision and accuracy of the means of the various water quality parameters improved as sampling frequency increased from quarterly to weekly sampling (Figs. 3.59-3.71). However, the degree to which a given sampling frequency affected precision and accuracy was highly variable among the various water quality

parameters (Table 3.4). Quarterly sampling provided reasonably accurate estimates of parameters such as temperature and salinity for all stations. For other parameters, the effect of sampling frequency was site-specific. For example, accurate estimates of water color could be made with quarterly sampling at three stations (BR, MB, and LP), but more frequent sampling would be required to achieve the same degree of accuracy at SN and SS, stations where there were both high levels and high variability in water color. For turbidity, quarterly sampling provided reasonable accuracy at BR; much more intensive sampling would be required at the remaining stations (every 2 months at LP, every 2 weeks at MB, SN, SS) to achieve similar accuracy. For nutrients, quarterly measurements were much more likely to give accurate estimates at some stations than at others, and more accurately for nitrogen than for phosphorus or silicate. The effect of sampling frequency on estimates of chlorophyll *a* was highly variable among stations; quarterly sampling provided $\pm 20\%$ accuracy at three stations (MB, SN, and LP).

While the previous analysis focused on accurate estimates of means, it also showed that increased sampling effort increased precision (i.e., variability around the means was reduced). The effect of improved precision is more important when comparison of sites, rather than estimates of water quality at a single site, is desired. ANOVA and T-K analyses demonstrated that increased precision resulted in an enhanced ability to distinguish water quality conditions among stations (Table 3.5). The extent to which increased sampling frequency resulted in meaningful improvements in statistical differences varied among various water quality parameters. At one extreme was temperature; significant differences among stations in temperature were only discernible when weekly sampling was employed.

In contrast, there were site-specific differences in some water quality parameters (color, TN, TDN, TP) that could be detected with quarterly sampling (Table 3.5). For example, a significant difference among stations for water color was not detectable with quarterly sampling (ANOVA was significant: $P = 0.03$, but T-K test did not detect what the station differences were). Those differences became apparent with sampling every 2 months and more distinct with monthly sampling. For water color, no further improvement in the ability to detect differences among stations occurred at the two most intensive sampling frequencies. No further improvement for TN and TDN occurred after sampling every 2 weeks and monthly, respectively; improvement for TP occurred up to weekly sampling.

Monthly sampling was required to detect initial differences among stations for 6 of the remaining 8 parameters; for the other factors (TDP and silicate) this ability occurred with sampling every 2 months (Table 3.5). Increased resolution among stations was detectable by further increases in sampling effort. For example, salinity differences among these stations were not detectable until sampling frequency was monthly; at that point, only the two most extreme stations were statistically different

from one another (T-K: $P < 0.05$). Sampling every 2 weeks improved the ability to identify significant differences among stations, which were further distinguished by weekly sampling.

3.5 Discussion

Previous measurements of various water quality parameters in IRL are scattered in the scientific literature and in agency reports. Historically, little attention has been paid to the problems of spatial and temporal variability of water quality within the lagoon. Given the presumed importance of water quality to the "health" of IRL, it is surprising that management agencies did not, until recently, place greater emphasis on obtaining synoptic water quality data for the lagoon. Previous water quality data from IRL have been synthesized by Windsor and Steward (1987) who, as part of the IRL Reconnaissance Report, reported primarily on the uncoordinated water quality sampling efforts conducted up to that time. In 1987, a lagoon-wide water quality monitoring network was initiated to conduct water quality sampling at stations throughout the lagoon (Steward et al. 1994). Water quality is currently being monitored monthly by St. Johns River Water Management District (SJRWMD) and quarterly by South Florida Water Management District (SFWMD). Data from that monitoring program have been analyzed by Woodward-Clyde (1994b). The present study is the first one to measure water quality parameters on a weekly basis at multiple stations from different portions of the lagoon.

The water quality data indicated a number of significant environmental gradients within IRL. Water quality patterns were consistent with the north-south order of stations, as most readily visualized by the dendrogram derived from the cluster analysis of stations. BR, the northernmost station, was usually at one end of the range for most water quality parameters: BR had the lowest mean temperature, color, turbidity, suspended solids, phosphorus, silicate, and chlorophyll *a*, and the highest nitrogen level. LP, the southernmost station, was usually on the other end of the water quality spectrum: LP had the highest salinity, turbidity, and suspended solids, and the lowest nitrogen level. TC had the lowest salinity, highest water color, and highest silicate concentration. The Sebastian stations (SN, SS) were most noteworthy in regards to their rapidly fluctuating salinities and elevated water color levels.

While a statistically significant north-south temperature differential was identified, it was relatively minor compared to the much larger magnitude of seasonal changes in temperature. The latter are likely to be quite important in determining seasonal changes in seagrass productivity (see Chapter 6), but are not likely to explain major differences in seagrass productivity among stations. However, temperature could be important in delineating the northern distribution of species in what is largely a tropical assemblage of seagrasses. Among the species present at these stations (see

Chapter 4), the most likely one to be impacted by temperature is *Thalassia testudinum* whose northern distribution along the Florida coast is near Sebastian Inlet in IRL. This northern limit could be caused by low temperature during the winter months; however, neither this study nor others have been designed to specifically address that hypothesis.

Salinity is likely to be a major factor for seagrass distribution and abundance in IRL. The impacts of freshwater discharges into the lagoon are not likely to be limited to the direct negative impacts of low salinity on seagrass productivity and survival. Rather, other environmental stresses are likely to co-vary with increased freshwater influences and primarily act through the mechanism of reduced light availability to seagrasses. Previous work has shown that the main contributors to the light attenuation in estuarine waters are dissolved yellow matter (i.e., color), phytoplankton chlorophyll *a*, and suspended solids (often operationally measured as turbidity), as well as water itself (Gallegos 1994). In this study, salinity was strongly and negatively correlated with color, TN, TDN, TP, TDP, silicate, and chlorophyll *a*, with the strongest relationship found with color. Woodward-Clyde (1994b) noted that color data from IRL are sparse; the current study significantly adds to what is known about color in IRL and directly relates increased color to reduced salinity associated with freshwater inputs.

Elevated nutrient levels associated with low salinity suggest that freshwater discharges into the lagoon are a significant source of nutrients to the system. A relatively rapid response to elevated nutrients is likely to be enhanced phytoplankton biomass, for which chlorophyll *a* is a proxy as well as an important attenuator of PAR. In contrast, salinity was positively correlated with suspended solids; this finding was probably due, at least in part, to increased suspended solids occurring during the winter (= dry season, higher salinities) as a result of winds associated with cold fronts and the resulting re-suspension of sediments in the lagoon. Segregation of the effects of these various attenuators of light are found in Chapter 7.

There are strong north-south nutrient gradients in IRL. Nitrogen was much higher in the north (BR) and lower in the south (LP), an observation that agrees well with the water quality synthesis of Woodward-Clyde (1994b). The nearly reverse pattern was observed for phosphorus that was lowest in the north (BR) and highest at the penultimate southern station (VB). A third pattern was observed for silicate that was highest at TC, lowest in the north (BR), and intermediate to the south (VB and LP). Higher silicate levels were strong correlated with lower salinity. This observation suggests that the distribution pattern of silicate was associated with freshwater influences.

Another important aspect of the nutrient status of IRL emerging from this study is the relative importance of phosphorus over nitrogen for most of the stations. Nitrogen concentrations were highest at BR, the most northern station, but, even there,

the multiple regression model indicated that phosphorus was the most important nutrient for determining chlorophyll *a* levels. Nitrogen was a secondary, but significant, factor at BR. SN was the only station where nitrogen was the most important parameter in the regression model; phosphorus was a secondary, but significant, factor. Elsewhere, the most important nutrient was phosphorus, with silicate a significant secondary factor at TC. These observations contrast with the perceived importance of nitrogen being the most likely nutrient limiting algal growth in IRL. For example, Hanisak (1990) determined that macroalgae are at least seasonally nitrogen-limited, but that study did not consider phosphorus status and was conducted at LP which did have the lowest nitrogen concentrations of the stations. Woodward-Clyde (1994b) noted that, despite high TP and low TN levels in that part of IRL (consistent with the findings of the present study), caution should be employed before concluding which nutrient limits algal growth in IRL. But nitrogen limitation may not be as widespread throughout the lagoon as previously thought. The relative and absolute roles of nitrogen and phosphorus as factors limiting algal growth in IRL merit additional study. This unresolved issue has major management implications.

The general spatial patterns of water quality among the stations in this study are consistent with those described by Woodward-Clyde (1994b). The major weakness of that previous water quality synthesis was lack of adequate consideration of temporal variability because of the relative low sampling frequency (quarterly) employed by the IRL monitoring network. However, the overall good agreement of spatial water quality patterns in the current study with those synthesized by Woodward-Clyde suggests that relationships among water quality parameters (this chapter) and their relationships with extinction coefficients (Chapter 7) could be broadly applied to the IRL water quality data base and be used in the development and verification of water quality models.

While all of the major potential attenuators of light (suspended solids, color, and water column chlorophyll *a*) interact to some extent, their seasonal patterns and their differences among stations were substantial enough to suggest that their roles in light attenuation could be segregated (this matter will be addressed in Chapter 7). For example, suspended solids were highest during winter, and color patterns were more related to wet vs. dry seasons, while chlorophyll *a* patterns were more seasonally variable than the other two PAR attenuators.

The value of turbidity measurements in SAV assessments has been questioned (Kenworthy and Haurert 1991). Turbidity is scaled on an artificial basis, and turbidity measurements have inherent weaknesses such as lowered values resulting from differential settling rates and presence of true color and inflated values resulting from air bubbles (EPA 1979). In the present study the relationship of turbidity with suspended solids (total, inorganic, or organic) was found to be highly significant.

Thus, turbidity measurements which can be made quickly and effectively in field monitoring efforts may serve as a good proxy of suspended solids in IRL.

The stratified water column sampling at the Sebastian stations indicated that, despite the occasional presence of surface vs. bottom gradients in water quality, integrated water column sampling was a good estimate of water quality parameters. When the data from both stations were pooled, significant differences between surface and bottom strata were found for several parameters: salinity, turbidity, TSS, ISS, and chlorophyll *a* were all lower, and color was higher, at the surface. Given the limited spatial and temporal magnitude of stratification in IRL, stratified water column sampling is not required in lagoon-wide water quality programs; integrated water column sampling should be an adequate characterization of water quality at any site in the lagoon. Stratified water column sampling may be of some value to the development of hydrodynamic and water quality models in "hot spots" of management concerns where pronounced, episodic freshwater inputs flow into IRL, such as near Sebastian River and Taylor Creek.

This study demonstrated the importance of conducting more than one year of water quality sampling to characterize sites in IRL. Variability in climate, primarily precipitation, is likely to lead to considerable interannual variability in some water quality parameters. The most significant interannual difference was the enormous decline in salinity at BR, apparently due to a large input of freshwater into the upper portion of IRL as a result of Tropical Storm Gordon. The lack of recovery to Year 1 salinity levels in Year 2 was probably due to the very long residence time of water in that portion of IRL (estimated to be on the order of one year by Smith 1993). The other factors that were significantly different between years at BR were all correlated with this decline in salinity and were consistent with freshwater impacts observed at other stations during the study. Considerable interannual variability of water quality in IRL has been previously noted (Windsor and Steward 1987, Woodward-Clyde 1994b). Therefore, a long-term water quality monitoring program should be maintained in IRL.

Given the various agencies involved in managing and monitoring IRL, it is important that there be standard methodology and appropriate quality assurance and quality control programs. An important issue is how often should a particular site be monitored to reasonably characterize its water quality? A major consideration is the purpose of the monitoring. An underlying assumption in this study was that water quality is important in that it determines, directly or indirectly, the survival and growth of seagrass in IRL. At the ecosystem level, the appropriate time scale to measure change in seagrass status (and hence, water quality) is probably on the order of years to decades; that is, while there will be occasional "good" and "bad" years for seagrass, long-term trends in seagrass and water quality status are the major items of interest. Similarly, it is important that assessment of how changes in management actions impact seagrass resources or water quality be determined over a period of time after

the action is taken. Development of appropriate models will help in evaluating the efficacy of various management activities.

To obtain meaningful estimates of long-term trends in water quality of IRL, seasonality needs to be considered, i.e., by sampling at appropriate times of the years. For example, twice-a-year (winter and summer) monitoring seems to provide an adequate characterization of SAV (Chapter 4); but how often is water quality sampling required to characterize a site?

Given that water quality parameters can change very rapidly (in a matter of hours to days) and, in most cases, also have overlying patterns of seasonality, year-round sampling would appear to be an absolute requirement, rather than trying to target a single time of the year to be “most representative” or “most important.” The data presented in Section 3.6 can be used in numerous ways to develop “what-if” scenarios. Important considerations on sampling frequency are the water quality parameters and stations of interest, as well as what the intent of the sampling is. Areas such as those represented by BR are usually quite stable in regards to water quality parameters. The major changes in water quality were usually slow, primarily associated with natural, seasonal changes. But BR also experienced the largest interannual change in water quality due to a sudden, large input of freshwater associated with a tropical storm. The impact of this freshwater was still observed one year later because of the limited flushing in that portion of the lagoon. On the other hand, water quality conditions at the Sebastian stations are extremely dynamic, changing and fluctuating much more rapidly due to their proximity to freshwater inputs from the Sebastian River and to high-salinity water through Sebastian Inlet. Other stations have intermediate conditions. Major changes in water quality parameters are due primarily to changes in freshwater inputs. Those changes are associated with natural forces, but accelerated by anthropogenic impacts. Storm events may be the most important triggers of changes in water quality; it would be desirable to incorporate an element of “post-storm” sampling into water quality monitoring programs.

The amount of sampling required to characterize a station is less than what is needed to detect differences among stations. Unless there is bias in making the measurements, precision will lead to accuracy (Sokal and Rohlf 1981). Monthly sampling gives a reasonably precise and accurate measurement of these water quality parameters, at least in the ability to characterize the stations in that analysis and detect differences among them. So, to the extent that these stations represent the continuum found in IRL, monthly water quality sampling is recommended for routine water quality efforts. More intensive sampling would be required for some purposes (e.g., model development and verification, identification of point-source impacts), but, given the considerable added expense, does not appear to be warranted for most monitoring.

The overall goal of this study was to relate water quality with SAV and PAR status. Those analyses are in Chapter 7. But at an initial, more qualitative level, it is clear that SAV within IRL experience a tremendous range of water quality conditions, both in terms of differences among stations and temporal changes at individual stations. The high degree of correlation among water quality parameters suggests that rapid assessment techniques may be possible, particularly with regard to specific questions, such as anthropogenic eutrophication (primarily nutrient enrichments) and light attenuation.

Station-specific differences in water quality, which appear to be driven by gradients associated primarily with the north-south orientation of IRL and location of major freshwater inputs, demonstrate the need for lagoon management on a segment-by-segment basis. However, the more important question is to what extent specific management actions taken will more broadly impact the lagoon. The answer to that question will require the development and verification of a lagoon-wide hydrodynamic model. Most importantly, the model needs to consider the enormous range in water quality patterns found throughout IRL, their complex interactions, and their impacts on SAV, which itself has considerable spatial and temporal variability (see Chapter 4).

3.6 Summary

Water quality sampling was conducted weekly at selected stations in Indian River Lagoon for 2 years. Integrated water column samples were analyzed for: temperature; salinity; color; turbidity; total, inorganic, and organic suspended solids; total and dissolved nitrogen; total and dissolved phosphorus; silicate; and chlorophyll *a*. At the Sebastian stations, 2 additional samples (surface = top 10 cm, bottom = 10 cm off bottom) were taken as well as the integrated samples because of the occasional existence of a stratified water column at those stations. The major results of this study are:

- (1) SAV within IRL experiences a tremendous range of water quality conditions, both in terms of differences among stations and temporal changes at individual stations.
- (2) Within IRL, there is a significant north-south temperature gradient. The most likely impacts of temperature on SAV are seasonal changes in seagrass productivity and determination of northern distribution limits.
- (3) Salinity patterns were variable among stations. At one extreme, BR was characterized by a relatively stable salinity throughout the first year of the study (90% of the salinity values were in the range of 26 to 32 ppt). A pronounced decline was associated with the passage of Tropical Storm Gordon in November

1994. The lack of a recovery to Year 1 salinity levels in Year 2 was due to the long residence time of water in that portion of IRL. Variability in salinity was greatest at SN and SS because of their proximity to large inputs of freshwater from the Sebastian River as well as inputs of high-salinity water through Sebastian Inlet. LP had the highest salinity among the stations.

- (4) Color patterns were variable among stations. At BR and MB, color was relatively stable and low, although higher in Year 2 than in Year 1. At TC, color was elevated during the wet season. Variability in color was greatest at SN and SS. Color was generally low at VB and LP, with increased levels observed during the later part of the wet season. The differences in color among stations were significant, with BR, MB, and LP significantly lower than TC, SN, and SS. Previous data on color from IRL are sparse. This study significantly adds to what is known about color in IRL and directly relates increased water color to reduced salinity associated with freshwater inputs.
- (5) Turbidity was elevated during periods of high winds: winter cold fronts and a tropical storm. BR and MB were significantly less turbid than TC, SN, VB, and LP; SS was intermediate between the two groupings of stations.
- (6) The seasonal patterns of suspended solids were similar to those of turbidity, with most of the suspended solids being inorganic. The variability in suspended solids at BR was less than that of the other stations. TSS was significantly greater at LP than at BR, MB, TC, and SS. ISS was significantly greater at SN, VB, and LP than at BR, MB, and TC. OSS was significantly greater at TC and LP than at the other stations.
- (7) Both total and dissolved nitrogen had limited seasonality with more variability during the wet season. Mean nitrogen concentrations were highest at BR, intermediate at MB and TC, and lowest at the four remaining stations. In all cases, most of the total nitrogen was in the dissolved form.
- (8) Total and dissolved phosphorus levels were low at BR throughout the year, with highest levels during the wet season. At the remaining stations, phosphorus levels were generally higher than at BR, with higher concentrations primarily in the wet season but with some significant pulses in winter. VB had significantly higher, and BR had significantly lower, mean phosphorus levels than the other stations. About half of the total phosphorus was in the dissolved form.
- (9) At BR, silicate was low throughout the year and had no evidence of seasonality, but was more elevated in Year 2. Silicate was higher at MB than at BR, with much higher levels during the wet season. Silicate patterns were similar at TC to MB in the wet season, but were more elevated in the dry season. Silicate levels at

SN and SS were considerably variable, but elevated, during the year. The patterns at VB and LP were intermediate among the other stations with higher levels generally present during late summer and fall (September-November). The mean silicate concentration was lowest at BR and LP, highest at TC, and intermediate at the other four stations. While distribution patterns of silicate and its impacts on diatom communities are likely to be of further scientific interest, the much greater importance of nitrogen and phosphorus, as determined by the current study, suggests that the incorporation of silicate into IRL water quality monitoring programs is not warranted at this time.

- (10) There were considerable temporal and spatial variations in chlorophyll *a* levels. Chlorophyll *a* was typically low at BR, but a phytoplankton bloom in December 1994 had the highest chlorophyll *a* for any station during the study. Seasonal patterns were more variable at the other stations, with a tendency to higher concentrations during the wet season. Mean chlorophyll *a* levels were higher at TC, VB, and LP than at BR, MB, and SS.
- (11) Stratified sampling at the Sebastian stations indicated that, despite the occasional presence of surface vs. bottom gradients in water quality, integrated water column sampling was a good estimate of water quality parameters. When the data from both stations were pooled, significant differences between surface and bottom strata were found for several parameters: salinity, turbidity, TSS, ISS, and chlorophyll *a* were all lower, and color was higher, at the surface. Integrated water column sampling should be an adequate characterization of water quality at any site in the lagoon.
- (12) The water quality data identified a number of significant environmental gradients within IRL. Cluster analysis indicated that the overall water quality relationships among the stations were consistent with their relative geographical location:
 - BR had the lowest mean temperature, color, turbidity, suspended solids, phosphorus, silicate, and chlorophyll *a*, and the highest nitrogen level.
 - LP was usually on the other end of the water quality spectrum: highest salinity, turbidity, and suspended solids, and the lowest nitrogen level.
 - TC had the lowest salinity, highest water color, and highest silicate level.
 - The Sebastian stations were most noteworthy in regards to their rapidly fluctuating salinities and elevated water color.
 - The water quality at MB and VB, consistent with their geographical locations, was intermediate among the other stations.
- (13) Correlation analyses revealed a high frequency of correlation among the various water quality parameters. In particular, salinity was found to have a number of highly significant correlations with other water quality parameters. Salinity was

strongly negatively correlated with color, TN, TDP, silicate, and chlorophyll *a*, but strongly positively correlated to TSS and ISS.

- (14) Linear regression models were used to describe the relationships between various combinations of water quality parameters. These models indicated that relationships among many water quality parameters were highly significant and, in some cases, were station-specific.
- Many of the most significant regression models involved salinity, including regressions with water color, TN, TDN, TP, TDP, silicate, and chlorophyll *a*. Elevated color levels were good indicators of freshwater inputs into IRL. Enhanced nutrient levels associated with low salinity suggest that freshwater discharges into the lagoon are a significant source of nutrients to the system.
 - Regression models for turbidity vs. total, inorganic, and organic suspended solids were highly significant. Turbidity measurements which can be made quickly and effectively in field monitoring efforts may serve as a good proxy of suspended solids in IRL.
- (15) Step-wise multiple regression analysis of chlorophyll *a* with TP, TN, and silicate indicated that, for the complete data set, phosphorus was the first significant factor to enter into the model, followed by nitrogen. For individual stations, phosphorus was usually the first and only factor to enter into the model. At SN, the first significant factor was nitrogen, followed by phosphorus. At TC, the first significant factor was phosphorus, followed by silicate. Nitrogen limitation may not be as widespread throughout the lagoon as previously thought. The relative and absolute roles of nitrogen and phosphorus as factors limiting algal growth in IRL merit additional study.
- (16) The good agreement of overall spatial water quality patterns in the current study with those synthesized by Woodward-Clyde (1994b) suggests that relationships among water quality parameters and their relationships with extinction coefficients could be broadly applied to the IRL water quality data base and be used in development and verification of water quality models.
- (17) This study demonstrated the importance of conducting more than one year of sampling to characterize sites. Interannual variability in climate, primarily precipitation, is likely to lead to considerable interannual variability in some water quality parameters. A long-term water quality monitoring program should be maintained in IRL.
- (18) The frequency of water quality sampling required to characterize a site in IRL is dependent upon location, the water quality parameters involved, and the desired levels of accuracy and precision. The amount of sampling required to characterize a station is less than what is needed to detect differences among

stations. To the extent that these stations represent the continuum found in IRL, monthly water quality sampling is recommended for routine water quality efforts. More intensive efforts would be required for some efforts (e.g., model development and verification, identification of point-source impacts), but the considerable added expense for most monitoring efforts does not appear to be warranted.

- (19) Station-specific differences in water quality, which appear to be driven by gradients associated with the north-south orientation of IRL and freshwater inputs, demonstrate the need for management of the lagoon on a segment by segment basis. Any lagoon-wide water quality or hydrodynamic models need to consider the enormous range in water quality patterns found throughout IRL, their complex interactions, and their impact on SAV. Future monitoring of water quality in IRL should focus on long-term changes associated with potential climatic changes and anthropogenic impacts, particularly those associated with freshwater discharges and the accompanying water quality impacts.

Table 3.1 Scenarios for analysis of water quality sampling frequency. Data in this analysis were obtained from weekly integrated water column samples (November 1993-November 1995). Analyses were restricted to the five stations that were sampled for the entire 2-year period.

Sampling Frequency	Number of Samples/Year	Samples Used from this Study
Weekly	52	All weekly samples
Biweekly	26	Samples from alternate weeks, beginning with week 1
Monthly	12	One sample per month (second weekly sample of each month)
Bimonthly	6	Subset of monthly samples (even-numbered months)
Quarterly	4	Subset of monthly samples (January, April, July, October)

Table 3.2 Correlation matrix of temperature (= Temp), salinity, color, turbidity, total suspended solids (= TSS), inorganic suspended solids (= ISS), organic suspended solids (= OSS), total nitrogen (= TN), total dissolved nitrogen (= TDN), total phosphorus (= TP), total dissolved phosphorus (= TDP), silicate, and chlorophyll a (= Chl). Data were obtained from weekly integrated water samples at all IRL stations (November 1993-November 1995). Values for each combination are Pearson correlation coefficients followed by level of significance.

	Salinity	Color	Turbid	TSS	ISS	OSS	TN	TDN	TP	TDP	Silicate	Chl
Temp	0.095 0.02	0.113 0.004	-0.192 0.0001	-0.094 0.02	-0.168 0.0001	0.099 0.02	-0.086 0.03	-0.114 0.005	0.184 0.0001	0.330 0.0001	0.247 0.0001	-0.009 0.82
Salinity		-0.582 0.0001	-0.059 0.14	0.344 0.0001	0.377 0.0001	0.153 0.002	-0.341 0.0001	-0.296 0.0001	-0.257 0.0001	-0.318 0.0001	-0.495 0.0001	-0.334 0.0001
Color			0.069 0.08	-0.229 0.0001	-0.224 0.0001	-0.139 0.001	0.040 0.32	0.028 0.49	0.408 0.0001	0.510 0.0001	0.376 0.0001	0.173 0.0001
Turbidity				0.769 0.0001	0.739 0.0001	0.675 0.0001	-0.032 0.44	-0.141 0.001	0.500 0.0001	0.005 0.91	0.105 0.01	0.511 0.0001
TSS					0.970 0.0001	0.829 0.0001	-0.181 0.0001	-0.257 0.0001	0.311 0.0001	-0.137 0.001	-0.111 0.010	0.291 0.0001
ISS						0.671 0.0001	-0.188 0.0001	-0.253 0.0001	0.290 0.0001	-0.159 0.0001	-0.131 0.001	0.219 0.0001
OSS							-0.137 0.001	-0.209 0.0001	0.365 0.0001	-0.003 0.94	-0.011 0.78	0.396 0.0001
TN								0.858 0.0001	0.012 0.77	0.073 0.07	0.006 0.87	0.080 0.05
TDN									-0.074 0.07	0.062 0.13	-0.020 0.63	-0.020 0.61
TP										0.770 0.0001	0.357 0.0001	0.524 0.0001
TDP											0.410 0.0001	0.242 0.0001
Silicate												0.220 0.0001

Table 3.3 Stepwise multiple regression models for chlorophyll *a*, as a function of total nitrogen (TN), total phosphorus (TP), and total silicate, for the complete data set (all stations) and for individual stations. Data were from weekly integrated water column samples (November 1993–November 1995). Individual variables needed a $P < 0.15$ to be considered for addition to the model and could be removed or added at subsequent steps. Variables were added one at a time as long as P for the model was < 0.05 .

Station	Step	Factor	Partial R ²	Model R ²	P
All	1	TP	0.267	0.267	0.0001
	2	TN	0.005	0.272	0.03
BR	1	TP	0.213	0.213	0.0001
MB	1	TP	0.232	0.232	0.0001
TC	1	TP	0.140	0.140	0.006
	2	Silicate	0.101	0.241	0.01
SN	1	TN	0.251	0.251	0.0001
	2	TP	0.081	0.332	0.001
SS	1	TP	0.208	0.208	0.0001
VB	1	TP	0.203	0.203	0.001
LP	1	TP	0.300	0.300	0.0001

Regression Equations

All: Chlorophyll *a* = 150.2 TP + 2.7 TN + 3.3

BR: Chlorophyll *a* = 303.1 TP + 1.9

MB: Chlorophyll *a* = 155.6 TP + 4.2

TC: Chlorophyll *a* = 144.7 TP - 1.8 Silicate + 17.6

SN: Chlorophyll *a* = 95.6 TP + 13.2 TN + 1.9

SS: Chlorophyll *a* = 110.5 TP + 6.4

VB: Chlorophyll *a* = 139.6 TP + 8.0

LP: Chlorophyll *a* = 186.9 TP + 2.0

Photosynthetically Active Radiation, Water Quality, and Submerged Aquatic Vegetation in IRL

Table 3.4 Minimal sampling frequency to achieve mean values within the range of $\pm 10\%$ and $\pm 20\%$ of the weekly means for various water quality parameters for all stations which were sampled for the entire 2 years of this study. Data in this analysis were from weekly integrated water column samples; see Table 3.1 for details on how data for each sampling frequency were derived. Codes for sampling frequency are: Q = quarterly, BM = bimonthly, M = monthly, BW = biweekly, W = weekly.

Parameter	Range	BR	MB	SN	SS	LP
Temperature	$\pm 10\%$	Q	Q	Q	Q	Q
	$\pm 20\%$	Q	Q	Q	Q	Q
Salinity	$\pm 10\%$	Q	Q	Q	Q	Q
	$\pm 20\%$	Q	Q	Q	Q	Q
Color	$\pm 10\%$	Q	Q	M	BM	Q
	$\pm 20\%$	Q	Q	BM	Q	Q
Turbidity	$\pm 10\%$	Q	BW	BW	BW	BM
	$\pm 20\%$	Q	BW	BW	BW	BM
TSS	$\pm 10\%$	Q	BW	BW	BW	BM
	$\pm 20\%$	Q	Q	Q	Q	BM
ISS	$\pm 10\%$	Q	BW	BW	BW	BM
	$\pm 20\%$	Q	Q	Q	Q	BM
OSS	$\pm 10\%$	Q	BW	BW	BW	Q
	$\pm 20\%$	Q	Q	BM	Q	Q
TN	$\pm 10\%$	M	Q	Q	Q	Q
	$\pm 20\%$	Q	Q	Q	Q	Q
TDN	$\pm 10\%$	BM	BM	Q	Q	Q
	$\pm 20\%$	Q	Q	Q	Q	Q
TP	$\pm 10\%$	Q	BW	BW	M	M
	$\pm 20\%$	Q	Q	Q	Q	Q
TDP	$\pm 10\%$	Q	Q	BM	BM	M
	$\pm 20\%$	Q	Q	Q	Q	Q
Silicate	$\pm 10\%$	BM	Q	Q	BW	BW
	$\pm 20\%$	BM	Q	Q	Q	Q
Chlorophyll <i>a</i>	$\pm 10\%$	BW	M	BW	BW	BW
	$\pm 20\%$	M	Q	Q	BM	Q

Table 3.5 Relationship of sampling frequency with the ability to statistically determine site-specific differences for water quality parameters. Data were from weekly integrated water column samples for all stations sampled for the entire 2 years of this study; see Table 3.1 for details on how data for each sampling frequency were derived. Codes for sampling frequency are: Q = quarterly, BM = bimonthly, M = monthly, BW = biweekly, W = weekly. For each line, P = probability of any significant difference among stations based on ANOVA; stations with identical letters are not significantly different (T-K: $P > 0.05$).

Parameter	Frequency	P	BR	MB	SN	SS	LP
Temperature	Q	0.90	a	a	a	a	a
	BM	0.83	a	a	a	a	a
	M	0.57	a	a	a	a	a
	BW	0.14	a	a	a	a	a
	W	0.004	a	ab	ab	b	b
Salinity	Q	0.30	a	a	a	a	a
	BM	0.11	a	a	a	a	a
	M	0.004	a	ab	ab	ab	b
	BW	0.0001	ab	a	bc	ab	c
	W	0.0001	a	b	a	a	c
Color	Q	0.03	a	a	a	a	a
	BM	0.001	a	a	b	b	ab
	M	0.0001	a	a	b	b	a
	BW	0.0001	a	a	b	b	a
	W	0.0001	a	a	b	b	a
Turbidity	Q	0.27	a	a	a	a	a
	BM	0.41	a	a	a	a	a
	M	0.05	a	ab	b	ab	ab
	BW	0.0001	a	ab	bc	ab	c
	W	0.0001	a	b	cd	bc	d
TSS	Q	0.25	a	a	a	a	a
	BM	0.36	a	a	a	a	a
	M	0.04	a	ab	ab	ab	b
	BW	0.0001	a	ab	bc	ab	c
	W	0.0001	a	ab	c	bc	d
ISS	Q	0.16	a	a	a	a	a
	BM	0.41	a	a	a	a	a
	M	0.04	a	ab	ab	ab	b
	BW	0.0001	a	ab	bc	ab	c
	W	0.0001	a	ab	c	bc	d

Table 3.5 (Continued)

Parameter	Frequency	P	BR	MB	SN	SS	LP
OSS	Q	0.45	a	a	a	a	a
	BM	0.18	a	a	a	a	a
	M	0.05	a	a	a	a	a
	BW	0.0001	a	ab	bc	ab	c
	W	0.0001	a	a	b	ab	c
TN	Q	0.02	a	ab	b	b	b
	BM	0.0002	a	ab	c	bc	c
	M	0.0001	a	a	b	b	b
	BW	0.0001	a	b	c	c	c
	W	0.0001	a	b	c	c	c
TDN	Q	0.0001	a	b	b	b	b
	BM	0.0001	a	ab	c	bc	c
	M	0.0001	a	b	c	c	c
	BW	0.0001	a	b	c	c	c
	W	0.0001	a	b	c	c	c
TP	Q	0.004	a	ab	b	ab	b
	BM	0.0001	a	b	b	b	b
	M	0.0001	a	b	b	b	b
	BW	0.0001	a	b	b	b	b
	W	0.0001	a	b	bc	bc	c
TDP	Q	0.18	a	a	a	a	a
	BM	0.03	a	ab	ab	ab	b
	M	0.002	a	b	b	b	b
	BW	0.0001	a	b	b	b	b
	W	0.0001	a	b	b	b	b
Silicate	Q	0.29	a	a	a	a	a
	BM	0.01	a	ab	ab	b	ab
	M	0.002	a	b	b	b	ab
	BW	0.0001	a	b	b	b	a
	W	0.0001	a	b	b	b	c
Chlorophyll <i>a</i>	Q	0.30	a	a	a	a	a
	BM	0.17	a	a	a	a	a
	M	0.020	a	ab	b	ab	ab
	BW	0.023	a	ab	b	ab	b
	W	0.0001	a	b	b	ab	b

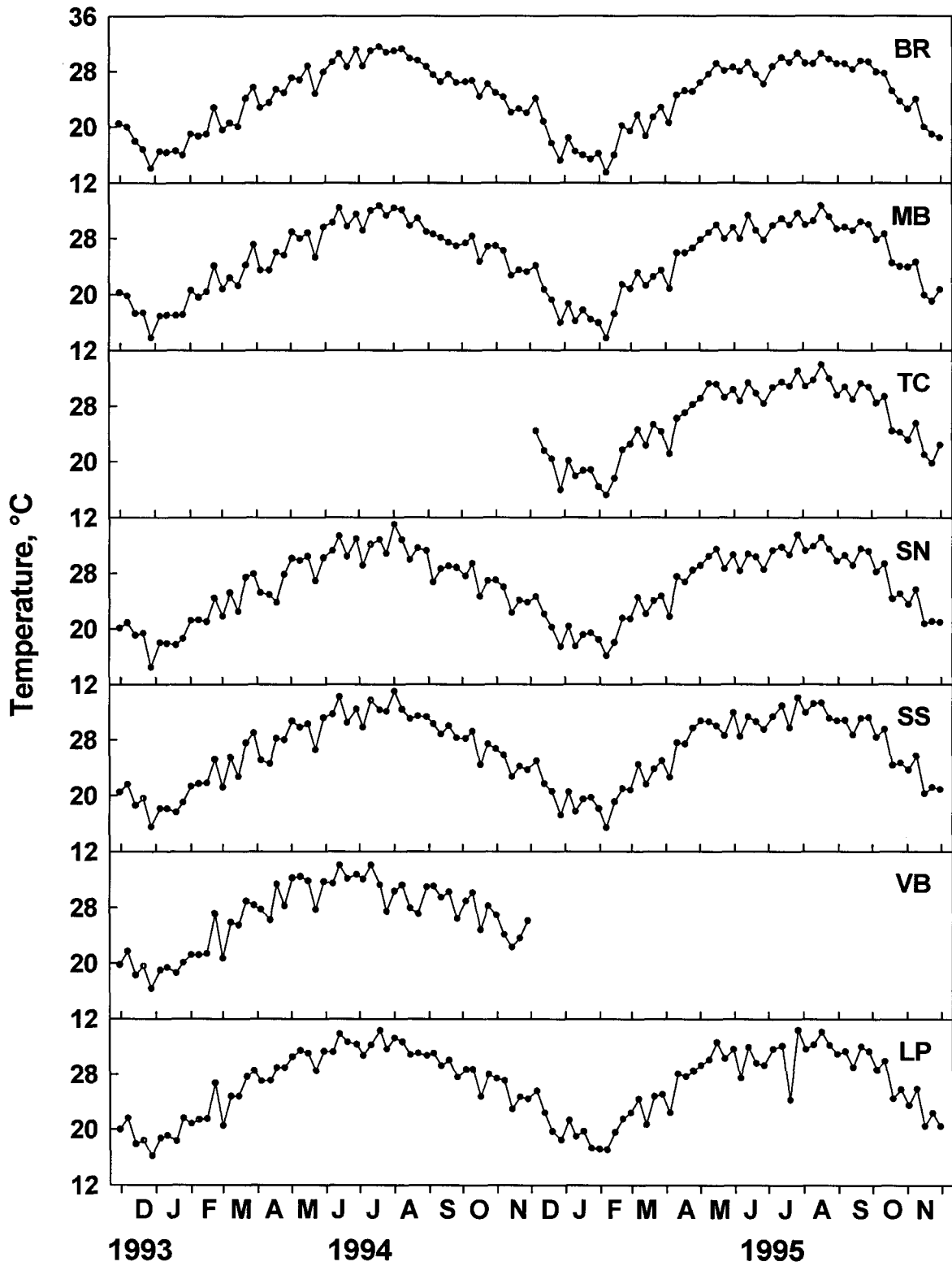


Fig. 3.1 Temperature of weekly integrated water column samples at IRL stations.

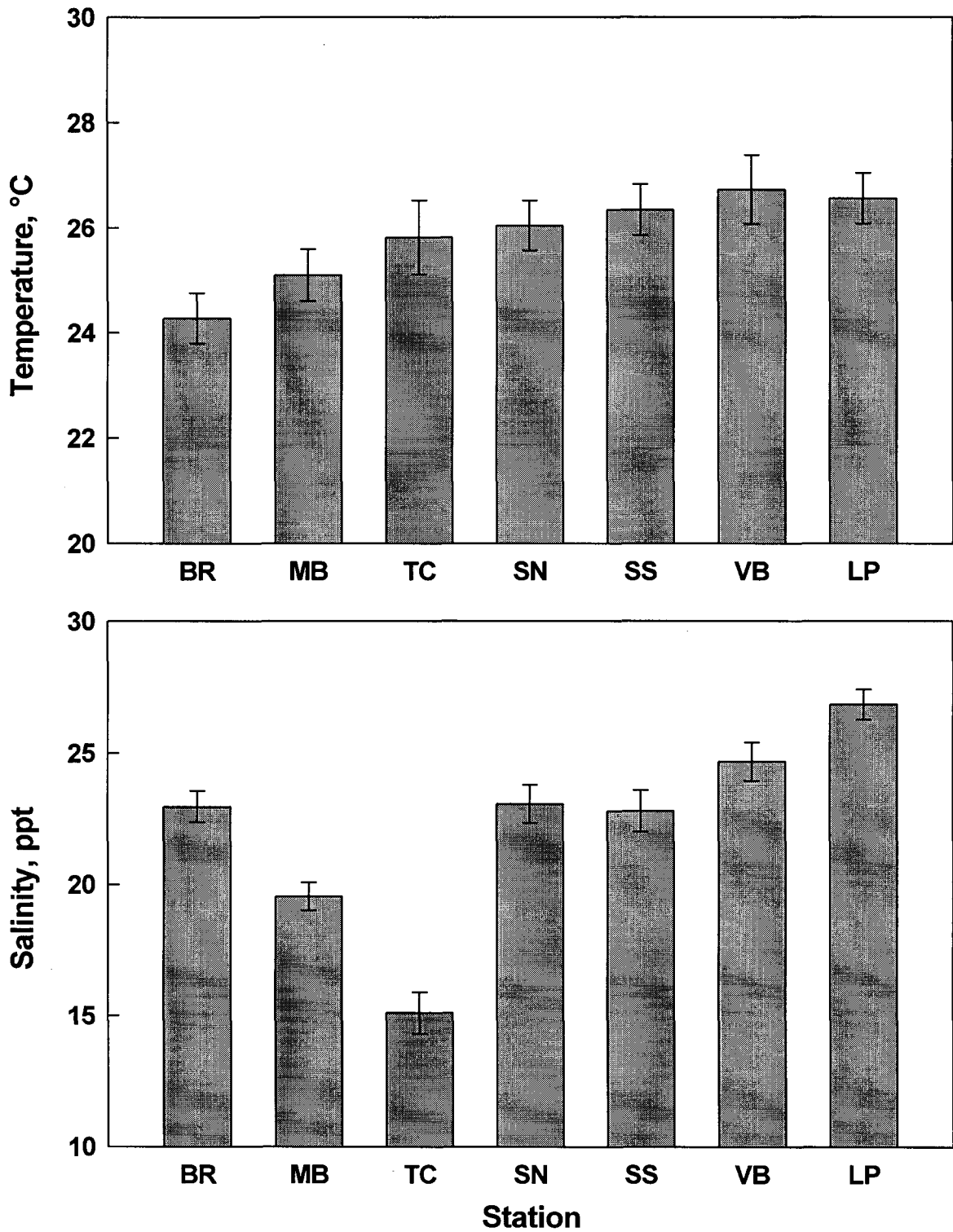


Fig. 3.2 Station means (\pm SE) for temperature and salinity of weekly integrated water column samples (both years of the study).

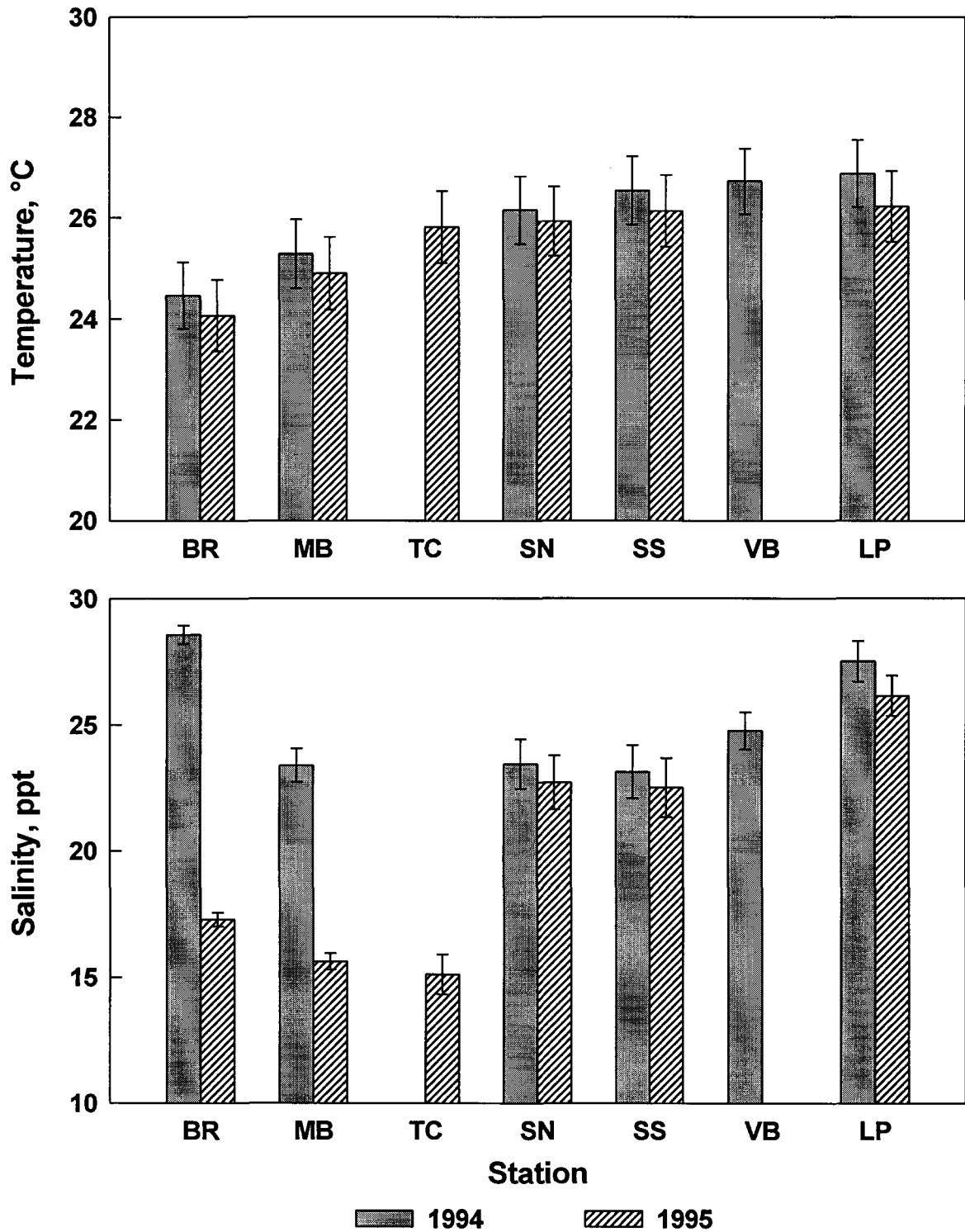


Fig. 3.3 Interannual variation in temperature and salinity based on station means (\pm SE) of weekly integrated water column samples.

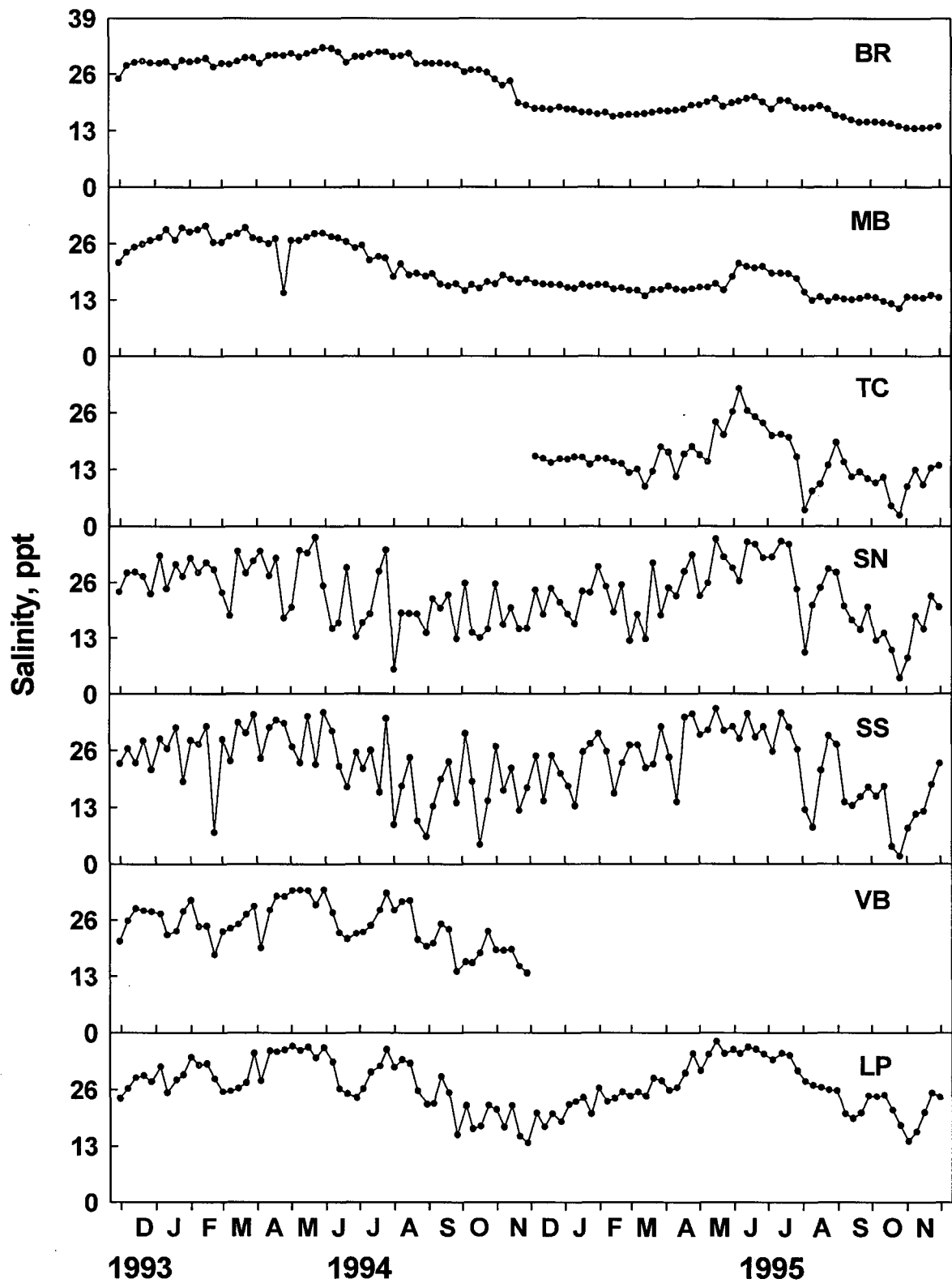


Fig. 3.4 Salinity of weekly integrated water column samples at IRL stations.

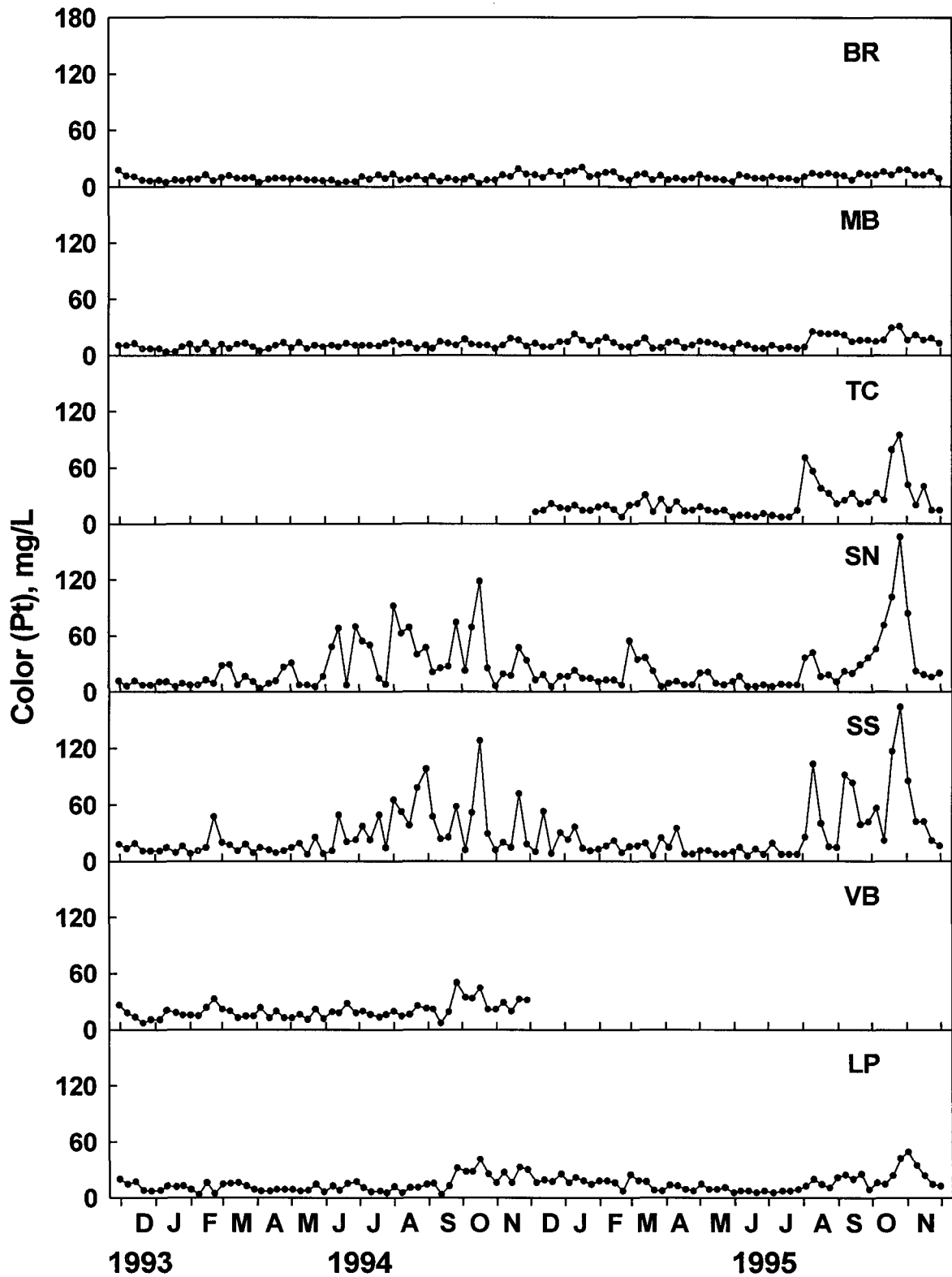


Fig. 3.5 Color of weekly integrated water column samples at IRL stations.

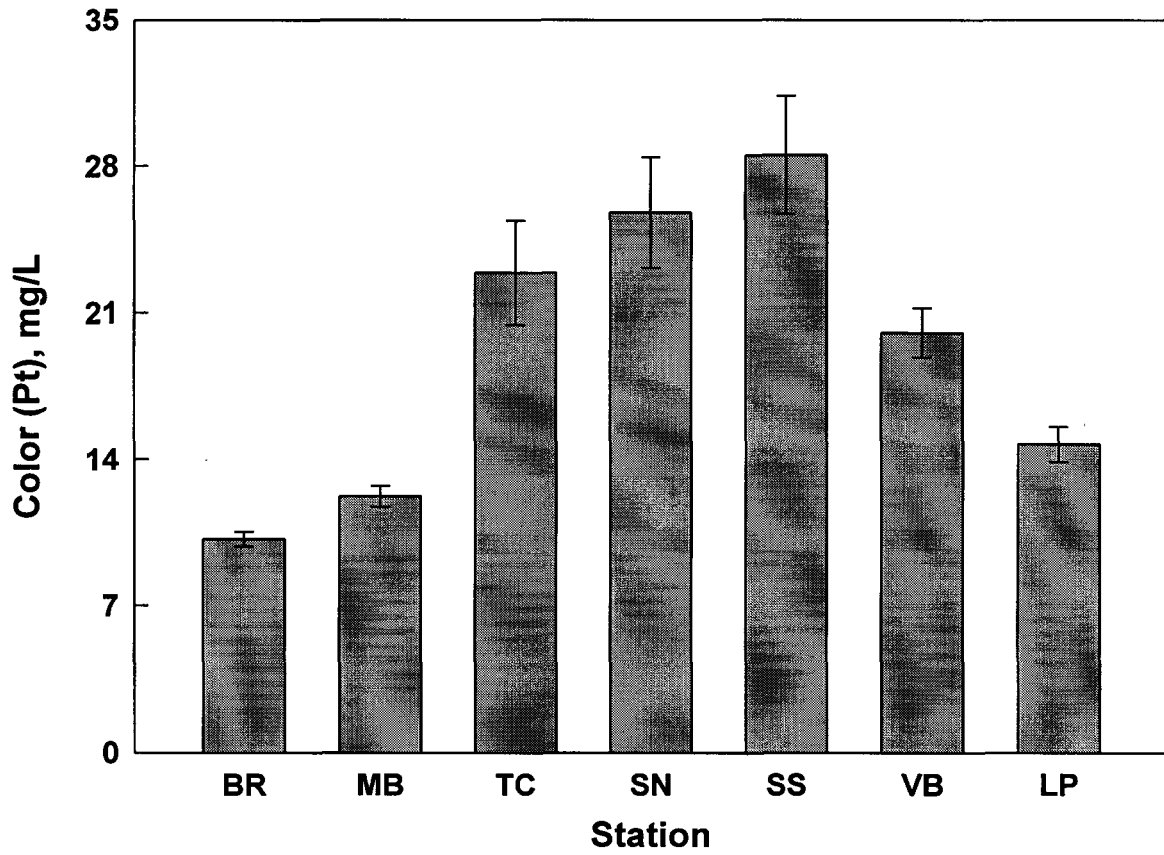


Fig. 3.6 Station means (\pm SE) for color of weekly integrated water column samples.

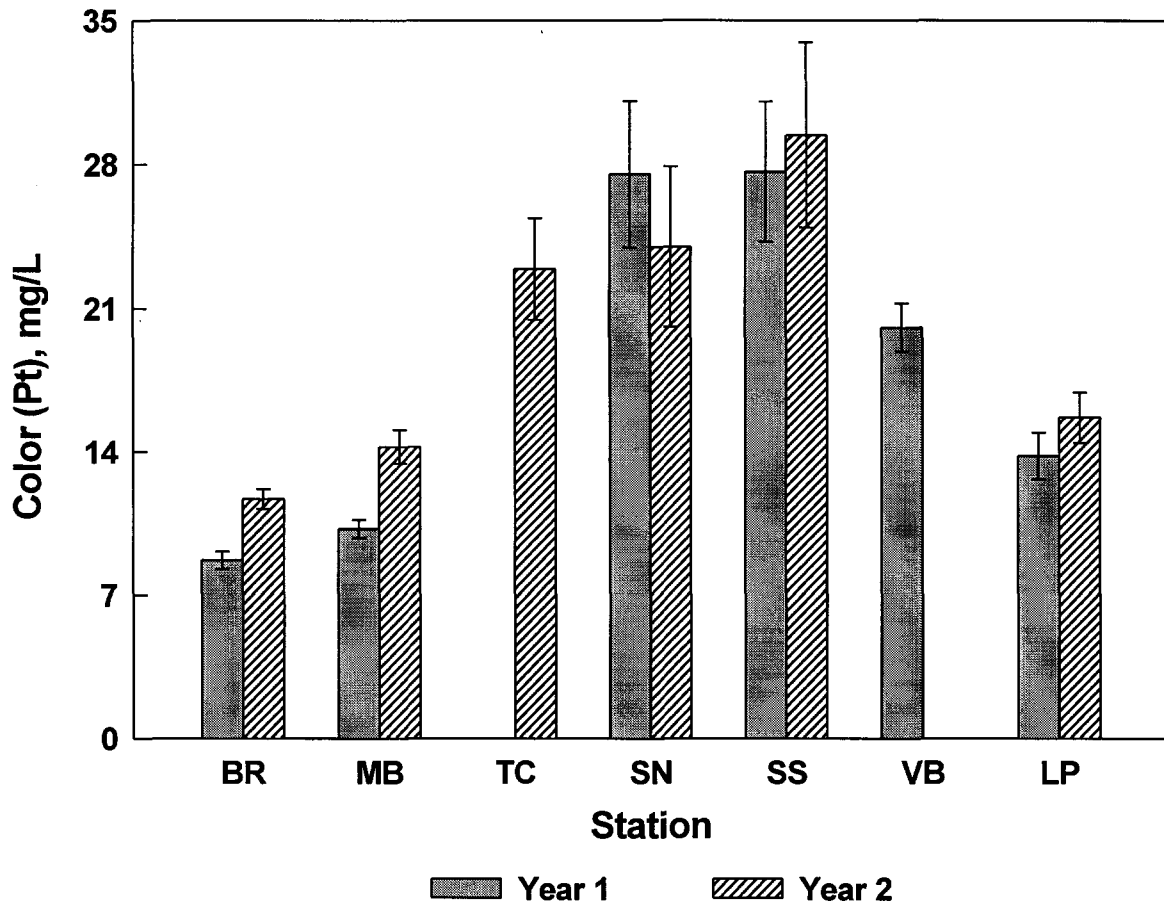


Fig. 3.7 Interannual variation in color based on station means (\pm SE) of weekly integrated water column samples.

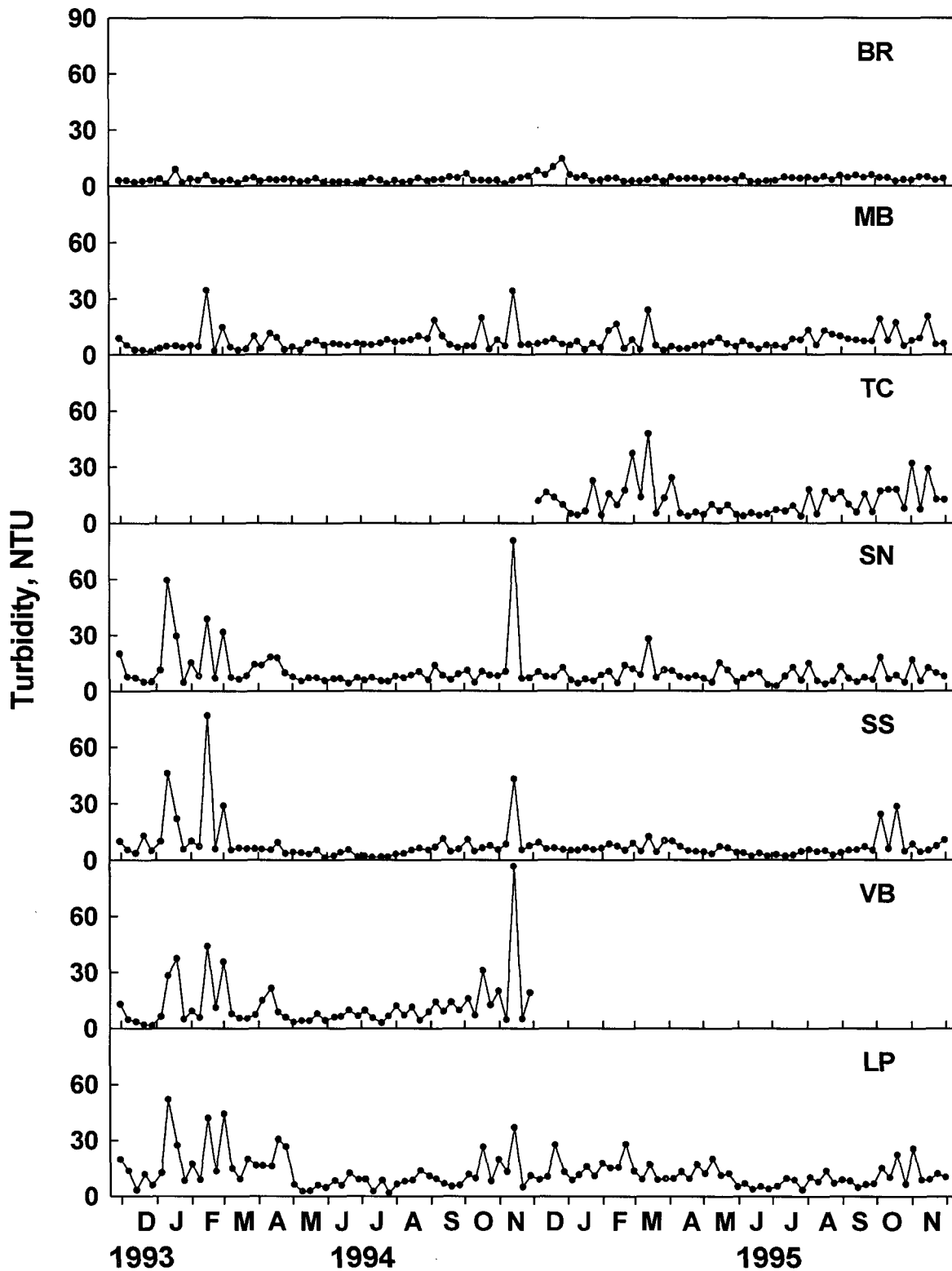


Fig. 3.8 Turbidity of weekly integrated water column samples at IRL stations.

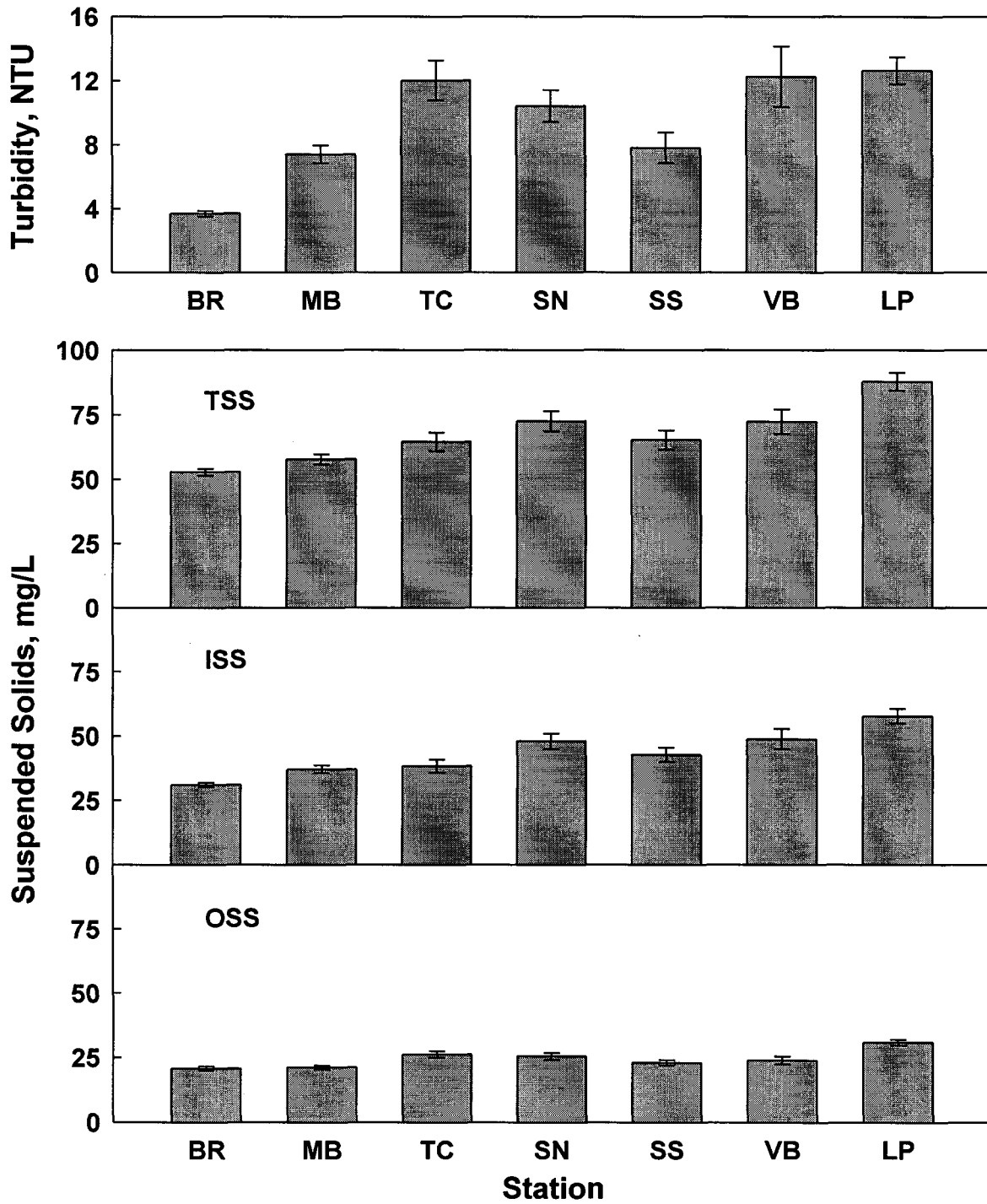


Fig. 3.9 Station means (\pm SE) for turbidity and total (TSS), inorganic (ISS), and organic (OSS) suspended solids of weekly integrated water column samples.

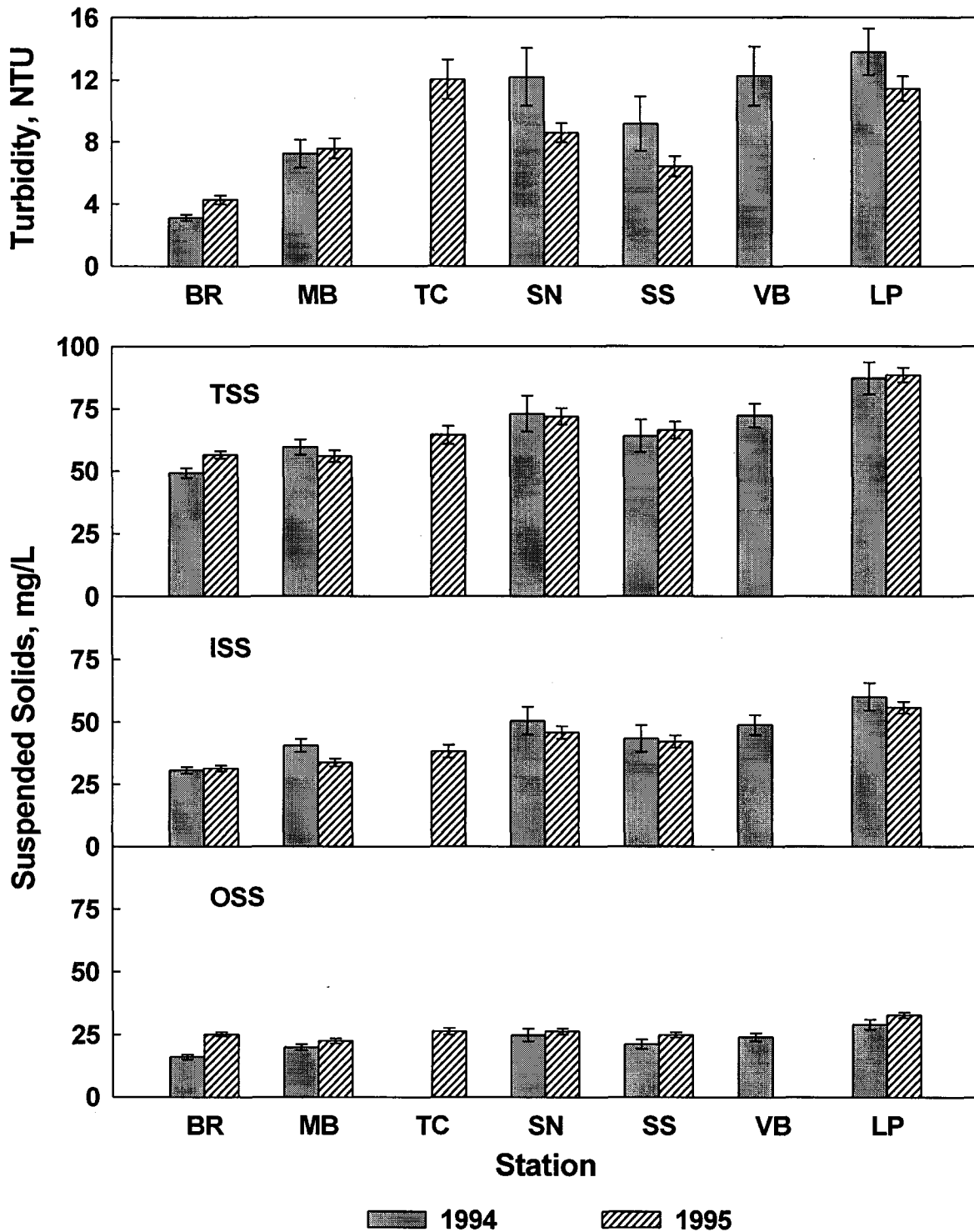


Fig. 3.10 Interannual variation in turbidity and total (TSS), inorganic (ISS), and organic (OSS) suspended solids based on station means (\pm SE) of weekly integrated water column samples.

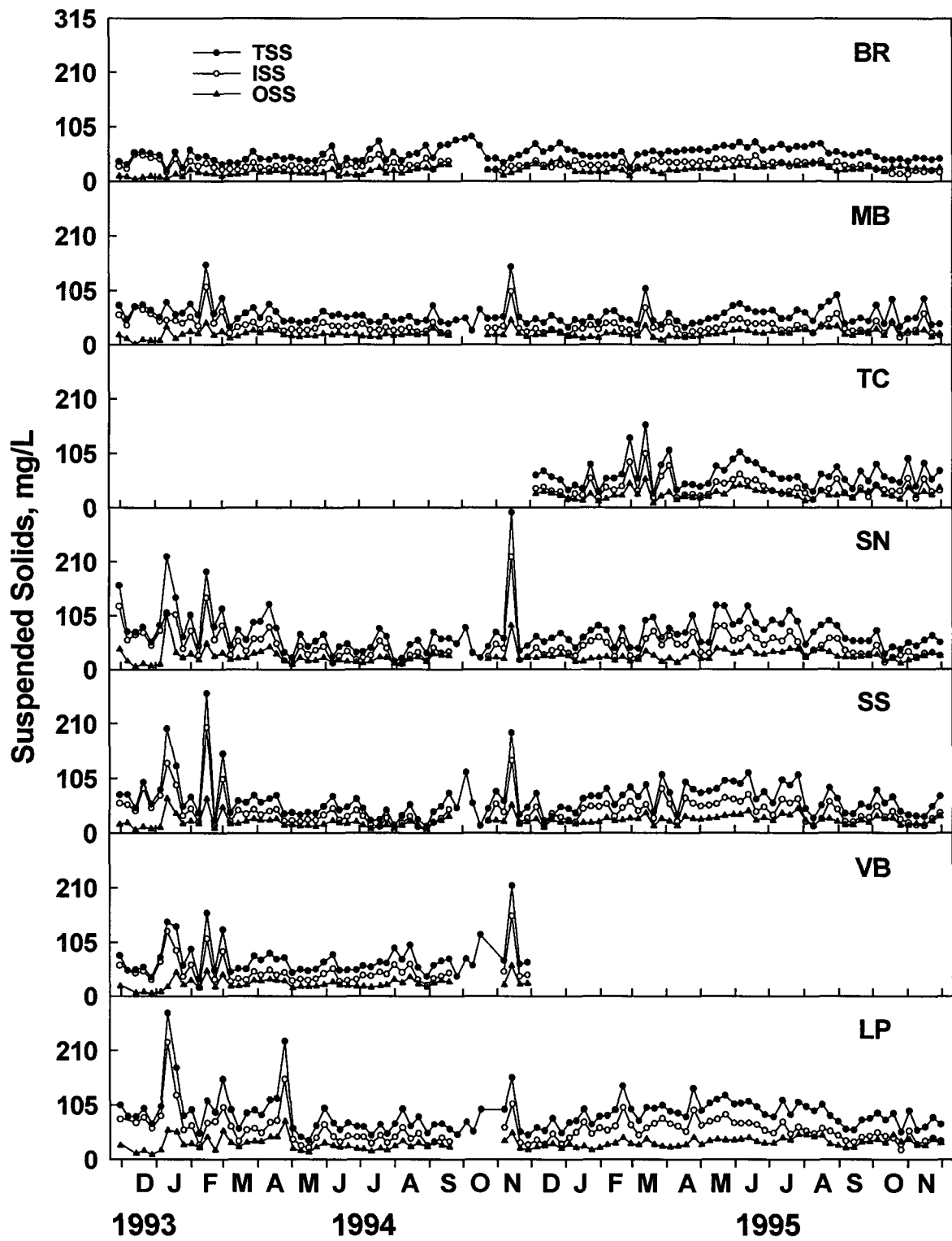


Fig. 3.11 Total (TSS), inorganic (ISS), and organic (OSS) suspended solids of weekly integrated water column samples at IRL stations.

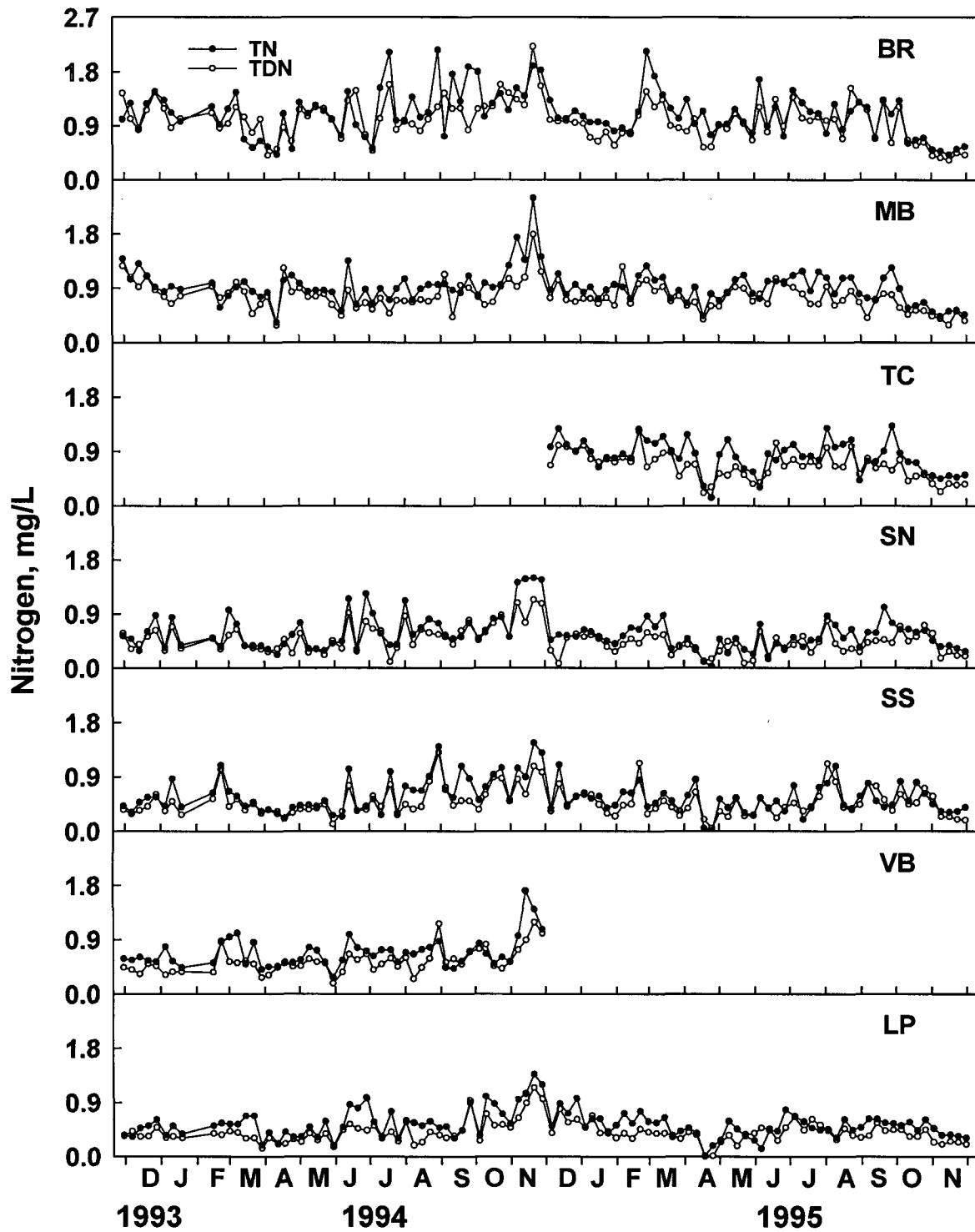


Fig. 3.12 Total (TN) and total dissolved nitrogen (TDN) concentrations of weekly integrated water column samples at IRL stations.

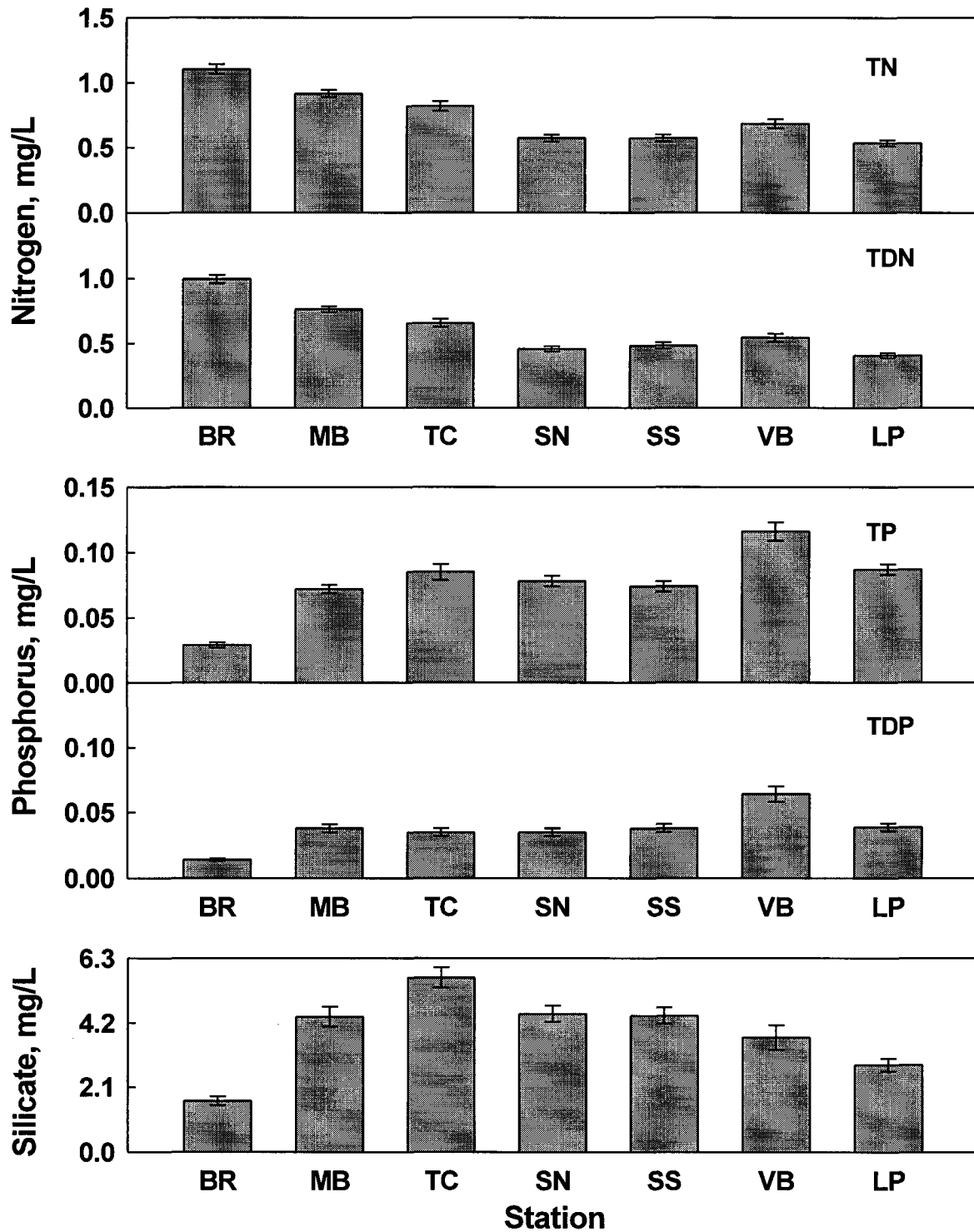


Fig. 3.13 Station means (\pm SE) for nutrient concentrations of weekly integrated water column samples: total (TN) and total dissolved nitrogen (TDN), total (TP) and total dissolved phosphorus (TDP), and total silicate.

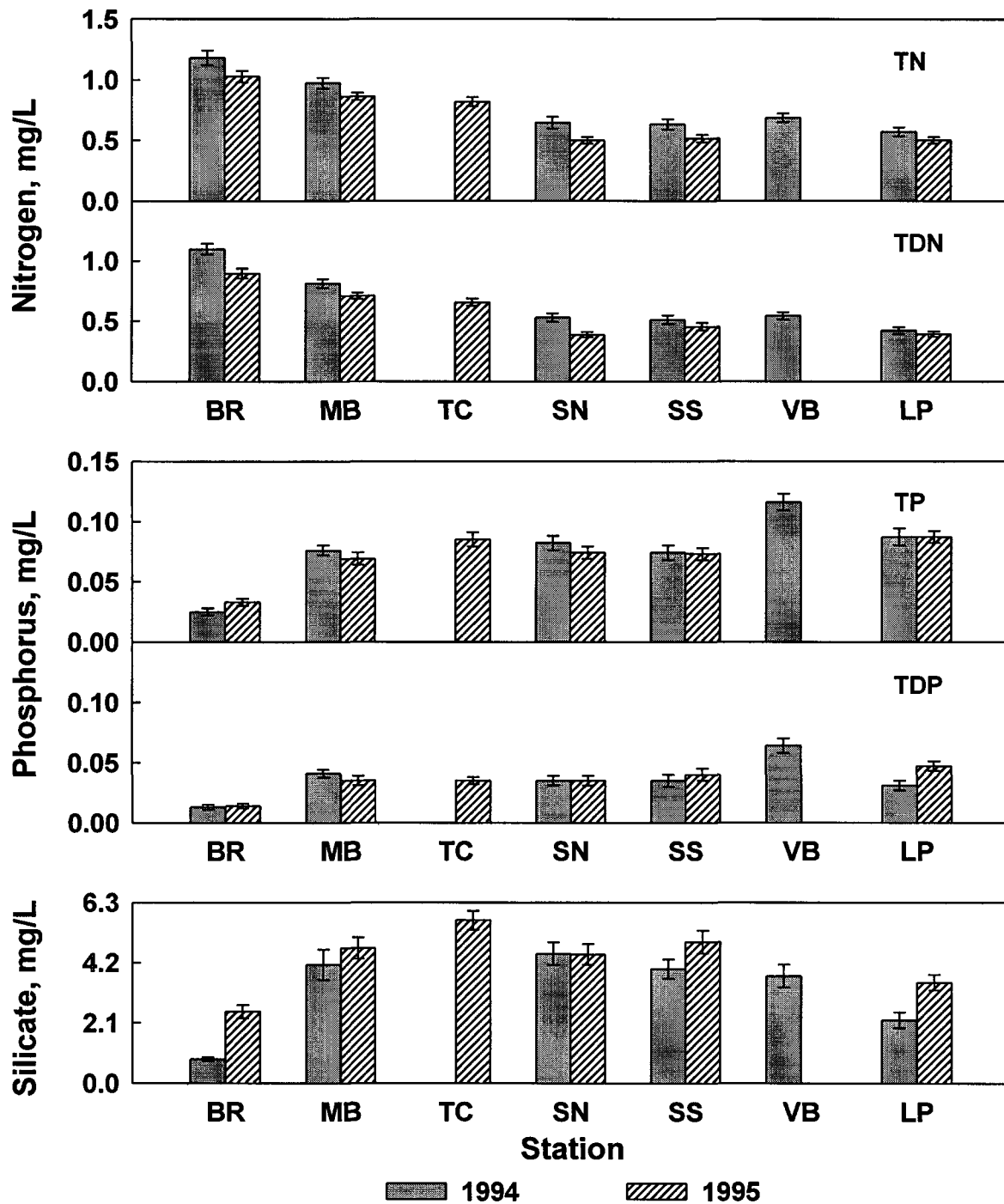


Fig 3.14 Interannual variation in nutrient concentrations based on station means (\pm SE) of weekly integrated water column samples: total (TN) and total dissolved nitrogen (TDN), total (TP) and total dissolved phosphorus (TDP), and total silicate.

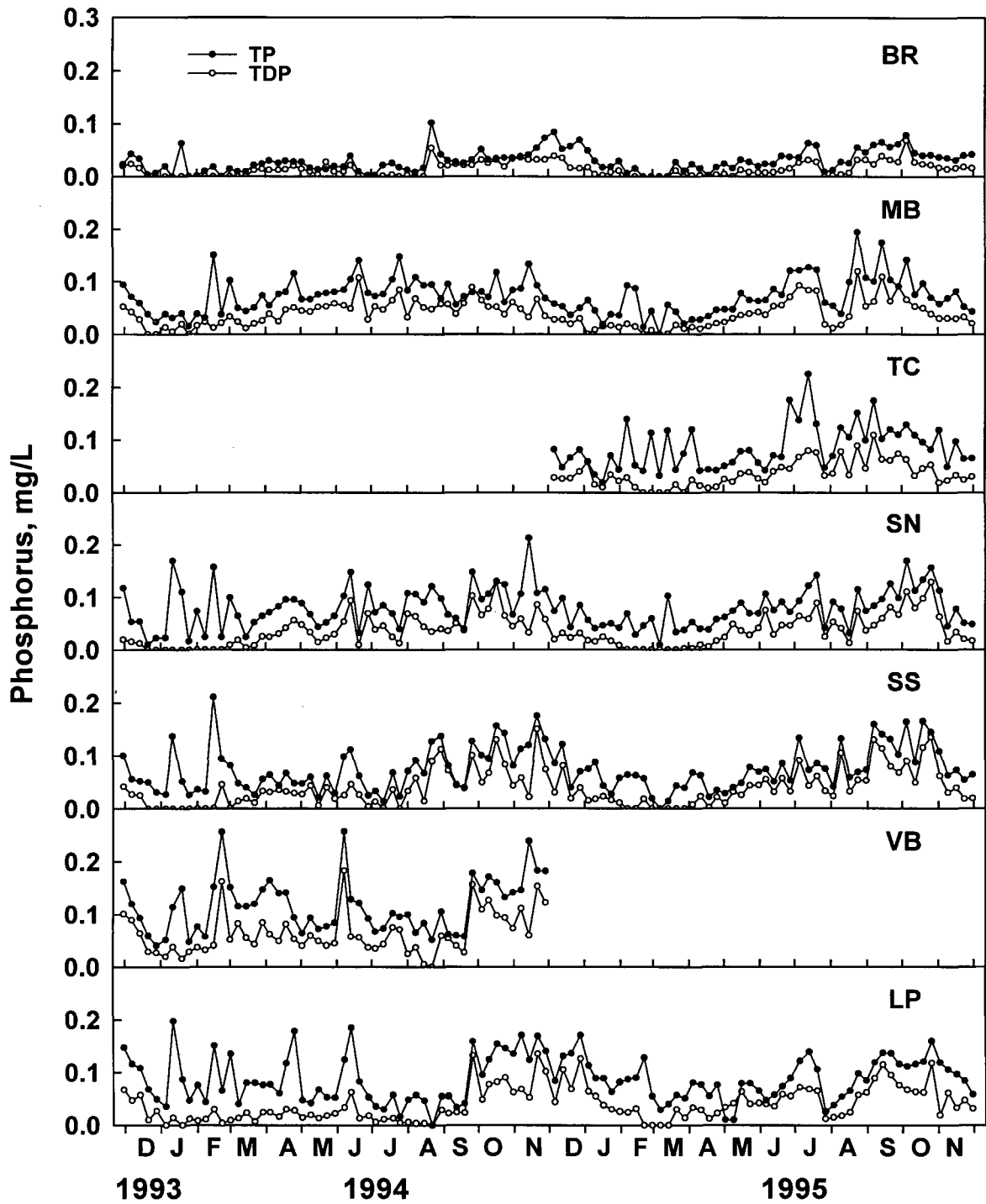


Fig. 3.15 Total (TP) and total dissolved phosphorus (TDP) concentration of weekly integrated water column samples at IRL stations.

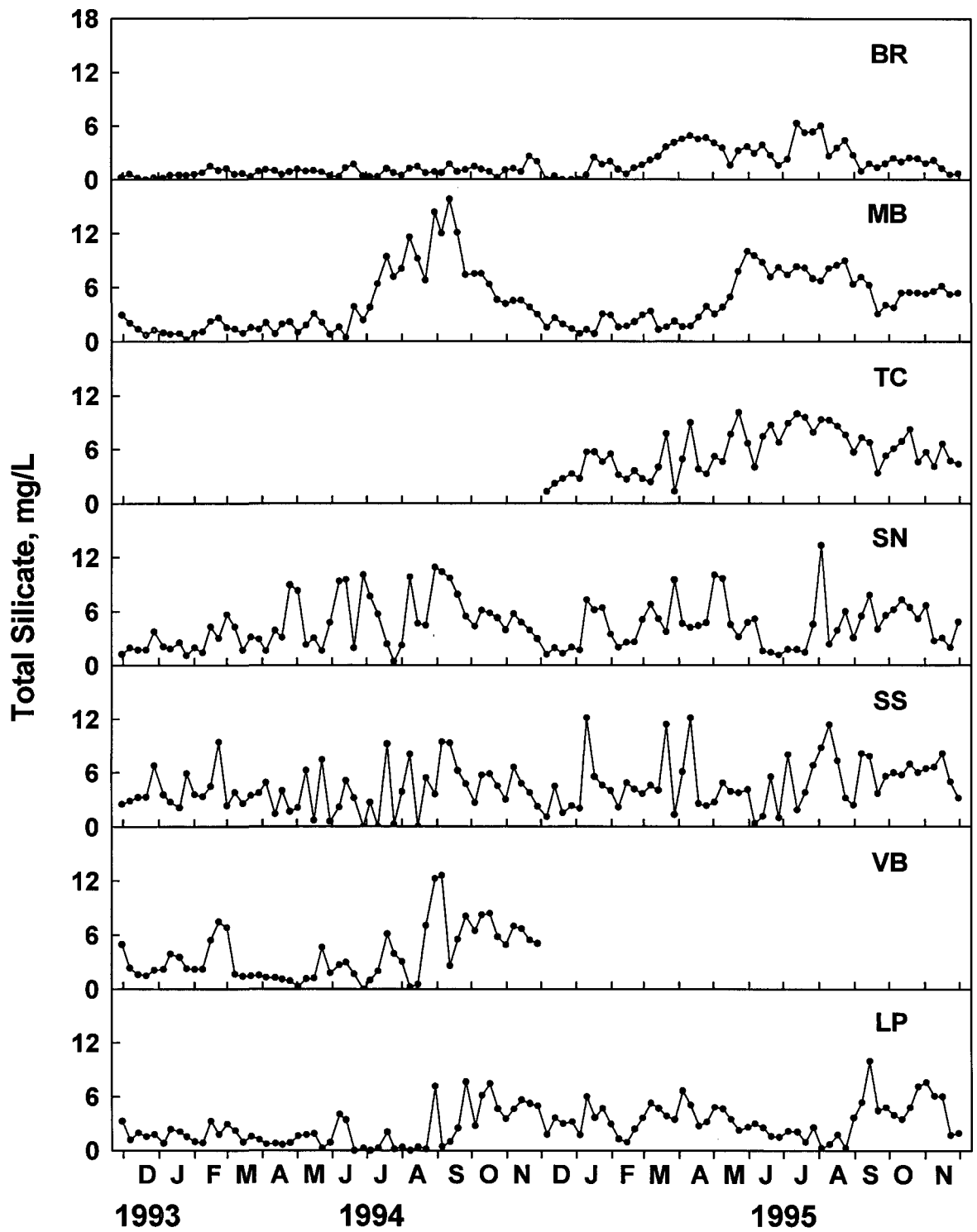


Fig. 3.16 Total silicate concentration of weekly integrated water column samples at IRL stations.

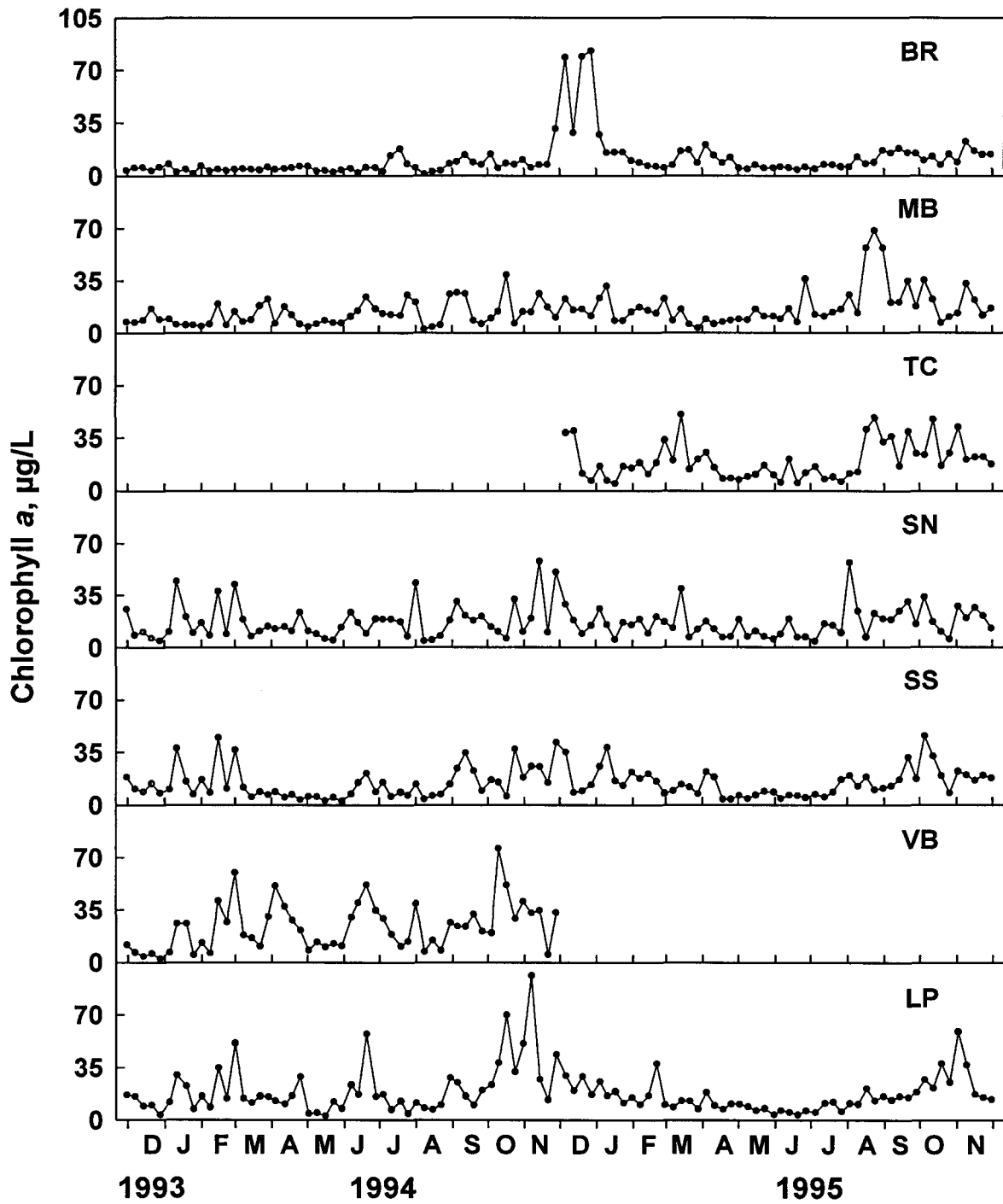


Fig. 3.17 Chlorophyll a concentration of weekly integrated water column samples at IRL stations.

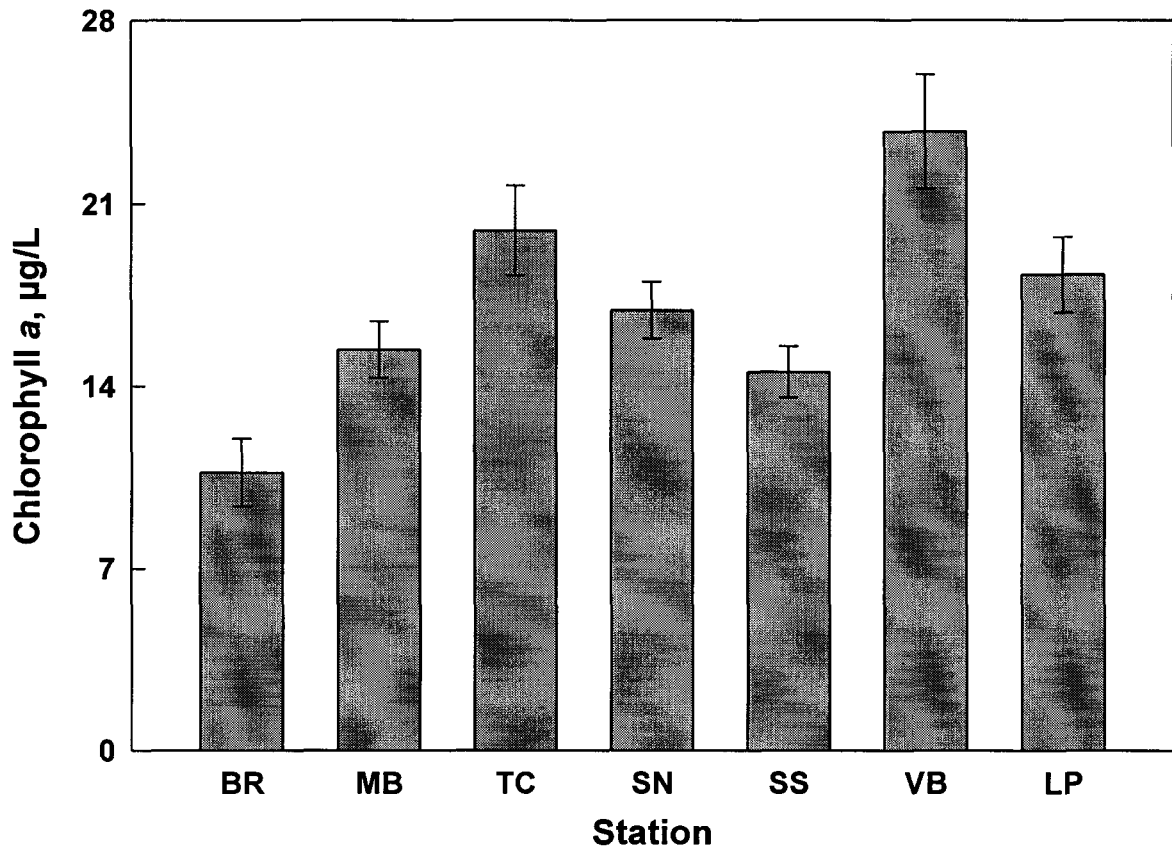


Fig. 3.18 Station means (\pm SE) for chlorophyll a concentration of weekly integrated water column samples.

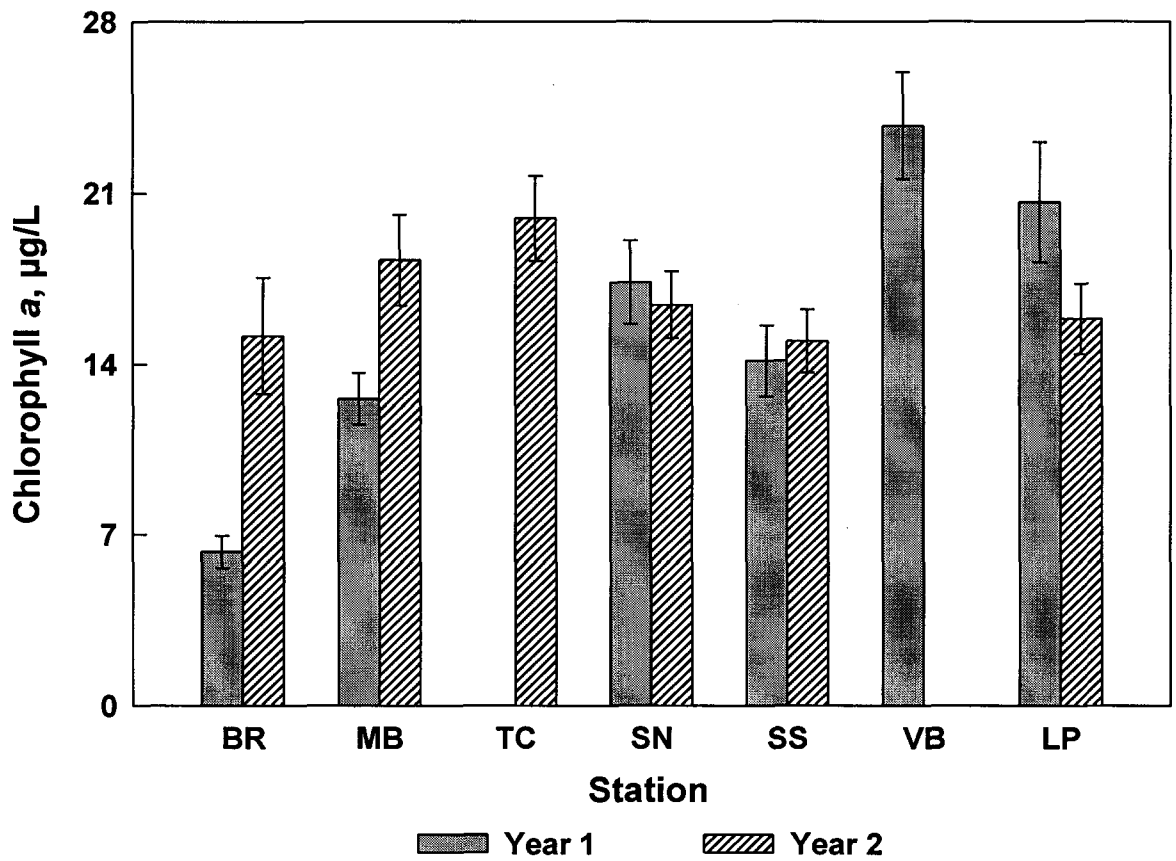


Fig. 3.19 Interannual variation in chlorophyll a concentration based on station means (\pm SE) of weekly integrated water column samples.

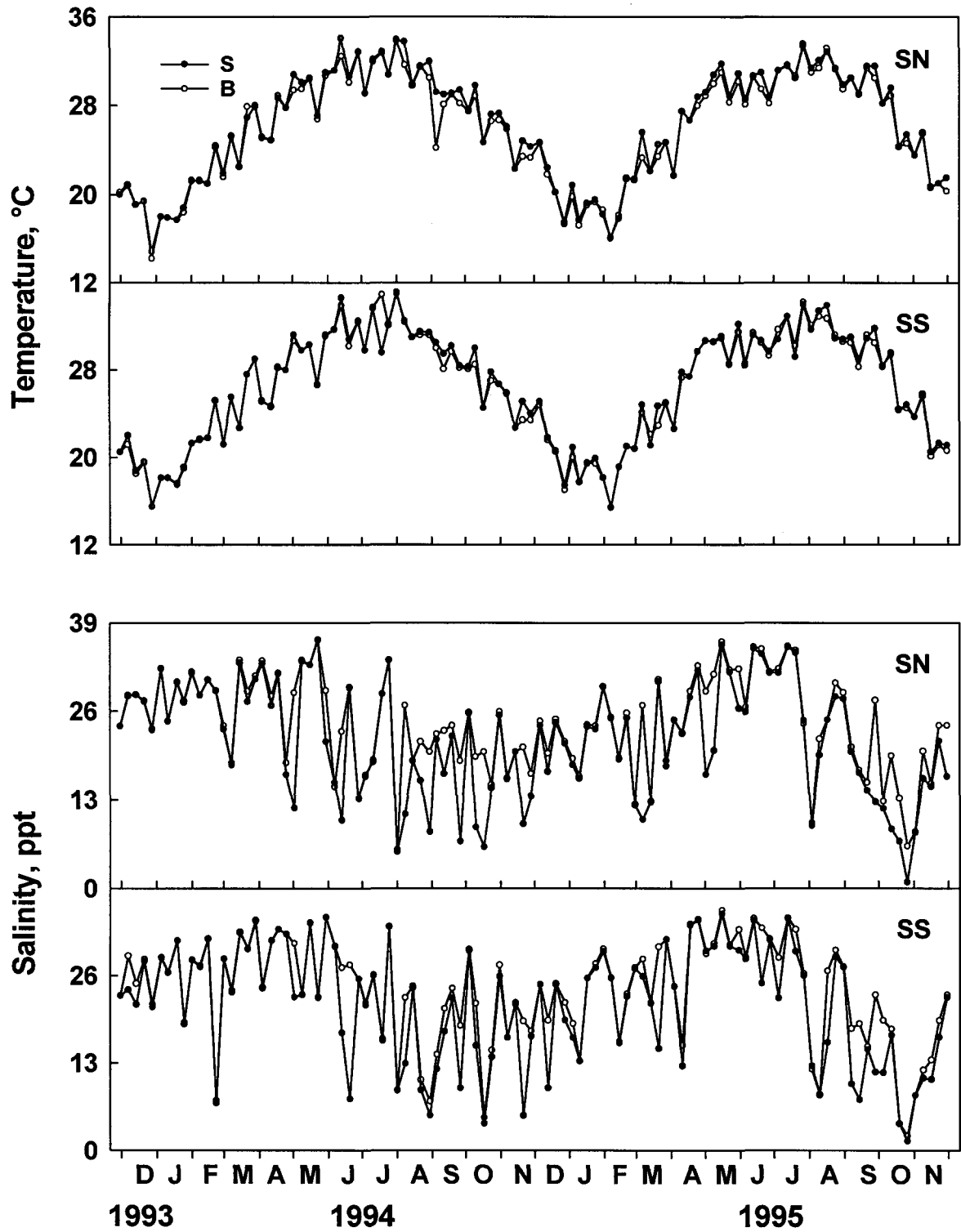


Fig. 3.20 Temperature and salinity of weekly surface and bottom water samples at SN and SS.

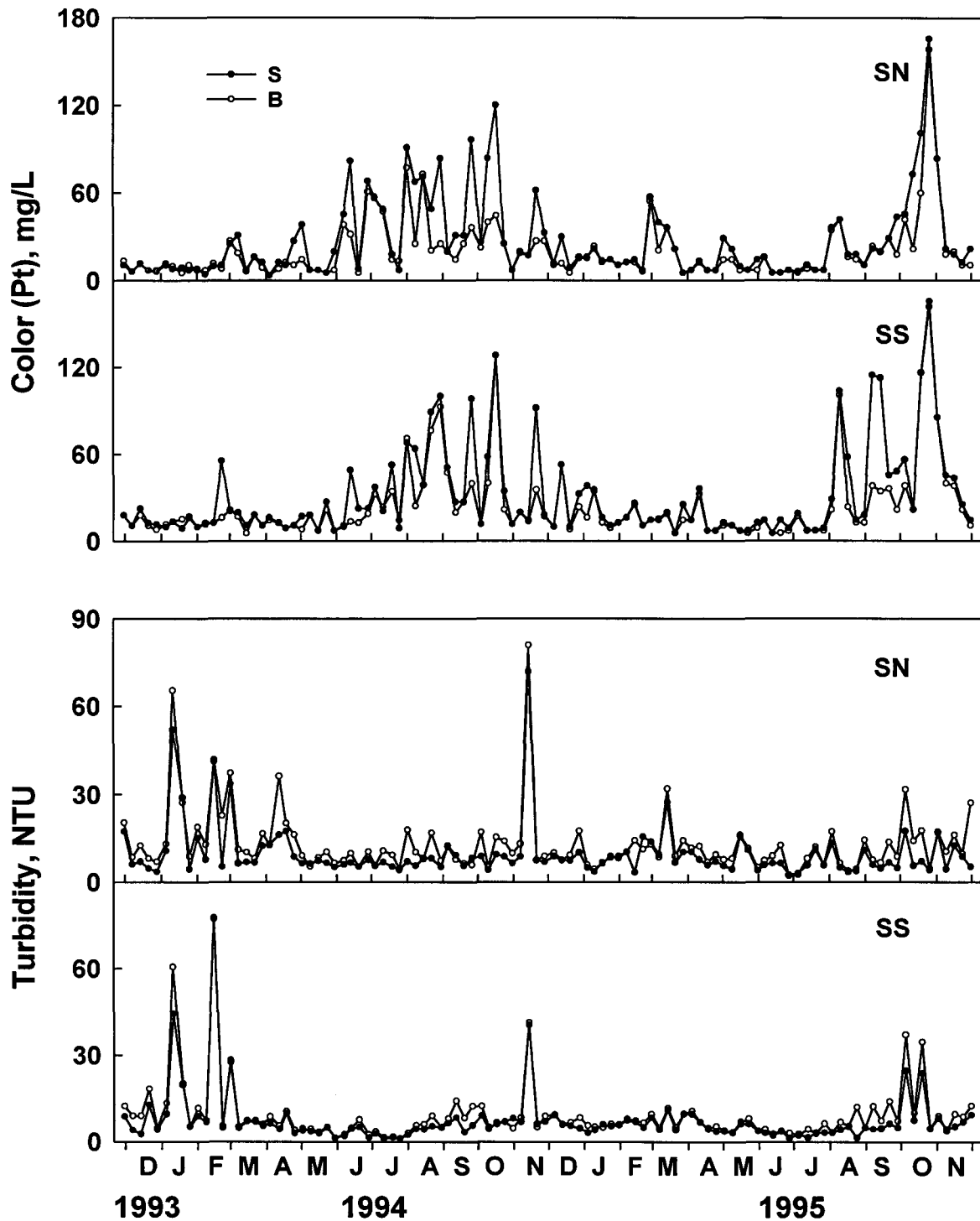


Fig. 3.21 Color and turbidity of weekly surface and bottom water samples at SN and SS.

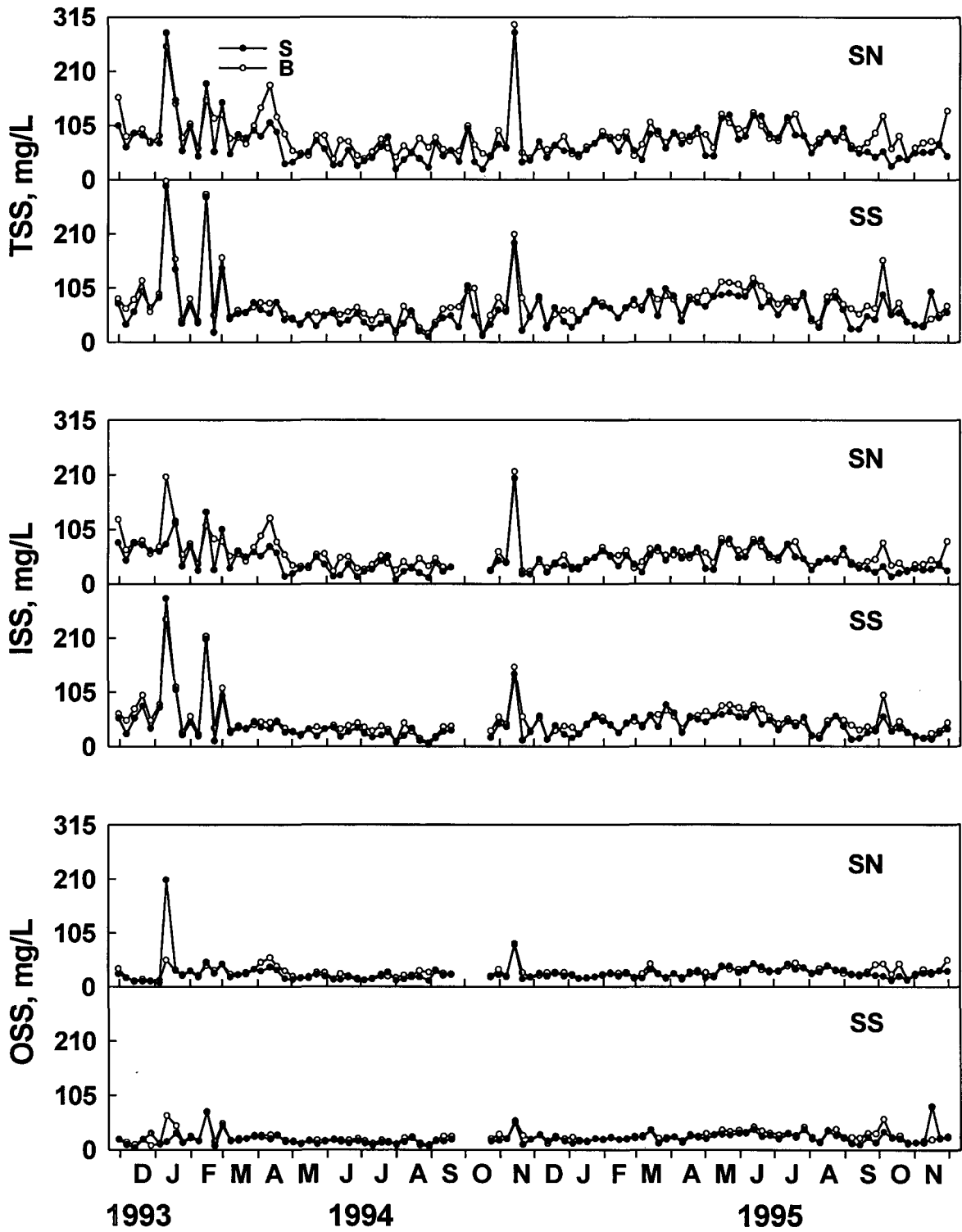


Fig. 3.22 Total (TSS), inorganic (ISS), and organic (OSS) suspended solids of weekly surface and bottom water samples at SN and SS.

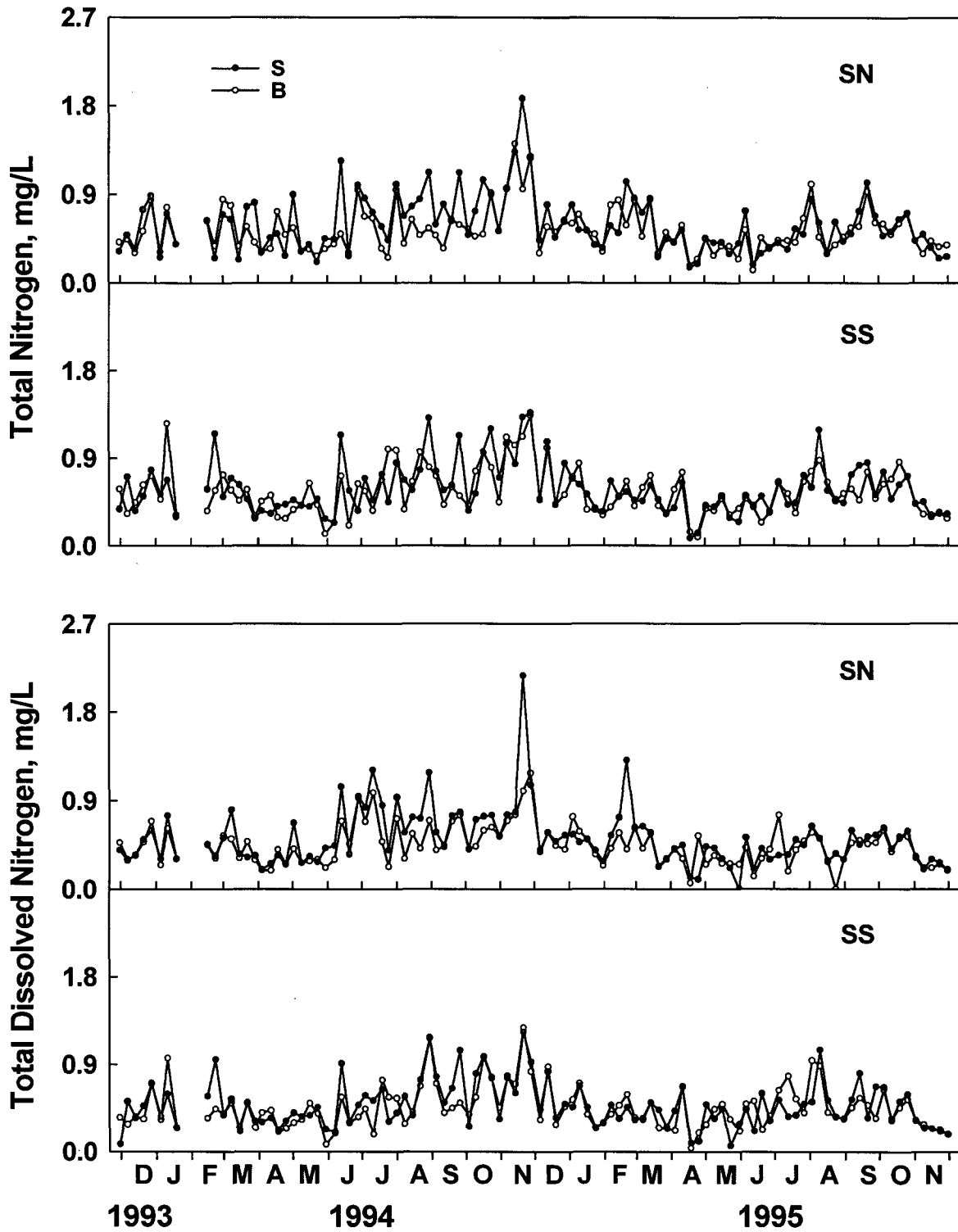


Fig. 3.23 Total and total dissolved nitrogen of weekly surface and bottom water samples at SN and SS.

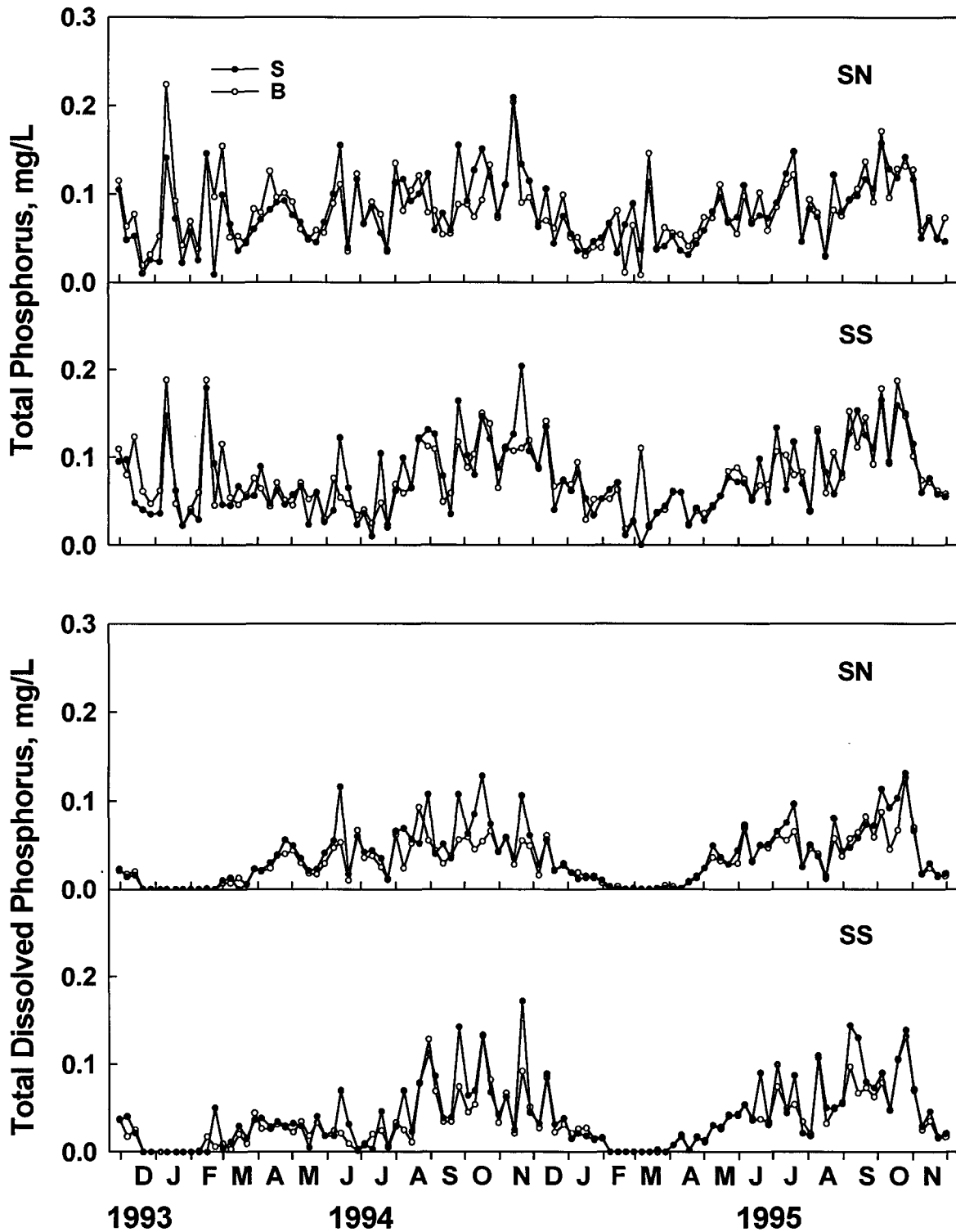


Fig. 3.24 Total and total dissolved phosphorus of weekly surface and bottom water samples at SN and SS.

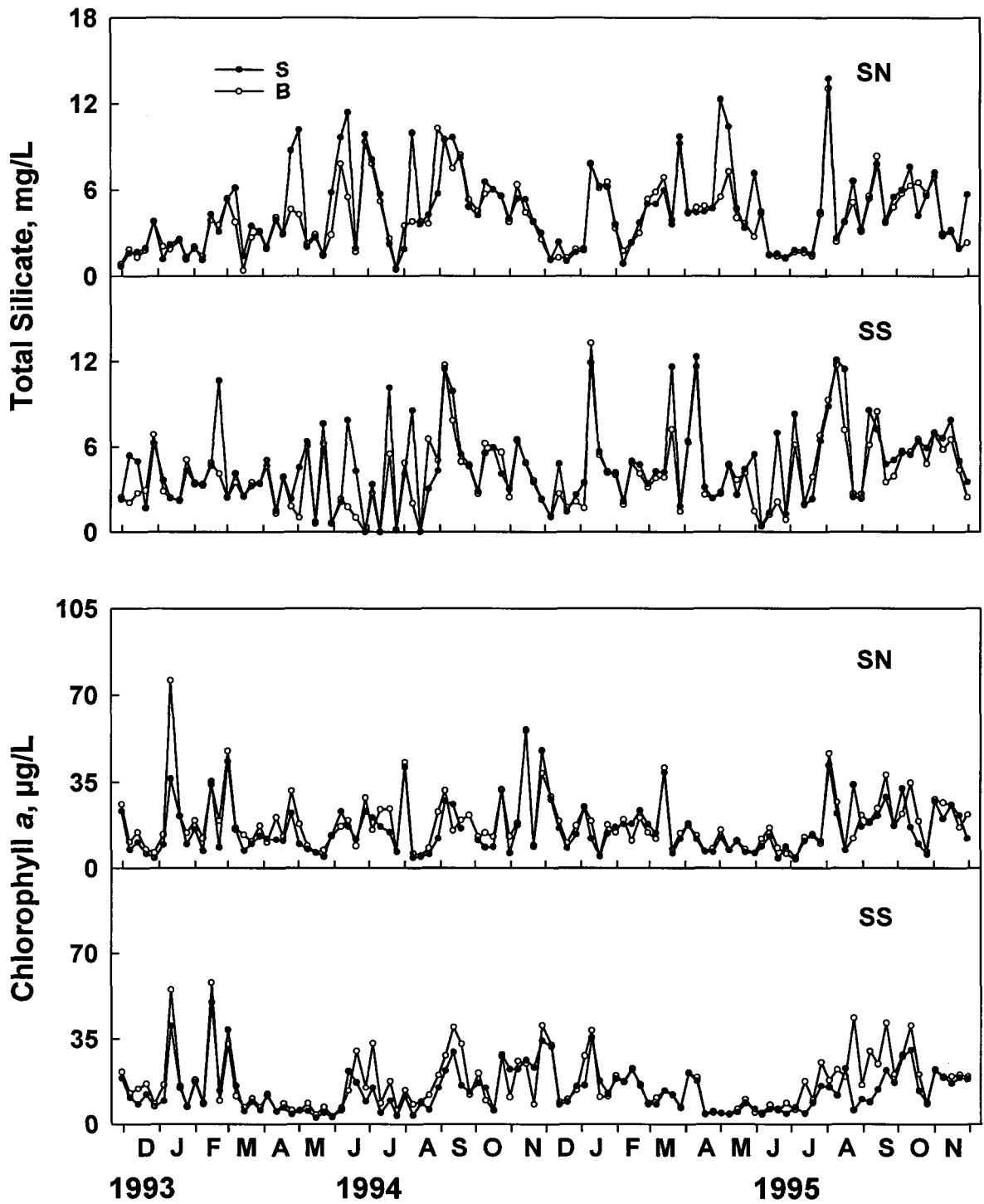


Fig. 3.25 Total silicate and chlorophyll *a* of weekly surface and bottom water samples at SN and SS.

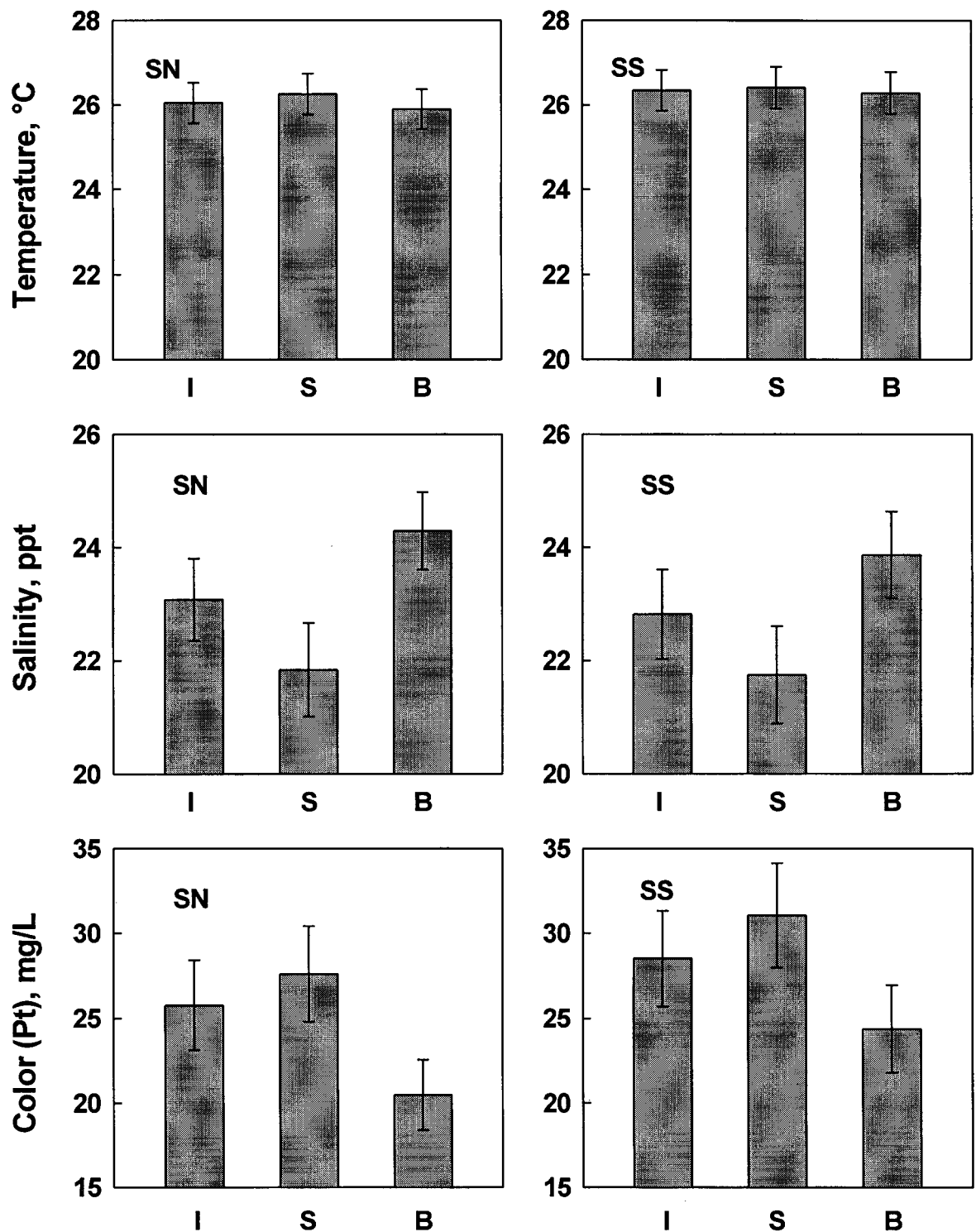


Fig. 3.26 Means (\pm SE) for temperature, salinity, and color of weekly stratified water column samples at SN and SS; I = integrated water column samples, S = surface samples, B = bottom samples.

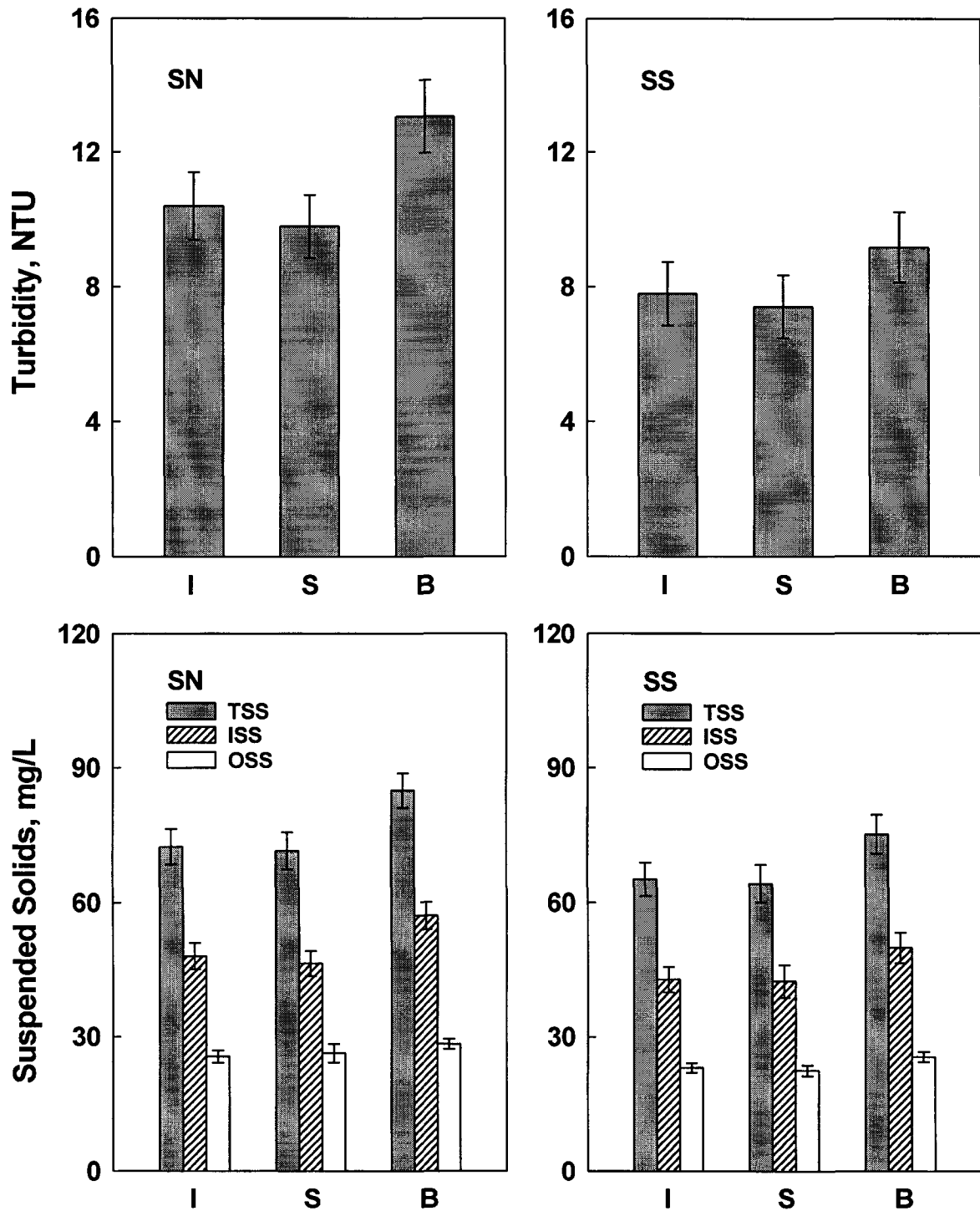


Fig. 3.27 Means (\pm SE) for turbidity and total (TSS), inorganic (ISS), and organic (OSS) suspended solids of weekly stratified water column samples at SN and SS; I = integrated water column samples, S = surface samples, B = bottom samples.

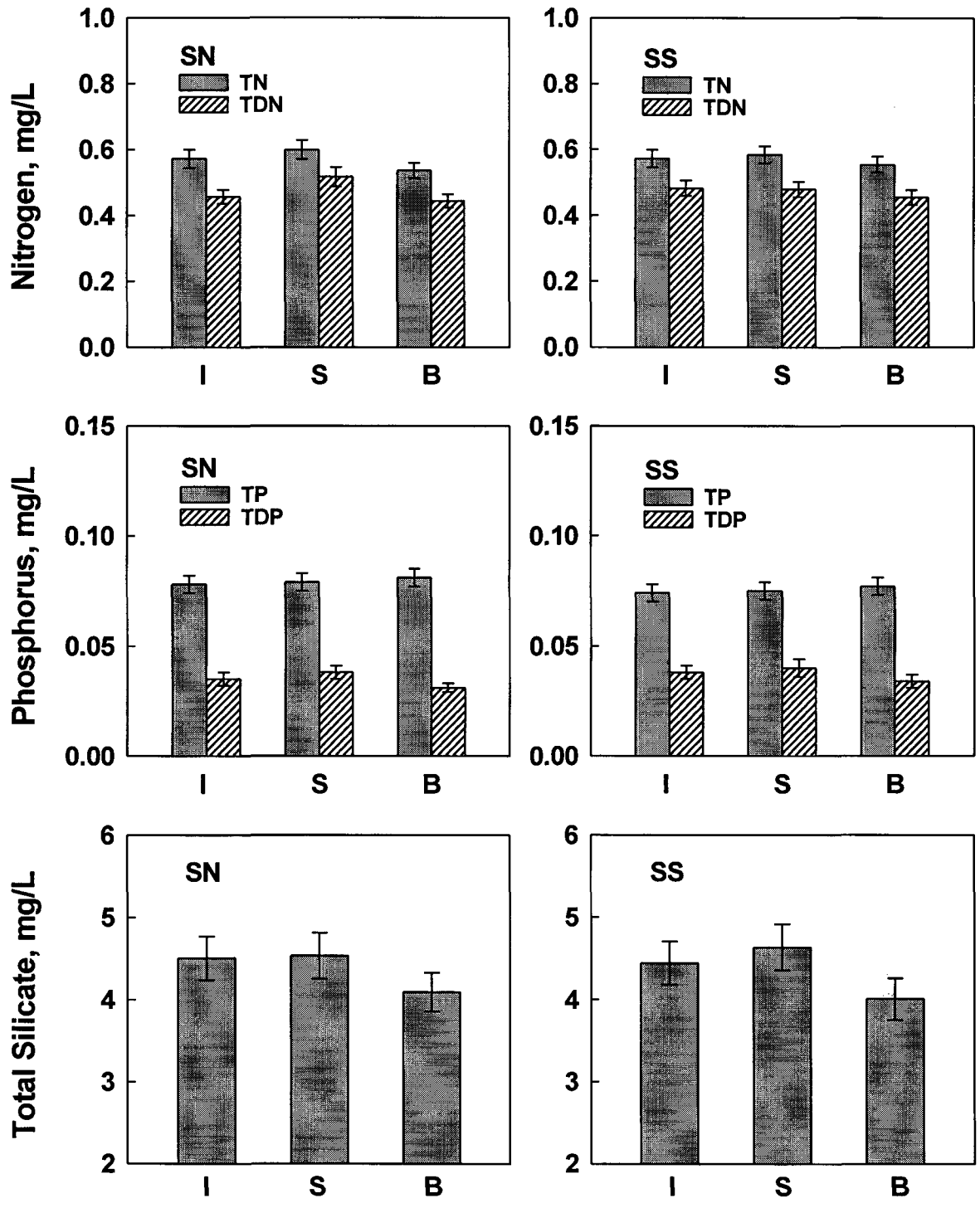


Fig. 3.28 Means (\pm SE) for nutrient concentrations of weekly stratified water column samples at SN and SS: total (TN) and total dissolved nitrogen (TDN), total (TP) and total dissolved phosphorus (TDP), and total silicate; I = integrated water column samples, S = surface samples, B = bottom samples.

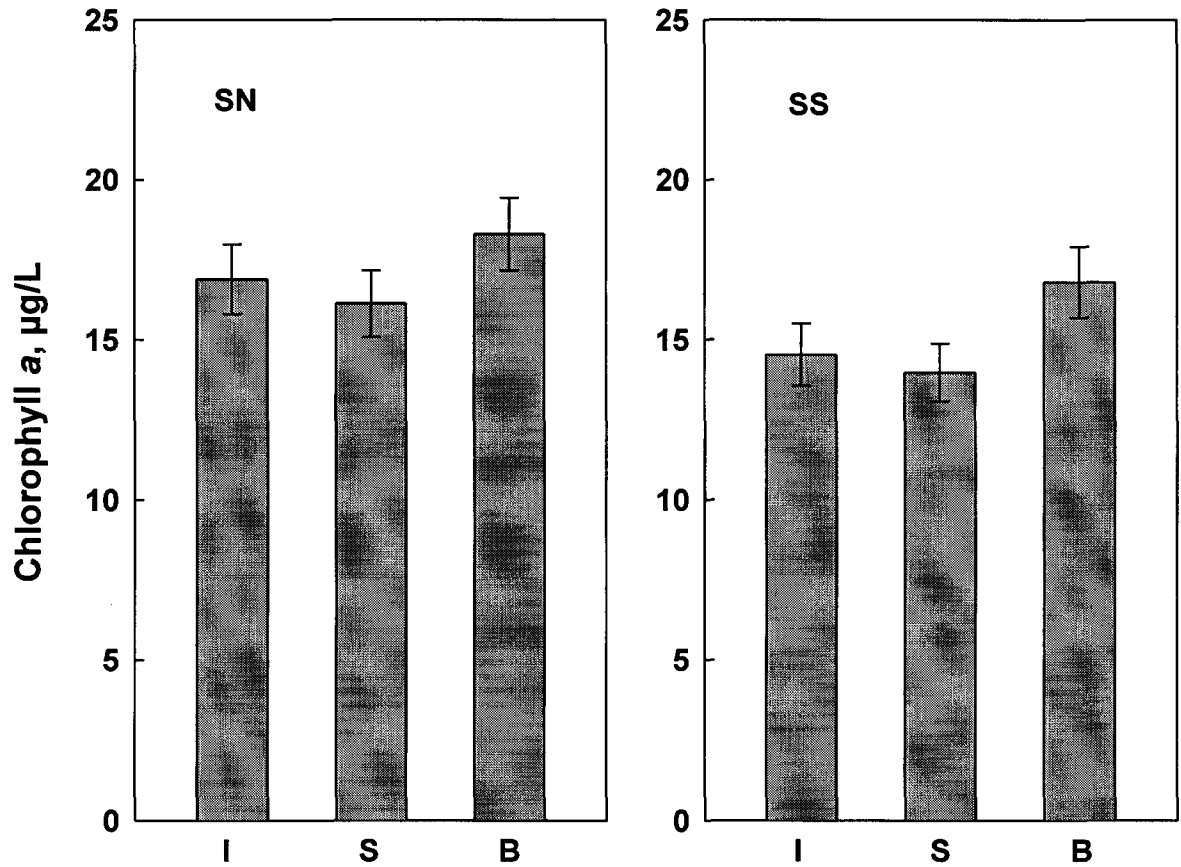


Fig. 3.29 Means (\pm SE) for chlorophyll *a* concentration of weekly stratified water column samples at SN and SS; I = integrated water column samples, S = surface samples, B = bottom samples.

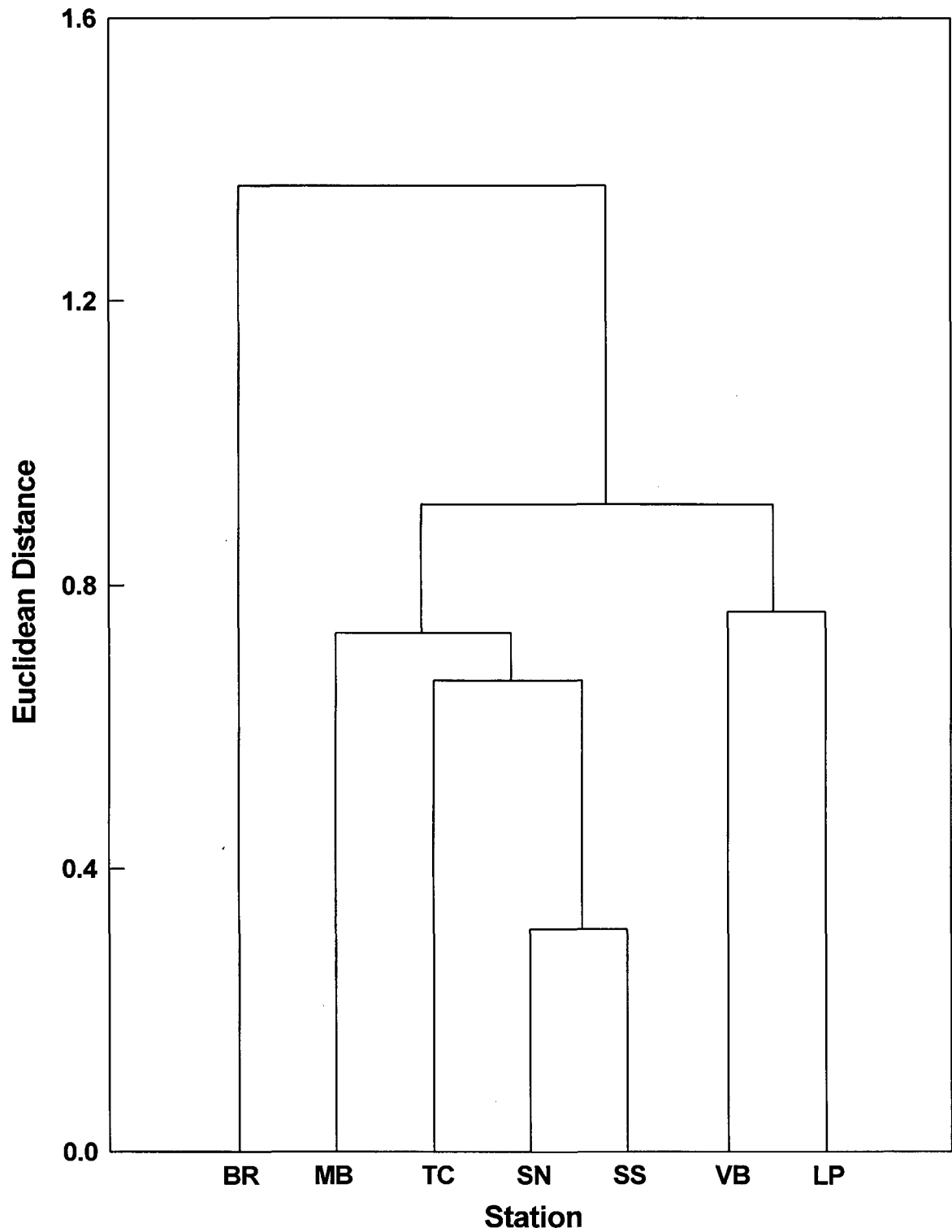


Fig. 3.30 Cluster analysis of IRL stations, based on weekly integrated water quality measurements (Years 1 and 2).

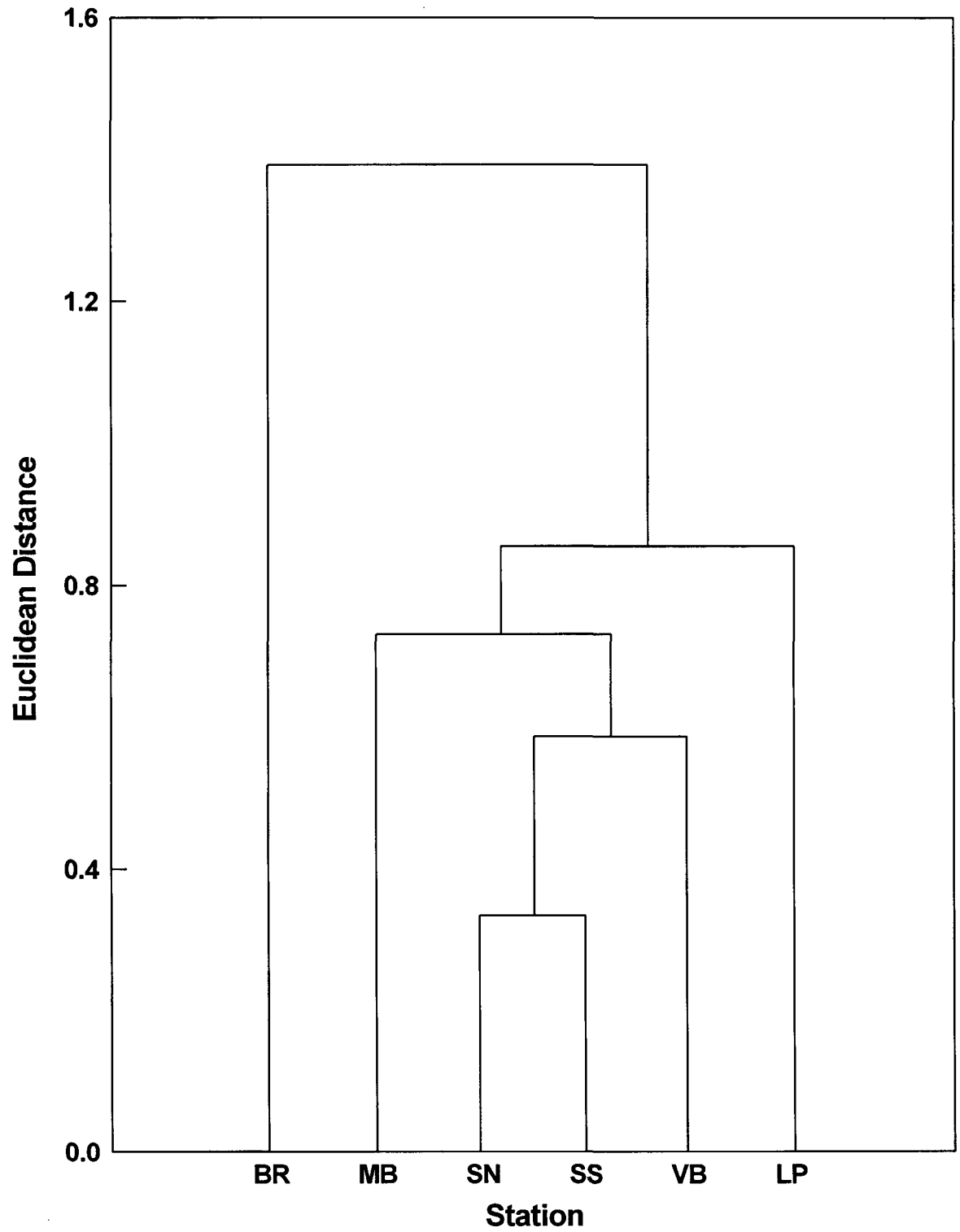


Fig. 3.31 Cluster analysis of IRL stations, based on weekly integrated water quality measurements (Year 1).

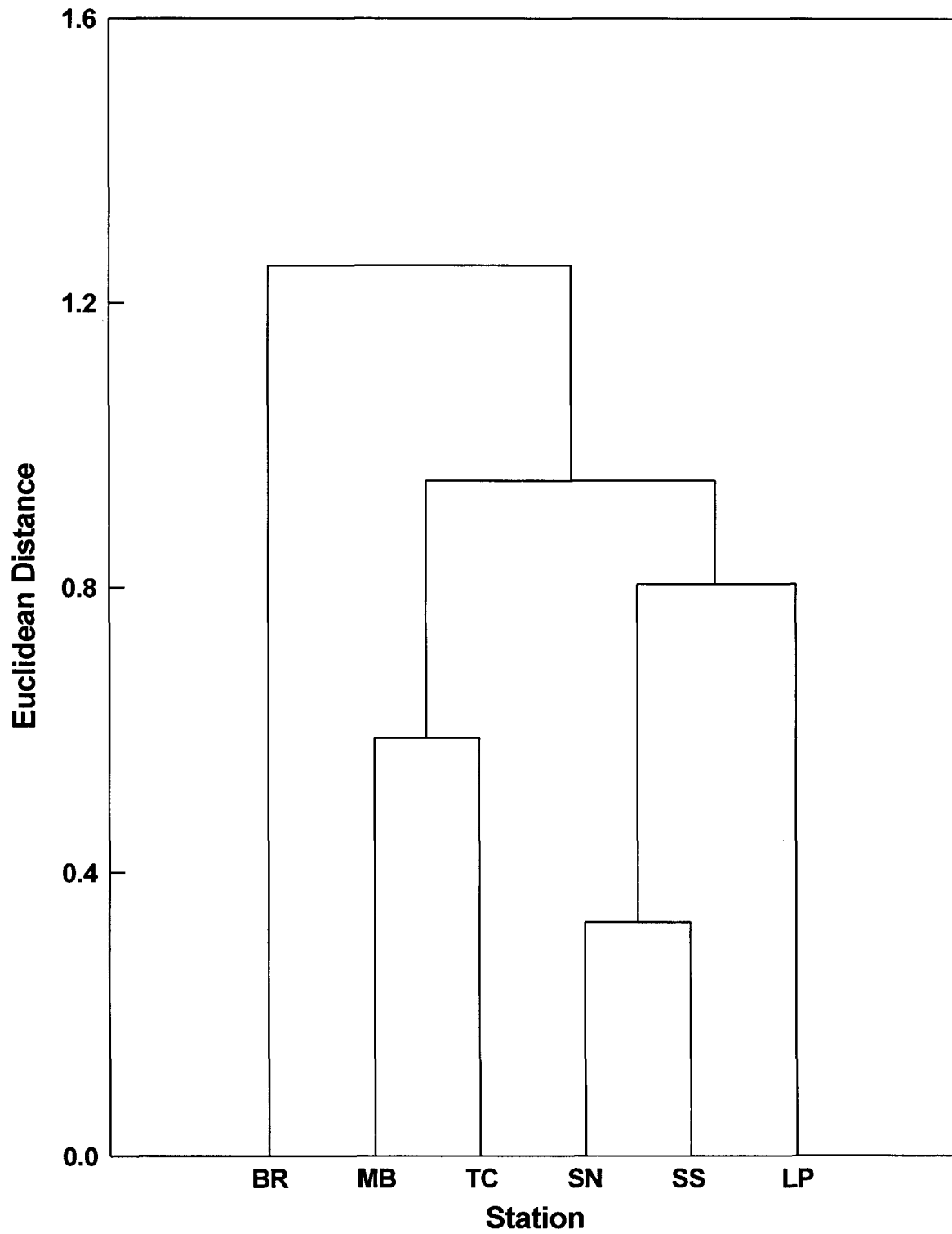


Fig. 3.32 Cluster analysis of IRL stations, based on weekly integrated water quality measurements (Year 2).

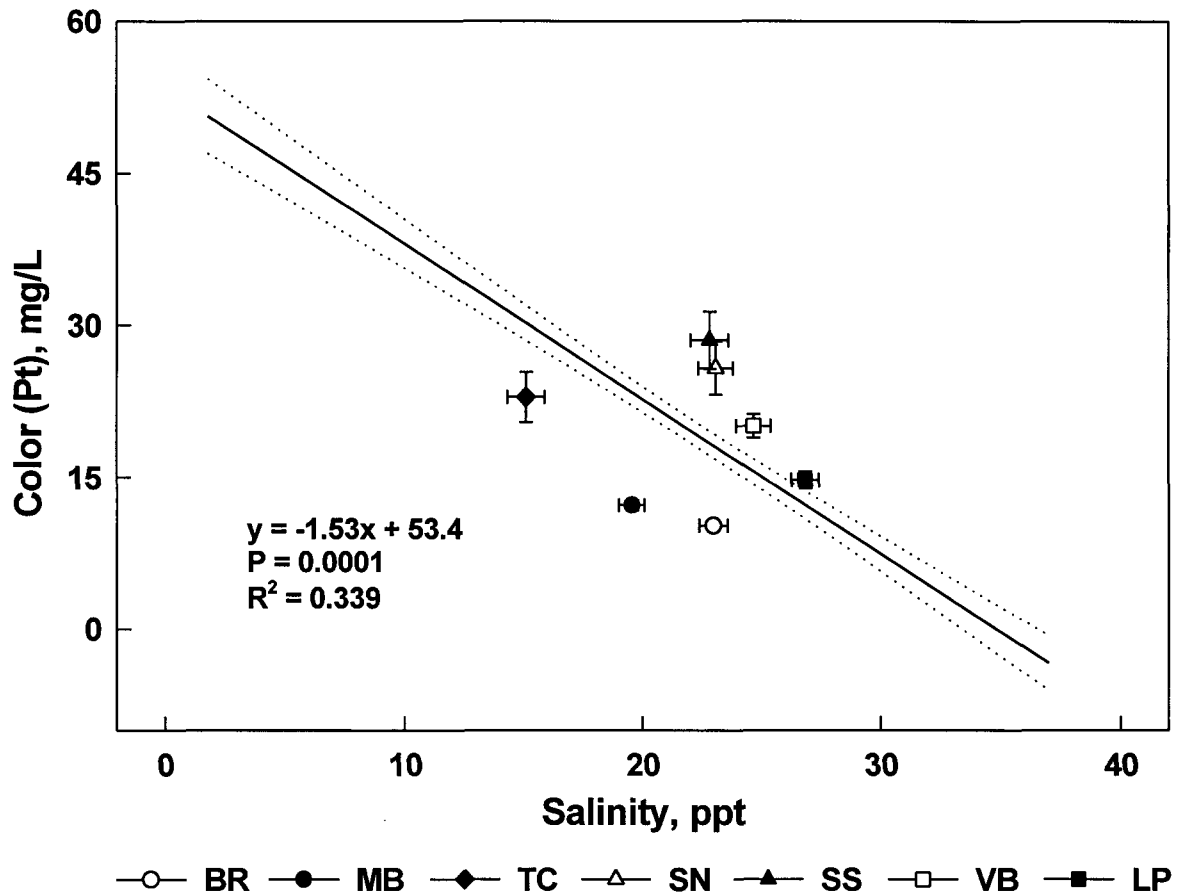


Fig. 3.33 Linear regression analysis of water color vs. salinity for the complete data set (all stations). Station means (\pm SE) for each variable are also presented, but all data were used in the regression model. Dotted lines indicate 95% confidence intervals of the regression line.

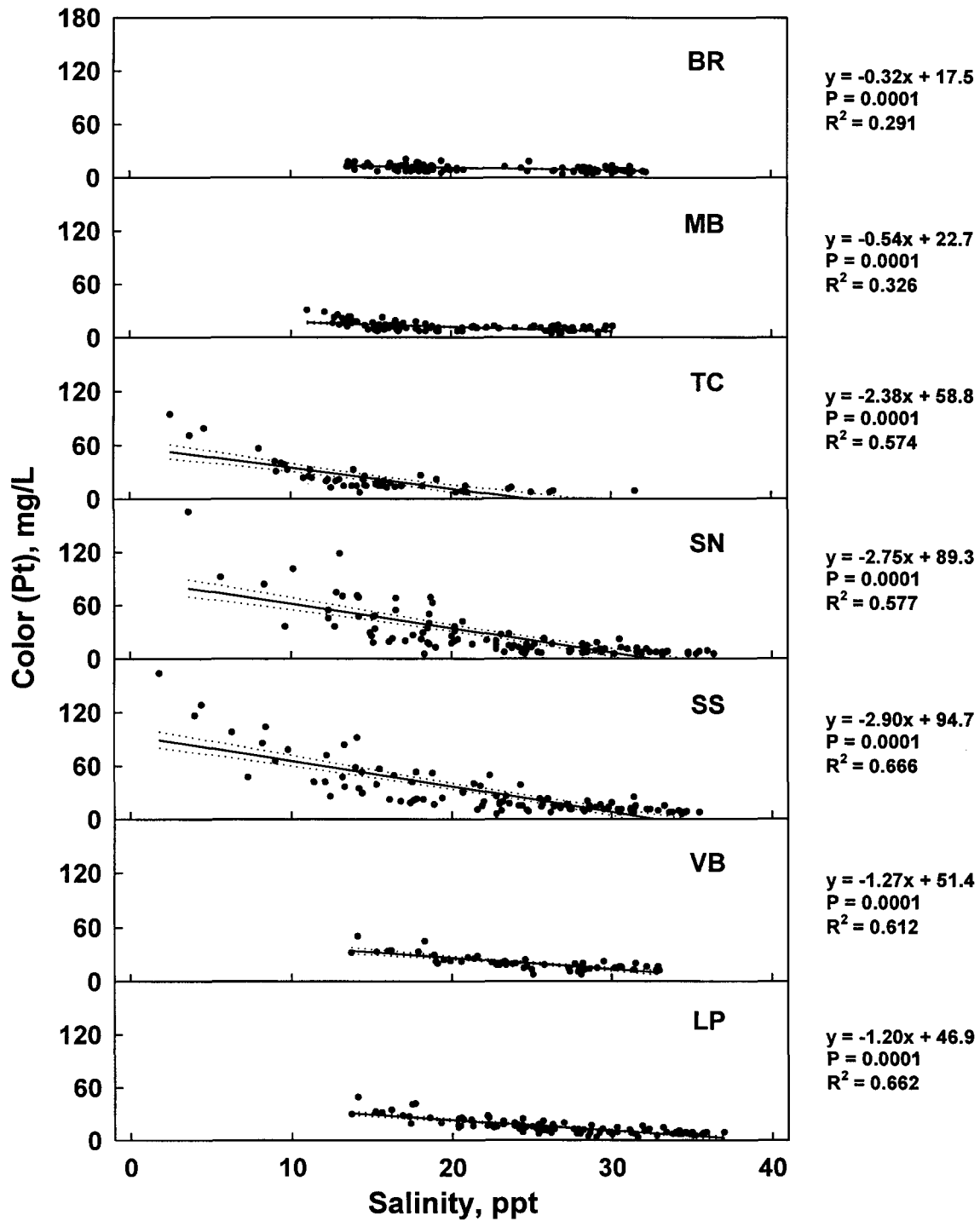


Fig. 3.34 Linear regression analysis of water color vs. salinity for each station. Dotted lines indicate 95% confidence intervals of the regression line.

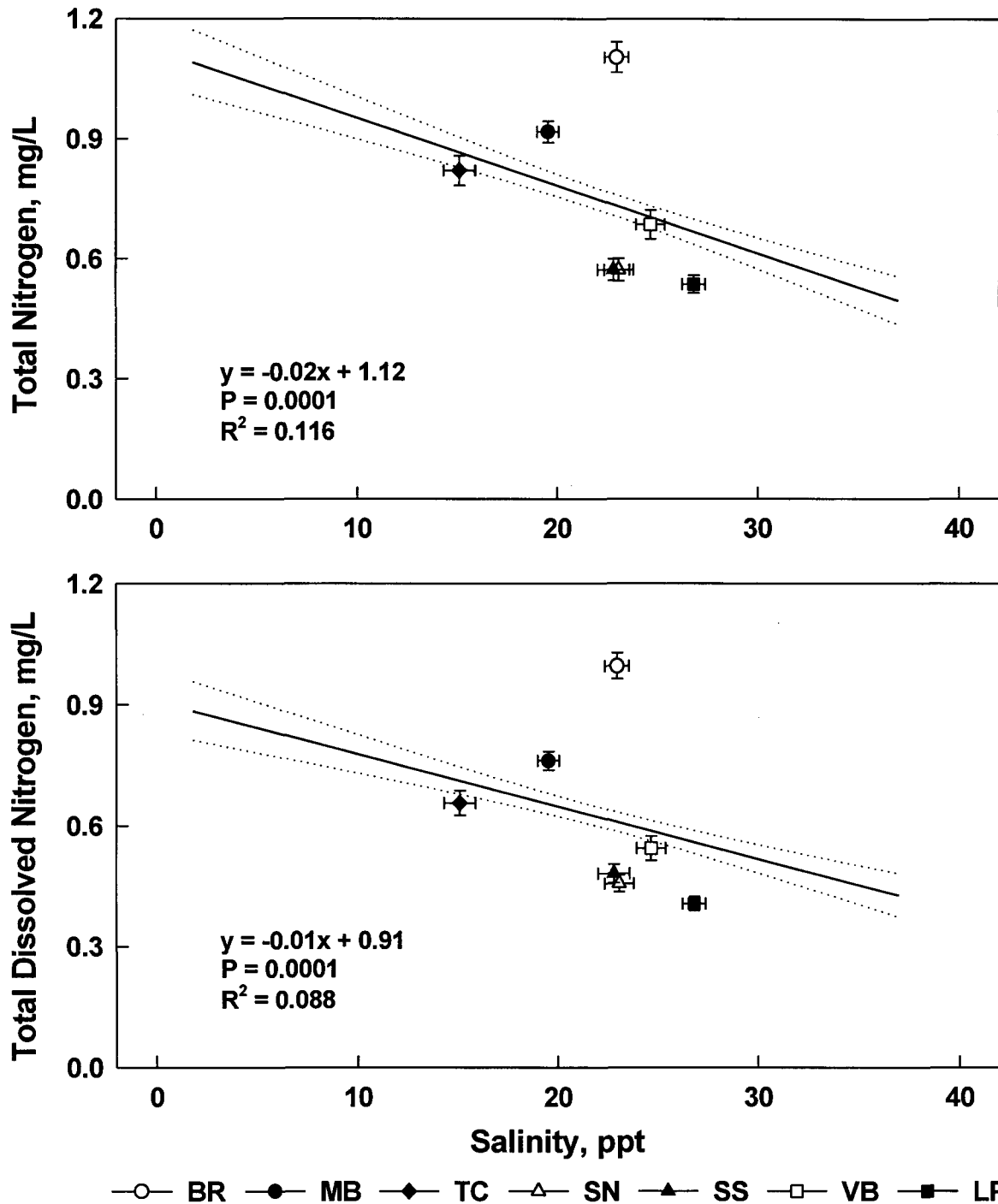


Fig. 3.35 Linear regression analyses of total and total dissolved nitrogen vs. salinity for the complete data set (all stations). Station means (\pm SE) for each variable are also presented, but all data were used in the regression models. Dotted lines indicate 95% confidence intervals of the regression line.

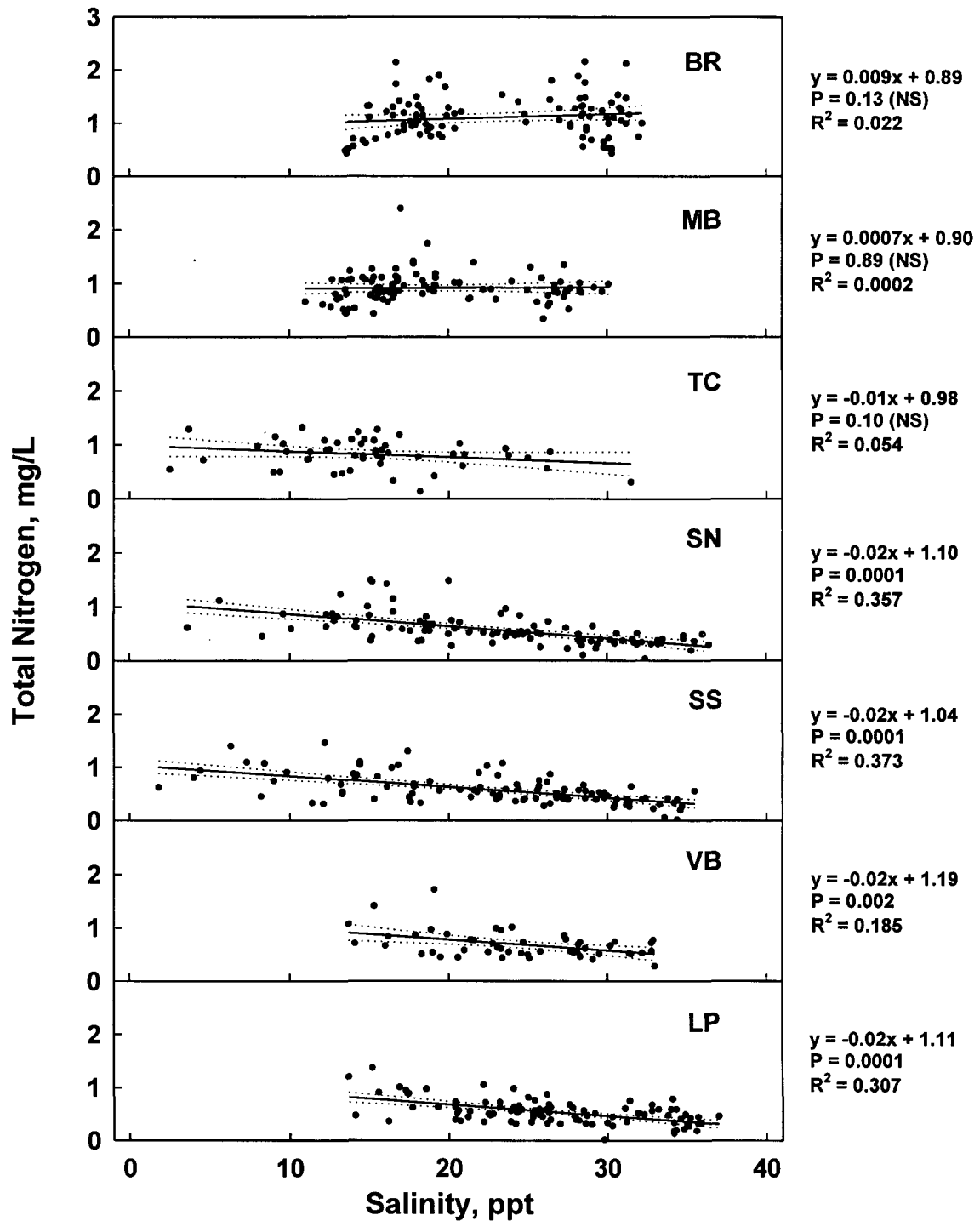


Fig. 3.36 Linear regression analysis of total nitrogen vs. salinity for each station. Dotted lines indicate 95% confidence intervals of the regression line.

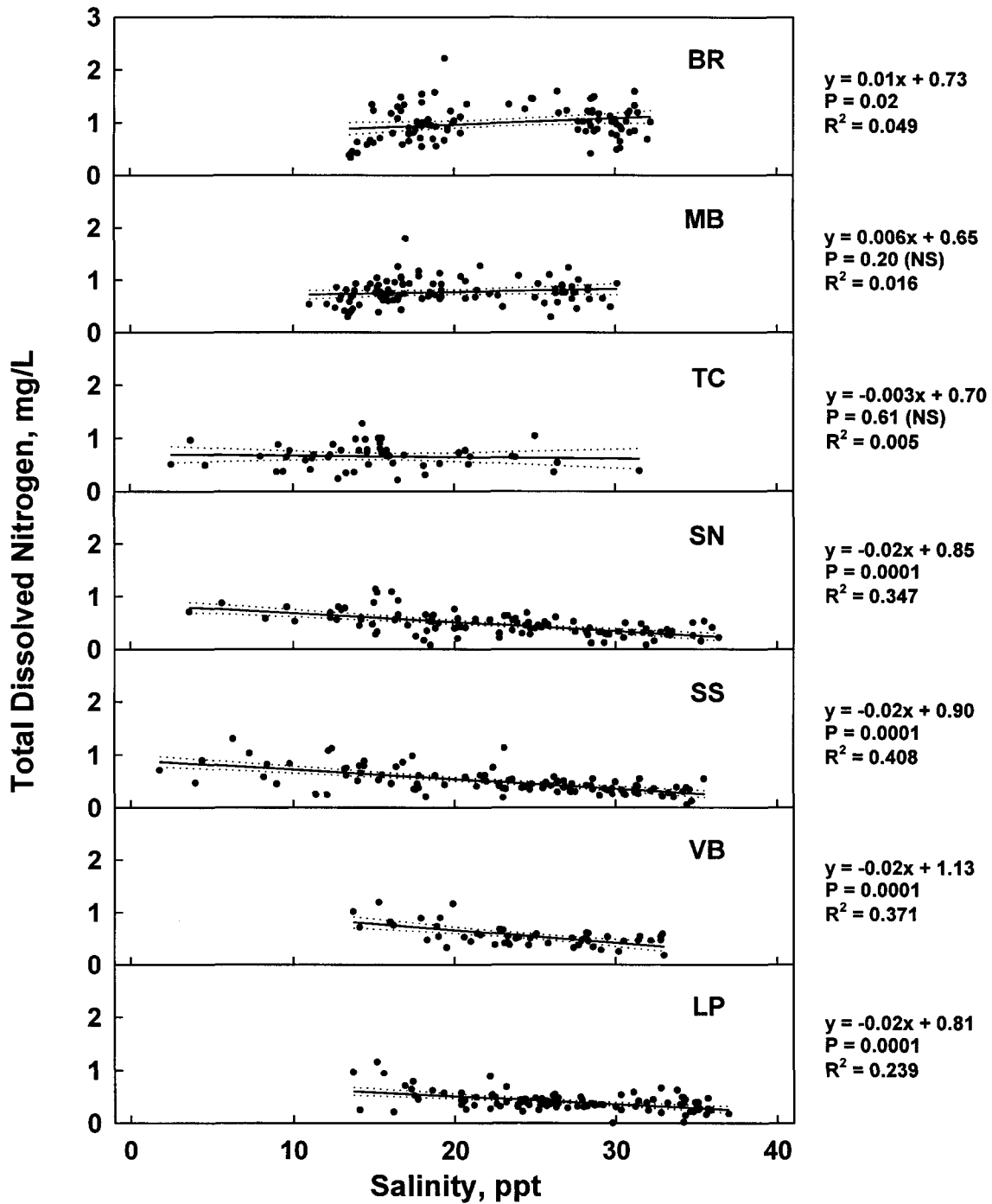


Fig. 3.37 Linear regression analysis of total dissolved nitrogen vs. salinity for each station. Dotted lines indicate 95% confidence intervals of the regression line.

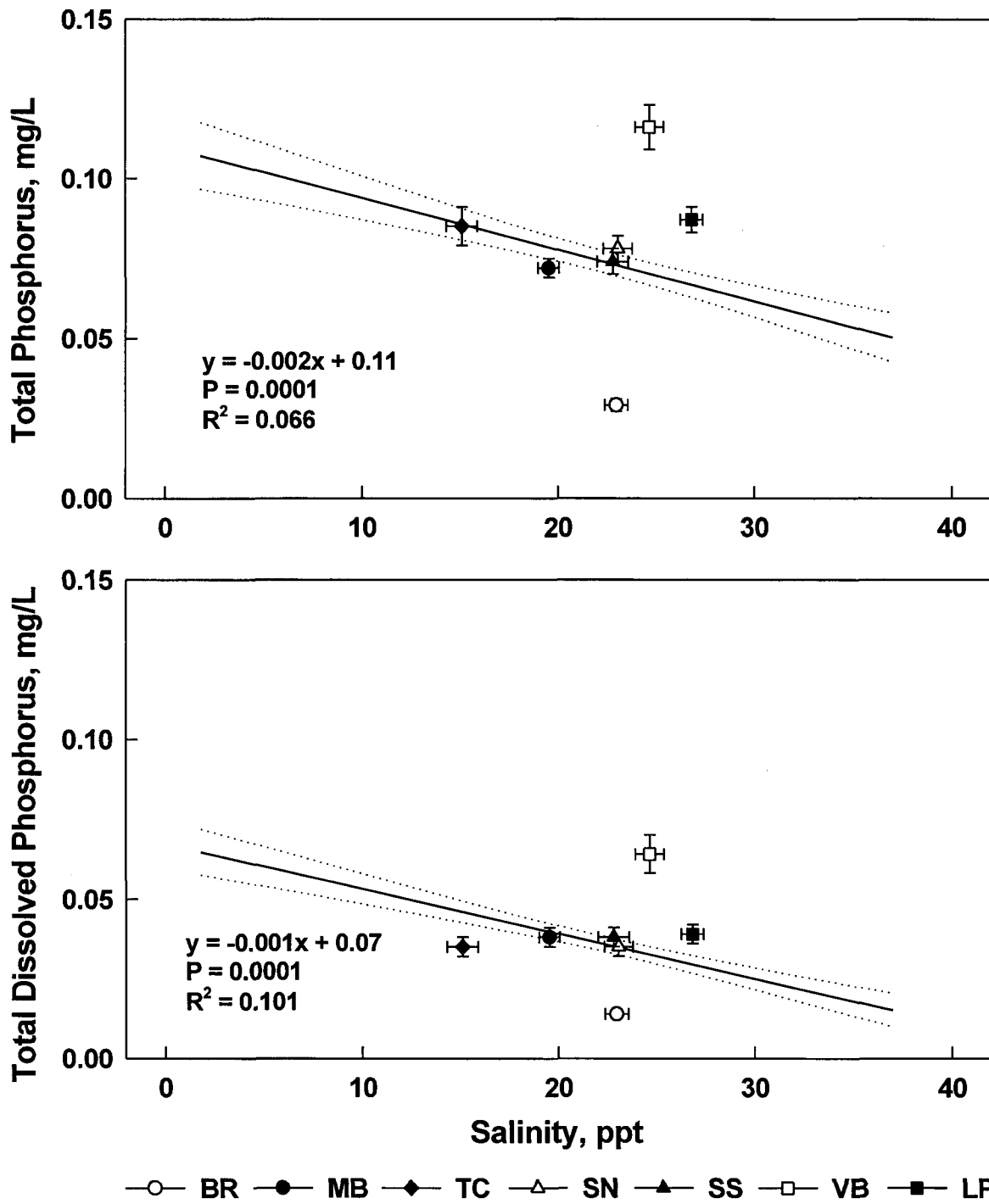


Fig. 3.38 Linear regression analyses of total and total dissolved phosphorus vs. salinity for the complete data set (all stations). Station means (\pm SE) for each variable are also presented, but all data were used in the regression models. Dotted lines indicate 95% confidence intervals of the regression line.

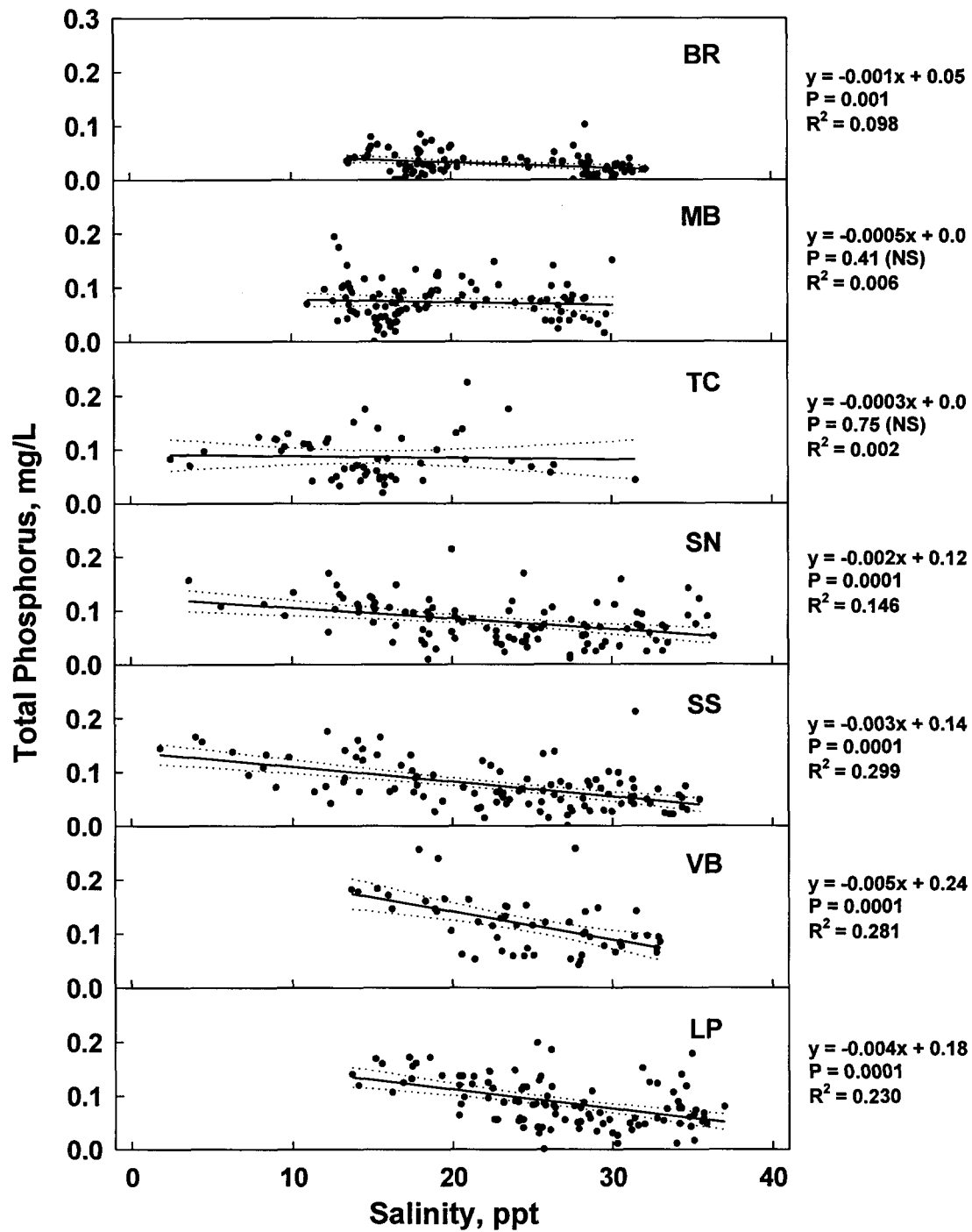


Fig. 3.39 Linear regression analysis of total phosphorus vs. salinity for each station. Dotted lines indicate 95% confidence intervals of the regression line.

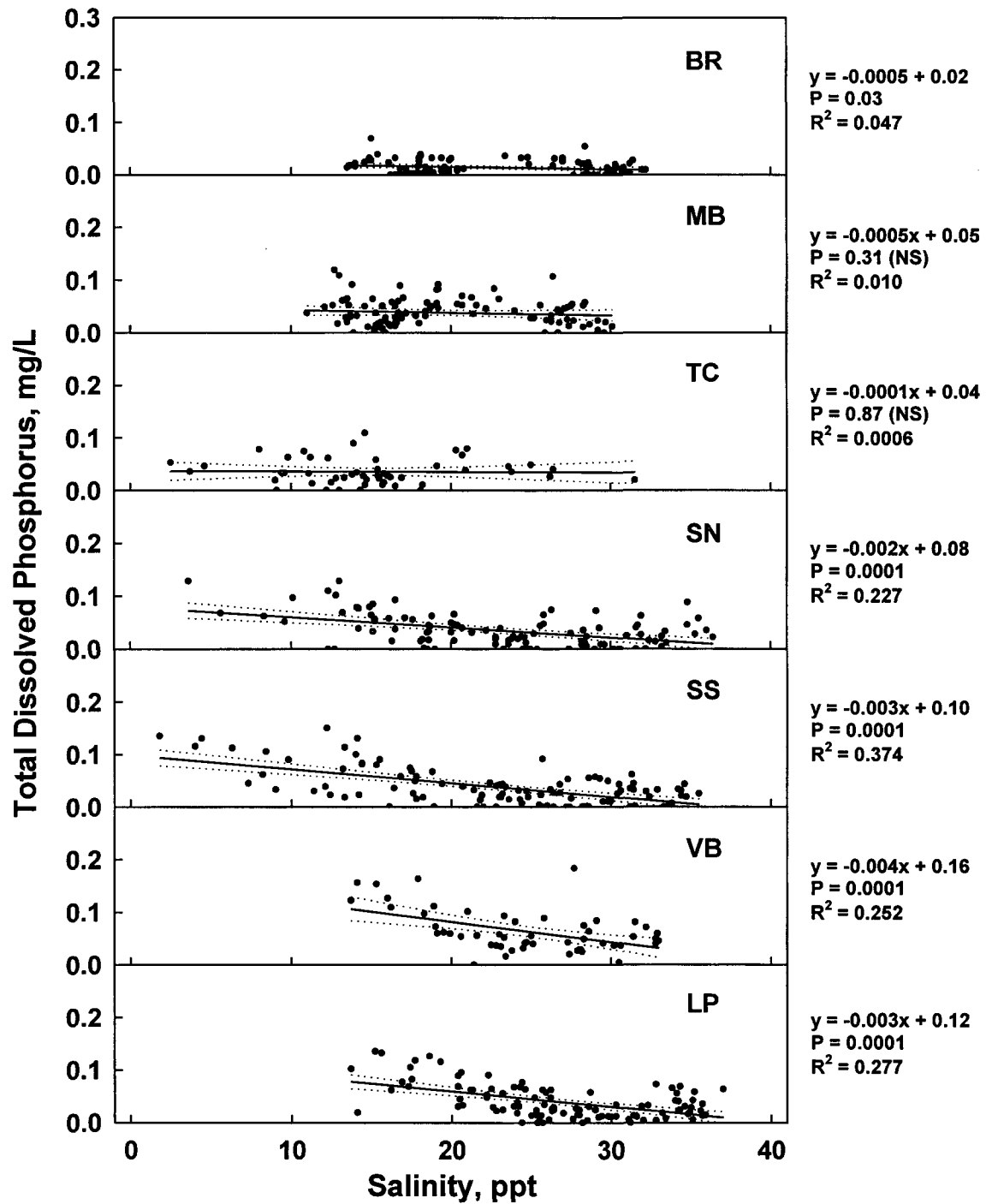


Fig. 3.40 Linear regression analysis of total dissolved phosphorus vs. salinity for each station. Dotted lines indicate 95% confidence intervals of the regression line.

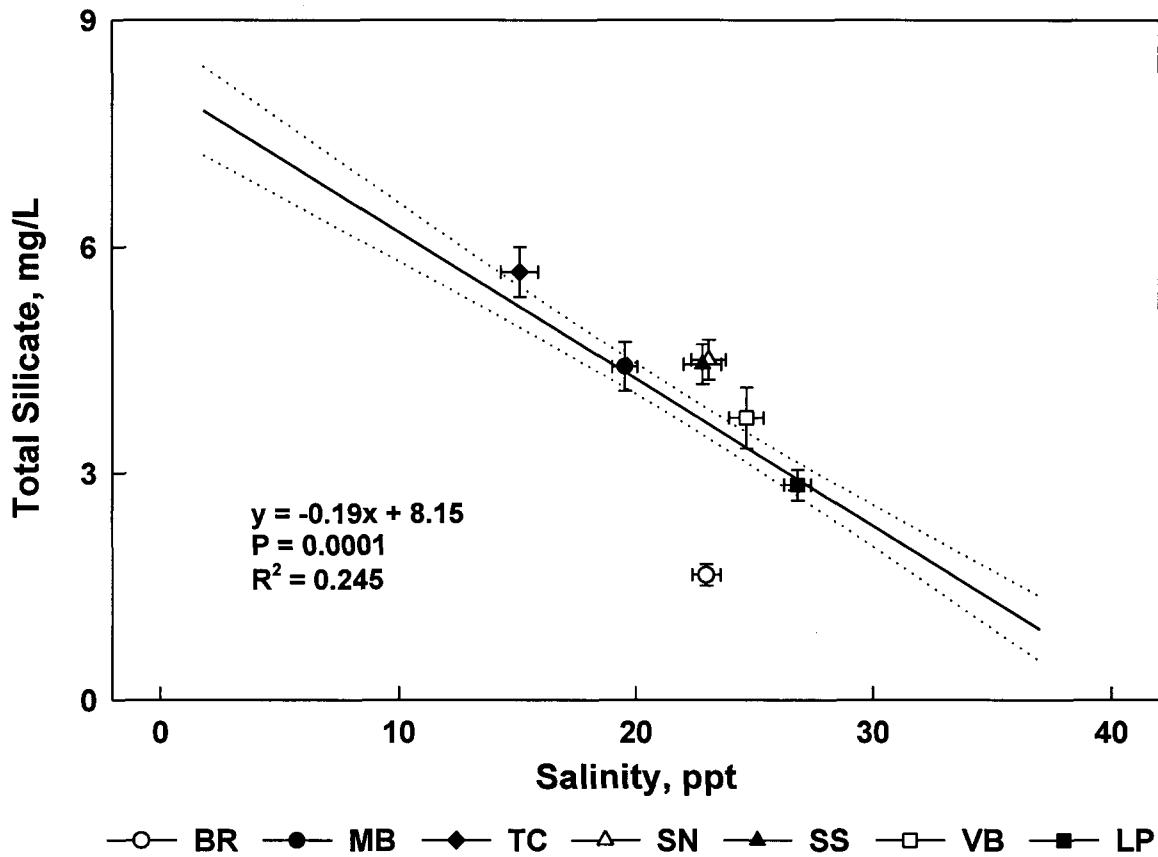


Fig. 3.41 Linear regression analysis of total silicate vs. salinity for the complete data set (all stations). Station means (\pm SE) for each variable are also presented, but all data were used in the regression model. Dotted lines indicate 95% confidence intervals of the regression line.

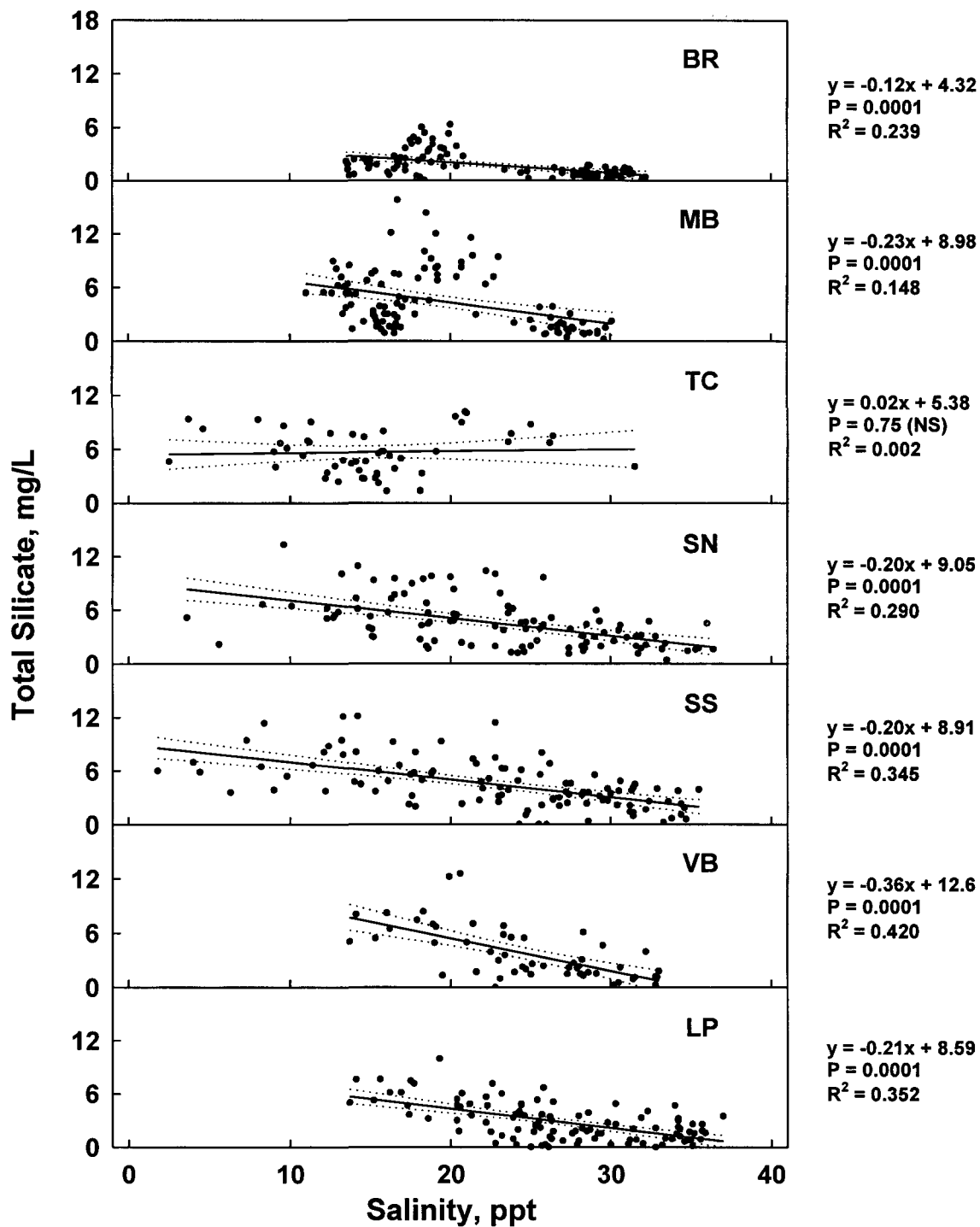


Fig. 3.42 Linear regression analysis of total silicate vs. salinity for each station. Dotted lines indicate 95% confidence intervals of the regression line.

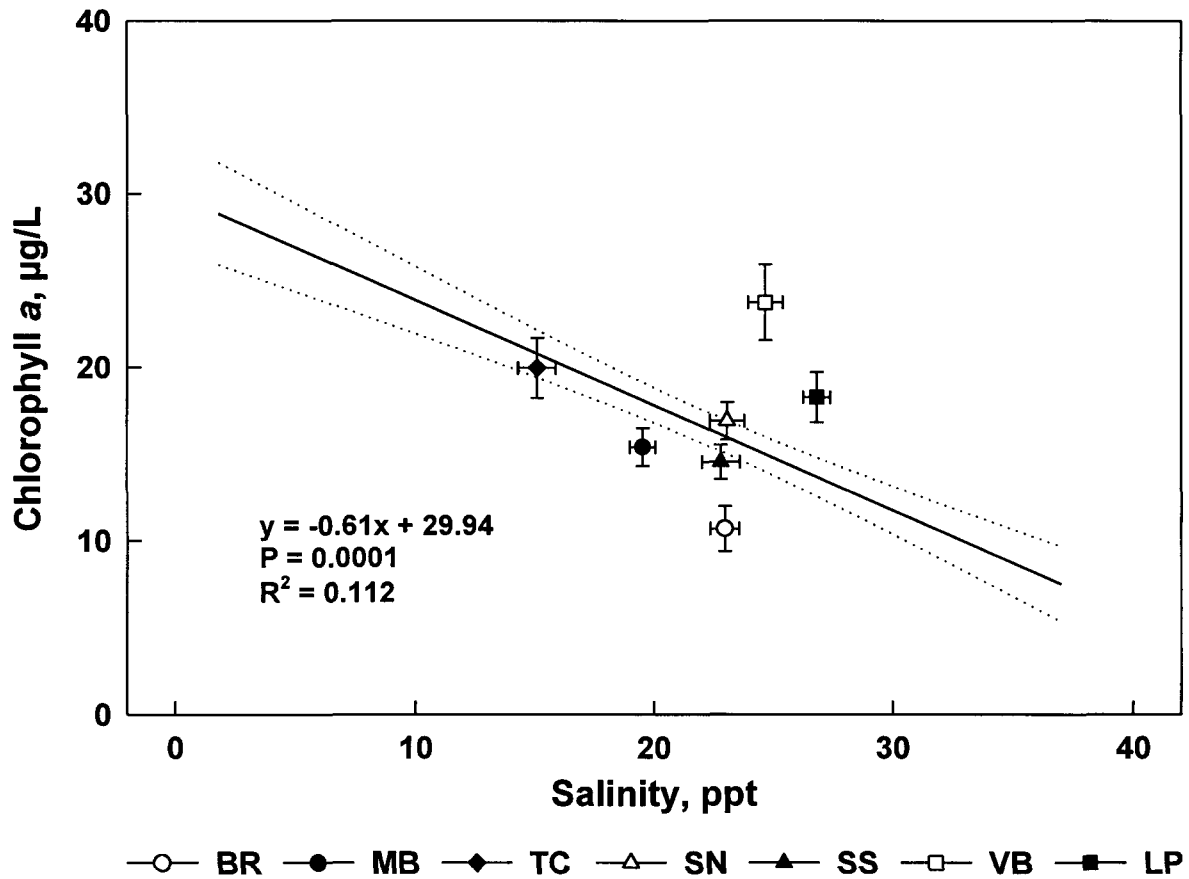


Fig. 3.43 Linear regression analysis of chlorophyll a vs. salinity for the complete data set (all stations). Station means (\pm SE) for each variable are also presented, but all data were used in the regression model. Dotted lines indicate 95% confidence intervals of the regression line.

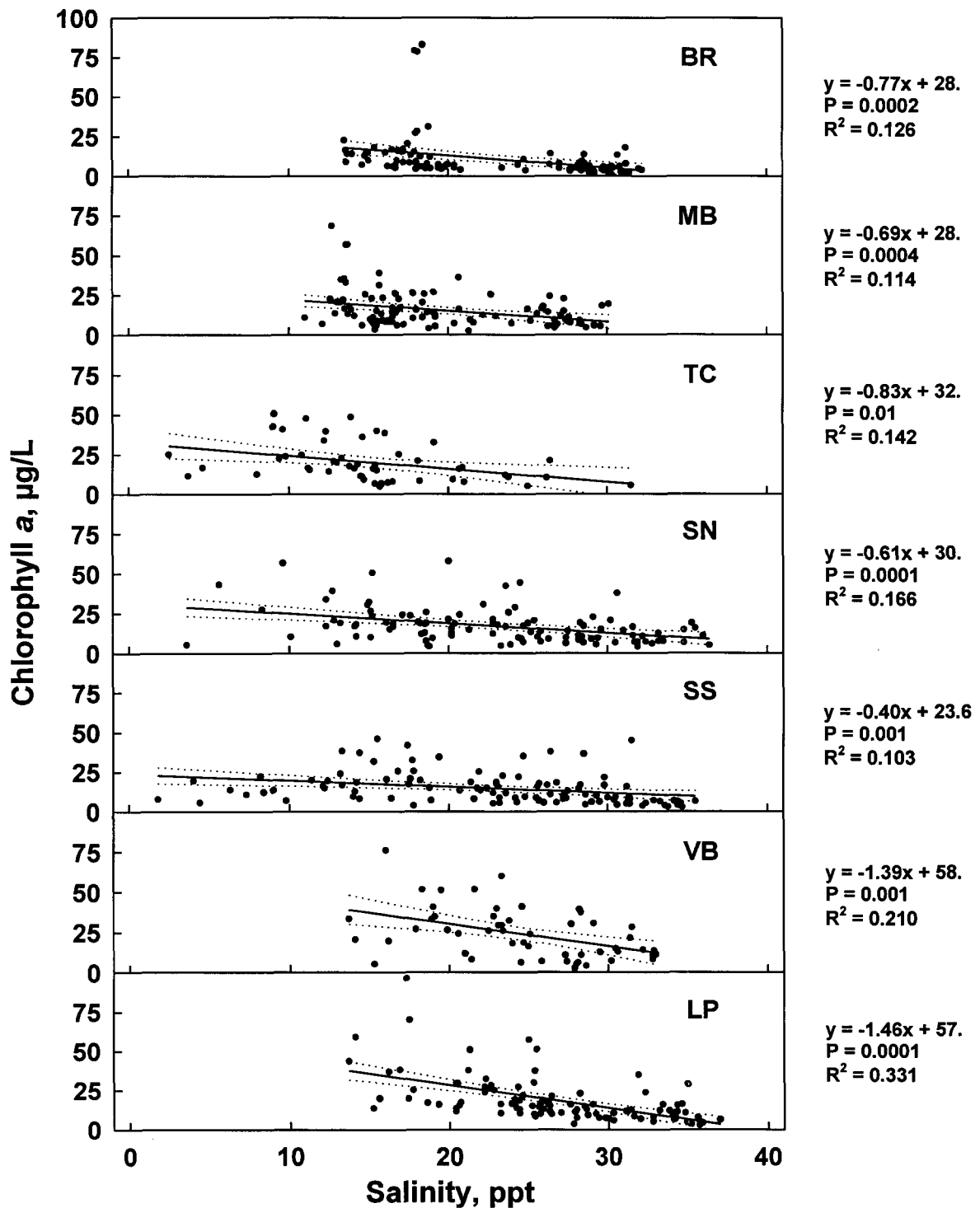


Fig. 3.44 Linear regression analysis of chlorophyll a vs. salinity for each station. Dotted lines indicate 95% confidence intervals of the regression line.

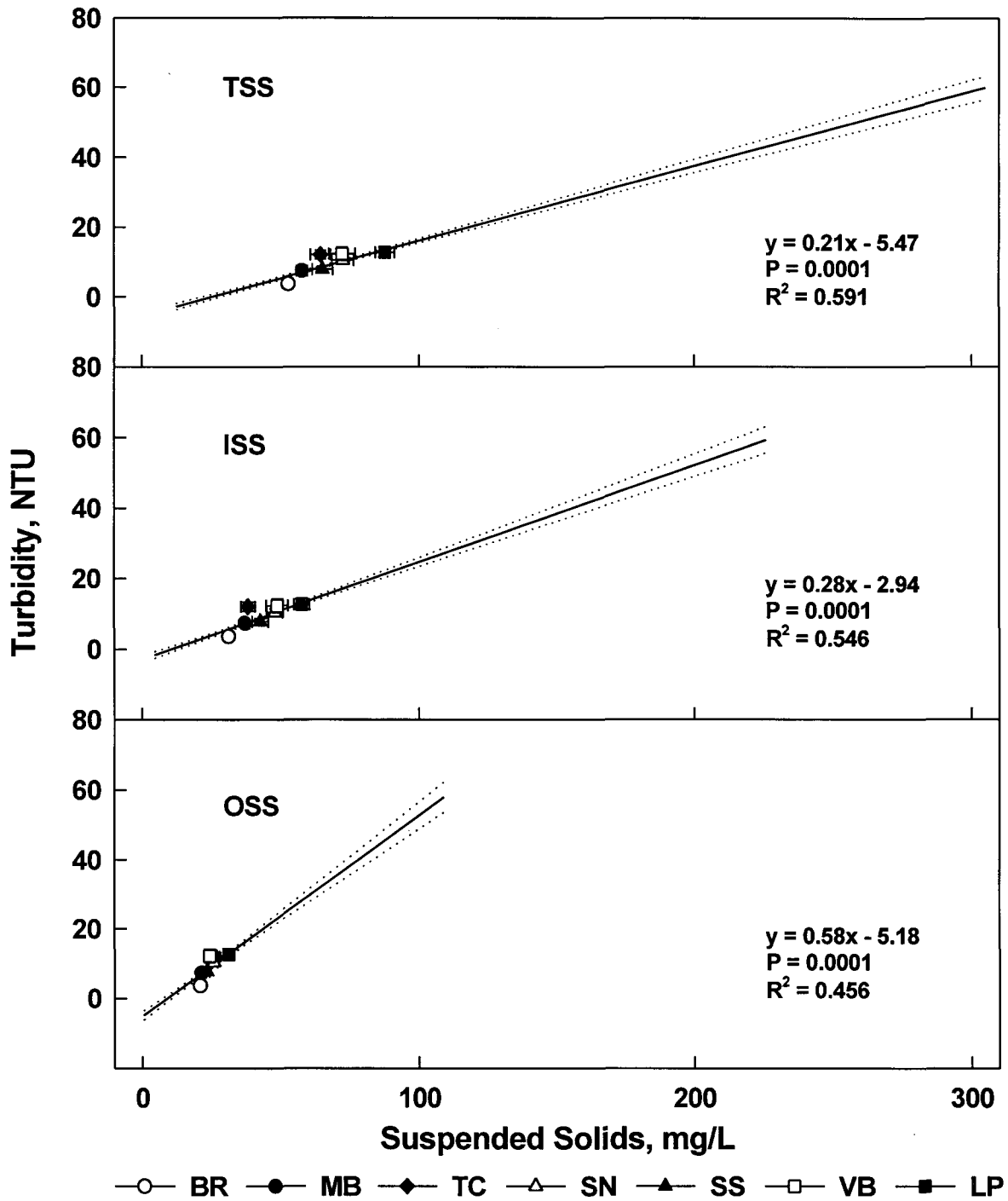


Fig. 3.45 Linear regression analyses of turbidity vs. total (TSS), inorganic (ISS), and organic (OSS) suspended solids for the complete data set (all stations). Station means (+SE) for each variable are also presented, but all data were used in the regression models. Dotted lines indicate 95% confidence intervals of the regression line.

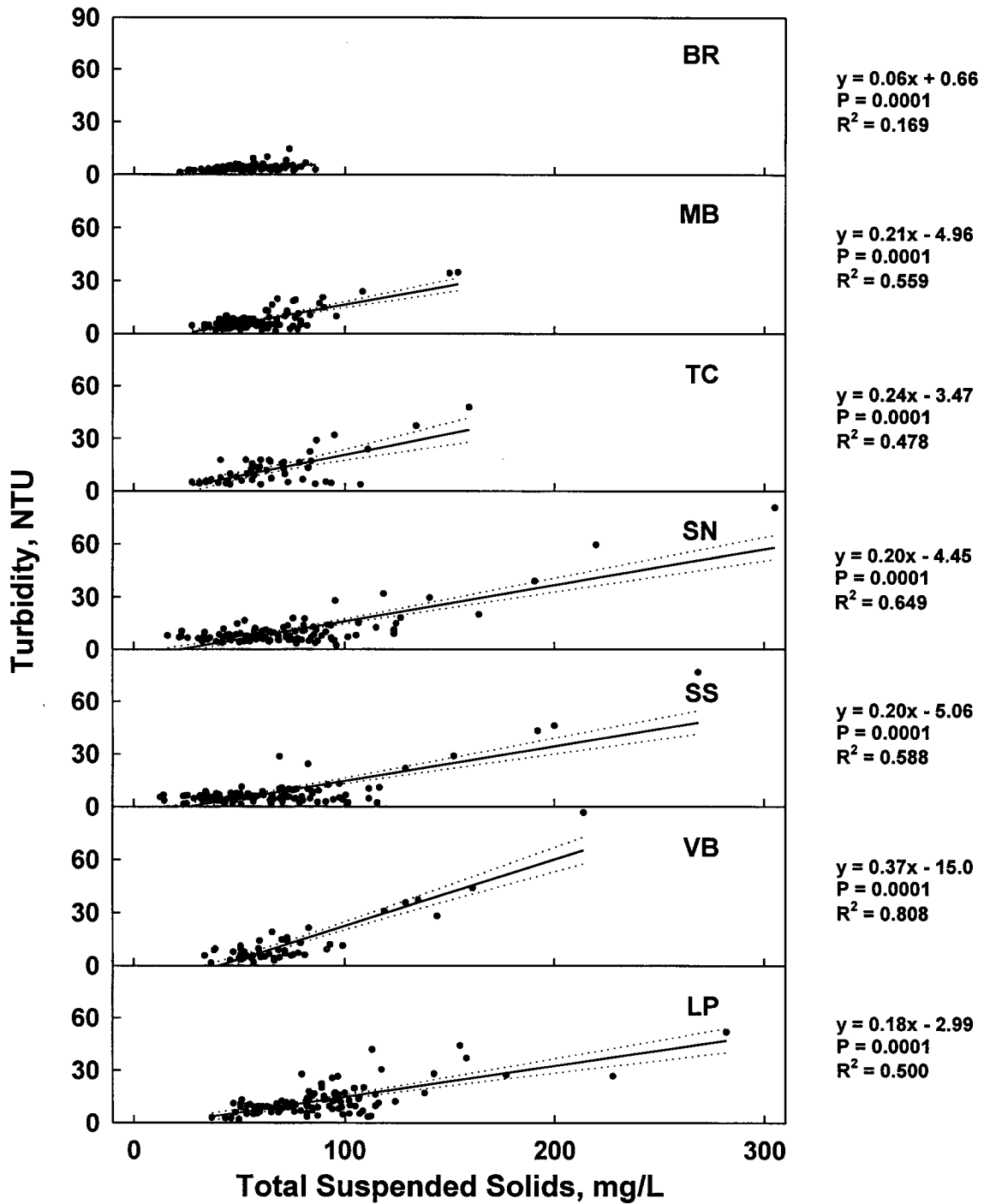


Fig. 3.46 Linear regression analysis of turbidity vs. total suspended solids for each station. Dotted lines indicate 95% confidence intervals of the regression line.

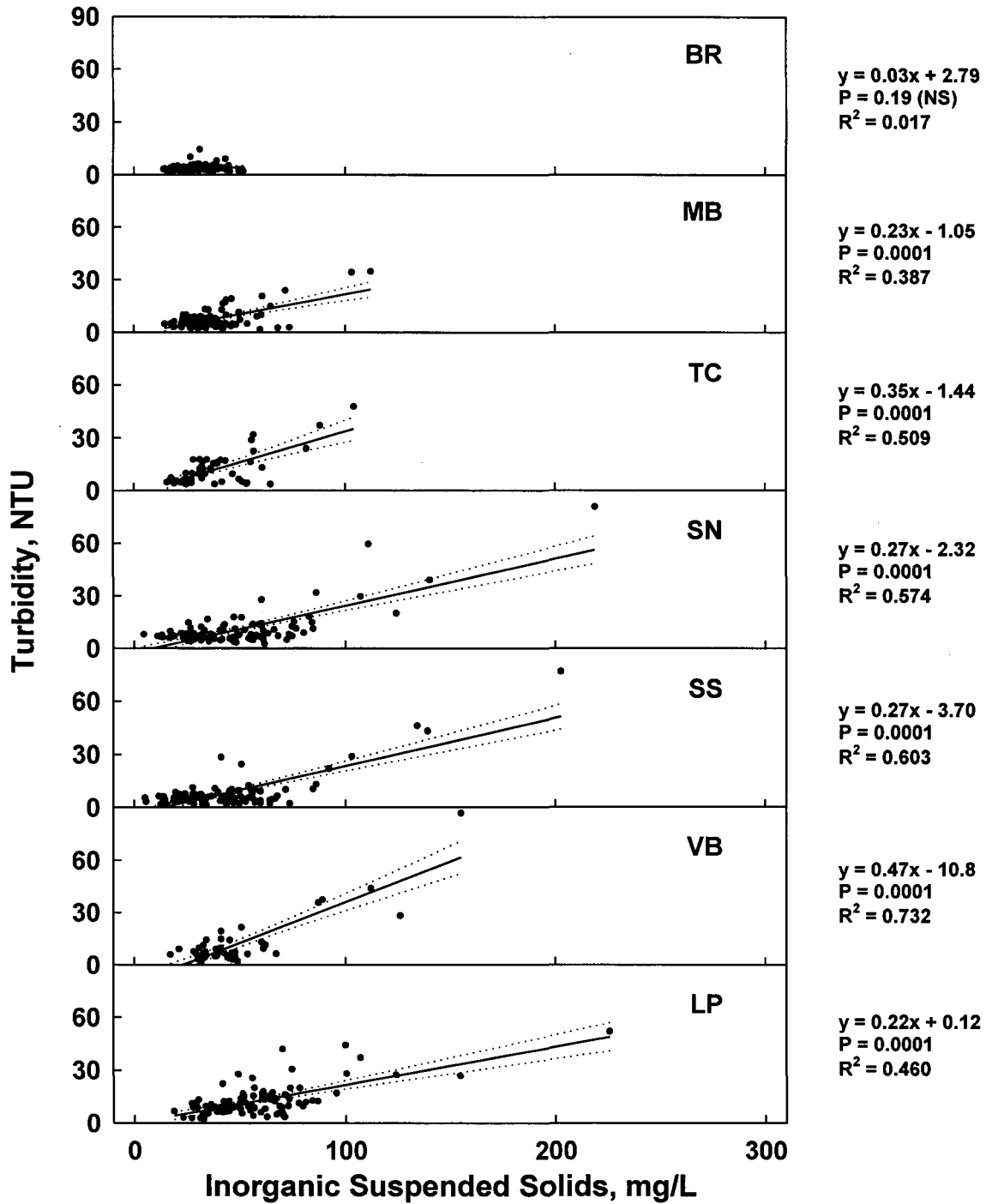


Fig. 3.47 Linear regression analysis of turbidity vs. inorganic suspended solids for each station. Dotted lines indicate 95% confidence intervals of the regression line.

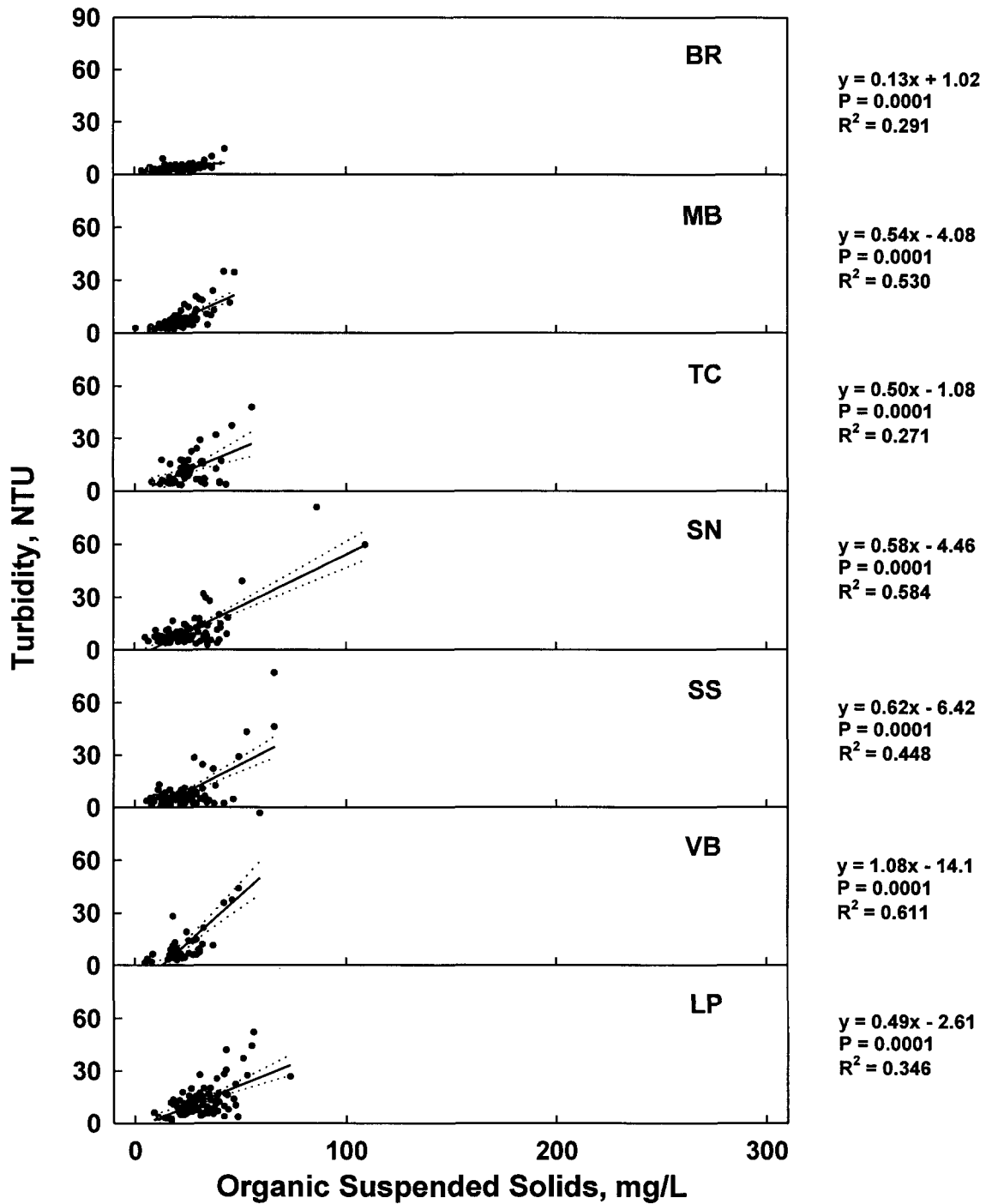


Fig. 3.48 Linear regression analysis of turbidity vs. organic suspended solids for each station. Dotted lines indicate 95% confidence intervals of the regression line.

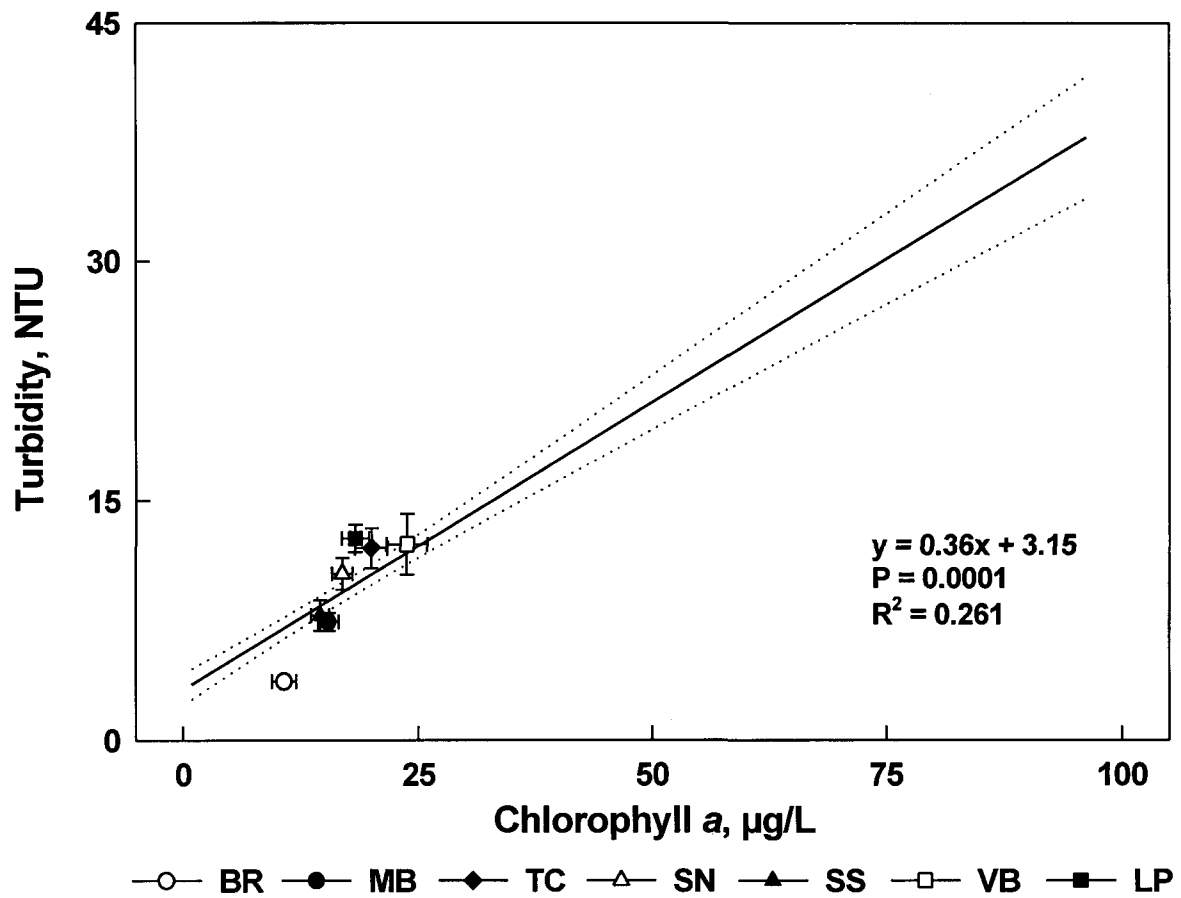


Fig. 3.49 Linear regression analysis of turbidity vs. chlorophyll a for the complete data set (all stations). Station means (\pm SE) for each variable are also presented, but all data were used in the regression model. Dotted lines indicate 95% confidence intervals of the regression line.

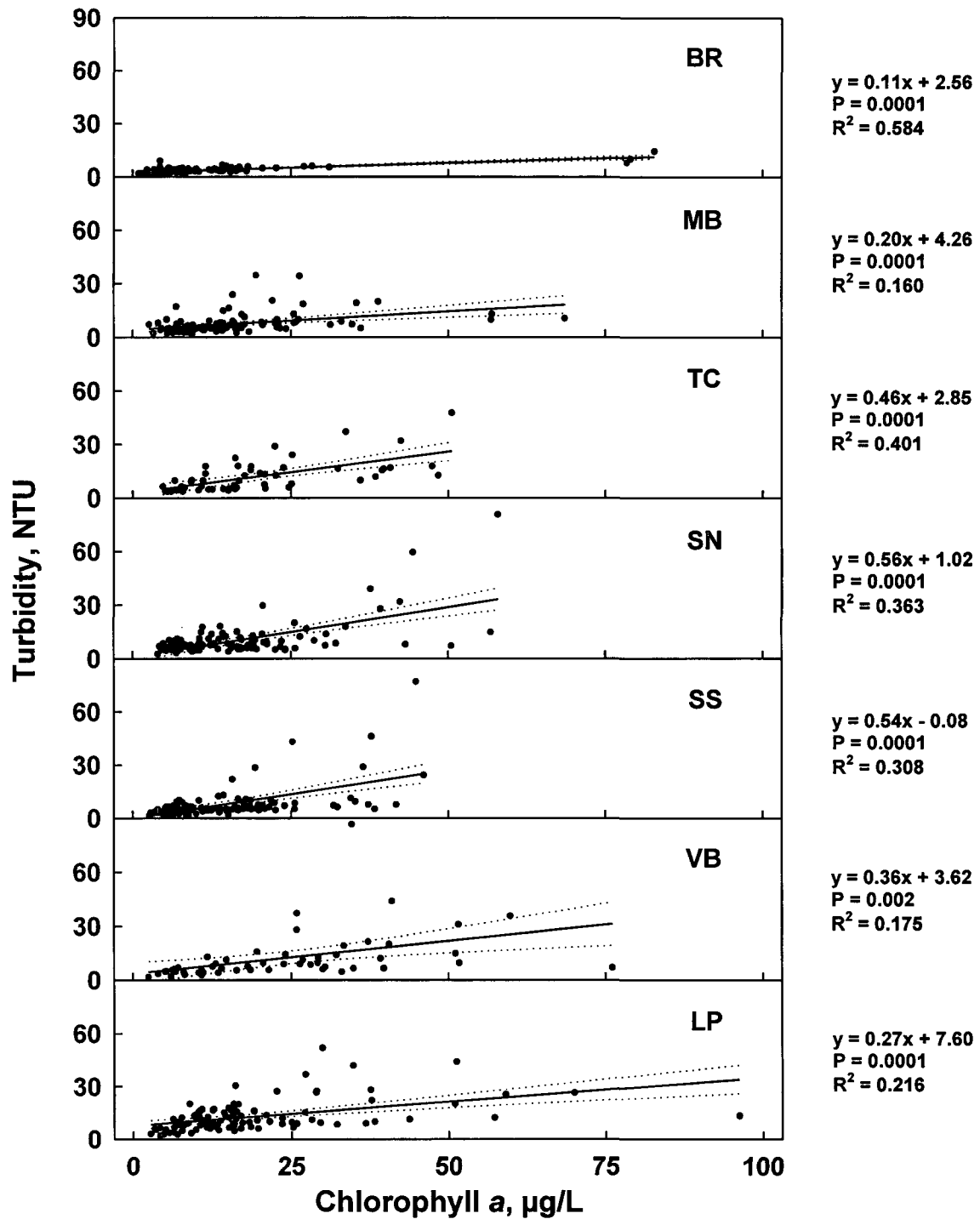


Fig. 3.50 Linear regression analysis of turbidity vs. chlorophyll *a* for each station. Dotted lines indicate 95% confidence intervals of the regression line.

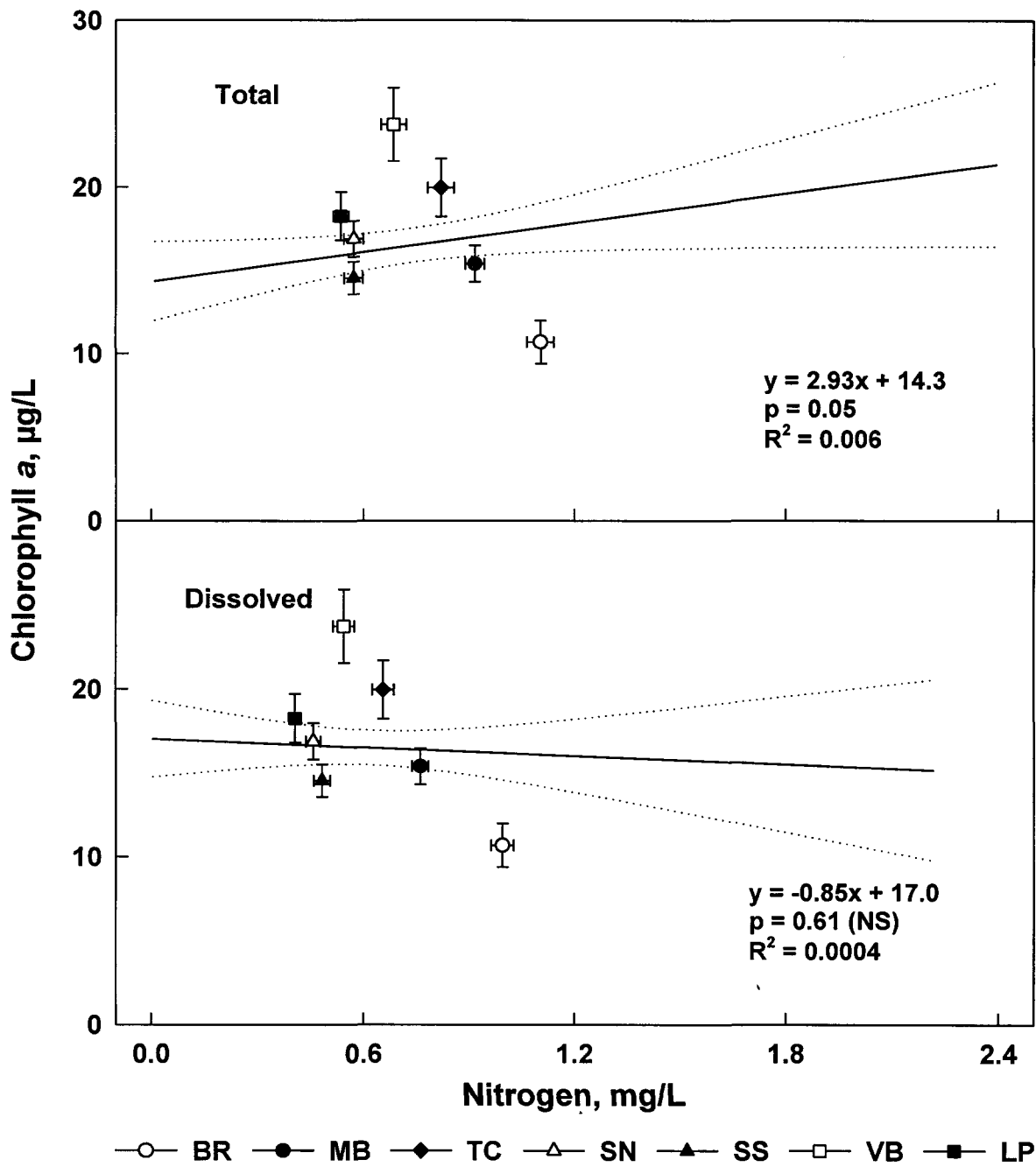


Fig. 3.51 Linear regression analyses of chlorophyll a vs. total (TN) and total dissolved nitrogen (TDN) for the complete data set (all stations). Station means (\pm SE) for each variable are also presented, but all data were used in the regression models. Dotted lines indicate 95% confidence intervals of the regression line.

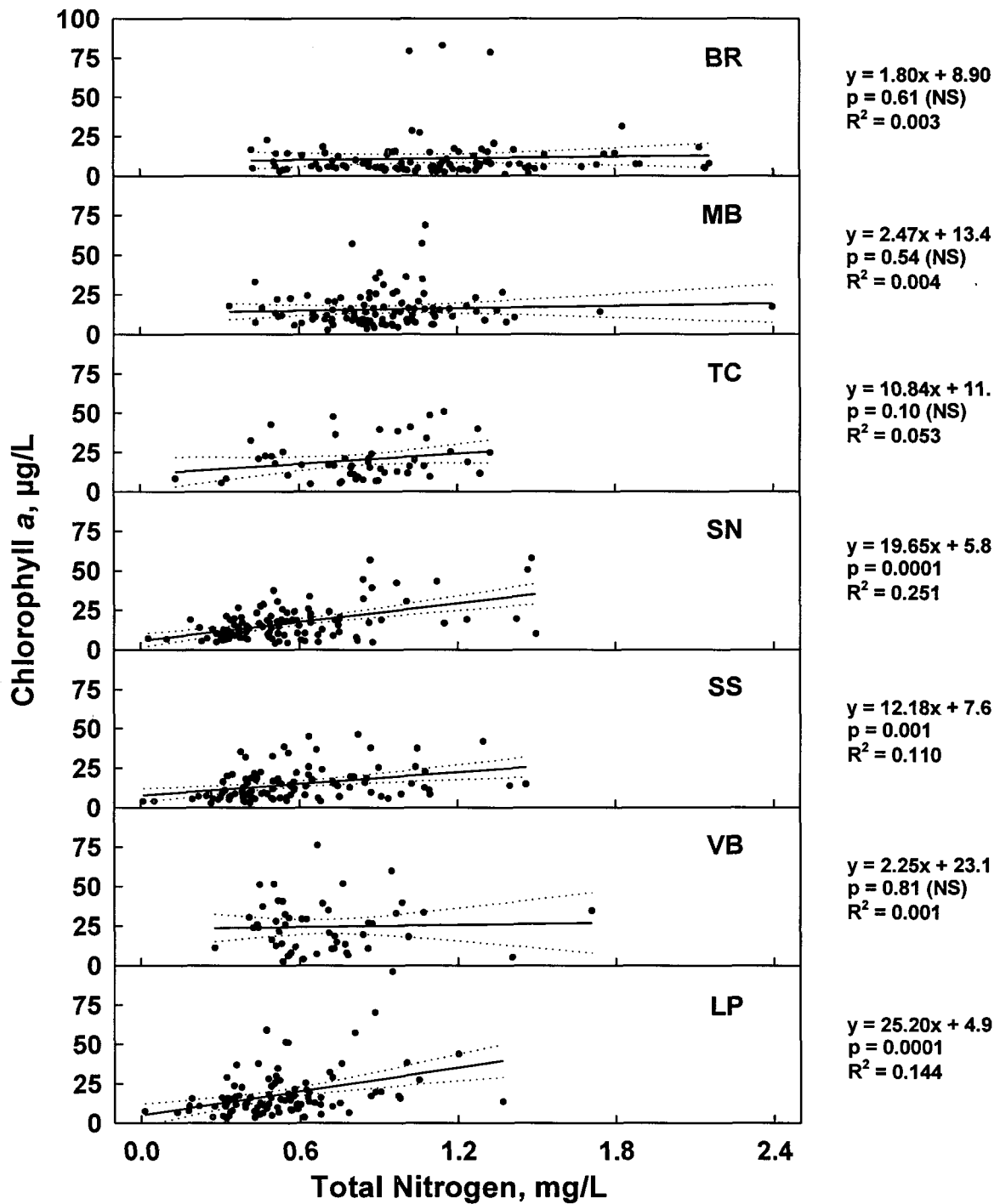


Fig. 3.52 Linear regression analysis of chlorophyll a vs. total nitrogen for each station. Dotted lines indicate 95% confidence intervals of the regression line.

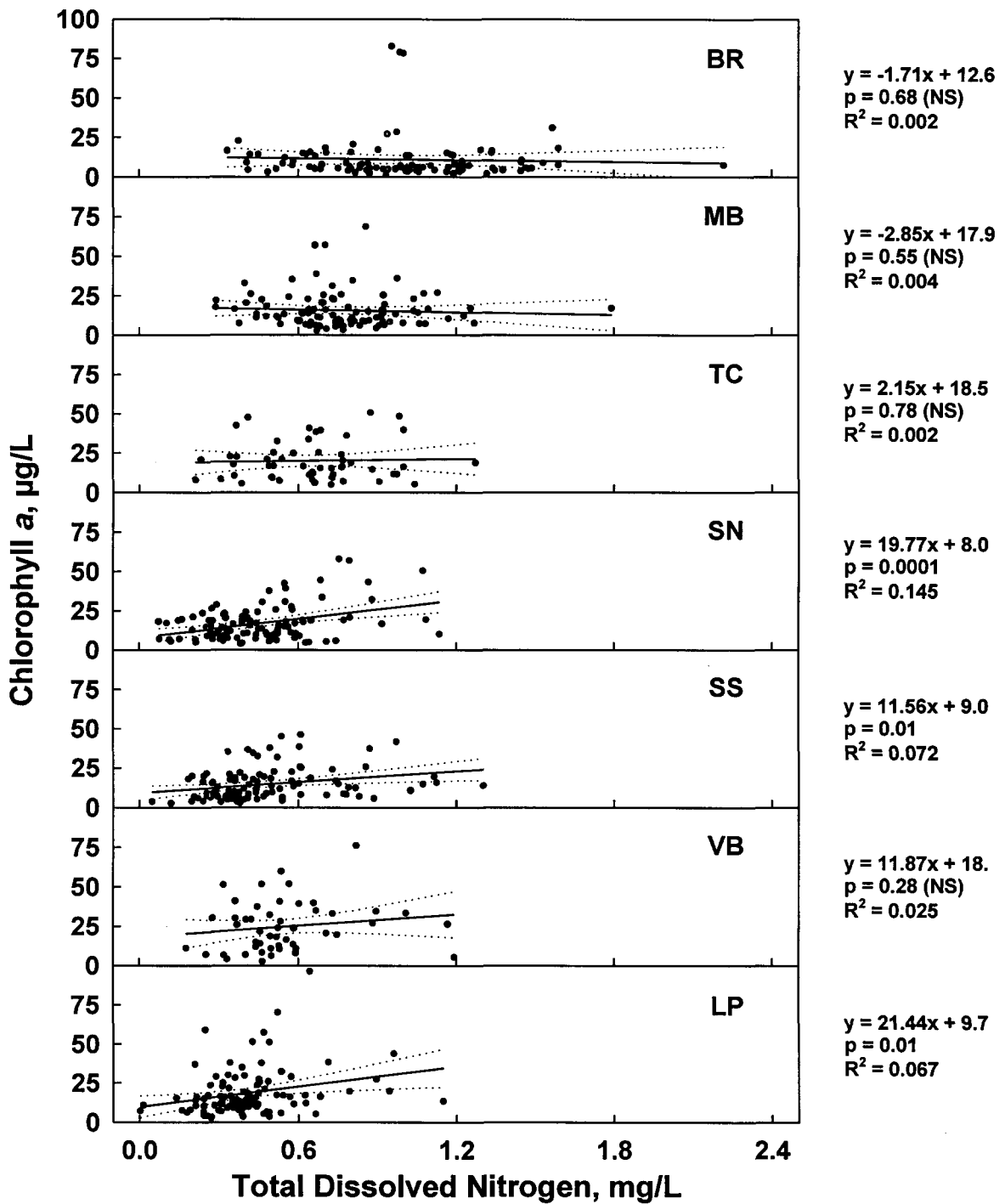


Fig. 3.53 Linear regression analysis of chlorophyll a vs. total dissolved nitrogen for each station. Dotted lines indicate 95% confidence intervals of the regression line.

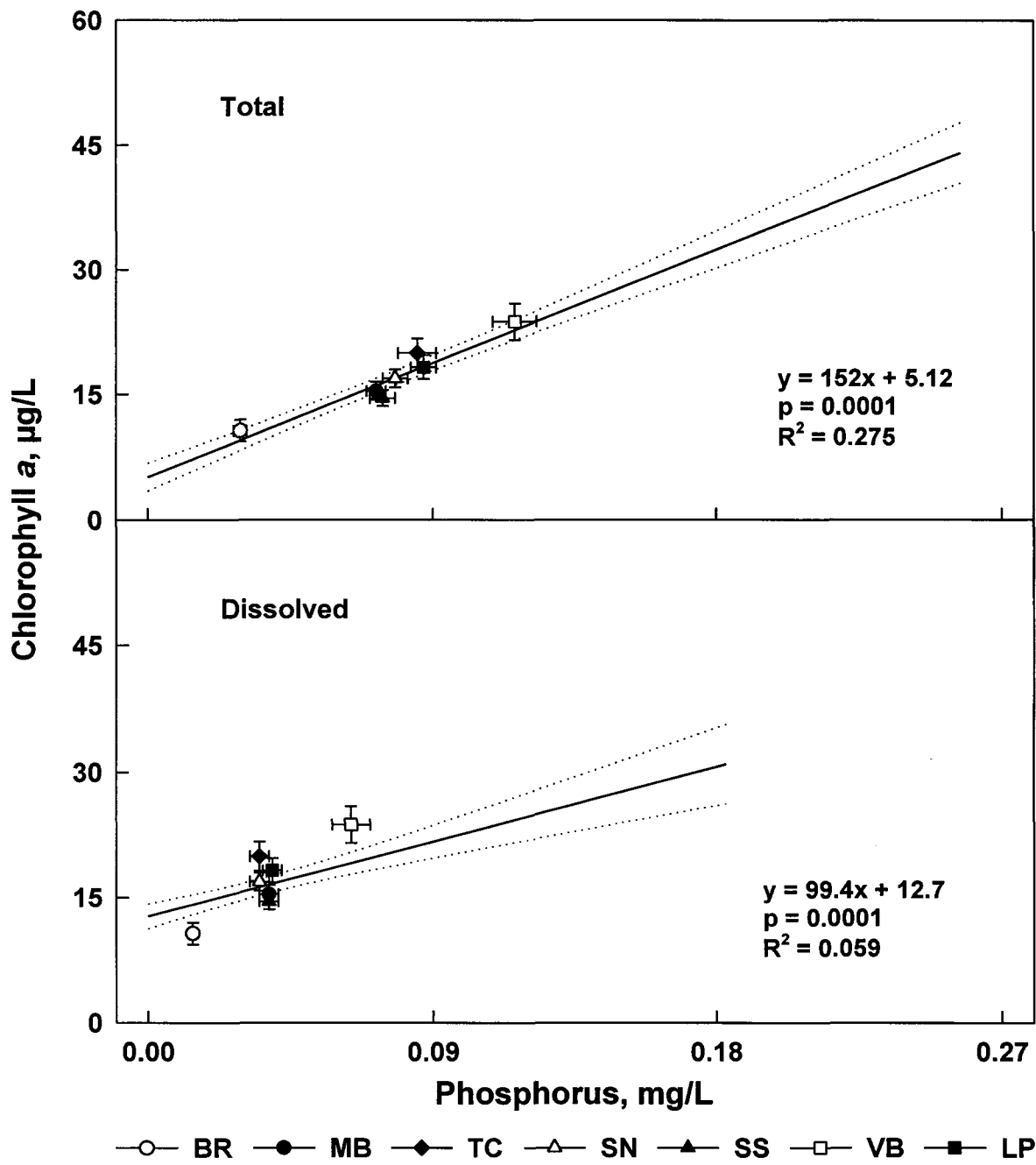


Fig. 3.54 Linear regression analyses of chlorophyll a vs. total (TP) and total dissolved phosphorus (TDP) for the complete data set (all stations). Station means (\pm SE) for each variable are also presented, but all data were used in the regression models. Dotted lines indicate 95% confidence intervals of the regression line.

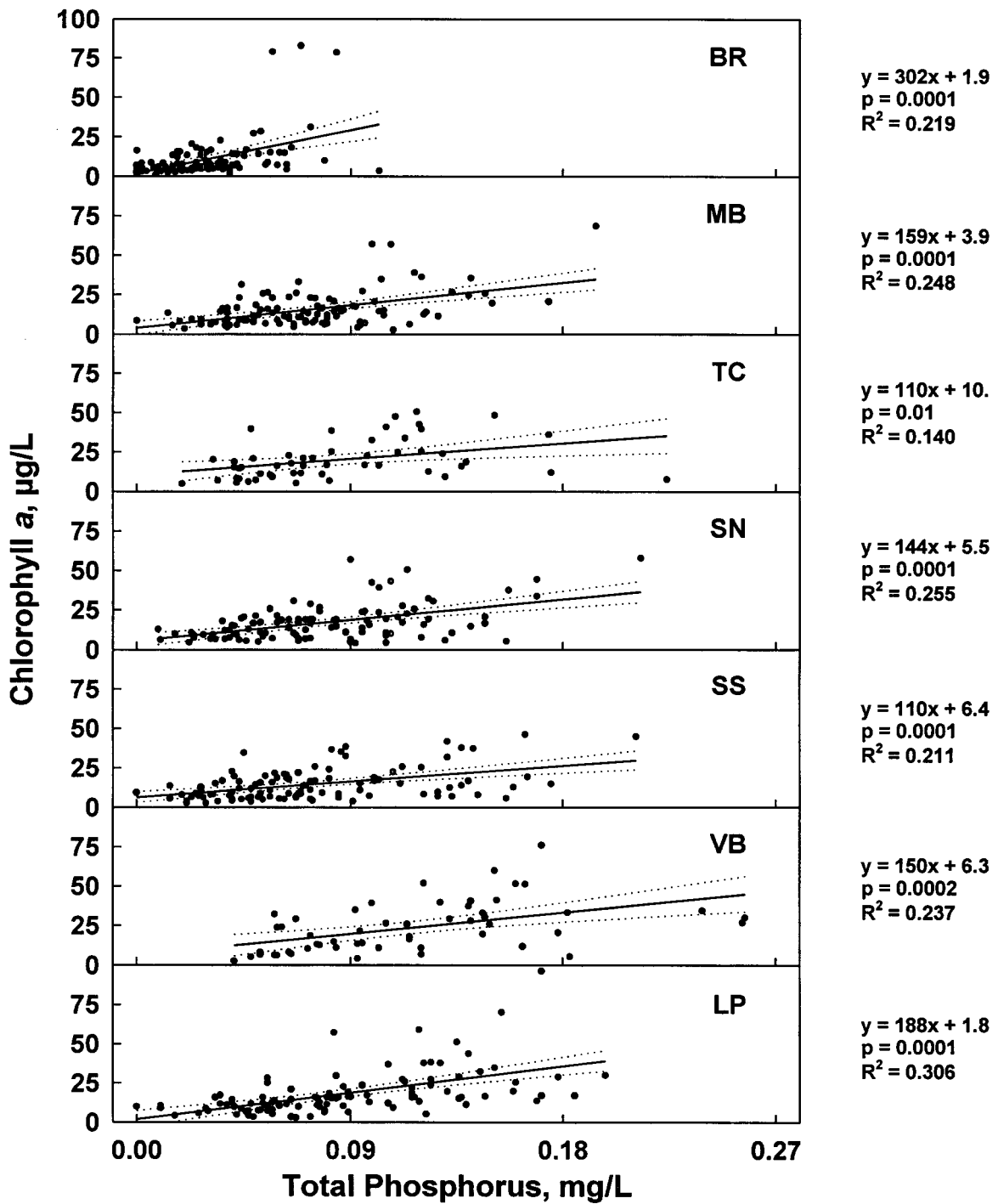


Fig. 3.55 Linear regression analysis of chlorophyll a vs. total phosphorus for each station. Dotted lines indicate 95% confidence intervals of the regression line.

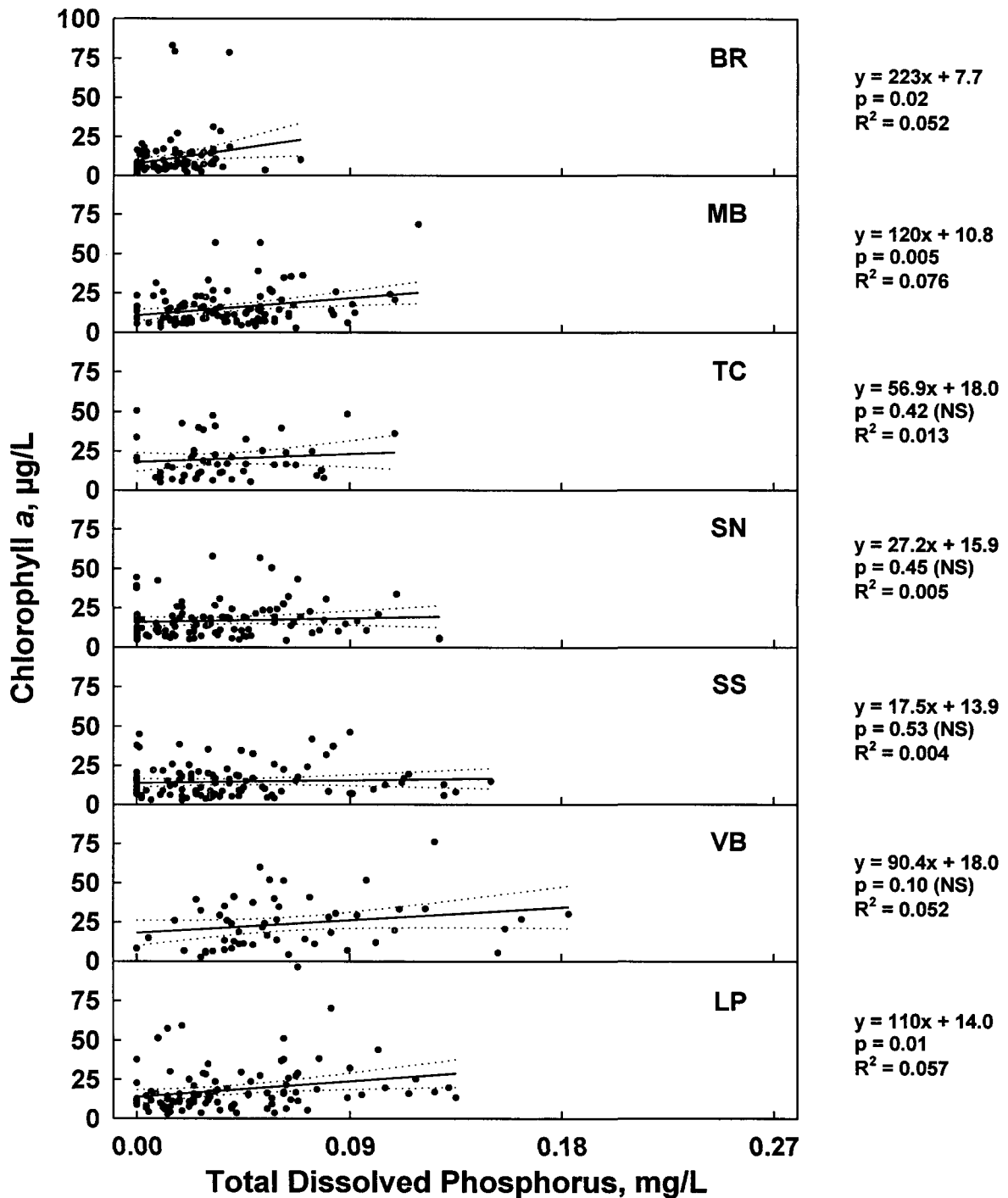


Fig. 3.56 Linear regression analysis of chlorophyll a vs. total dissolved phosphorus for each station. Dotted lines indicate 95% confidence intervals of the regression line.

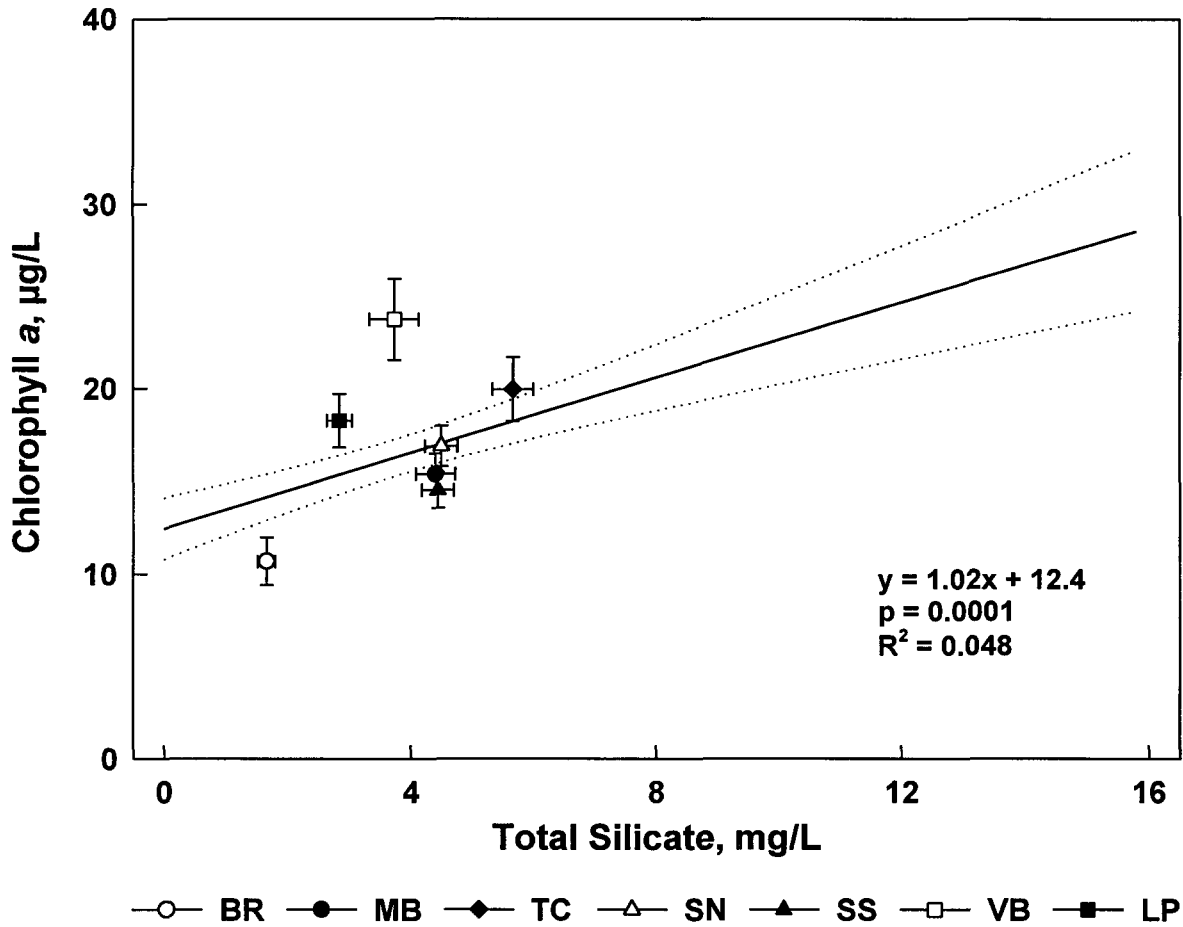


Fig. 3.57 Linear regression analyses of chlorophyll a vs. total silicate for the complete data set (all stations). Station means (\pm SE) for each variable are also presented, but all data were used in the regression model. Dotted lines indicate 95% confidence intervals of the regression line.

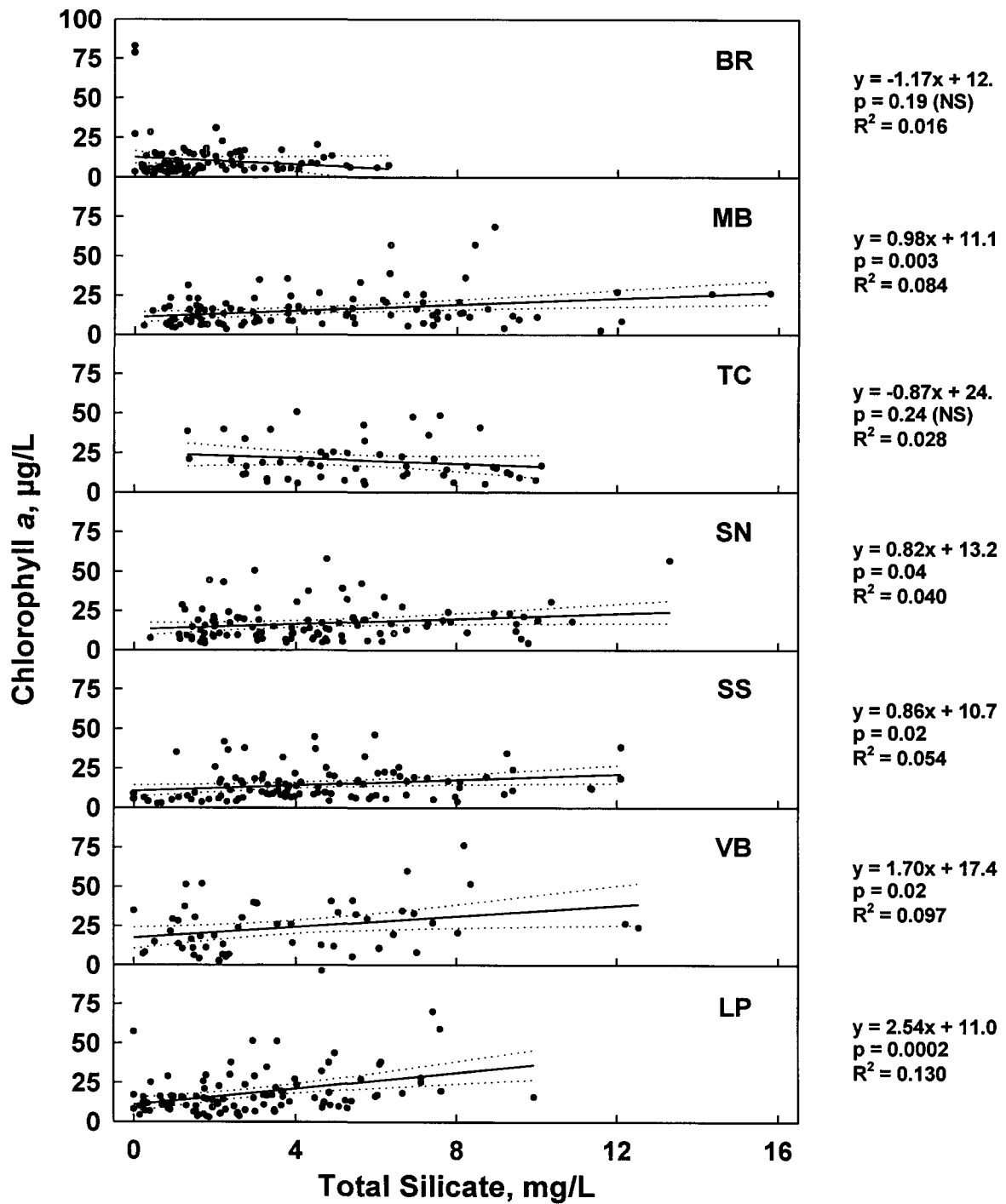


Fig. 3.58 Linear regression analysis of chlorophyll a vs. total silicate for each station. Dotted lines indicate 95% confidence intervals of the regression line.

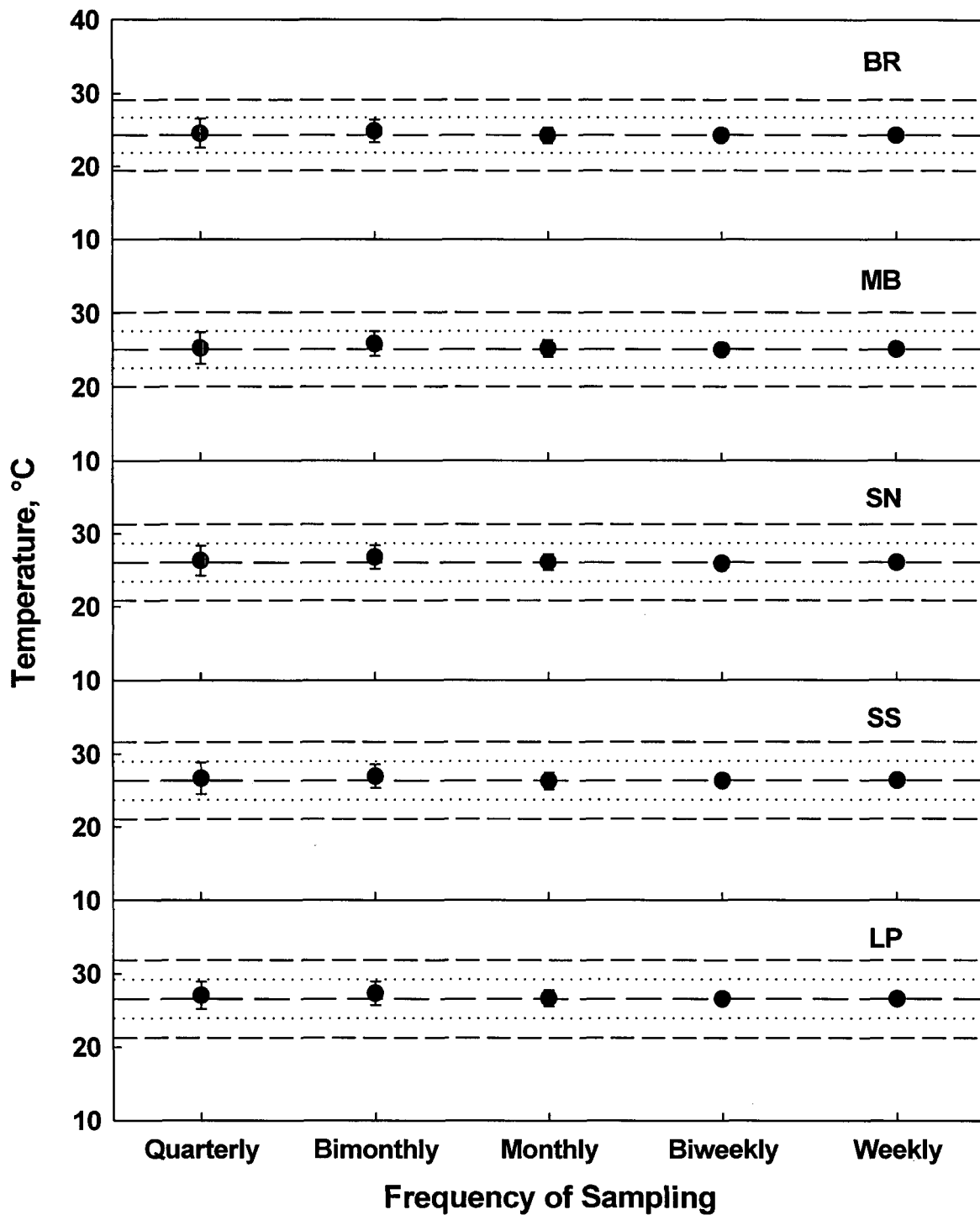


Fig. 3.59 Station means (\pm SE) for temperature as a function of sampling frequency. The center line indicates the mean value for weekly sampling; the dotted lines and outer broken lines indicate values that are $\pm 10\%$ and $\pm 20\%$ of the weekly means, respectively.

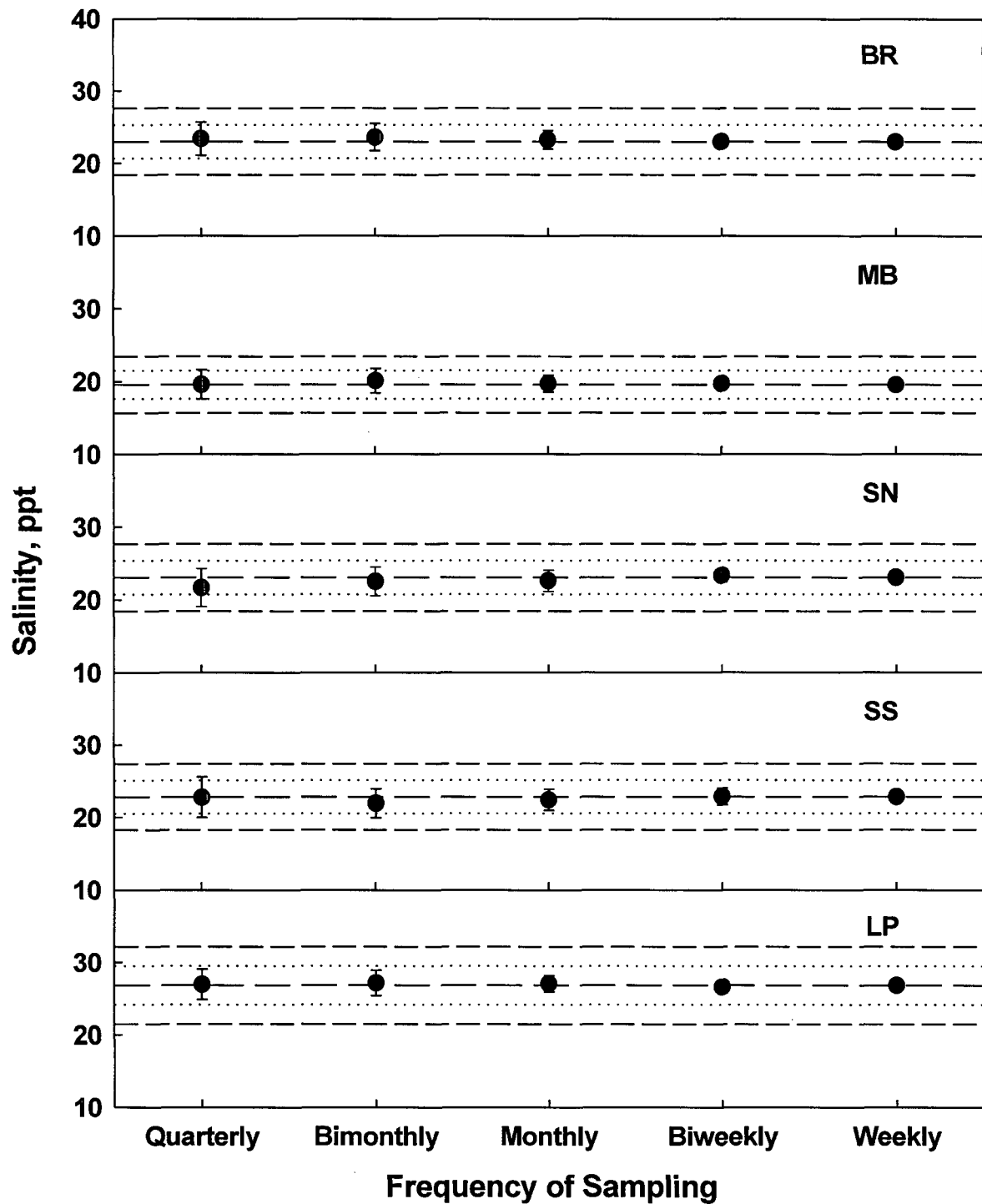


Fig. 3.60 Station means (\pm SE) for salinity as a function of sampling frequency. The center line indicates the mean value for weekly sampling; the dotted lines and outer broken lines indicate values that are $\pm 10\%$ and $\pm 20\%$ of the weekly means, respectively.

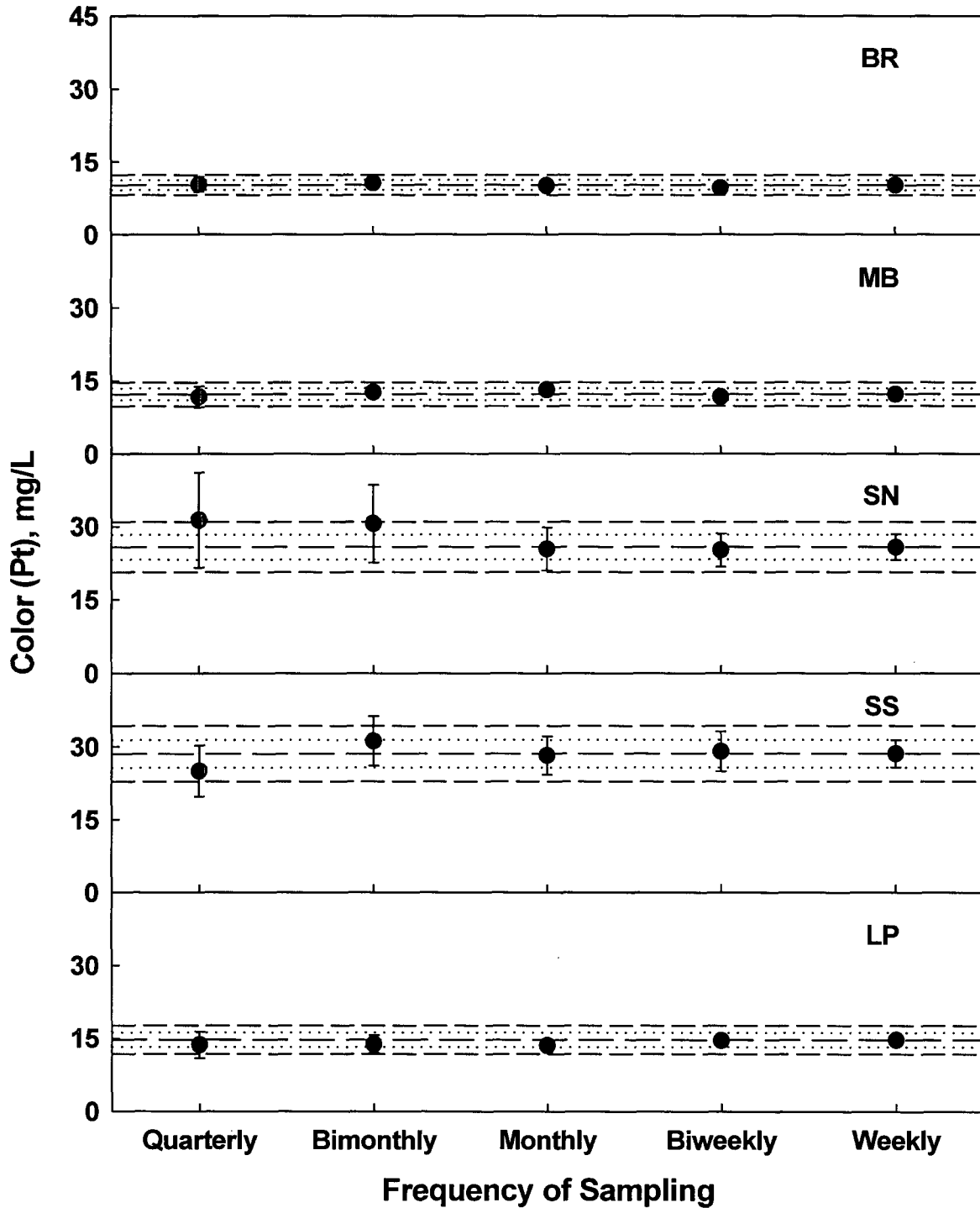


Fig. 3.61 Station means (\pm SE) for color as a function of sampling frequency. The center line indicates the mean value for weekly sampling; the dotted lines and outer broken lines indicate values that are $\pm 10\%$ and $\pm 20\%$ of the weekly means, respectively.

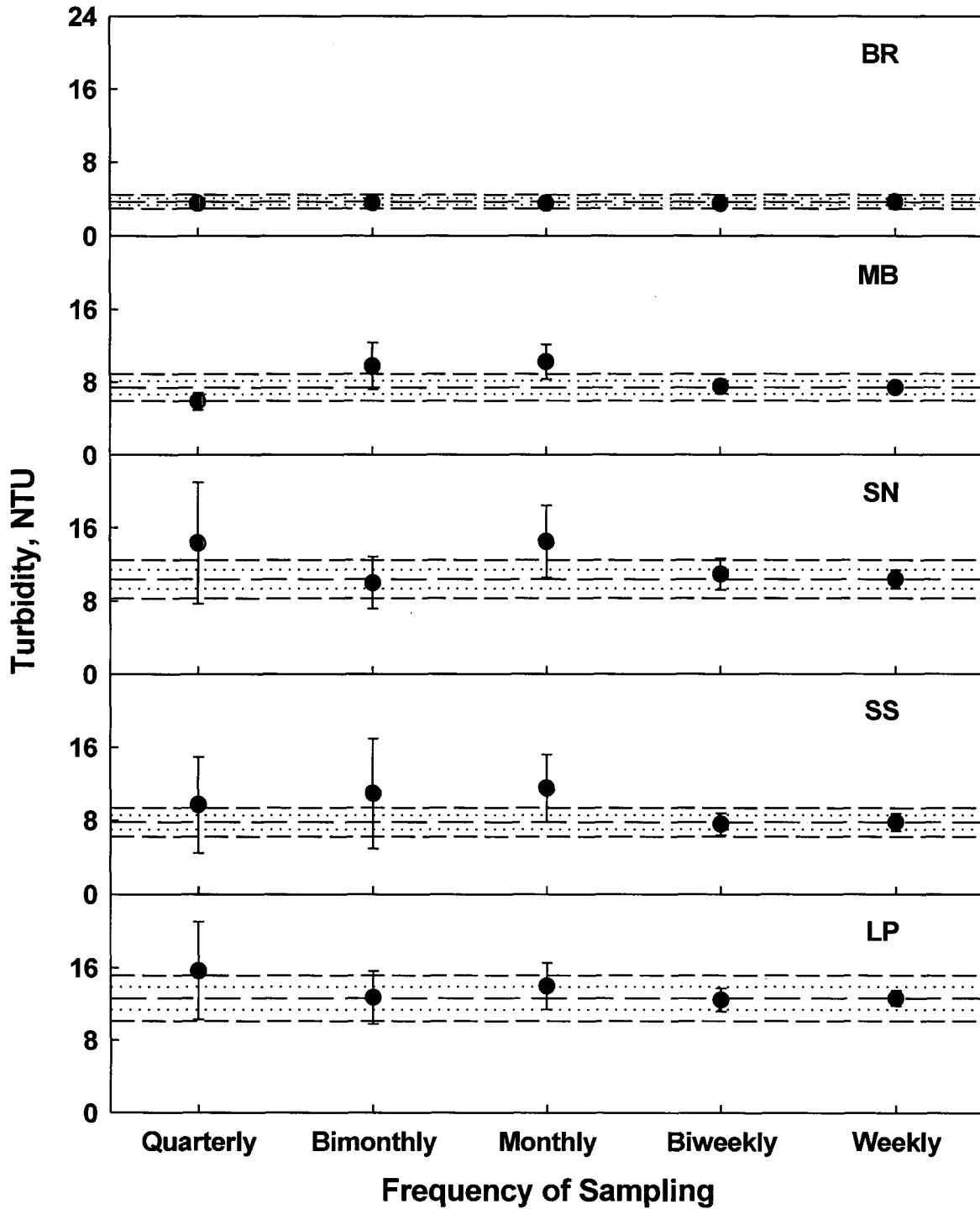


Fig. 3.62 Station means (\pm SE) for turbidity as a function of sampling frequency. The center line indicates the mean value for weekly sampling; the dotted lines and outer broken lines indicate values that are $\pm 10\%$ and $\pm 20\%$ of the weekly means, respectively.

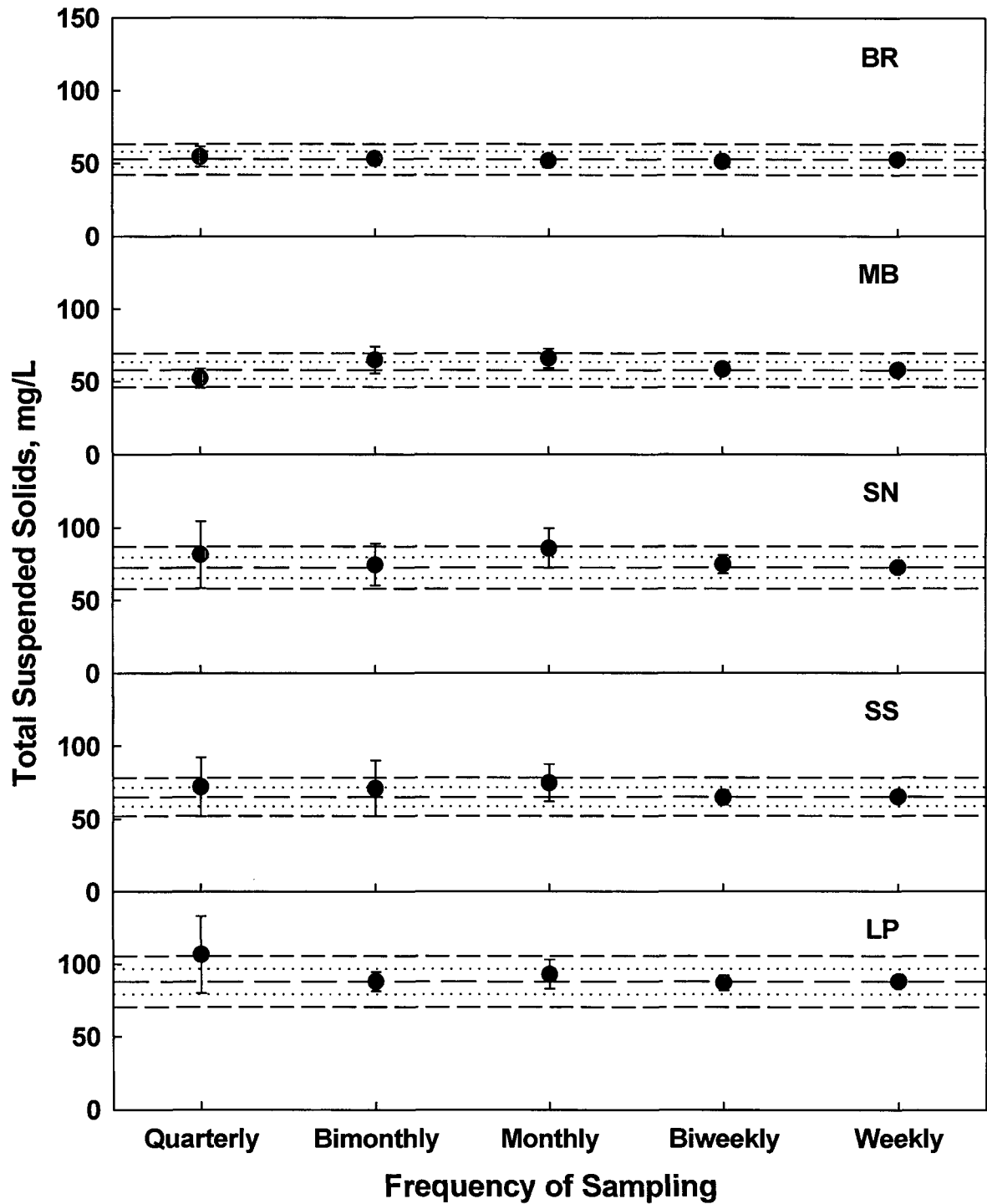


Fig. 3.63 Station means (\pm SE) for total suspended solids as a function of sampling frequency. The center line indicates the mean value for weekly sampling; the dotted lines and outer broken lines indicate values that are $\pm 10\%$ and $\pm 20\%$ of the weekly means, respectively.

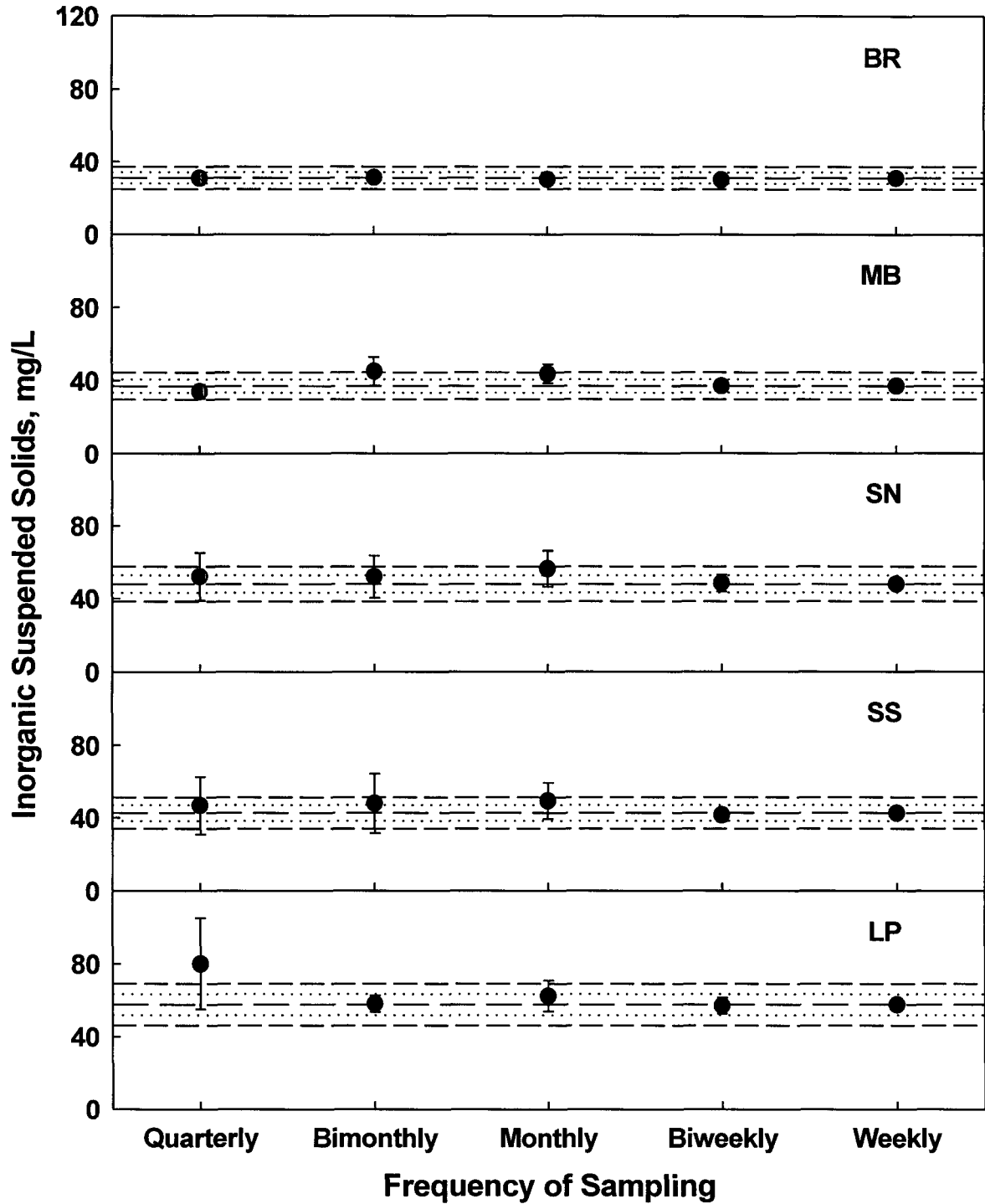


Fig. 3.64 Station means (\pm SE) for inorganic suspended solids as a function of sampling frequency. The center line indicates the mean value for weekly sampling; the dotted lines and outer broken lines indicate values that are $\pm 10\%$ and $\pm 20\%$ of the weekly means, respectively.

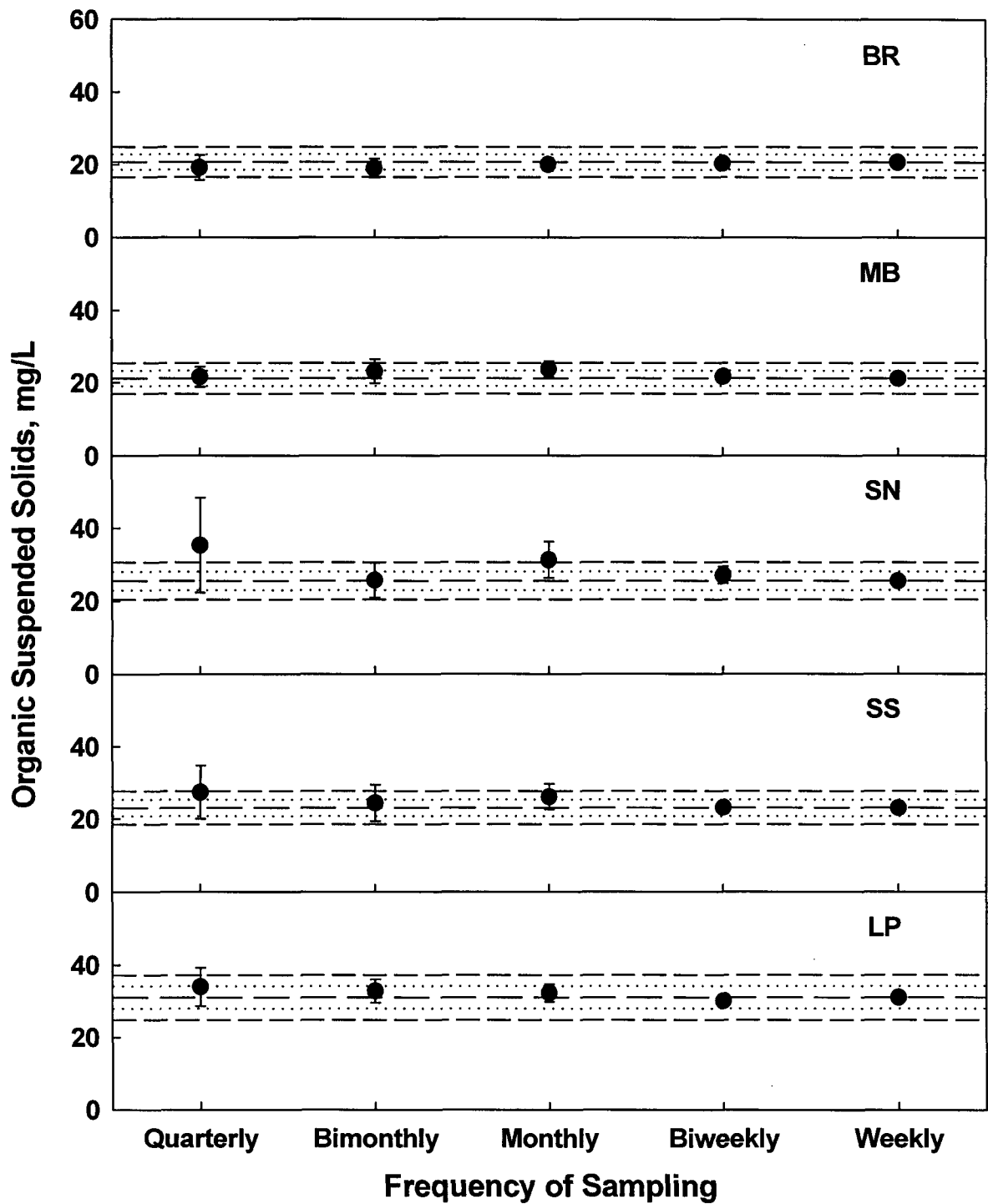


Fig. 3.65 Station means (\pm SE) for organic suspended solids as a function of sampling frequency. The center line indicates the mean value for weekly sampling; the dotted lines and outer broken lines indicate values that are $\pm 10\%$ and $\pm 20\%$ of the weekly means, respectively.

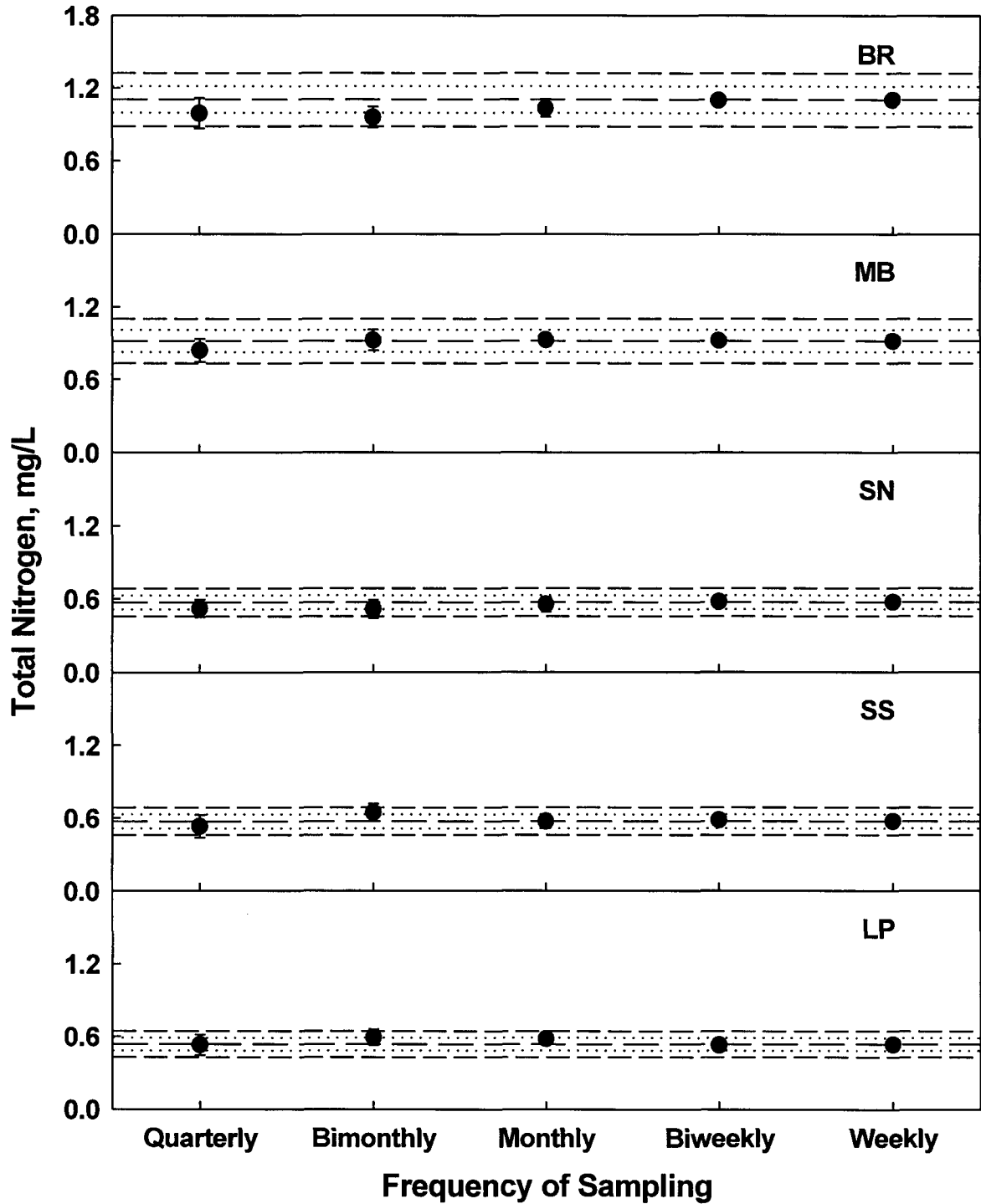


Fig. 3.66 Station means (\pm SE) for total nitrogen as a function of sampling frequency. The center line indicates the mean value for weekly sampling; the dotted lines and outer broken lines indicate values that are $\pm 10\%$ and $\pm 20\%$ of the weekly means, respectively.

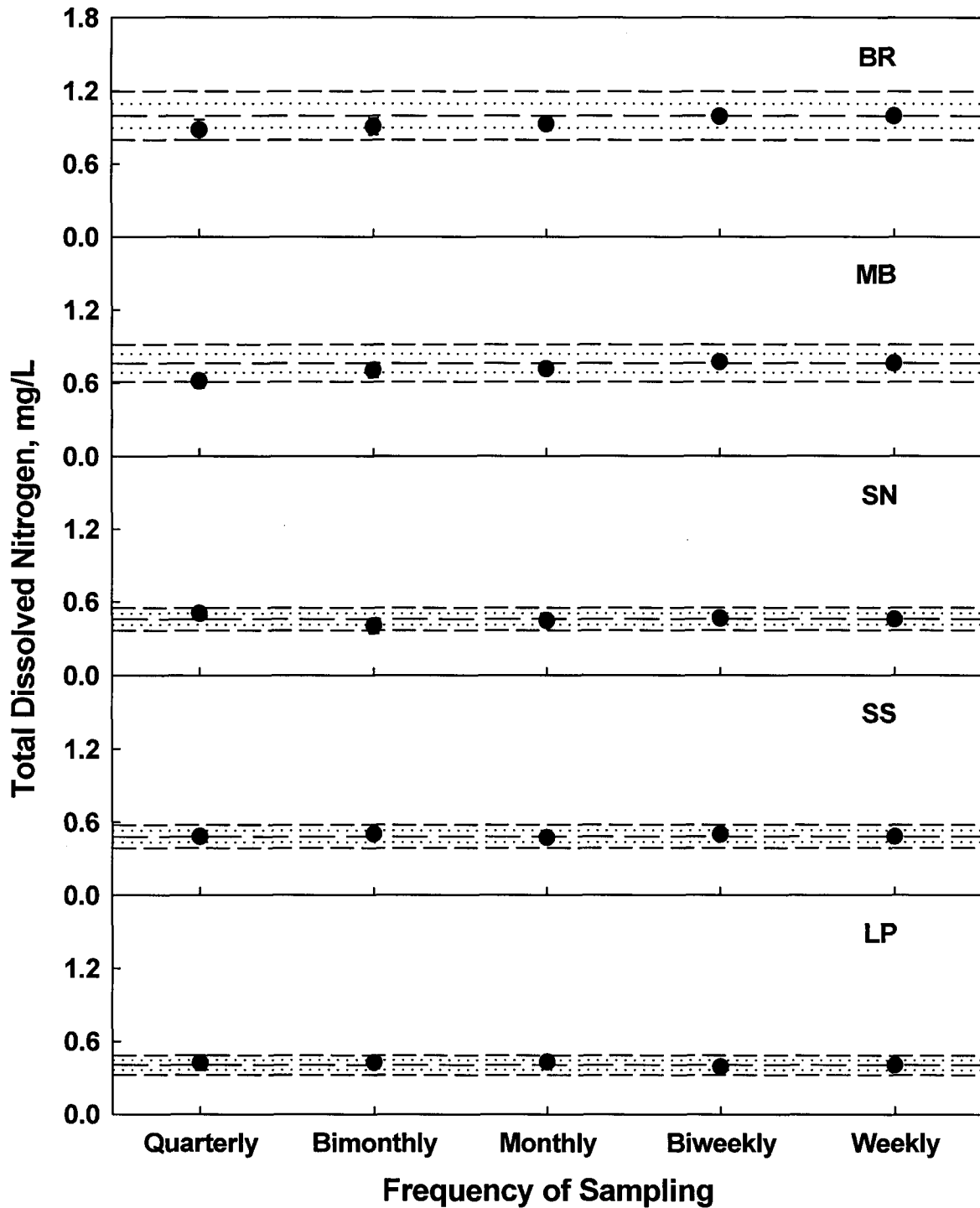


Fig. 3.67 Station means (\pm SE) for total dissolved nitrogen as a function of sampling frequency. The center line indicates the mean value for weekly sampling; the dotted lines and outer broken lines indicate values that are $\pm 10\%$ and $\pm 20\%$ of the weekly means, respectively.

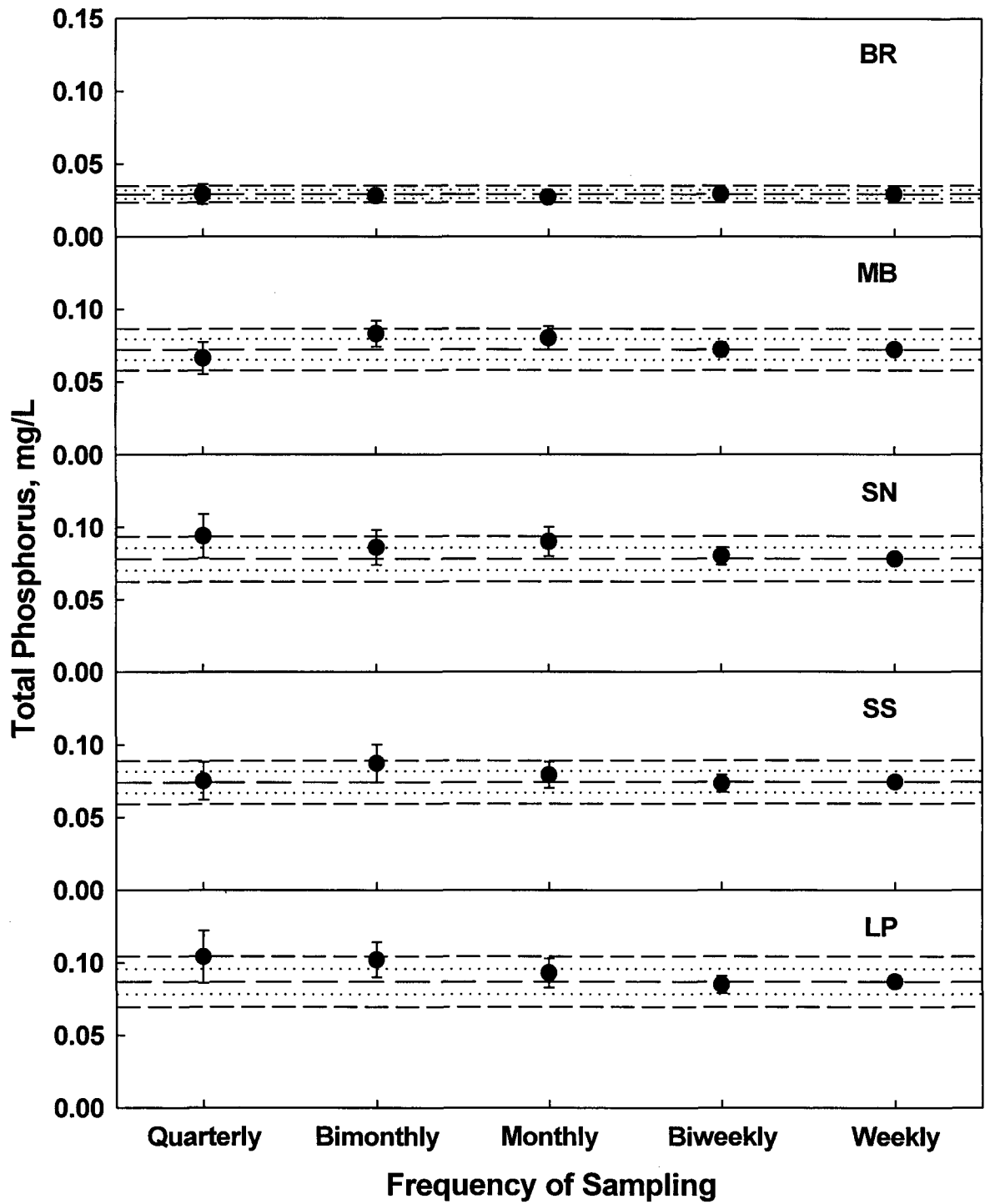


Fig. 3.68 Station means (\pm SE) for total phosphorus as a function of sampling frequency. The center line indicates the mean value for weekly sampling; the dotted lines and outer broken lines indicate values that are $\pm 10\%$ and $\pm 20\%$ of the weekly means, respectively.

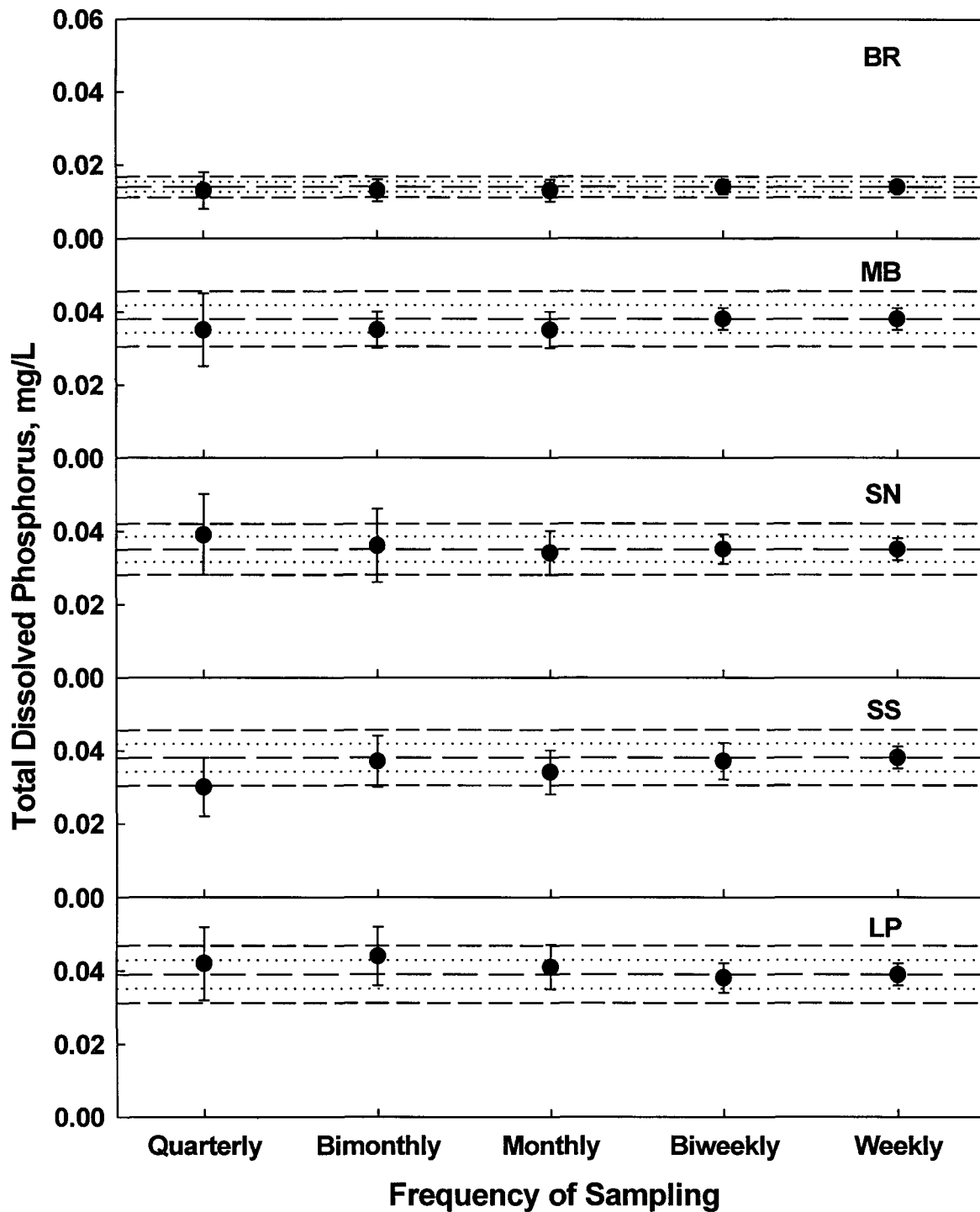


Fig. 3.69 Station means (\pm SE) for total dissolved phosphorus as a function of sampling frequency. The center line indicates the mean value for weekly sampling; the dotted lines and outer broken lines indicate values that are \pm 10% and \pm 20% of the weekly means, respectively.

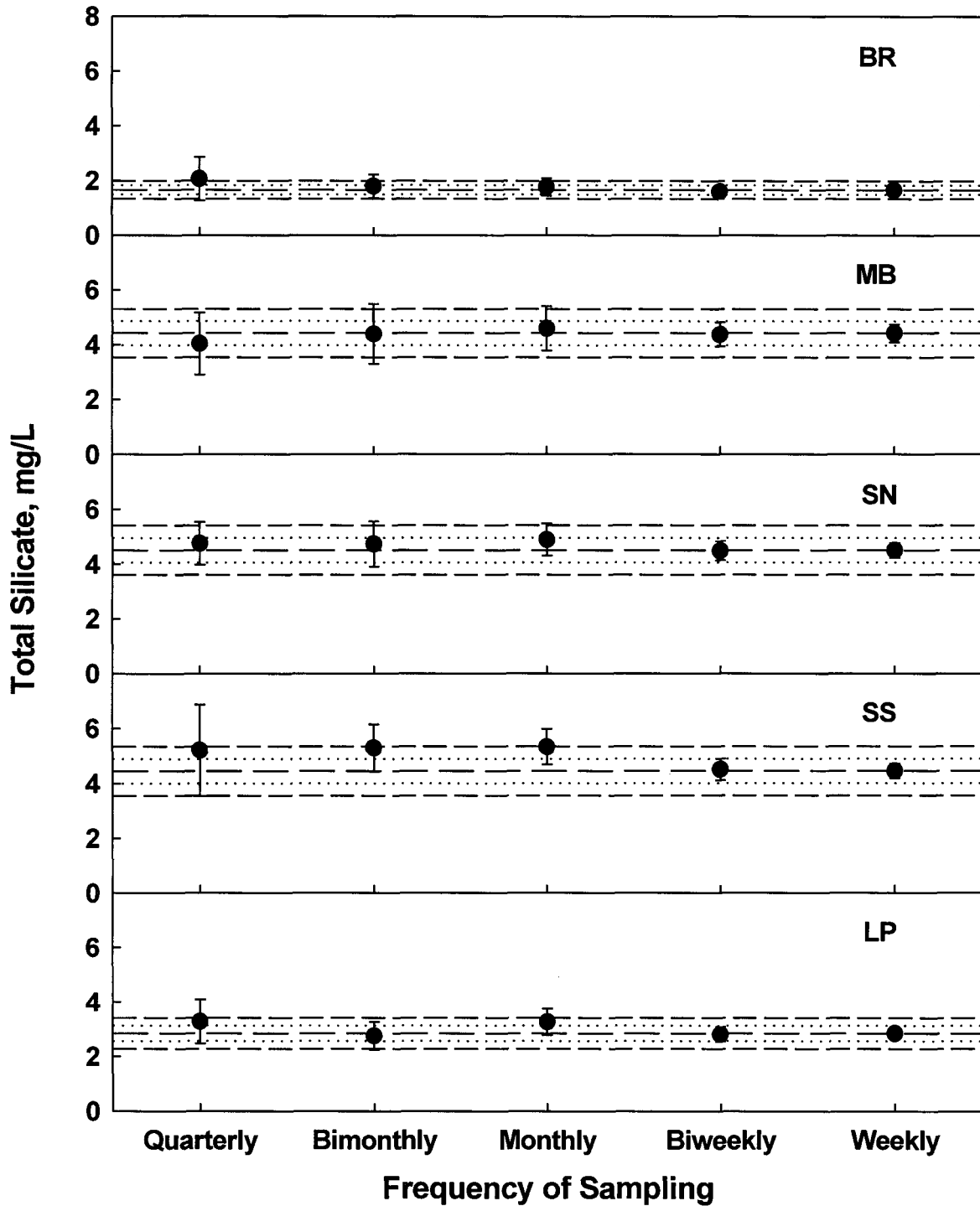


Fig. 3.70 Station means (\pm SE) for total silicate as a function of sampling frequency. The center line indicates the mean value for weekly sampling; the dotted lines and outer broken lines indicate values that are $\pm 10\%$ and $\pm 20\%$ of the weekly means, respectively.

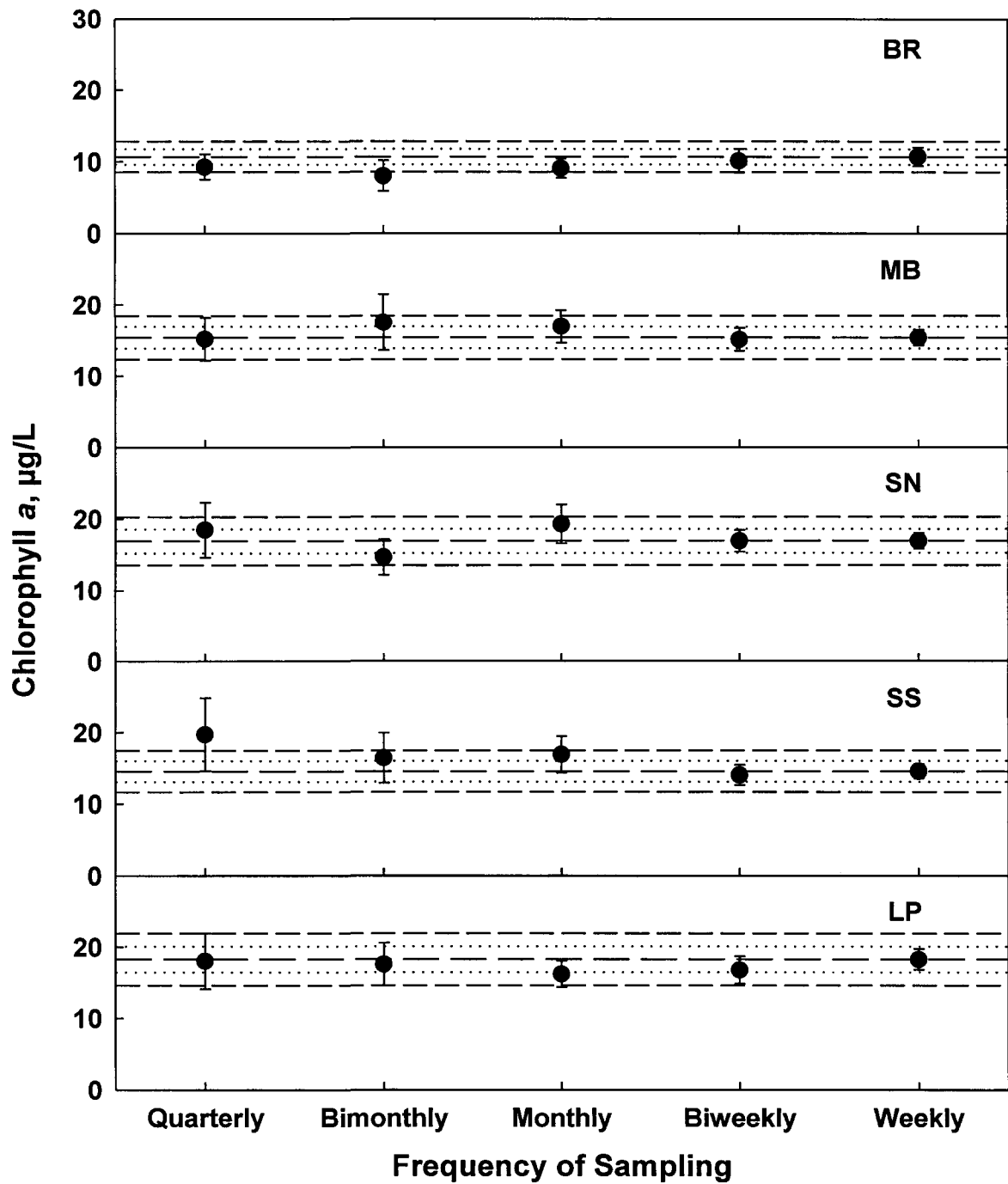


Fig. 3.71 Station means (\pm SE) for chlorophyll *a* as a function of sampling frequency. The center line indicates the mean value for weekly sampling; the dotted lines and outer broken lines indicate values that are $\pm 10\%$ and $\pm 20\%$ of the weekly means, respectively.

Chapter 4: SAV

4.1 Introduction

In the marine environment, the term "Submerged Aquatic Vegetation" (SAV) primarily refers to seagrasses, but may also include macroscopic algae. Seagrasses are angiosperms (flowering plants). Accordingly, they have vascular tissue and plant organs (roots, stems, leaves). Macroscopic algae, or macroalgae, lack these organs and do not have flowers. While macroalgae are morphologically simpler, they are genetically much more diverse than seagrasses.

The ecological importance of seagrasses in estuaries and coastal zones throughout the world is well established (e.g., Wood et al. 1969, Thayer et al. 1984, Larkum et al. 1989). Seagrasses have major impacts on other biotic resources, including fisheries, with considerable economic significance (e.g., Gilmore 1987, Livingston 1987, Durako et al. 1988). The recognition that healthy seagrass habitat is required for the ecological functioning and the economical viability of estuarine and coastal ecosystems has triggered significant interest in a better understanding and management of this resource.

Seagrass is a critical component of Indian River Lagoon (IRL), playing important roles in biological productivity and species diversity (Dawes et al. 1995). Attaining and maintaining a functioning macrophyte-based ecosystem is a high priority for lagoon management (IRLNEP 1993, Steward et al. 1994). IRL has approximately 100,000 acres of seagrasses (Dawes et al. 1995). All seven species of Florida/Caribbean seagrasses are present: *Halodule wrightii*, *Syringodium filiforme*, *Thalassia testudinum*, *Halophila engelmannii*, *Halophila decipiens*, *Halophila johnsonii*, and *Ruppia maritima*.

This study did not attempt to fully characterize IRL's SAV resource. Rather, measurements were made to quantify SAV at selected sites chosen to represent a wide range of light (Chapter 2), water quality (Chapter 3), and SAV (this chapter) conditions, with the objective of ultimately relating SAV status at those sites to ambient light and water quality conditions (Chapter 7). Sampling occurred at quarterly intervals for 2 years to determine seasonal and interannual variability in SAV parameters,

This chapter presents the principal SAV data collected at the monitoring stations and quantifies the interrelationships of SAV parameters. In subsequent chapters, additional characterization of SAV is presented: epiphyte loads (Chapter 5) and primary productivity (Chapter 6). Relationships between SAV, water quality, and underwater light are presented in Chapter 7.

4.2 Task Description

Task 4: To quantify the SAV resource at selected stations in Indian River Lagoon quarterly for 2 years.

4.3 Methods

SAV sampling was conducted quarterly at the IRL monitoring stations (see Chapter 1 for station locations) for parameters which may respond to changes in PAR and water quality: species composition, percent cover, canopy height, shoot density, above- and below-ground biomass of seagrass, and macroalgal biomass. Nine quarterly samplings were made over a 2-year period (Table 4.1).

Sampling for percent cover and canopy was conducted by the District as part of its lagoon-wide seagrass monitoring program (Virnstein and Morris 1996). At each station, a permanent transect ("Transect 1" = "Whole-bed Transect") was established perpendicular to the shoreline and extended to just beyond the "deep edge" of the seagrass bed. Each transect was videotaped (no results reported herein; videotapes are archived at the District), and estimates of percent cover and canopy height made along the transects, typically at 10-m intervals, but more frequently for shorter transects (i.e., BR and MB) and less frequently for the longest transect (LP). Percent cover was estimated by visual assessment of the presence or absence of each seagrass species in a 1-m² quadrat subdivided into 100 square cells; the percentage of cells with a given species present was considered its percent cover. Canopy height (mean of 3 measurements) was determined with a metered PVC pole for each seagrass species present. At all stations but MB and TC, Transect 1 was also sampled for shoot density and biomass (this chapter), epiphytes (Chapter 5), and grazers (Chapter 8) by HBOI.

Two additional transects, both 20-m long and perpendicular to Transect 1, were established at all stations but MB and TC. The rationale for these short transects was that one ("Transect 2" = "Mid-bed Transect") was at the location of the PAR (Chapter 2) and water quality (Chapter 3) sampling, and the other ("Transect 3" = "Deep-edge Transect") was at the "deep-edge" of the seagrass bed. Transect 2 began about 1 m from the mid-bed PAR sensor array and ran at the same depth as the array, parallel to shore; Transect 3 ran along the "deep edge" of the seagrass bed as delineated by the District (Bob Virnstein) at the start of sampling. At MB and TC, sampling by HBOI was limited to Transect 2 because of the small seagrass population, a minimal depth gradient along Transect 1, and no identifiable "deep edge".

Sampling locations along each transect for biomass, epiphytes, and grazers were determined by random numbers. For each station except MB and TC, 10 samples were taken along Transect 1 and 6 each along Transects 2 and 3; more

samples were taken along Transect 1 because of its greater length and depth gradient relative to the other transects. At MB and TC, 10 samples were taken along Transect 2. Thus, for most stations, a total of 22 samples were taken, and at MB and TC, 10 samples were taken, for a total of 120 samples each quarter in Year 1 and 108 samples each quarter in Year 2 (Table 1; the difference in the number of samples between years was due to VB being sampled only in Year 1, and TC only in Year 2).

This sampling effort was much greater than what had been initially proposed. Sampling was conducted for 9 quarters; the contract called for only 6 quarters of sampling. Moreover, each quarterly sampling effort was twice that specified in the contract ($n = 10$ per station, 6 stations); the additional sampling was performed to assess variability within each bed, including "mid-bed" (Transect 2) and "deep edge" (Transect 3). So, while the contract called for the analysis of 360 samples (6 sampling events @6 stations x 10 samples per station), a total of 1,042 samples (Table 1), nearly 3 times the number of samples originally proposed, were collected and analyzed.

SAV samples were collected with PVC corers (15.4 cm in diameter, 186 cm² in area), sieved on a 1-mm mesh sieve to remove sediment, placed in individual, labeled plastic bags on ice, and frozen until processed. Seagrass shoot density (expressed as shoots/m² for each species) was determined from counts of the number of shoots of each species in each core. Seagrass biomass (g dry weight/m²) from the cores was sorted to species, partitioned into above-ground (shoots and blades) and below-ground (roots and rhizomes) biomass, dried at 80°C to constant weight, and weighed. Total macroalgal biomass from the cores was also dried and weighed.

In this report, data are presented as means \pm standard errors (SE). Statistical analyses were performed with SAS statistical software (SAS Institute 1988). Statistical significance among means was tested with analysis of variance (ANOVA). When ANOVA indicated the existence of significant differences, the Tukey-Kramer test (T-K) determined which means were significantly different. Prior to performing ANOVA, data were transformed (Sokal and Rohlf 1981) with the logarithmic (for shoot counts and biomass) or the arcsine transformation (for percent cover). The minimal level of significance for any analysis was $P \leq 0.05$.

The relationship among selected SAV parameters for each seagrass species was determined by correlation and linear regression analyses (Sokal and Rohlf 1981). Stepwise multiple regression (Sokal and Rohlf 1981) determined the relationship of above-ground, below-ground, and total biomass (dependent variables) to more rapidly measured parameters, i.e., shoot density, cover, and canopy height (independent variables). The data used for these analyses were species means for each station-season combination (excluding Transect 3).

4.4 Results

The presentation of results begins with the overall patterns of each SAV parameter measured for the entire seagrass community and its component species, without regard to station, season, or transect (Section 4.4.1). Overall station means for the seagrass community and its component species, for all samples collected, without regard to season or transect (Section 4.4.2), complete the overview. Analysis of the entire data set demonstrates the effect of transect location (Section 4.4.3). After adjustments are made for transect effect, seasonality in SAV parameters is presented (Section 4.4.4). Comparisons among stations and years are made (Section 4.4.5). Lastly, results of correlation, linear regression, and multiple regression analyses are presented that define the relationships among key SAV parameters (Section 4.4.6).

4.4.1 Seagrass Overview

Four seagrass species were present in this study: *Halodule wrightii*, *Syringodium filiforme*, *Thalassia testudinum*, and *Halophila engelmannii*. *H. wrightii* was the only species found at all sites. *S. filiforme* was found primarily at 3 sites (BR, VB, and LP), with occasional occurrence at SS. *T. testudinum* was limited to VB and LP. *H. engelmannii* was present in small amounts at BR and infrequently encountered at SN and SS.

In terms of cover, *H. wrightii* (Fig. 4.1) was the most abundant seagrass (grand mean cover for all samples in the study = $39 \pm 1\%$), followed by *T. testudinum* ($8 \pm 1\%$), *S. filiforme* ($4 \pm 1\%$), and *H. engelmannii* ($0.2 \pm 0.1\%$); species covers were all significantly different (ANOVA: $P = 0.0001$; T-K: $P \leq 0.05$). The grand means for canopy height of *T. testudinum* (0.27 ± 0.01 m) and *S. filiforme* (0.22 ± 0.01 m) were twice that of *H. wrightii* (0.12 ± 0.01 m) and five times that of *H. engelmannii* (0.05 ± 0.01 m).

The grand mean for total seagrass density for all collections ($n = 1,042$ cores) was 852 ± 39 shoots/m² (Fig 4.1). Shoot densities and all three biomass parameters of the four species were all significantly different from each other (ANOVA: $P = 0.0001$); *H. wrightii* was the densest seagrass, followed in order by *S. filiforme*, *T. testudinum*, and *H. engelmannii* (T-K: $P \leq 0.05$). In terms of biomass, *H. wrightii* still predominated, but was followed in order by *T. testudinum*, *S. filiforme*, and *H. engelmannii*. The grand mean for total biomass for all species was 77.0 ± 4.6 g dry weight/m². The ratio of above:below-ground biomass averaged 0.53 for all collections; this ratio increased from 0.42 for *H. wrightii* to 0.62 for *S. filiforme* and 0.72 for *T. testudinum*. The more diminutive *H. engelmannii* was unique in having more above- than below-ground biomass (ratio = 1.69).

4.4.2 Station Overview

Seagrass communities

Seagrass cover data (Figs. 4.2-4.9) indicated mixed populations of seagrass at 3 stations: BR (Fig. 4.2), primarily *H. wrightii* and *S. filiforme*, with a small population of *H. engelmannii*; VB (Fig. 4.7), primarily *T. testudinum* and *H. wrightii*, with a small population of *S. filiforme*; and LP (Fig. 4.8), equal amounts of *H. wrightii*, *T. testudinum*, and *S. filiforme*. Seagrass at MB (Fig. 4.3), TC (Fig. 4.4), SN (Fig. 4.5), and SS (Fig. 4.6) was exclusively, or nearly so, *H. wrightii*. Trace amounts of *H. engelmannii* were recorded at SN, as were *H. engelmannii* and *S. filiforme* at SS. Canopy height of the seagrass community was a function of species composition (Fig. 4.9); for any given species, canopy height was relatively constant among stations, with the most notable exception being the relatively small canopy height of *H. wrightii* at MB and TC.

The mean depth of seagrass at the stations ranged between 0.58 and 0.87 m (Table 4.2). The mean "deep edge" of the seagrass beds was greatest at BR (1.48 m) and least at MB (0.75 m). From MB south to LP, this depth increased. The "deep edge" of seagrass at any location was rarely as sharply delineated as this term implies; herein, the "deep edge" refers to the deepest point of discontinuity between vegetated and unvegetated bottom along a depth profile, but individual plants could commonly be found deeper than the "deep edge." The linear extent from shore of the seagrass beds was not only a function of depth of the "deep edge," but also bottom profiles (Figs. 4.2-4.8); the narrowest seagrass beds were at BR (the bed with the deepest edge) and MB (the shallowest bed).

Seagrass species within mixed communities had station-specific patterns of depth zonation. At BR (Fig. 4.2), *H. wrightii* declined with depth as *S. filiforme* became more abundant; *H. engelmannii* was most common at mid-depths. At VB (Fig. 4.8), *H. wrightii* dominated the shallow end of the site, was replaced by *T. testudinum* at intermediate depths, and dominated again in deeper water. *S. filiforme*, when present, was found in deeper water. At LP (Fig. 4.8), *S. filiforme* was much more abundant than at VB and largely replaced *H. wrightii* in deeper water.

There were significant differences (ANOVA: $P = 0.0001$) in seagrass parameters among stations (Fig. 4.10). Shoot density was highest at BR (1994 ± 146 shoots/m²), lowest at MB (82 ± 20 shoots/m²), and intermediate at the other stations (311 ± 60 to 752 ± 66 shoots/m²). Station-specific patterns in biomass were similar to those of shoot density, with the exception that VB had a significantly higher above-ground biomass than the other intermediate stations. Above-ground biomass was maximal at VB (74.2 ± 11.1 g dry weight/m²) and BR (41.5 ± 3.7 g dry weight/m²) and minimal at MB (0.8 ± 0.2 g dry weight/m²). Below-ground biomass was maximal at VB

(114.3 ± 15.4 g dry weight/m²) and BR (109.7 ± 9.7 g dry weight/m²) and minimal at MB (1.6 ± 0.4 g dry weight/m²). Total biomass was maximal at VB (188.6 ± 26.0 g dry weight/m²) and BR (151.2 ± 12.7 g dry weight/m²) and minimal at MB (2.5 ± 0.6 g dry weight/m²). Some of the differences among stations in total seagrass shoot density and biomass were due to differences in species composition at the stations, e.g., a shoot of *T. testudinum* has much more biomass than a shoot of *H. wrightii*.

Halodule wrightii

H. wrightii (Fig. 4.11) was the only seagrass species present at all stations. Both mean cover and shoot density were highest at BR, SS, and SN, intermediate at LP and VB, and lowest at MB and TC (ANOVA: $P = 0.0001$; T-K: $P \leq 0.05$). Biomass parameters followed the same general pattern, although all three biomass means were significantly higher at BR than at SS and SN (ANOVA: $P = 0.0001$; T-K: $P \leq 0.05$). Cover of *H. wrightii* was 5-10 times higher at BR ($62 \pm 6\%$), SS ($56 \pm 2\%$), and SN ($55 \pm 3\%$) than at MB ($14 \pm 1\%$) and TC ($6 \pm 2\%$). Canopy height at MB (0.07 ± 0.01 m) and TC (0.06 ± 0.01 m) was only half that of the other stations (0.12 ± 0.01 to 0.16 ± 0.01 m). Shoot density (1542 ± 141 shoots/m²), above-ground biomass (29.6 ± 3.1 g dry weight/m²), below-ground biomass (89.3 ± 9.4 g dry weight/m²), and total biomass (118.9 ± 12.0 g dry weight/m²) were maximal at BR.

Syringodium filiforme

The next most widespread seagrass species was *S. filiforme* (Fig. 4.12), which was a major component of the seagrass community at BR and LP, and present in small amounts at VB and SS. Mean cover was significantly greater (ANOVA: $P = 0.0001$) at BR ($30 \pm 6\%$) than at LP ($19 \pm 3\%$), but differences among these two stations in shoot density (BR: 411 ± 44 shoots/m²; LP: 353 ± 37 shoots/m²), above-ground biomass (BR: 10.8 ± 1.4 g dry weight/m²; LP: 10.2 ± 1.3 g dry weight/m²), below-ground biomass (BR: 19.7 ± 2.3 g dry weight/m²; LP: 13.8 ± 1.6 g dry weight/m²), total biomass (BR: 30.5 ± 3.6 g dry weight/m²; LP: 24.0 ± 2.7 g dry weight/m²), and canopy height (BR: 0.20 ± 0.03 m; LP: 0.23 ± 0.01 m) were not significant (ANOVA: $P > 0.05$).

Thalassia testudinum

T. testudinum (Fig. 4.13), which only grows south of Sebastian Inlet, was restricted to the two southernmost stations. Cover ($49 \pm 4\%$), shoot density (165 ± 25 shoots/m²), above-ground biomass (66.0 ± 11.4 g dry weight/m²), below-ground biomass (95.7 ± 16.0 g dry weight/m²), and total biomass (161.7 ± 26.8 g dry weight/m²) were significantly higher (ANOVA: $P = 0.0001$; T-K: $P \leq 0.05$) at VB than at LP. Canopy height did not significantly vary between these stations (VB: 0.27 ± 0.01 m; LP: 0.26 ± 0.01 m).

Halophila engelmannii

With the exception of a couple of samples at SN and SS, *H. engelmannii* (Fig. 4.14) was collected only at BR, with a mean cover of $3 \pm 1\%$, canopy height of 0.05 ± 0.01 m, shoot density of 41 ± 16 shoots/m², above-ground biomass of 1.1 ± 0.4 g dry weight/m², below-ground biomass of 0.7 ± 0.3 g dry weight/m², and total biomass of 1.8 ± 0.6 g dry weight/m².

Macroalgae

The grand mean macroalgal cover for all stations (Fig. 4.15) was $15 \pm 1\%$, with the lowest mean at BR ($1 \pm 1\%$) and the highest mean at VB ($41 \pm 4\%$). The grand mean macroalgal biomass was 17.0 ± 2.0 g dry weight/m², almost all of which was composed of unattached, "drift" algae; 65% (11.0 ± 1.3 g dry weight/m²) of the total belonged to the red algal genus *Gracilaria*. Macroalgal abundance increased along the north-south gradient of stations, ranging from 0.7 ± 0.2 g dry weight/m² at BR to 35.6 ± 6.4 and 41.5 ± 11.5 g dry weight/m² at LP and VB, respectively.

Although species composition of macroalgae was beyond the scope of the project, there was evidence of shifts along the north-south gradient: no *Gracilaria* was collected at the most northern station (BR), only *Gracilaria* was collected in measurable quantities at TC, and the percentage of *Gracilaria* (73-76%) was higher at intermediate stations (MB, SN, SS) than at the southernmost stations (VB, LP; 58-59%).

4.4.3 Transect Differences in SAV

In addition to differences in species composition, within-site and temporal variability confounds an assessment of differences in SAV among sites. In this section, the entire data set of SAV parameters is presented for each station-transect-month combination (Figs. 4.16-4.37). Transect differences in SAV parameters are examined both for the whole seagrass community and its component species prior to assessments of seasonality (Section 4.3.4) and differences among stations and years (Section 4.3.5). Specifically, this section addresses the question: are there differences in SAV among transects at any time or station?

Seagrass communities

For the total seagrass community (Figs. 4.16-4.19), at any one station and time, there were usually no significant differences (ANOVA: $P > 0.05$) in SAV parameters between Transects 1 ("whole bed") and 2 ("mid-bed"). The only exceptions to the equality of Transects 1 and 2 were: (1) at BR, below-ground (Fig. 4.18) and total

biomass (Fig. 4.19) for Transect 1 were greater than those of Transect 2 for one collection (May 1995); and (2) at VB, above-ground biomass (Fig. 4.17) for Transect 2 was greater than that of Transect 1 for one collection (August 1994) and shoot density (Fig. 4.16) of Transect 2 was greater than that of Transect 1 for another collection (November 1994). In general, shoot density and biomass were usually greater (ANOVA: $P = 0.0001$; T-K: $P \leq 0.05$) at both Transects 1 and 2 than at Transect 3 (the "deep edge").

Halodule wrightii

There were no significant differences (ANOVA: $P > 0.05$) between Transects 1 and 2 in either shoot density or biomass of *H. wrightii* (Figs. 4.20-4.23) for any station-season combination, with one exception: at BR, below-ground (Fig. 4.22) and total biomass (Fig. 4.23) for Transect 1 were greater than those of Transect 2 in May 1995.

The May 1995 collection was also the only one at BR where the values for the SAV parameters at Transects 1 and 2 did not always exceed those of Transect 3. At the two Sebastian stations (SN and SS), there were significant differences (ANOVA: $P < 0.05$) in SAV parameters among transects at times (usually in collections made in the months of May and August when seagrass was growing well, and Transect 3 had significantly less seagrass than the other transects). At VB, there were no significant differences in SAV parameters among transects (ANOVA: $P > 0.05$). At LP, the only significant differences between Transect 3 and the other transects were in February 1996 when Transect 3 had a higher shoot density (Fig. 4.20) and higher above-ground biomass (Fig. 4.21) than Transect 1 and higher below-ground (Fig. 4.22) and total biomass (Fig. 4.23) than both Transects 1 and 2.

Syringodium filiforme

Shoot density and biomass of *S. filiforme* (Figs. 4.24-4.27) for Transects 1 and 2 were statistically equal for any station-season combination (ANOVA: $P > 0.05$), with two exceptions (February 1995, November 1995) at BR where biomass values, but not shoot density, were greater for Transect 2 than for Transect 1.

Sometimes Transect 3 had significantly lower shoot density and biomass parameters than the other transects (ANOVA: $P = 0.0001$; T-K: $P \leq 0.05$). At BR, in August 1994 and November 1994, Transect 3 had lower shoot density and biomass than the other transects, and in February 1995, Transect 3 had lower biomass, but not shoot density, than the other transects. At LP, in February 1994, 1995, and 1996, and April 1994, Transect 3 had lower shoot density and biomass than the other transects.

Thalassia testudinum

Shoot density and biomass of *T. testudinum* (Figs. 4.28–4.31) for Transects 1 and 2 were always statistically equal (ANOVA: $P > 0.05$) at both stations where it occurred, with one exception. In August 1994, shoot density and biomass at VB were higher for Transect 2 than for Transect 1.

At VB, there generally were significant reductions in shoot density and biomass along Transect 3 compared to the other transects (ANOVA: $P = 0.0001$; T-K: $P \leq 0.05$), except in February 1994 and 1995, when there were no significant differences among transects (ANOVA: $P > 0.05$). At LP, because of relatively lower values for all parameters and a heterogeneous distribution of *T. testudinum*, there were no significant differences among transects (ANOVA: $P > 0.05$).

Halophila engelmannii

Transect-specific effects on the SAV parameters for *H. engelmannii* (Figs. 4.32–4.35) were not significant (ANOVA: $P > 0.05$).

Macroalgae

There were some significant differences among transects in total macroalgal biomass (Fig. 4.36), primarily in regards to Transect 3. Macroalgal biomass of Transects 1 and 2 was always equal for each station-season combination (ANOVA: $P > 0.05$), with three exceptions. At SN, in February 1994 and August 1994, algal biomass along Transect 2 was significantly lower than the other two transects (ANOVA: $P = 0.002$; T-K: $P \leq 0.05$). At LP, in April 1994, biomass along Transect 2 was significantly higher than that of Transect 1 (ANOVA: $P = 0.0001$; T-K: $P \leq 0.05$).

For most stations, there was generally no significant difference between Transect 3 and the other transects (ANOVA: $P > 0.05$), but macroalgal biomass along Transect 3 was usually significantly higher at SN and significantly lower at LP (ANOVA: $P \leq 0.05$; T-K: $P \leq 0.05$).

The dominant component of the macroalgal community, *Gracilaria* spp. (Fig. 4.37), had patterns similar to those of the whole macroalgal community.

4.4.4 Seasonality of SAV

Because there were almost always no differences in shoot density or biomass between Transects 1 and 2, but frequent differences among those transects and

Transect 3, data from Transects 1 and 2 were combined for the remaining analyses. These data (Figs. 4.38-4.43) were used to assess seasonality of SAV (this section) and to compare SAV among stations and years (Section 4.3.5). These analyses eliminate the confounding effect of depth (Transect 3) at the stations and also incorporate cover and canopy height data (from Transect 1) collected by the District (L. Morris et al.). Specifically, this section addresses the question: is there seasonality in SAV parameters measured at any station?

Seagrass communities

Seasonal patterns in SAV parameters for the total seagrass community varied among stations (Fig. 4.38). At BR, the most notable temporal differences among SAV parameters were associated with a large decline in seagrass between February 1995 and May 1995 (see Fig. 4.2). Shoot density was the least variable parameter, with May 1995 having a significantly lower density than all other months (ANOVA: $P = 0.0001$; T-K: $P \leq 0.05$). Before the decline, above-ground biomass was significantly greater in August 1994 than in other months (ANOVA: $P = 0.0001$; T-K: $P \leq 0.05$), but there were no significant differences among months in below-ground or total biomass (ANOVA: $P > 0.05$). Following the seagrass decline (August 1995 to February 1996), shoot density returned to earlier levels, but none of the biomass parameters returned to pre-decline levels (ANOVA: $P = 0.0001$; T-K: $P \leq 0.05$).

At MB (Fig. 4.38), there were limited differences in shoot density among months (ANOVA: $P = 0.04$; but T-K could not detect any significant differences, $P > 0.05$). Similarly, while there were significant temporal differences in biomass (ANOVA: $P = 0.001$, 0.01 , and 0.004 , respectively, for above-ground, below-ground, and total biomass), only the extreme endpoints were significantly different (T-K: $P \leq 0.05$) from one another (April 1994 was significantly different from all other months for above-ground biomass and significantly different from November 1995 and February 1996 for below-ground and total biomass).

At TC (Fig. 4.38), shoot density and biomass were significantly higher in May 1995 and August 1995 than in other months (ANOVA: $P = 0.0001$; T-K: $P \leq 0.05$).

At SN (Fig. 4.38), shoot density, below-ground biomass, and total biomass were significantly lower during November 1994 to May 1995 and during November 1995 to February 1996 than in other months (ANOVA: $P = 0.0001$; T-K: $P \leq 0.05$).

At SS (Fig. 4.38), shoot density and biomass patterns were similar to those at SN (ANOVA: $P = 0.0001$; T-K: $P \leq 0.05$), with the exception that shoot density and above-ground biomass (but not below-ground and total biomass) in May 1995 were not depressed, as they were at SN.

At VB and LP (Fig. 4.38), shoot density and biomass did not significantly vary (ANOVA: $P > 0.05$). The apparent seasonal differences in biomass at VB were not significant because of the large variability in those parameters (the largest at any station).

Halodule wrightii

As *H. wrightii* was the dominant seagrass species in the study, the variable temporal patterns observed among stations for the overall seagrass community were also found for *H. wrightii* (Fig. 4.39). Overall seasonal patterns were notably altered as the result of the decline during 1995, most severely at BR.

At BR (Fig. 4.39), there were no significant differences in cover over time (ANOVA: $P > 0.05$). Canopy height was significantly greater in August 1994 and November 1994 than in other months (ANOVA: $P = 0.0001$; T-K: $P \leq 0.05$). Shoot density and all seagrass biomass parameters were significantly lower in May 1995 than in all other months (ANOVA: $P = 0.0001$; T-K: $P \leq 0.05$). Before the decline, there were no significant differences among months (February 1994 through February 1995) in above-ground, below-ground, or total biomass (T-K: $P \geq 0.05$). Following the decline, shoot density returned to earlier levels. *H. wrightii* was beginning to recover by the end of the study, as above-ground, below-ground, and total biomass were all significantly higher in February 1996 than the low levels recorded in May 1995 (ANOVA: $P = 0.0001$; T-K: $P \leq 0.05$).

At MB (Fig. 4.39), cover was significantly higher in April 1994 and August 1995 (ANOVA: $P = 0.0001$; T-K: $P \leq 0.05$). Canopy height was highest in April 1994 and August 1994 and lowest in November 1995 (ANOVA: $P = 0.0001$; T-K: $P \leq 0.05$). [Note: Canopy height was not measured by the District at this station in February 1994.] There were minimal significant differences in shoot density among months (ANOVA: $P = 0.04$; but T-K could not detect any differences among months at $P = 0.05$). Similar to cover, above-ground biomass was significantly higher in April 1995 and August 1995 (ANOVA: $P = 0.001$, T-K: $P \leq 0.05$). Differences among months for below-ground and total biomass were less distinct; in both cases, the only significant difference was higher biomass in April 1994 than in November 1995 and February 1996 (ANOVA: $P = 0.01$, 0.004 , respectively, for below-ground and total biomass; T-K: $P \leq 0.05$).

At TC (Fig. 4.39), differences in cover and canopy height among months were not significant (ANOVA: $P > 0.05$). Shoot density and biomass were significantly higher in May 1995 and August 1995 (ANOVA: $P = 0.0001$; T-K: $P \leq 0.05$).

At SN (Fig. 4.39), cover was highest from April to November 1994 and in August 1995 and lowest in November 1995 (ANOVA: $P = 0.0001$; T-K: $P \leq 0.05$).

There was a consistent seasonal pattern in canopy height (ANOVA: $P = 0.0001$; T-K: $P \leq 0.05$): highest during summer (August 1994 and 1995), intermediate during spring (April 1994 and May 1995), and lowest during fall (November 1994 and 1995) and winter (February 1994, 1995, and 1996). While there were highly significant differences among months for shoot density, below-ground biomass, and total biomass (ANOVA: $P = 0.0001$), their seasonal patterns were less distinct than, but generally similar to, those for cover and canopy.

At SS (Fig. 4.39), cover was always higher during spring and summer than during fall and winter. Canopy height followed the same seasonal patterns as at SN but was greater in August 1995 than in August 1994 and greater in April 1994 than in May 1995 (ANOVA: $P = 0.0001$; T-K: $P \leq 0.05$). Differences among months for shoot density, below-ground biomass, and total biomass (ANOVA: $P = 0.0001$) were highly significant, with seasonal patterns less distinct, but generally following that of cover.

At VB (Fig. 4.39), the only significant difference for any parameter was for canopy height, which was maximal in August 1994 and minimal in February 1994 and November 1994 (ANOVA: $P = 0.0001$; T-K: $P \leq 0.05$).

At LP (Fig. 4.39), the only significant difference for any parameter was for canopy height which was reduced during the winter, particularly during February 1995 (ANOVA: $P = 0.0001$; T-K: $P \leq 0.05$). The apparent peaks at LP in August were not significant because of the high degree of variability at that time.

Syringodium filiforme

There was little statistically detected seasonality in most SAV parameters for *S. filiforme* (Fig. 4.40), but a significant decline in *S. filiforme* occurred during 1995 at BR.

At BR (Fig. 4.40), the decline in cover that occurred between February 1995 and May 1995 was not significant (ANOVA: $P > 0.05$), probably because of the low sample size for cover along the transects at this station (see Fig. 4.2). Canopy height (Fig. 4.40) was significantly higher in August 1994 than in all other months except April 1994 and November 1994 (ANOVA: $P = 0.0001$; T-K: $P \leq 0.05$). Shoot density, below-ground biomass, and total biomass were significantly higher from February 1994 to February 1995 (i.e., before the seagrass decline at this station) than during the remainder of the study (ANOVA: $P = 0.0001$; T-K: $P \leq 0.05$). During the first year, above-ground biomass was significantly higher during August 1994 and November 1994 than during February 1994 and 1995 (ANOVA: $P = 0.0001$; T-K: $P \leq 0.05$). Unlike *H. wrightii*, *S. filiforme* did not begin to recover by the end of the study, as shoot density and biomass in February 1996 were not significantly different from the low levels recorded in May 1995 (T-K: $P \geq 0.05$).

At LP (Fig. 4.40), the only significant difference for any parameter was for canopy height which was highest (ANOVA: $P = 0.0001$; T-K: $P \leq 0.05$) during summer (August 1994 and 1995) and spring (April 1994 and May 1995).

Thalassia testudinum

The only SAV parameter of *T. testudinum* (Fig. 4.41) that significantly varied through time was canopy height (ANOVA: $P = 0.0001$; T-K: $P \leq 0.05$). At VB, canopy height was higher in April 1994 than in February and November 1994 (ANOVA: $P = 0.001$; T-K: $P \leq 0.05$). At LP, canopy height was significantly higher in August 1994 than in November 1994 and February 1995 and 1996 (ANOVA: $P = 0.001$; T-K: $P \leq 0.05$). The apparent differences in shoot density and biomass at VB were not significant because of large variability in those parameters, due to the spatial heterogeneity of *T. testudinum* at this station.

Halophila engelmannii

BR was the only station with significant amounts of *H. engelmannii* (Fig 4.42). Its presence was limited to the first year of the study, prior to the precipitous decline in seagrass at that station. There were no significant differences in cover and canopy among months (ANOVA: $P > 0.05$), probably because of the low sample size for cover along the transects at this station (see Fig. 4.2). The only month in which shoot density and biomass were significantly different was August 1994 when values for these parameters all peaked (ANOVA: $P = 0.001$ for shoot density, above-ground biomass, and total biomass, 0.0002 for below-ground biomass; T-K: $P \leq 0.05$). This relatively low ability to detect statistical significance in *H. engelmannii* was due to its highly patchy distribution, when it was present.

Macroalgae

Despite strong seasonal patterns at individual stations, there was no consistent temporal pattern in macroalgal cover and biomass (Fig. 4.43). At each station, the patterns of *Gracilaria* biomass and total macroalgal biomass were similar.

At BR (Fig. 4.43), macroalgal cover was significantly higher in November 1994 than in other months (ANOVA: $P = 0.01$; T-K: $P \leq 0.05$). Biomass was significantly higher in November 1994 than in May 1995, November 1995, and February 1996 (ANOVA: $P = 0.02$; T-K: $P \leq 0.05$)

At MB (Fig. 4.43), macroalgal cover was highest in November 1994 and February 1995 (ANOVA: $P = 0.0001$; T-K: $P \leq 0.05$). Biomass was significantly higher in November 1994 than February 1994, August 1995, November 1995, and February 1996 (ANOVA: $P = 0.02$; T-K: $P \leq 0.05$)

At TC (Fig. 4.43), macroalgal cover and biomass were higher in August 1995 than in all other months (ANOVA: $P = 0.001$; T-K: $P \leq 0.05$).

At SN (Fig. 4.43), macroalgal cover was highest in April 1994 and February 1995 and lowest in November 1995 (ANOVA: $P = 0.0001$; T-K: $P \leq 0.05$). The only significant difference for biomass among months was August 1995 being higher than February 1996 (ANOVA: $P = 0.002$; T-K: $P \leq 0.05$).

At SS (Fig. 4.43), macroalgal cover was highest in February 1994 and 1995 and lowest in August 1994, November 1994 and 1995, and February 1996 (ANOVA: $P = 0.0001$; T-K: $P \leq 0.05$). Biomass was significantly higher in August 1994 and August 1995 than in November 1994 (ANOVA: $P = 0.0001$; T-K: $P \leq 0.05$).

At VB (Fig. 4.43), macroalgal cover was maximal in February 1994 and minimal in November 1994 (ANOVA: $P = 0.02$; T-K: $P \leq 0.05$). Biomass did not significantly vary among months (ANOVA: $P > 0.05$).

At LP (Fig. 4.43), macroalgal cover was higher in February 1994 and April 1994 than in all other months (ANOVA: $P = 0.0001$; T-K: $P \leq 0.05$). Biomass was significantly higher in February 1994 and April 1994 than in February 1996 (ANOVA: $P = 0.0001$; T-K: $P \leq 0.05$).

4.4.5 Comparisons of SAV among Stations and Years

The previous two sections addressed small-scale spatial (within station) and temporal (between sampling months or seasons) differences in SAV parameters. This section addresses larger-scale spatial (among stations) and temporal differences (among years). Specifically, this section addresses the question: what are the differences in SAV among stations and among years?

Seagrass community

At the community-level, shoot density during both years (Fig. 4.44) was significantly highest at BR, intermediate at SN, SS, VB, and LP, lower at TC, and lowest at MB (ANOVA: $P = 0.0001$; T-K: $P \leq 0.05$). Biomass followed the same order, except that, due to the influence of *T. testudinum* at VB and LP, above-ground, below-ground, and total biomass at BR and VB were equivalent (T-K: $P \geq 0.05$), and above-ground biomass was significantly greater at LP than at SN and SS (ANOVA: $P = 0.0001$; T-K: $P \leq 0.05$).

The amount of interannual variability in SAV parameters varied among stations (Fig. 4.44). At BR, shoot density and biomass declined considerably in 1995 (41%,

61%, 55%, and 56%, respectively, for shoot density, above-ground, below-ground and total biomass; ANOVA: $P = 0.0001$). At MB and SS, biomass also significantly declined (% decline, respectively, for above-ground, below-ground and total biomass: at MB, 80%, 71%, and 74%; at SS, 47%, 55%, and 52%; ANOVA, respectively, for above-ground, below-ground and total biomass: at MB, $P = 0.02, 0.04, 0.04$; at SS, $P = 0.04, 0.0001, \text{ and } 0.0003$), but shoot density did not (ANOVA: $P > 0.05$). At SN, below-ground and total biomass significantly declined (% decline = 57% and 42%; ANOVA: $P = 0.01, 0.04$, respectively), but shoot density and above-ground biomass did not (ANOVA: $P > 0.05$). At LP, SAV parameters did not vary significantly among years (ANOVA: $P > 0.05$).

Halodule wrightii

Cover of *H. wrightii* (Fig. 4.45) was highest at BR, SN, and SS and lowest at TC (ANOVA: $P = 0.0001$; T-K: $P \leq 0.05$). Canopy height was lower at MB and TC than at all other stations (ANOVA: $P = 0.0001$; T-K: $P \leq 0.05$). Shoot density and biomass were always highest at BR, followed by SN and SS, then by VB and TC, and finally by LP and MB (ANOVA: $P = 0.0001$; T-K: $P \leq 0.05$).

The amount of interannual variability in SAV parameters varied among stations. At BR (Fig. 4.45), cover did not significantly vary between years (ANOVA: $P > 0.05$). Interannual differences were significant for canopy height, shoot density, and all biomass parameters, with considerable declines in 1995 (% decline, respectively for canopy height, shoot density above-ground, below-ground and total biomass: 39%, 28%, 52%, 56%, and 50%; ANOVA: 0.002 for canopy height, 0.0001 for all other parameters).

At MB (Fig. 4.45), canopy height and above-ground biomass, below-ground biomass, and total biomass significantly declined in 1995 (% decline: 25%, 80%, 71%, and 74%, respectively; ANOVA: $P = 0.0001, 0.02, 0.04, 0.04$, respectively), but cover and shoot density did not (ANOVA: $P > 0.05$).

At SN (Fig. 4.45), cover, below-ground biomass, and total biomass significantly declined in 1995 (% decline = 44%, 57%, and 42%, respectively; ANOVA: $P = 0.0001, 0.01, 0.04$, respectively), but canopy height, shoot density, and above-ground biomass did not (ANOVA: $P > 0.05$).

At SS (Fig. 4.45), cover and above-ground biomass, below-ground biomass, and total biomass significantly declined in 1995 (% decline: 22%, 47%, 55%, and 52%, respectively; ANOVA: $P = 0.0004, 0.04, 0.0001, \text{ and } 0.0003$, respectively), but canopy height and shoot density did not (ANOVA: $P > 0.05$).

At LP (Fig. 4.45), SAV parameters did not significantly vary among years (ANOVA: $P > 0.05$).

Syringodium filiforme

S. filiforme (Fig. 4.46) was a major component of the seagrass community only at BR and LP. Overall, cover was significantly higher at BR than at LP (ANOVA: $P = 0.0001$; T-K: $P \leq 0.05$), but differences between these stations in canopy height, shoot density, and biomass were not significant (ANOVA: $P > 0.05$).

S. filiforme declined precipitously at BR during 1995 (Fig. 4.46). All SAV parameters at this station were significantly lower during 1995 than in 1994 (% decline for cover, canopy height, shoot density, above-ground biomass, below-ground biomass, and total biomass: 68%, 54%, 75%, 81%, 77%, and 78%, respectively; ANOVA: $P = 0.0001$). At LP, SAV parameters did not vary significantly among years (ANOVA: $P > 0.05$).

Interannual differences at BR impacted the comparison of SAV parameters between BR and LP (Fig. 4.46). During 1994, all SAV parameters were significantly higher at BR than at LP (ANOVA: $P = 0.0001$; T-K: $P \leq 0.05$), but during 1995, this pattern was completely reversed, i.e., values for all SAV parameters were significantly higher at LP than at BR (ANOVA: $P = 0.0001$; T-K: $P \leq 0.05$).

Thalassia testudinum

T. testudinum (Fig. 4.47) was restricted to the southernmost stations, VB and LP. All SAV parameters were significantly higher at VB than at LP (ANOVA: $P = 0.0001$; T-K: $P \leq 0.05$), with one exception. Canopy height did not vary significantly among stations (ANOVA: $P > 0.05$). At LP, SAV parameters did not vary significantly among years (ANOVA: $P > 0.05$).

Halophila engelmannii

H. engelmannii was consistently present at BR in 1994, but absent in 1995 (Fig. 4.48). Despite a relatively low frequency of occurrence, the higher SAV values in 1994 were statistically significant (ANOVA, respectively for cover, shoot density, above-ground biomass, below-ground biomass, and total biomass: $P = 0.0001$, 0.0003, 0.001, 0.002, 0.001).

Macroalgae

Macroalgal cover, total macroalgal biomass, and *Gracilaria* biomass (Fig. 4.49) increased along the north-south gradient of stations: lowest at BR and MB, highest at

VB and LP, and intermediate at the other stations (ANOVA: $P = 0.0001$; T-K: $P \leq 0.05$).

The only significant interannual differences occurred at LP (Fig. 4.49), where macroalgal cover, total macroalgal biomass, and *Gracilaria* biomass were all significantly higher in 1994 than in 1995 (ANOVA: $P = 0.0001$, 0.0004 , 0.0005 , respectively).

4.4.6 Correlation and Regression Analyses of SAV Parameters

Based on correlation analyses of shoot density, biomass, cover, and canopy height for each of the major seagrass species (Tables 4.3-4.5), shoot density, biomass, and cover were all highly correlated. The correlation of canopy height to the other parameters was much lower, but significant for *H. wrightii* with all other parameters and for *S. filiforme* with all other parameters except cover. Most of the relationships among these parameters are also presented graphically as linear regressions (Figs. 4.50-4.58).

The relationship and predictive capability of using certain SAV parameters that are more rapidly obtained (i.e., shoot density, cover, canopy height) than others that are much more time consuming (i.e., above-, below-, and total biomass) was determined with multiple regression. Step-wise multiple regressions were computed for each species except *H. engelmannii*, because of its low sampling frequency (Tables 4.6-4.8). Shoot density was the most significant factor to predict each of the biomass parameters. Canopy height was a secondary factor that significantly improved models for above-ground biomass of all species and for total biomass of *H. wrightii*. Cover was a secondary factor that significantly improved the model for below-ground biomass of *S. filiforme*.

4.5 Discussion

Despite the importance of SAV, there are surprisingly few published data on SAV parameters in Indian River Lagoon (reviewed by Dawes et al. 1995), and little attention has been paid to the problems of spatial and temporal variability of SAV in the lagoon. The present study appears to be the first to measure a wide variety of SAV parameters, and to consider spatial and temporal variability, at representative stations from different portions of the lagoon. The sampling problems inherent in this variability not only have limited previous scientific investigations on the SAV resource, but also confounds its management.

IRL has the highest seagrass biodiversity in the Caribbean region, with 7 species (Dawes et al. 1995). Only 4 species were encountered in the present study: *H. wrightii*, *S. filiforme*, *T. testudinum*, and *H. engelmannii*. The first 3 species are the most abundant species in IRL (Dawes et al. 1995). *H. engelmannii* was limited to a relatively small number of individuals under the canopy of larger seagrasses. Not found at any station were *Halophila decipiens*, *Halophila johnsonii*, and *Ruppia maritima*. The northern distribution of these species of *Halophila* is believed to be near Sebastian Inlet; *Ruppia*, while present throughout IRL, tends to be more abundant in northern IRL, and is probably the least abundant seagrass in the lagoon (Virnstein and Cairns 1986). Relative to the whole lagoon, this study overstates the relative abundance of *T. testudinum* (possibly at the expense of *S. filiforme*) due to the selection of the 2 southern stations; the northern limit of *T. testudinum* is near Sebastian Inlet, and 70% (areal coverage) of SAV occurs in the northern IRL, north of Cocoa (Woodward-Clyde Consultants 1994a). Yet, when present, *T. testudinum* is a dominant species, and this dominance increases further in South Florida (Zieman 1987).

Seagrass seasonality is a factor that must be considered when making site comparisons of SAV. This study found seagrass maxima in August, observations consistent with previous studies that have demonstrated rapid seagrass growth in spring and maximal standing stock in summer (Virnstein and Carbonara 1985; Dawes et al. 1995). What may be unusual in this data set is the rapid decline in seagrass, particularly at the Sebastian stations, between August and November 1994, followed by a general decline in most seagrasses parameters at most stations during 1995.

The seagrass decline at BR was precipitous. *H. wrightii* did begin to recover later in 1995, but *S. filiforme* did not, and *H. engelmannii* was not found for the remainder of the study. The cause of this decline appears to be related to sharply reduced salinities during 1995 associated with high rainfall and run-off. This interaction will be addressed further in Chapter 7.

BR, VB, and LP had appreciable amounts of more than one species of seagrass. At those sites, vertical zonation, typical of what has been previously observed in IRL (Dawes et al. 1995) was present, with *H. wrightii* more abundant in shallow water, but replaced by other species in deeper water, a pattern common in South Florida (Zieman 1987). However, at times, *H. wrightii* was a common component along the "deep-edge"; this pattern suggests that some factor, other than light (i.e., competition with other seagrass species), is responsible for its disjunct depth distribution.

Comparisons of SAV abundance data collected in this study with previous work are difficult because of differences in locations, parameters measured (most previous studies measured only 1 or 2 SAV parameters), or sampling design (e.g., while some

studies sampled dense monospecific beds, the present study sampled randomly along designated transects). Most previous data on seagrass abundance in IRL have been above-ground biomass from sites in the southern part of the lagoon, between Vero Beach and Fort Pierce Inlet. In this study, there was a large range in seagrass abundance among stations; stations with mixed seagrass communities had the highest cover and biomass.

The maximal above-ground biomass for *H. wrightii* (102.2 ± 17.5 g dry weight/m², at BR in August 1994) was within the range given by Virnstein and Carbonara (1985) for beds of *H. wrightii* at Link Port, higher than other measurements at Link Port (Heffernan and Gibson 1983), Vero Beach (Heffernan and Gibson 1983), and the Fort Pierce Harbor area (Hanisak in Gilmore and Hanisak 1991), but lower than at Jim Island near Fort Pierce Inlet (Heffernan and Gibson 1983). The widespread distribution of *H. wrightii* is due to a number of reasons, but, probably most relevant to this study, is its greater tolerance to salinity changes, such as what might be expected at the Sebastian stations. A fine-scale mapping study near Taylor Creek in Fort Pierce (Hanisak in Gilmore and Hanisak 1991) demonstrated that *H. wrightii* tolerated lower salinities better than other seagrass species in the community. *H. wrightii* also showed its relative resiliency in this study; following low salinity stress, *H. wrightii* was the first species to begin to recover at BR following its precipitous decline during 1995.

The highest above-ground biomass for *S. filiforme* in the present study was 42.9 ± 9.0 g dry weight/m² (at BR in August 1994), a value similar to previous maxima reported for this species at Link Port (Heffernan and Gibson 1983, Virnstein and Carbonara 1985) and higher than that reported for Jim Island (Heffernan and Gibson 1983) and the Fort Pierce Harbor area (Hanisak in Gilmore and Hanisak 1991). However, the highest above-ground biomass at LP (23.6 ± 8.3 g dry weight/m², August 1994) in this study is only about half the maximum reported by Virnstein and Carbonara (1985) for monospecific beds of *S. filiforme* at this site.

The maximal above-ground biomass for *T. testudinum* (168.0 ± 45.8 g dry weight/m², at VB in August 1994) was about mid-range for values reported by Virnstein and Carbonara (1985) from monospecific stands of *T. testudinum* at Link Port. However, the maximal value at VB is higher than other measurements at Link Port, Vero Beach, and Jim Island (Heffernan and Gibson 1983). The maximal value for *T. testudinum* at LP is much lower than that reported for monospecific beds at the site by Virnstein and Carbonara (1985); however, those authors realized that biomass varied significantly among different density beds, and, for example, they used a 20% biomass estimate for low-density beds. Relative to maps made mostly in 1980 (Virnstein and Carbonara 1985), seagrass at this site overall appears relatively stable through time, but *T. testudinum* appears to have expanded its distribution over the last 20 years.

Even less studied than seagrass in IRL is another component of SAV: benthic macroalgae. In seagrass beds of IRL, the macroalgal community consists primarily of unattached "drift algae", mostly red algae, especially *Gracilaria* spp. (Benz et al. 1979; Virnstein and Carbonara 1985; Hanisak in Gilmore and Hanisak 1991; Hanisak, unpublished). Maximal biomass values reported in this study (123.0 ± 42.7 g dry weight/m², at LP in April 1994) were considerably higher than those reported from seagrass beds at Jim Island (Benz et al. 1979) and the Fort Pierce Harbor area, and are about 2.5 times higher than maximal bed-wise values reported previously at Link Port (Virnstein and Carbonara 1985). However, the seasonality of macroalgae at LP agrees well with the previous study at this site (Virnstein and Carbonara 1985): a winter maximum and summer minimum. The inverse pattern occurred in the northern lagoon, but given the large amount of interannual variability that can occur at a single site (Virnstein and Carbonara 1985 observed a 25-fold increase between April maxima in successive years), the north-south gradient in macroalgal abundance and other perceived patterns should be confirmed.

The high amount of correlation among individual SAV parameters suggests that they do not all need to be measured to adequately assess SAV in the lagoon. Which SAV parameters should be measured? The problem is that each SAV parameter measured provides a different type of information. Biomass data are generally the preferred metric for measuring standing stock of many types of plants when their harvesting can be readily accomplished. Biomass for individual species can be added to obtain a total community value; in contrast, some parameters such as shoot density are not as meaningful in mixed species communities because of considerable variability in size and biomass of the component species. In this study, it appeared that above-ground biomass responded to seasonal and spatial changes more readily than below-ground biomass, but the latter may be a better measure of long-term success at a site. The major limitation of biomass as the primary SAV metric is that harvesting and subsequent processing are tedious and time consuming, and probably not feasible if a large number of sites are being sampled.

Multiple regression analyses indicated significant, predictive relationships between seagrass biomass and parameters that can be measured more rapidly (i.e., shoot density, cover, canopy height). Shoot density was the most significant factor to predict each of the biomass parameters for individual species. Canopy height was a secondary factor that significantly improved models for above-ground biomass of all three species and total biomass of *H. wrightii*. Cover was a secondary factor that significantly improved models for below-ground biomass of *S. filiforme*. These analyses suggest that shoot density may be the best parameter among those that can be relatively rapidly assessed in the field to estimate seagrass biomass, a parameter which requires large amounts of processing time. It might be desirable to increase the number of shoot density estimates in the ongoing District seagrass transect monitoring program to increase the ability to predict seagrass biomass.

Differences in species composition make comparisons of the total seagrass community among stations difficult. Species composition is clearly an important factor influencing SAV measurements due to differences in size and resource allocation among species. It is ironic that the high seagrass biodiversity of IRL may actually hinder its management. While, at least initially, site comparisons can be made by species, ultimately parameters such as above-ground biomass and cover, which incorporate all species, will need to be used for modeling SAV in the lagoon. In addition to being botanically significant, above-ground biomass probably has greater ecological significance (i.e., as an index of available food and habitat) than other SAV parameters measured. Among rapid assessment parameters, cover is probably the most ecologically meaningful one, as it, too, provides an estimate of habitat availability. The high degree of correlation among SAV parameters suggests that rapid assessment techniques for assessing SAV status and changes through time, such as the District's current monitoring of permanent transects (over 70 sites in IRL), are appropriate. The considerable interannual differences observed in this 2-year study demonstrate the importance of long-term seagrass monitoring (i.e., over many years) in IRL.

Future monitoring might also place greater emphasis on *H. wrightii*. Not only is *H. wrightii* the most widespread and abundant seagrass in the lagoon, but it also is more tolerant to environmental stress than other seagrasses and is the initial colonizer in seagrass communities. Greater recognition and study of the role of *H. wrightii* in the lagoon is needed. For example, recent work has demonstrated that *H. wrightii* may be the preferred seagrass habitat for the spotted sea trout (Gilmore, unpublished). During the start-up reconnaissance for this project, large amounts of *H. wrightii* were observed in the Crane Creek area of Melbourne, at sites where no seagrass may have been present since the early 1980's (Conrad White, personal communication). Was this "bloom" a sign of significant improvement in environmental conditions for seagrass in that part of the lagoon? Moreover, as demonstrated by the rapid decline of *H. wrightii* at the Sebastian stations in fall 1994 and at BR shortly thereafter, and its subsequent recovery at these stations, *H. wrightii* quickly responds to changes in water quality. Thus, *H. wrightii* is a promising seagrass indicator of changing environmental conditions, be they good or bad.

4.6 Summary

SAV at the PAR monitoring stations in IRL was quantified quarterly for 2 years for parameters which should respond to changes in PAR and water quality: species composition, percent cover, canopy height, shoot density, above- and below-ground biomass of seagrass, and macroalgal biomass. The major results of this study were:

- (1) Species composition, spatial (i.e., within-site) and temporal (i.e., seasonal, interannual) variability at the stations confounded an assessment of differences in SAV among sites.
- (2) Mixed populations of seagrass occurred at 3 stations: BR, primarily *H. wrightii* and *S. filiforme*, with a small population of *H. engelmannii*; VB, primarily *T. testudinum* and *H. wrightii*, with a small population of *S. filiforme*; and LP, equal amounts of *H. wrightii*, *T. testudinum*, and *S. filiforme*. Seagrass at MB, TC, SN, and SS was exclusively, or nearly so, *H. wrightii*. Species composition was an important factor influencing SAV measurements due to differences in size and resource allocation among species.
- (3) Mixed seagrass communities had site-specific patterns of depth zonation. At BR, *H. wrightii* declined with depth as *S. filiforme* became more abundant; *H. engelmannii* was most common at mid-depths. At VB, *H. wrightii* dominated the shallow end of the site, was replaced by *T. testudinum* at intermediate depths, and dominated again near the deep edge of the bed. The small amount of *S. filiforme* present tended to be near the deeper end of the bed. At LP, *S. filiforme* was much more abundant than at VB and largely replaced *H. wrightii* in deeper water.
- (4) At most stations, 3 transects were established to examine spatial variability of seagrass at the stations. "Mid-bed" transects agreed well with "whole bed" transects in regards to SAV parameters. SAV generally declined along the "deep edge" transect. Data from the first 2 transects were combined for seasonal, interannual, and interstation comparisons of SAV.
- (5) The most common seasonal pattern for SAV parameters was August maxima and November minima.
- (6) There were significant interannual differences in SAV parameters, with a considerable decline at most stations during 1995. The decline at BR was precipitous; *H. wrightii* began to recover later in the year, but *S. filiforme* and *H. engelmannii* did not. The cause of this decline appears to be related to sharply reduced salinities during 1995 associated with high rainfall and run-off.
- (7) Shoot density of the total seagrass community was highest at BR, intermediate at SN, SS, VB, and LP, lower at TC, and lowest at MB. Biomass followed the same order, except that, due to the influence of *T. testudinum* at VB and LP, above-ground, below-ground, and total biomass at VB were equivalent to those at BR, and above-ground biomass was significantly greater at LP than at SN and SS.
- (8) *H. wrightii* was the predominant seagrass overall and the only seagrass species present at all stations. Cover was highest at BR, SN, and SS and lowest at TC.

Canopy height was lower at MB and TC than at all other stations. Shoot density and all seagrass biomass parameters were always highest at BR, followed by SN and SS, then by VB and TC, and finally by LP and MB. The amount of interannual variability for these SAV parameters varied among stations.

- (9) The next most widespread seagrass species was *S. filiforme*, which was a major component of the seagrass community at BR and LP, and present in small amounts at VB and SS. During 1995, *S. filiforme* precipitously declined at BR and did not recover. All SAV parameters at this station were significantly lower during 1995 than in 1994. There were no significant interannual differences for any of these parameters at LP. Interannual differences at BR impacted the comparison of SAV parameters between BR and LP. During 1994, all SAV parameters were significantly higher at BR than at LP, but during 1995, this pattern was reversed.
- (10) *T. testudinum*, restricted to the southernmost stations, was more abundant at VB than at LP. All SAV parameters were significantly higher at VB than at LP, with one exception. Canopy height did not vary significantly among stations. Interannual differences in SAV parameters did not occur.
- (11) *H. engelmannii* was consistently present at BR during 1994, but absent in 1995. Despite a relatively low frequency of occurrence, the higher SAV values in 1994 were statistically significant.
- (12) The macroalgal community at these stations was almost exclusively unattached, "drift" algae; 65% of the total belonged to the red algal genus *Gracilaria*. Macroalgal abundance increased along the north-south gradient of stations. As with seagrass, there were varying degrees of macroalgal seasonality. The only significant interannual difference occurred at LP, where macroalgal cover, total macroalgal biomass, and *Gracilaria* biomass were all significantly higher in 1994 than in 1995.
- (13) Correlation analyses of shoot density, above-ground biomass, below-ground biomass, total biomass, cover, and canopy height for each of the 3 major seagrass species indicated that shoot density and the biomass parameters were all highly correlated. The correlation of canopy height to the other parameters was much lower, but significant for *H. wrightii* with all other parameters and for *S. filiforme* with all other parameters except cover.
- (14) The relationship and predictive capability of certain SAV parameters that are more rapidly obtained (i.e., shoot density, cover, canopy height) than others that are much more time consuming (i.e., above-ground, below-ground, and total biomass) was determined with multiple regression. Shoot density was the most

significant factor to predict each of the biomass parameters. Canopy height was a secondary factor that significantly improved models for above-ground biomass of all species and total biomass of *H. wrightii*. Cover was a secondary factor that significantly improved models for below-ground biomass of *S. filiforme*.

- (15) Differences in species composition make comparisons of the total seagrass community among stations difficult. While, at least initially, site comparisons can be made by species, ultimately parameters such as above-ground biomass and cover, which incorporate all species, will be needed to model SAV in the lagoon. Above-ground biomass probably has greater ecological significance (i.e., as an index of available food and habitat) than other SAV parameters measured. Among rapid assessment parameters, cover is probably the most ecologically meaningful one, as it, too, provides an estimate of habitat availability.
- (16) Because of the predominance of *H. wrightii* in the lagoon, its wide environmental tolerance, and its important ecological roles, *H. wrightii* is a promising candidate for a seagrass indicator of changing environmental conditions.
- (17) Continued long-term monitoring of seagrass in IRL is recommended. The existing monitoring program (Vimstein and Morris 1996) seems adequate to detect long-term trends in SAV status of interest to resource managers.

Table 4.1 Dates of quarterly SAV samplings. VB was sampled only during 1994 and February 1995 and TC was sampled only during 1995 and February 1996. For convenience elsewhere in this chapter, the collections are referred to by the designations under "Sampling Event". The total number of samples for the entire study was n = 1,042.

Sampling Event	Sampling Dates	Number of Samples per Station						
		BR	MB	TC	SN	SS	VB	LP
February 1994	February 8-12, 1994	22	10	—	22	22	22	22
April 1994	April 25-29, 1994	22	10	—	22	22	22	22
August 1994	August 5-9, 1994	22	10	—	22	22	22	22
November 1994	October 28 - November 3, 1994	22	10	—	22	22	22	22
February 1995	January 30 - February 3, 1995	22	10	10	22	22	22	22
May 1995	May 8-10, 1995	22	10	10	22	22	—	22
August 1995	August 14-16, 1995	22	10	10	22	22	—	22
November 1995	November 27-29, 1995	22	10	10	22	22	—	22
February 1996	February 8-13, 1996	22	10	10	22	22	—	22
Station Totals		198	90	50	198	198	110	198

Table 4.2 Mean depth (m) of seagrass beds and depth (m), distance from shore (m), and species present at the "deep edge" at IRL stations during the quarterly SAV samplings.

Station	Month	Mean Depth (m)	"Deep Edge" of Seagrass Bed		
			Depth (m)	Distance from Shore (m)	Species
BR	2/94	0.67	1.67	28	<i>H. wrightii</i> , <i>S. filiforme</i>
	4/94	0.73	1.76	28	<i>H. wrightii</i> , <i>S. filiforme</i>
	8/94	0.74	1.75	28	<i>H. wrightii</i> , <i>S. filiforme</i>
	11/94	0.96	1.95	28	<i>H. wrightii</i> , <i>S. filiforme</i>
	2/95	0.63	1.41	27	<i>H. wrightii</i> , <i>S. filiforme</i>
	5/95	0.78	1.39	26	<i>H. wrightii</i> , <i>S. filiforme</i>
	8/95	0.95	1.48	25	<i>H. wrightii</i> , <i>S. filiforme</i>
	11/95	0.72	1.05	25	<i>H. wrightii</i>
	2/96	0.66	0.90	20	<i>H. wrightii</i>
	Mean	0.76	1.48	26	
MB	2/94	ND	ND	32	<i>H. wrightii</i>
	4/94	0.57	0.67	32	<i>H. wrightii</i>
	8/94	0.59	0.83	37	<i>H. wrightii</i>
	11/94	0.78	0.93	32	<i>H. wrightii</i>
	2/95	0.38	0.54	32	<i>H. wrightii</i>
	5/95	0.54	0.72	32	<i>H. wrightii</i>
	8/95	0.79	1.04	30	<i>H. wrightii</i>
	11/95	0.56	0.70	30	<i>H. wrightii</i>
	2/96	0.39	0.54	30	<i>H. wrightii</i>
	Mean	0.58	0.75	32	

ND = Not Determined

Table 4.2 (Continued)

Station	Month	Mean Depth (m)	"Deep Edge" of Seagrass Bed		Species
			Depth (m)	Distance from Shore (m)	
TC	2/95	0.64	0.85	80	<i>H. wrightii</i>
	5/95	0.70	0.77	70	<i>H. wrightii</i>
	8/95	1.00	1.02	50	<i>H. wrightii</i>
	11/95	0.78	0.78	70	<i>H. wrightii</i>
	2/96	0.55	0.44	20	<i>H. wrightii</i>
	Mean	0.73	0.77	58	
	SN	2/94	0.48	0.85	140
4/94		0.61	0.83	130	<i>H. wrightii</i>
8/94		0.73	1.17	140	<i>H. wrightii</i>
11/94		0.79	1.04	138	<i>H. wrightii</i>
2/95		0.51	0.93	140	<i>H. wrightii</i>
5/95		0.59	0.86	130	<i>H. wrightii</i>
8/95		0.95	1.18	130	<i>H. wrightii</i>
11/95		0.70	0.91	130	<i>H. wrightii</i>
2/96		0.49	0.85	140	<i>H. wrightii</i>
Mean		0.65	0.96	135	
SS		2/94	0.64	0.96	400
	4/94	0.78	1.10	400	<i>H. wrightii</i>
	8/94	0.87	1.22	400	<i>H. wrightii</i>
	11/94	0.96	1.30	400	<i>H. wrightii</i>
	2/95	0.69	1.00	400	<i>H. wrightii</i>
	5/95	0.71	1.03	400	<i>H. wrightii</i>
	8/95	1.00	1.35	390	<i>H. wrightii</i>
	11/95	0.85	1.20	400	<i>H. wrightii</i>
	2/96	0.68	1.10	400	<i>H. wrightii</i>
	Mean	0.80	1.14	399	

Table 4.2 (Continued)

Station	Month	Mean Depth (m)	"Deep Edge" of Seagrass Bed		
			Depth (m)	Distance from Shore (m)	Species
VB	2/94	0.72	0.98	230	<i>H. wrightii</i> , <i>S. filiforme</i>
	4/94	0.74	1.05	230	<i>H. wrightii</i>
	8/94	0.98	1.30	240	<i>H. wrightii</i> , <i>S. filiforme</i>
	11/94	1.04	1.20	244	<i>H. wrightii</i>
	Mean	0.87	1.13	236	
LP	2/94	0.53	1.10	500	<i>H. wrightii</i> , <i>S. filiforme</i>
	4/94	0.80	1.38	500	<i>H. wrightii</i> , <i>S. filiforme</i>
	8/94	1.01	1.63	500	<i>H. wrightii</i> , <i>S. filiforme</i>
	11/94	0.85	1.25	500	<i>H. wrightii</i> , <i>S. filiforme</i>
	2/95	0.70	1.12	500	<i>H. wrightii</i> , <i>S. filiforme</i>
	5/95	0.73	1.18	500	<i>H. wrightii</i> , <i>S. filiforme</i>
	8/95	0.98	1.64	500	<i>H. wrightii</i> , <i>S. filiforme</i>
	11/95	0.78	1.30	500	<i>H. wrightii</i> , <i>S. filiforme</i>
	2/96	0.79	1.36	500	<i>H. wrightii</i> , <i>S. filiforme</i>
	Mean	0.80	1.33	500	

Table 4.3 *Halodule wrightii*. Correlation matrix of shoot density (shoots/m²), above-ground, below-ground, and total biomass (g dry weight/m²), cover (%), and canopy height (m). Data used in this analysis were mean station values (derived from Transects 1 and 2) from each quarterly SAV sampling. Values for each combination are Pearson correlation coefficients followed by level of significance.

Parameter	Above-ground Biomass	Below-ground Biomass	Total Biomass	Cover	Canopy Height
Shoot Density	0.782 0.0001	0.819 0.0001	0.846 0.0001	0.761 0.0001	0.362 0.01
Above-ground Biomass		0.782 0.0001	0.888 0.0001	0.704 0.0001	0.672 0.0001
Below-ground Biomass			0.981 0.0001	0.624 0.0001	0.325 0.02
Total Biomass				0.677 0.0001	0.448 0.001
Cover					0.561 0.0001

Table 4.4 *Syringodium filiforme*. Correlation matrix of shoot density (shoots/m²), above-ground, below-ground, and total biomass (g dry weight/m²), cover (%), and canopy height (m). Data used in this analysis were mean station values (derived from Transects 1 and 2) from each quarterly SAV sampling. Values for each combination are Pearson correlation coefficients followed by level of significance.

Parameter	Above-ground Biomass	Below-ground Biomass	Total Biomass	Cover	Canopy Height
Shoot Density	0.867 0.0001	0.948 0.0001	0.945 0.0001	0.913 0.0001	0.555 0.02
Above-ground Biomass		0.869 0.0001	0.952 0.0001	0.838 0.0001	0.769 0.0002
Below-ground Biomass			0.979 0.0001	0.934 0.0001	0.488 0.04
Total Biomass				0.925 0.0001	0.623 0.001
Cover					0.453 0.06

Table 4.5 *Thalassia testudinum*. Correlation matrix of shoot density (shoots/m²), above-ground, below-ground, and total biomass (g dry weight/m²), cover (%), and canopy height (m). Data used in this analysis were mean station values (derived from Transects 1 and 2) from each quarterly SAV sampling. Values for each combination are Pearson correlation coefficients followed by level of significance.

Parameter	Above-ground Biomass	Below-ground Biomass	Total Biomass	Cover	Canopy Height
Shoot Density	0.957 0.0001	0.960 0.0001	0.965 0.0001	0.861 0.0002	0.219 0.47
Above-ground Biomass		0.970 0.0001	0.990 0.0001	0.776 0.002	0.379 0.20
Below-ground Biomass			0.995 0.0001	0.810 0.001	0.278 0.36
Total Biomass				0.802 0.001	0.321 0.28
Cover					0.227 0.46

Table 4.6 *Halodule wrightii*. Stepwise multiple regression models for above-ground, below-ground, and total biomass (g dry weight/m²), as a function of shoot density (shoots/m²), cover (%), and canopy height (m). Data used in this analysis were mean station values (derived from Transects 1 and 2) from each quarterly SAV sampling. Individual variables had to have a P value < 0.15 to be considered for addition to the model and could be removed or added at subsequent steps. Variables were added one at a time as long as P for the model was <0.05.

Parameter	Step	Factor	Partial R ²	Model R ²	P
Above-ground Biomass	1	Shoot Density	0.606	0.606	0.0001
	2	Shoot Density Canopy Height	0.174	0.781	0.0001
Below-ground Biomass	1	Shoot Density	0.667	0.667	0.0001
Total Biomass	1	Shoot Density	0.712	0.712	0.0001
	2	Shoot Density Canopy Height	0.023	0.735	0.04

Regression Equations:

$$\text{Above-ground Biomass} = 0.02 \text{ Shoot Density} + 151.4 \text{ Canopy Height} - 16.1$$

$$\text{Below-ground Biomass} = 0.05 \text{ Shoot Density} - 3.7$$

$$\text{Total Biomass} = 0.07 \text{ Shoot Density} + 181.0 \text{ Canopy Height} - 22.8$$

Table 4.7 *Syringodium filiforme*. Stepwise multiple regression models for above-ground, below-ground, and total biomass (g dry weight/m²), as a function of shoot density (shoots/m²), cover (%), and canopy height (m). Data used in this analysis were mean station values (derived from Transects 1 and 2) from each quarterly SAV sampling. Individual variables had to have a P value < 0.15 to be considered for addition to the model and could be removed or added at subsequent steps. Variables were added one at a time as long as P for the model was <0.05.

Parameter	Step	Factor	Partial R ²	Model R ²	P
Above-ground Biomass	1	Shoot Density	0.725	0.725	0.0001
	2	Shoot Density Canopy Height	0.127	0.852	0.03
Below-ground Biomass	1	Shoot Density	0.887	0.887	0.0001
	2	Shoot Density Cover	0.032	0.918	0.03
Total Biomass	1	Shoot Density	0.882	0.882	0.0001

Regression Equations:

$$\text{Above-ground Biomass} = 0.02 \text{ Shoot Density} + 47.1 \text{ Canopy Height} - 7.8$$

$$\text{Below-ground Biomass} = 0.03 \text{ Shoot Density} + 0.33 \text{ Cover} - 3.0$$

$$\text{Total Biomass} = 0.09 \text{ Shoot Density} - 5.5$$

Table 4.8 *Thalassia testudinum*. Stepwise multiple regression models for above-ground, below-ground, and total biomass (g dry weight/m²), as a function of shoot density (shoots/m²), cover (%), and canopy height (m). Data used in this analysis were mean station values (derived from Transects 1 and 2) from each quarterly SAV sampling. Individual variables had to have a P value < 0.15 to be considered for addition to the model and could be removed or added at subsequent steps. Variables were added one at a time as long as P for the model was <0.05.

Parameter	Step	Factor	Partial R ²	Model R ²	P
Above-ground Biomass	1	Shoot Density	0.924	0.924	0.0001
	2	Shoot Density Canopy Height	0.030	0.953	0.0001
Below-ground Biomass	1	Shoot Density	0.922	0.922	0.0001
Total Biomass	1	Shoot Density	0.937	0.937	0.0001

Regression Equations:

$$\text{Above-ground Biomass} = 0.45 \text{ Shoot Density} + 138.1 \text{ Canopy Height} - 40.4$$

$$\text{Below-ground Biomass} = 0.67 \text{ Shoot Density} - 9.7$$

$$\text{Total Biomass} = 1.1 \text{ Shoot Density} - 15.0$$

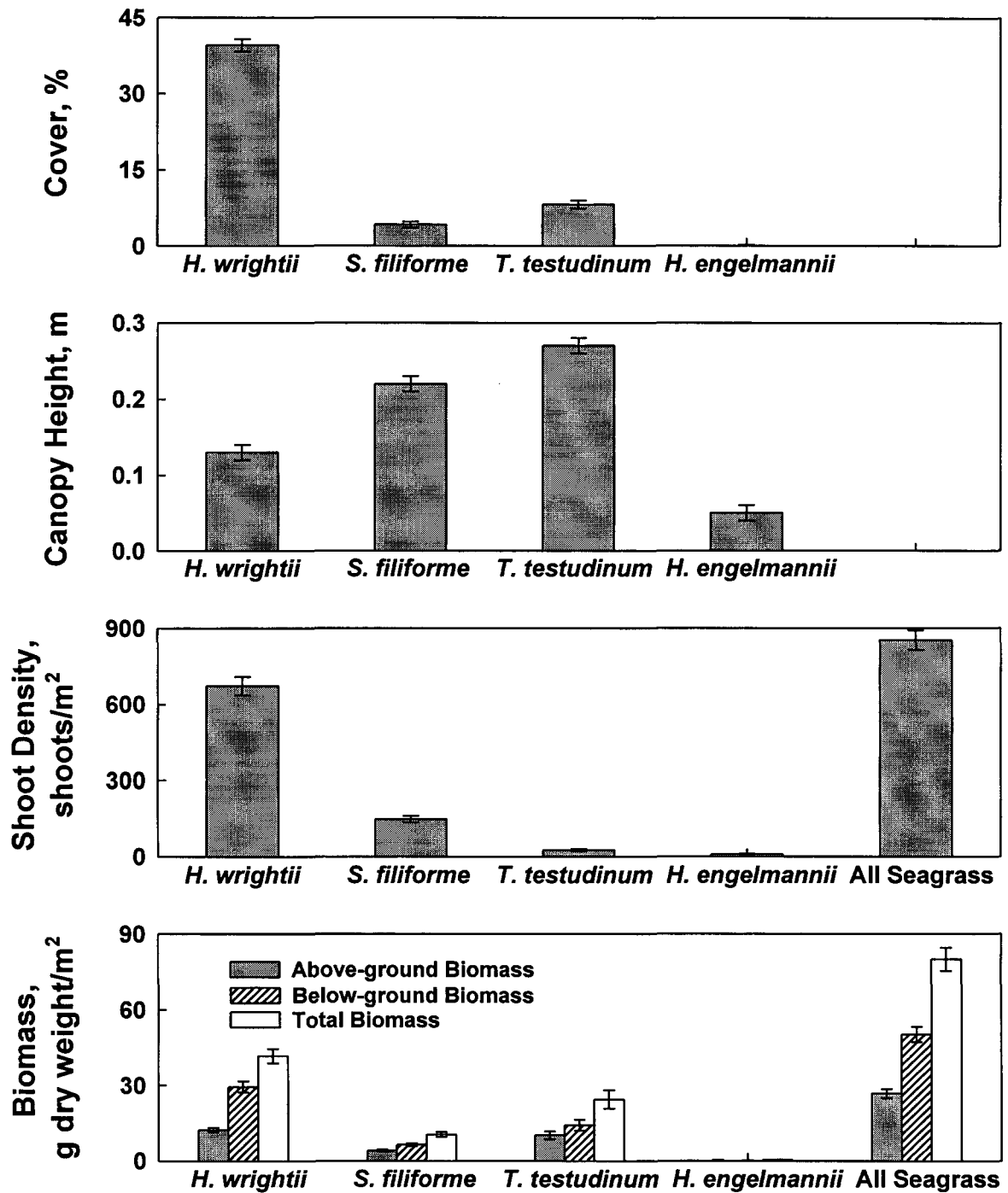


Fig. 4.1 Grand means (\pm SE) for cover, canopy height, shoot density, and above-ground, below-ground, and total biomass by species, and (for shoot density and biomass) all species of seagrass, for the entire study.

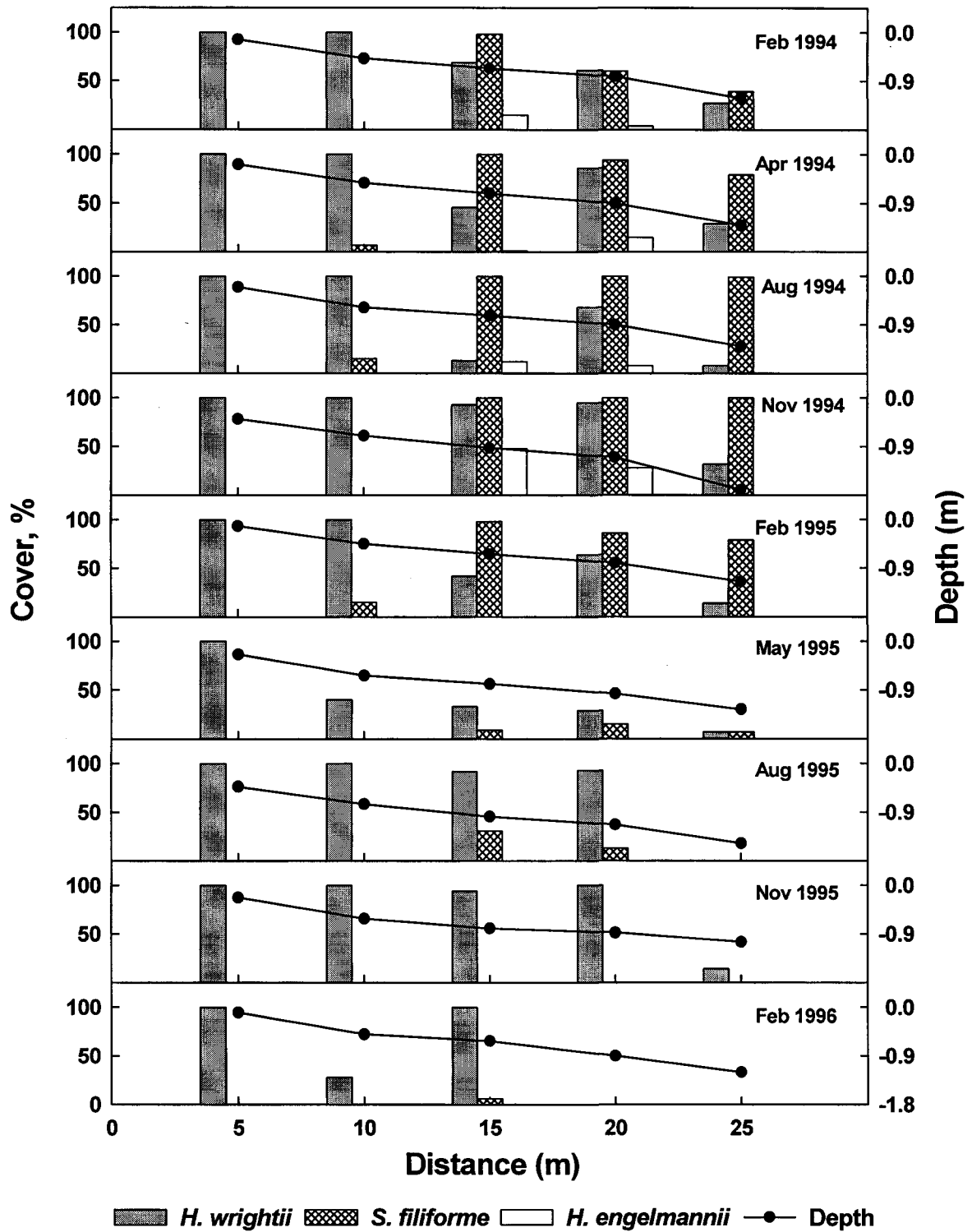


Fig. 4.2 Seagrass cover, by species and season, vs. depth and distance from shore at BR. Data were collected and provided by SJRWMD (L. Morris et al.).

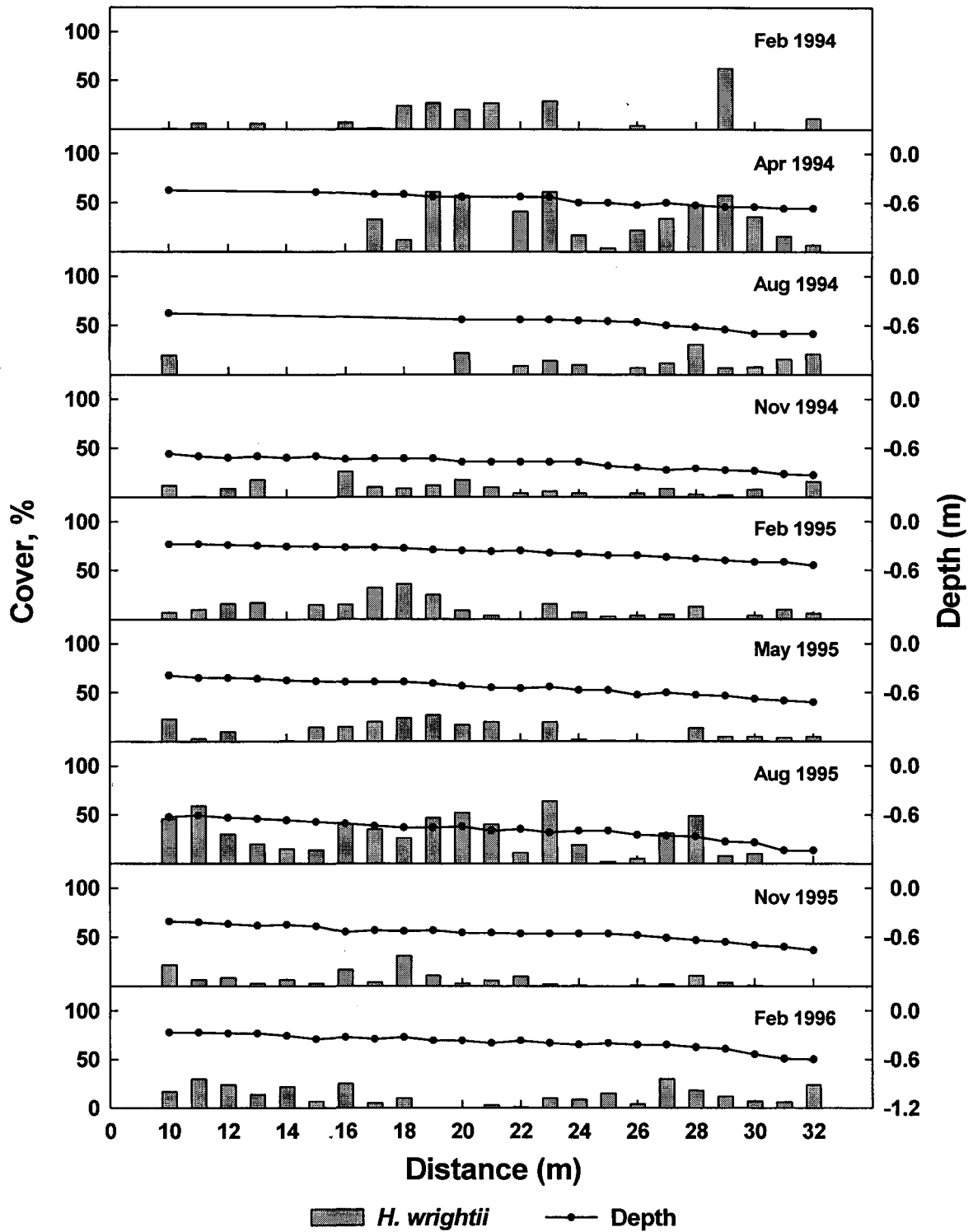


Fig. 4.3 Seagrass cover, by species and season, vs. depth and distance from shore at MB. Data were collected and provided by SJRWMD (L. Morris et al.).

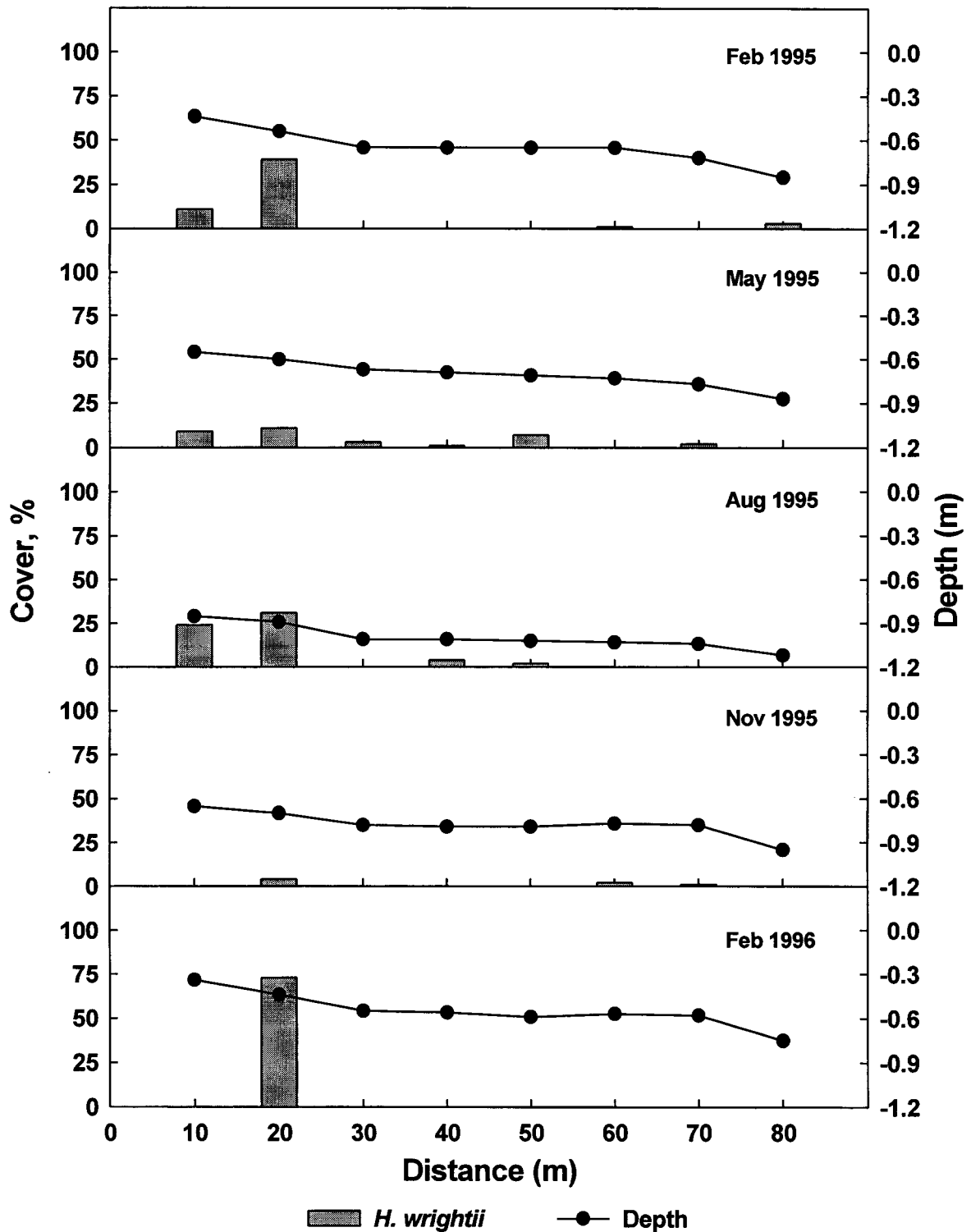


Fig. 4.4 Seagrass cover, by species and season, vs. depth and distance from shore at TC. Data were collected and provided by SJRWMD (L. Morris et al.).

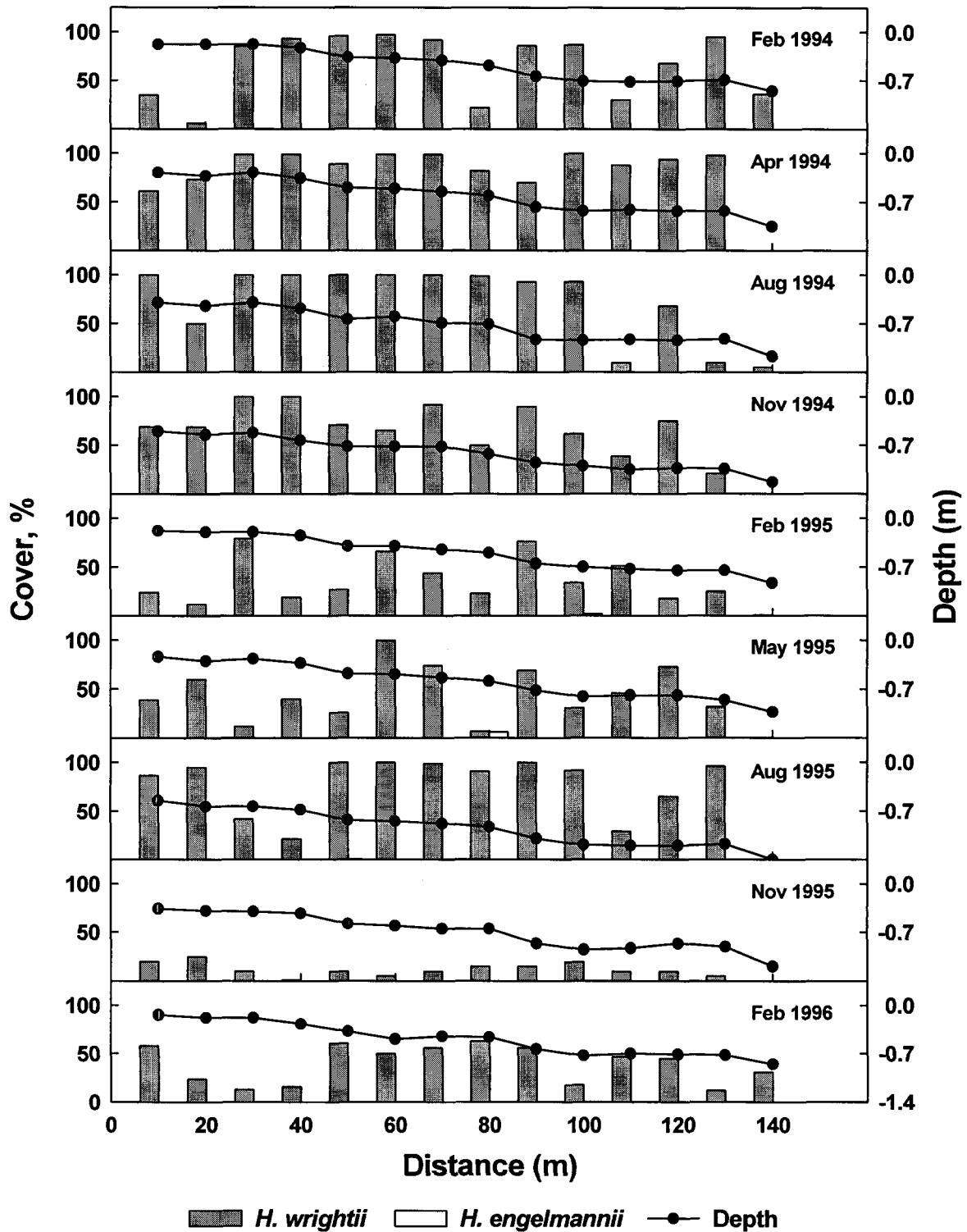


Fig. 4.5 Seagrass cover, by species and season, vs. depth and distance from shore at SN. Data were collected and provided by SJRWMD (L. Morris et al.).

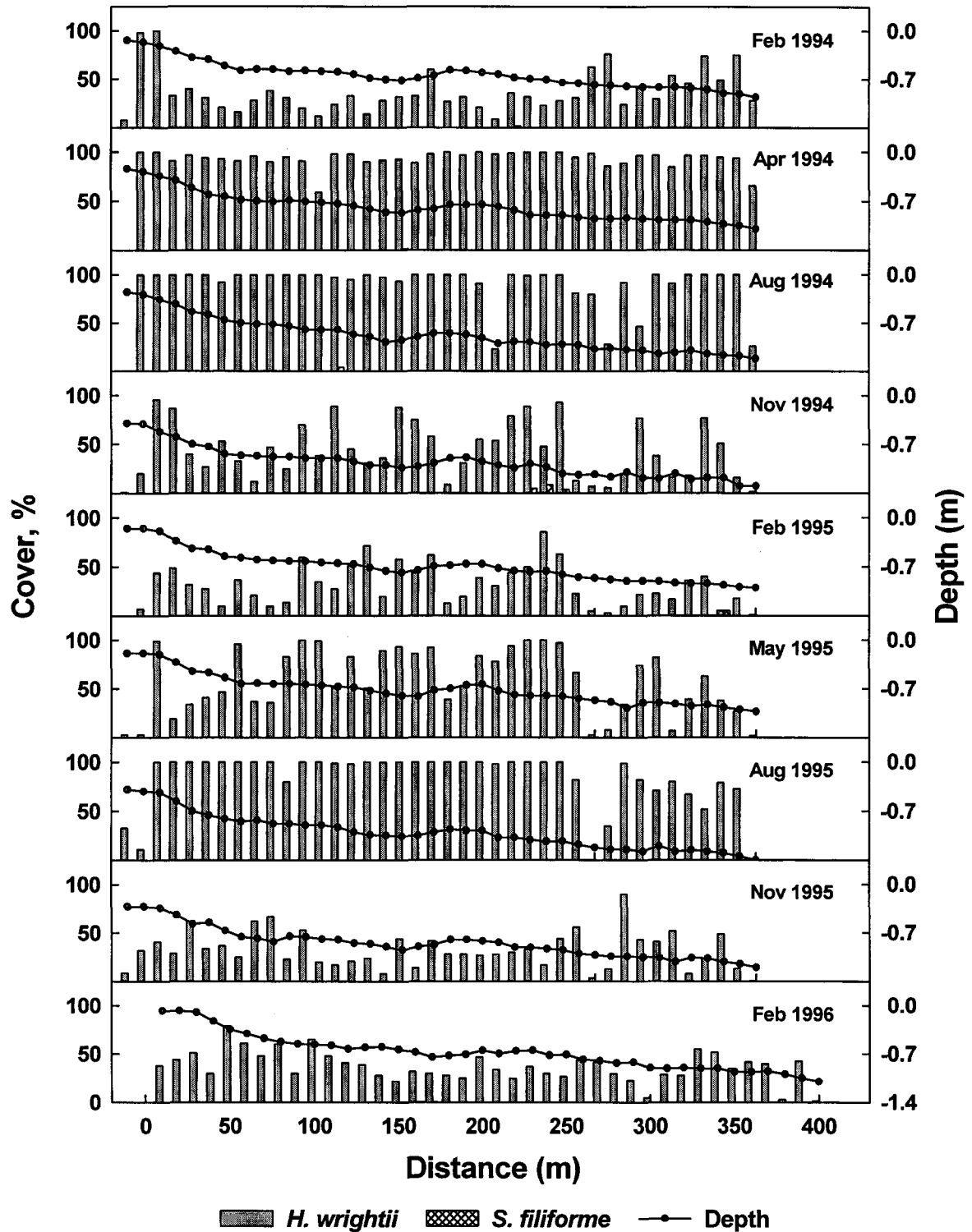


Fig. 4.6 Seagrass cover, by species and season, vs. depth and distance from shore at SS. Data were collected and provided by SJRWMD (L. Morris et al.).

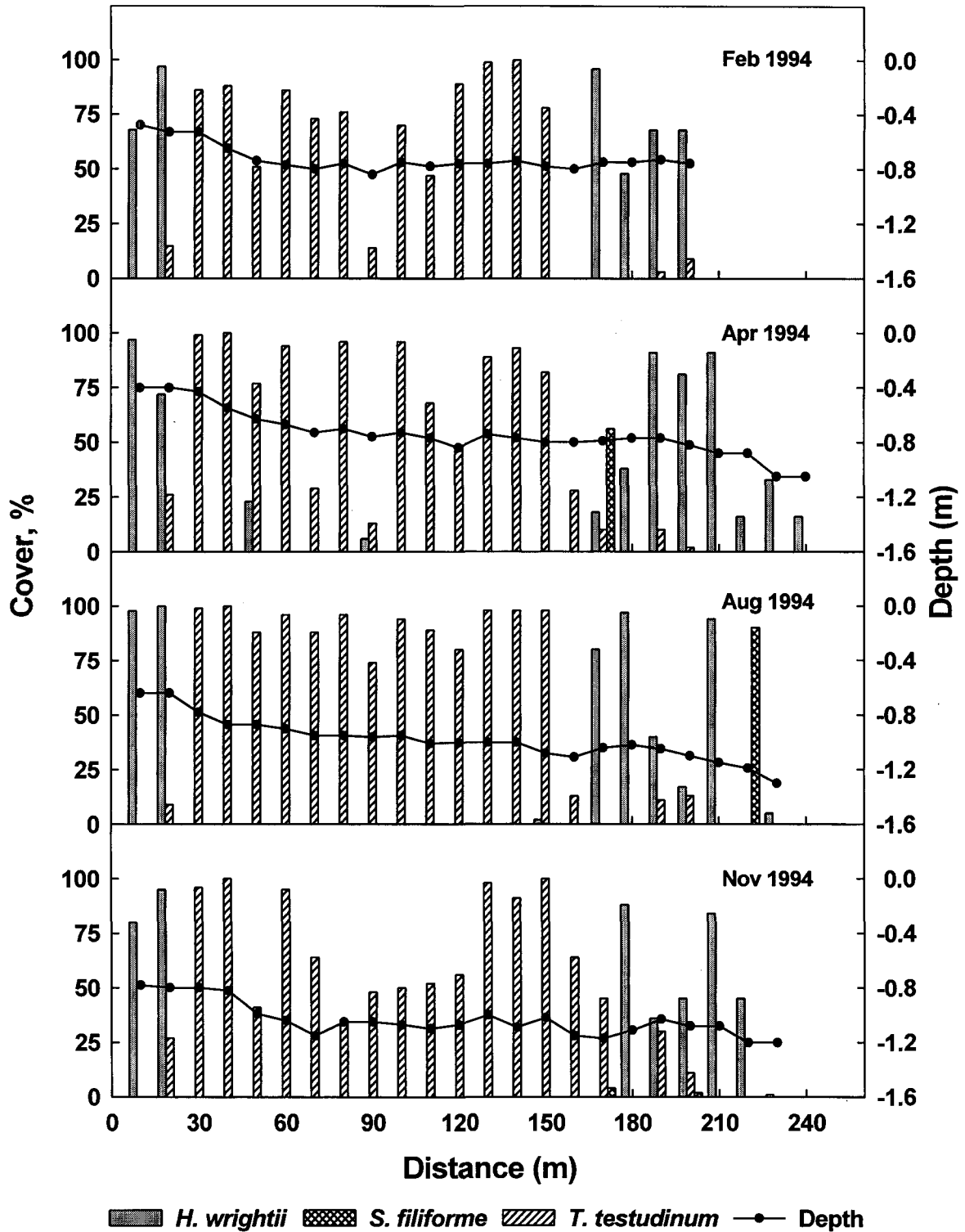


Fig. 4.7 Seagrass cover, by species and season, vs. depth and distance from shore at VB. Data were collected and provided by SJRWMD (L. Morris et al.).

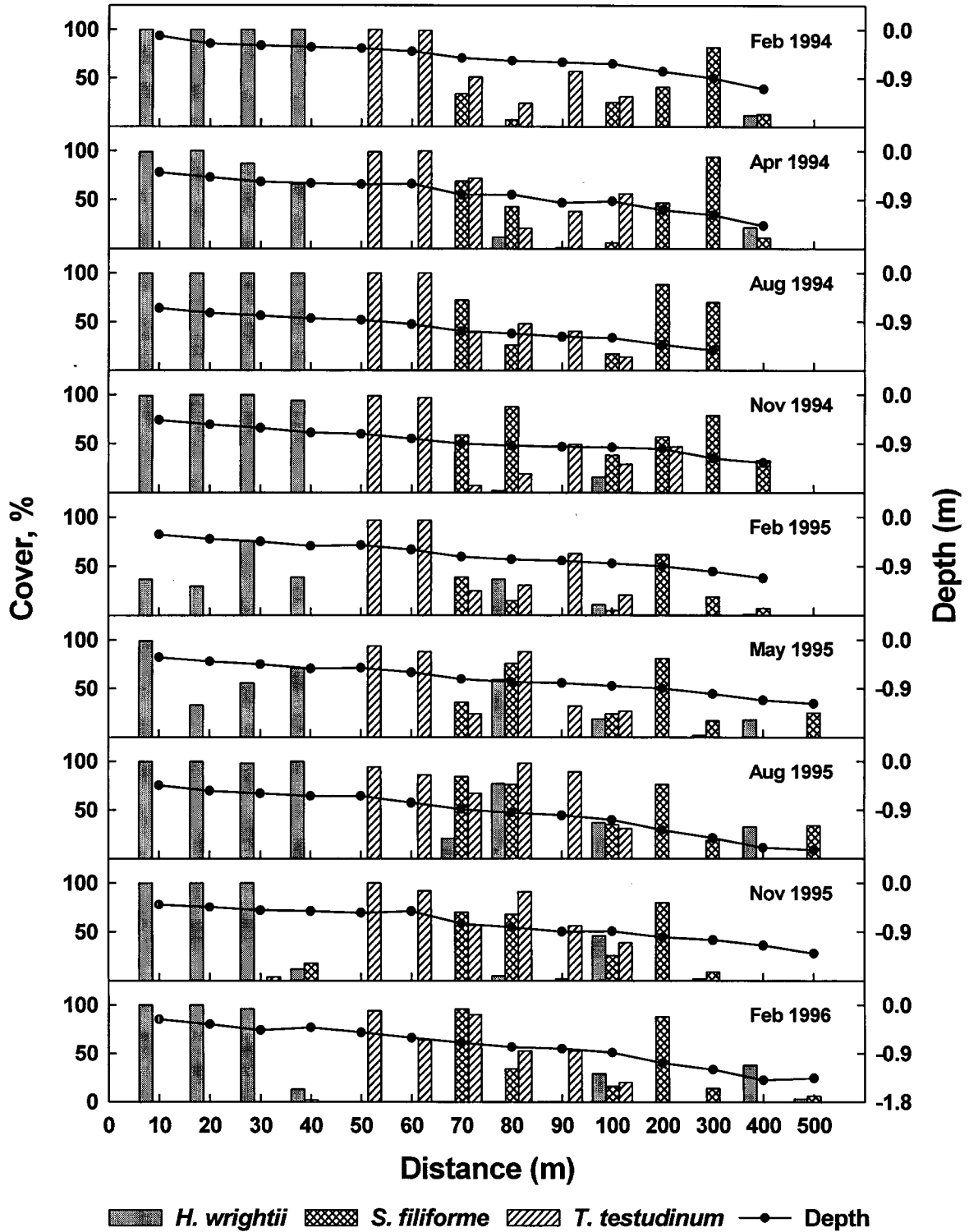


Fig. 4.8 Seagrass cover, by species and season, vs. depth and distance from shore at LP. Data were collected and provided by SJRWMD (L. Morris et al.).

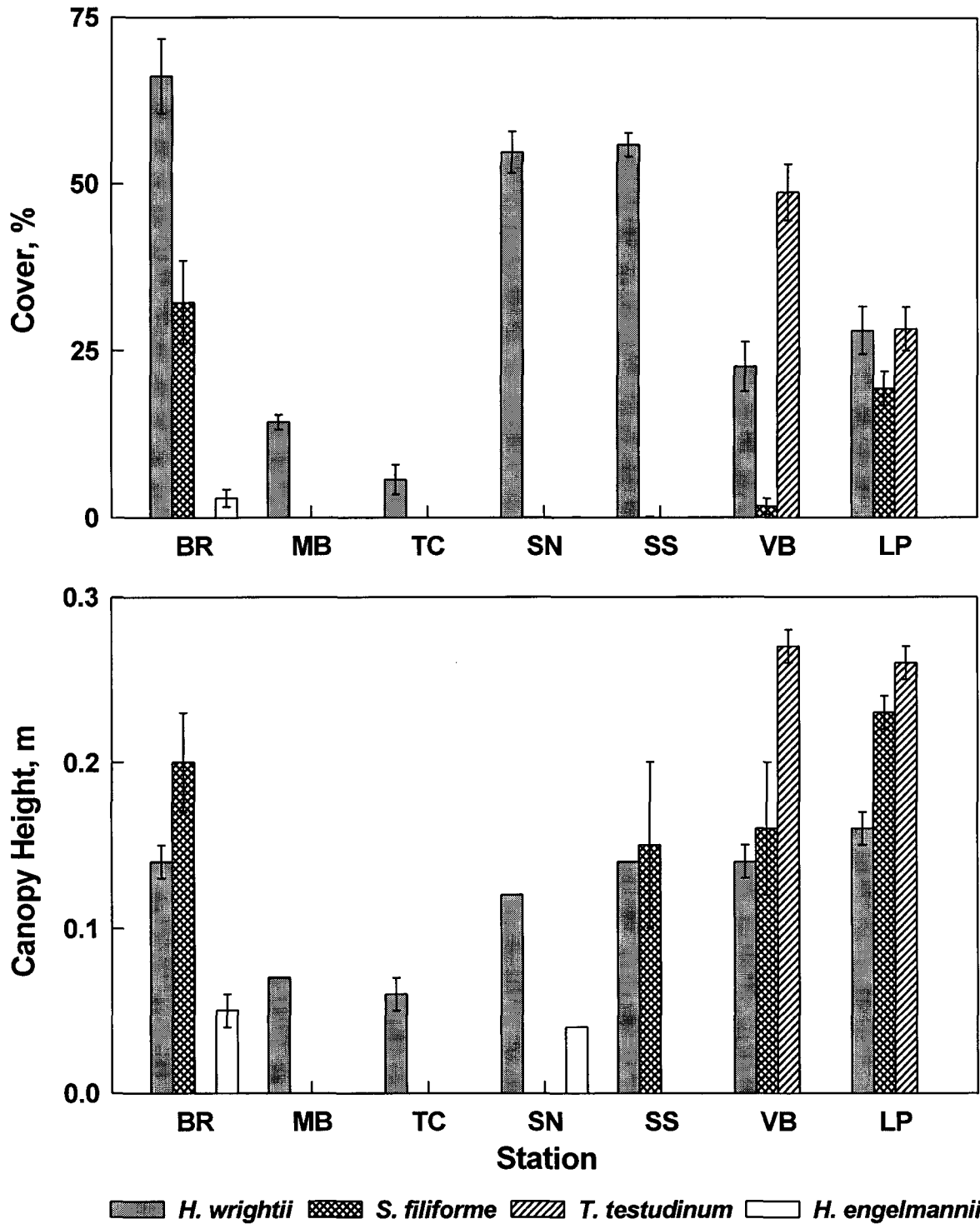


Fig. 4.9 Station means (\pm SE) for cover and canopy height of *Halodule wrightii*, *Halophila engelmannii*, *Syringodium filiforme*, and *Thalassia testudinum*, for the entire study.

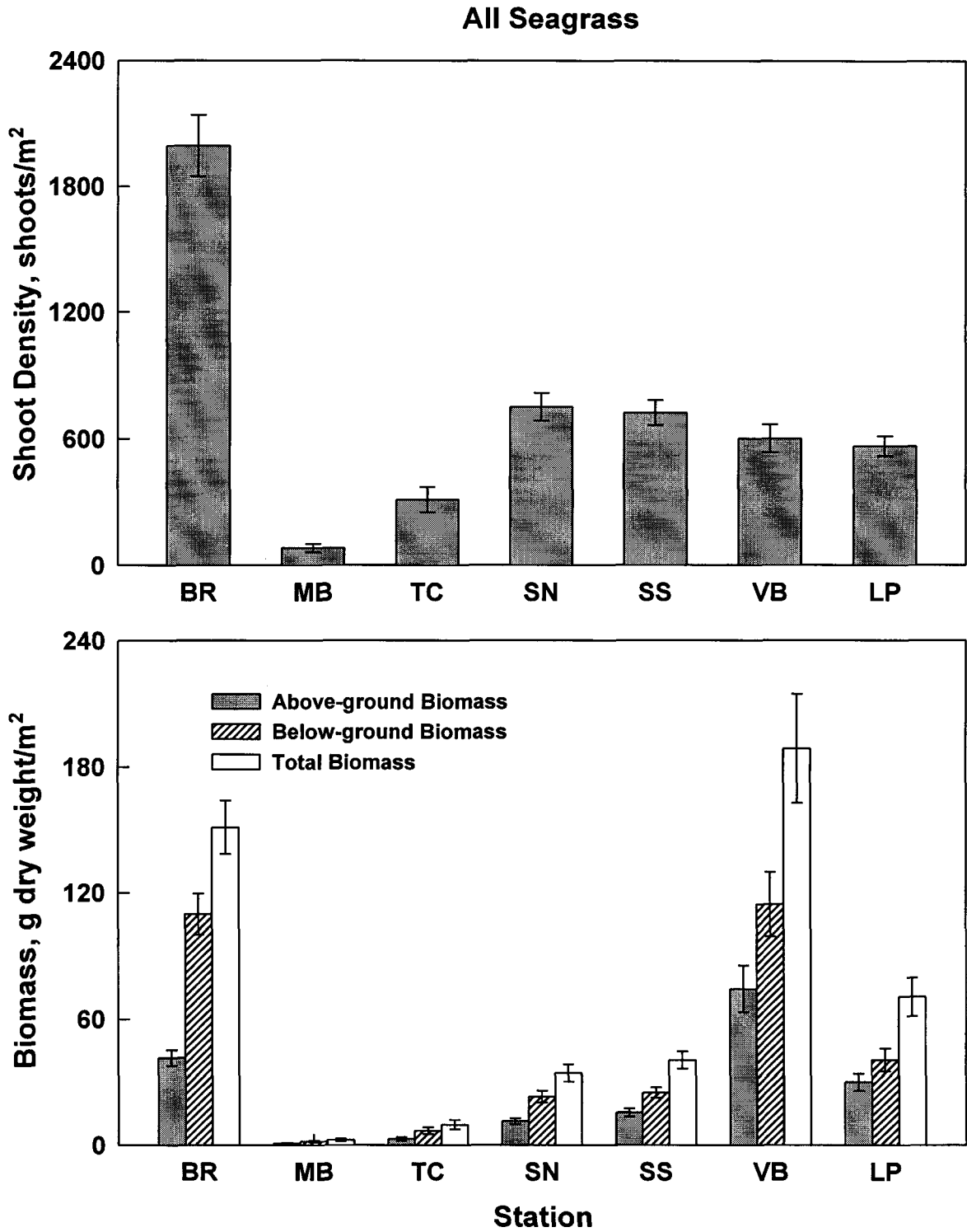


Fig. 4.10 Station means (\pm SE) for shoot density and above-ground, below-ground, and total biomass of the seagrass community, by season and transect.

Halodule wrightii

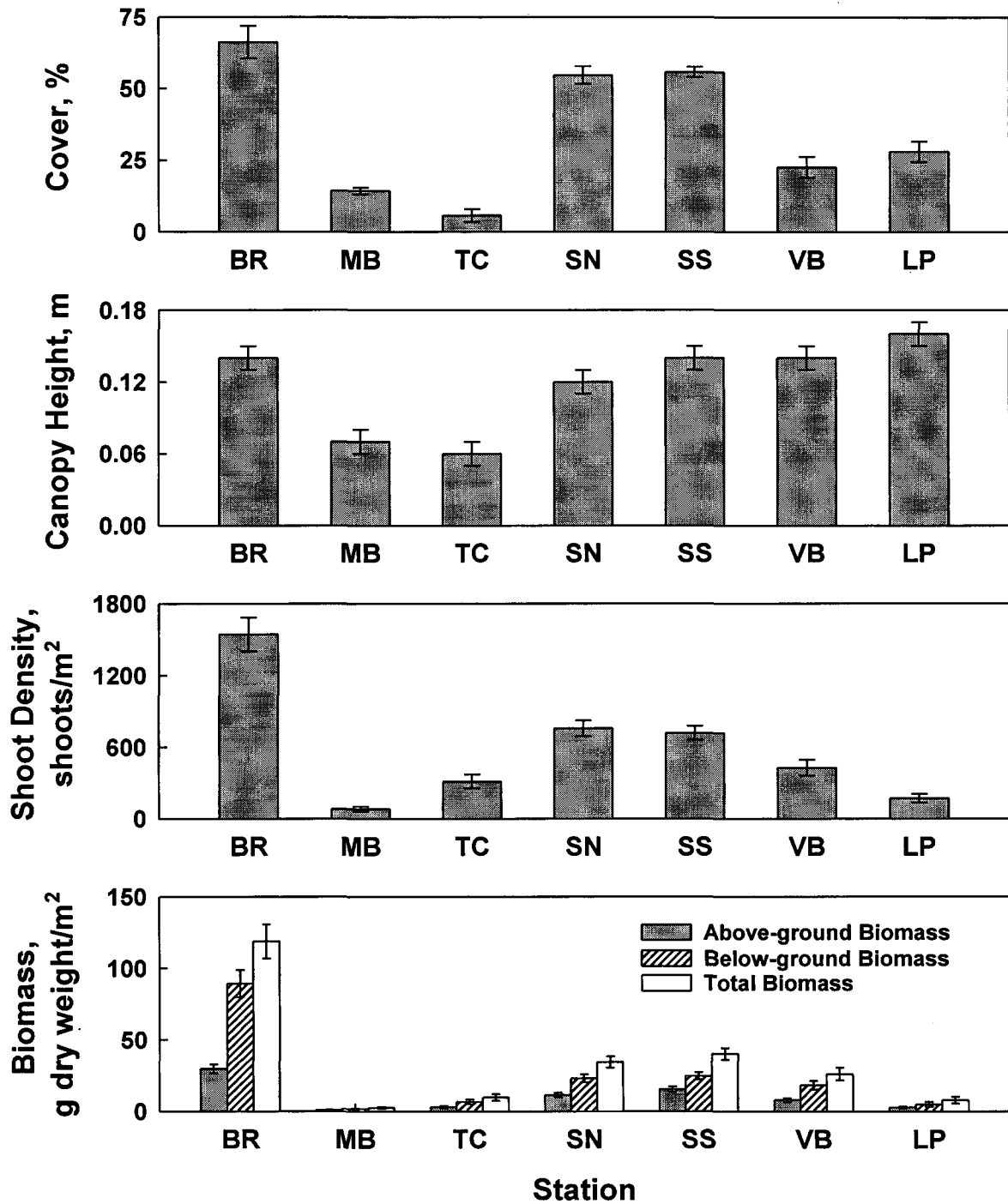


Fig. 4.11 Station means (\pm SE) for cover, canopy height, shoot density, and above-ground, below-ground, and total biomass of *Halodule wrightii*, by season and transect.

Syringodium filiforme

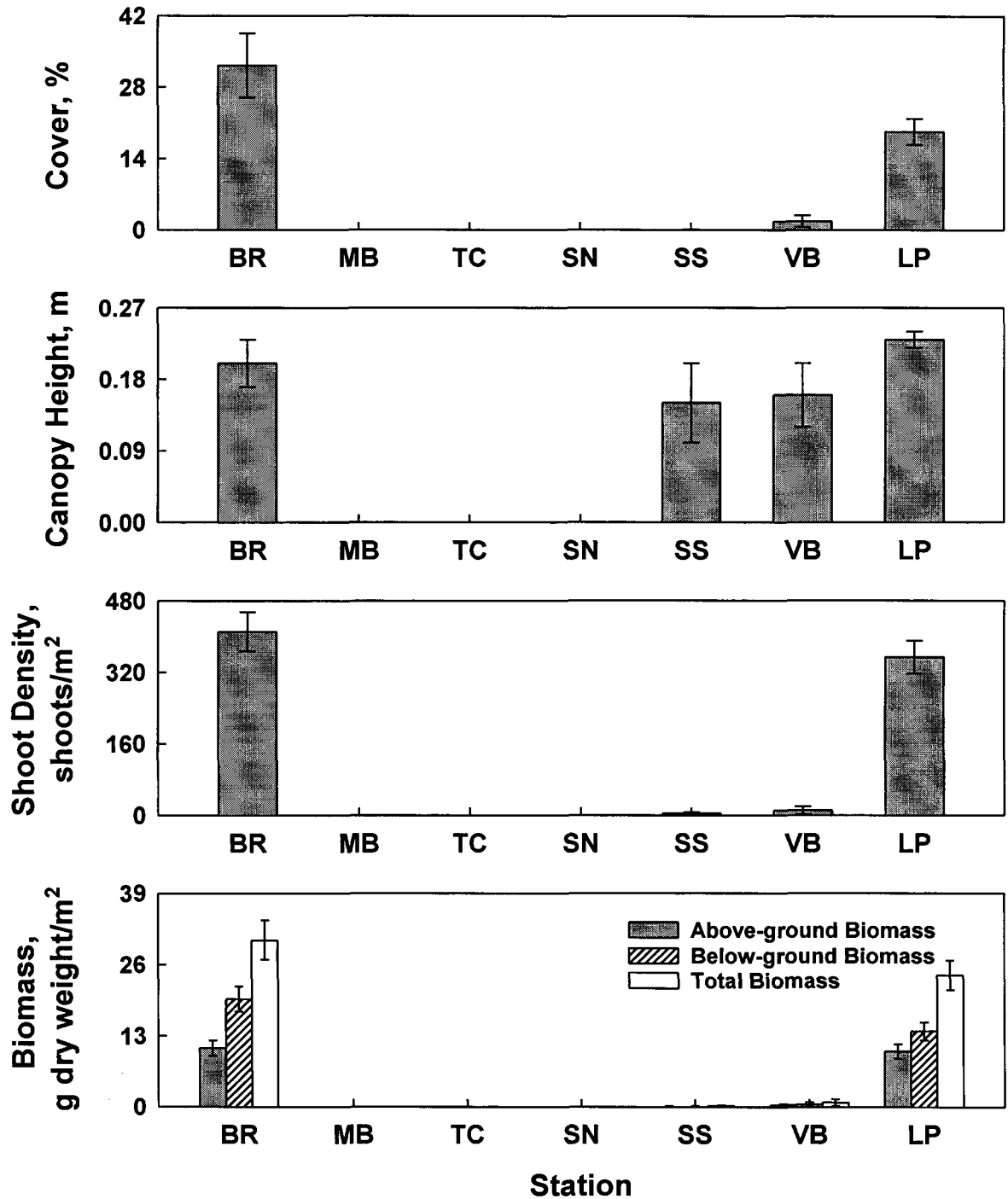


Fig. 4.12 Station means (\pm SE) for cover, canopy height, shoot density, and above-ground, below-ground, and total biomass of *Syringodium filiforme*, by season and transect.

Thalassia testudinum

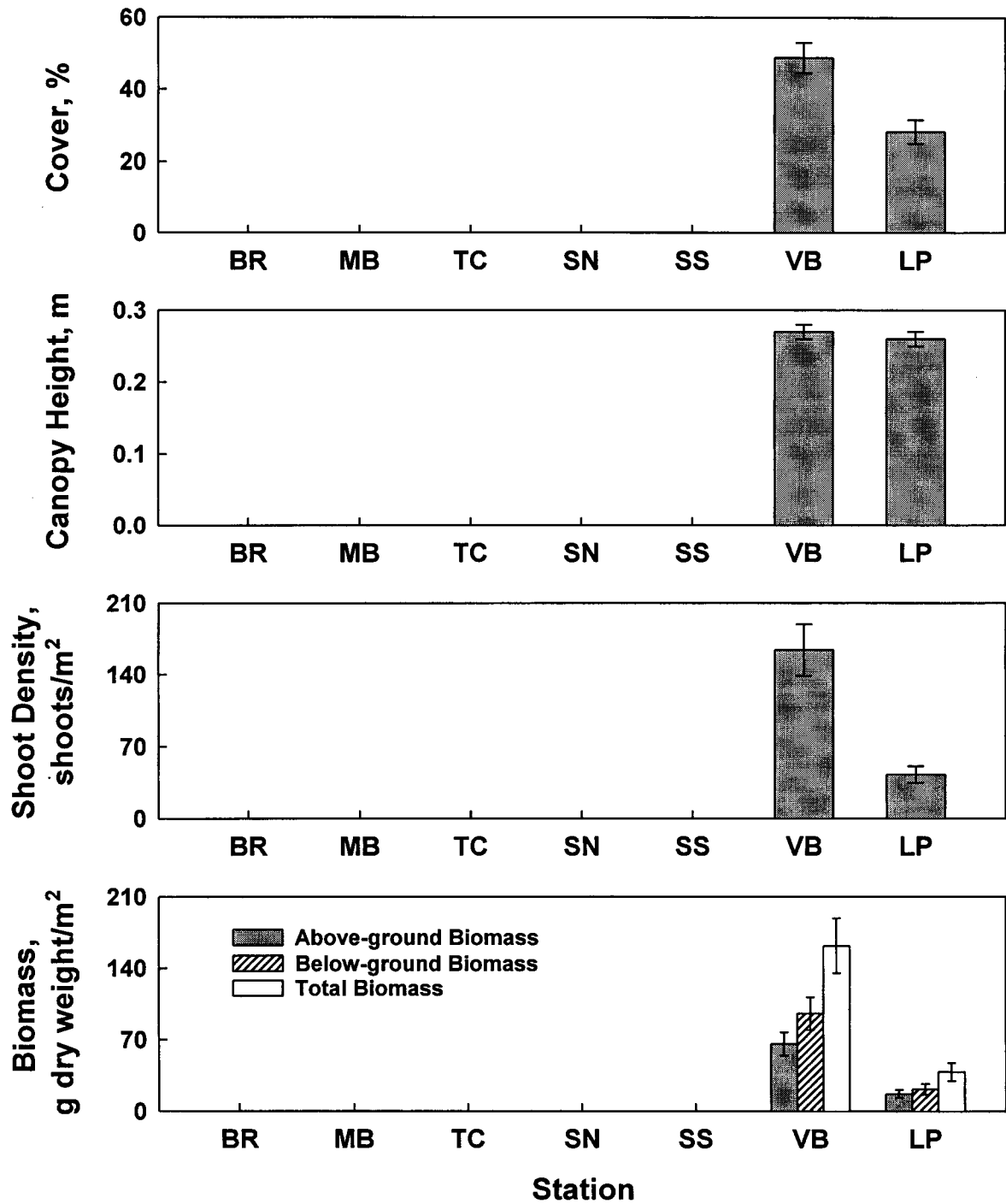


Fig. 4.13 Station means (\pm SE) for cover, canopy height, shoot density, and above-ground, below-ground, and total biomass of *Thalassia testudinum*, by season and transect.

Halophila engelmannii

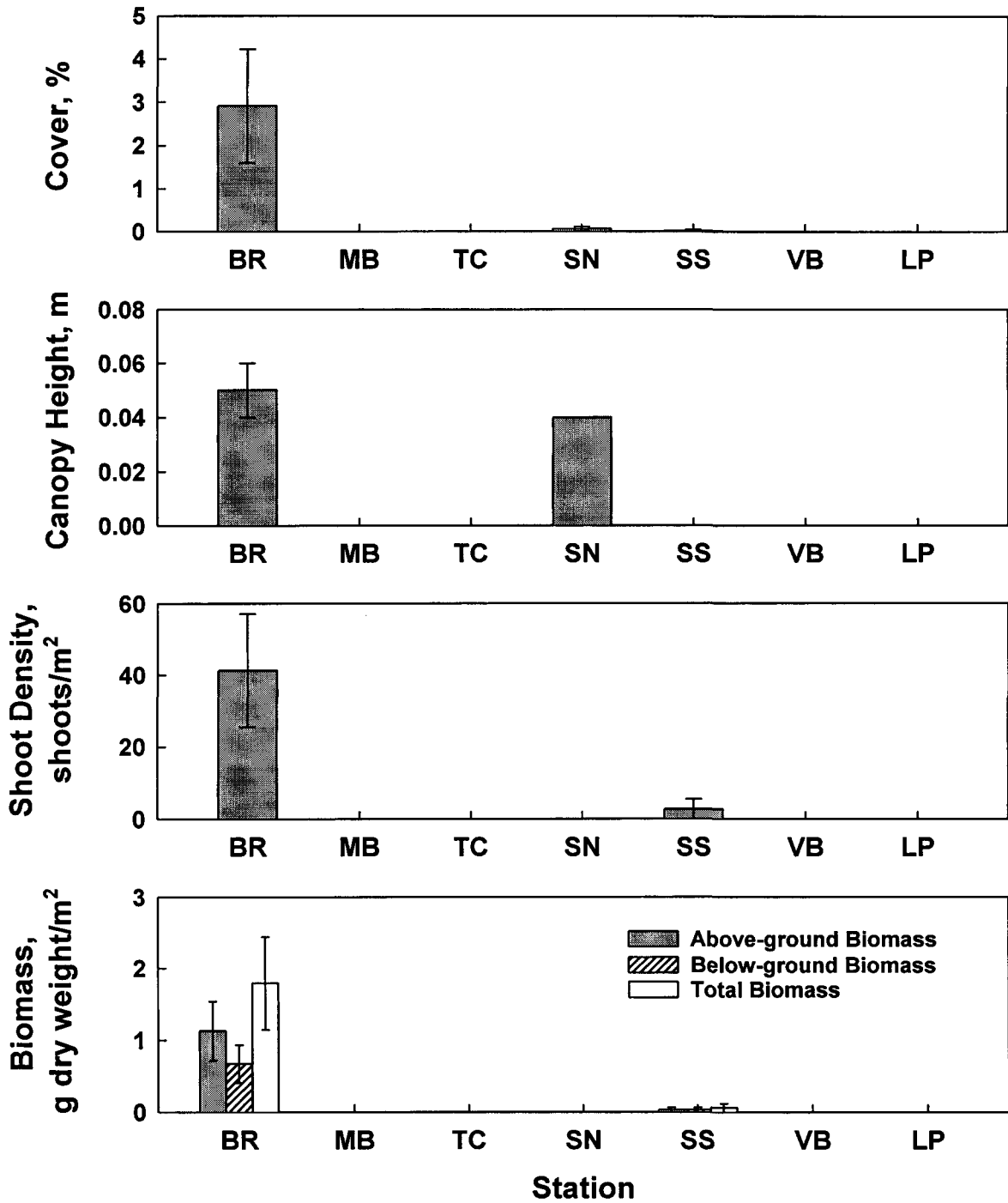


Fig. 4.14 Station means (\pm SE) for cover, canopy height, shoot density, and above-ground, below-ground, and total biomass of *Halophila engelmannii*, by season and transect.

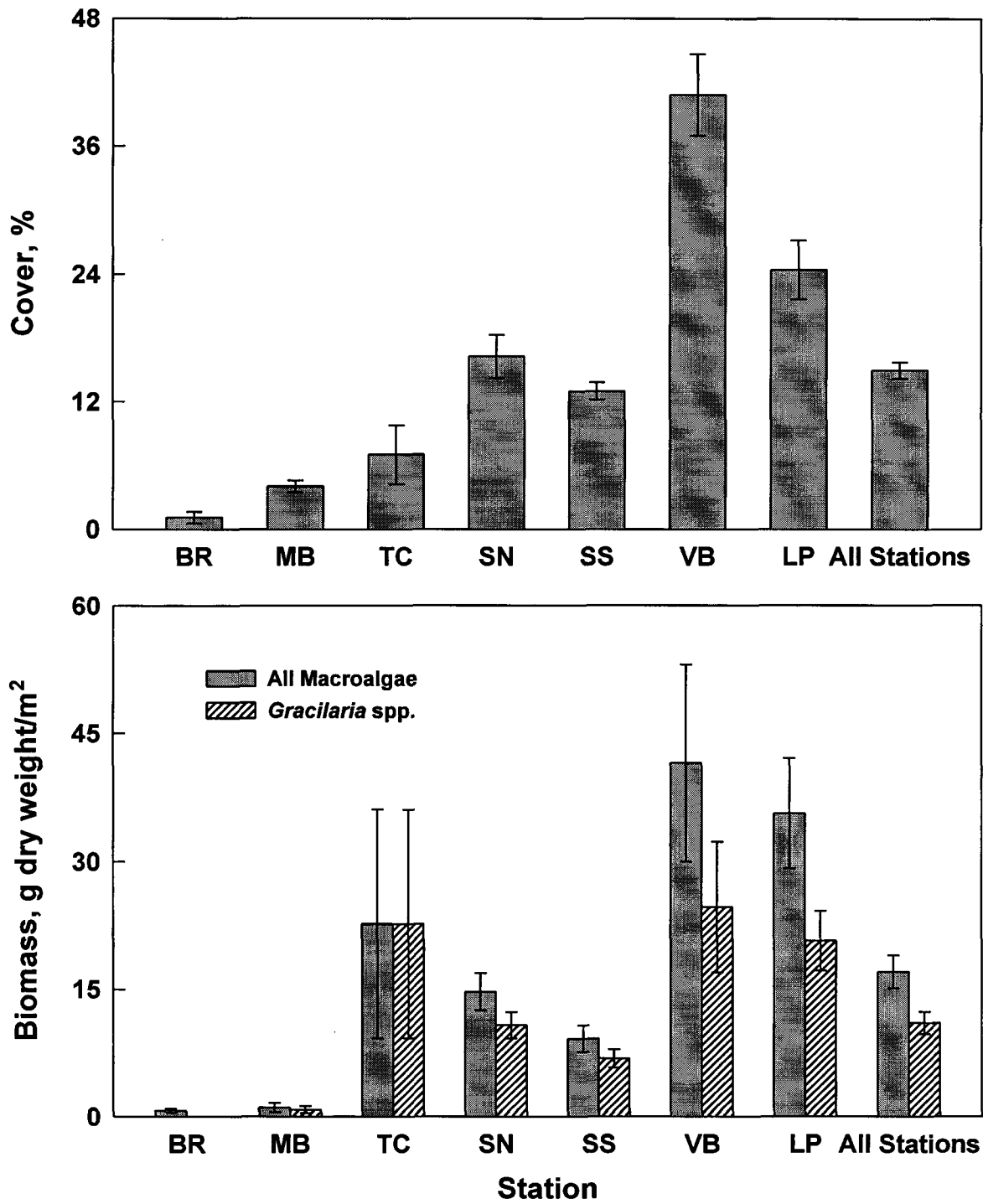


Fig. 4.15 Station means (\pm SE) for cover and biomass of all macroalgae and biomass of *Gracilaria* spp., by season and transect.

All Seagrass

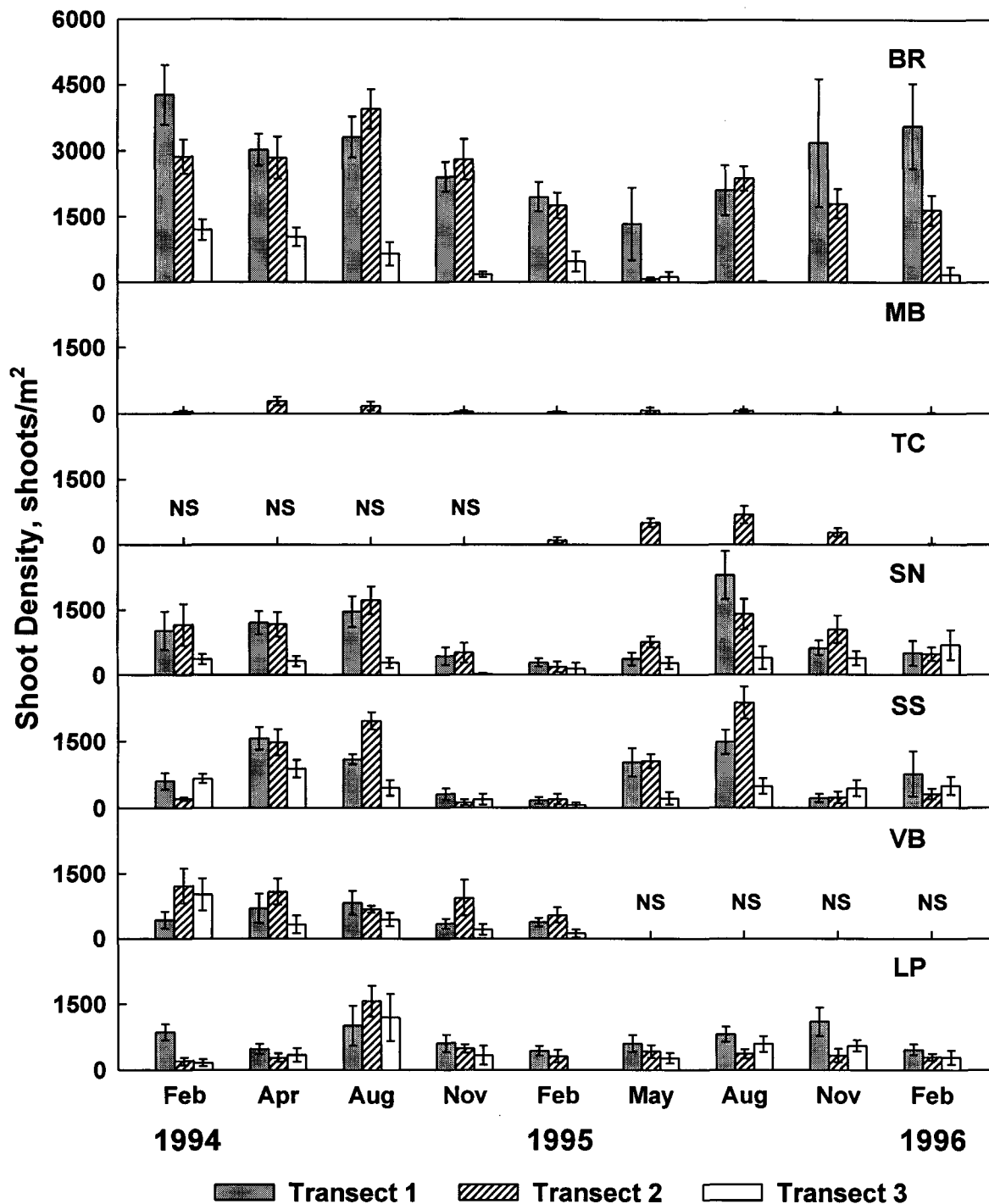


Fig. 4.16 Shoot density of the seagrass community, by station, transect, and season. Data are means (\pm SE) for all station-transect-season combinations; NS = not sampled (VB was sampled only during Year 1, TC only during Year 2).

All Seagrass

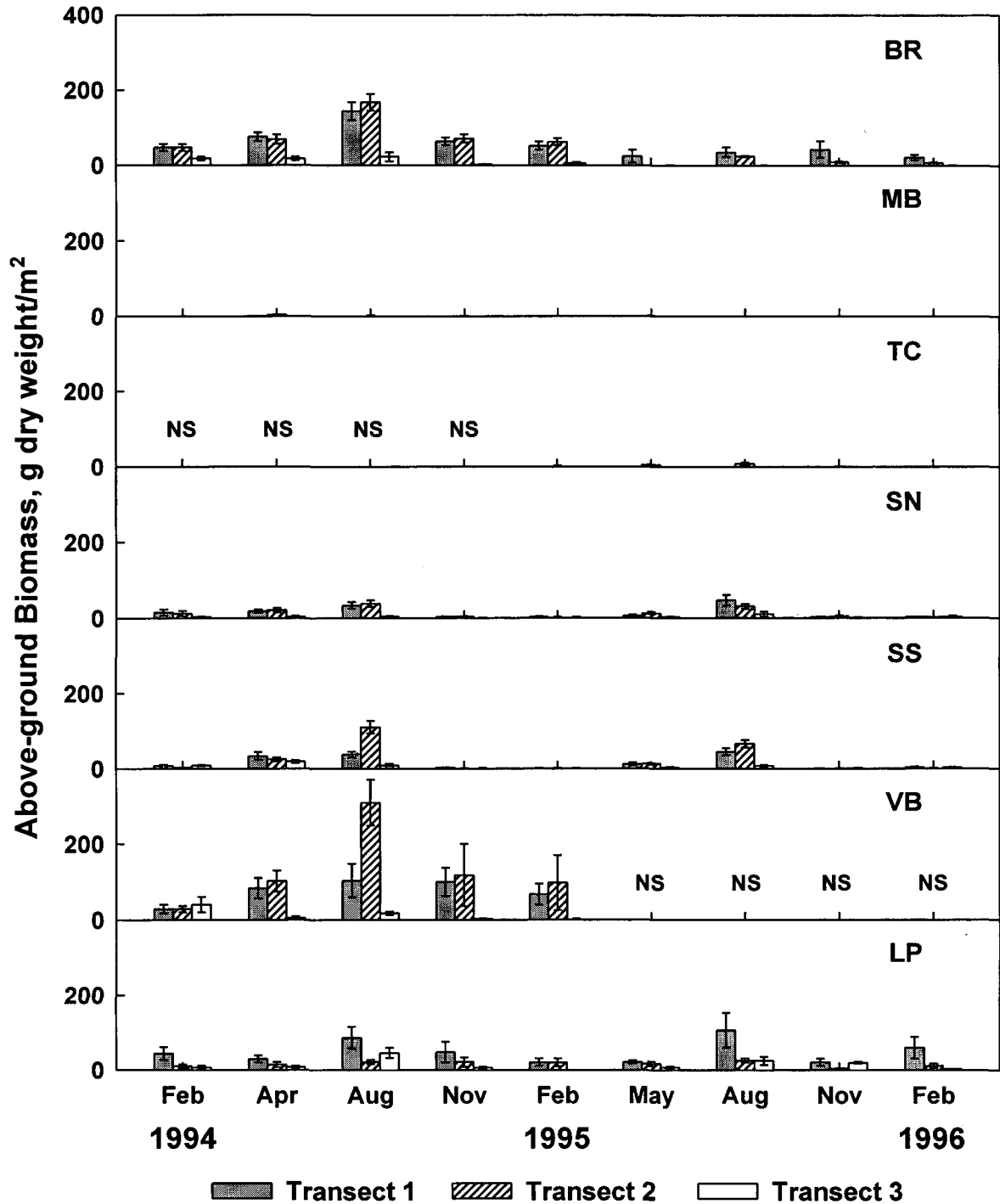


Fig. 4.17 Above-ground biomass of the seagrass community, by station, transect, and season. Data are means (\pm SE) for all station-transect-season combinations; NS = not sampled (VB was sampled only during Year 1, TC only during Year 2).

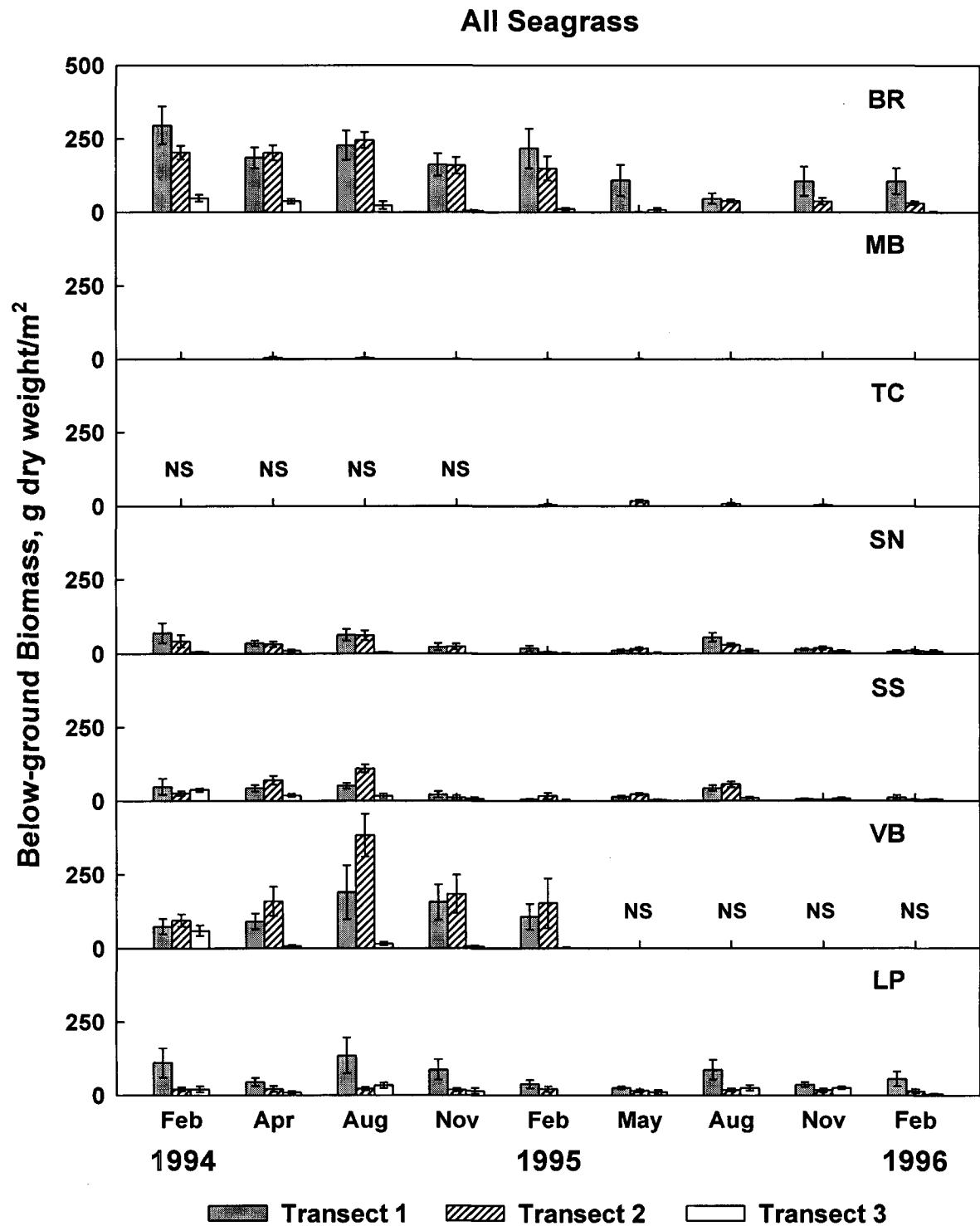


Fig. 4.18 Below-ground biomass of the seagrass community, by station, transect, and season. Data are means (\pm SE) for all station-transect-season combinations; NS = not sampled (VB was sampled only during Year 1, TC only during Year 2).

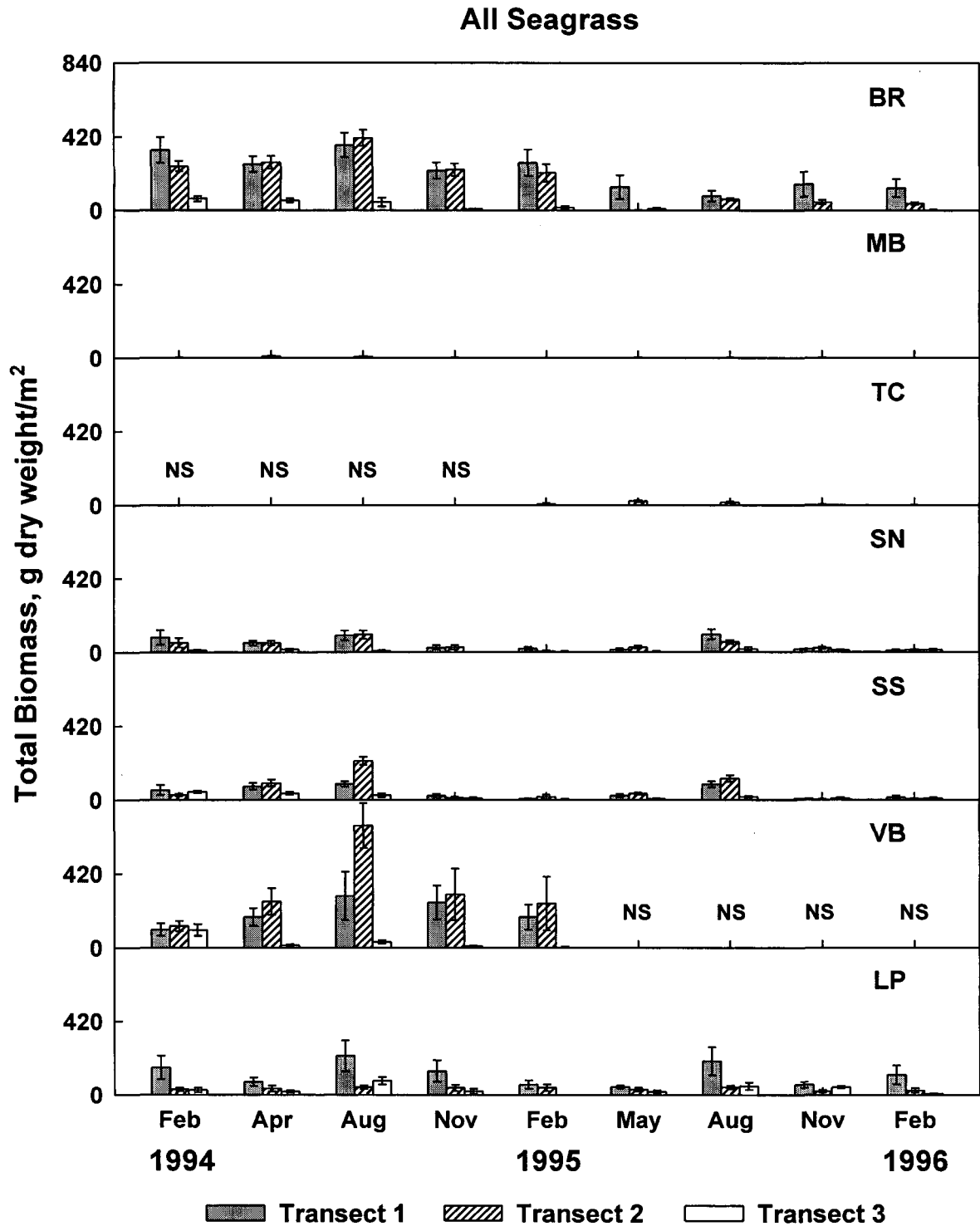


Fig. 4.19 Total biomass of the seagrass community, by station, transect, and season. Data are means (\pm SE) for all station-transect-season combinations; NS = not sampled (VB was sampled only during Year 1, TC only during Year 2).

Halodule wrightii

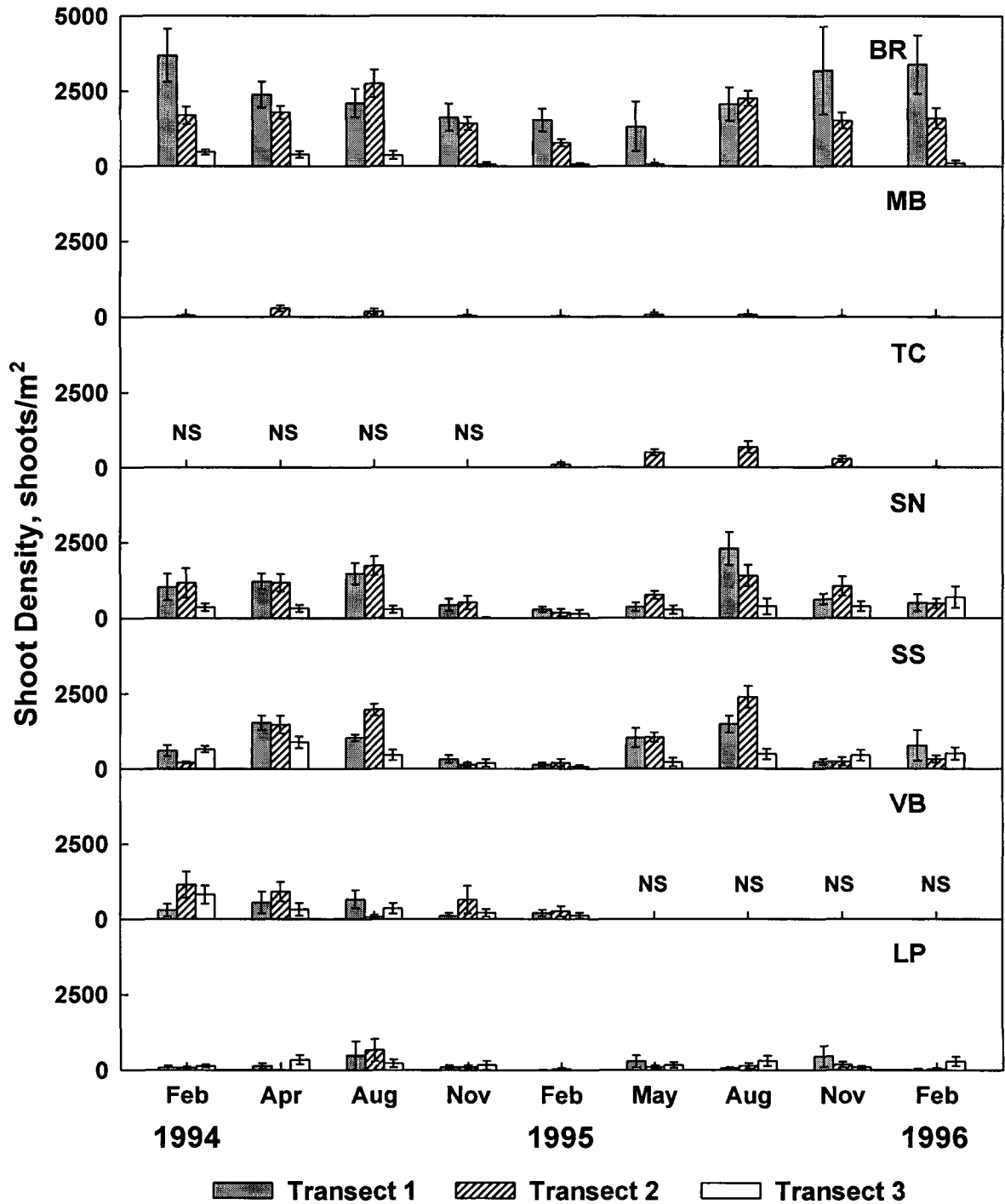


Fig. 4.20 Shoot density of *Halodule wrightii*, by station, transect, and season. Data are means (\pm SE) for all station-transect-season combinations; NS = not sampled (VB was sampled only during Year 1, TC only during Year 2).

Halodule wrightii

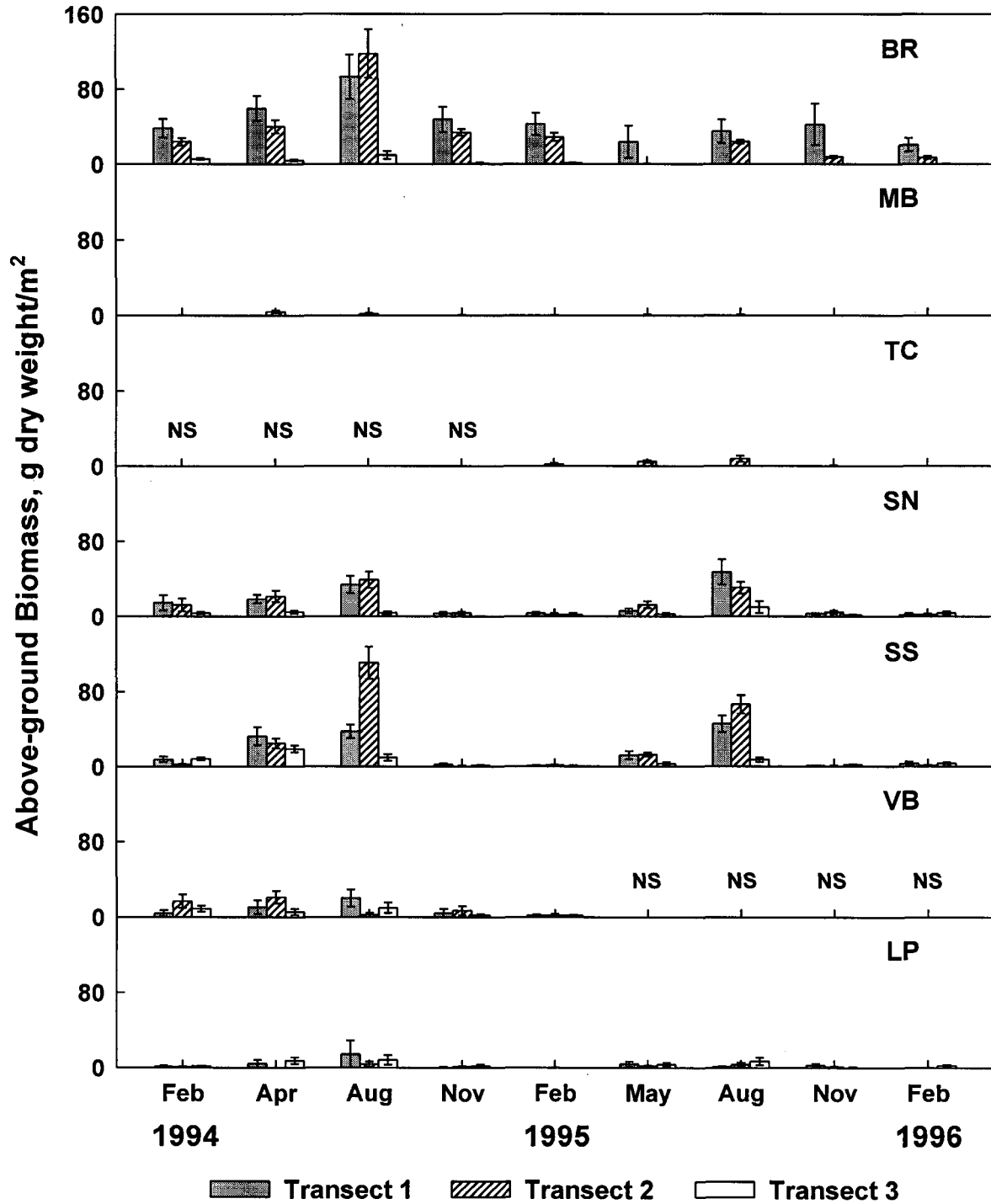


Fig. 4.21 Above-ground biomass of *Halodule wrightii*, by station, transect, and season. Data are means (\pm SE) for all station-transect-season combinations; NS = not sampled (VB was sampled only during Year 1, TC only during Year 2).

Halodule wrightii

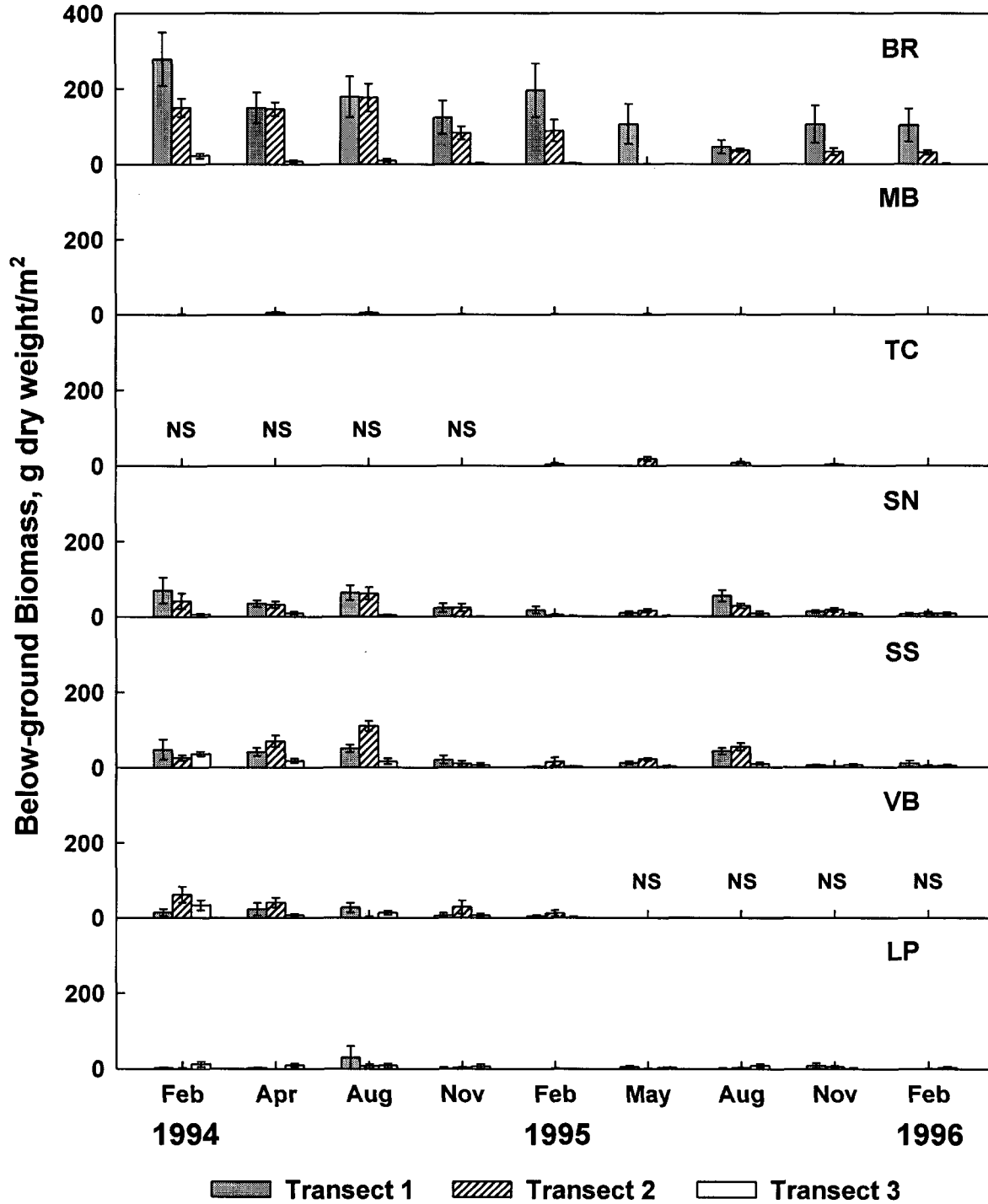


Fig. 4.22 Below-ground biomass of *Halodule wrightii*, by station, transect, and season. Data are means (\pm SE) for all station-transect-season combinations; NS = not sampled (VB was sampled only during Year 1, TC only during Year 2).

Halodule wrightii

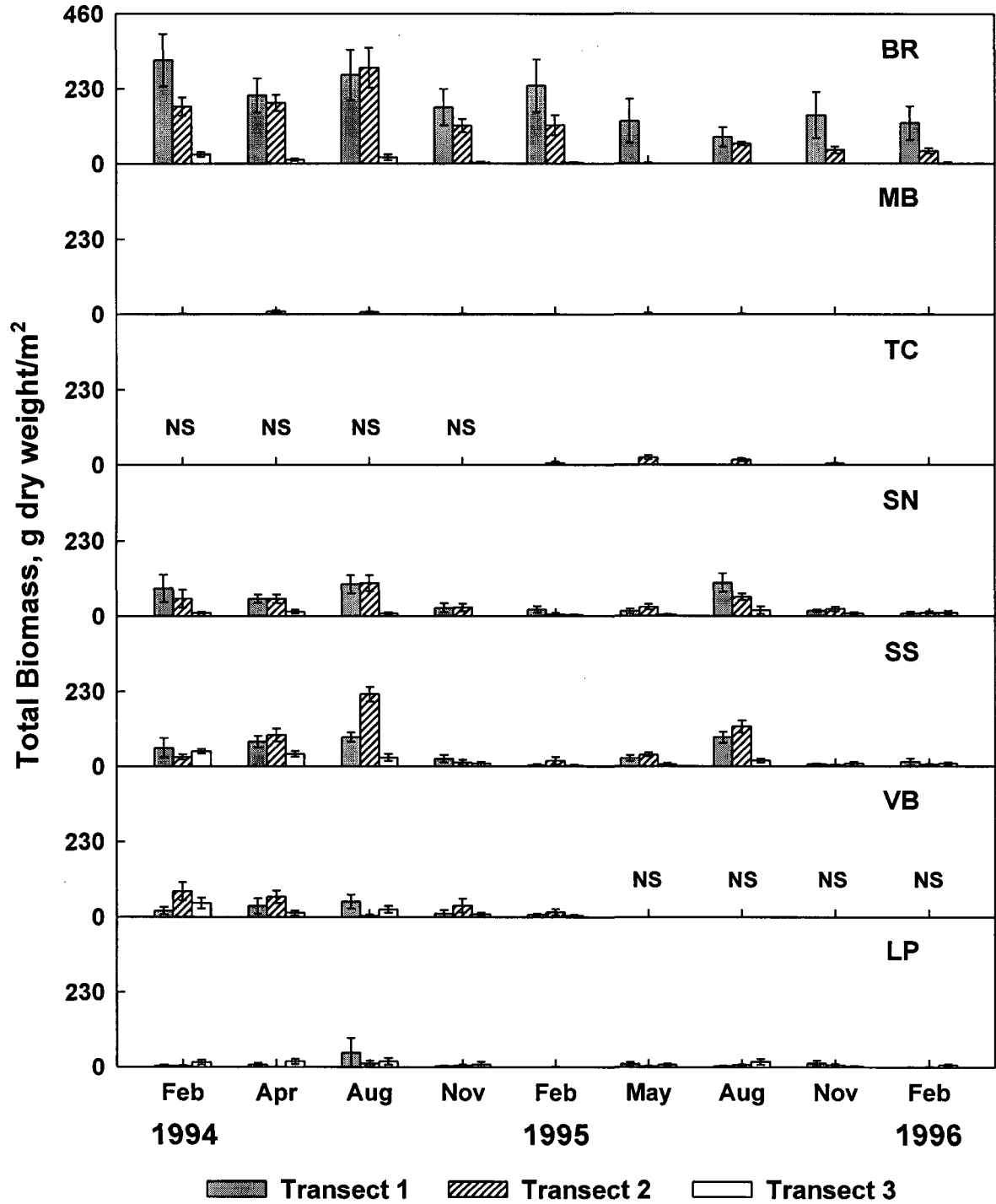


Fig. 4.23 Total biomass of *Halodule wrightii*, by station, transect, and season. Data are means (\pm SE) for all station-transect-season combinations; NS = not sampled (VB was sampled only during Year 1, TC only during Year 2).

Syringodium filiforme

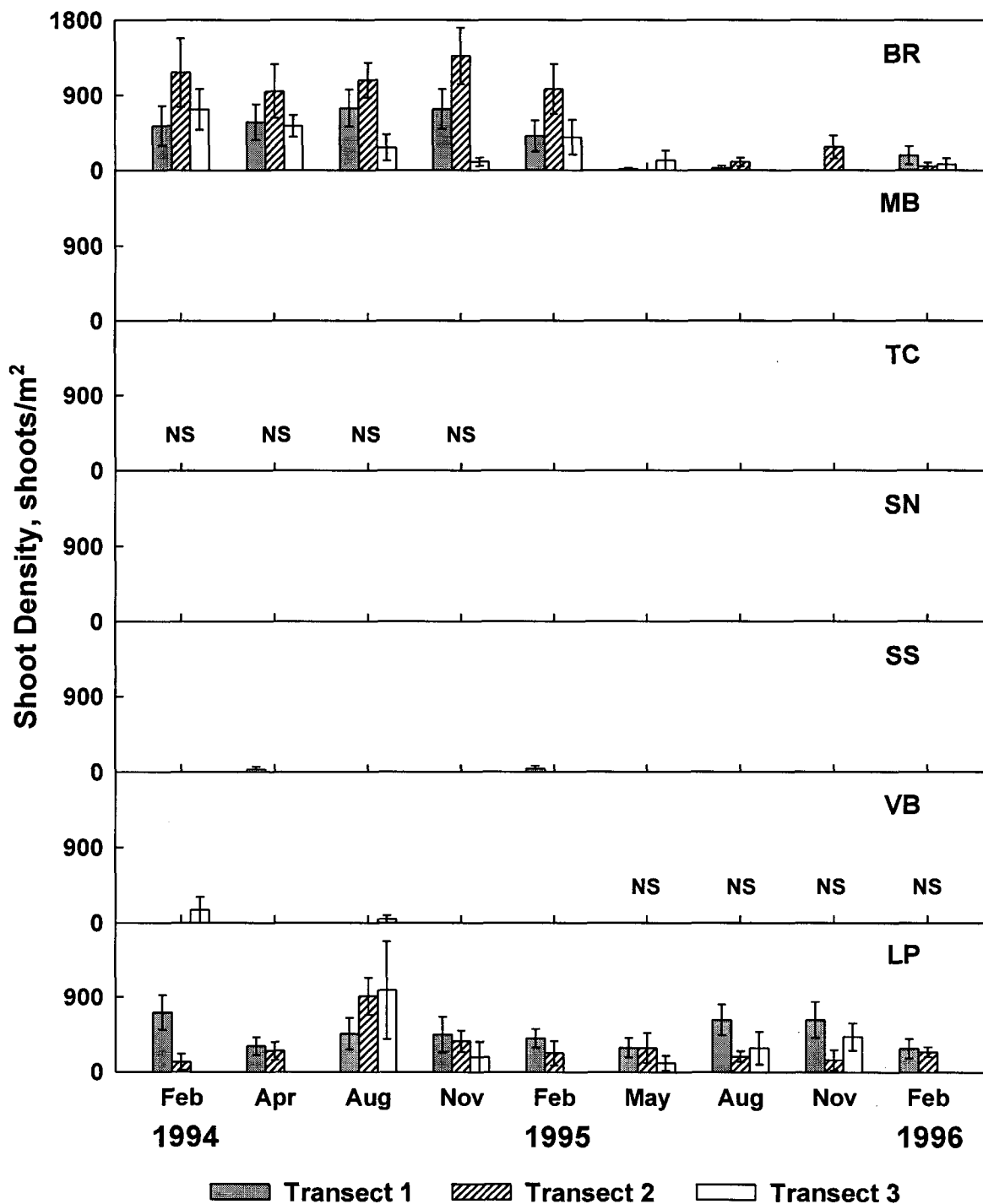


Fig. 4.24 Shoot density of *Syringodium filiforme*, by station, transect, and season. Data are means (\pm SE) for all station-transect-season combinations; NS = not sampled (VB was sampled only during Year 1, TC only during Year 2).

Syringodium filiforme

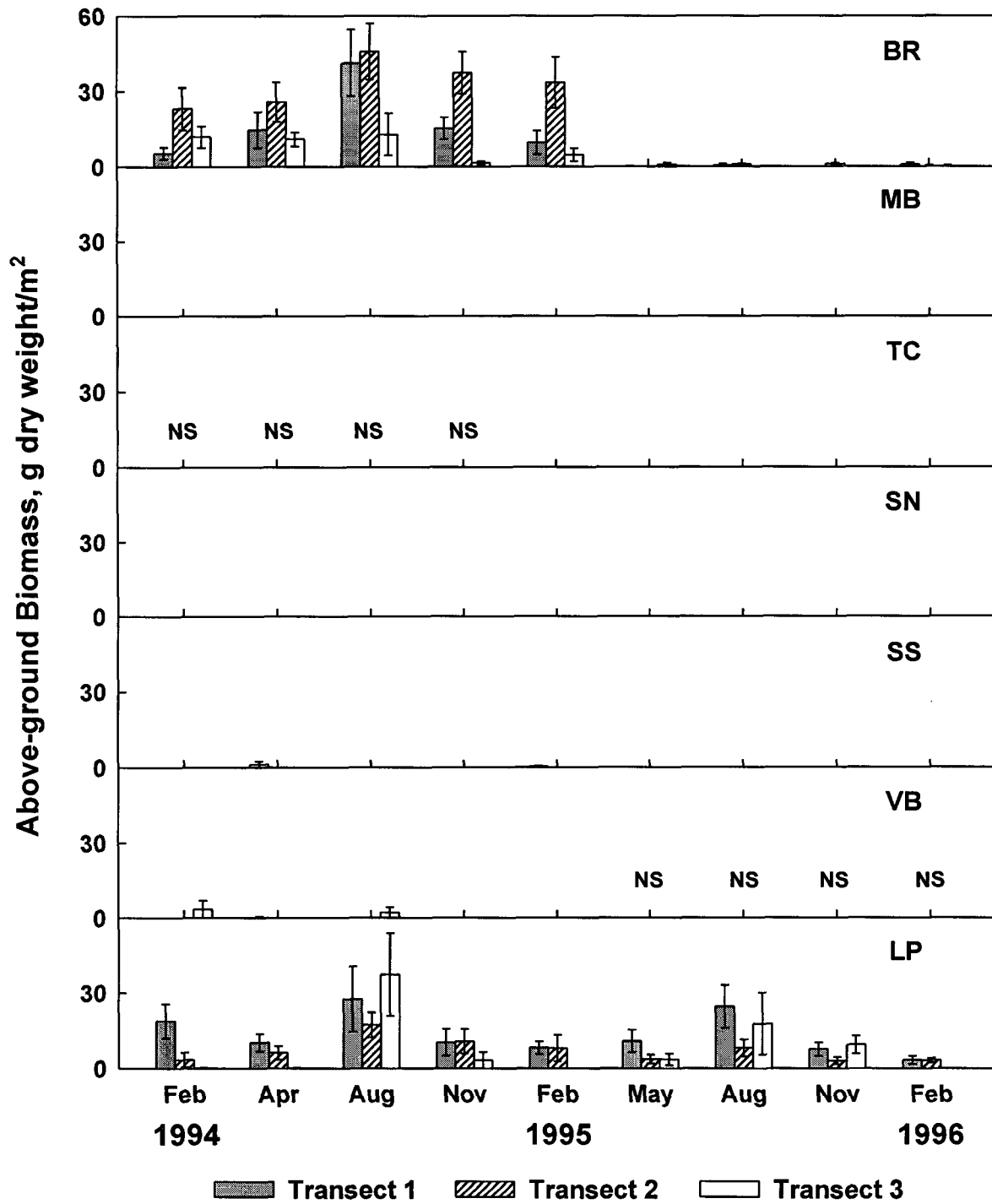


Fig. 4.25 Above-ground biomass of *Syringodium filiforme*, by station, transect, and season. Data are means (\pm SE) for all station-transect-season combinations; NS = not sampled (VB was sampled only during Year 1, TC only during Year 2).

Syringodium filiforme

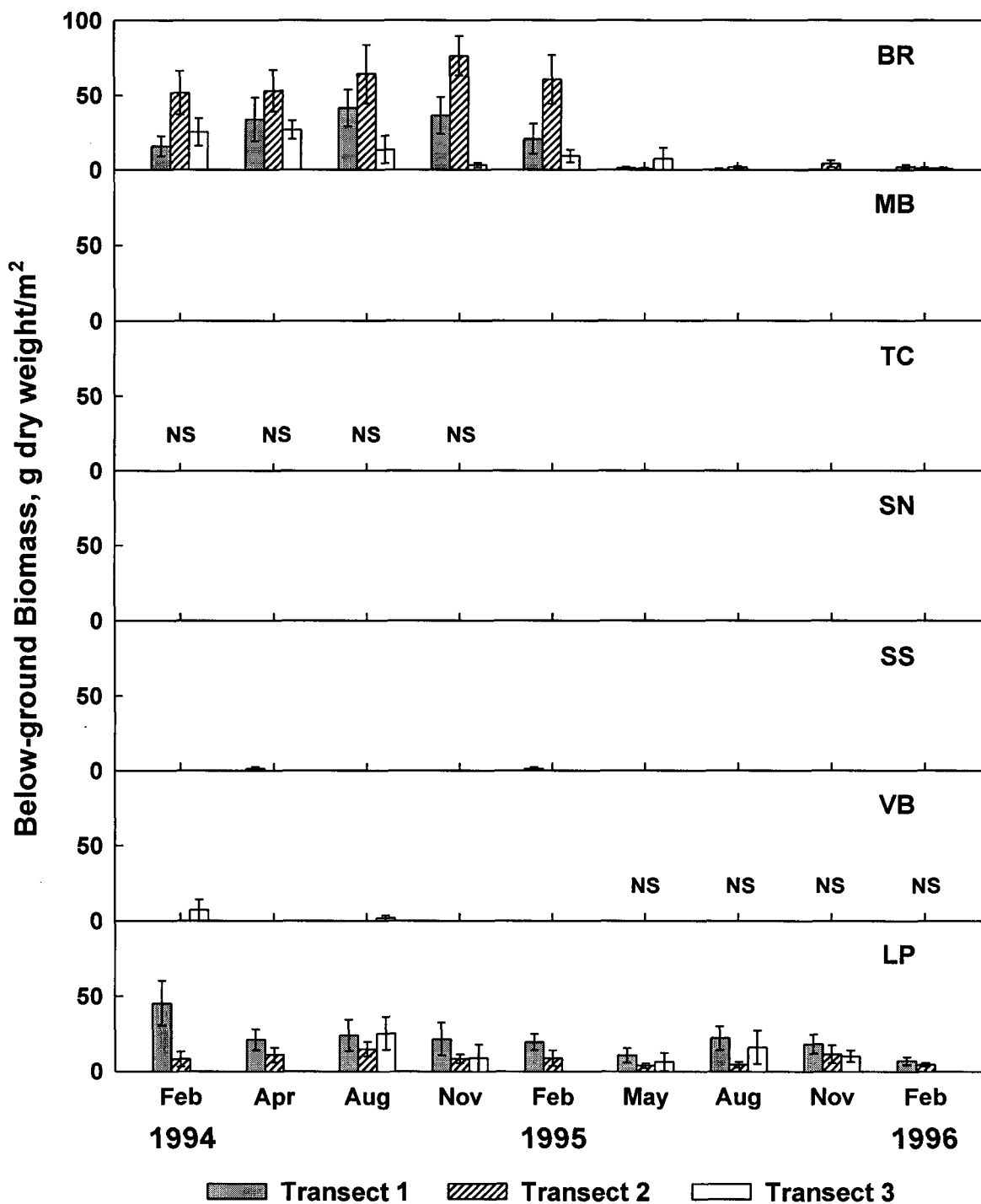


Fig. 4.26 Below-ground biomass of *Syringodium filiforme*, by station, transect, and season. Data are means (\pm SE) for all station-transect-season combinations; NS = not sampled (VB was sampled only during Year 1, TC only during Year 2).

Syringodium filiforme

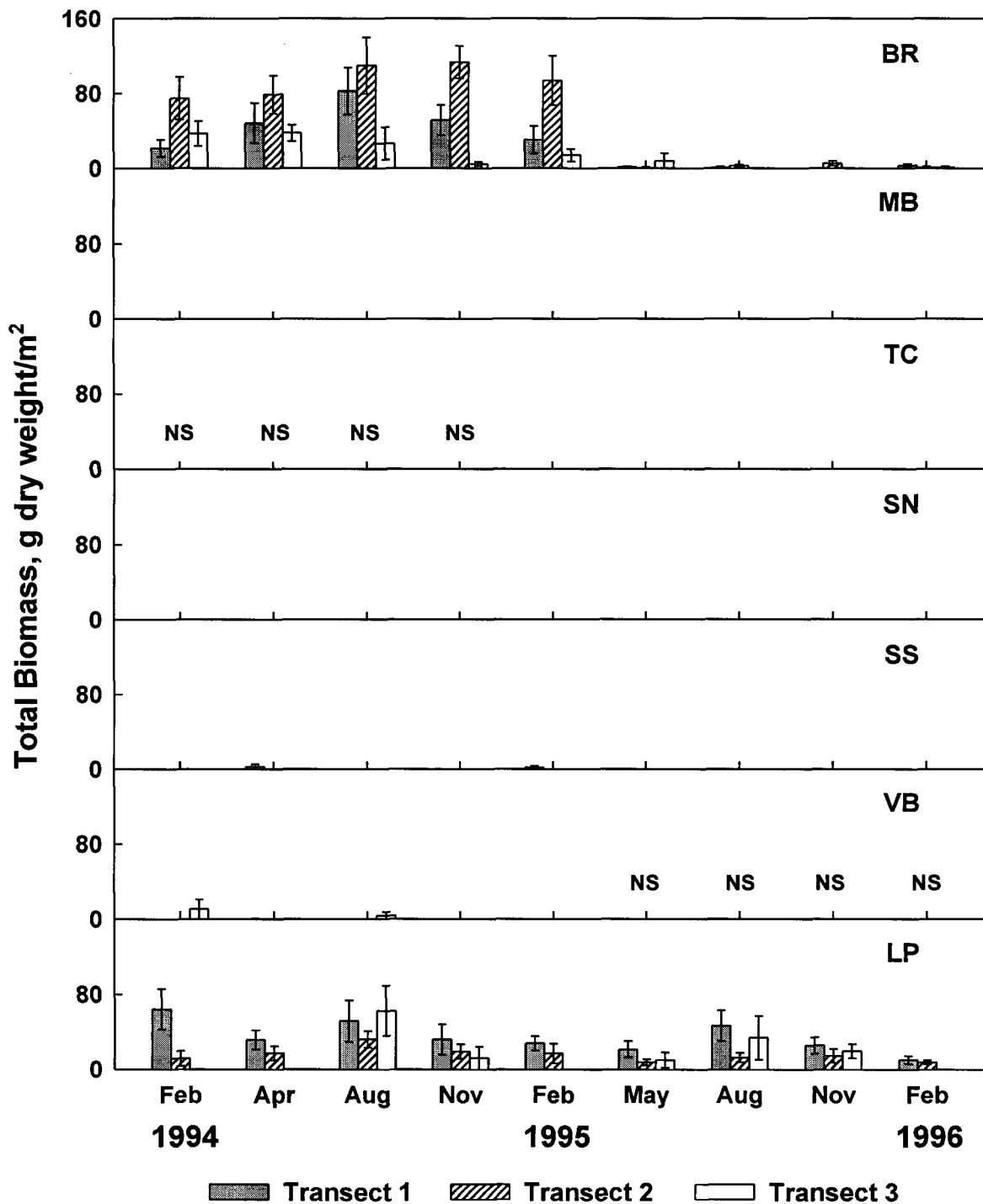


Fig. 4.27 Total biomass of *Syringodium filiforme*, by station, transect, and season. Data are means (\pm SE) for all station-transect-season combinations; NS = not sampled (VB was sampled only during Year 1, TC only during Year 2).

Thalassia testudinum

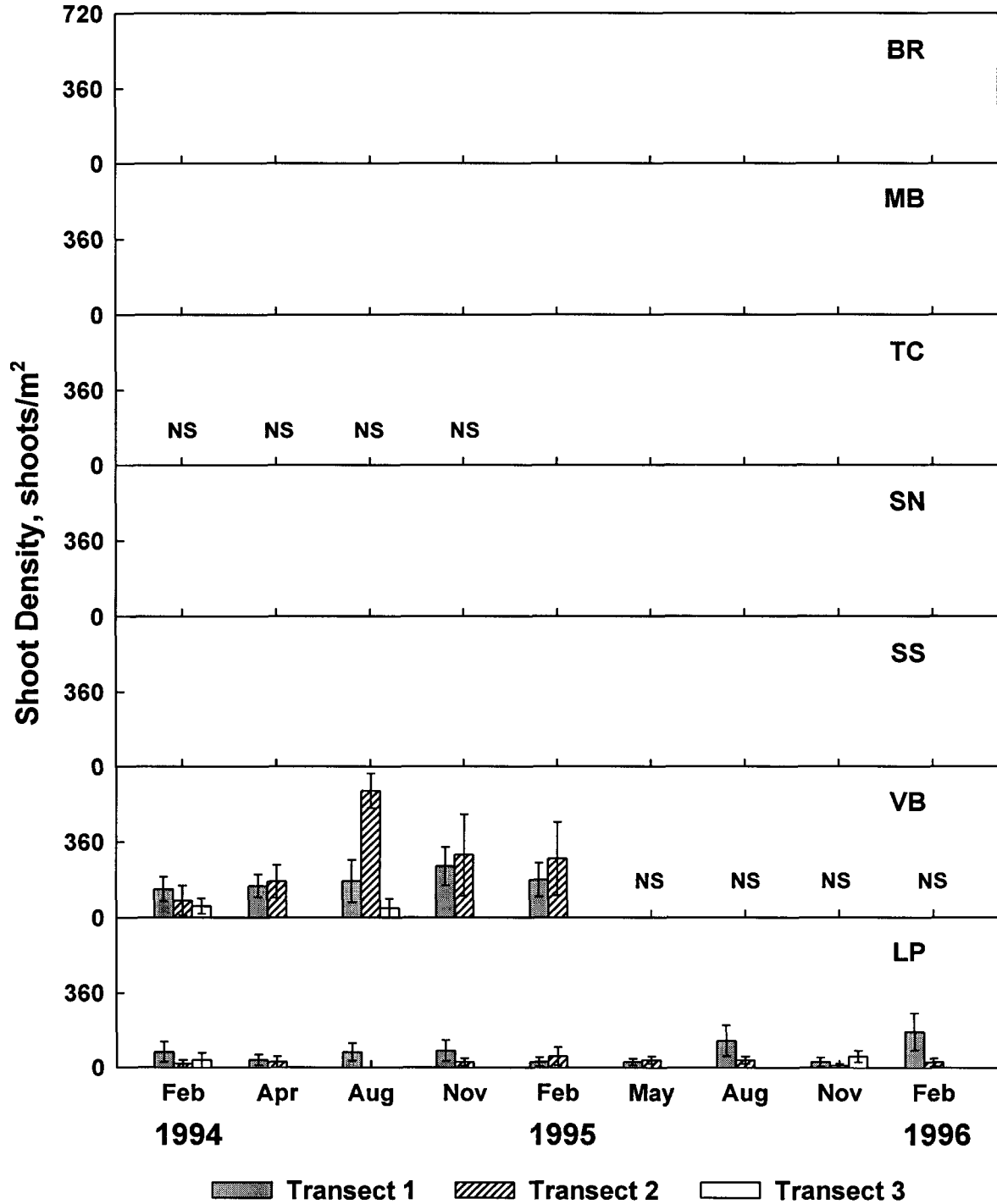


Fig. 4.28 Shoot density of *Thalassia testudinum*, by station, transect, and season. Data are means (\pm SE) for all station-transect-season combinations; NS = not sampled (VB was sampled only during Year 1, TC only during Year 2).

Thalassia testudinum

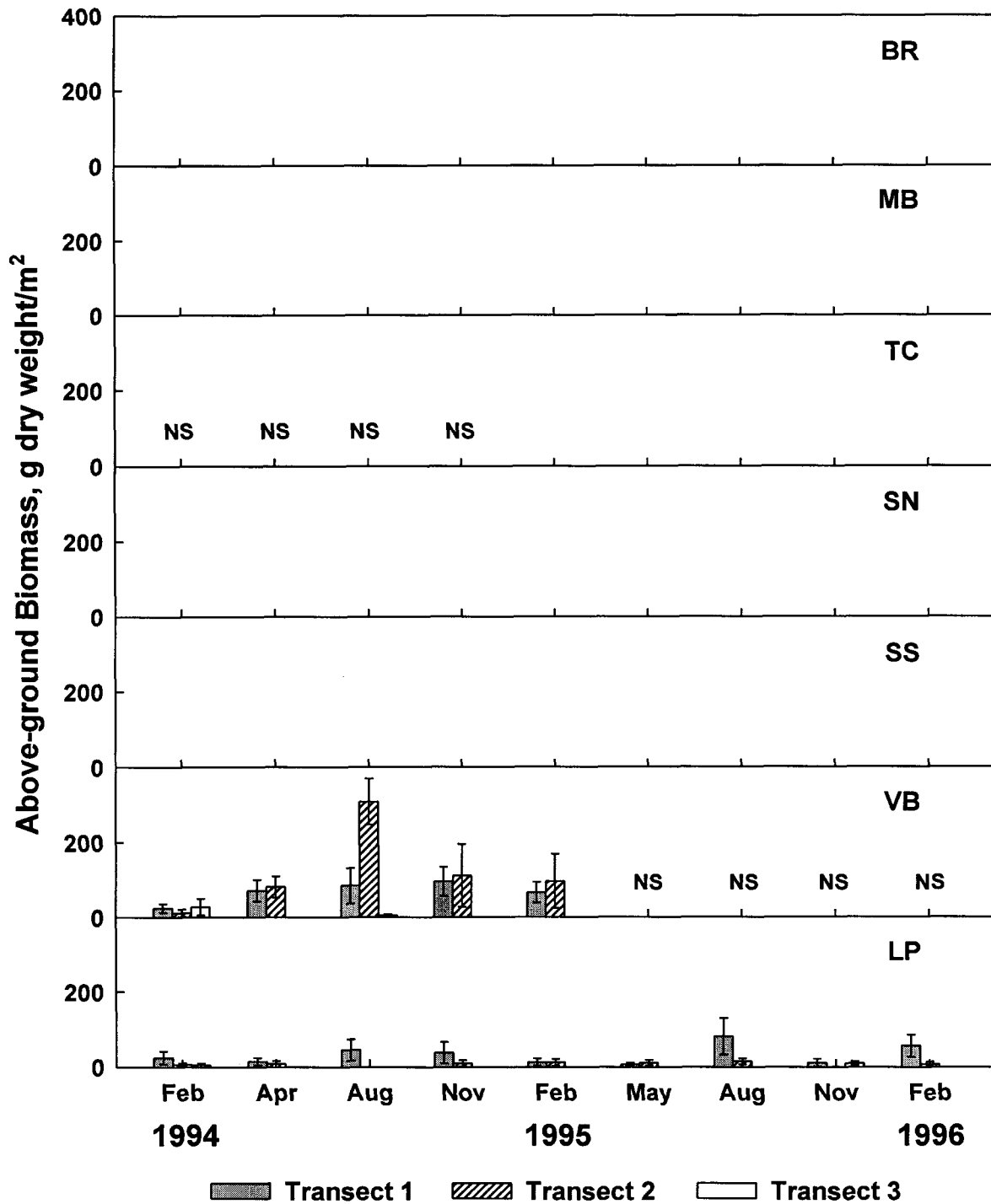


Fig. 4.29 Above-ground biomass of *Thalassia testudinum*, by station, transect, and season. Data are means (\pm SE) for all station-transect-season combinations; NS = not sampled (VB was sampled only during Year 1, TC only during Year 2).

Thalassia testudinum

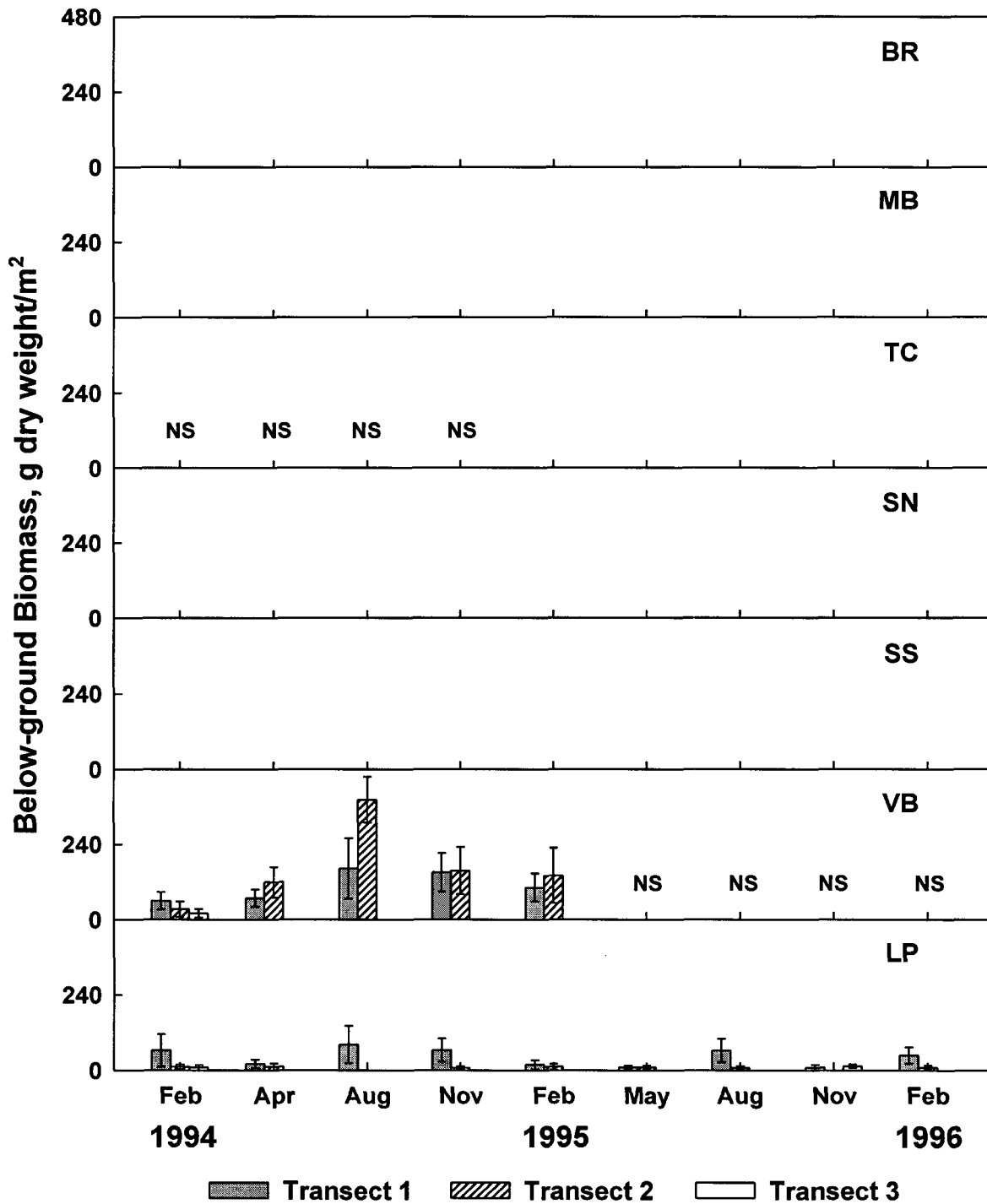


Fig. 4.30 Below-ground biomass of *Thalassia testudinum*, by station, transect, and season. Data are means (\pm SE) for all station-transect-season combinations; NS = not sampled (VB was sampled only during Year 1, TC only during Year 2).

Thalassia testudinum

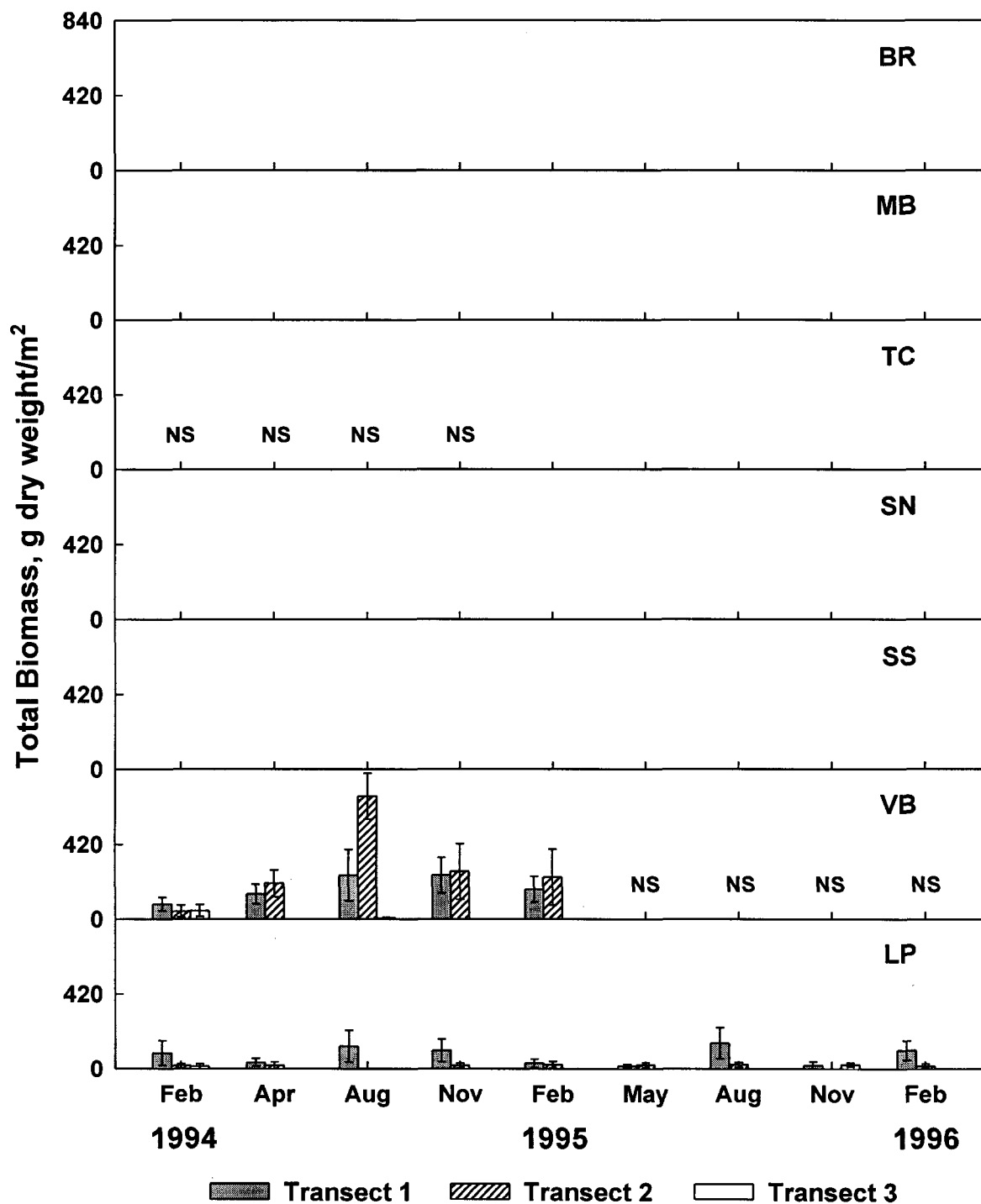


Fig. 4.31 Total biomass of *Thalassia testudinum*, by station, transect, and season. Data are means (\pm SE) for all station-transect-season combinations; NS = not sampled (VB was sampled only during Year 1, TC only during Year 2).

Halophila engelmannii

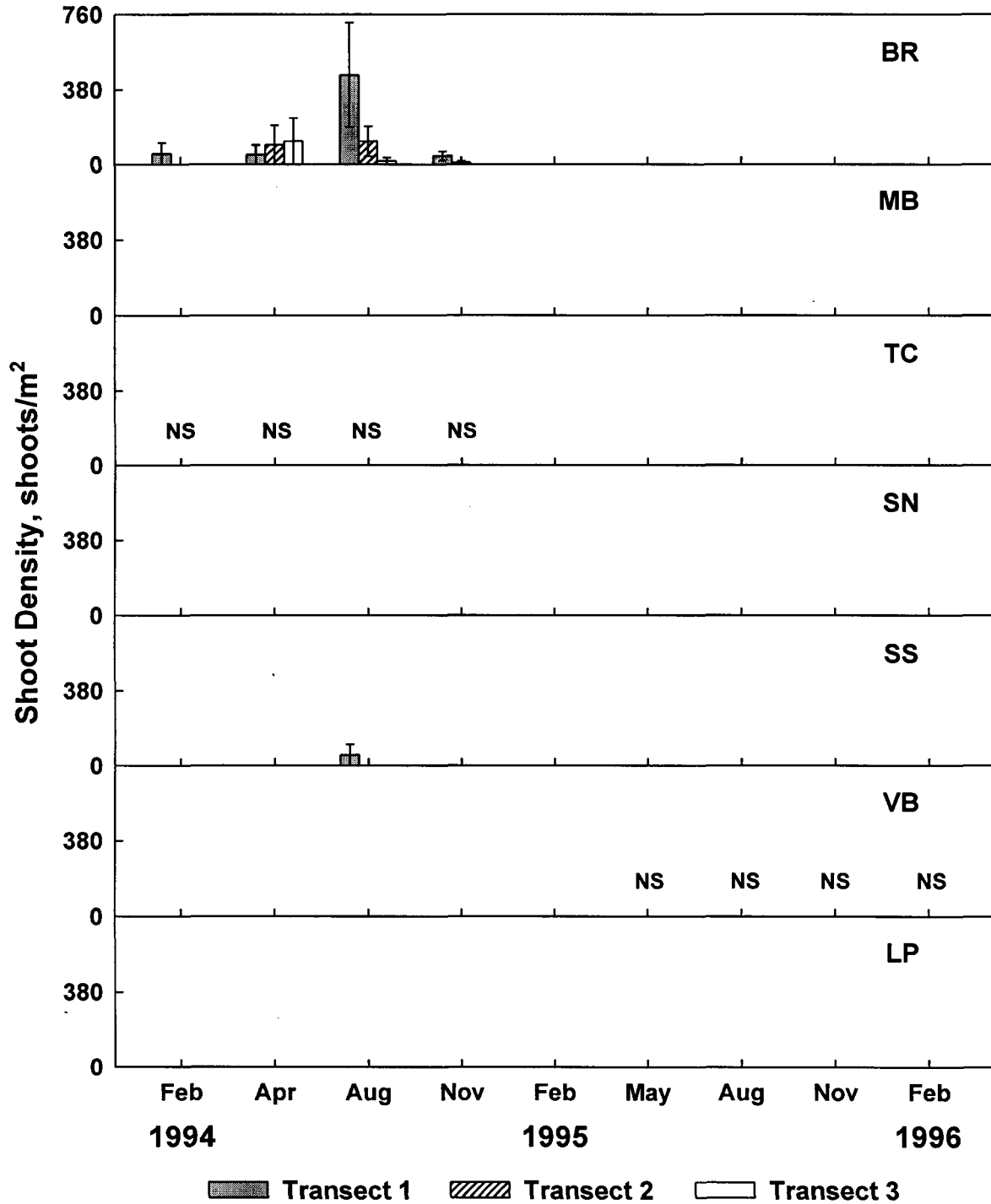


Fig. 4.32 Shoot density of *Halophila engelmannii*, by station, transect, and season. Data are means (\pm SE) for all station-transect-season combinations; NS = not sampled (VB was sampled only during Year 1, TC only during Year 2).

Halophila engelmannii

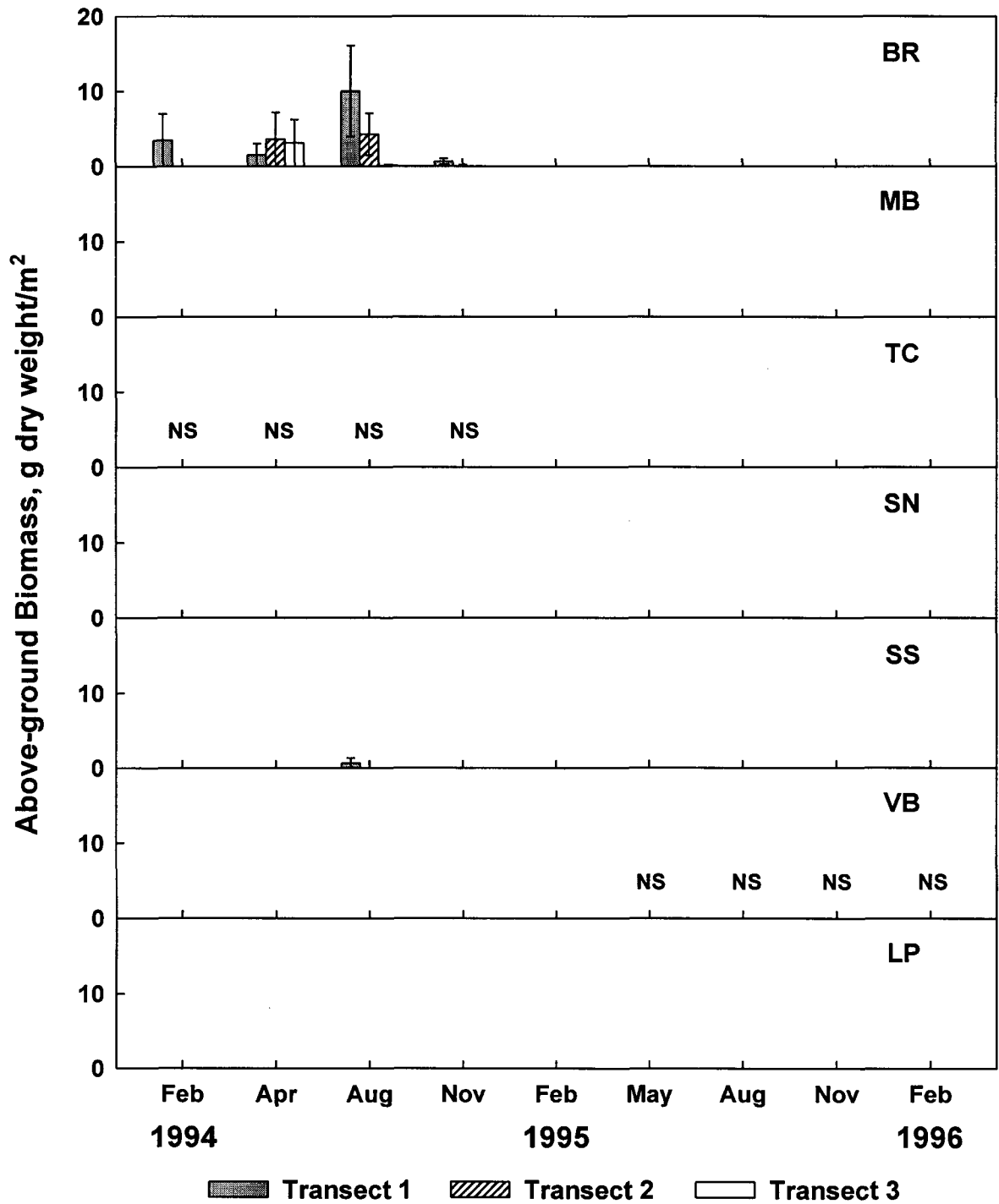


Fig. 4.33 Above-ground biomass of *Halophila engelmannii*, by station, transect, and season. Data are means (\pm SE) for all station-transect-season combinations; NS = not sampled (VB was sampled only during Year 1, TC only during Year 2).

Halophila engelmannii

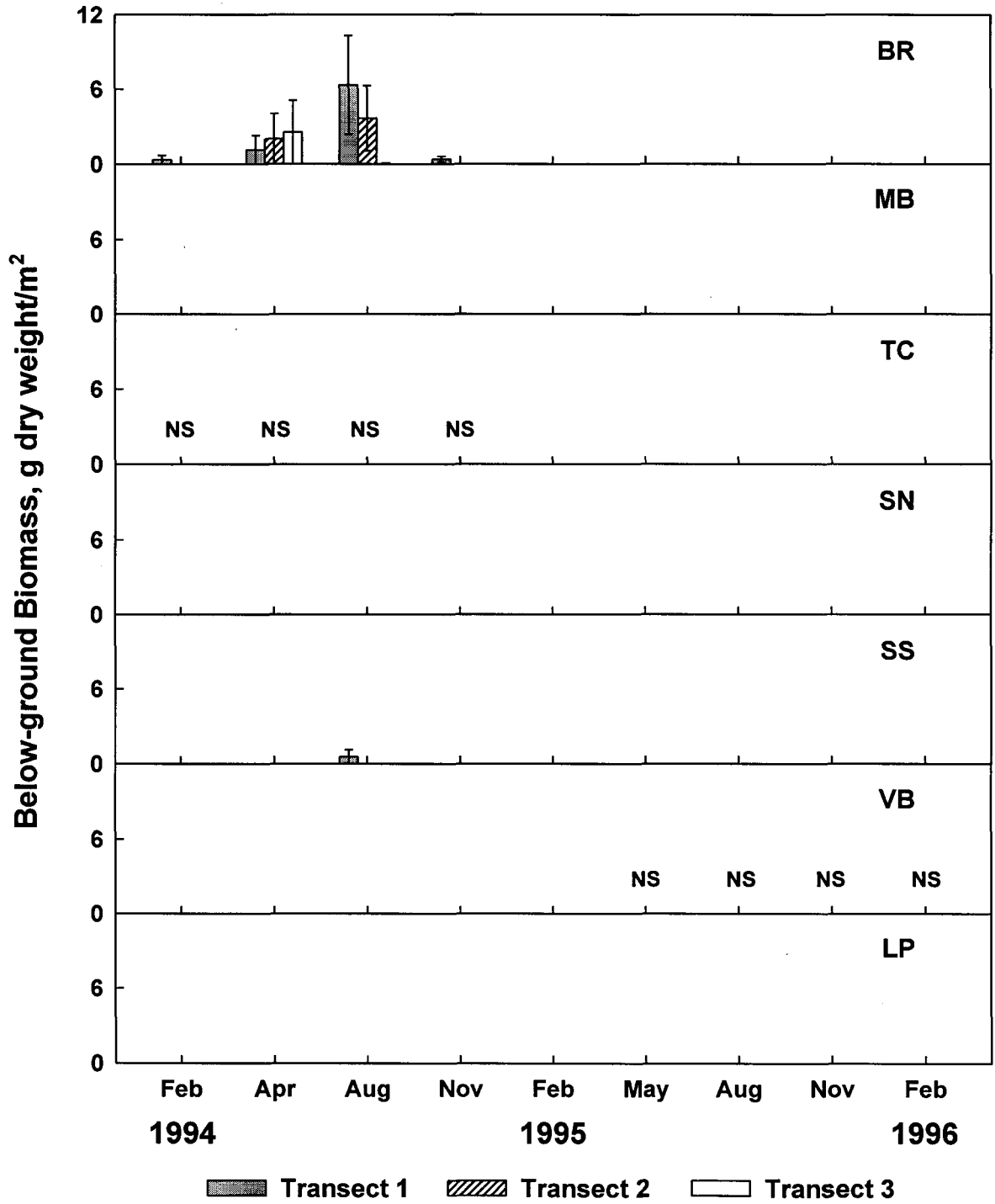


Fig. 4.34 Below-ground biomass of *Halophila engelmannii*, by station, transect, and season. Data are means (\pm SE) for all station-transect-season combinations; NS = not sampled (VB was sampled only during Year 1, TC only during Year 2).

Halophila engelmannii

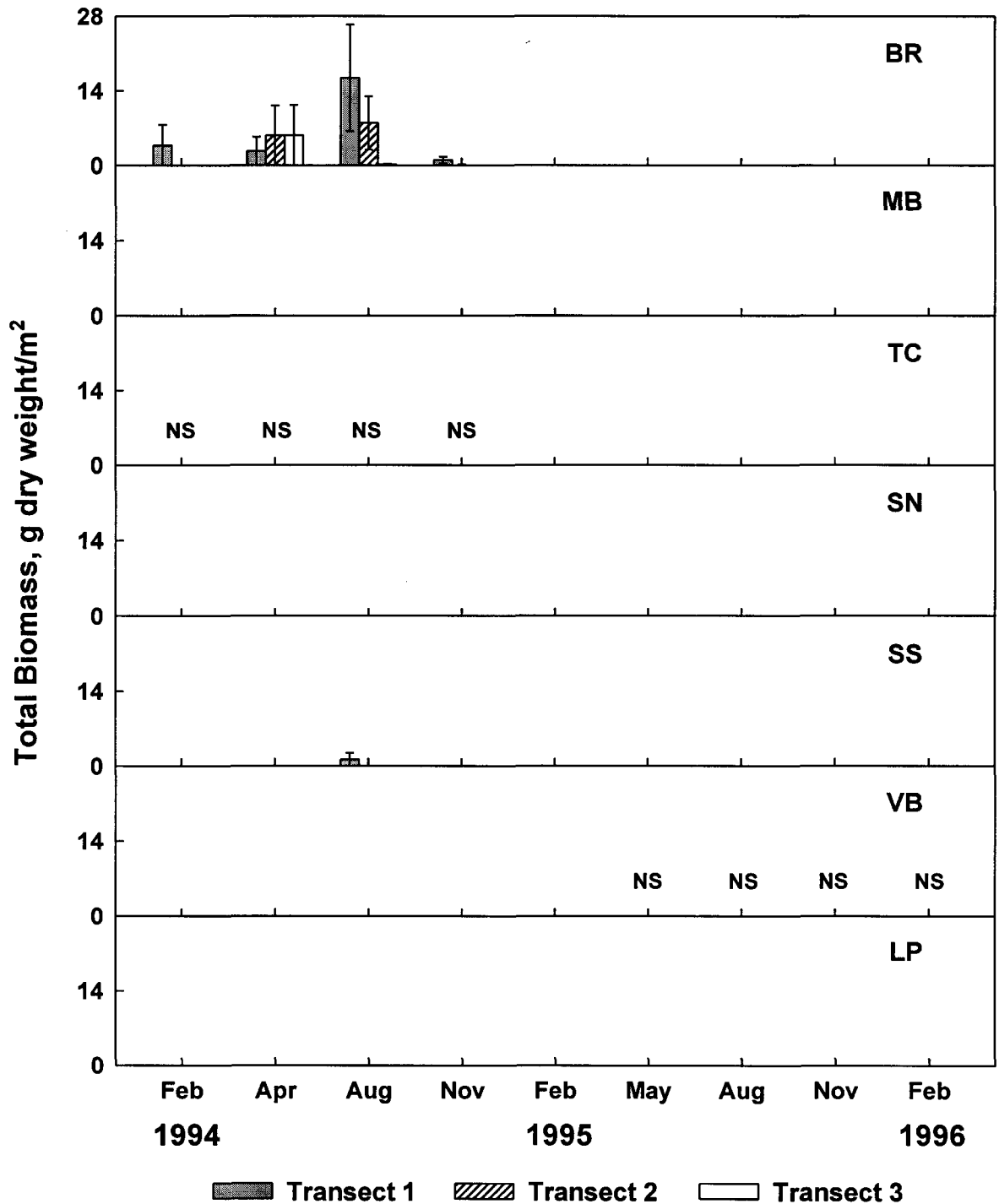


Fig. 4.35 Total biomass of *Halophila engelmannii*, by station, transect, and season. Data are means (\pm SE) for all station-transect-season combinations; NS = not sampled (VB was sampled only during Year 1, TC only during Year 2).

All Macroalgae

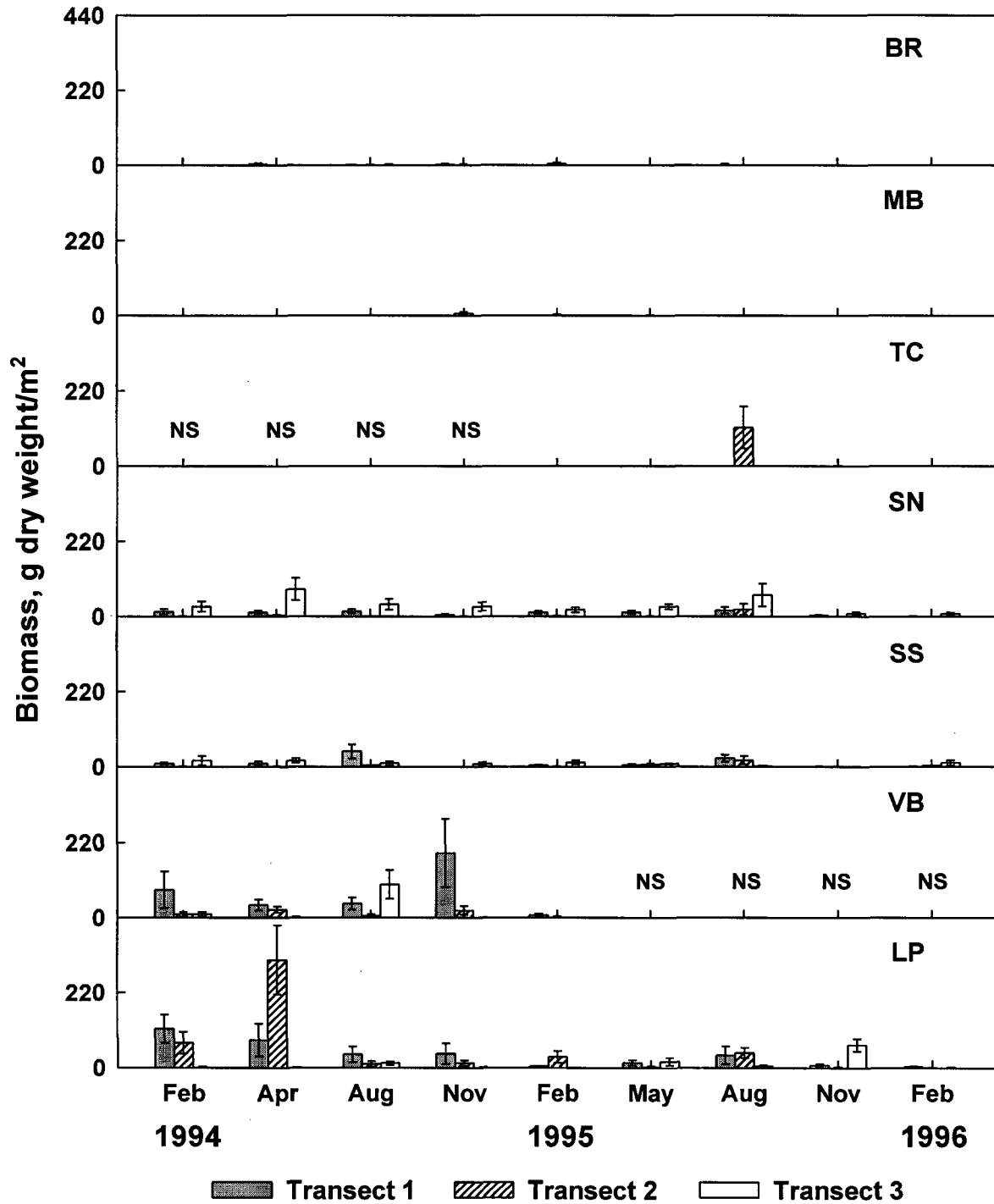


Fig. 4.36 Total biomass of all macroalgae, by station, transect, and season. Data are means (\pm SE) for all station-transect-season combinations; NS = not sampled (VB was sampled only during Year 1, TC only during Year 2).

Gracilaria spp.

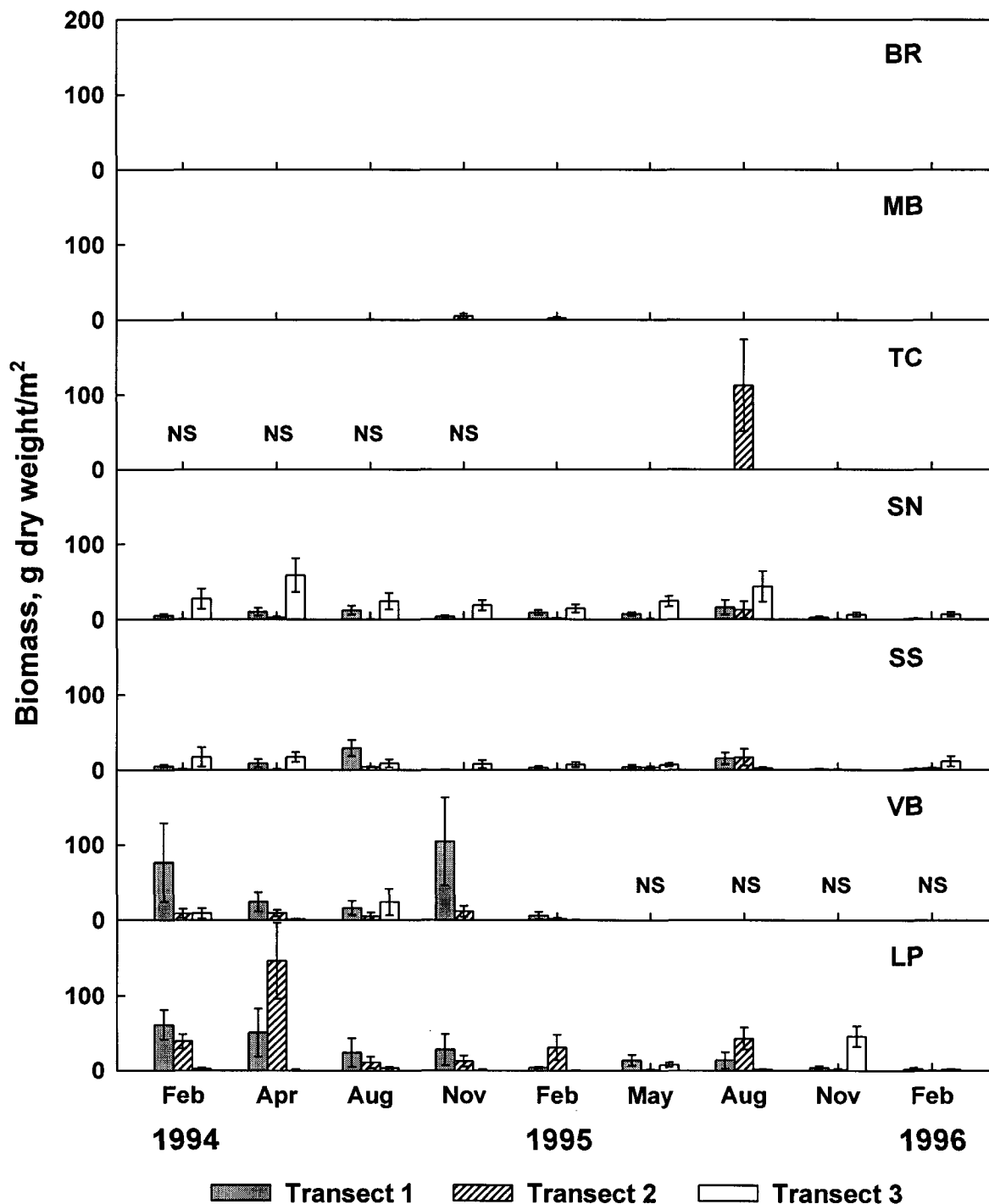


Fig. 4.37 Total biomass of *Gracilaria* spp., by station, transect, and season. Data are means (\pm SE) for all station-transect-season combinations; NS = not sampled (VB was sampled only during Year 1, TC only during Year 2).

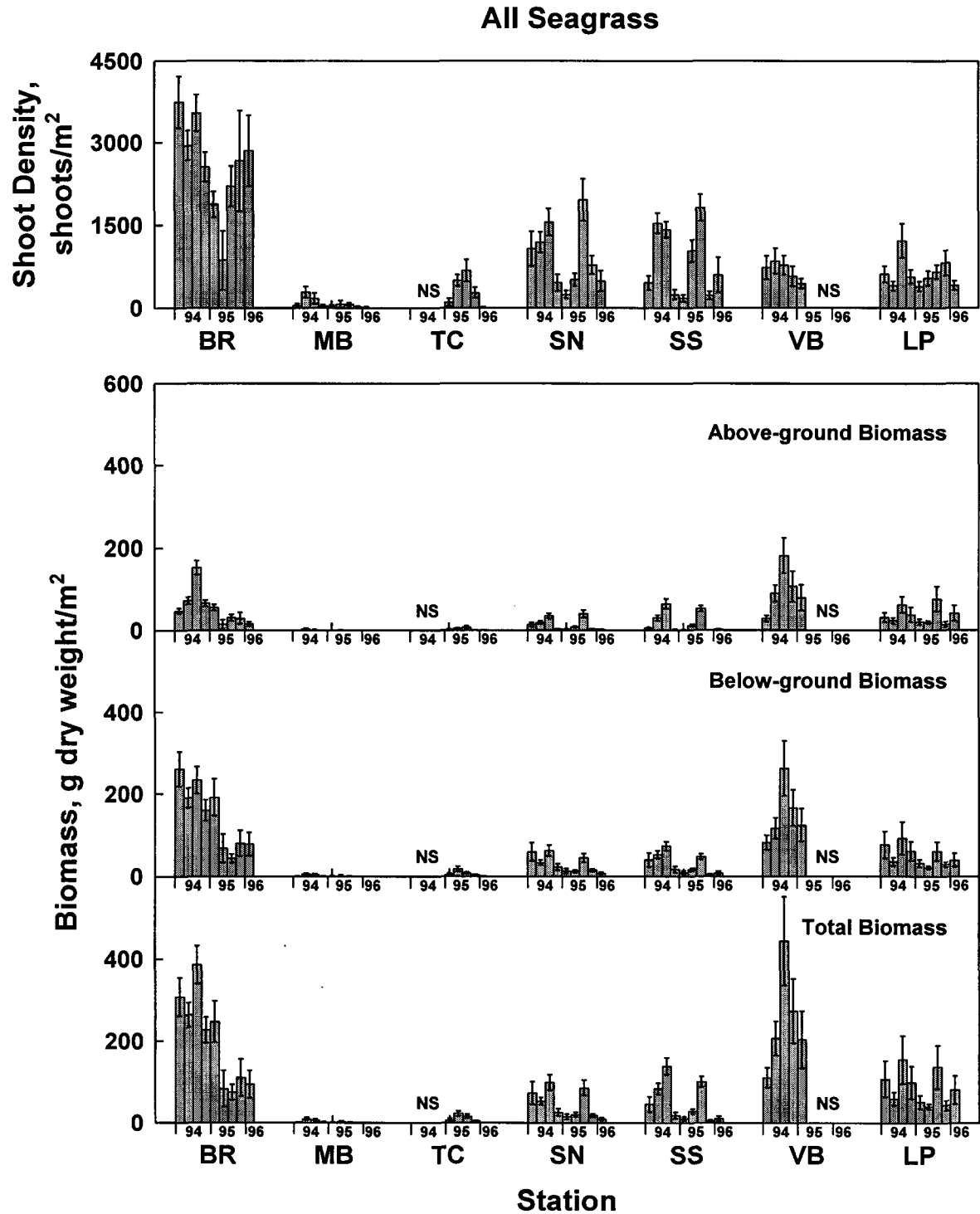


Fig. 4.38 Shoot density and above-ground, below-ground, and total biomass of the seagrass community, by station and season. Data are means (\pm SE) for Transects 1 and 2; NS = not sampled (VB was sampled only during Year 1, TC only during Year 2).

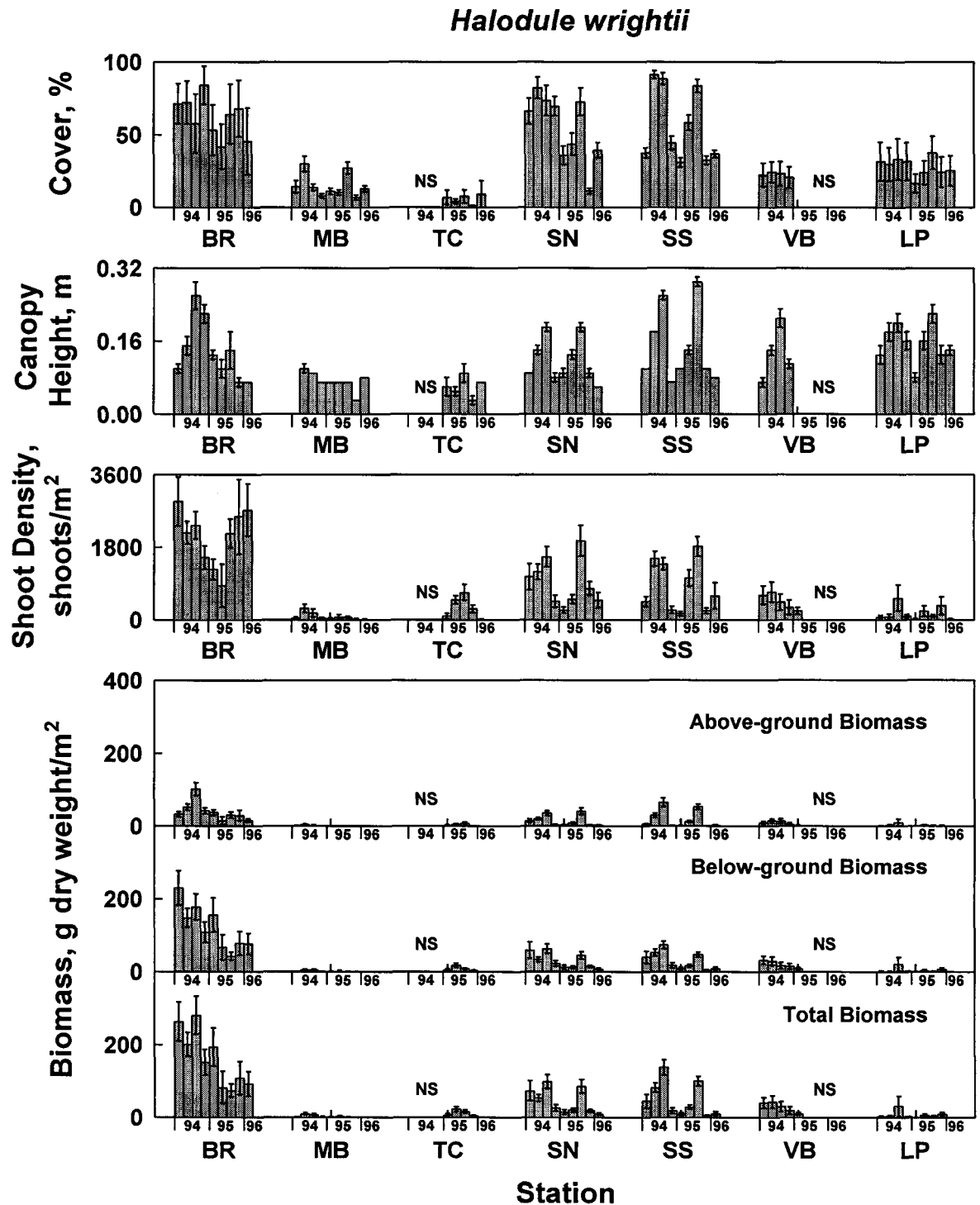


Fig. 4.39 Cover, canopy height, shoot density, and above-ground, below-ground, and total biomass of *Halodule wrightii*, by station and season. Data are means (\pm SE) for Transects 1 and 2; NS = not sampled (VB was sampled only during Year 1, TC only during Year 2).

Syringodium filiforme

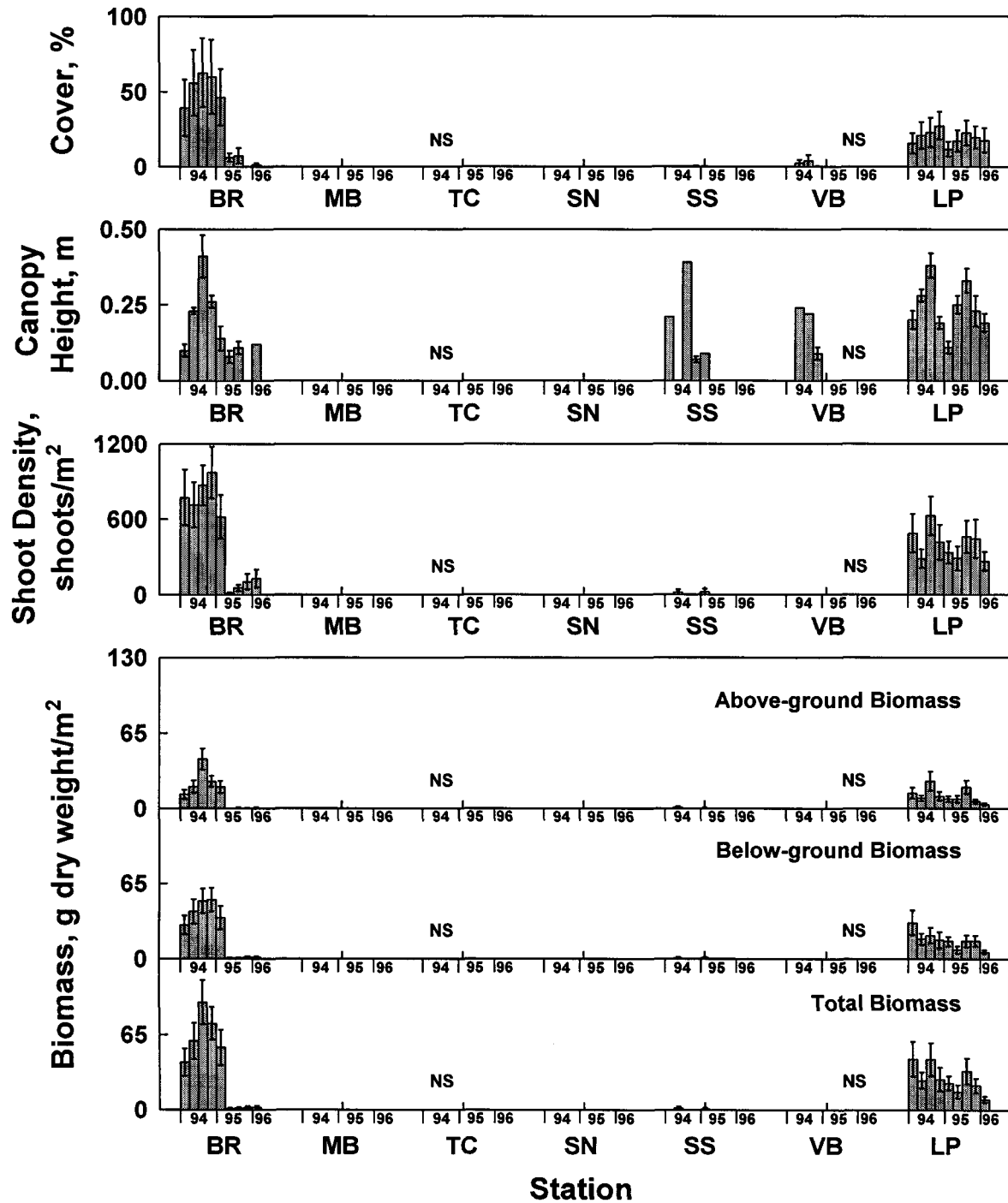


Fig. 4.40 Cover, canopy height, shoot density, and above-ground, below-ground, and total biomass of *Syringodium filiforme*, by station and season. Data are means (\pm SE) for Transects 1 and 2; NS = not sampled (VB was sampled only during Year 1, TC only during Year 2).

Thalassia testudinum

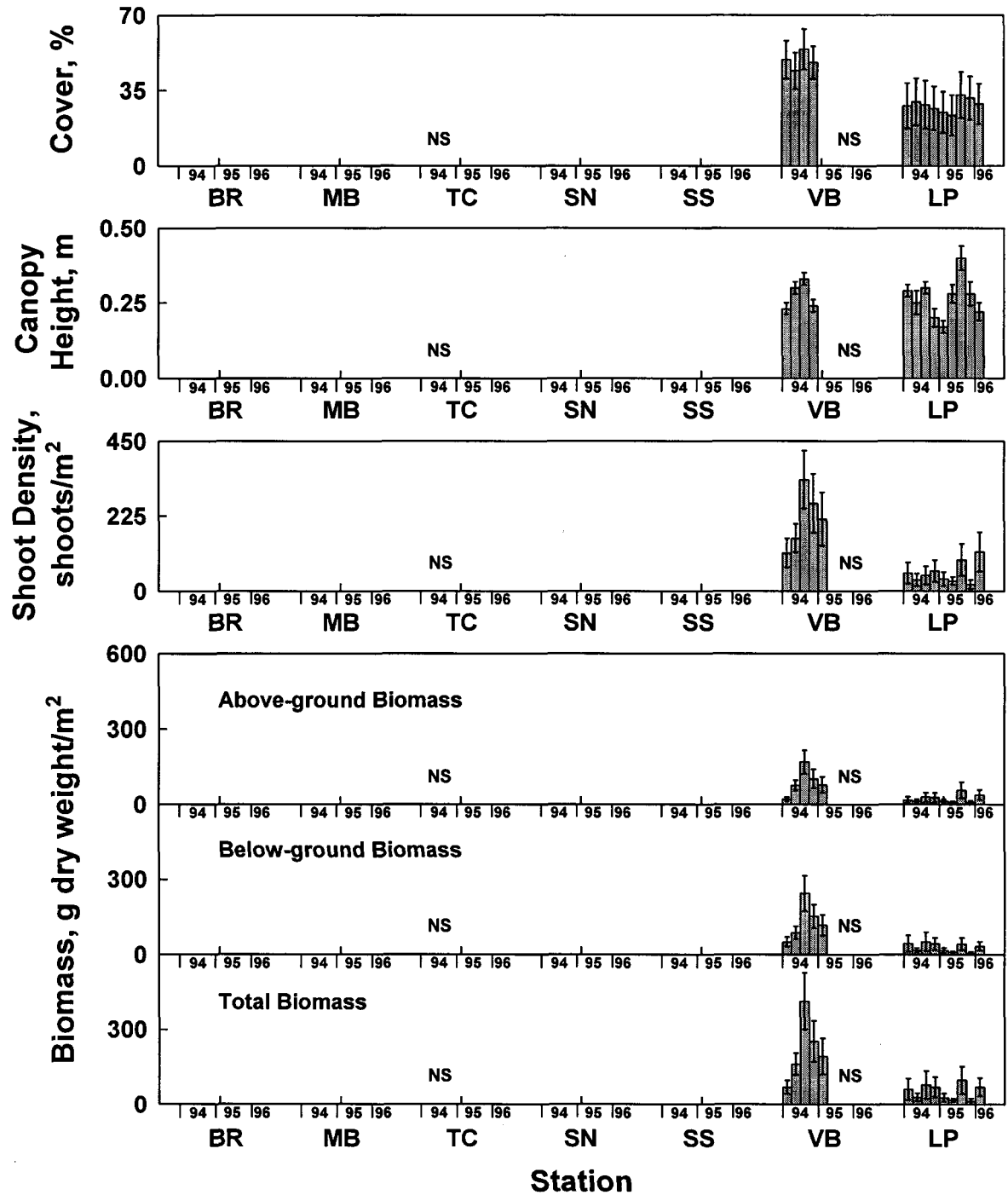


Fig. 4.41 Cover, canopy height, shoot density, and above-ground, below-ground, and total biomass of *Thalassia testudinum*, by station and season. Data are means (\pm SE) for Transects 1 and 2; NS = not sampled (VB was sampled only during Year 1, TC only during Year 2).

Halophila engelmannii

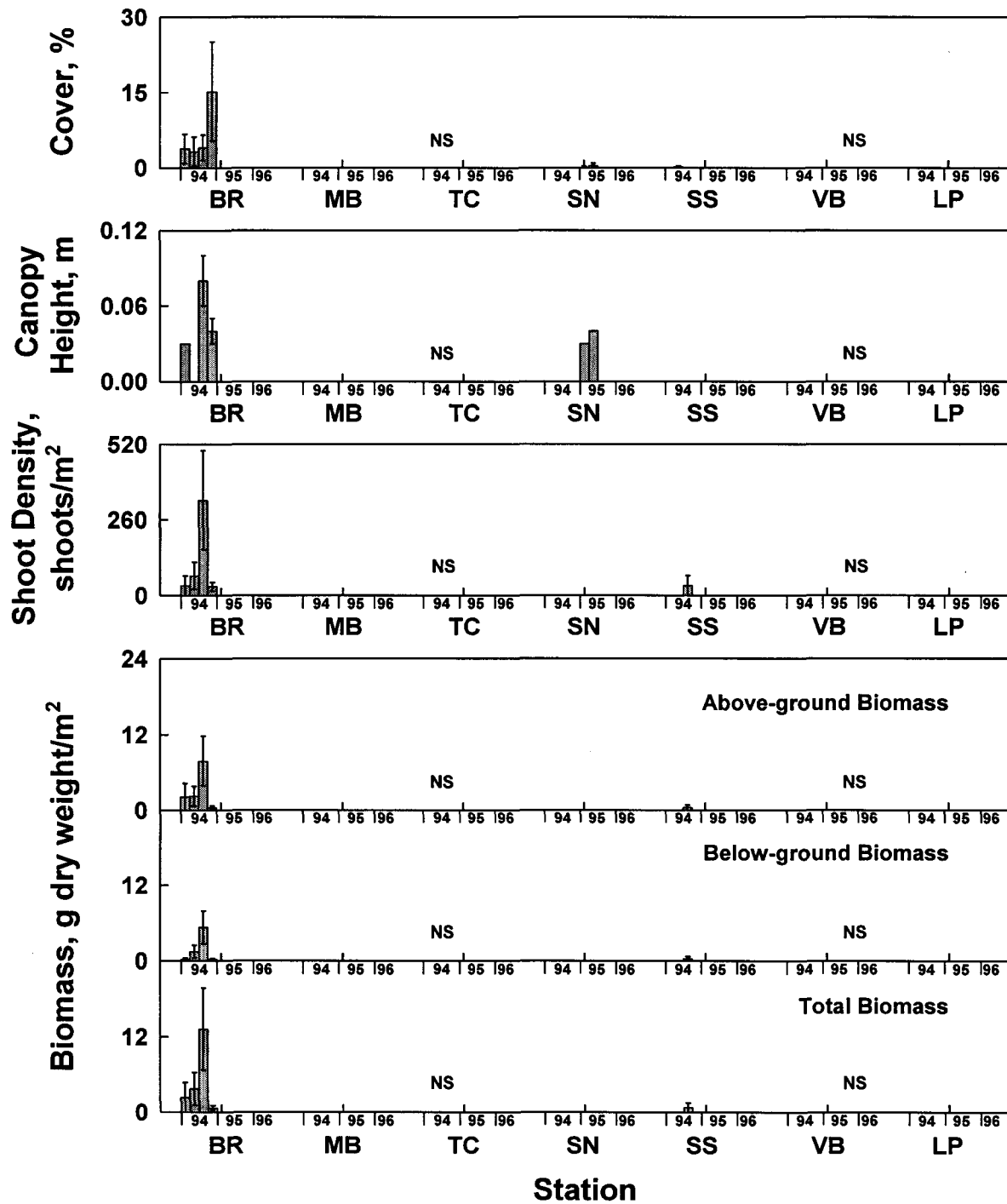


Fig. 4.42 Cover, canopy height, shoot density, and above-ground, below-ground, and total biomass of *Halophila engelmannii*, by station and season. Data are means (\pm SE) for Transects 1 and 2; NS = not sampled (VB was sampled only during Year 1, TC only during Year 2).

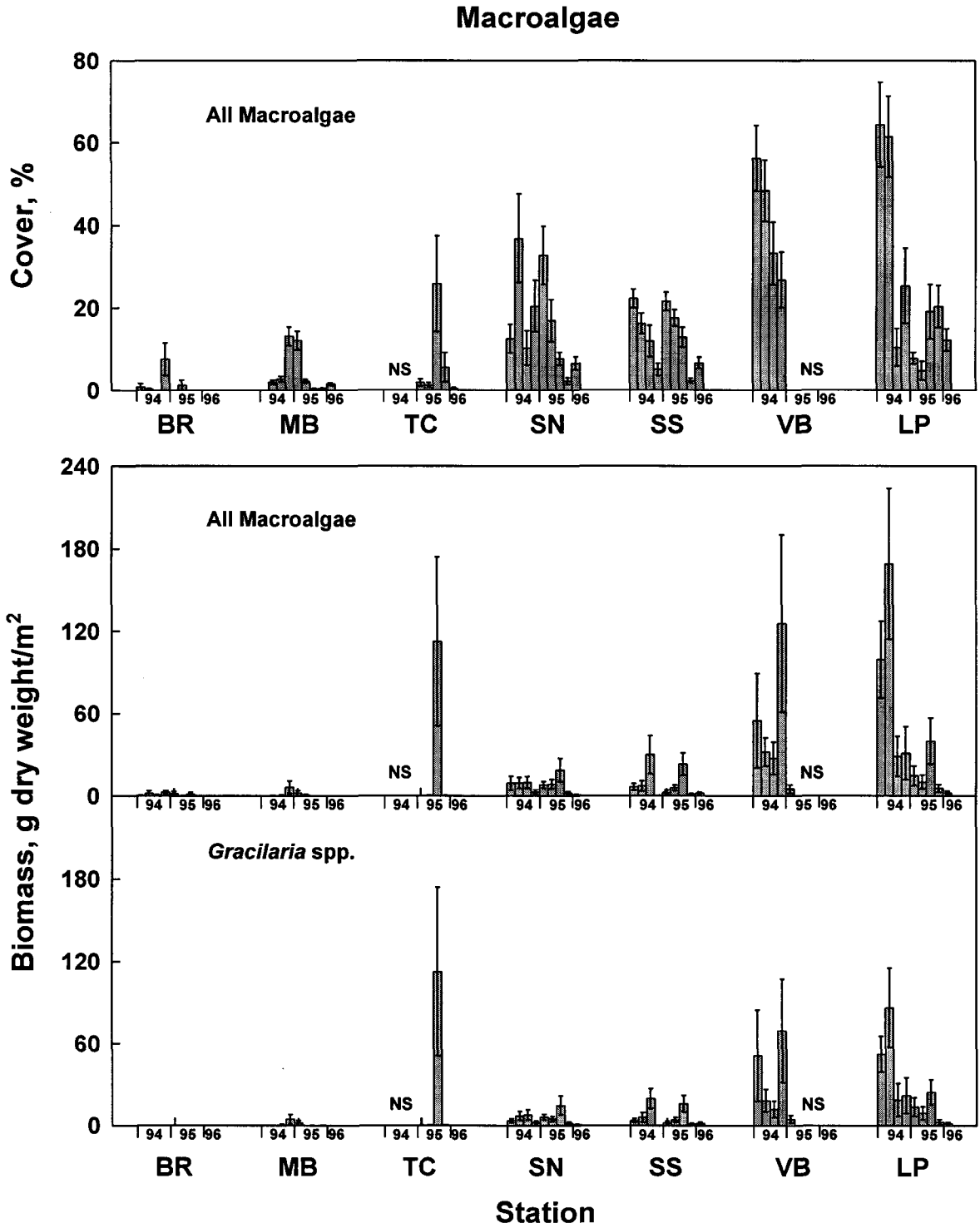


Fig. 4.43 Cover and biomass of all macroalgae and biomass of *Gracilaria* spp., by station and season. Data are means (\pm SE) for Transects 1 and 2; NS = not sampled (VB was sampled only during Year 1, TC only during Year 2).

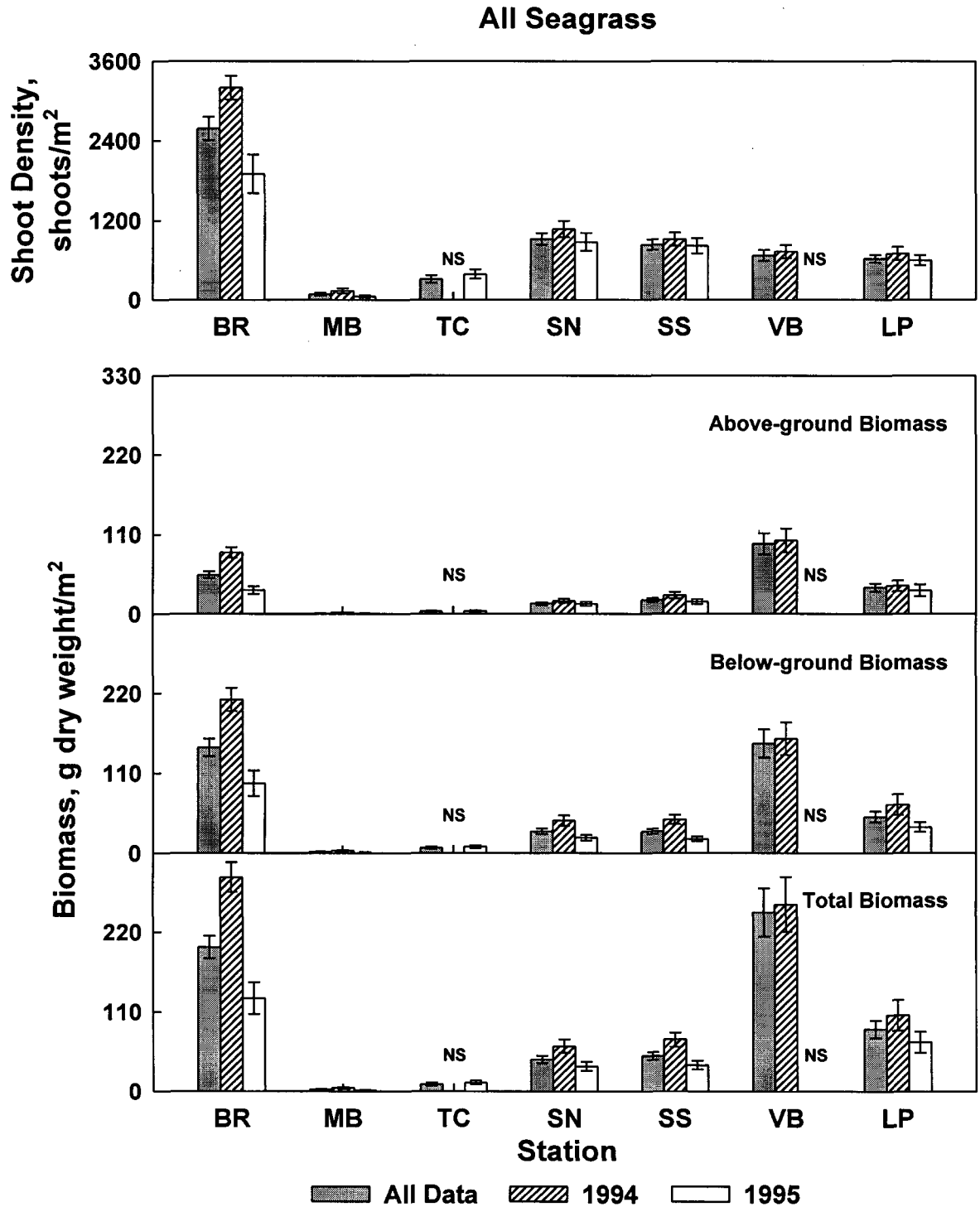


Fig. 4.44 Interannual variation in shoot density and above-ground, below-ground, and total biomass of the seagrass community based on station means (\pm SE) for Transects 1 and 2; NS = not sampled (VB was sampled only during Year 1, TC only during Year 2).

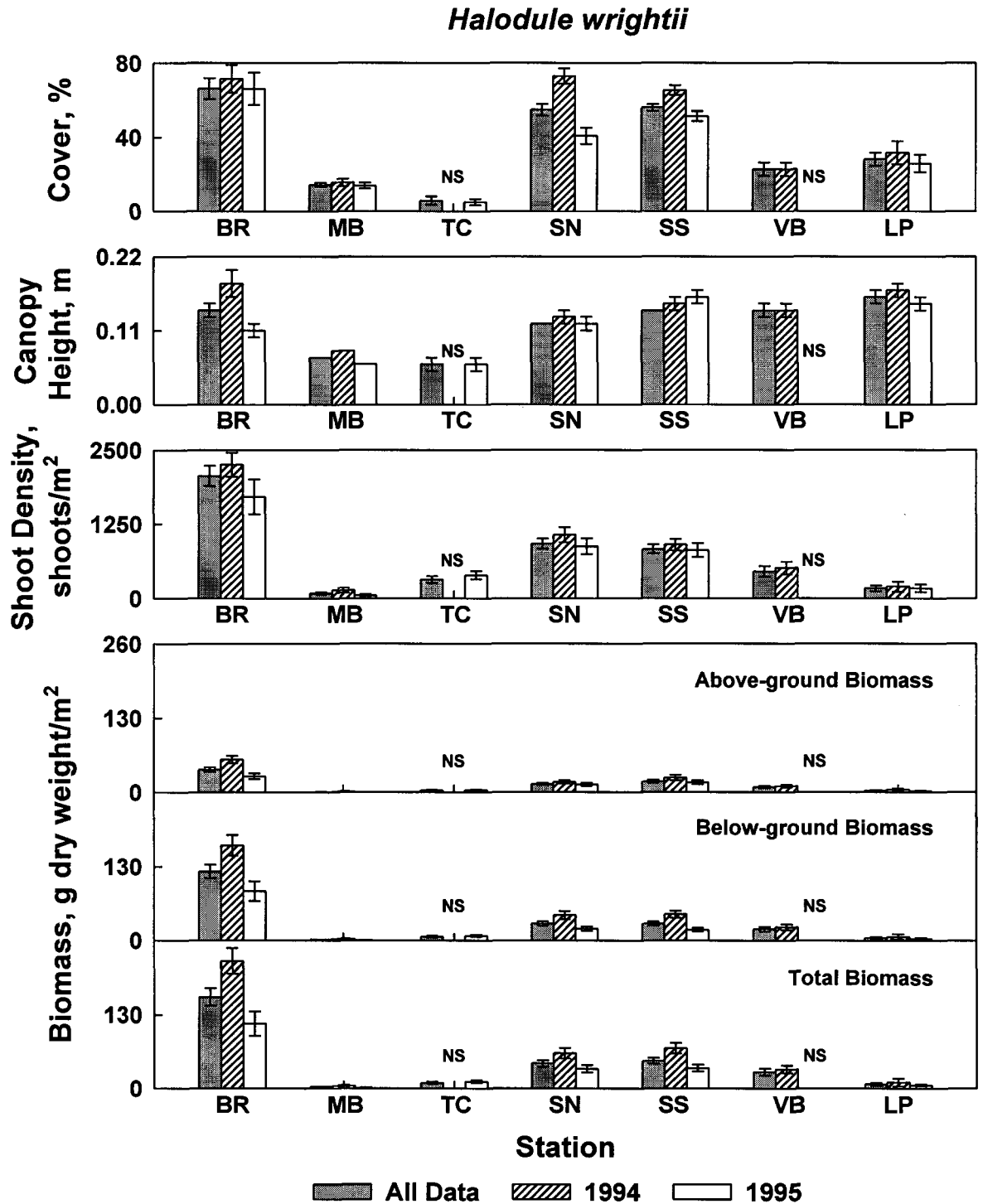


Fig. 4.45 Interannual variation in cover, canopy height, shoot density, above-ground, below-ground, and total biomass of *Halodule wrightii* based on station means (\pm SE) for Transects 1 and 2; NS = not sampled (VB was sampled only during Year 1, TC only during Year 2).

Syringodium filiforme

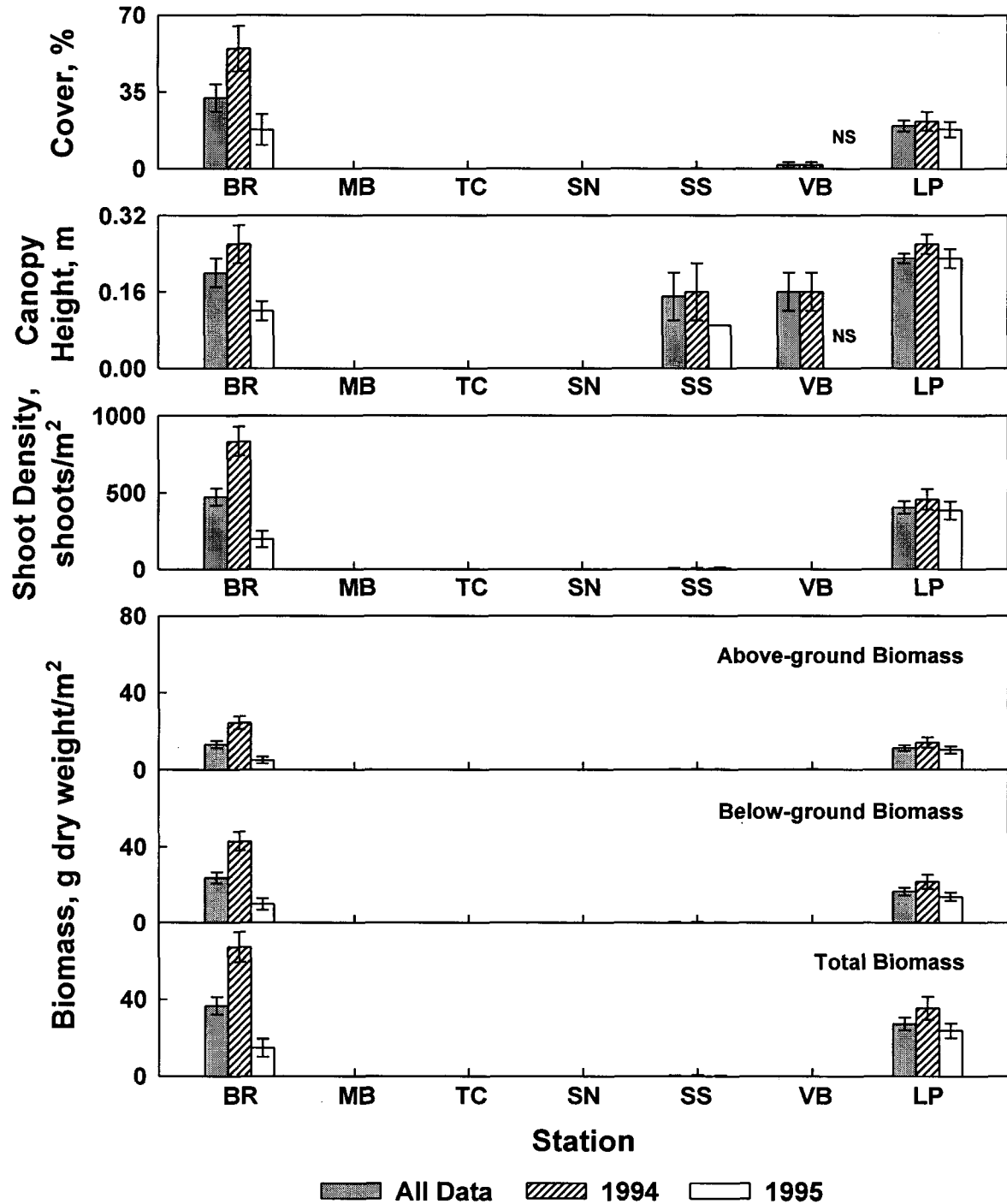


Fig. 4.46 Interannual variation in cover, canopy height, shoot density, above-ground, below-ground, and total biomass of *Syringodium filiforme* based on station means (\pm SE) for Transects 1 and 2; NS = not sampled (VB was sampled only during Year 1, TC only during Year 2).

Thalassia testudinum

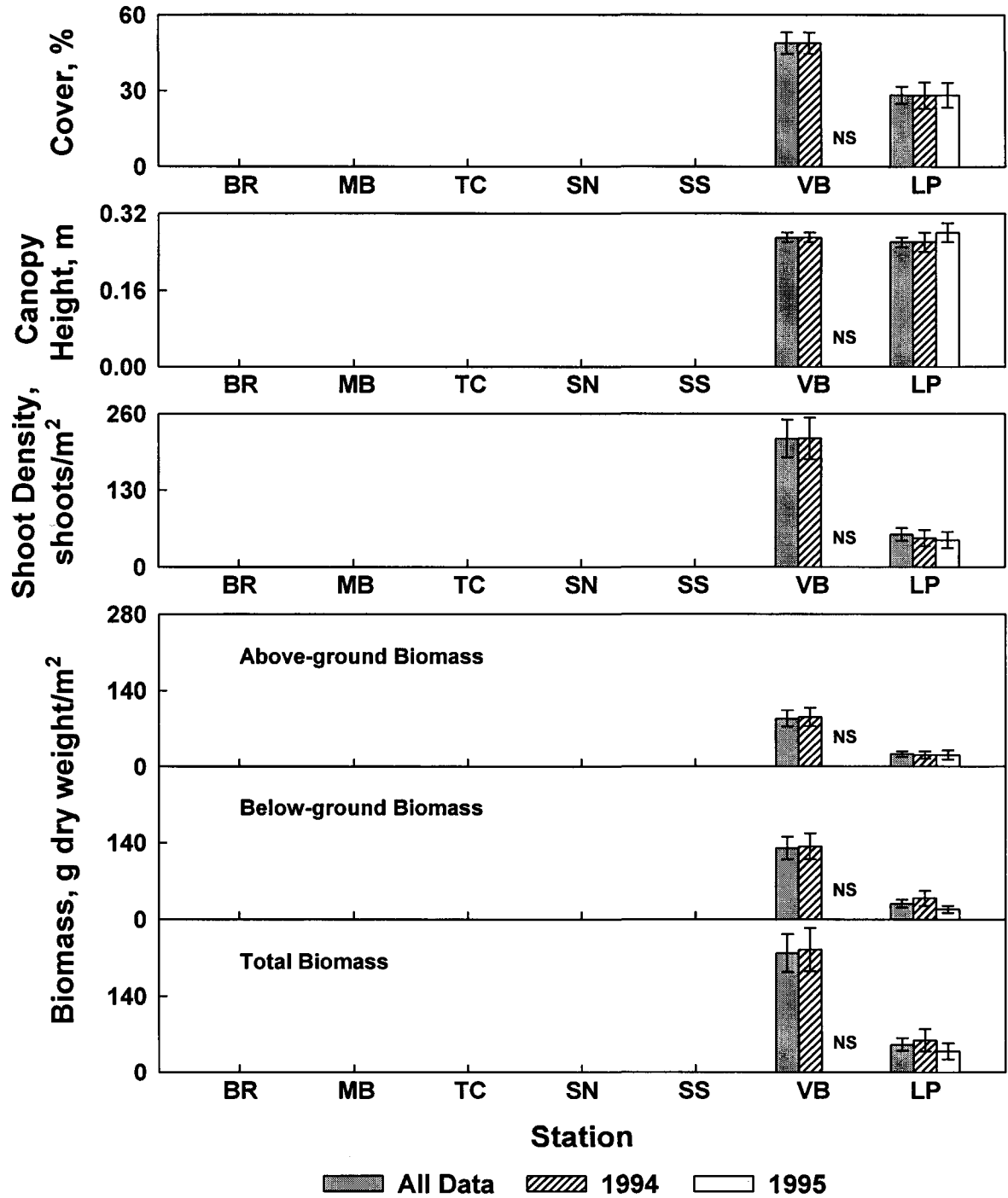


Fig. 4.47 Interannual variation in cover, canopy height, shoot density, above-ground, below-ground, and total biomass of *Thalassia testudinum* based on station means (\pm SE) for Transects 1 and 2; NS = not sampled (VB was sampled only during Year 1, TC only during Year 2).

Halophila engelmannii

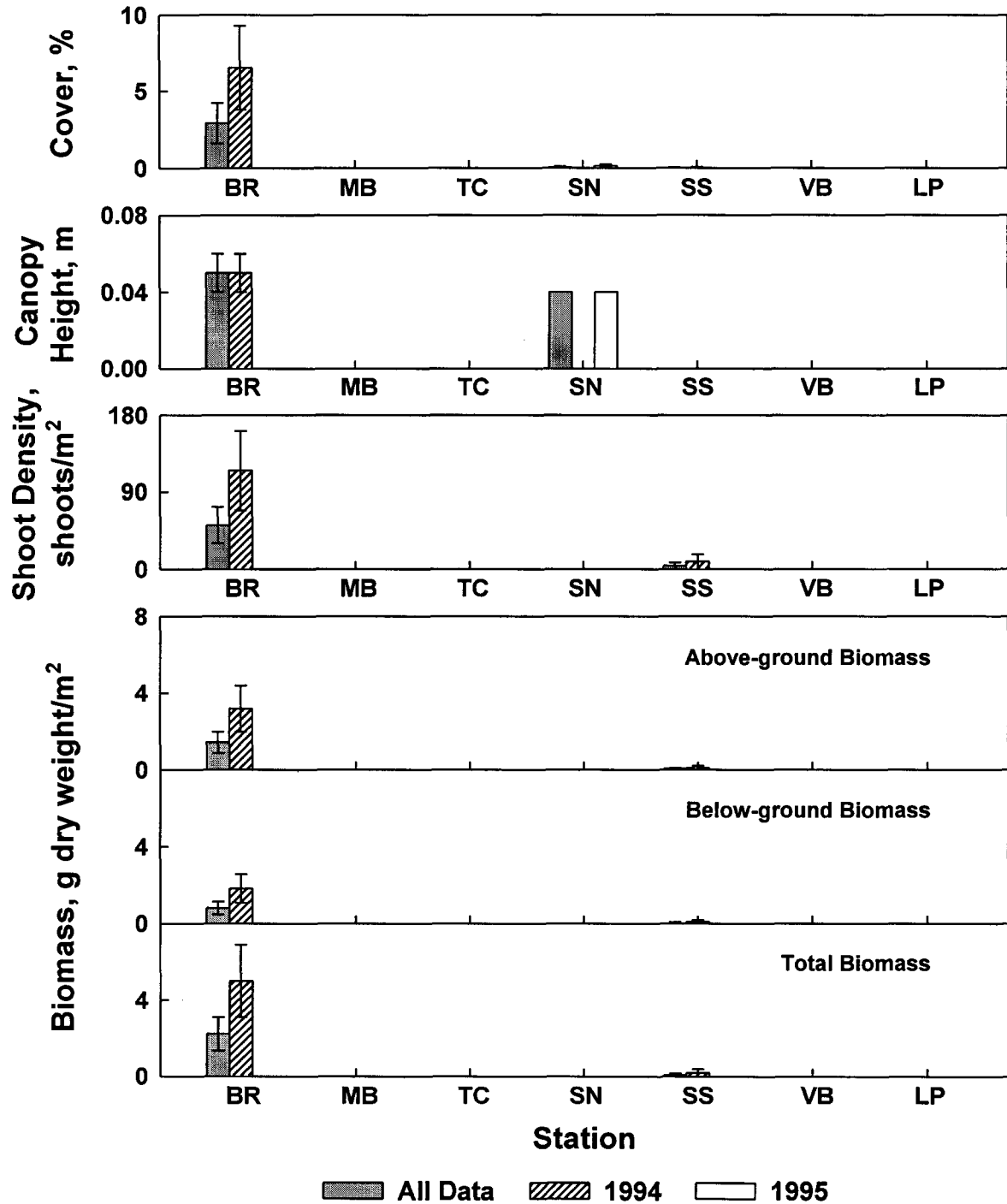


Fig. 4.48 Interannual variation in cover, canopy height, shoot density, above-ground, below-ground, and total biomass of *Halophila engelmannii* based on station means (\pm SE) for Transects 1 and 2; NS = not sampled (VB was sampled only during Year 1, TC only during Year 2).

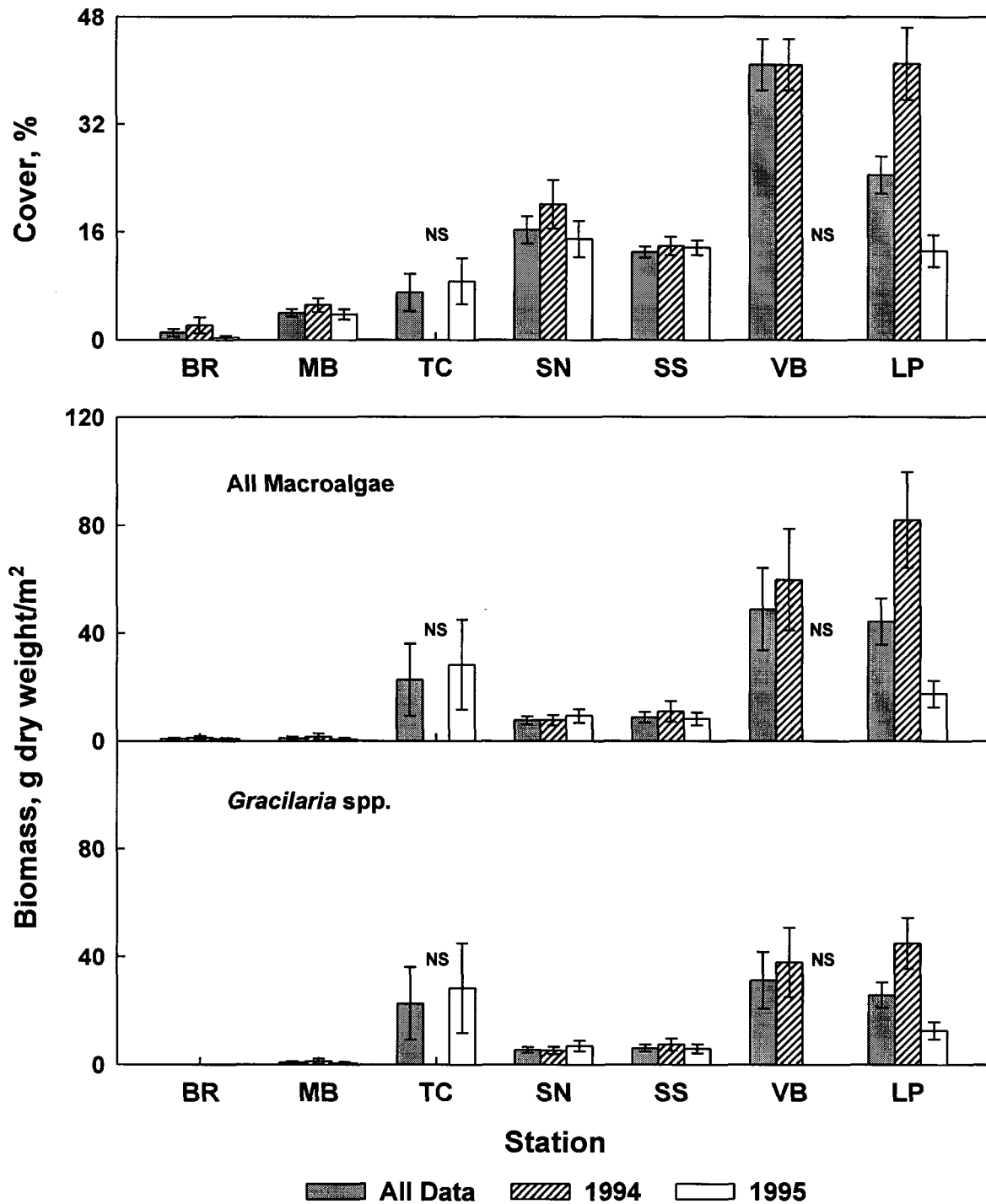


Fig. 4.49 Interannual variation in cover and biomass of all macroalgae and biomass of *Gracilaria* spp. based on station means (\pm SE) for Transects 1 and 2; NS = not sampled (VB was sampled only during Year 1, TC only during Year 2).

Halodule wrightii

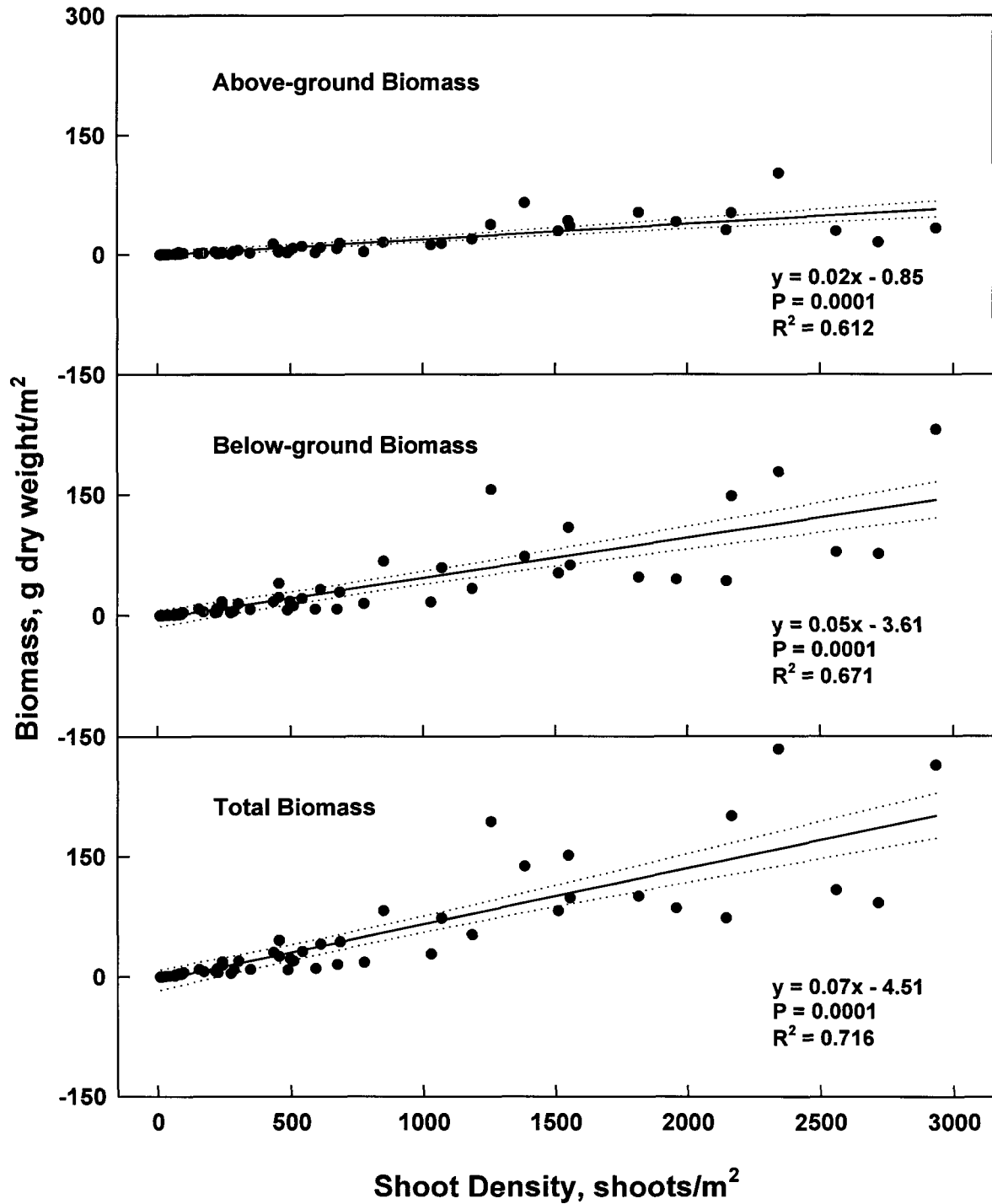


Fig. 4.50 Linear regressions of above-ground, below-ground, and total biomass vs. shoot density of *Halodule wrightii*, based on seasonal station means. Dotted lines indicate 95% confidence intervals of the regression line.

Syringodium filiforme

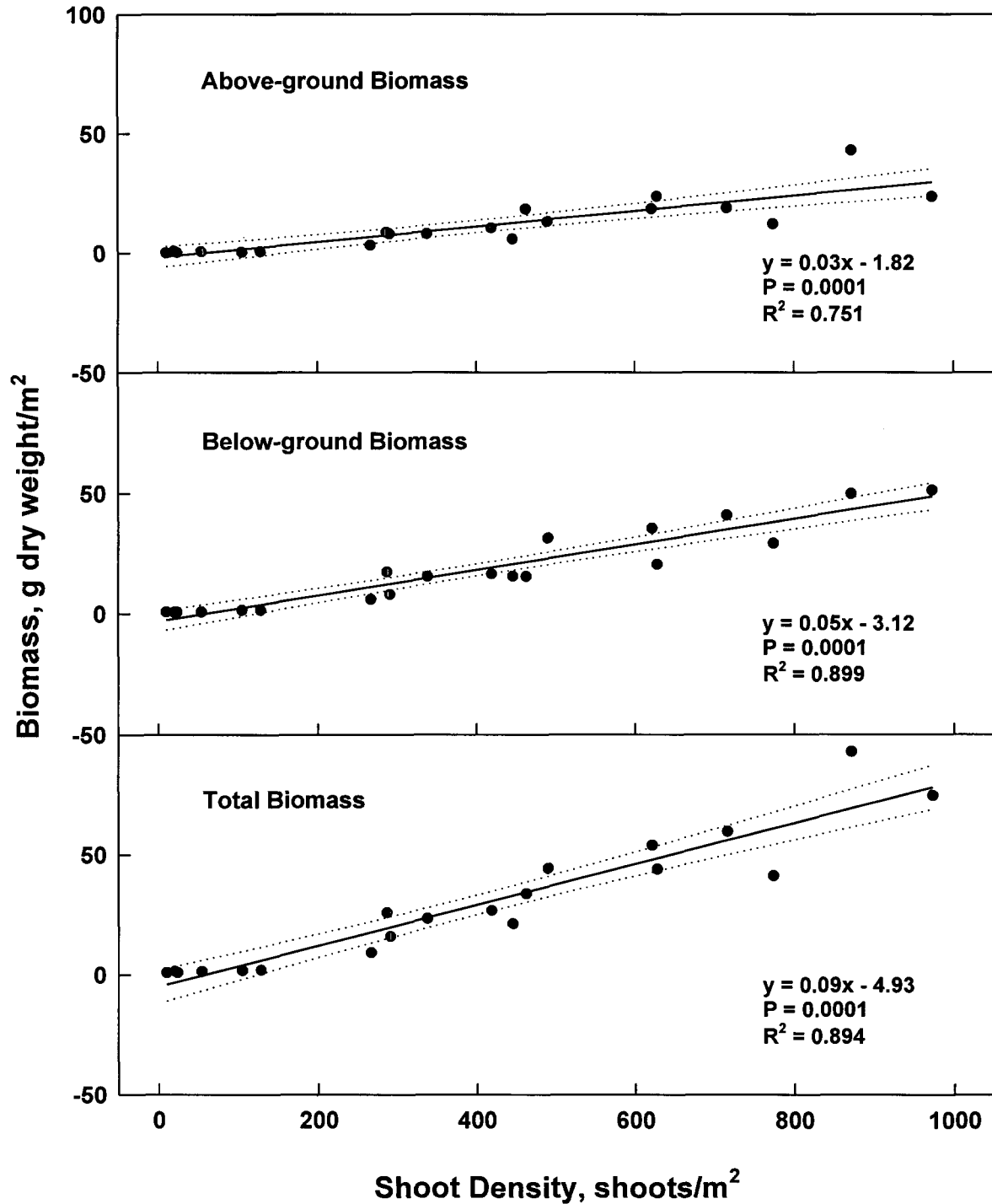


Fig. 4.51 Linear regressions of above-ground, below-ground, and total biomass vs. shoot density of *Syringodium filiforme*, based on seasonal station means. Dotted lines indicate 95% confidence intervals of the regression line.

Thalassia testudinum

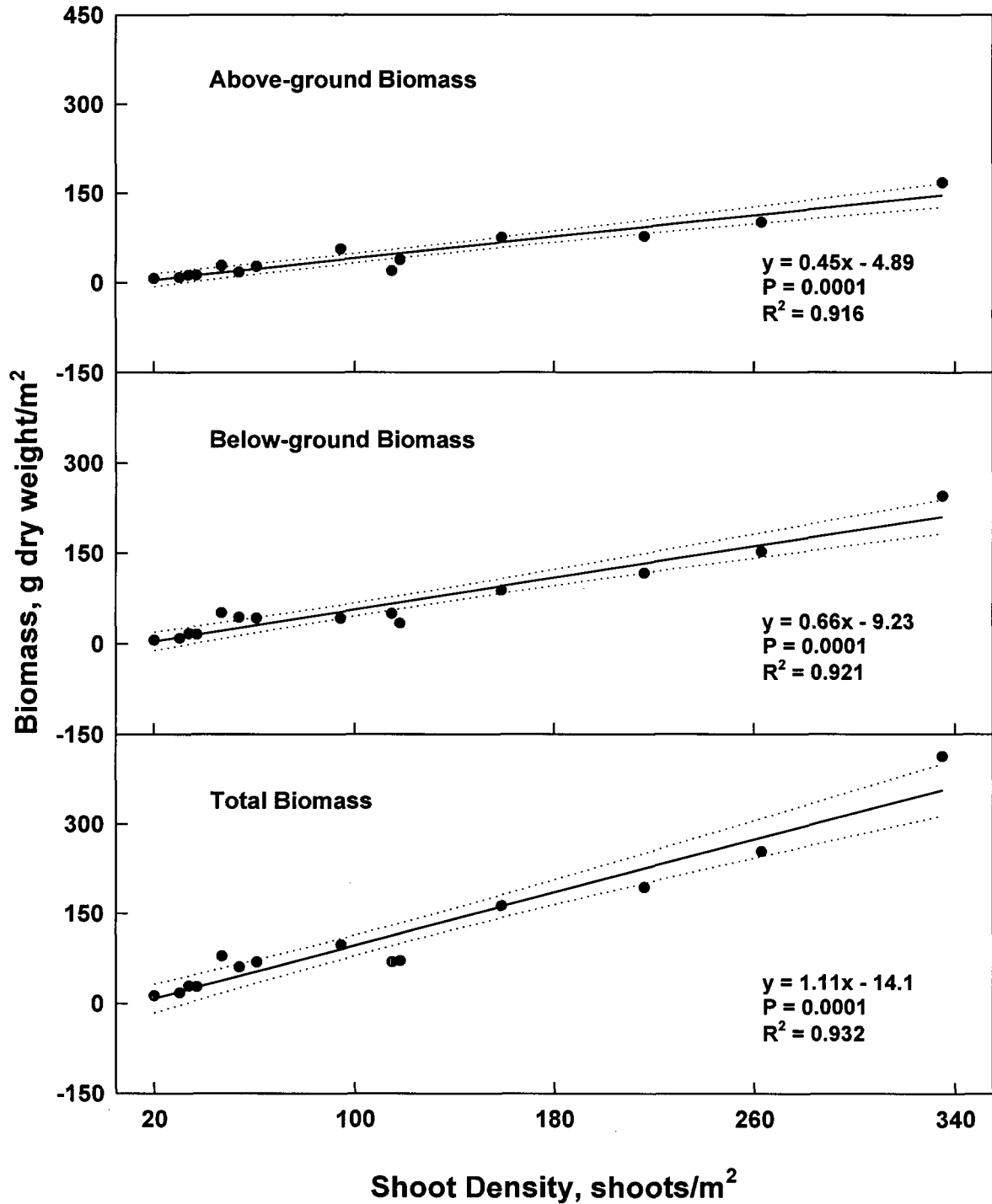


Fig. 4.52 Linear regressions of above-ground, below-ground, and total biomass vs. shoot density of *Thalassia testudinum*, based on seasonal station means. Dotted lines indicate 95% confidence intervals of the regression line.

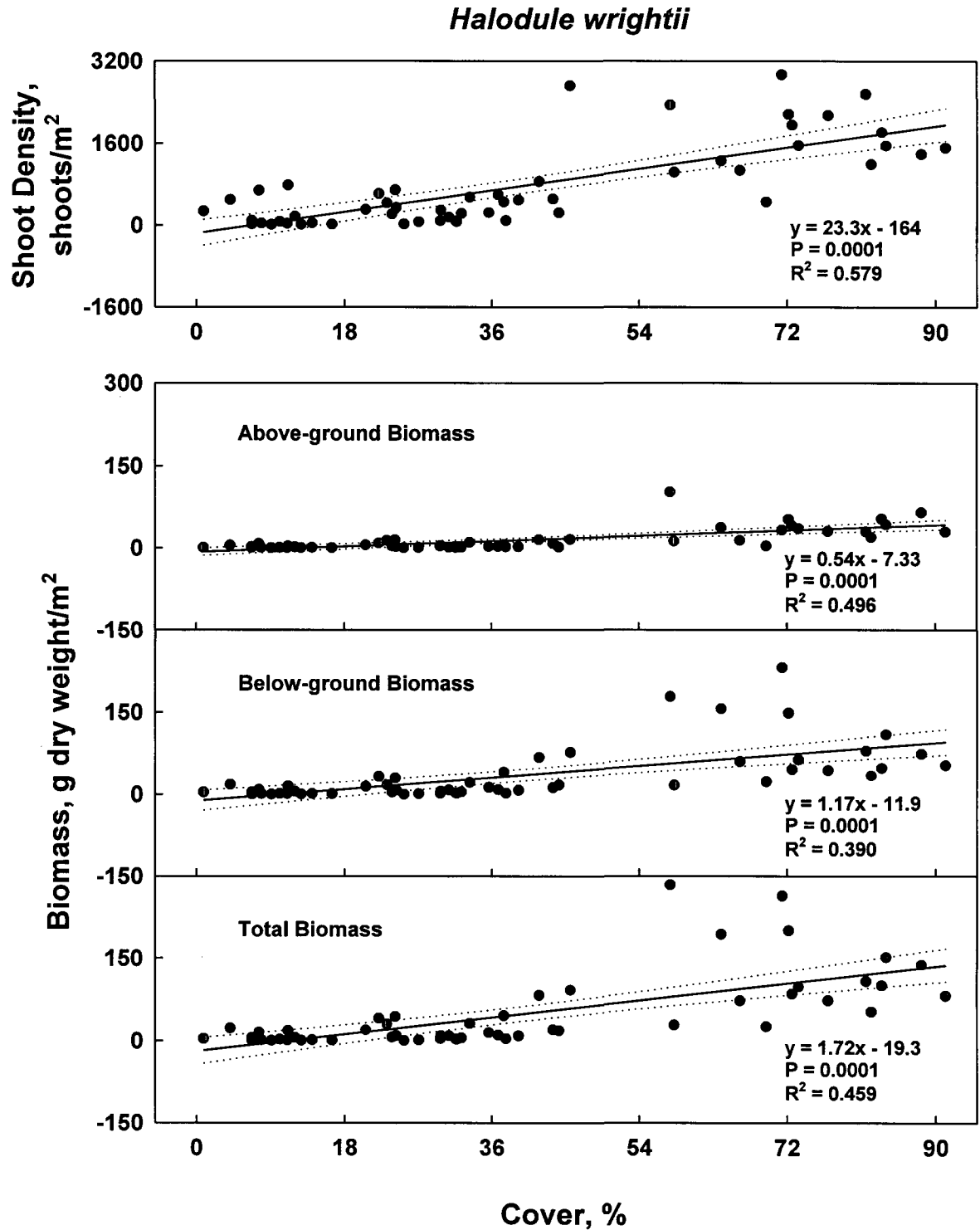


Fig. 4.53 Linear regressions of shoot density, above-ground, below-ground, and total biomass vs. cover of *Halodule wrightii*, based on seasonal station means. Dotted lines indicate 95% confidence intervals of the regression line.

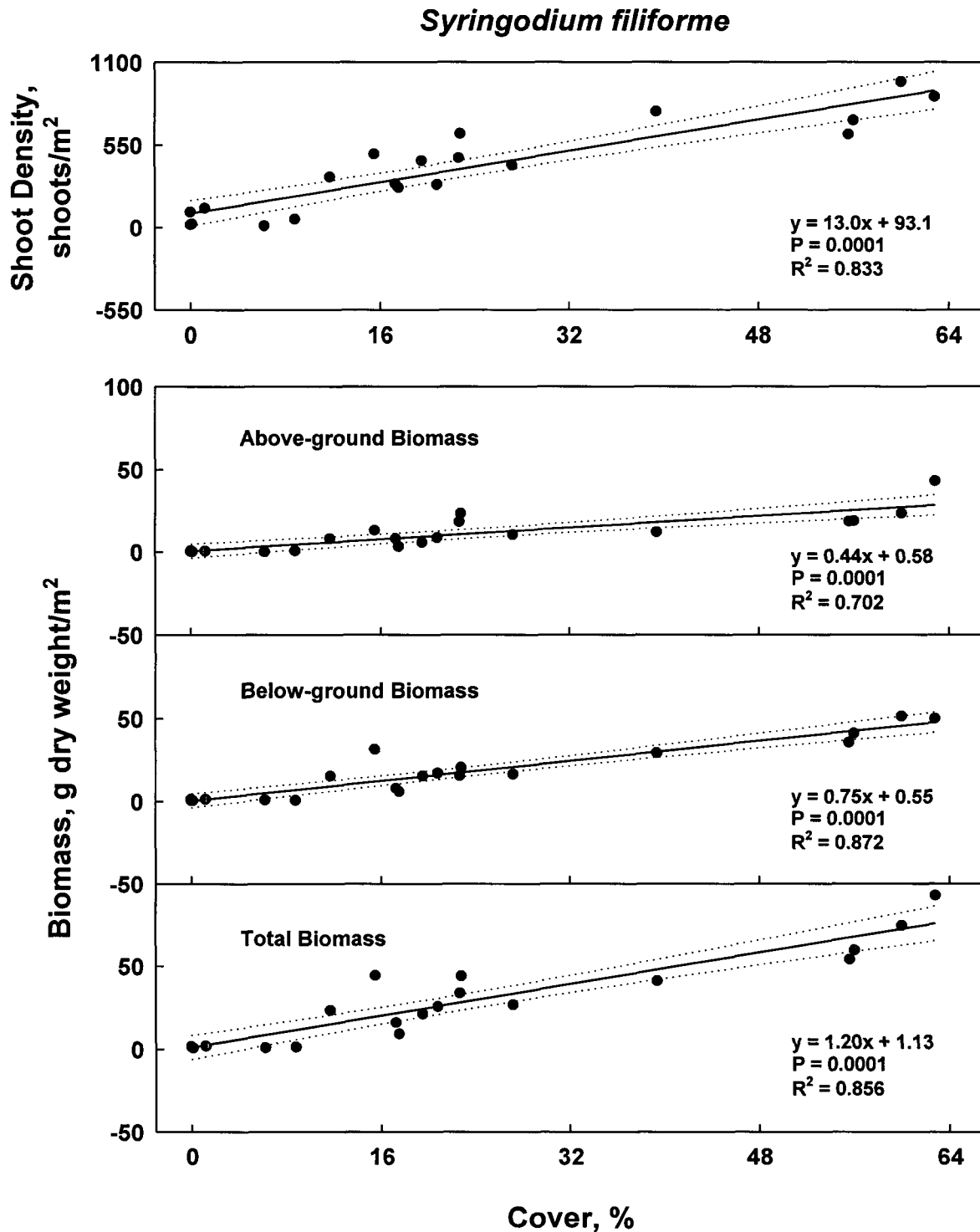


Fig. 4.54 Linear regressions of shoot density, above-ground, below-ground, and total biomass vs. cover of *Syringodium filiforme*, based on seasonal station means. Dotted lines indicate 95% confidence intervals of the regression line.

Thalassia testudinum

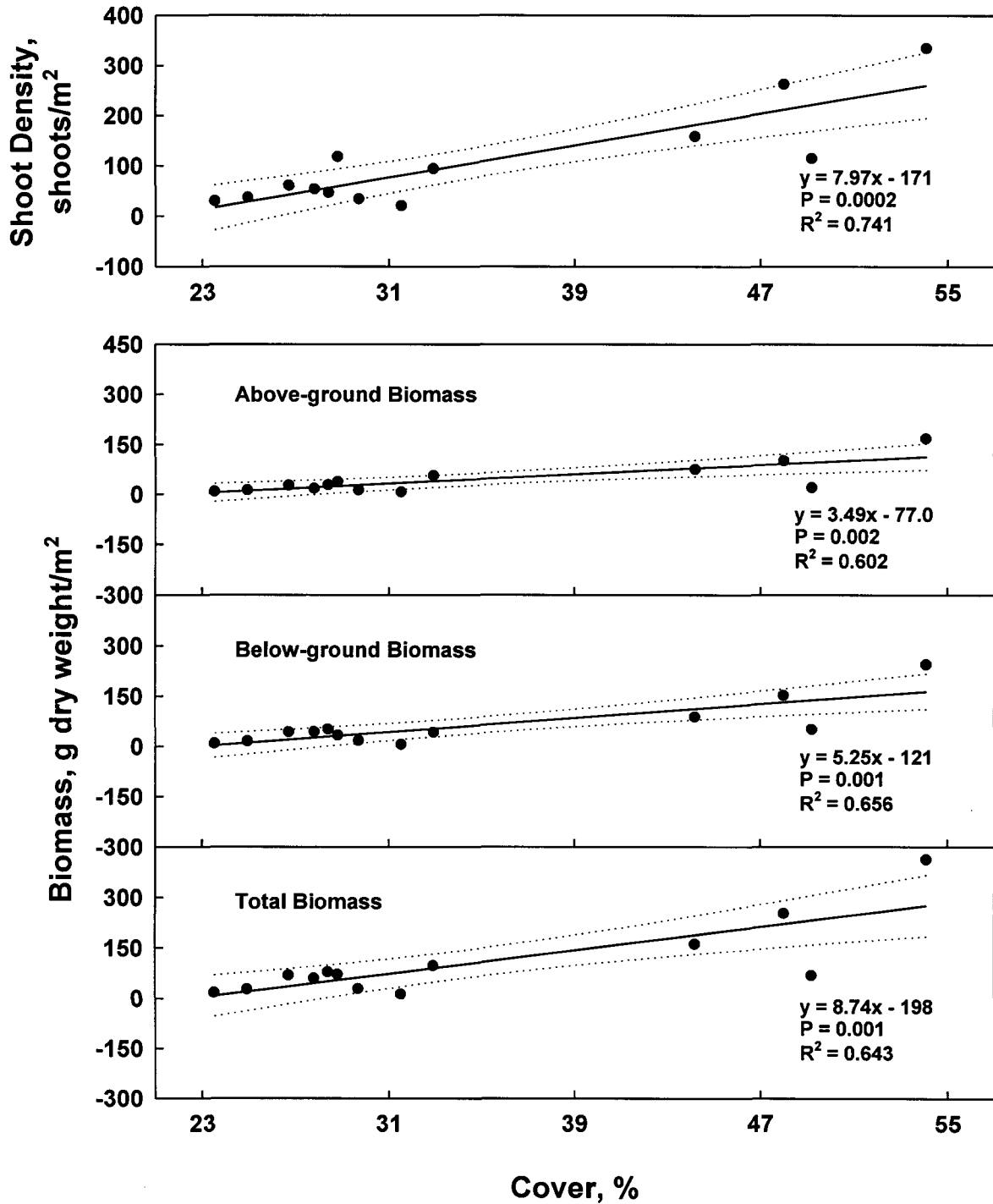


Fig. 4.55 Linear regressions of shoot density, above-ground, below-ground, and total biomass vs. cover of *Thalassia testudinum*, based on seasonal station means. Dotted lines indicate 95% confidence intervals of the regression line.

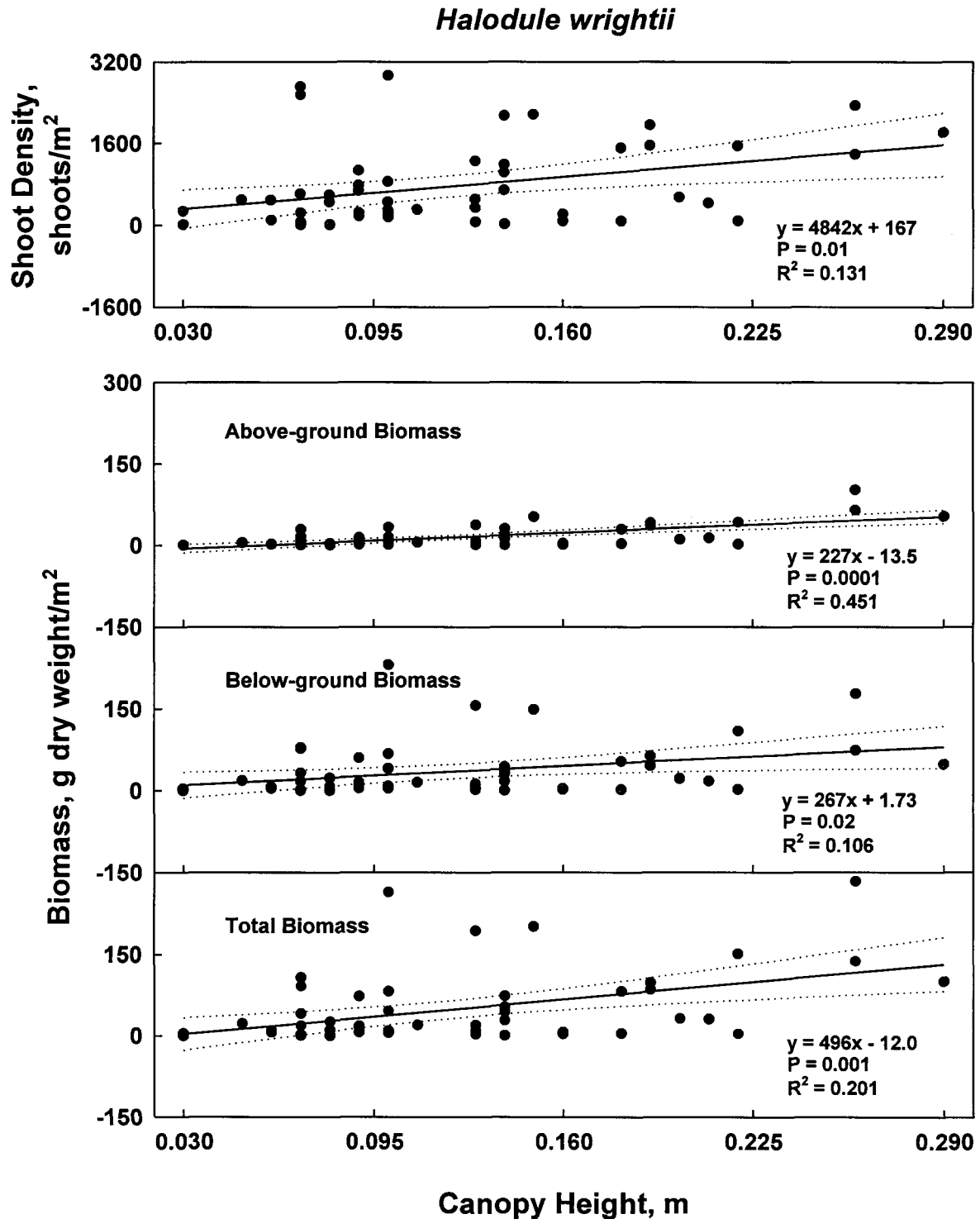


Fig. 4.56 Linear regressions of shoot density, above-ground, below-ground, and total biomass vs. canopy height of *Halodule wrightii*, based on seasonal station means. Dotted lines indicate 95% confidence intervals of the regression line.

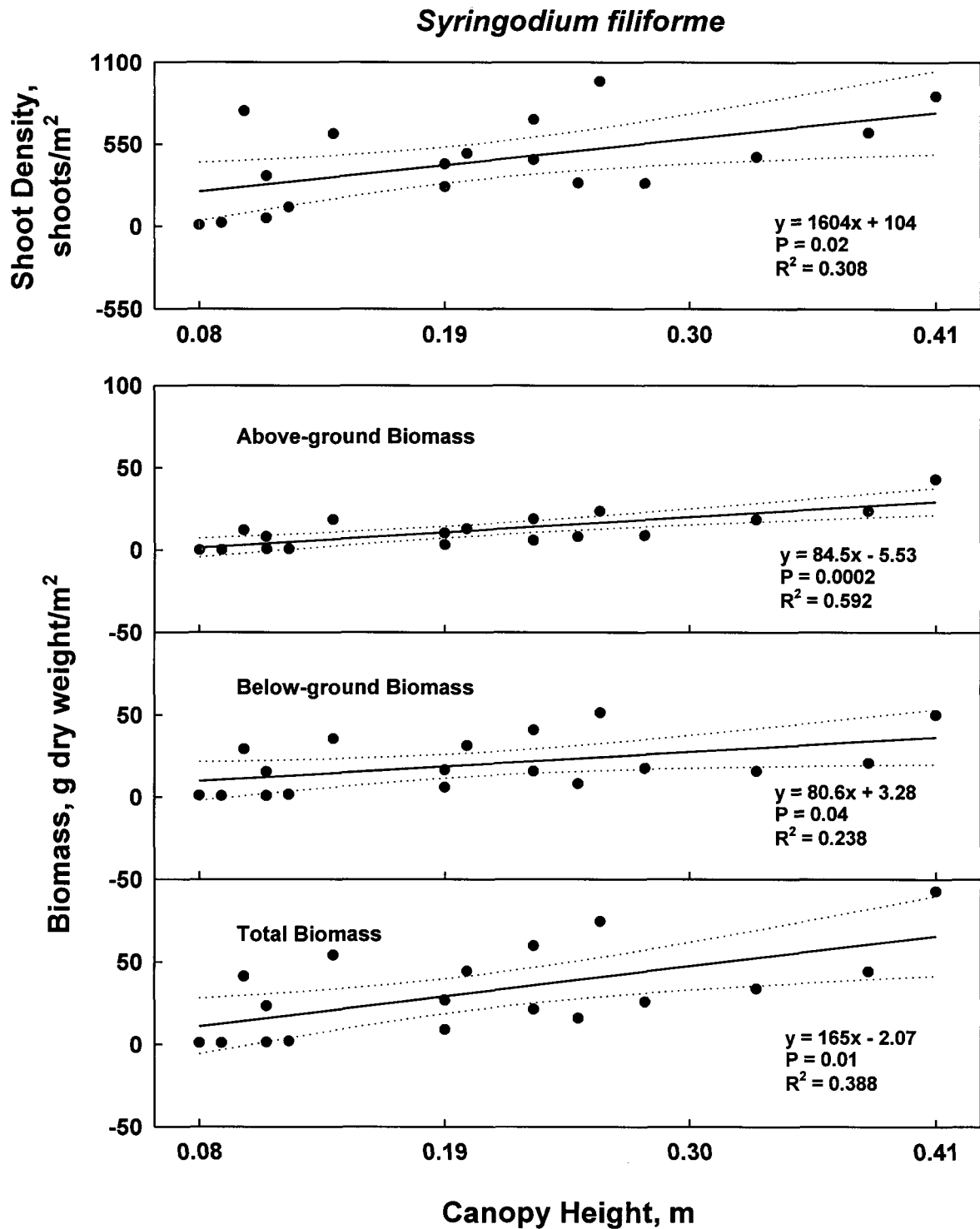


Fig. 4.57 Linear regressions of shoot density, above-ground, below-ground, and total biomass vs. canopy height of *Syringodium filiforme*, based on seasonal station means. Dotted lines indicate 95% confidence intervals of the regression line.

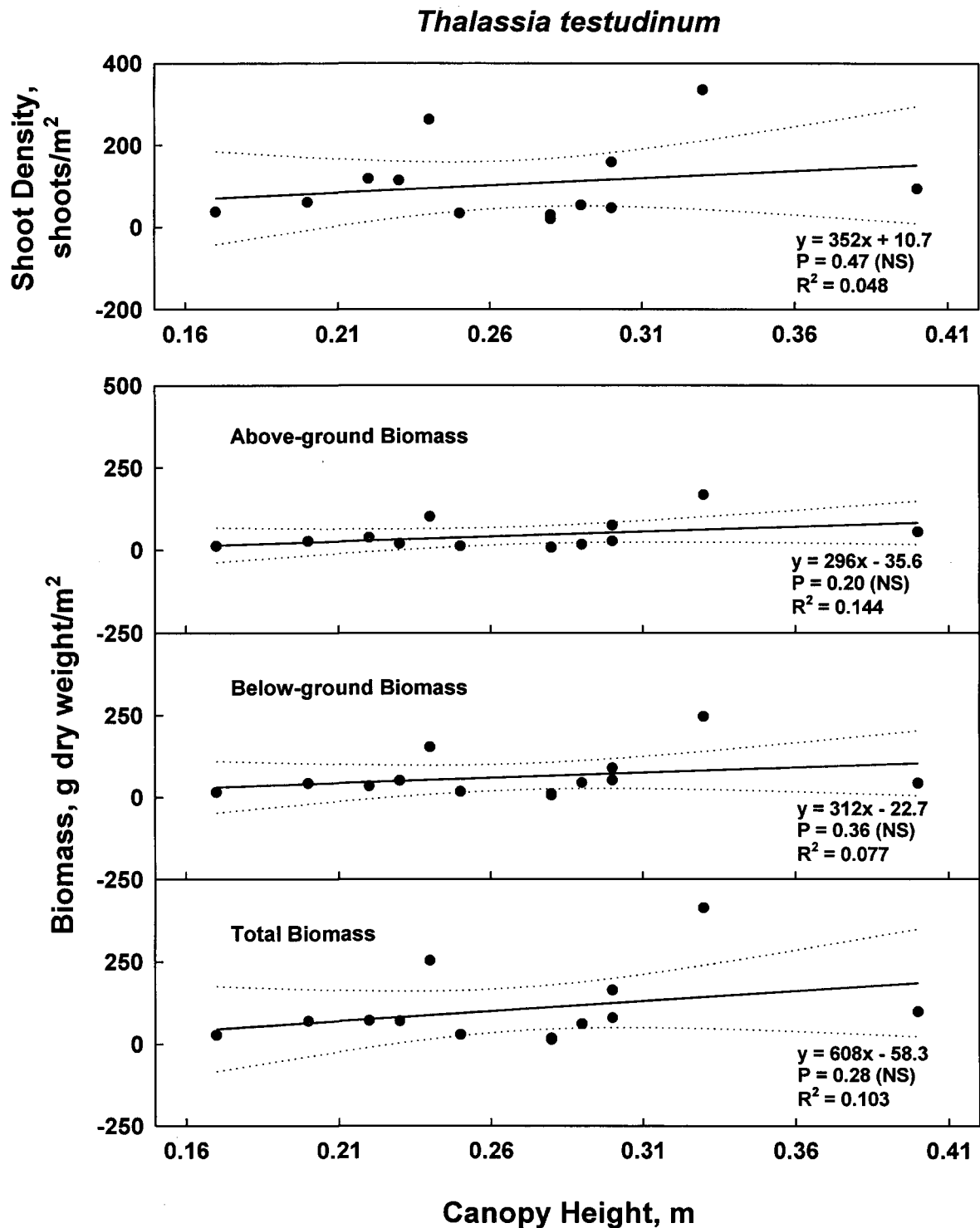


Fig. 4.58 Linear regressions of shoot density, above-ground, below-ground, and total biomass vs. canopy height of *Thalassia testudinum*, based on seasonal station means. Dotted lines indicate 95% confidence intervals of the regression line.

Chapter 5: Epiphytes

5.1 Introduction

Epiphytes are organisms that grow on plants. Seagrass epiphyte communities are complex assemblages of organisms that have been little studied in IRL (Hall and Eiseman 1981; see review in Harden 1994). Epiphytes may be important in relationships involving PAR, water quality, and SAV, as epiphytes reduce the amount of light available to their seagrass hosts. For example, increased nutrient inputs might indirectly limit seagrass by stimulating the growth of epiphytic algae on seagrass leaves. Excessive epiphytes may cause lower shoot densities, lower leaf area, and lower seagrass biomass by reducing the amount of light the leaves receive.

The primary purpose of this portion of the study was to determine if there were significant differences in the abundance of seagrass epiphytes among the PAR monitoring stations. Interactions of epiphytes, seagrasses, and water quality are addressed in Chapters 7 and 8.

5.2 Task Description

Task 5: To quantify the epiphyte load on seagrass shoots at selected stations in Indian River Lagoon quarterly for 1 year.

5.3 Methods

During the quarterly SAV sampling (see Chapter 4), seagrass shoots were collected for epiphyte analyses along all transects at the 6 Year-1 stations. At each station, a permanent transect ("Transect 1" or "Whole-bed Transect") was established perpendicular to the shoreline and extended to the "deep edge" of the seagrass beds. Two additional transects, both 20-m long and perpendicular to Transect 1, were established at all stations except MB (which had only a single, mid-bed transect). Transect 2 ("Mid-bed Transect") began about 1 m from the mid-bed PAR sensor array and ran at the same depth as the array, parallel to shore; Transect 3 ("Deep-edge Transect") ran along the "deep edge" of the bed as delineated by the District (Bob Virnstein) at the start of sampling.

Sampling locations for epiphytes along each transect were determined by random numbers. For each station except MB, 10 samples were taken along Transect 1, and 6 samples were taken along Transects 2 and 3. Each sample was

placed in a pre-labeled plastic bag on ice in a darkened cooler and kept frozen until processed.

Epiphytes were quantified on the above-ground seagrass fraction as delineated by the presence of photosynthetic tissue (herein, loosely referred to as shoots). The originally proposed technique for epiphyte removal was a mechanical one, which was found to give unreliable (i.e., inconsistent) removal of epiphytes. Harden (1994) also had difficulty in removing epiphytes from IRL samples with mechanical techniques. In the current study, epiphyte removal was optimized with a combined chemical/mechanical technique.

A pretreatment of MES buffer (0.1 M, pH = 5.5) dissolved carbonates and hydrolyzed polysaccharide-protein matrices used by calcareous algae and diatoms for attachment. Photosynthetic portions of seagrasses were placed on ice blocks and 1-3 mL of buffer was pipetted over the shoot. The buffer solution with seagrass was kept in the dark for 5 minutes and placed on a dissecting microscope. Epiphytes were removed by scraping the leaf surface with a rubber-tipped spatula while viewed at 100-150x magnification. Sand grains and dead leaf material were removed from the slurry prior to analyses. The epiphyte slurry was subsampled to estimate chlorophyll *a* content and dry weight. Removal of the sand and detrital contaminants facilitated grinding of the chlorophyll samples (and avoided breaking the grinding apparatus) and permitted direct comparison of biomass (dry weight) with chlorophyll measures.

Chlorophyll *a* was determined spectrophotometrically with the trichromatic equations of SCOR/UNESCO (1966). Seagrass and epiphyte samples were dried at 60°C. Dry weights were measured on a Mettler balance (accuracy = 0.0002 g, precision = 0.0001 g). Because both seagrass and epiphyte fractions were treated with an acidification step whereby carbonates were removed, all dry weights were carbonate-free. Epiphyte weight data were normalized to above-ground seagrass biomass to facilitate comparisons among species.

A minimum of 6 shoots per seagrass species present from each transect at each station was processed. The number of shoots processed was a function of species composition at the random coordinates and the number of whole, undamaged plants following collection, transport, and freezing. If there were several shoots collected within a single bag, leaf blades could not always be assigned to a single shoot with certainty and those samples were not processed. On average, more than 16 shoots were processed from each transect.

In this report, data are presented as means \pm standard errors (SE). When $n < 3$ for a species, data were not plotted; statistical analyses used the entire data set. Statistical analyses were performed with SAS statistical software (SAS Institute 1988). Statistical significance among means was tested with analysis of variance (ANOVA).

Photosynthetically Active Radiation, Water Quality, and Submerged Aquatic Vegetation in IRL

When ANOVA indicated the existence of significant differences, the Tukey-Kramer test (T-K) determined which means were significantly different. Prior to ANOVA, data were logarithmically transformed (Sokal and Rohlf 1981) to obtain normally distributed data. Pearson correlations were calculated to identify relationships between epiphyte and shoot dry weight, between chlorophyll/shoot and shoot dry weight, and between epiphytic chlorophyll /shoot and epiphyte dry weight. The minimal level of significance for any analysis was $P \leq 0.05$.

5.4 Results

5.4.1 Overview

The epiphyte load of 769 shoots was determined. *Halodule wrightii* was the most frequently sampled seagrass (517 samples = 67.2 % of the total), followed by *Syringodium filiforme* (157 samples = 20.4%), *Thalassia testudinum* (80 samples = 10.4%), and *Halophila engelmannii* (15 samples = 2.0%). *H. wrightii* was encountered on every sampling date at all locations, whereas the distribution of other species was more localized. Four epiphyte parameters were calculated from the raw data and analyzed: epiphytic chlorophyll/shoot (Fig. 5.1), epiphytic chlorophyll/g dry weight epiphyte (Fig. 5.2), epiphytic chlorophyll/g shoot dry weight (Fig. 5.3), and the ratio of epiphyte:seagrass dry weight (Fig. 5.4).

For all seagrass species combined, epiphytic chlorophyll averaged >50 mg chl *a*/seagrass shoot (Figure 5.5, top). Epiphytic chlorophyll averaged >0.3 g chl *a*/g epiphyte dry weight (Figure 5.5, bottom) and >1.3 g chl *a*/g shoot dry weight (Figure 5.6, top). Mean epiphyte:shoot dry weight ratios were >9 (Figure 5.6, bottom). Correlation analyses (Table 5.1) indicated significant relationships between epiphyte and shoot dry weight, between chlorophyll/shoot and shoot dry weight, and between epiphytic chlorophyll/shoot and epiphyte dry weight ($P = 0.0001$).

5.4.2 Seagrass Species-Specific Patterns in Epiphyte Parameters

Both epiphytic chlorophyll/shoot (Fig. 5.5, top) and epiphytic chlorophyll/epiphyte dry weight (Figure 5.5, bottom) were much higher for *T. testudinum* than the other seagrass species. When epiphytic chlorophyll was normalized to shoot dry weight (Fig. 5.6, top), *T. testudinum* had the highest epiphytic chlorophyll (2.3 g chl *a*/g shoot dry weight), followed by *H. wrightii* (1.3 g chl *a*/g shoot dry weight), *S. filiforme* (1.2 g chl *a*/g shoot dry weight), and *H. engelmannii* (0.5 g chl *a*/g shoot dry weight). The epiphyte:shoot dry weight ratio for *H. wrightii* (10.8) was the highest of the 4 seagrass species, followed in order by *H. engelmannii*, *S. filiforme*, and *T. testudinum* (Fig. 5.6, bottom).

Correlations between epiphyte and shoot dry weight were significant for all species except *H. engelmannii* (Table 5.2). Positive correlations between epiphytic dry weight and epiphytic chlorophyll/shoot, as well as the relationship between epiphytic chlorophyll/shoot and shoot dry weight, were significant for *H. wrightii* and *S. filiforme*, but not for the other species. In subsequent data analyses and figures, epiphytic chlorophyll and epiphytic dry weight were normalized to shoot dry weight to facilitate comparisons among seagrass species.

5.4.3 Differences in Epiphyte Loads among Transects

There were no consistent patterns in epiphyte loads among transects, either on a chlorophyll (Fig. 5.7) or dry weight (Fig. 5.8) basis. For example, epiphytic chlorophyll normalized to shoot dry weight for *H. wrightii* was maximal at the deep-edge transect 3 at BR, but not at any of the other sites (Fig. 5.7).

5.4.4 Seasonality of Epiphytes

Chlorophyll *a* data normalized to shoot dry weight for the 4 sampling events (Fig. 5.9) indicated that epiphytic chlorophyll on *H. wrightii* was highest in August and November, while epiphytic chlorophyll on *T. testudinum* peaked in August. Seasonal patterns of *S. filiforme* epiphytic chlorophyll were not as distinct. Seasonal patterns in epiphyte:shoot dry weight ratios (Fig. 5.10) were less discernible than those for epiphytic chlorophyll.

Because the majority of the samples were from *H. wrightii* (517 of 769 samples), further analysis was conducted on the epiphytic load of this species. ANOVA indicated significant seasonal patterns in epiphytic chlorophyll/g dry weight of *H. wrightii* at all stations and transects (Table 5.3). In most cases, the highest epiphyte load was found in November (T-K: $P < 0.05$).

5.4.5 Differences in Epiphyte Loads among Stations

When epiphytic chlorophyll values were normalized to dry weight of all seagrass shoots (Fig. 5.11, top), values for each station except MB were similar. Epiphyte:shoot dry weight ratios (Fig. 5.11, bottom) were higher at MB, SS, and SN, where *H. wrightii* was dominant, than at BR, VB, and LP, which had mixed seagrass communities.

Epiphytic chlorophyll *a*/shoot dry weight of *H. wrightii* was highest at BR and lowest at MB (Fig. 5.12, top). Epiphytic chlorophyll/shoot dry weight of *S. filiforme* was

higher at LP than at BR. Epiphytic chlorophyll/shoot dry weight of *T. testudinum* was higher at VB than at LP. Epiphyte:shoot dry weight ratios did not significantly vary among stations for *H. wrightii*, *S. filiforme*, or *T. testudinum* (Fig. 5.12, bottom).

Multivariate analysis of variance tested for differences in epiphytic biomass as a function of month and station. Because the majority of the samples were from *H. wrightii* and the only transect common to all stations was the mid-bed Transect 2, the data set was reduced prior to analyses ($n = 204$ samples of *H. wrightii*). Analyses were run with epiphytic chlorophyll/g shoot dry weight as the dependent variable and month and station as independent variables. The results of this analysis indicated that month explained significant variance in the dependent variable ($P = 0.0001$). Highest epiphyte load was in November, followed by August, and lastly by February and April (T-K: $P < 0.05$). Thus, epiphyte seasonality within stations was a more significant factor than differences among stations.

5.5 Discussion

Methodologies to separate epiphytes from seagrasses in previous studies have included several mechanical and chemical treatment procedures. As pointed out by several researchers (reviewed in Gough and Woelkerling 1976, Meulemans 1988), no single technique to remove epiphytes is appropriate for all subsequent analyses. The technique in this work differs from those in other studies, including a previous study of IRL epiphytes (Harden 1994). Most investigators (e.g., Moncreiff et al. 1992, Harden 1994) did not remove carbonates from samples prior to determining dry weights, as was done in the current study. This study also involved the microscopic examination of seagrass shoots and subsequent removal of sand and detritus; no removal information was provided in other studies.

Although this study sampled more intensively than most studies, given the large potential variability within the epiphyte community, some differences among seasons, transects, and/or stations might not have been detected. The sample size was much greater than the 6 shoots/site contractually required and as recommended by Harden (1994). Even with 250% oversampling (15 samples per transect), sampling may not have adequately characterized epiphyte abundance.

There are few previous data on epiphyte loads in IRL. Harden (1994) reported epiphyte:seagrass dry weight ratios around 2 for his study of IRL seagrass epiphytes, lower than the current study where these ratios were greater than 9. A recent study by Miller (1997) focused on the epiphyte loads of *H. wrightii* along 12 transects in IRL, from May to September 1996. As with most studies on seagrass epiphytes, Miller (1997) did not find a consistent spatial pattern in epiphyte loads (i.e., geographical orientation of stations, mid-bed vs. deep edge). In general, she found highest epiphyte

levels in the northern and middle sections of IRL, but not all stations in those sections had high levels. She also generally found lower epiphyte loads on *H. wrightii* at deep-edge locations. Miller (1997) found little temporal differences at her stations over her 5-month study, that was limited to the wet, summer season. Significant seasonality was found in the current study, with higher levels found during summer and fall than during the rest of the year.

Miller (1997) reported epiphyte loads in terms of g ash-free dry weight/g shoot dry weight. Using an estimated ash-free composition of 28%, a value she used for comparisons with other data, her range of epiphyte loads, reported as 0.35 to 1.20 g ash-free dry weight/g shoot dry weight, can be converted to a range of 1.25 to 4.29 g dry weight/g shoot dry weight. This range is considerably below the year-round mean for *H. wrightii* (10.8 g dry weight/g shoot dry weight) found in the current study. Some of this discrepancy is due to heavy epiphyte loads in November 1995. Also, as Miller (1997) reported, interannual differences in epiphyte load can be significant at any one site. Although interannual differences in epiphyte load were beyond the scope of the current project, Miller's observation that interannual variability in epiphytes did not alter relative differences among stations is relevant to an understanding of epiphyte-seagrass relationships in IRL.

The high biodiversity of seagrass in IRL makes comparison with less complex systems difficult. Moncreiff et al. (1992) reported epiphyte:seagrass dry weight ratios around 4 for *H. wrightii* in Mississippi Sound. Epiphytic chlorophyll content has not been routinely determined for seagrass epiphytes. Data on chlorophyll content for epiphytes on submersed freshwater plants (Zimba 1995) were higher than those of seagrasses in IRL, even when normalized to dry weight units. Peaks in epiphyte abundance on *T. testudinum* occurred in August, similar to the summer peak reported by Thorhaug (1974). In that work, as *T. testudinum* ceased growing, epiphytic red algal biomass increased, and it was hypothesized that nutrients were released to the algae from the senescent seagrass. Macauley et al. (1988) reported peak epiphytic biomass (dry weight and chlorophyll) on *T. testudinum* in the northern Gulf of Mexico over a 3-year period during winter to late spring.

Epiphyte loads were primarily a function of the size (biomass) of the host species; epiphyte and host dry weights were positively correlated. This result suggests that epiphyte abundance is controlled by the surface area of each seagrass species available for colonization, and that epiphytes might not decrease seagrass biomass (i.e., if light levels after attenuation by epiphytes are still above the light saturation requirement for the seagrass). The seagrass species-specific relationship with epiphytes was in all cases positive; however, the strength of the relationship differed among seagrass species.

There were no consistent patterns among transects in epiphyte loads, either on a chlorophyll or dry weight basis. The relatively small differences among stations suggests that the epiphyte component within IRL seagrass beds is much more stable than might be expected for these algae which have such rapid turnover times. Although epiphytes are often considered to have a negative impact on seagrass in that they attenuate PAR, there is no obvious relationship between epiphyte load (this chapter) and seagrass abundance (Chapter 4); this relationship will be explored more in a subsequent chapter (Chapter 7).

5.6 Summary

Epiphytic biomass at 6 sites within IRL were quantified concurrently with SAV parameters on a quarterly basis for 1 year. The major results from this study were:

- (1) For all species combined, epiphytic chlorophyll averaged over 50 mg chl *a*/ shoot. Epiphytic chlorophyll exceeded 0.3 g chl *a*/g epiphyte dry weight and exceeded 1.3 g chl *a*/g shoot dry weight. Epiphyte:shoot dry weight ratios were over 9.
- (2) Correlation analyses indicated significant relationships between epiphyte and shoot dry weight, between epiphytic chlorophyll/shoot and shoot dry weight, and between epiphytic chlorophyll/shoot and epiphyte dry weight.
- (3) Epiphytic chlorophyll/shoot was much higher on *T. testudinum* than on the other seagrass species. When epiphytic chlorophyll was normalized to shoot dry weight or to epiphyte dry weight, *T. testudinum* had the highest epiphytic chlorophyll/g shoot dry weight, followed by *H. wrightii*, *S. filiforme*, and *H. engelmannii*. *H. wrightii* had the highest epiphyte:shoot dry weight ratio, followed in order by *H. engelmannii*, *S. filiforme*, and *T. testudinum*.
- (4) There were no consistent patterns in epiphyte loads among transects, either on a chlorophyll or dry weight basis.
- (5) Chlorophyll *a* data normalized to shoot dry weight for the 4 sampling events indicated that epiphytic biomass on *H. wrightii* was highest in August and November, whereas epiphytic biomass on *T. testudinum* peaked in August. Seasonal patterns of epiphytic chlorophyll on *S. filiforme* were not as distinct. Seasonal patterns in epiphyte:shoot dry weight ratios were less discernible than those for epiphytic chlorophyll.
- (6) When epiphytic chlorophyll values were normalized to dry weight of all seagrass shoots, values for each station except MB were similar. Epiphyte:shoot dry weight

ratios were higher at MB, SS, and SN, where *H. wrightii* was dominant, than at BR, VB, and LP, which had mixed seagrass communities.

- (7) Epiphytic chlorophyll/shoot dry weight of *H. wrightii* was highest at BR and lowest at MB. Epiphytic chlorophyll/shoot dry weight of *S. filiforme* was higher at LP than at BR. Epiphytic chlorophyll/shoot dry weight of *T. testudinum* was higher at VB than at LP. Epiphyte:shoot dry weight ratios did not significantly vary among stations for *H. wrightii*, *S. filiforme*, or *T. testudinum*.
- (8) Multivariate analysis of variance tested for differences in epiphytic biomass as a function of month and station. The results of this analysis indicated that month explained significant variance in the dependent variable. Highest epiphyte load was in November, followed by August, and lastly by February and April (T-K: $P = 0.0001$). Thus, epiphyte seasonality within stations was a more significant factor than differences among stations.

Table 5.1 Correlation matrix of shoot dry weight (g), epiphyte dry weight (g), and epiphytic chlorophyll/shoot (mg chl *a*/seagrass shoot). Matrix results are for all data (n = 769). Values for each combination are Pearson correlation coefficients followed by level of significance.

Variable	Epiphyte Dry Weight	Epiphytic Chlorophyll/Shoot
Shoot Dry Weight	0.503 (0.0001)	0.310 (0.0001)
Epiphyte Dry Weight		0.166 (0.0001)

Table 5.2 Correlation matrix of shoot dry weight (g), epiphyte dry weight (g), and epiphytic chlorophyll/shoot (mg chl *a*/seagrass shoot), for each seagrass species. Matrix results are for all data (n = 769). Values for each combination are Pearson correlation coefficients followed by level of significance.

Species	n	Variable	Epiphyte Dry Weight	Epiphytic Chlorophyll/Shoot
<i>H. wrightii</i>	517	Shoot Dry Weight	0.214 (0.0001)	0.103 (0.0192)
		Epiphyte Dry Weight		0.252 (0.0001)
<i>S. filiforme</i>	157	Shoot Dry Weight	0.400 (0.0001)	0.311 (0.0001)
		Epiphyte Dry Weight		0.405 (0.0001)
<i>T. testudinum</i>	80	Shoot Dry Weight	0.491 (0.0001)	-0.006 (0.95)
		Epiphyte Dry Weight		-0.099 (0.38)
<i>H. engelmannii</i>	15	Shoot Dry Weight	0.027 (0.92)	0.134 (0.63)
		Epiphyte Dry Weight		-0.579 (0.38)

Table 5.3 *Halodule wrightii*. Groupings of months sampled resulting from Tukey range test following ANOVA for epiphytic chlorophyll/shoot dry weight (g chl *a*/g shoot dry weight). Significant differences were tested at P = 0.05. Months are listed from highest to lowest means. Months having common underlines are not significantly different.

Station	Transect	Months			
BR	1	<u>Aug</u>	<u>Nov</u>	<u>Apr</u>	<u>Feb</u>
	2	<u>Nov</u>	<u>Aug</u>	<u>Feb</u>	<u>Apr</u>
	3	<u>Feb</u>	<u>Apr</u>		
MB	2	<u>Nov</u>	<u>Aug</u>	<u>Feb</u>	<u>Apr</u>
SN	1	<u>Nov</u>	<u>Aug</u>	<u>Feb</u>	<u>Apr</u>
	2	<u>Nov</u>	<u>Aug</u>	<u>Feb</u>	<u>Aug</u>
	3	<u>Nov</u>	<u>Aug</u>	<u>Apr</u>	<u>Feb</u>
SS	1	<u>Nov</u>	<u>Apr</u>	<u>Feb</u>	<u>Aug</u>
	2	<u>Nov</u>	<u>Apr</u>	<u>Feb</u>	<u>Aug</u>
	3	<u>Nov</u>	<u>Feb</u>	<u>Aug</u>	<u>Apr</u>
VB	1	<u>Nov</u>	<u>Aug</u>	<u>Feb</u>	<u>Apr</u>
	2	<u>Nov</u>	<u>Aug</u>	<u>Feb</u>	<u>Aug</u>
	3	<u>Nov</u>	<u>Feb</u>	<u>Aug</u>	<u>Apr</u>
LP	1	<u>Aug</u>	<u>Nov</u>	<u>Apr</u>	<u>Feb</u>
	2	<u>Apr</u>	<u>Aug</u>		
	3	<u>Aug</u>	<u>Nov</u>	<u>Apr</u>	<u>Feb</u>

All Seagrass Species

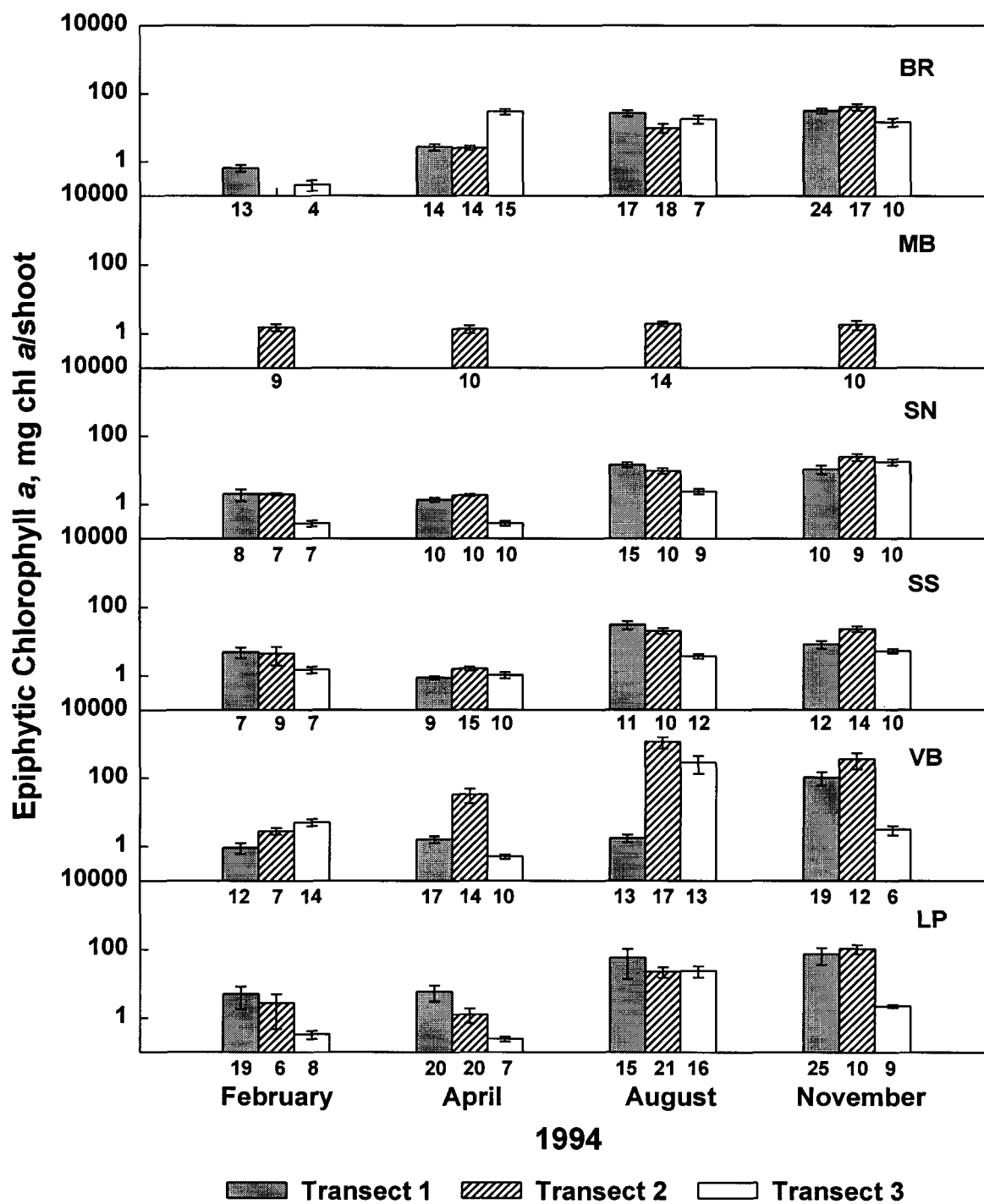


Fig. 5.1 Epiphytic chlorophyll a on a per seagrass shoot basis (log scale) by station, transect, and season for all seagrass species combined. Data are means (\pm SE) for all station-transect-season combinations, with the number of replicates below the horizontal axes for each combination.

All Seagrass Species

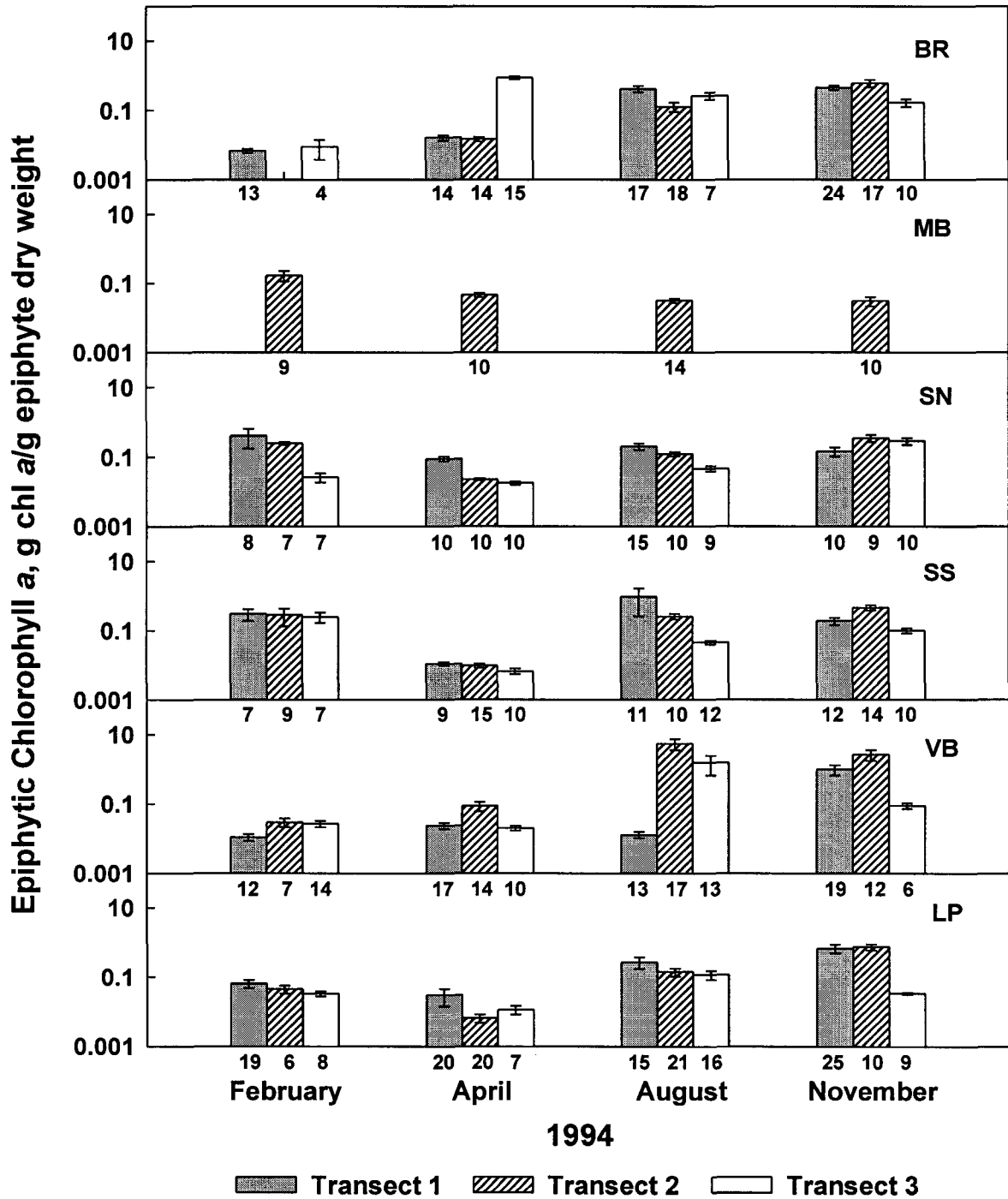


Fig. 5.2 Epiphytic chlorophyll a normalized to epiphyte dry weight (log scale) by station, transect, and season for all seagrass species combined. Data are means (\pm SE) for all station-transect-season combinations, with the number of replicates below the horizontal axes for each combination.

All Seagrass Species

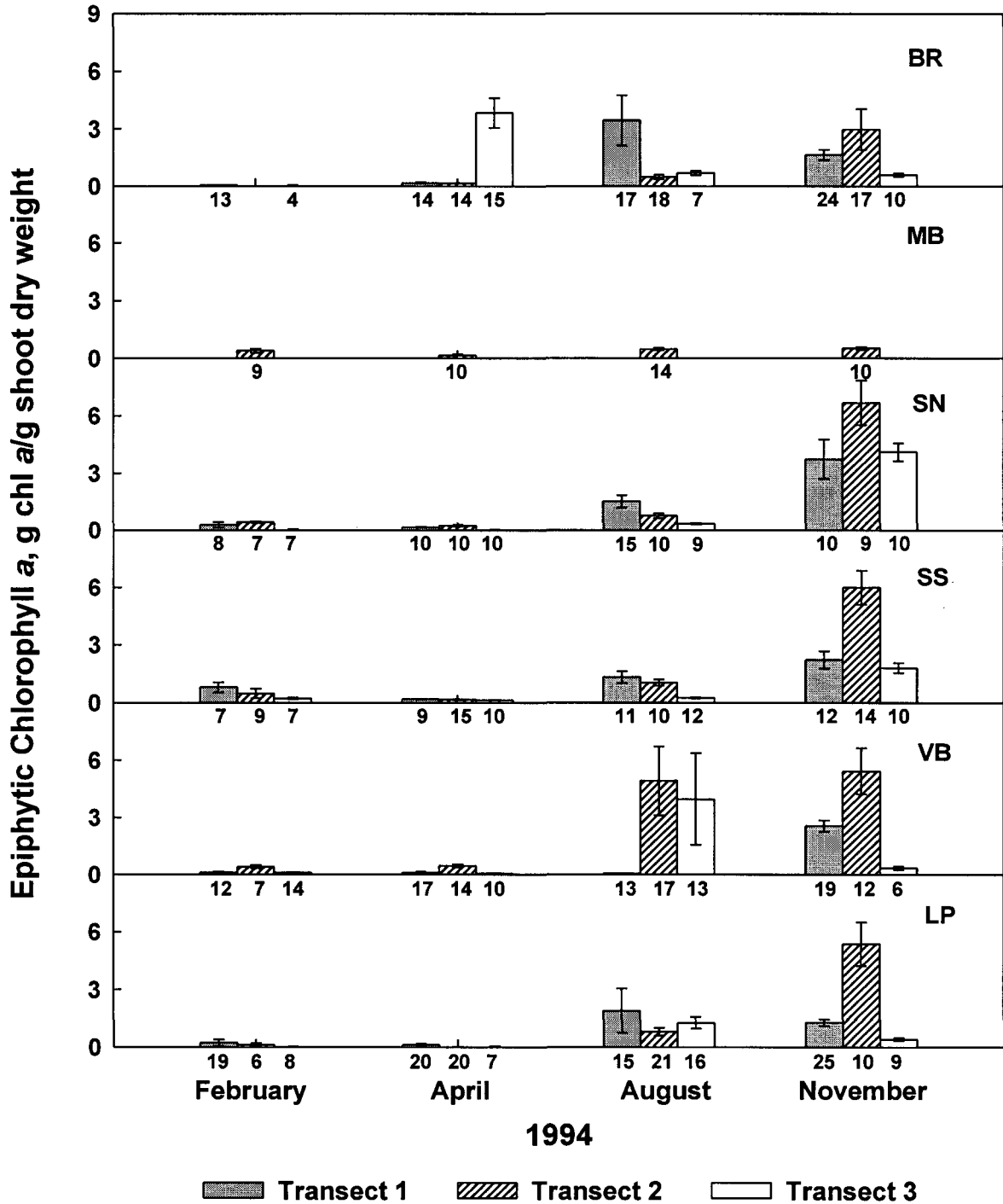


Fig. 5.3 Epiphytic chlorophyll *a* normalized to seagrass shoot dry weight by station, transect, and season for all seagrass species combined. Data are means (\pm SE) for all station-transect-season combinations, with the number of replicates below the horizontal axes for each combination.

All Seagrass Species

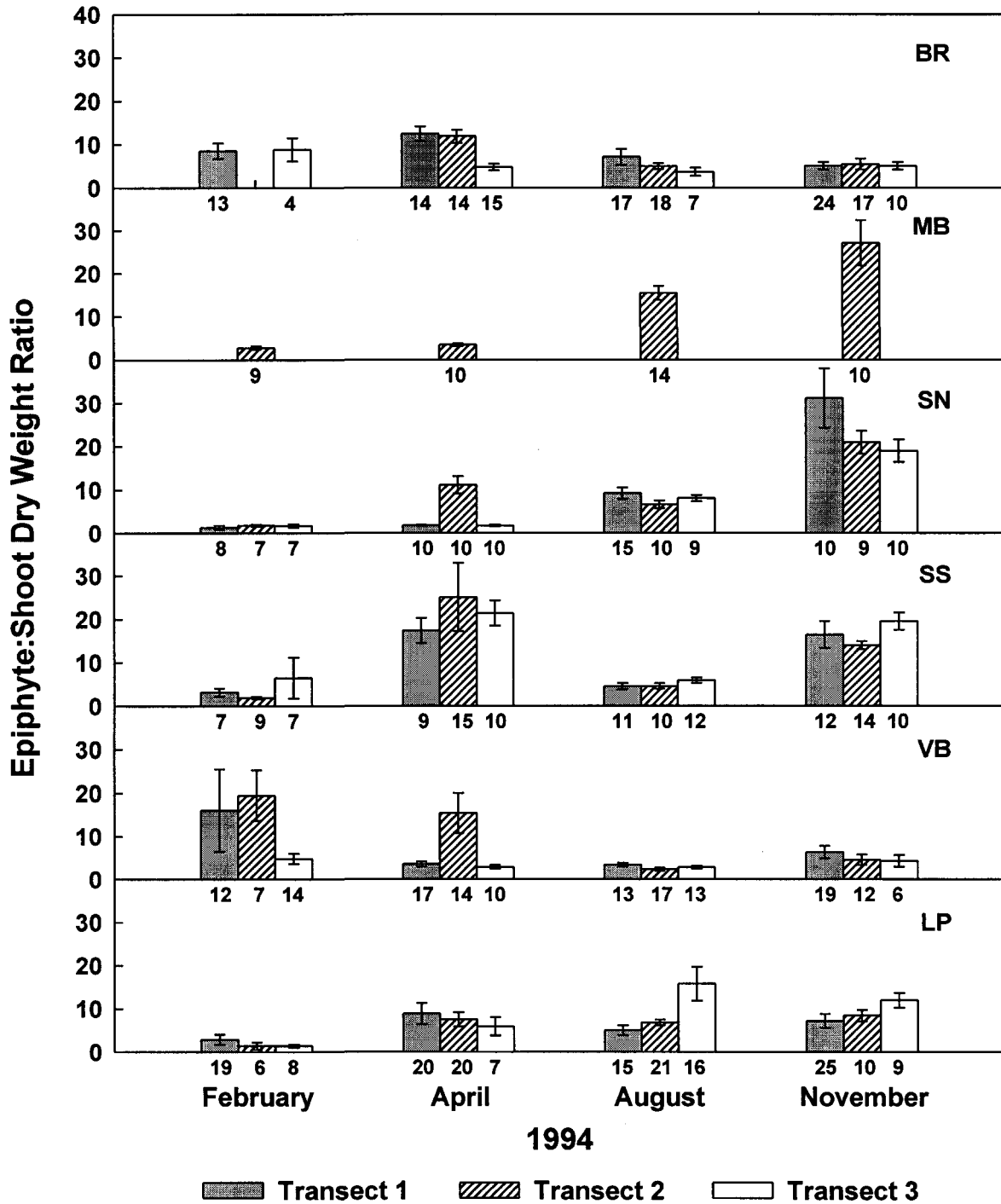


Fig. 5.4 Epiphyte:seagrass shoot dry weight ratio by station, transect, and season for all seagrass species combined. Data are means (\pm SE) for all station-transect-season combinations, with the number of replicates below the horizontal axes for each combination.

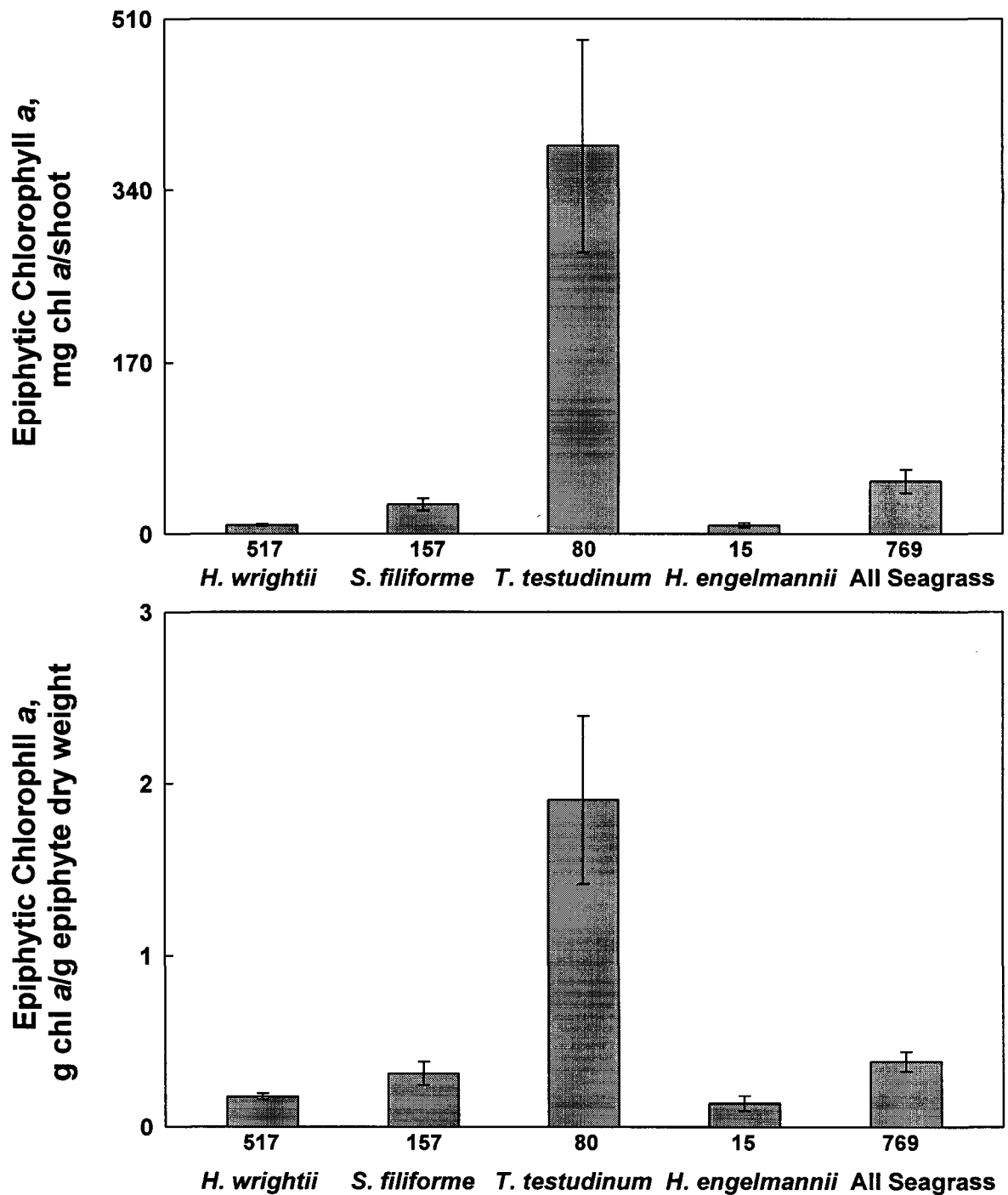


Fig. 5.5 Top: Epiphytic chlorophyll a on a per seagrass shoot basis. Bottom: Epiphytic chlorophyll a normalized to epiphyte dry weight. Data are means (\pm SE) by seagrass species, and for all species combined, for the entire study, with the number of replicates below the horizontal axes for each combination.

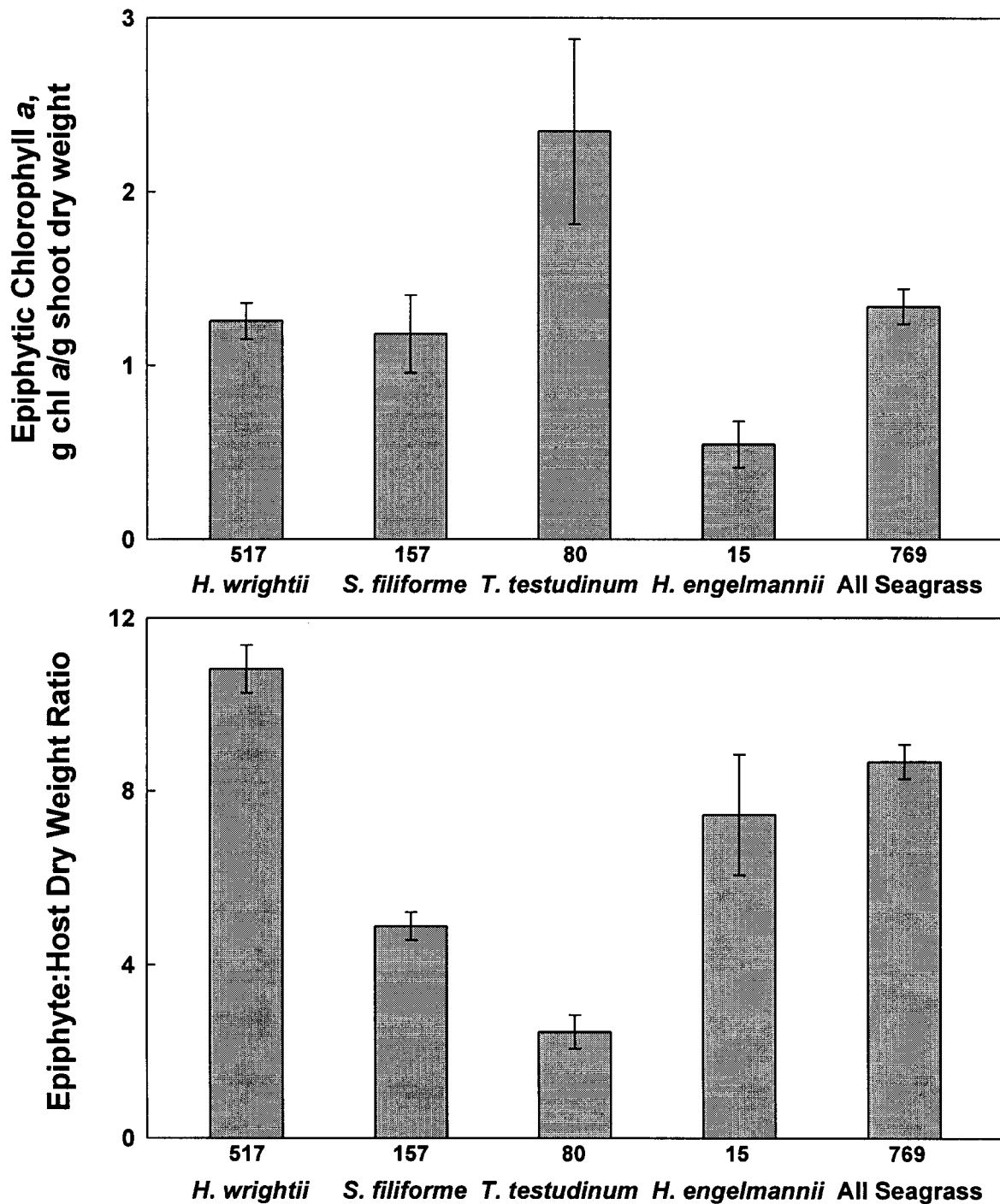


Fig. 5.6 Top: Epiphytic chlorophyll a normalized to seagrass shoot dry weight. Bottom: Epiphyte:seagrass shoot dry weight ratio. Data are means (\pm SE) by species, and for all species combined, for the entire study, with the number of replicates below the horizontal axes for each combination.

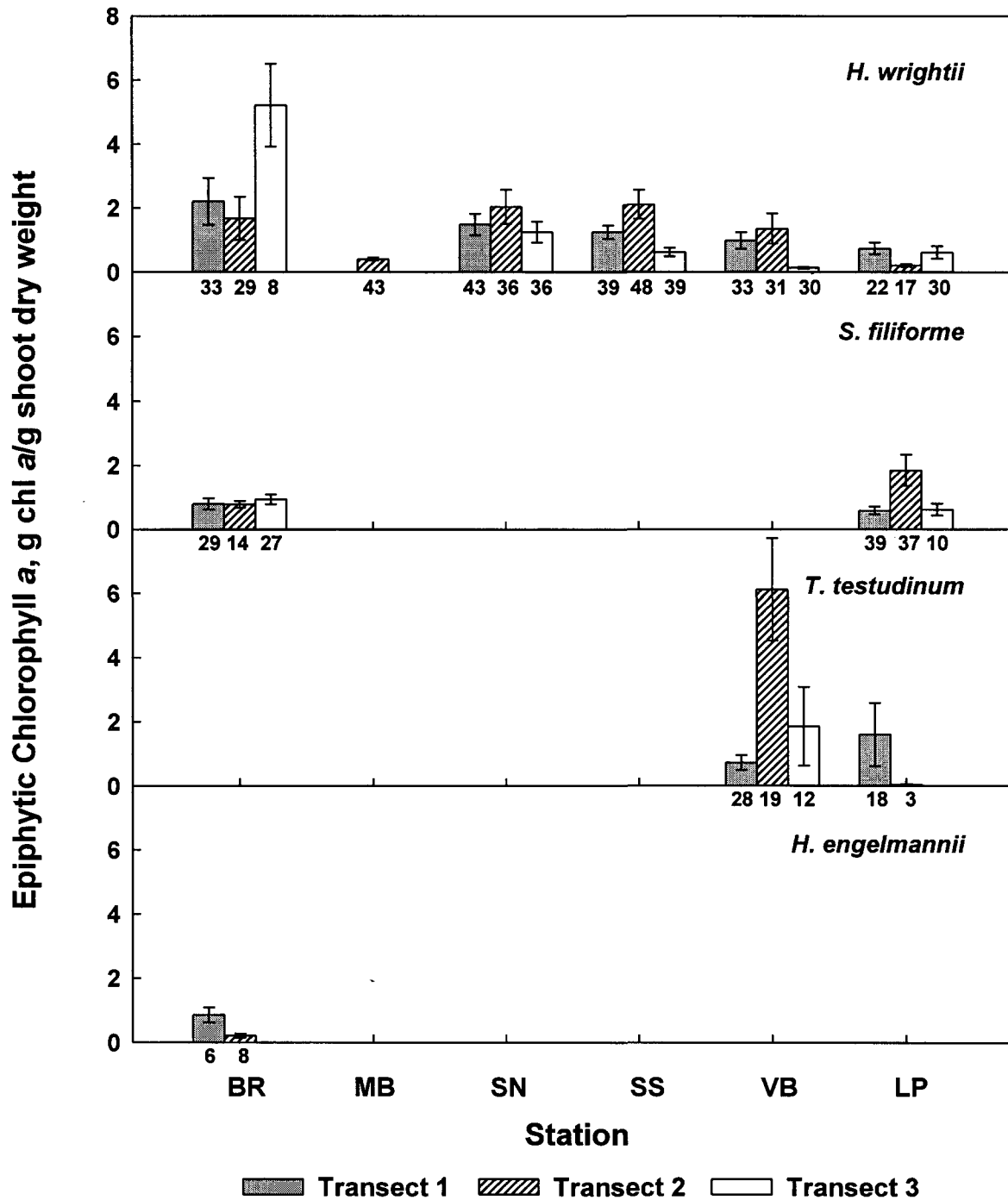


Fig. 5.7 Epiphytic chlorophyll *a* normalized to seagrass shoot dry weight by species, station, and transect. Data are means (\pm SE) by species for all species-station-transect combinations, with the number of replicates below the horizontal axes for each combination.

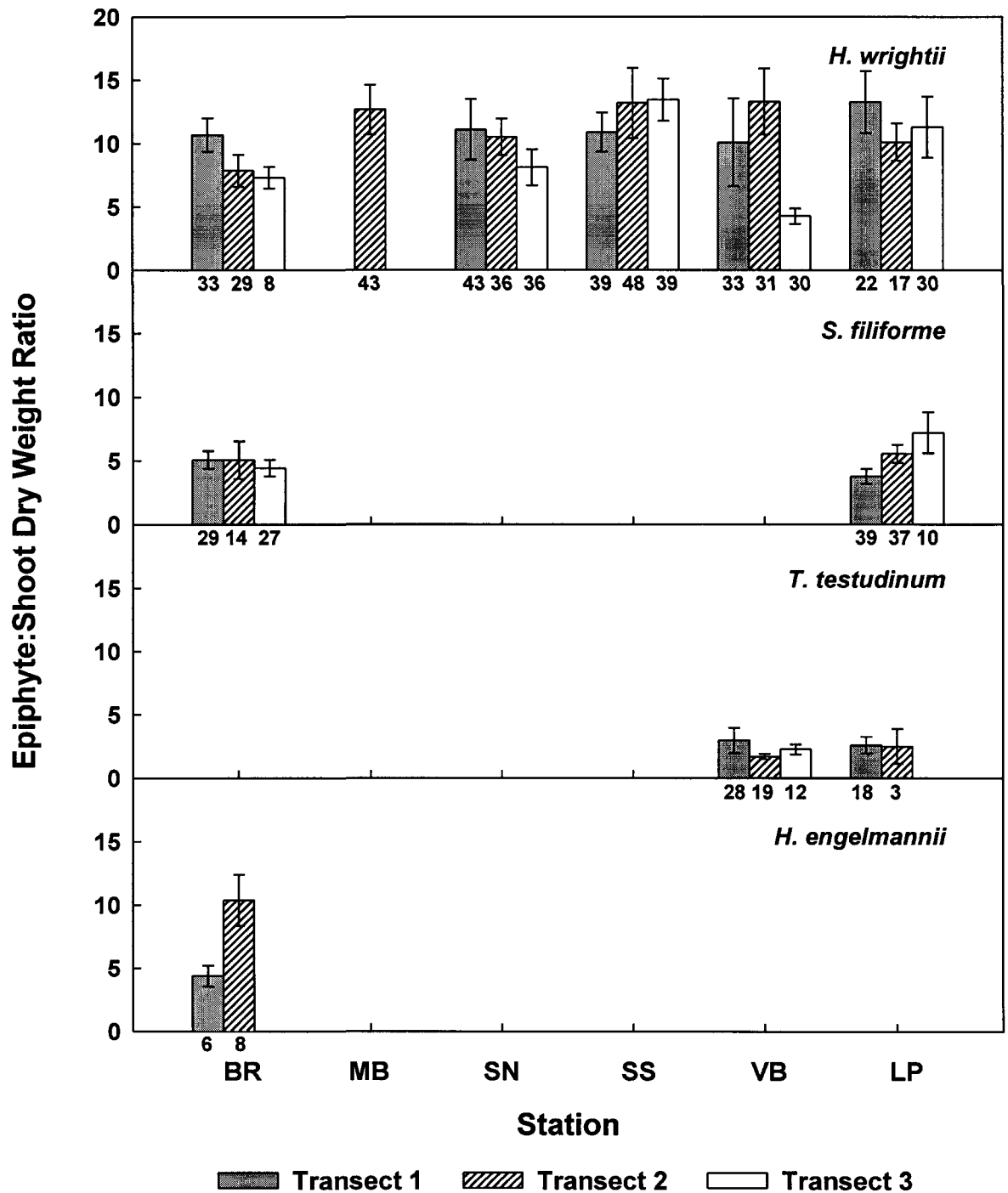


Fig. 5.8 Epiphyte:shoot dry weight ratios by species, station, and transect. Data are means (\pm SE) by species for all species-station-transect combinations, with the number of replicates below the horizontal axes for each combination.

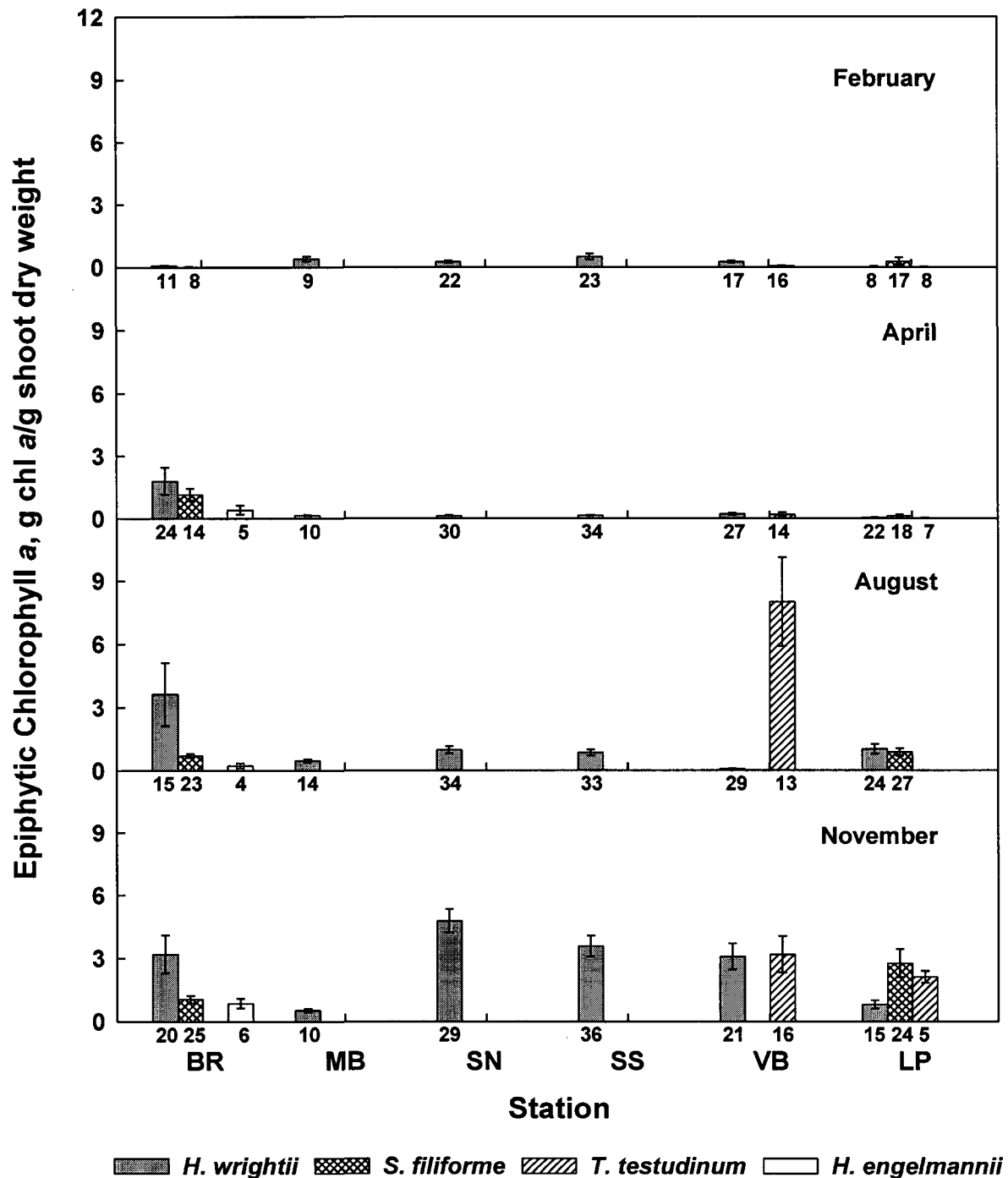


Fig. 5.9 Epiphytic chlorophyll a normalized to seagrass shoot dry weight by species, station, and season. Data are means (\pm SE) by species for all species-station-season combinations, with the number of replicates below the horizontal axes for each combination.

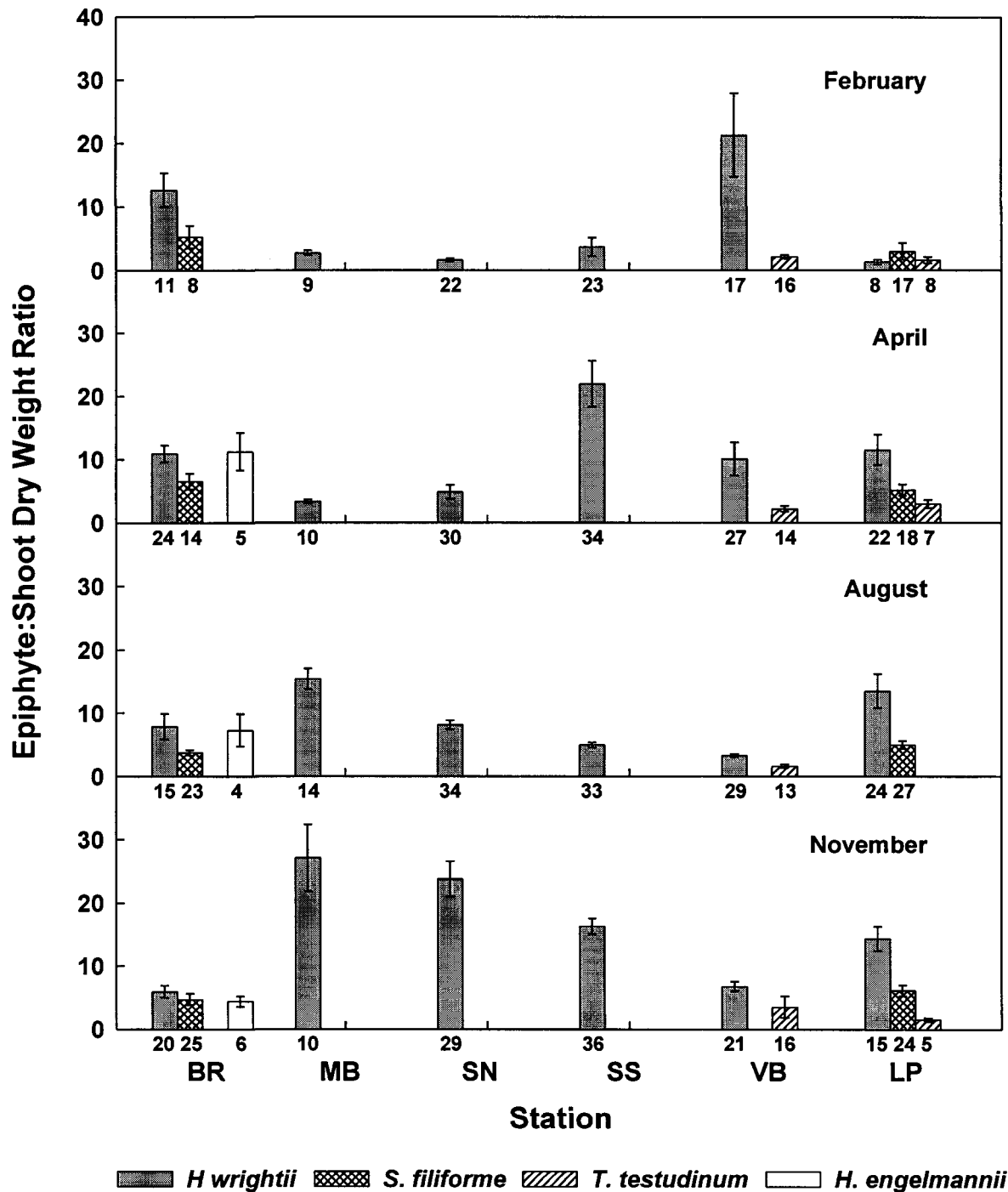


Fig. 5.10 Epiphyte:shoot dry weight ratios by species, station, and season. Data are means (\pm SE) by species for all species-station-season combinations, with the number of replicates below the horizontal axes for each combination.

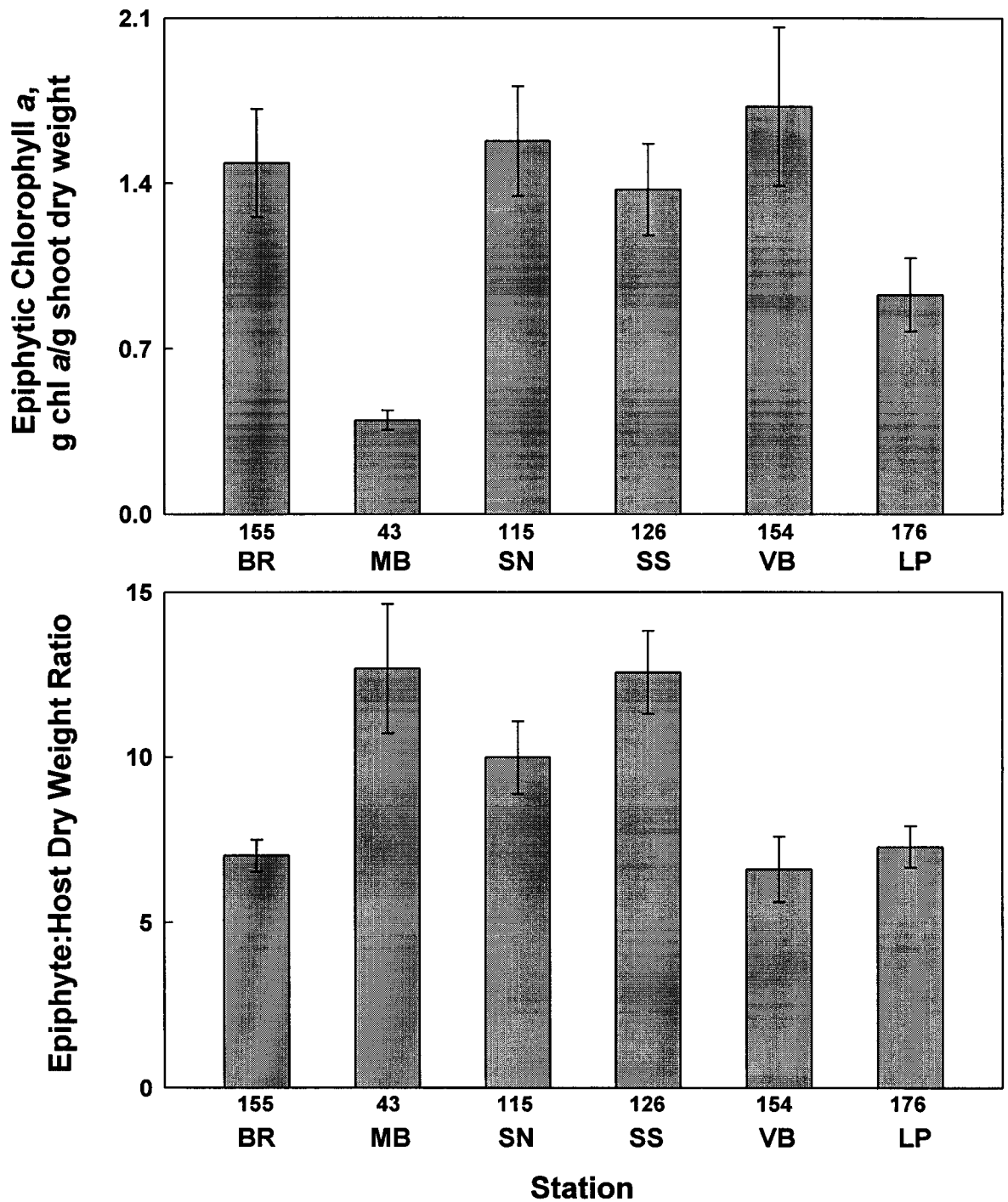


Fig. 5.11 Top: Epiphytic chlorophyll a normalized to seagrass shoot dry weight. Bottom: Epiphyte:seagrass shoot dry weight ratio. Data are means (\pm SE) by station, for all species combined, for the entire study, with the number of replicates below the horizontal axes for each combination.

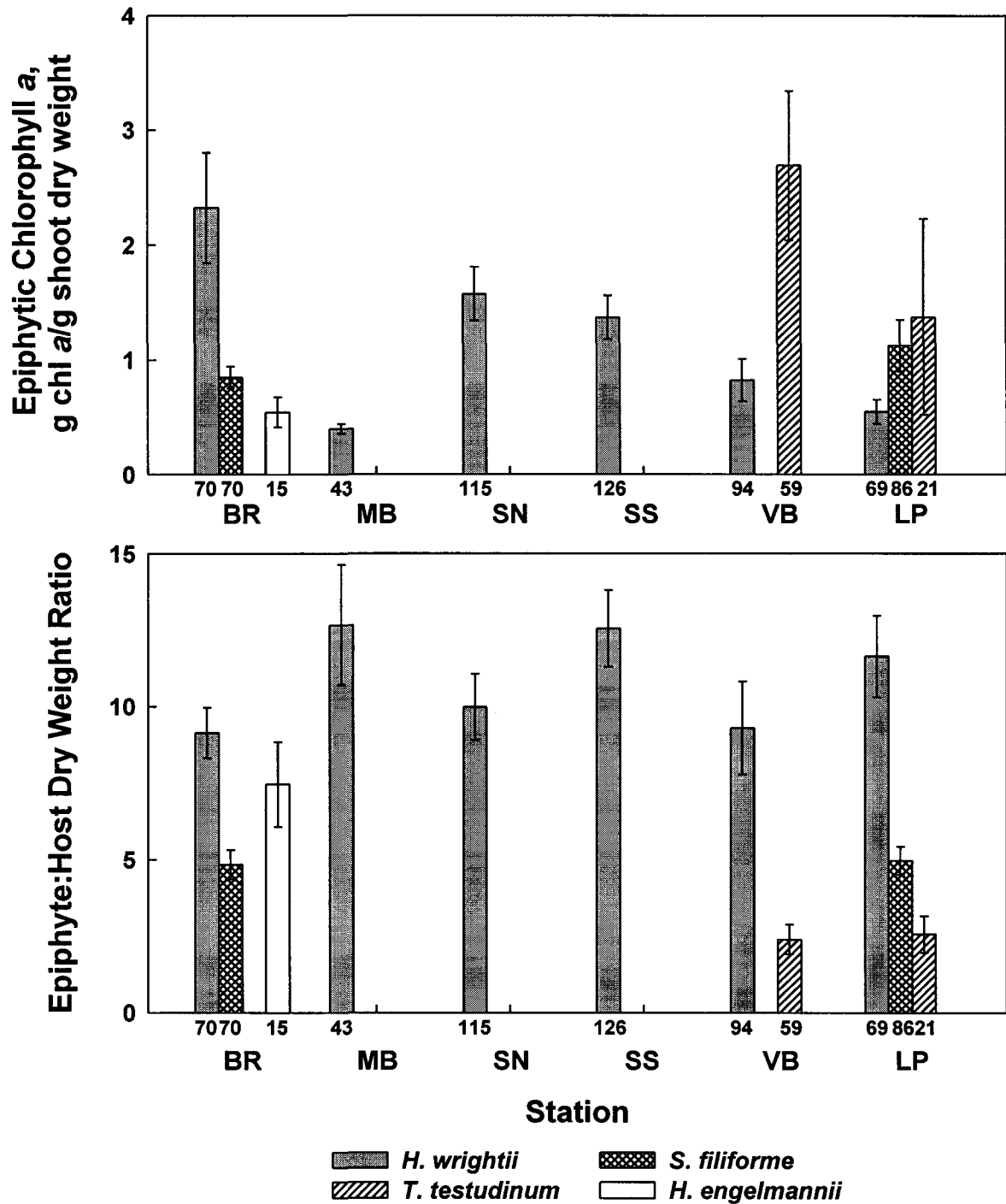


Fig. 5.12 Top: Epiphytic chlorophyll a normalized to seagrass shoot dry weight. Bottom: Epiphyte:seagrass shoot dry weight ratio. Data are means (\pm SE) by station, for each species, with the number of replicates below the horizontal axes for each combination.

Chapter 6: Primary Productivity

6.1 Introduction

Seagrass beds are generally considered to be among the most productive marine systems. There have been few previous studies that have estimated seagrass primary productivity in IRL (Virnstein 1982, Heffernan and Gibson 1983, Rice et al. 1983, Jensen and Gibson 1986).

In this study, primary productivity was considered a parameter that might be useful in an evaluation of SAV status within IRL. The primary productivities of seagrass and epiphytes were measured seasonally at the 6 Year 1 monitoring stations, with the major intent of comparing their productivities among stations. In addition, comparisons of primary productivity on an areal basis were made for seagrass, epiphytes, phytoplankton, and benthic microalgae.

6.2 Task Description

Task 6: To quantify the productivity of seagrass and seagrass epiphytes at selected stations in Indian River Lagoon quarterly for 1 year.

6.3 Methods

Measurements of primary productivity were made at the 6 IRL monitoring stations during the Year 1 quarterly sampling of SAV (see Chapter 4) by Dr. Paul Zimba (University of Florida). In addition to the contractually obligated measurements on seagrasses and epiphytes, the primary productivities of phytoplankton in the water column and benthic microalgae in the sediments were also measured. For each season, at least 5 incubations were made along both the "mid-bed" Transect 2 and the "deep-edge" Transect 3 at each station (with the exception of MB which had only a single, mid-bed transect) for each seagrass species present. Differences in seagrass distribution (see Chapter 4) resulted in different seagrass species being incubated at the stations.

Productivity measurements followed the procedures of Kemp et al. (1986), as modified by Moncreiff et al. (1992). During the first incubation period (February 1994), separate plexiglass incubation chambers were used for the seagrass-epiphyte complex, phytoplankton, and sediments. After a review of the results, all subsequent incubations were made for the 4 productivity components with a single chamber. The chambers (20 cm high) were patterned after the oxygen chambers of Cahoon and

Cooke (1992), who measured the primary productivity in sediments off of North Carolina. Chamber diameters were either 5 or 10 cm depending on seagrass size and canopy height. Each cylindrical chamber had a stirring assembly attached to the top; water movement external to the chamber turned the internal stirrer.

^{14}C -labeled sodium bicarbonate was used as a tracer of carbon assimilation. Incubations lasted 2 h, typically between 1000 and 1400 h. Chambers were placed over seagrass plants and allowed to acclimate for 5 min. Septa-stoppered ports in the chambers were used for tracer injections. 1-mL tuberculin syringes were loaded with stock tracer and injected into each chamber. Chambers were mixed by the stirring apparatus, and a second syringe was used to remove the time-zero activity sample.

All cylinders were processed similarly. Onboard the boat or onshore, 0.5 mL of each activity sample was added to phenethylamine (carbon trapping solution) in scintillation vials. Incubations were terminated by addition of acetic acid:methanol solution. An end-of-incubation phytoplankton sample (5 mL) was removed from each encapsulated core, placed on ice, and transported to the laboratory.

In the laboratory, seawater was removed from each core by siphon, and each productivity component collected. A 2.1-cm diameter syringe core (1-cm deep) was used to sample sediments; these sediment cores were immediately frozen. Seagrass plants were removed from sediments and frozen.

Sediment and phytoplankton samples were digested with a hydrogen peroxide solution (final concentration 10%). Samples were dried, scintillation cocktail was added, and the samples were counted with a Beckman LSC counter. Seagrass samples were processed by removal of epiphytes with MES buffer (0.1 M, pH = 5.5; see Chapter 5). Seagrass and epiphyte samples were also digested with hydrogen peroxide, dried, and counted on a LSC counter.

Carbon uptake by seagrass and epiphytes was individually calculated as mg C g dry weight above-ground seagrass $^{-1}$ h $^{-1}$. Areal productivities of seagrass and epiphytes were calculated by multiplying their respective mean carbon uptakes with mean above-ground seagrass biomass (g dry weight/m 2) for the appropriate station and transect (data from Chapter 4). These areal productivity estimates (g C m $^{-2}$ h $^{-1}$) were compared with the areal productivity of phytoplankton and benthic microalgae.

In this report, data are presented as means \pm standard errors (SE). Statistical analyses were performed with SAS statistical software (SAS Institute 1988). Statistical significance among means was tested with analysis of variance (ANOVA). When ANOVA indicated the existence of significant differences, the Tukey-Kramer test (T-K) determined which means were significantly different. Prior to ANOVA, data were

logarithmically transformed (Sokal and Rohlf 1981) to obtain normally distributed data. The minimal level of significance for any analysis was $P \leq 0.05$.

6.4 Results

The presentation of results begins with overall comparisons of productivity among seagrass species (Section 6.3.1), followed by examination of patterns in productivity among seasons (Section 6.3.2), transects (Section 6.3.3), and stations (Section 6.3.4). Lastly, the primary productivity data are coupled with above-ground seagrass biomass (Chapter 4) to calculate primary productivity on an areal (per m²) basis and to compare the primary productivities of seagrass, epiphytes, phytoplankton, and benthic microalgae at the 6 stations (Section 6.3.5).

6.4.1 Comparison of Productivity among Seagrass Species

A total of 374 seagrass shoots was processed for carbon uptake and attached epiphyte productivity. *Halodule wrightii* was the most frequently sampled seagrass (241 samples = 64.4% of the total), followed by *Syringodium filiforme* (76 samples = 20.3%), *Thalassia testudinum* (44 samples = 11.8%), and *Halophila engelmannii* (13 samples = 3.5%). *H. wrightii* was the only seagrass present at all transects and stations and was nearly evenly sampled at the mid-bed Transect 2 (131 samples) and deep-edge Transect 3 (110 samples).

The primary productivity for all seagrass species combined (grand mean) was 9.48 ± 0.73 mg C g dry weight⁻¹ h⁻¹ (Fig. 6.1). There were no significant differences in productivity among the major species of seagrass (*H. wrightii*, *S. filiforme*, and *T. testudinum*), but the productivity of *H. engelmannii* was significantly lower.

Similarly, epiphyte productivity did not vary significantly among *H. wrightii*, *S. filiforme*, and *T. testudinum*; epiphyte productivity on *H. engelmannii* was significantly lower. Epiphyte primary productivity for all seagrass species combined (grand mean) was 13.42 ± 0.95 mg C g dry weight⁻¹ h⁻¹, a value 41.6% greater than that of the host seagrass. Seagrass epiphyte productivity was greater than each of their respective host seagrass species, ranging from 1.07x for *S. filiforme* to 2.30x for *H. engelmannii*.

6.4.2 Comparison of Productivity among Seasons

For all stations and transects, the highest productivity for seagrass (Figs. 6.2-6.3) and epiphytes (Figs. 6.4-6.5) occurred in April or August. The most notable

features of the ratio of epiphyte:seagrass productivity (Figs. 6.6-6.7) were elevated values in November, particularly at the Sebastian stations.

6.4.3 Comparison of Productivity between Transects

The significance of differences between transects varied throughout the year for both seagrass (Figs. 6.8-6.9) and epiphyte productivities (Figs. 6.10-6.11). When productivities were low (February and November), they did not vary significantly (ANOVA: $P > 0.05$) between the mid-bed Transect 2 and the deep-edge Transect 3. When productivities were high (April and August), they were often significantly higher for the mid-bed Transect 2 than the deep-edge Transect 3, especially for *H. wrightii* (Figs. 6.8, 6.10).

6.4.4 Comparison of Productivity among Stations

Differences in the primary productivities of seagrasses and epiphytes were not seasonally consistent among stations. At the mid-bed Transect 2, when primary productivity was low (February and November), seagrass (Fig. 6.2) and epiphyte productivities (Fig. 6.4) did not significantly vary among stations (ANOVA: $P > 0.05$). In April, seagrass productivity was highest at MB and VB and lowest at BR and SS (Fig. 6.2); epiphyte productivity was highest at VB and lowest at SS (Fig. 6.4). In August, seagrass (Fig. 6.2) and epiphyte productivities (Fig. 6.4) were both higher at BR, MB, and SN than at SS and VB.

At the deep-edge Transect 3, seagrass productivity did not significantly vary (ANOVA: $P > 0.05$) among stations within any season (Fig. 6.3). Epiphyte productivity varied among stations, with epiphyte productivity at SN being lower than the other stations in April, but higher than the other stations in August (Fig. 6.5).

6.4.5 Comparison of the Primary Productivities of Seagrass, Epiphytes, Phytoplankton, and Benthic Microalgae

Overall, the primary productivities of seagrass and epiphytes, on an areal basis, were much greater (15-30 times) than those of phytoplankton and benthic microalgae (Fig. 6.14). Mean areal primary productivity ($\text{g C m}^{-2} \text{h}^{-1}$) for all incubations was 0.76 ± 0.11 for seagrass, 1.01 ± 0.14 for epiphytes, 0.03 ± 0.002 for phytoplankton, and 0.05 ± 0.002 for benthic microalgae. Thus, seagrasses and their epiphytes accounted for 96% of the carbon fixed (41% and 55%, for seagrass and epiphytes, respectively).

Additional analyses of areal primary productivity were conducted for the mid-bed Transect 2. Areal primary productivity was highest at VB and lowest at MB (Fig. 6.15). Seagrass productivity ranged from 36% (MB) to 46% (BR) of the total areal primary productivity. The areal primary productivities of seagrass and epiphytes were higher in April and August than in February and November (Figs. 6.16-6.17).

6.5 Discussion

Dawes et al. (1995) reviewed the previous, limited, measurements of seagrass primary productivity made in IRL, which tend to be higher than those of comparable systems in Florida (i.e., Tampa Bay). Heffernan and Gibson (1983) measured the productivities of the larger species of seagrass, as well as those of epiphytes, benthic microalgae, and phytoplankton, at 3 stations (Jim Island, Link Port, and Vero Beach) in March and July. Relative to the other autotrophic components in the lagoon, these previous studies noted a large amount of spatial and temporal variability in seagrass productivity. Comparable to the seasonality patterns observed in the present study, both seagrass and epiphyte productivity were much higher in July than in March. Estimates of seagrass productivity ranged from 7% (Jensen and Gibson 1986) to 86% (calculated from Heffernan and Gibson 1983) of the carbon fixed at a site. In the present study, the mean percent contribution of seagrasses to total autotrophic productivity (41%) was in the middle of the previously reported range for IRL, with a relatively narrow range (36-46%) among stations.

The lack of pattern in carbon fixation among stations (i.e., no patterns in February and November, no consistent patterns in June and August) suggests that primary productivity, as measured in this study, has limited value as an index of SAV conditions. The observed differences among stations in areal productivity were more influenced by differences in seagrass above-ground biomass (Chapter 4) than in carbon fixation. The lack of pattern in short-term carbon acquisition, particularly in June and August when productivity was high, may be due to one or more reasons. During each quarter, incubations were made during a single week, but incubations were not performed on the same day at all stations, or under the same weather conditions. Photosynthetic measurements were conducted over a brief period (2 hours) that varied among stations in local weather conditions (e.g., cloud cover, cold fronts) which may override longer term environmental conditions (water quality parameters and K) that influence growth over a period of weeks to months. These field measurements also did not consider the complex physiological source-sink interactions that exist within clones of seagrass; photosynthetic performance of individual shoots may relate more to the carbon storage status in the rhizomes than the ambient conditions to which the shoots are exposed.

Other seagrass parameters (percent cover, biomass, or growth rates) are much more likely to be effective biological integrators of environmental conditions in an IRL monitoring program. To be more useful, productivity measurements would have to be performed much more frequently than the quarterly measurements made in this study. If incorporating ^{14}C measurements into a monitoring program is considered in the future, care must be taken to standardize the methodology to effectively make temporal and spatial comparisons within the lagoon.

6.6 Summary

Primary productivity was measured quarterly for 1 year at the 6 monitoring stations to assess carbon incorporation by seagrass and associated epiphytes, with the major intent of comparing their productivities among stations. In addition, comparisons of primary productivity were made on an areal basis for seagrass, epiphytes, phytoplankton, and benthic microalgae. The major results from this study are:

- (1) The primary productivity for all seagrass species combined (grand mean) was 9.48 ± 0.73 mg C g dry weight $^{-1}$ h $^{-1}$. There were no significant differences in productivity among the major species of seagrass (*H. wrightii*, *S. filiforme*, and *T. testudinum*); the productivity of *H. engelmannii* was significantly lower.
- (2) There were no significant differences in the productivity of epiphytes among *H. wrightii*, *S. filiforme*, and *T. testudinum*; the productivity of epiphytes on *H. engelmannii* was significantly lower. Epiphyte primary productivity for all seagrass species combined (grand mean) was 13.42 ± 0.95 mg C g dry weight $^{-1}$ h $^{-1}$, a value 41.6% greater than seagrass productivity. Epiphyte productivity was greater than each of their respective host seagrass species, ranging from 1.07x for *S. filiforme* to 2.30x for *H. engelmannii*.
- (3) For all stations and transects, highest seagrass and epiphyte productivities were in May or August. The ratio of epiphyte:seagrass productivity was elevated in November, particularly at the Sebastian stations.
- (4) The significance of differences between transects varied throughout the year for both seagrass and epiphyte productivities. When productivities were low (February and November), they did not vary between the mid-bed Transect 2 and the deep-edge Transect 3. When productivities were high (April and August), they were often significantly higher for the mid-bed Transect 2 than the deep-edge Transect 3, especially for *H. wrightii*.

- (5) Differences in the primary productivities of seagrasses and epiphytes were not seasonally consistent among stations. At the mid-bed Transect 2, when primary productivities were low (February and November), they did not vary among stations. In April, seagrass productivity was highest at MB and VB and lowest at BR and SS; epiphyte productivity was highest at VB and lowest at SS. In August, seagrass and epiphyte productivities were both higher at BR, MB, and SN than at SS and VB. At the deep-edge Transect 3, seagrass productivity did not significantly vary among stations within any season. Epiphyte productivity varied slightly among stations, with epiphyte productivity at SN being lower than the other stations in April, but higher than the other stations in August.
- (6) Overall, the primary productivities of seagrass and epiphytes, on an areal basis, were much greater (15-30 times) than those of phytoplankton and benthic microalgae. Mean areal productivity ($\text{g C m}^{-2} \text{ h}^{-1}$) for all incubations was 0.76 ± 0.11 for seagrass, 1.01 ± 0.14 for epiphytes, 0.03 ± 0.002 for phytoplankton, and 0.05 ± 0.002 for benthic microalgae. Thus, seagrasses and their epiphytes accounted for 96% of the carbon fixed (41% and 55%, for seagrass and epiphytes, respectively).
- (7) Areal primary productivity was highest at VB and lowest at MB. Seagrass productivity ranged from 36% (MB) to 46% (BR) of the total areal primary productivity at these stations. The areal primary productivities of seagrass and epiphytes were higher in April and August than in February and November.
- (8) The lack of pattern in carbon fixation among stations suggests that primary productivity, as measured in this study, has limited value as an index of SAV conditions. Other seagrass measurements (percent cover, biomass or growth rates) are much more likely to be effective biological integrators of environmental conditions in an IRL monitoring program. To be more useful, measurements of primary productivity would have to be performed much more frequently than the quarterly measurements made in this study. If incorporating ^{14}C measurements into a monitoring program is considered in the future, care must be taken to standardize the methodology to effectively make temporal and spatial comparisons within the lagoon.

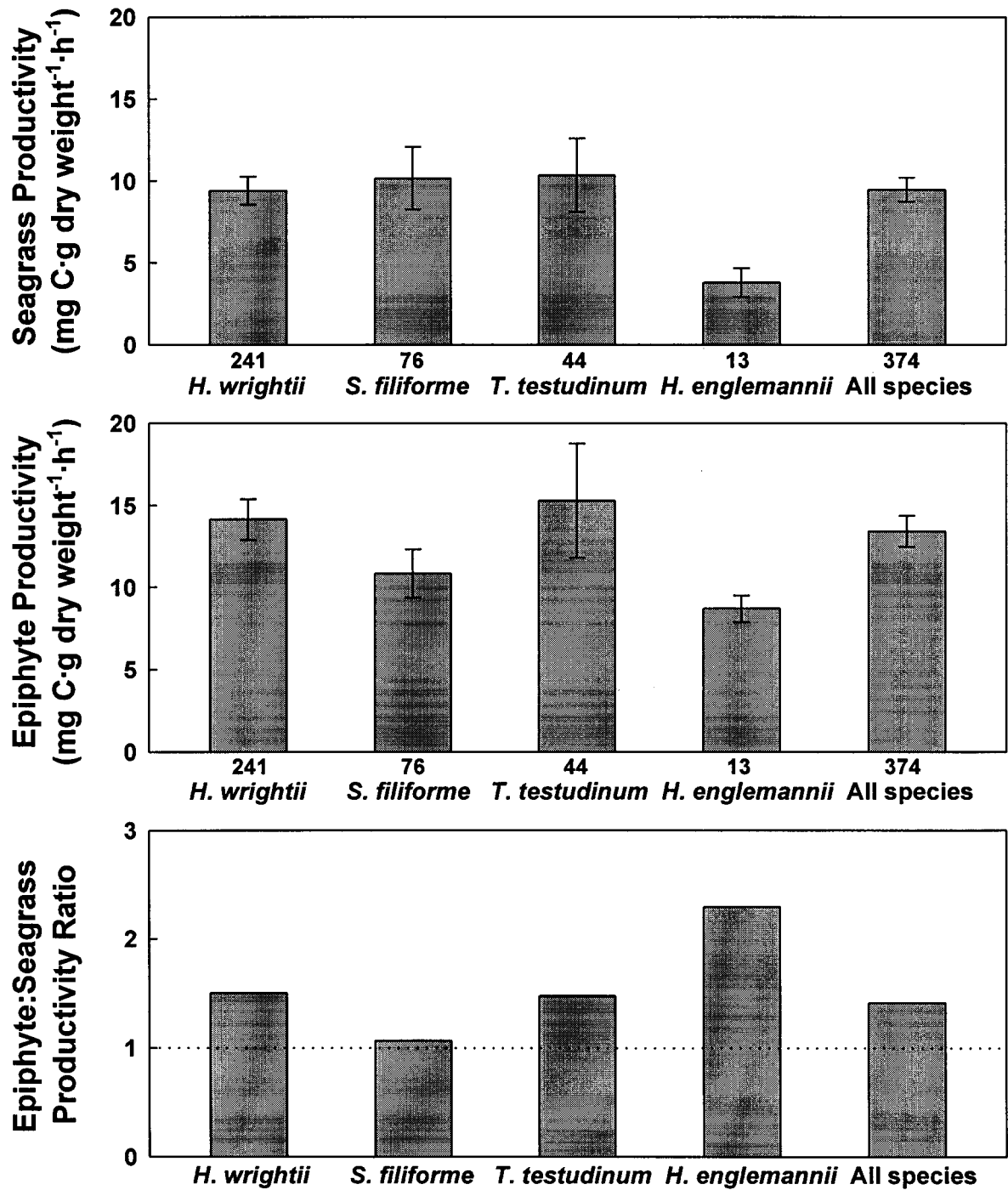


Fig. 6.1 Seagrass and epiphyte productivity and ratio of epiphyte:seagrass productivity. Data are means (\pm SE) by species and for all species combined, for the entire study, with the number of replicates below the horizontal axes for each combination. Dotted line indicates equal productivity of seagrass and epiphytes.

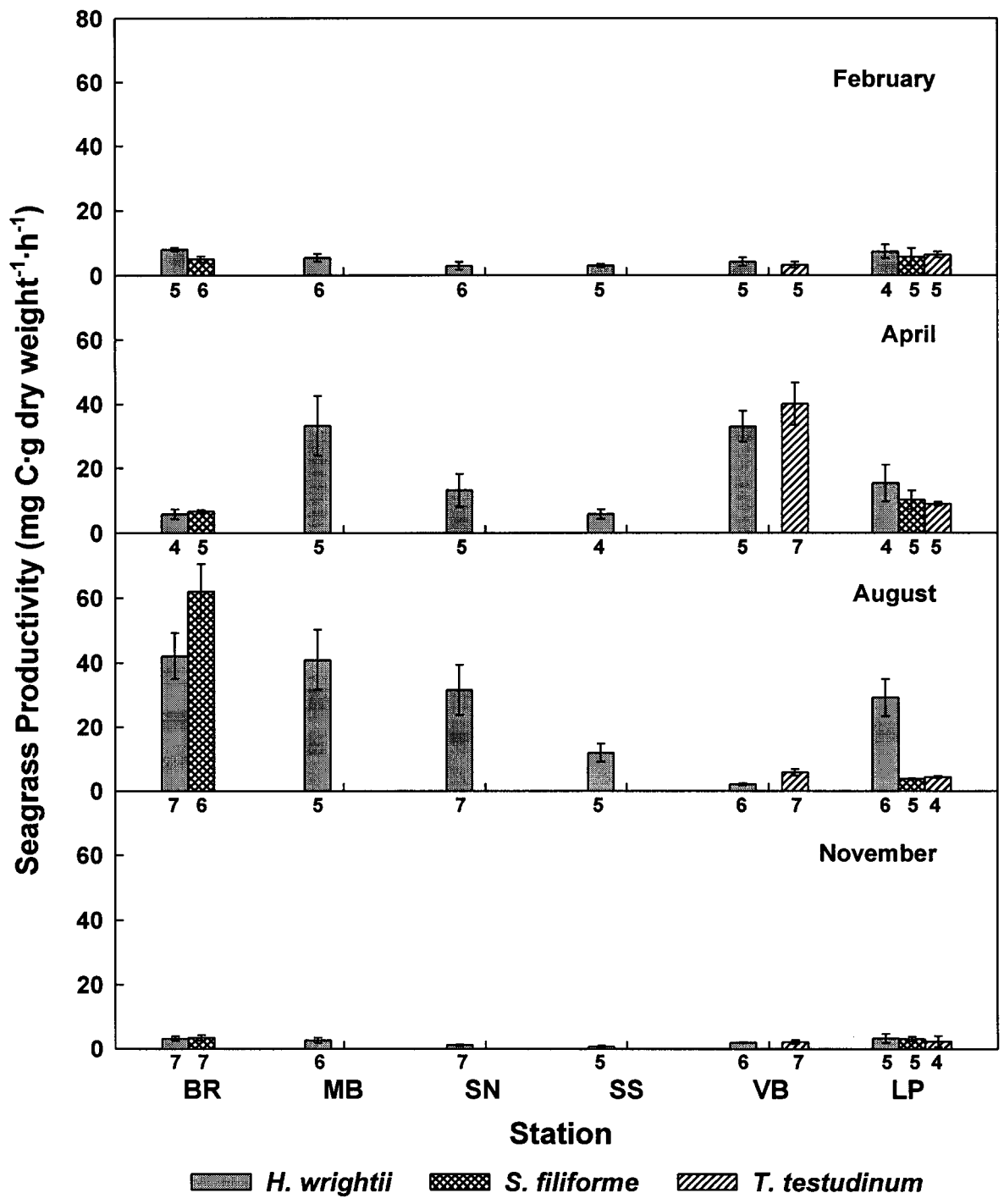


Fig. 6.2 Seagrass productivity, by month, station, and seagrass species, for the “mid-bed” Transect 2. Data are means (\pm SE) for all month-station-species combinations, with the number of replicates below the horizontal axes for each combination.

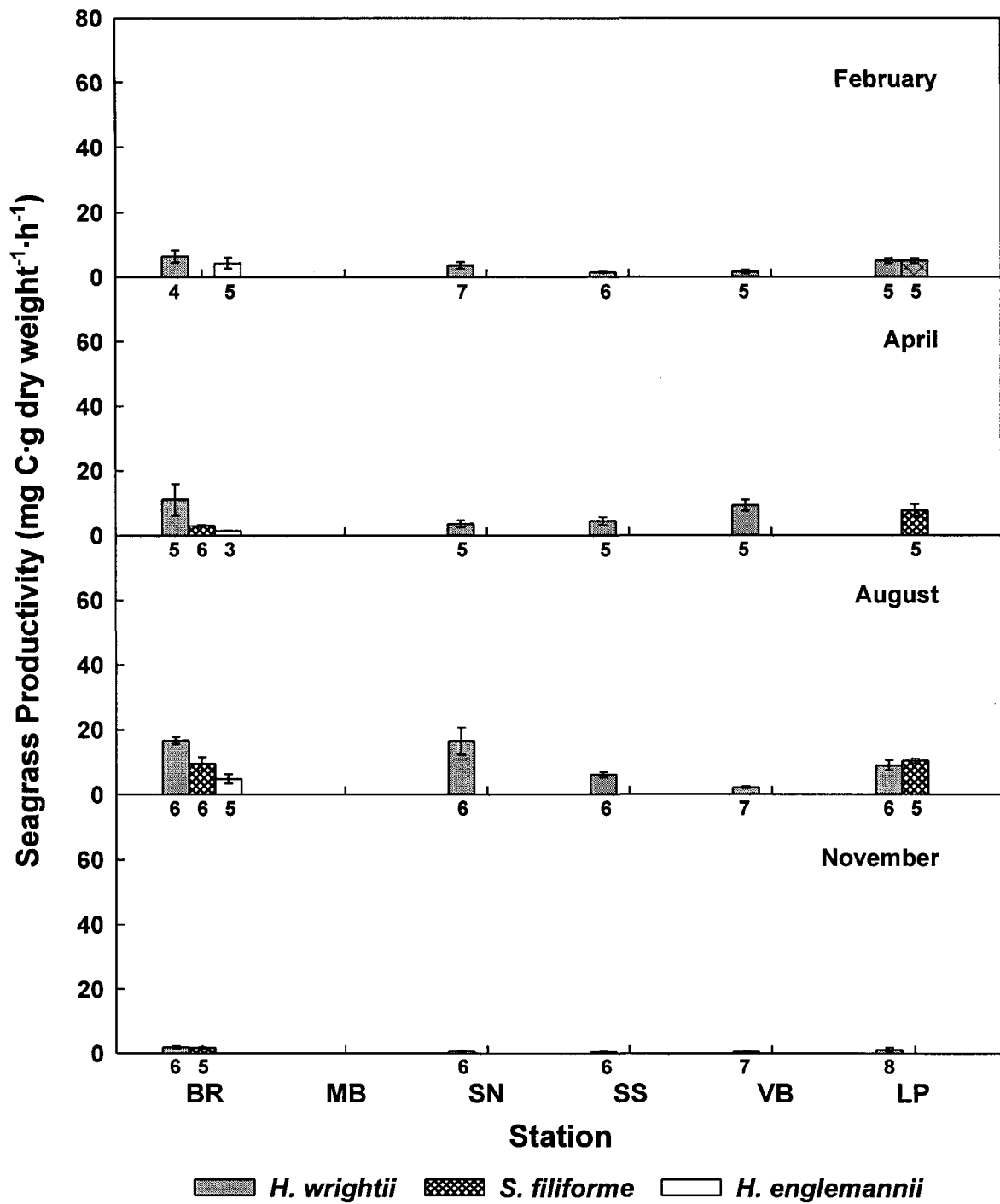


Fig. 6.3 Seagrass productivity, by month, station, and seagrass species, for the “deep-edge” Transect 3. Data are means (\pm SE) for all month-station-species combinations, with the number of replicates below the horizontal axes for each combination.

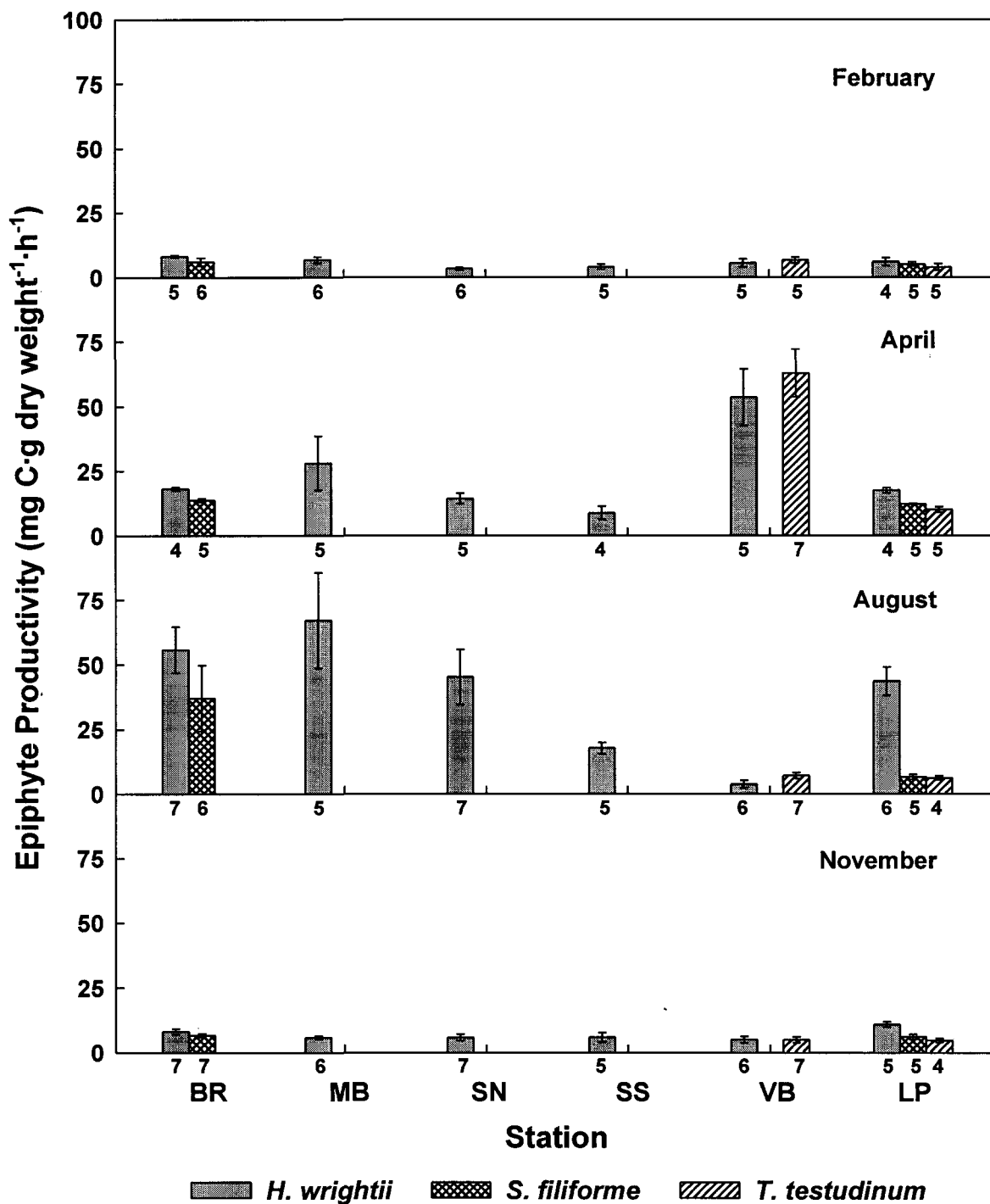


Fig. 6.4 Epiphyte productivity, by month, station, and seagrass species, for the “mid-bed” Transect 2. Data are means (+SE) for all month-station-species combinations, with the number of replicates below the horizontal axes for each combination.

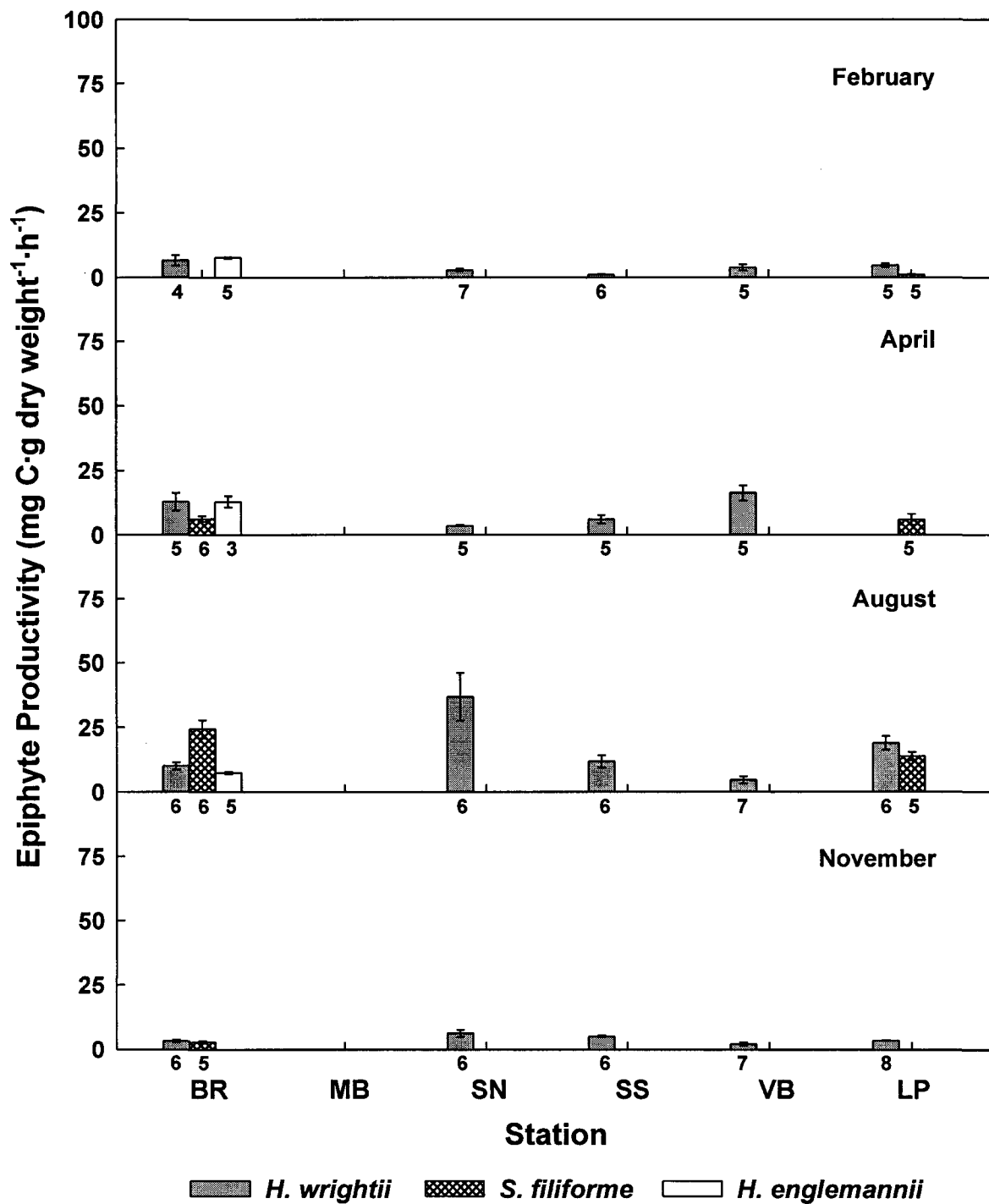


Fig. 6.5 Epiphyte productivity, by month, station, and seagrass species, for the “deep-edge” Transect 3. Data are means (\pm SE) for all month-station-species combinations, with the number of replicates below the horizontal axes for each combination.

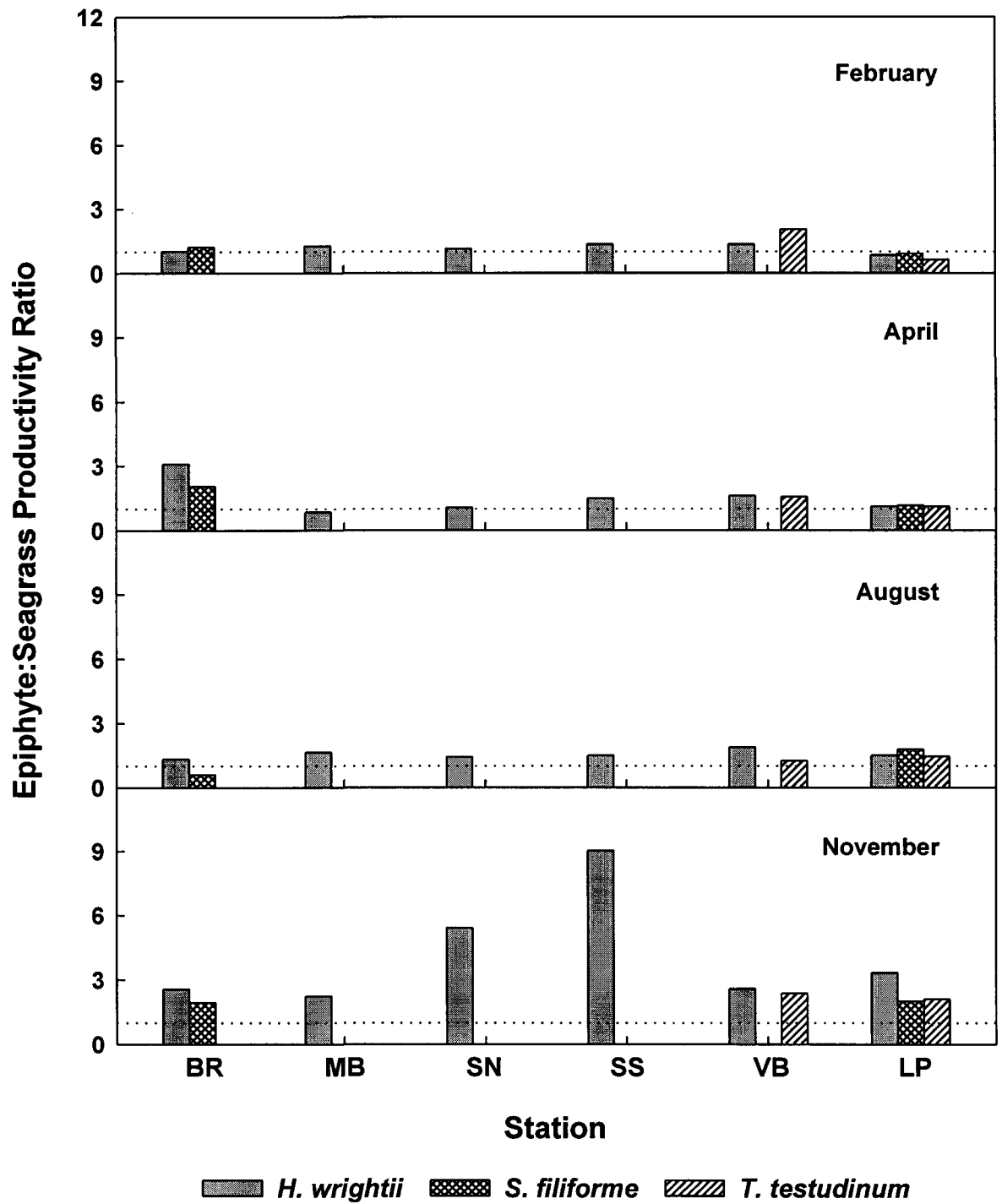


Fig. 6.6 Ratio of epiphyte:seagrass productivity, by month, station, and seagrass species, for the "mid-bed" Transect 2. Data are ratios of means presented in Figs. 6.2 and 6.4. Dotted line indicates equal productivity of seagrass and epiphytes.

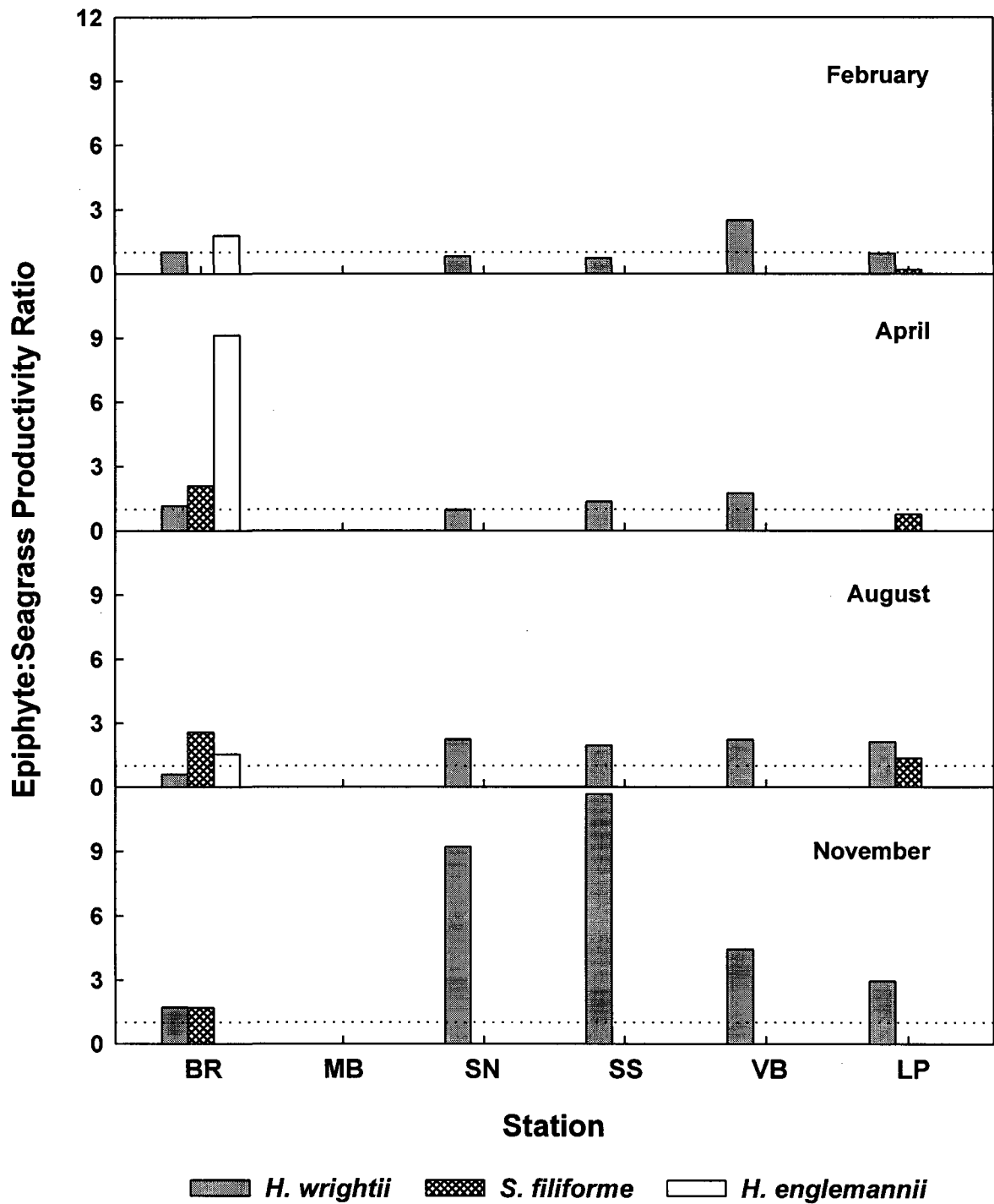


Fig. 6.7 Ratio of epiphyte:seagrass productivity, by month, station, and seagrass species, for the "deep-edge" Transect 3. Data are ratios of means presented in Figs. 6.3 and 6.5. Dotted line indicates equal productivity of seagrass and epiphytes.

Halodule wrightii

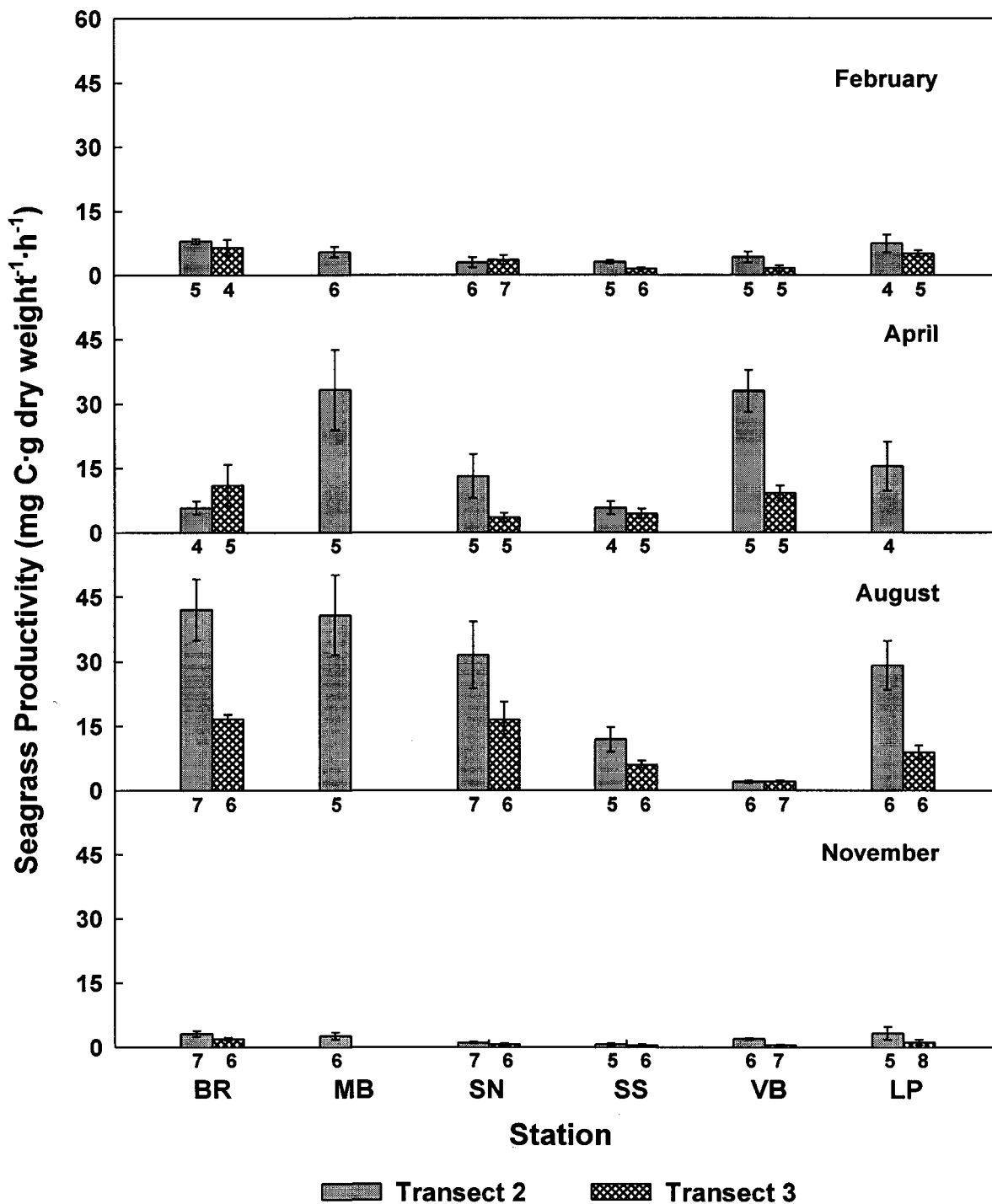


Fig. 6.8 Seagrass productivity by month, station, and transect for *Halodule wrightii*. Data are means (\pm SE) for all month-station-transect combinations, with the number of replicates below the horizontal axes for each combination.

Syringodium filiforme

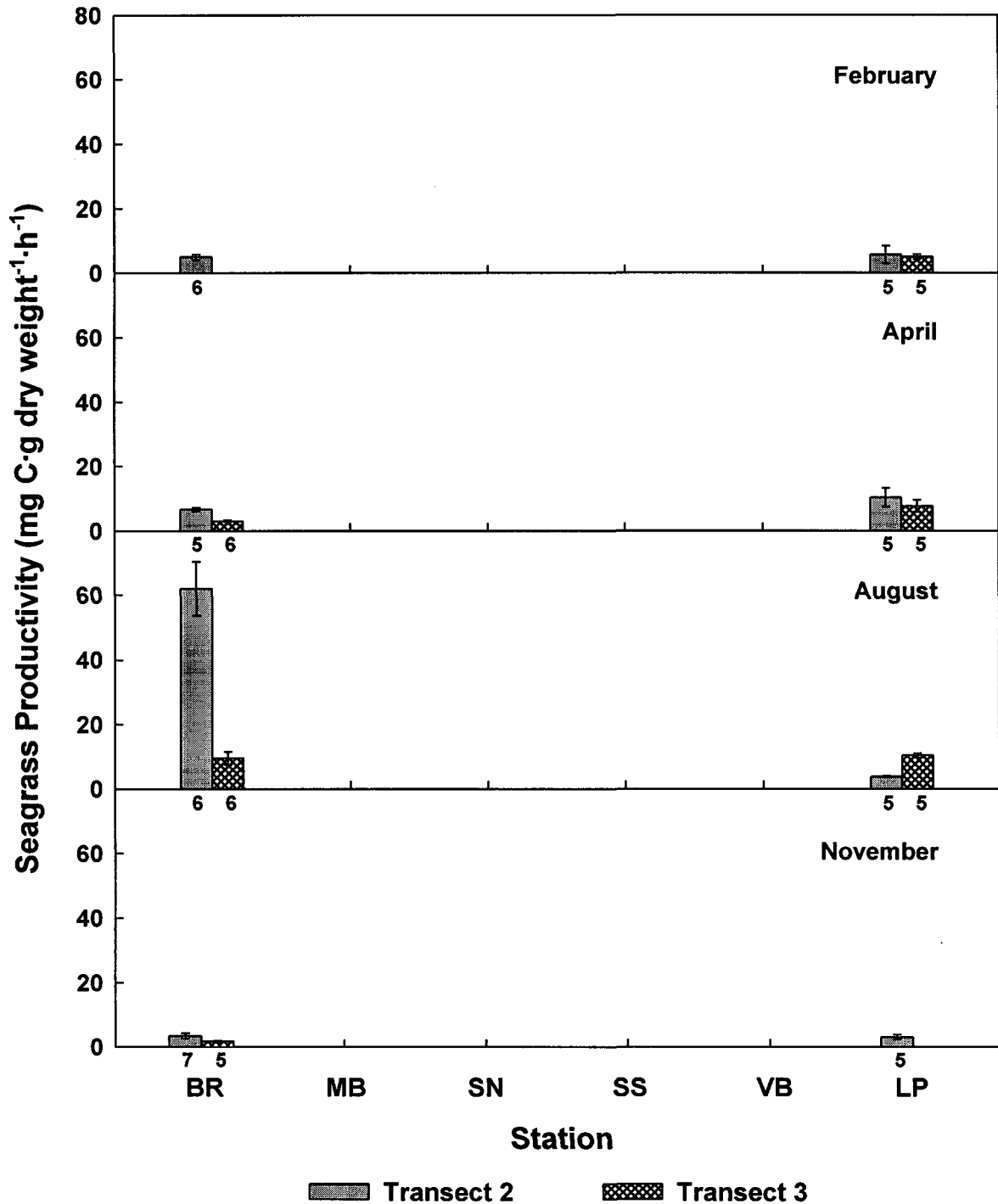


Fig. 6.9 Seagrass productivity by month, station, and transect for *Syringodium filiforme*. Data are means (+SE) for all month-station-transect combinations, with the number of replicates below the horizontal axes for each combination.

Halodule wrightii

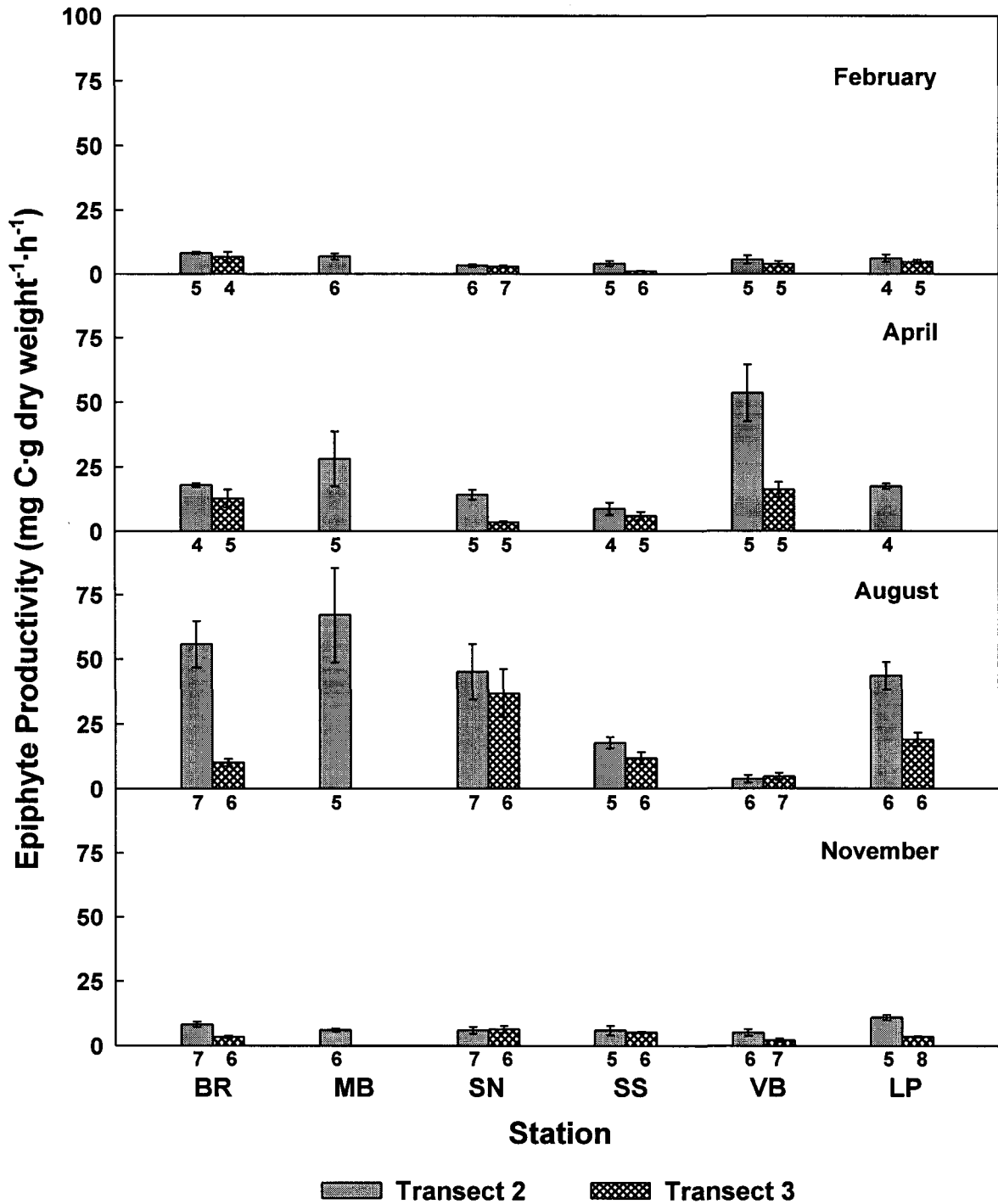


Fig. 6.10 Epiphyte productivity by month, station, and transect for *Halodule wrightii*. Data are means (\pm SE) for all month-station-transect combinations, with the number of replicates below the horizontal axes for each combination.

Syringodium filiforme

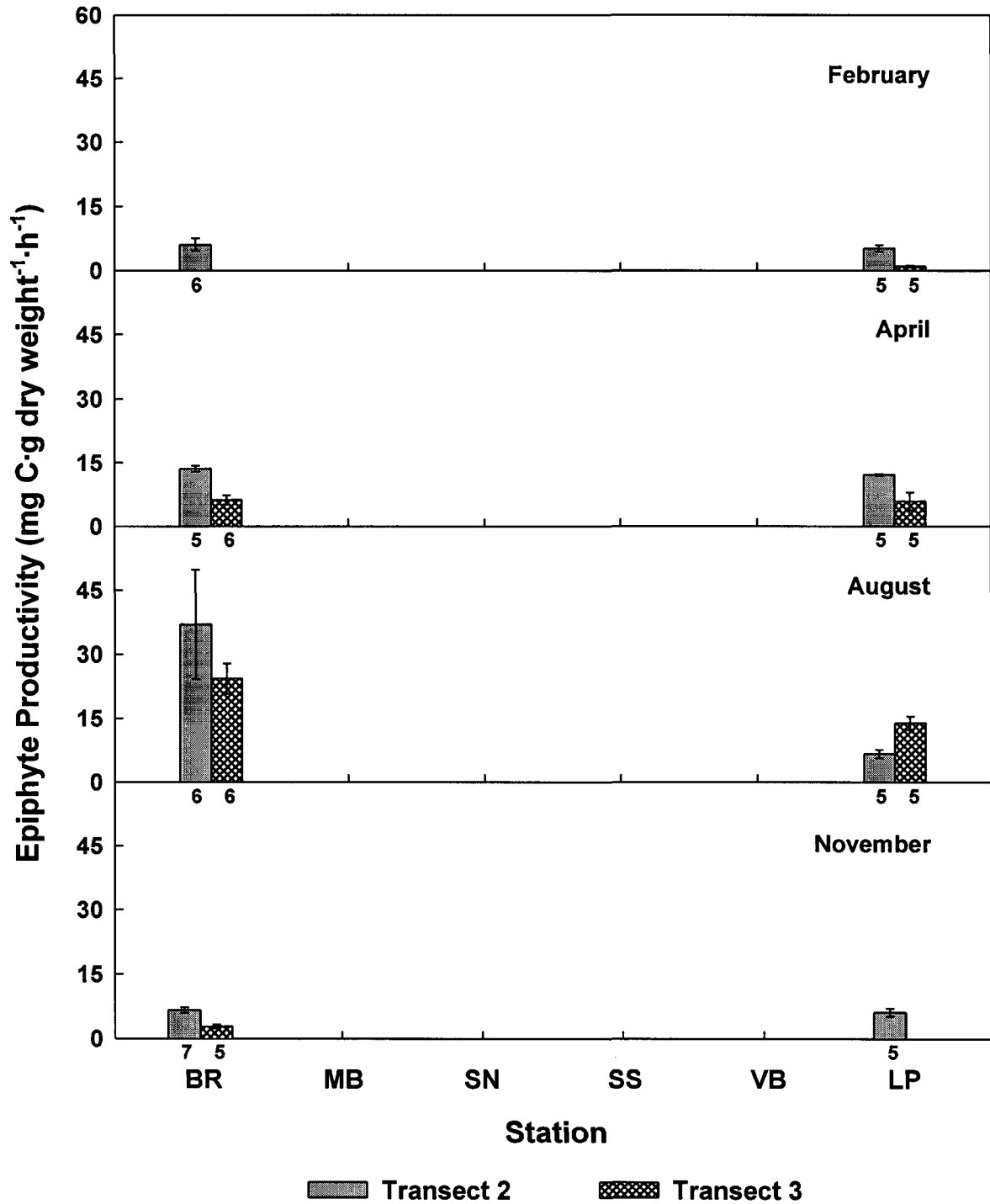


Fig. 6.11 Epiphyte productivity by month, station, and transect for *Syringodium filiforme*. Data are means (\pm SE) for all month-station-transect combinations, with the number of replicates below the horizontal axes for each combination.

Halodule wrightii

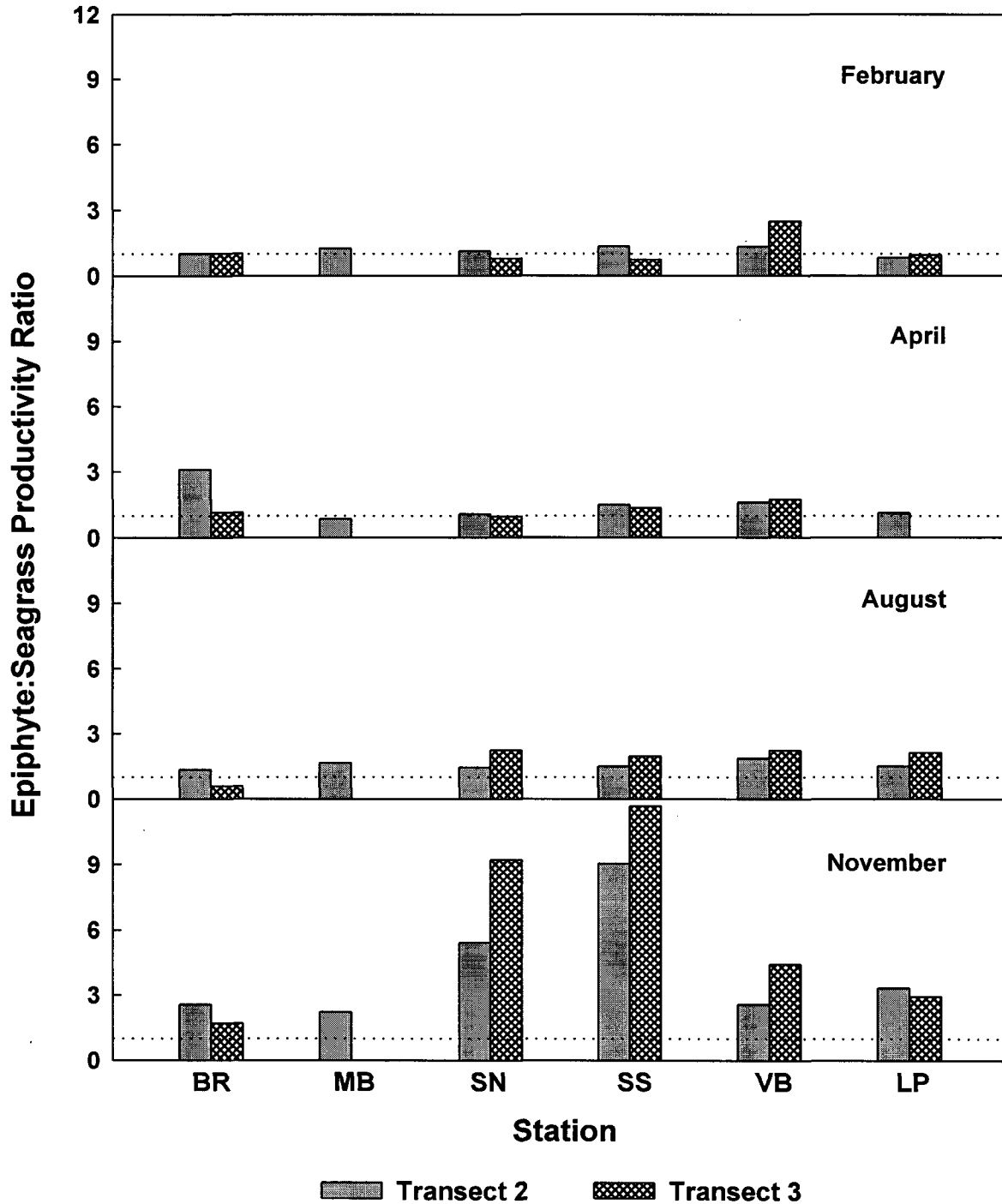


Fig. 6.12 Ratio of epiphyte:seagrass productivity by month, station, and transect for *Halodule wrightii*. Data are ratios of means presented in Figs. 6.8 and 6.10. Dotted line indicates equal productivity of seagrass and epiphytes.

Syringodium filiforme

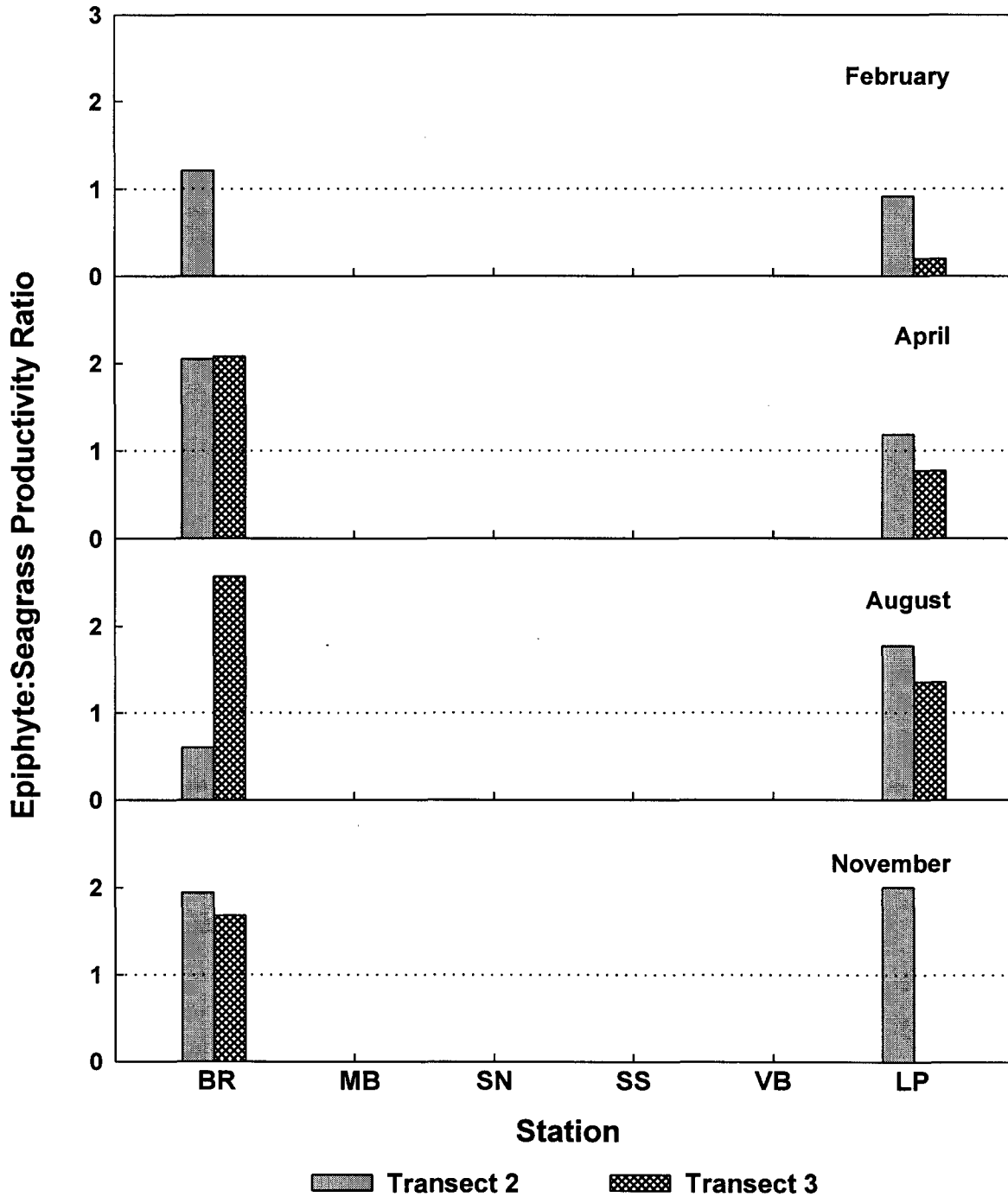


Fig. 6.13 Ratio of epiphyte:seagrass productivity by month, station, and transect for *Syringodium filiforme*. Data are ratios of means presented in Figs. 6.9 and 6.11. Dotted line indicates equal productivity of seagrass and epiphytes.

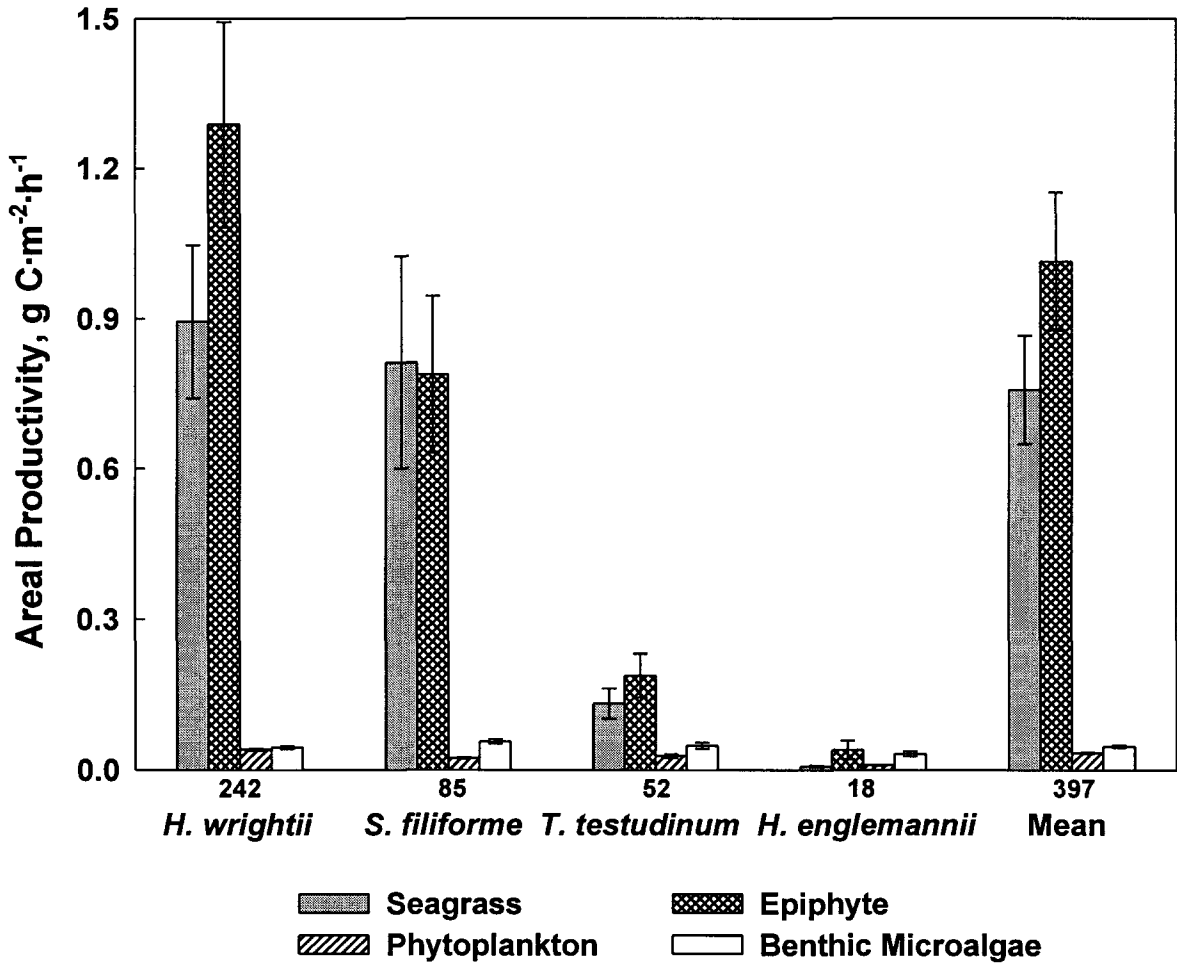


Fig. 6.14 Areal seagrass productivity. Data are means (\pm SE) by species, and for all species combined, for the entire study, with the number of replicates below the horizontal axis.

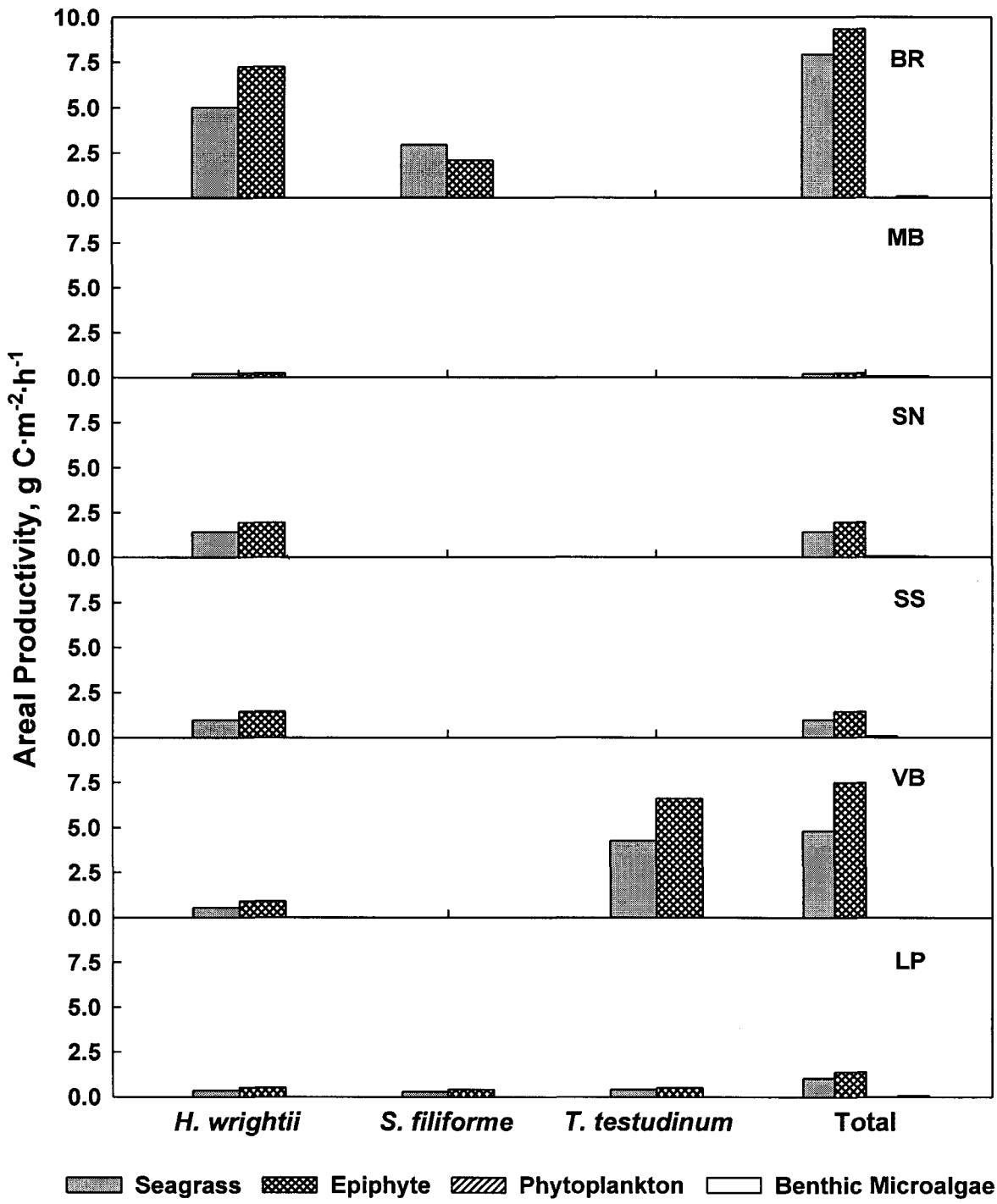


Fig. 6.15 Areal productivity of seagrass by species, epiphytes, phytoplankton, and benthic microalgae, by station, for the “mid-bed” Transect 2. Data are means for all station-species combinations.

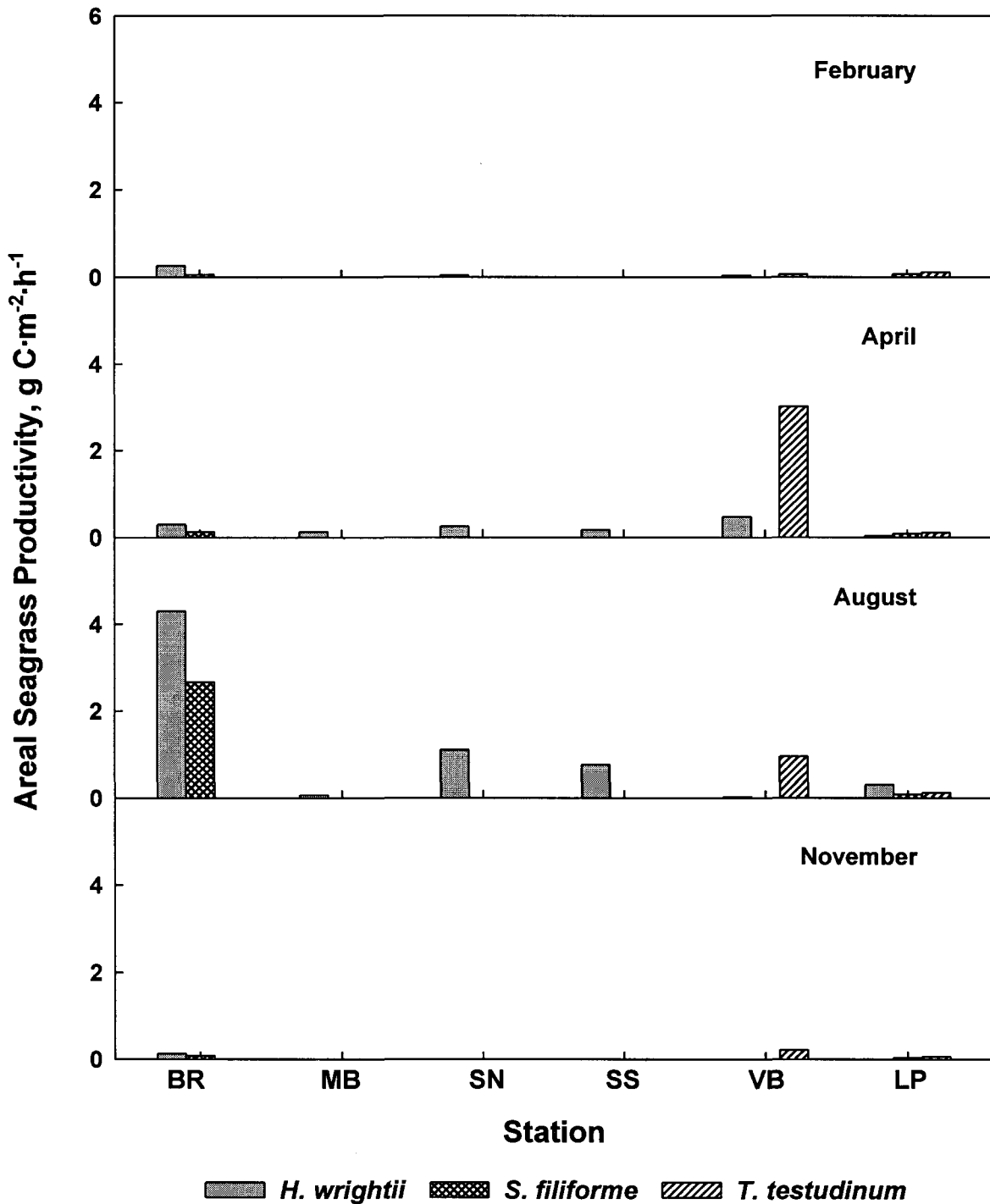


Fig. 6.16 Areal productivity of seagrass, by station and seagrass species, for the "mid-bed" Transect 2.

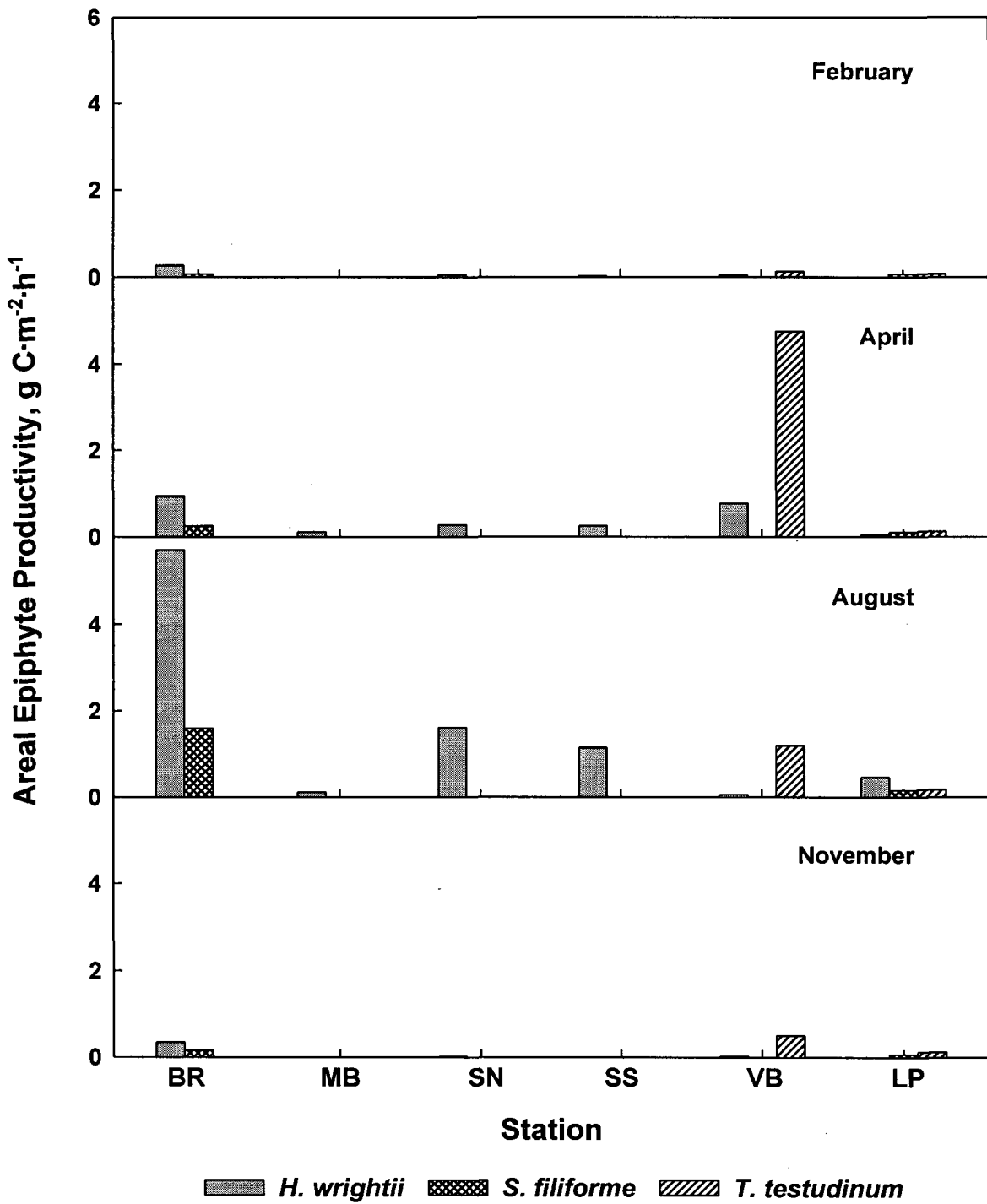


Fig. 6.17 Areal productivity of epiphytes, by station and seagrass species, for the "mid-bed" Transect 2.

Chapter 7: Relationships of Light Attenuation, Water Quality, and SAV

7.1 Introduction

Previously (Chapters 2 through 6), data for PAR and light attenuation, water quality, seagrass abundance, and epiphyte loads were analyzed for temporal and spatial variability within and among the IRL monitoring stations. This chapter uses correlation and regression analyses to identify and define relationships among seagrass abundance, light attenuation, and water quality.

7.2 Task Description

Task 7: To analyze data collected as part of the previous tasks to address the relationships between PAR, light attenuation, seagrass, epiphytes, and water quality.

7.3 Methods

The data analyzed in this chapter were collected as part of previous tasks (see Chapter 2 for PAR and K, Chapter 3 for water quality, Chapter 4 for seagrass, Chapter 5 for epiphytes, and Chapter 6 for productivity). Parameters used were:

- Underwater PAR (= S2 sensor, top of seagrass canopy, mid-bed)
- Vertical light attenuation coefficient (K; measured from the S1 and S2 sensors)
- Water quality parameters
 - Temperature
 - Salinity
 - Color
 - Turbidity
 - Total (TSS), inorganic (ISS), and organic suspended solids (OSS)
 - Total (TN) and total dissolved nitrogen (TDN) concentrations
 - Total (TP) and total dissolved phosphorus (TDP) concentrations
 - Total silicate concentration
 - Chlorophyll a concentration
- Seagrass abundance
 - Seagrass cover (%)
 - Seagrass above-ground biomass (g dry weight/m²)
 - Epiphyte load (g dry weight epiphyte/g dry weight above-ground biomass)

Photosynthetically Active Radiation, Water Quality, and Submerged Aquatic Vegetation in IRL

Relationships among these parameters were determined with correlation and linear regression analyses (Sokal and Rohlf 1981), performed with SAS statistical software (SAS Institute 1988). The minimal level of statistical significance for all analyses was $P \leq 0.05$.

Correlation analyses and linear regression analyses were used to identify the relationships of underwater PAR and vertical light attenuation coefficient (K) with the water quality parameters. The data in these analyses were weekly water quality data and the PAR and K measurements made during the water quality sampling; data were excluded from analyses whenever there were any problems or anomalies with the PAR equipment and the resulting data (see Chapter 2). Stepwise multiple regression models (Sokal and Rohlf 1981) determined the relationships of underwater PAR and K (dependent variables) with the water quality parameters; these analyses identified and partitioned the effects of the various water quality parameters on underwater PAR and light attenuation.

Correlation analyses and linear regression analyses were also used to identify the relationships of seagrass abundance and epiphyte load with underwater PAR and K and the relationships of seagrass abundance and epiphyte load with the water quality parameters. Because seagrass standing crop and epiphyte loads are due to environmental conditions over a period of weeks to months and because seagrass and epiphytes measurements were made seasonally, mean seasonal values for PAR, K, and water quality parameters were used for these analyses, along with seasonal measurements of seagrass abundance and epiphyte load. Seasonal means were determined using the month that seagrass and epiphyte sampling had occurred and the antecedent two months (i.e., Winter = December through February, Spring = March through May, Summer = June through August, Fall = September through November).

7.4 Results

The presentation of results includes the relationships of PAR and K with various water quality parameters (Sections 7.4.1-7.4.3), followed by the relationships of seagrass abundance and epiphyte load with PAR and K (Section 7.4.4), and the relationships of seagrass abundance and epiphyte load with water quality parameters (Section 7.4.5). In all cases, the relationships presented include both those for all data (all stations combined) and the data for each individual station.

7.4.1 Correlation Analyses of Underwater PAR and K with Water Quality Parameters

Correlation Analysis (All Stations)

Correlation analyses for PAR and K with the weekly water quality data revealed a high frequency of correlation with various water quality parameters for the combined data set from all stations ("all"; Tables 7.1 and 7.2). There was a significant ($P < 0.05$) correlation of underwater PAR with 12 of the 13 water quality parameters under consideration (Table 7.1); only the correlation of underwater PAR with TN was not significant ($P > 0.05$). All of the significant correlations were highly significant (usually $P = 0.0001$), except for TDN ($P = 0.03$), and, with the exception of temperature, salinity, TN, and TDN, were negative. Five of the significant correlations had a correlation coefficient above 0.3; those correlations were between PAR and salinity, color, turbidity, TP, and chlorophyll *a*. Chlorophyll *a* had the highest correlation with PAR ($r = -0.406$, $P = 0.0001$).

For the combined data set (all stations), K was significantly ($P < 0.05$) correlated with all 13 water quality parameters (Table 7.2). The significant correlations were all highly significant (usually $P = 0.0001$), with the exception of TN ($P = 0.047$), and, except for temperature, salinity, TN, and TDN, were positive. Seven of the significant correlations had a correlation coefficient above 0.3; those correlations were between K and color, turbidity, TSS, ISS, OSS, TP, and chlorophyll *a*. Turbidity had the highest correlation with K ($r = 0.657$, $P = 0.0001$).

Correlation Analysis (By Stations) - Temperature and Salinity

Temperature and salinity are physical factors that would not be expected to be direct attenuators of light, and that have previously been shown to co-vary with many of the water quality parameters measured in this study (see Chapter 3). The positive correlation of temperature with underwater PAR (Table 7.1) was significant at all stations except BR; the negative correlation of temperature with K (Table 7.2) was significant at 2 stations (SS and LP). The positive correlation of salinity with underwater PAR (Table 7.1) was highly significant at all stations; the negative correlation of salinity with K (Table 7.2) was significant at all stations except BR (where $P = 0.08$).

Correlation Analysis (By Stations) - Color, Turbidity, Suspended Solids, and Chlorophyll *a*

Color, turbidity, suspended solids, and chlorophyll are generally recognized as the most significant direct attenuators of light in aquatic systems. All significant correlations with any of these parameters were negative for underwater PAR (Table 7.1) and positive for K (Table 7.2).

The negative correlation of color with underwater PAR (Table 7.1) was significant at all stations. The positive correlation of color with K was significant at all stations (Table 7.2).

The negative correlation of turbidity with underwater PAR (Table 7.1) was significant at all stations. The positive correlation of turbidity with K (Table 7.2) was highly significant at all stations. The correlation of K with turbidity was higher than that of all other water quality parameters at all stations, except BR, where the correlation coefficient of K with turbidity ($r = 0.337$, $P = 0.001$) was slightly lower than that of K with TP ($r = 0.355$, $P = 0.0003$).

The negative correlation of TSS with PAR (Table 7.1) was significant only at MB ($r = -0.303$, $P = 0.002$). The negative correlation of ISS with PAR (Table 7.1) was significant at MB ($r = -0.234$, $P = 0.02$) and VB ($r = -0.439$, $P = 0.02$). The negative correlation of OSS with PAR (Table 7.1) was significant at BR ($r = -0.306$, $P = 0.003$) and MB ($r = -0.371$, $P = 0.0001$). The positive correlations of both TSS and ISS with K (Table 7.2) were significant at all stations except BR and TC. The positive correlation of OSS with K (Table 7.2) was significant at all stations but BR, TC, and VB (at VB, the relationship was almost significant; $P = 0.07$).

The negative correlation of chlorophyll *a* with underwater PAR (Table 7.1) was significant at all stations, except VB. The positive correlation of chlorophyll *a* with K (Table 7.2) was significant at all stations, except MB, where this relationship was nearly significant ($P = 0.08$).

Correlation Analysis (By Stations) - Nutrients

As with temperature and salinity, nutrients do not directly attenuate light, but they are likely to be correlated with underwater PAR and/or K because nutrients influence the growth of phytoplankton, which are more directly related to light attenuation, i.e., turbidity, suspended solids, and chlorophyll (see Chapter 3 for chlorophyll-nutrient relationships).

The negative correlations of total nitrogen (TN) and total dissolved nitrogen (TDN) with PAR (Table 7.1) and the positive correlations of TN and TDN with K (Table 7.2) were significant only at SN and SS.

The negative correlation of total phosphorus (TP) with underwater PAR (Table 7.1) was significant at all stations, except TC and VB (at VB, this relationship was almost significant: $r = -0.323$, $P = 0.06$). The negative correlation of total dissolved phosphorus (TDP) with underwater PAR (Table 7.1) was significant at 4 stations: BR, SN, SS, and LP. The positive correlation of TP with K (Table 7.2) was significant at all stations, except TC and VB (at TC, this relationship was almost significant: $r = 0.271$, $P = 0.06$). The positive correlation of TDP with K (Table 7.2) was significant only at BR.

The negative correlation of total silicate with underwater PAR (Table 7.1) was significant at 3 stations: SS, VB, and LP. The positive correlation of total silicate with K (Table 7.2) was significant at 2 stations: VB and LP.

Relationship of Underwater PAR and K

Comparisons of the two sets of correlations (Tables 7.1 and 7.2) revealed that underwater PAR and K were both significantly correlated to various water quality parameters. Not surprisingly, the relationship of any water quality parameter with PAR was inverse to that of its relationship with K. When K was regressed against underwater PAR, there was a highly significant relationship ($P = 0.0001$), but this relationship explained only 25.4% of the observed variance for all data combined (Fig. 7.1) and from 13.5% (BR) to 36.4% (TC) for individual stations (Fig. 7.2). For relationships with water quality, K was a more useful parameter than PAR (which is strongly influenced by seasonal and diel cycles of ambient light, see Chapter 2); thus, most of the remaining presentation of results in this section will focus on the significant relationships of K with various water quality parameters.

Correlation Analysis - Station Comparisons

Of the station-specific relationships of K with the 13 water quality parameters (Table 7.2), SS had 11 significant relationships, SN and LP had 10, MB and VB 7, BR 6, and TC only 4. The positive correlations of K with color and turbidity were significant at all 7 stations. Six stations had significant correlations: (1) between K and salinity (the exception was BR, where the relationship was almost significant; $r = -0.179$, $P = 0.08$), and (2) between K and chlorophyll *a* (the exception was MB, where the relationship was almost significant; $r = 0.174$, $P = 0.08$). Five stations had significant correlations: (1) between K and TSS (the exceptions were BR and TC), (2) between K and ISS (the exceptions were BR and TC), and (3) between K and TP (the exceptions were TC and VB). Four stations had significant correlations between K and OSS (the exceptions were BR, TC, and VB). The remaining, significant, station-specific relationships with K were found only at 1 or 2 stations: (1) temperature, only at SS and LP, (2) TN and TDN, both only at SN and SS, and (3) TDP, only at BR.

7.4.2 Linear Regression Analyses of K with Water Quality Parameters

Linear regressions of the relationships between underwater PAR and K with the individual water quality parameters were conducted on the complete data set (all stations) as well as on a station-specific basis. These linear regression models are presented graphically, first for PAR (Figs. 7.3-7.24) and then for K (Figs. 7.25-7.46), in the same order the data were previously presented (Tables 7.1, Table 7.2). Overall, as previously mentioned, the relationships of K with water quality parameters were both more

significant, and more relevant, than the relationships of PAR with water quality, so the subsequent presentation of results in this section will be limited to K.

Temperature and K

The negative relationship between temperature and K was significant for the overall data set (Fig. 7.25), but the amount of variance explained by this regression was rather small ($R^2 = 0.015$). This relationship was significant only at SS and LP (Fig. 7.26); the amount of variance explained ($R^2 = 0.079$ at SS, 0.172 at LP) was relatively low.

Salinity and K

While the relationship between salinity and K was highly significant ($P = 0.0001$) for the overall data set (Fig. 7.27), the amount of variance explained by this regression was rather small ($R^2 = 0.065$). This regression was significant at all stations but BR (Fig. 7.28), but the amount of variance explained was usually low (R^2 ranged from 0.058 at MB to 0.179 at VB), with a much stronger relationship at TC ($R^2 = 0.403$; $P = 0.0001$).

Color and K

While the relationship between color and K was highly significant ($P = 0.0001$) for the overall data set (Fig. 7.29), the amount of variance explained by this regression was small ($R^2 = 0.114$). While this regression was significant, with positive slopes, at all stations (Fig. 7.30), this relationship was much stronger at TC ($R^2 = 0.299$) than at the other stations (R^2 ranged from 0.053 at SN to 0.150 at VB).

Turbidity and K

The relationship between turbidity and K was highly significant ($P = 0.0001$) for the overall data set (Fig. 7.31); the amount of variance explained by this regression was high ($R^2 = 0.431$). This regression was also highly significant ($P = 0.0001$, except at BR where $P = 0.001$) at all stations (Fig. 7.32), with positive slopes and a high amount of variance explained by the relationship (R^2 ranged from 0.380 at LP to 0.515 at SS, except BR where $R^2 = 0.114$).

Suspended Solids and K

Regression models for K vs. total, inorganic, and organic suspended solids were all highly significant ($P = 0.0001$) for the complete data set (all stations; Fig. 7.33). The regression with K was stronger for ISS ($R^2 = 0.141$) than for OSS ($R^2 = 0.095$); the slope of K vs. OSS was steeper than that of K vs. ISS. With the exception of BR and TC (where no regressions with K were significant; $P > 0.05$) and OSS at VB, the regression models for K vs. TSS, ISS, and OSS were all significant (Fig. 7.34-7.36). The amount of variance

explained by the significant relationships of K and TSS (Fig. 7.34) at the stations varied substantially (R^2 ranged from 0.060 at SN to 0.330 at MB). Regression relationships with K were stronger (higher R^2 values) for ISS (Fig. 7.35) than for OSS (Fig. 7.36) at TC, SS, VB, and LP, but not at BR, MB and SN.

Nitrogen and K

The relationships between TN and K, as well as between TDN and K, were significant for the overall data set (Figs. 7.37), but the amount of variance explained by these regressions was small ($R^2 = 0.007$ and 0.013 , respectively, for TN and TDN). The regressions of K with TN (Fig. 7.38) and TDN (Fig. 7.39) were significant only at SN and SS, and in both cases, the amount of variance explained was low (R^2 ranged from 0.058 to 0.151).

Phosphorus and K

The relationships between TP and K and between TDP and K were both highly significant for the overall data set (Figs. 7.40), but the amount of variance explained by TP ($R^2 = 0.186$) was much greater than that by TDP ($R^2 = 0.022$). The relationship between K and TP was highly significant at all stations but TC and VB (Fig. 7.41). The relationship between K and TDP was significant ($R^2 = 0.071$; $P = 0.01$) only at BR (Fig. 7.42).

Silicate and K

The relationship between K and total silicate was highly significant ($P = 0.0001$) for the overall data set (Fig. 7.43), but accounted for a small amount of the observed variance ($R^2 = 0.044$). This relationship was significant only at VB and LP (Fig. 7.44), and was stronger at VB ($R^2 = 0.193$) than at LP ($R^2 = 0.110$).

Chlorophyll *a* and K

The relationship between K and chlorophyll *a* was highly significant ($P = 0.0001$) for the overall data set (Fig. 7.45) and significant, usually highly so, at all stations but MB, where $P = 0.08$ (Fig. 7.46). R^2 was highest at TC ($R^2 = 0.400$).

7.4.3 Multiple Regression Analyses of Underwater PAR and K with Water Quality Parameters

Multiple regression analysis of underwater PAR and water quality parameters indicated that for the complete data set (all stations, Table 7.3), chlorophyll *a* was the first, and most significant, factor to enter the model, followed by color, temperature, OSS, TDP, and TDN. This model had an R^2 value of 0.384.

In contrast, salinity was the initial parameter to enter station-specific models at 5 stations (Table 7.3); the exceptions were BR, where salinity entered the model after TP, and SS, where salinity did not enter the model at all. At SS, chlorophyll *a* was the first factor to enter the model. Temperature and phosphorus (as either P or TDP) were also factors in 5 station-specific models (exceptions were BR and VB for temperature, VB and LP for phosphorus). R^2 for the models ranged from 0.409 (VB) to 0.581 (SS).

Multiple regression analysis of K with the water quality parameters indicated that, for the complete data set (all stations, Table 7.4), turbidity was the first significant factor to enter the model, followed by color, ISS, salinity, and TSS. This model had a R^2 value of 0.540.

Turbidity was also the initial parameter to enter station-specific models at 5 stations (Table 7.3); however, turbidity was not a factor in models at BR and VB. At BR, TP was the first factor to enter the model, followed by silicate and salinity. At VB, ISS was the first factor to enter the model, followed by salinity. Salinity was a factor in 5 station-specific models (exceptions were TC and SS). ISS was a factor in 3 models (TC, VB, and LP). Color was a factor in 2 models (TC and SS). TSS, OSS, and TDN were each factors in 1 station-specific model (TSS at MB, OSS and TDN at SN). R^2 for the station-specific models ranged from 0.212 (BR) to 0.728 (SS).

7.4.4 Relationships of Seagrass Abundance and Epiphyte Load with Underwater PAR and K

For the full data set (all stations), there was a significant correlation between PAR and seagrass above-ground biomass, but no significant correlations between PAR with seagrass cover or epiphyte load (Table 7.5). For the full data set, there was a significant correlation between K and both seagrass cover and above-ground biomass, but no significant correlations between K with epiphyte load (Table 7.6). Regression analysis (Fig. 7.47) indicated that the increase in seagrass cover with decreasing K was significant ($P = 0.005$; $R^2 = 0.161$), but the relationship of cover with PAR was not. The increase in seagrass above-ground biomass (Fig. 7.48) with increasing PAR, or decreasing K, was significant ($P = 0.04$ for PAR, 0.01 for K), although R^2 values were relatively low (0.090 and 0.126, respectively). Regression analysis showed no significant relationship of epiphyte load with either PAR or K (Fig. 7.49).

The only site-specific significant correlation between PAR and seagrass cover, seagrass above-ground biomass, or epiphyte load was with cover at SS (Table 7.5). Regression analysis demonstrated a significant positive relationship ($P = 0.047$; $R^2 = 0.510$) of cover with PAR at that station (Fig. 7.50).

The only site-specific significant correlation between K and seagrass cover, seagrass above-ground biomass, or epiphyte load was with biomass at LP (Table 7.6); the relationship of K and cover at LP was almost significant ($P = 0.07$). Regression analysis demonstrated a significant negative relationship ($P = 0.01$; $R^2 = 0.751$) of seagrass biomass with K at that station (Fig. 7.51).

7.4.5 Relationships of Seagrass Abundance and Epiphyte Load with Water Quality Parameters

For the full data set (all stations), seagrass cover was significantly correlated with salinity, total phosphorus, and silicate (Table 7.7) and seagrass above-ground biomass was significantly correlated with temperature, salinity, and silicate (Table 7.8). The correlations with temperature and salinity were all positive, while those with phosphorus and silicate were negative. Regression analysis indicated that the amount of variance explained by regression models of seagrass above-ground biomass with temperature (Fig. 7.52) and phosphorus (Fig. 7.53) was relatively small ($R^2 = 0.118$ and 0.095 , respectively for salinity and TP). Stronger models were found with salinity (Fig. 7.54) for both cover ($R^2 = 0.293$) and seagrass above-ground biomass ($R^2 = 0.166$) and with silicate (Fig. 7.55) for both cover ($R^2 = 0.307$) and seagrass above-ground biomass ($R^2 = 0.150$). The only water quality parameter to be significantly related to epiphyte load for the full data set was silicate (Table 7.9; Fig. 7.56; $R^2 = 0.175$).

Of the 91 combinations of stations and water quality parameters, there were only 4 significant site-specific correlations between seagrass cover and the various water quality parameters (Table 7.7). Significant correlations were with temperature at SS and LP, silicate at BR, and chlorophyll *a* at SS. The amount of variance explained by the regression models for these relationships (Figs. 7.57-7.58; Fig. 7.59, top panel) was high (R^2 values ranged from 0.510 to 0.772).

Of the 91 combinations of stations and water quality parameters, there were only 4 significant site-specific correlations between seagrass above-ground biomass and the various water quality parameters (Table 7.8). Significant correlations were with temperature at SS, salinity at BR, turbidity at TC, and chlorophyll *a* at SS. The amount of variance explained by the regression models for these relationships (Figs. 7.60-7.62; Fig. 7.59, bottom panel) was high (R^2 values ranged from 0.488 to 0.963).

Of the 91 combinations of stations and water quality parameters, there were only 3 significant site-specific correlations between epiphyte load and the various water quality parameters (Table 7.9). Significant correlations were with salinity, color, and chlorophyll *a* at MB. The amount of variance explained by the regression models for these relationships (Fig. 7.63) was high (R^2 values ranged from 0.905 to 0.987).

7.5 Discussion

This study demonstrated a high frequency of correlation of underwater PAR and vertical light attenuation coefficients with various water quality parameters. While underwater PAR, not light attenuation, is what seagrasses directly respond to, underwater PAR is strongly influenced by seasonal and diel cycles of ambient light, as well as by attenuation within the water column. Thus, attenuation coefficients appear to be much more useful than measurements of PAR in addressing water quality effects on underwater light availability. All 13 water quality parameters in this study were found to be significantly correlated to K. K was most significantly related to turbidity, color, suspended solids (TSS, ISS, and OSS), TP, and chlorophyll *a*.

Turbidity (and/or suspended solids), color, and chlorophyll are generally recognized as the most significant direct attenuators of light in aquatic systems. In this study, each of these parameters individually was significantly related to reduced underwater PAR and increased K, but turbidity was the most significant attenuator of light in IRL. Given the high degree of correlation of turbidity with suspended solids (see Chapter 3), it was not surprising to find strong relationships of K with TSS, ISS, and OSS. ISS had a greater impact on K than OSS because the former were more abundant (see also Chapter 3); but on a per unit weight basis, OSS attenuated more light (i.e., there was a greater slope with K).

Multiple regression analysis of K and water quality parameters indicated that for the complete data set, turbidity was the first significant factor to enter the model, followed by color, ISS, salinity, and TSS. Suspended solids are clearly responsible for most of the light attenuation by the water column in IRL. High levels of suspended solids were associated with wind events (see Chapter 3). As most of these suspended solids are probably "natural" in origin, the only appropriate management action might be to reduce sediments from entering the system (e.g., via storm water retention).

While the relationships between color and chlorophyll *a* and K are both highly significant, the amount of variance explained by the regressions was smaller than that of turbidity. The role of color as a light attenuator is secondary to that of turbidity/suspended solids. While color is associated with freshwater inputs (see Chapter 3), color is primarily a natural phenomenon associated with decaying vegetation in freshwater systems. Perhaps the most interesting finding from this analysis is that chlorophyll was not part of the overall model, an observation that suggests that management action addressing phytoplankton blooms (e.g., alteration of nutrient inputs) currently would not significantly improve light clarity.

While nutrients are not direct attenuators of light, they are likely to be correlated with K because nutrients influence the growth of phytoplankton, which are more closely related to the direct attenuators of light, i.e., turbidity (and/or suspended solids) and chlorophyll. Based on the results of this study, the relationships of K with nutrients are less important than those with the major attenuators discussed above. Moreover, there were differences among nutrient types in their relationships to observed light attenuation, and the relationship of any one nutrient with K was variable among the stations.

The most significant nutrient effect was found for phosphorus: the relationships between K and TP and TDP were both highly significant, with TP having a stronger correlation. One might expect a greater correlation with TDP than with TP as the former is more likely related to chlorophyll production (i.e., phytoplankton use dissolved, not particulate, phosphorus), but the reason for this apparent paradox may simply be that TP is more related to particulate material in the water column which is a significant attenuator of light. In contrast, TDN for the overall data set was more significantly related to K than TN, and correlations between K and nitrogen were lower than those between K and phosphorus. Among stations, the regressions of K with TN and TDN were significant only at the Sebastian stations. The relationship between K and total silicate was highly significant for the overall data set. Among stations, this relationship was significant only at the 3 southernmost stations.

This study established several direct links between seagrass abundance and both PAR and K. For the full data set, there were significant correlations and regressions between PAR and seagrass above-ground biomass and between K and both seagrass cover and above-ground biomass. There were only a few significant site-specific relationships found between seagrass abundance or epiphyte load with PAR and K; greater statistical resolution might be seen with longer-term sampling or larger sample sizes.

This study also identified significant relationships between seagrass abundance and water quality parameters. For the full data set, seagrass cover was significantly correlated with salinity, total phosphorus, and silicate, and above-ground seagrass biomass was significantly correlated with temperature, salinity, and silicate. The correlations with temperature and salinity were all positive, while those with phosphorus and silicate were negative. The amount of variance explained by regression models of above-ground biomass with temperature and phosphorus was relatively small. Stronger models were found with salinity for both cover and above-ground biomass and with silicate for both cover and above-ground biomass.

The only water quality parameter to be significantly related to epiphyte load for the full data set was silicate. As diatoms (the only algae that require silicon) are a significant component of epiphyte communities in IRL, this relationship is not surprising, but finding no relationship with other nutrients is. The absence of stronger relationships between

nutrients and epiphytes may be due to the mediating role of grazers (see Chapter 8). Again, because of the relatively low sampling effort for seagrass abundance and epiphyte load relative to the more intensive weekly sampling for water quality, there were only a few significant, site-specific relationships between seagrass abundance or epiphyte load and individual water quality parameters.

The overall goal of this study was to relate water quality with seagrass and PAR status in IRL. This study has demonstrated that seagrass within IRL experiences a tremendous range of water quality conditions, both in terms of differences among stations and temporal changes at individual stations. Relationships between light attenuation and water quality have been established. This study found that considerable differences in water quality and underwater light exist throughout IRL. Both correlation and multiple regression analyses clearly showed station-specific differences, which demonstrates the need for a segment-by-segment approach to water quality management in IRL.

Now that initial relationships between water quality and light attenuation have been established for different sites in IRL, it would be desirable to verify those relationships over a broader area. Based on results presented in this chapter, turbidity and color are environmental factors that could be quickly and effectively measured in field monitoring efforts as rapid assessments of water quality parameters that determine light attenuation. Other important water quality parameters, e.g., nutrients and chlorophyll, are more time consuming to measure, but because they are less important to light attenuation in IRL, they probably do not need to be measured as often, if light attenuation is the chief issue of concern.

The relationships of light and water quality with seagrass were not as well defined in this study, probably because the numbers of sampling events and stations were low, relative to the large amount of spatial and temporal variability that exists in seagrass communities throughout IRL. One way to improve the understanding of light attenuation and water quality with seagrass abundance might be frequent water quality analyses at the sites of the District's extensive monitoring network of seagrass transects. Rapid assessments of light, water quality, and seagrass are recommended for future monitoring efforts in IRL. Such assessments would provide a fairly simply obtained, yet meaningful, synoptic evaluation of a large area of the lagoon.

7.6 Summary

Previously (Chapters 2 through 6), data for PAR and light attenuation, water quality, seagrass, and epiphytes were analyzed for temporal and spatial variability within and among the IRL monitoring stations. This chapter identifies and defines the key relationships among light attenuation, water quality, and seagrass abundance. The major results of this study are:

Photosynthetically Active Radiation, Water Quality, and Submerged Aquatic Vegetation in IRL

- (1) Correlation analyses for PAR and vertical light attenuation coefficients (K) with water quality data revealed a high frequency of correlation with various water quality parameters. Light attenuation coefficients were much more useful than PAR measurements in addressing water quality effects on underwater light availability; correlations between water quality parameters with K were more significant statistically than those with underwater PAR. When water quality parameters were examined individually, K was most significantly related to turbidity, suspended solids (TSS, ISS, and OSS), color, chlorophyll *a*, and TP.
- (2) Of the station-specific relationships of K with the water quality parameters, positive correlations with both color and turbidity were significant at all 7 stations. Six stations had significant correlations: (1) between K and salinity (the exception was BR), and (2) between K and chlorophyll *a* (the exception was MB).
- (3) The most significant attenuator of light in IRL was turbidity. Strong relationships also existed between K and total, organic and inorganic suspended solids, which were all highly correlated to turbidity. Inorganic suspended solids had a greater impact on K than did organics because they were more abundant; but on a per unit weight basis, organic solids attenuated more light.
- (4) Color and chlorophyll had smaller roles as attenuators of light in IRL. While the relationships between both parameters and K were highly significant, the amount of variance explained by the regressions was much smaller than that for turbidity. The impact of color and chlorophyll on light attenuation is likely to be quite variable throughout IRL because of their large amount of spatial and temporal variability.
- (5) The relationships of K with nutrients were less important than those with turbidity, color, and chlorophyll. There were differences among nutrient types in their relationships to observed light attenuation, and the relationship of any one nutrient with light attenuation was variable among stations. The most significant nutrient effect was found for phosphorus (and more so for TP than TDP). The relationship with TP may be attributed to attenuation by the particulate fraction.
- (6) Multiple regression analysis of K and water quality parameters indicated that, for the complete data set, turbidity was the first significant factor to enter the model, followed by color, ISS, salinity, and TSS. Chlorophyll was not part of the model; this observation suggests that management action addressing phytoplankton blooms (e.g., reduction of current nutrient inputs) would not significantly improve light clarity.
- (7) Multiple regression analyses of water quality parameters and K showed station-specific differences, which demonstrate the need for a segment-by-segment approach to water quality management in IRL.

- (8) For the full data set, there were significant correlations and regressions between PAR and above-ground seagrass biomass and between K and both seagrass cover and above-ground biomass. There were only a few significant site-specific relationships found between seagrass abundance or epiphyte load with PAR and K; greater statistical resolution might be seen with longer-term sampling or larger sample sizes.
- (9) For the full data set, seagrass cover was significantly correlated with salinity, total phosphorus, and silicate, and seagrass above-ground biomass was significantly correlated with temperature, salinity, and silicate. The relationships with temperature and salinity were all positive, while those with phosphorus and silicate were negative. The only water quality parameter significantly related to epiphyte load for the full data set was silicate. As diatoms (the only algae that require silicon) are a significant component of epiphyte communities in IRL, this relationship is not surprising, but finding no relationship with other nutrients is. The absence of stronger relationships between nutrients and epiphytes may be due to the mediating role of grazers.
- (10) Turbidity and color are water quality parameters that are important to light attenuation and that can be quickly measured in field monitoring efforts as rapid assessments of water quality. Now that initial relationships between water quality and light attenuation have been established for different sites in IRL, it would be desirable to determine those relationships over a broader area. Rapid assessment of light, water quality, and seagrass, perhaps in relationship to the District's extensive monitoring network of seagrass transects, would provide a fairly simply obtained, yet meaningful, synoptic evaluation of a large area of the lagoon.

Table 7.1 Correlation coefficients of underwater PAR with temperature, salinity, color, turbidity, total suspended solids (TSS), inorganic suspended solids (ISS), organic suspended solids (OSS), total nitrogen (TN), total dissolved nitrogen (TDN), total phosphorus (TP), total dissolved phosphorus (TDP), total silicate, and chlorophyll *a*, for all stations, and by station. Water quality data were from weekly integrated water samples (November 1993–November 1995); PAR values were 15-minute mean values during each water sampling. Values for each combination are Pearson correlation coefficients, level of significance, and (n).

	All	BR	MB	TC	SN	SS	VB	LP
Temperature	0.228 0.0001 (578)	0.168 0.10 (98)	0.288 0.003 (104)	0.328 0.02 (49)	0.232 0.02 (102)	0.366 0.0003 (95)	0.386 0.02 (34)	0.567 0.0001 (96)
Salinity	0.304 0.0001 (578)	0.442 0.0001 (98)	0.455 0.0001 (104)	0.519 0.0001 (49)	0.559 0.0001 (102)	0.541 0.0001 (95)	0.490 0.003 (34)	0.611 0.0001 (96)
Color	-0.365 0.0001 (578)	-0.358 0.0003 (98)	-0.409 0.0001 (104)	-0.357 0.01 (49)	-0.468 0.0001 (102)	-0.429 0.0001 (95)	-0.402 0.02 (34)	-0.470 0.0001 (96)
Turbidity	-0.396 0.0001 (578)	-0.428 0.0001 (98)	-0.406 0.0001 (104)	-0.311 0.03 (49)	-0.348 0.0003 (102)	-0.331 0.001 (95)	-0.359 0.04 (34)	0.433 0.0001 (96)
TSS	-0.195 0.0001 (574)	-0.187 0.07 (98)	-0.303 0.002 (104)	0.087 0.55 (49)	0.011 0.92 (102)	0.010 0.92 (92)	-0.260 0.15 (32)	-0.063 0.55 (94)
ISS	-0.187 0.0001 (551)	0.033 0.75 (94)	-0.234 0.02 (100)	0.102 0.49 (49)	0.008 0.93 (98)	-0.021 0.85 (92)	-0.439 0.02 (28)	-0.091 0.39 (90)
OSS	-0.221 0.0001 (551)	-0.306 0.003 (94)	-0.371 0.0001 (100)	0.045 0.76 (49)	-0.090 0.38 (98)	-0.001 0.99 (92)	-0.072 0.71 (28)	-0.008 0.94 (90)
TN	0.048 0.25 (578)	-0.020 0.85 (98)	-0.141 0.15 (104)	-0.102 0.48 (49)	-0.462 0.0001 (102)	-0.396 0.0001 (95)	-0.209 0.23 (34)	-0.334 0.001 (96)
TDN	0.093 0.03 (578)	0.027 0.79 (98)	-0.099 0.32 (104)	-0.207 0.15 (49)	-0.447 0.0001 (102)	-0.389 0.0001 (95)	-0.167 0.34 (34)	-0.255 0.01 (96)
TP	-0.390 0.0001 (578)	-0.526 0.0001 (98)	-0.215 0.03 (104)	-0.097 0.51 (49)	-0.542 0.0001 (102)	-0.543 0.0001 (95)	-0.323 0.06 (34)	-0.398 0.0001 (96)
TDP	-0.254 0.0001 (578)	-0.454 0.0001 (98)	-0.071 0.47 (104)	-0.174 0.23 (49)	-0.357 0.0002 (102)	-0.327 0.001 (95)	-0.252 0.15 (34)	-0.274 0.01 (96)
Silicate	-0.122 0.003 (578)	-0.059 0.57 (98)	-0.106 0.29 (104)	0.150 0.30 (49)	-0.134 0.18 (102)	-0.241 0.02 (95)	-0.375 0.03 (34)	-0.333 0.001 (96)
Chlorophyll <i>a</i>	-0.406 0.0001 (578)	-0.433 0.0001 (98)	-0.332 0.001 (104)	-0.404 0.004 (49)	-0.470 0.0001 (102)	-0.563 0.0001 (95)	-0.183 0.30 (34)	-0.459 0.0001 (96)

Table 7.2 Correlation coefficients of vertical light attenuation coefficient (K) with temperature, salinity, color, turbidity, total suspended solids (TSS), inorganic suspended solids (ISS), organic suspended solids (OSS), total nitrogen (TN), total dissolved nitrogen (TDN), total phosphorus (TP), total dissolved phosphorus (TDP), total silicate, and chlorophyll a, for all stations, and by station. Water quality data were from weekly integrated water samples (November 1993-November 1995); K values were calculated from 15-minute mean PAR values during each water sampling. Values for each combination are Pearson correlation coefficients, level of significance, and (n).

	All	BR	MB	TC	SN	SS	VB	LP
Temperature	-0.119 0.004 (577)	0.021 0.84 (98)	-0.022 0.83 (104)	-0.180 0.22 (49)	-0.165 0.10 (102)	-0.281 0.01 (94)	-0.209 0.23 (34)	-0.415 0.0001 (96)
Salinity	-0.255 0.0001 (577)	-0.179 0.08 (98)	-0.241 0.01 (104)	-0.635 0.0001 (49)	-0.300 0.002 (102)	-0.356 0.0004 (94)	-0.423 0.01 (34)	-0.322 0.001 (96)
Color	0.337 0.0001 (577)	0.244 0.02 (98)	0.313 0.001 (104)	0.547 0.0001 (49)	0.230 0.02 (102)	0.366 0.0003 (94)	0.397 0.02 (34)	0.309 0.002 (96)
Turbidity	0.657 0.0001 (577)	0.337 0.001 (98)	0.706 0.0001 (104)	0.648 0.0001 (49)	0.676 0.0001 (102)	0.717 0.0001 (94)	0.693 0.0001 (34)	0.616 0.0001 (96)
TSS	0.376 0.0001 (573)	0.070 0.50 (98)	0.574 0.0001 (104)	0.196 0.18 (49)	0.245 0.01 (102)	0.270 0.01 (94)	0.564 0.001 (32)	0.494 0.0001 (94)
ISS	0.376 0.0001 (550)	-0.004 0.97 (94)	0.456 0.0001 (100)	0.207 0.15 (49)	0.213 0.03 (98)	0.282 0.01 (91)	0.704 0.0001 (28)	0.521 0.0001 (90)
OSS	0.308 0.0001 (550)	0.133 0.20 (94)	0.582 0.0001 (100)	0.141 0.33 (49)	0.266 0.01 (98)	0.217 0.04 (91)	0.346 0.07 (28)	0.293 0.01 (90)
TN	-0.083 0.047 (577)	-0.129 0.20 (98)	0.044 0.66 (104)	0.182 0.21 (49)	0.338 0.001 (102)	0.296 0.004 (94)	0.058 0.74 (34)	0.087 0.40 (96)
TDN	-0.114 0.01 (577)	-0.113 0.27 (98)	0.054 0.59 (104)	0.143 0.33 (49)	0.389 0.0001 (102)	0.242 0.02 (94)	0.065 0.71 (34)	0.058 0.57 (96)
TP	0.431 0.0001 (577)	0.355 0.0003 (98)	0.346 0.0003 (104)	0.271 0.06 (49)	0.459 0.0001 (102)	0.412 0.0001 (94)	0.209 0.24 (34)	0.371 0.0002 (96)
TDP	0.147 0.0004 (577)	0.266 0.01 (98)	0.007 0.94 (104)	0.090 0.54 (49)	0.032 0.75 (102)	0.137 0.19 (94)	-0.008 0.97 (34)	0.069 0.51 (96)
Silicate	0.211 0.0001 (577)	-0.192 0.06 (98)	0.139 0.16 (104)	-0.055 0.71 (49)	0.085 0.39 (102)	0.099 0.34 (94)	0.440 0.01 (34)	0.332 0.001 (96)
Chlorophyll a	0.415 0.0001 (577)	0.332 0.001 (98)	0.174 0.08 (104)	0.632 0.0001 (49)	0.499 0.0001 (102)	0.482 0.0001 (94)	0.397 0.02 (34)	0.391 0.0001 (96)

Table 7.3 Stepwise multiple regression models for underwater PAR with temperature, salinity, color, turbidity, total suspended solids (=TSS), inorganic suspended solids (=ISS), organic suspended solids (=OSS), total nitrogen (=TN), total dissolved nitrogen (=TDN), total phosphorus (=TP), total dissolved phosphorus (=TDP), total silicate, and chlorophyll a, for all stations, and by station. Water quality data were from weekly integrated water samples (November 1993-November 1995); PAR values were 15-minute mean values during each water sampling. Individual variables had to have a P value <0.15 to be considered for addition to the model and could be removed or added at subsequent steps. Variables were added one at a time as long as P for the model was <0.05.

Station	Step	Factor	Partial R ²	Model R ²	P
All	1	Chlorophyll a	0.162	0.162	0.0001
	2	Color	0.072	0.234	0.0001
	3	Temperature	0.079	0.312	0.0001
	4	OSS	0.047	0.359	0.0001
	5	TDP	0.017	0.376	0.0001
	6	TDN	0.008	0.384	0.01
BR	1	TP	0.275	0.275	0.0001
	2	Salinity	0.100	0.375	0.0003
	3	Silicate	0.072	0.447	0.001
MB	1	Salinity	0.196	0.196	0.0001
	2	TSS	0.167	0.364	0.0001
	3	Temperature	0.098	0.461	0.0001
	4	TDP	0.077	0.538	0.0001
	5	OSS	0.024	0.563	0.02
TC	1	Salinity	0.270	0.270	0.0001
	2	Temperature	0.048	0.318	0.08
	3	TDP	0.115	0.433	0.004
	4	Chlorophyll a	0.054	0.487	0.04
SN	1	Salinity	0.293	0.293	0.0001
	2	ISS	0.165	0.458	0.0001
	3	TP	0.039	0.498	0.01
	4	Temperature	0.074	0.572	0.0001
SS	1	Chlorophyll a	0.343	0.343	0.0001
	2	Color	0.116	0.459	0.0001
	3	Temperature	0.100	0.559	0.0001
	4	TP	0.022	0.581	0.03
VB	1	Salinity	0.207	0.207	0.02
	2	ISS	0.202	0.409	0.01
LP	1	Salinity	0.348	0.348	0.0001
	2	Temperature	0.152	0.500	0.0001
	3	Turbidity	0.057	0.558	0.001

Regression Equations

All: PAR = 41.2 Temperature - 9.80 Color - 12.2 OSS + 151.8 TDN - 3179 TDP - 10.4 Chl a + 374.9

BR: PAR = 38.7 Salinity - 8716 TP + 100.7 Silicate + 188.5

MB: PAR = 74.9 Temperature +50.5 Salinity - 4.6 TSS - 22.1 OSS - 8927 TDP - 661.4

TC: PAR = 46.3 Temperature +33.4 Salinity - 8171 TDP - 11.0 Chl a - 436.8

SN: PAR = 27.2 Temperature + 26.7 Salinity - 2.6 ISS - 4540 TP - 324.7

SS: PAR = 38.1 Temperature - 6.62 Color - 3038 TP - 19.0 Chl a + 441.5

VB: PAR = 49.1 Salinity - 9.7 ISS - 4.1

LP: PAR = 27.3 Temperature + 30.9 Salinity - 14.3 Turbidity - 926.7

Photosynthetically Active Radiation, Water Quality, and Submerged Aquatic Vegetation in IRL

Table 7.4 Stepwise multiple regression models for vertical light attenuation coefficient (K) with temperature, salinity, color, turbidity, total suspended solids (=TSS), inorganic suspended solids (=ISS), organic suspended solids (=OSS), total nitrogen (=TN), dissolved nitrogen (=TDN), total phosphorus (=TP), dissolved phosphorus (=TDP), total silicate, and chlorophyll a, for all stations, and by station. Water quality data were from weekly integrated water samples (November 1993-November 1995); PAR values were 15-minute mean values during each water sampling. Individual variables had to have a P value < 0.15 to be considered for addition to the model and could be removed or added at subsequent steps. Variables were added one at a time as long as P for the model was <0.05.

Station	Step	Factor	Partial R ²	Model R ²	P
All	1	Turbidity	0.430	0.430	0.0001
	2	Color	0.096	0.526	0.0001
	3	ISS	0.003	0.529	0.07
	4	Salinity	0.006	0.536	0.01
	5	TSS	0.005	0.540	0.02
BR	1	TP	0.127	0.127	0.0004
	2	Silicate	0.040	0.167	0.04
	3	Salinity	0.045	0.212	0.03
MB	1	Turbidity	0.500	0.500	0.0001
	2	Salinity	0.018	0.518	0.06
	3	Chlorophyll a TSS	0.025	0.543	0.02
	4		0.032	0.575	0.01
TC	1	Turbidity	0.420	0.420	0.0001
	2	Color	0.169	0.589	0.0001
	3	ISS	0.060	0.649	0.01
	4	Chlorophyll a	0.033	0.682	0.04
SN	1	Turbidity	0.470	0.470	0.0001
	2	Salinity	0.121	0.590	0.0001
	3	OSS	0.032	0.622	0.01
	4	TDN	0.019	0.641	0.03
SS	1	Turbidity	0.524	0.524	0.0001
	2	Color	0.204	0.728	0.0001
VB	1	ISS	0.496	0.496	0.0001
	2	Salinity	0.146	0.642	0.004
LP	1	Turbidity	0.352	0.352	0.0001
	2	Silicate	0.090	0.442	0.003
	3	ISS	0.050	0.492	0.005
	4	Salinity	0.053	0.545	0.002

Regression Equations

- All: $K = -0.02 \text{ Salinity} + 0.02 \text{ Color} + 0.10 \text{ Turbidity} - 0.01 \text{ TSS} + 0.02 \text{ ISS} + 0.88$
 BR: $K = -0.03 \text{ Salinity} + 10.3 \text{ TP} - 0.17 \text{ Silicate} + 1.59$
 MB: $K = -0.05 \text{ Salinity} + 0.09 \text{ Turbidity} + 0.02 \text{ TSS} - 0.02 \text{ Chl } a + 1.59$
 TC: $K = 0.02 \text{ Color} + 0.08 \text{ Turbidity} - 0.02 \text{ ISS} + 0.02 \text{ Chl } a + 0.71$
 SN: $K = -0.03 \text{ Salinity} + 0.17 \text{ Turbidity} - 0.03 \text{ OSS} + 1.15 \text{ TDN} + 2.03$
 SS: $K = 0.02 \text{ Color} + 0.15 \text{ Turbidity} + 0.14$
 VB: $K = -0.10 \text{ Salinity} + 0.04 \text{ ISS} + 2.58$
 LP: $K = -0.05 \text{ Salinity} + 0.03 \text{ Turbidity} + 0.02 \text{ ISS} + 0.10 \text{ Silicate} + 1.79$

Table 7.5 Correlation coefficients of seagrass cover, seagrass above-ground biomass, and epiphyte loads with underwater PAR for all stations, and by station. Seagrass and epiphyte data are from seasonal sampling. PAR values were mean values during each season. Values for each combination are Pearson correlation coefficients, level of significance, and (n). Epiphyte load was measured only during Year 1.

	All	BR	MB	TC	SN	SS	VB	LP
Seagrass Cover	0.149	-0.022	0.323	0.619	0.506	0.714	0.455	0.452
	0.31	0.96	0.44	0.38	0.20	0.047	0.54	0.26
	(48)	(8)	(8)	(4)	(8)	(8)	(4)	(8)
Seagrass Biomass	0.300	0.434	0.686	0.810	0.537	0.546	0.311	0.555
	0.04	0.28	0.06	0.19	0.17	0.16	0.69	0.15
	(48)	(8)	(8)	(4)	(8)	(8)	(4)	(8)
Epiphyte Load	-0.109	0.398	-0.771	—	-0.446	0.539	0.147	0.136
	0.61	0.60	0.23		0.55	0.46	0.85	0.86
	(24)	(4)	(4)		(4)	(4)	(4)	(4)

Table 7.6 Correlation coefficients of seagrass cover, seagrass above-ground biomass, and epiphyte loads with vertical light attenuation coefficient (K) for all stations, and by station. Seagrass and epiphyte data are from seasonal sampling. PAR values were mean values during each season. Values for each combination are Pearson correlation coefficients, level of significance, and (n). Epiphyte load was measured only during Year 1.

	All	BR	MB	TC	SN	SS	VB	LP
Seagrass Cover	-0.401 0.005 (48)	-0.032 0.94 (8)	0.280 0.50 (8)	-0.605 0.39 (4)	-0.569 0.14 (8)	-0.213 0.61 (8)	-0.487 0.51 (4)	-0.666 0.07 (8)
Seagrass Biomass	-0.355 0.01 (48)	0.044 0.92 (8)	-0.406 0.32 (8)	-0.676 0.32 (4)	-0.529 0.18 (8)	-0.163 0.70 (8)	-0.196 0.80 (4)	-0.867 0.01 (8)
Epiphyte Load	0.067 0.75 (24)	-0.869 0.13 (4)	0.945 0.06 (4)	—	-0.020 0.98 (4)	-0.724 0.28 (4)	-0.275 0.73 (4)	0.006 0.99 (4)

Table 7.7 Correlation coefficients of seagrass cover with temperature, salinity, color, turbidity, total suspended solids (=TSS), inorganic suspended solids (=ISS), organic suspended solids (=OSS), total nitrogen (=TN), dissolved nitrogen (=TDN), total phosphorus (=TP), dissolved phosphorus (=TDP), total silicate, and chlorophyll a, for all stations, and by station. Biomass data were from the seasonal samplings. Water quality data were seasonal averages of the weekly integrated water samples (November 1993-November 1995). Values for each combination are Pearson correlation coefficients and level of significance, and (n).

	All	BR	MB	TC	SN	SS	VB	LP
Temperature	0.128	-0.095	0.286	-0.015	0.323	0.791	0.481	0.714
	0.39	0.82	0.49	0.98	0.44	0.02	0.52	0.05
	(48)	(8)	(8)	(4)	(8)	(8)	(4)	(8)
Salinity	0.541	0.638	-0.109	0.832	0.598	0.500	0.322	0.266
	0.0001	0.09	0.80	0.17	0.12	0.21	0.68	0.52
	(48)	(8)	(8)	(4)	(8)	(8)	(4)	(8)
Color	-0.194	-0.225	0.089	-0.741	-0.340	-0.242	-0.319	-0.142
	0.19	0.59	0.83	0.26	0.41	0.56	0.68	0.74
	(48)	(8)	(8)	(4)	(8)	(8)	(4)	(8)
Turbidity	-0.268	-0.125	-0.271	-0.722	0.197	-0.676	-0.654	-0.503
	0.07	0.77	0.52	0.28	0.64	0.07	0.35	0.20
	(48)	(8)	(8)	(4)	(8)	(8)	(4)	(8)
TSS	0.031	-0.231	-0.270	0.163	0.288	-0.316	-0.518	-0.116
	0.83	0.58	0.52	0.84	0.49	0.45	0.48	0.78
	(48)	(8)	(8)	(4)	(8)	(8)	(4)	(8)
ISS	0.003	-0.317	0.032	0.383	0.316	-0.347	-0.467	-0.208
	0.98	0.44	0.94	0.62	0.45	0.40	0.53	0.62
	(48)	(8)	(8)	(4)	(8)	(8)	(4)	(8)
OSS	0.002	-0.365	0.614	-0.388	0.223	-0.272	-0.494	0.374
	0.99	0.37	0.11	0.61	0.59	0.51	0.51	0.36
	(48)	(8)	(8)	(4)	(8)	(8)	(4)	(8)
TN	0.109	0.479	0.057	0.881	0.118	-0.257	0.073	0.079
	0.46	0.23	0.89	0.12	0.78	0.54	0.93	0.85
	(48)	(8)	(8)	(4)	(8)	(8)	(4)	(8)
TDN	0.192	0.602	0.051	0.865	0.220	-0.230	-0.089	0.197
	0.19	0.11	0.90	0.13	0.60	0.58	0.91	0.64
	(48)	(8)	(8)	(4)	(8)	(8)	(4)	(8)
TP	-0.308	0.106	0.193	-0.068	-0.040	-0.422	-0.653	-0.052
	0.03	0.80	0.65	0.93	0.93	0.30	0.35	0.90
	(48)	(8)	(8)	(4)	(8)	(8)	(4)	(8)
TDP	-0.188	0.282	0.125	-0.067	-0.131	-0.102	-0.557	0.036
	0.20	0.50	0.77	0.93	0.76	0.81	0.44	0.93
	(48)	(8)	(8)	(4)	(8)	(8)	(4)	(8)
Silicate	-0.554	-0.754	0.234	0.138	-0.178	-0.561	-0.287	-0.308
	0.0001	0.03	0.58	0.86	0.67	0.15	0.71	0.46
	(48)	(8)	(8)	(4)	(8)	(8)	(4)	(8)
Chlorophyll a	-0.225	-0.021	0.569	-0.813	-0.268	-0.879	-0.101	0.055
	0.12	0.96	0.14	0.19	0.52	0.004	0.90	0.90
	(48)	(8)	(8)	(4)	(8)	(8)	(4)	(8)

Table 7.8 Correlation coefficients of seagrass above-ground biomass with temperature, salinity, color, turbidity, total suspended solids (=TSS), inorganic suspended solids (=ISS), organic suspended solids (=OSS), total nitrogen (=TN), dissolved nitrogen (=TDN), total phosphorus (=TP), dissolved phosphorus (=TDP), total silicate, and chlorophyll a, for all stations, and by station. Biomass data were from the seasonal samplings. Water quality data were seasonal averages of the weekly integrated water samples (November 1993-November 1995). Values for each combination are Pearson correlation coefficients and level of significance, and (n).

	All	BR	MB	TC	SN	SS	VB	LP
Temperature	0.344	0.369	0.283	0.718	0.686	0.786	0.888	0.602
	0.02	0.37	0.50	0.28	0.06	0.02	0.11	0.11
	(48)	(8)	(8)	(4)	(8)	(8)	(4)	(8)
Salinity	0.407	0.699	0.653	0.912	0.394	0.264	-0.053	0.353
	0.004	0.05	0.08	0.09	0.33	0.53	0.95	0.39
	(48)	(8)	(8)	(4)	(8)	(8)	(4)	(8)
Color	-0.129	-0.421	-0.474	-0.417	-0.067	-0.043	0.172	-0.396
	0.38	0.30	0.24	0.58	0.88	0.92	0.83	0.33
	(48)	(8)	(8)	(4)	(8)	(8)	(4)	(8)
Turbidity	-0.225	-0.510	-0.605	-0.981	-0.390	-0.651	-0.446	-0.601
	0.12	0.20	0.11	0.02	0.34	0.08	0.55	0.12
	(48)	(8)	(8)	(4)	(8)	(8)	(4)	(8)
TSS	-0.058	-0.249	-0.226	0.818	0.018	-0.337	-0.566	-0.082
	0.70	0.55	0.59	0.18	0.97	0.41	0.43	0.85
	(48)	(8)	(8)	(4)	(8)	(8)	(4)	(8)
ISS	-0.066	-0.015	-0.184	0.667	-0.081	-0.368	-0.636	-0.130
	0.66	0.97	0.66	0.33	0.85	0.37	0.36	0.76
	(48)	(8)	(8)	(4)	(8)	(8)	(4)	(8)
OSS	-0.063	-0.377	-0.214	0.216	0.057	-0.295	0.136	0.141
	0.67	0.36	0.61	0.78	0.89	0.48	0.86	0.74
	(48)	(8)	(8)	(4)	(8)	(8)	(4)	(8)
TN	0.138	0.293	-0.167	0.224	-0.089	-0.097	0.468	0.198
	0.35	0.48	0.69	0.78	0.83	0.82	0.53	0.64
	(48)	(8)	(8)	(4)	(8)	(8)	(4)	(8)
TDN	0.160	0.223	-0.074	0.160	-0.108	-0.011	0.447	0.322
	0.28	0.60	0.86	0.84	0.80	0.98	0.55	0.44
	(48)	(8)	(8)	(4)	(8)	(8)	(4)	(8)
TP	-0.033	-0.163	0.091	0.275	0.136	-0.250	-0.094	-0.314
	0.82	0.70	0.83	0.73	0.75	0.55	0.91	0.45
	(48)	(8)	(8)	(4)	(8)	(8)	(4)	(8)
TDP	0.050	-0.104	0.115	0.166	0.126	-0.047	0.041	-0.150
	0.73	0.81	0.79	0.83	0.77	0.91	0.96	0.72
	(48)	(8)	(8)	(4)	(8)	(8)	(4)	(8)
Silicate	-0.387	-0.574	-0.279	0.736	-0.061	-0.515	0.070	-0.531
	0.01	0.14	0.50	0.26	0.89	0.19	0.93	0.18
	(48)	(8)	(8)	(4)	(8)	(8)	(4)	(8)
Chlorophyll a	-0.018	-0.197	-0.392	-0.703	-0.328	-0.715	0.520	-0.202
	0.90	0.64	0.34	0.30	0.43	0.05	0.48	0.63
	(48)	(8)	(8)	(4)	(8)	(8)	(4)	(8)

Photosynthetically Active Radiation, Water Quality, and Submerged Aquatic Vegetation in IRL

Table 7.9 Correlation coefficients of epiphyte load with temperature, salinity, color, turbidity, total suspended solids (=TSS), inorganic suspended solids (=ISS), organic suspended solids (=OSS), total nitrogen (=TN), dissolved nitrogen (=TDN), total phosphorus (=TP), dissolved phosphorus (=TDP), total silicate, and chlorophyll *a*, for all stations, and by station. Biomass data were from the seasonal samplings. Water quality data were seasonal averages of the weekly integrated water samples (November 1993-November 1995). Values for each combination are Pearson correlation coefficients and level of significance, and (n).

	All	BR	MB	SN	SS	VB	LP
Temperature	0.131	-0.451	0.518	0.316	0.249	-0.711	0.813
	0.54	0.55	0.48	0.68	0.75	0.29	0.19
	(24)	(4)	(4)	(4)	(4)	(4)	(4)
Salinity	-0.252	0.393	-0.994	-0.537	0.471	0.505	-0.292
	0.23	0.61	0.01	0.46	0.53	0.50	0.71
	(24)	(4)	(4)	(4)	(4)	(4)	(4)
Color	0.077	-0.460	0.951	0.391	-0.330	-0.600	0.426
	0.72	0.54	0.048	0.61	0.67	0.40	0.57
	(24)	(4)	(4)	(4)	(4)	(4)	(4)
Turbidity	-0.118	0.130	0.859	-0.075	-0.474	-0.014	-0.772
	0.58	0.87	0.14	0.93	0.53	0.99	0.23
	(24)	(4)	(4)	(4)	(4)	(4)	(4)
TSS	-0.293	-0.797	-0.399	-0.285	-0.397	0.157	-0.812
	0.16	0.20	0.60	0.72	0.60	0.84	0.19
	(24)	(4)	(4)	(4)	(4)	(4)	(4)
ISS	-0.258	-0.475	-0.380	-0.210	-0.430	0.273	-0.887
	0.22	0.52	0.62	0.79	0.57	0.73	0.11
	(24)	(4)	(4)	(4)	(4)	(4)	(4)
OSS	-0.049	-0.498	0.771	0.320	-0.139	-0.521	0.014
	0.82	0.50	0.23	0.68	0.86	0.48	0.99
	(24)	(4)	(4)	(4)	(4)	(4)	(4)
TN	0.028	-0.858	0.695	0.567	-0.363	-0.818	0.488
	0.89	0.14	0.31	0.43	0.64	0.18	0.51
	(24)	(4)	(4)	(4)	(4)	(4)	(4)
TDN	-0.015	-0.578	0.246	0.689	-0.356	-0.802	0.361
	0.94	0.42	0.75	0.31	0.65	0.20	0.64
	(24)	(4)	(4)	(4)	(4)	(4)	(4)
TP	0.121	-0.602	0.710	0.690	-0.284	-0.326	0.015
	0.57	0.40	0.29	0.31	0.72	0.67	0.99
	(24)	(4)	(4)	(4)	(4)	(4)	(4)
TDP	0.338	-0.383	0.791	0.844	0.249	-0.448	0.451
	0.11	0.62	0.21	0.16	0.75	0.55	0.55
	(24)	(4)	(4)	(4)	(4)	(4)	(4)
Silicate	0.419	-0.503	0.943	0.604	-0.081	-0.518	0.317
	0.04	0.50	0.06	0.40	0.92	0.48	0.68
	(24)	(4)	(4)	(4)	(4)	(4)	(4)
Chlorophyll <i>a</i>	-0.034	-0.668	0.982	0.491	-0.419	-0.823	0.335
	0.88	0.33	0.02	0.51	0.58	0.18	0.67
	(24)	(4)	(4)	(4)	(4)	(4)	(4)

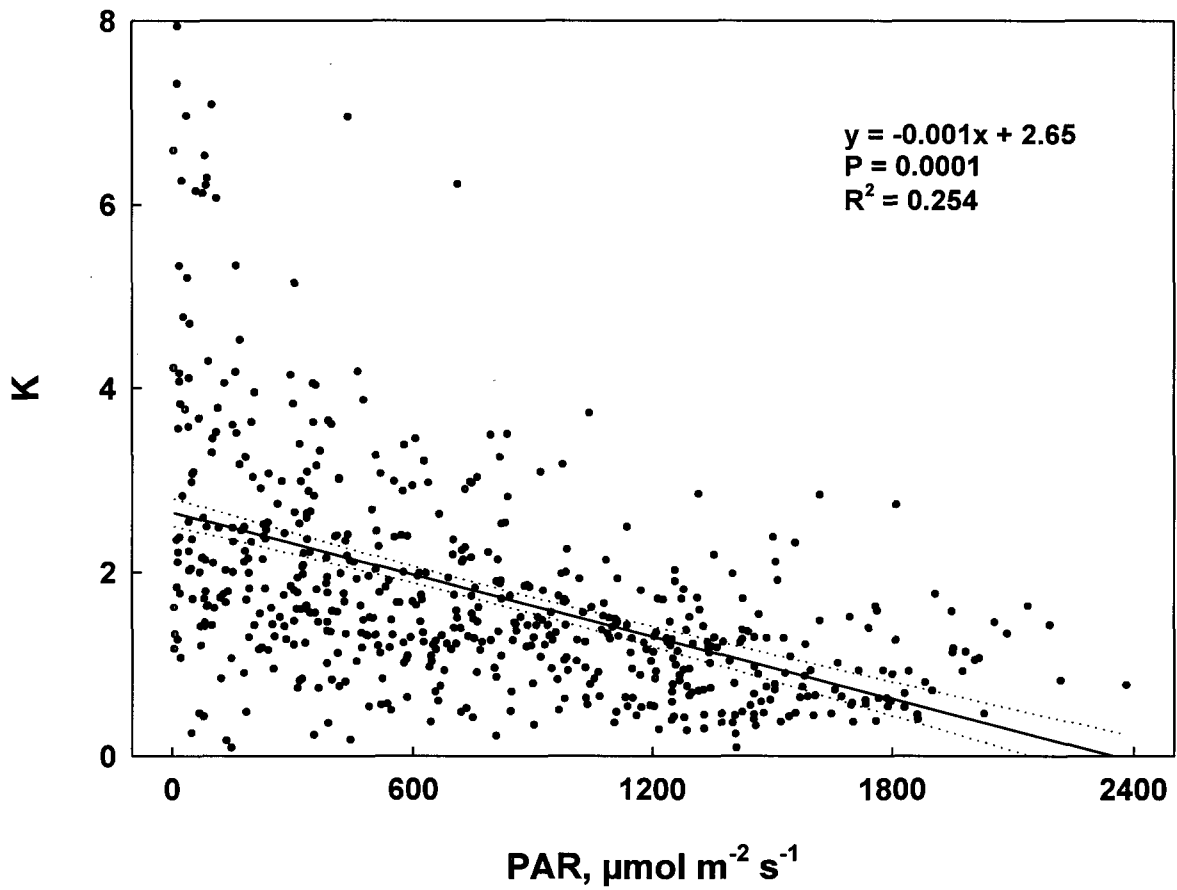


Fig. 7.1 Linear regression analysis of light attenuation coefficient (K) vs. underwater PAR based on weekly water quality sampling at IRL monitoring stations (all stations combined). Dotted lines indicate 95% confidence intervals of the regression line.

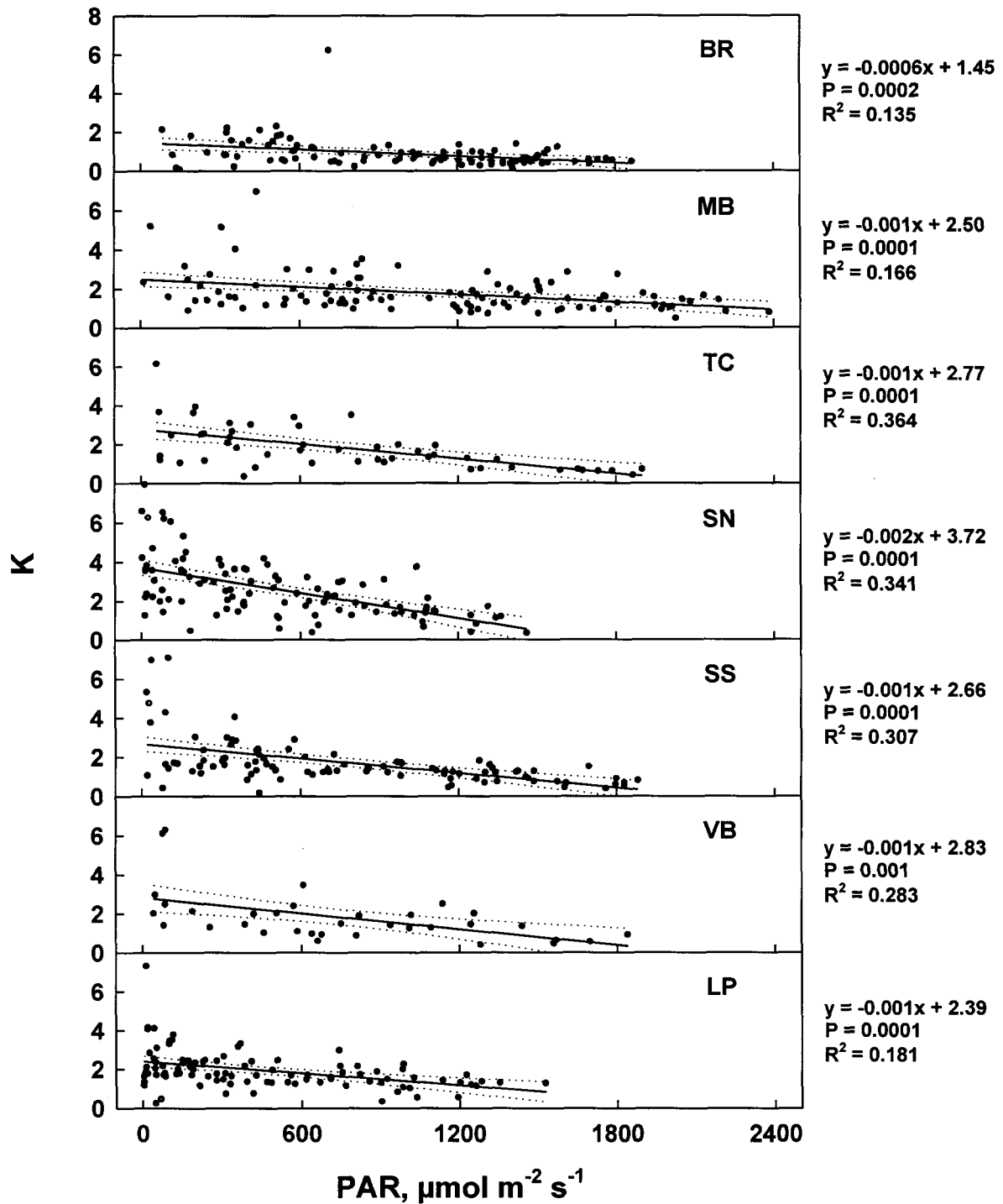


Fig. 7.2 Linear regression analysis of light attenuation coefficient (K) vs. underwater PAR based on weekly water quality sampling at each IRL monitoring station. Dotted lines indicate 95% confidence intervals of the regression line.

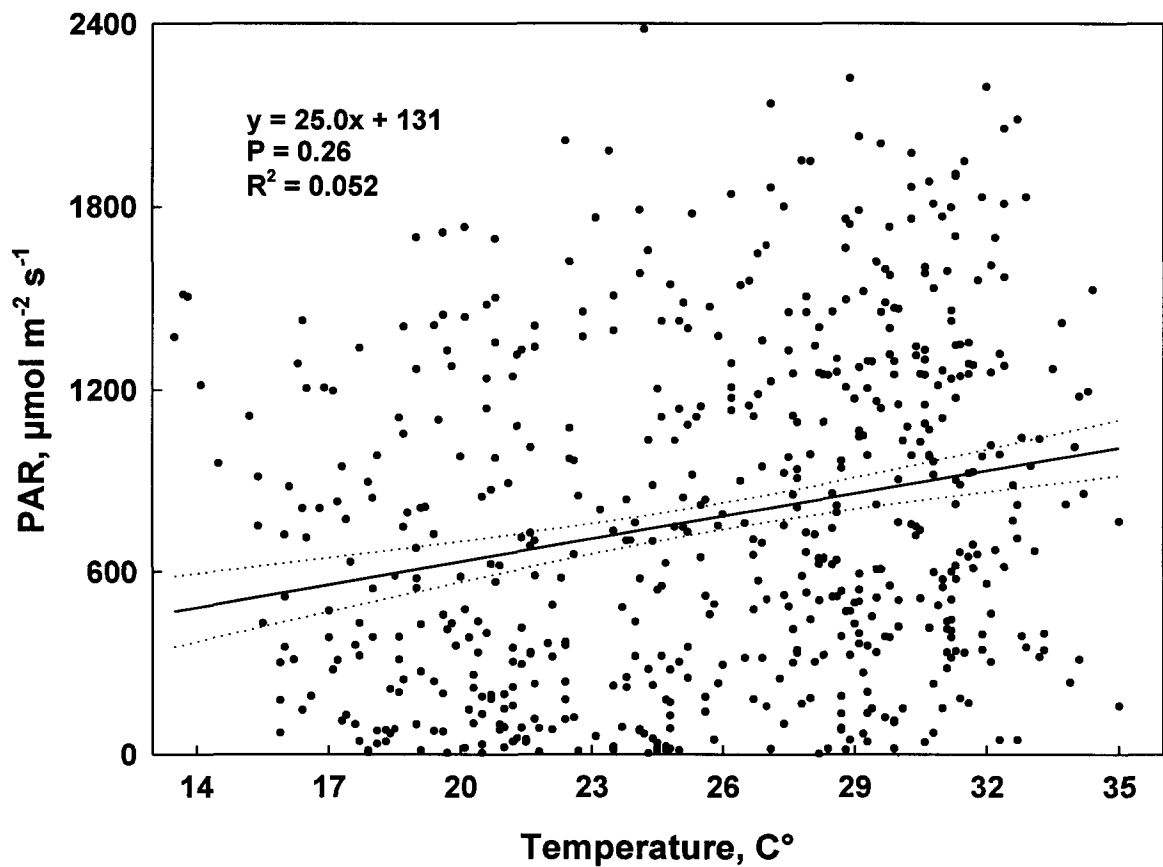


Fig. 7.3 Linear regression analysis of underwater PAR vs. temperature based on weekly water quality sampling at IRL monitoring stations (all stations combined). Dotted lines indicate 95% confidence intervals of the regression line.

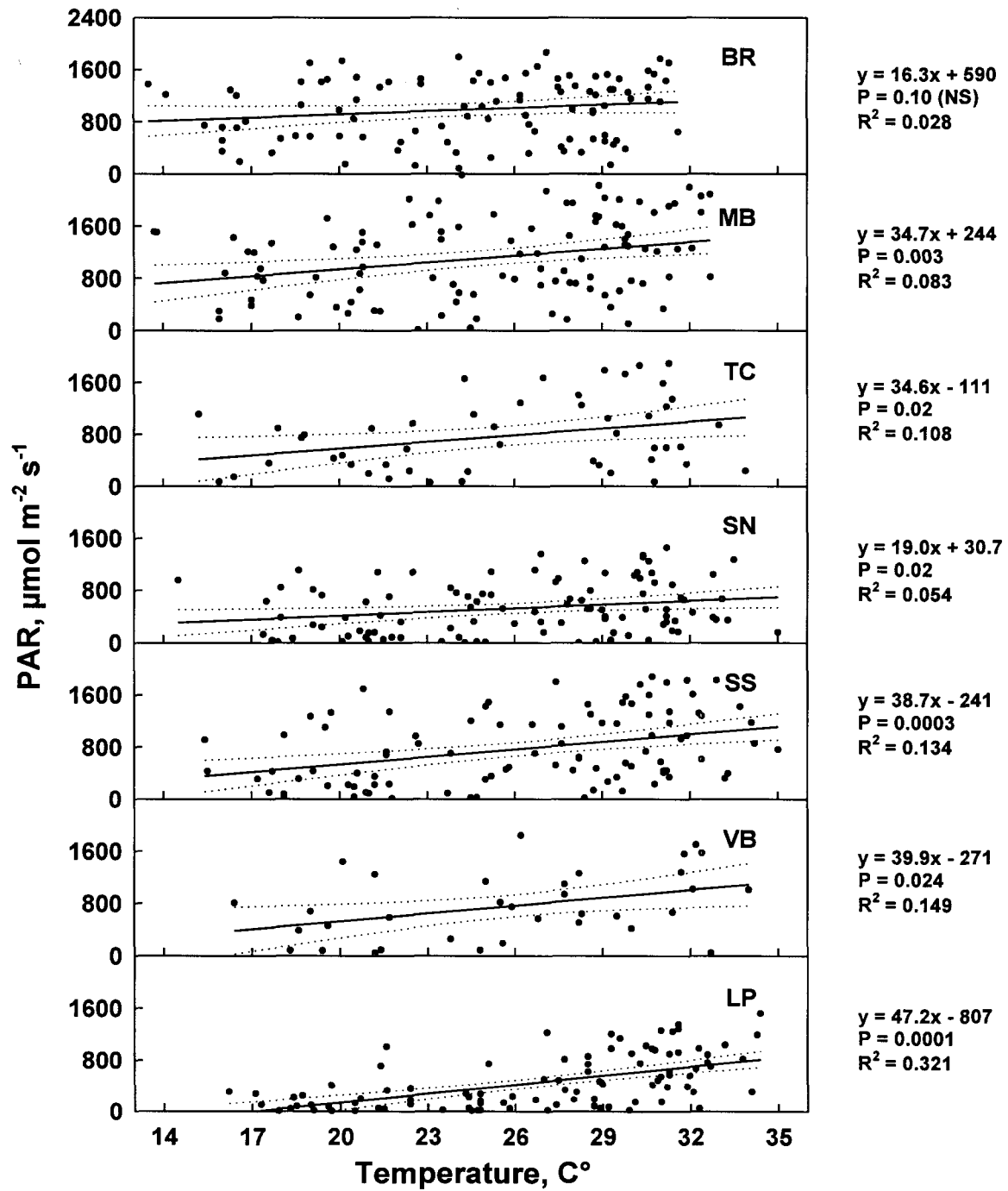


Fig. 7.4 Linear regression analysis of underwater PAR vs. temperature based on weekly water quality sampling at each IRL monitoring station. Dotted lines indicate 95% confidence intervals of the regression line.

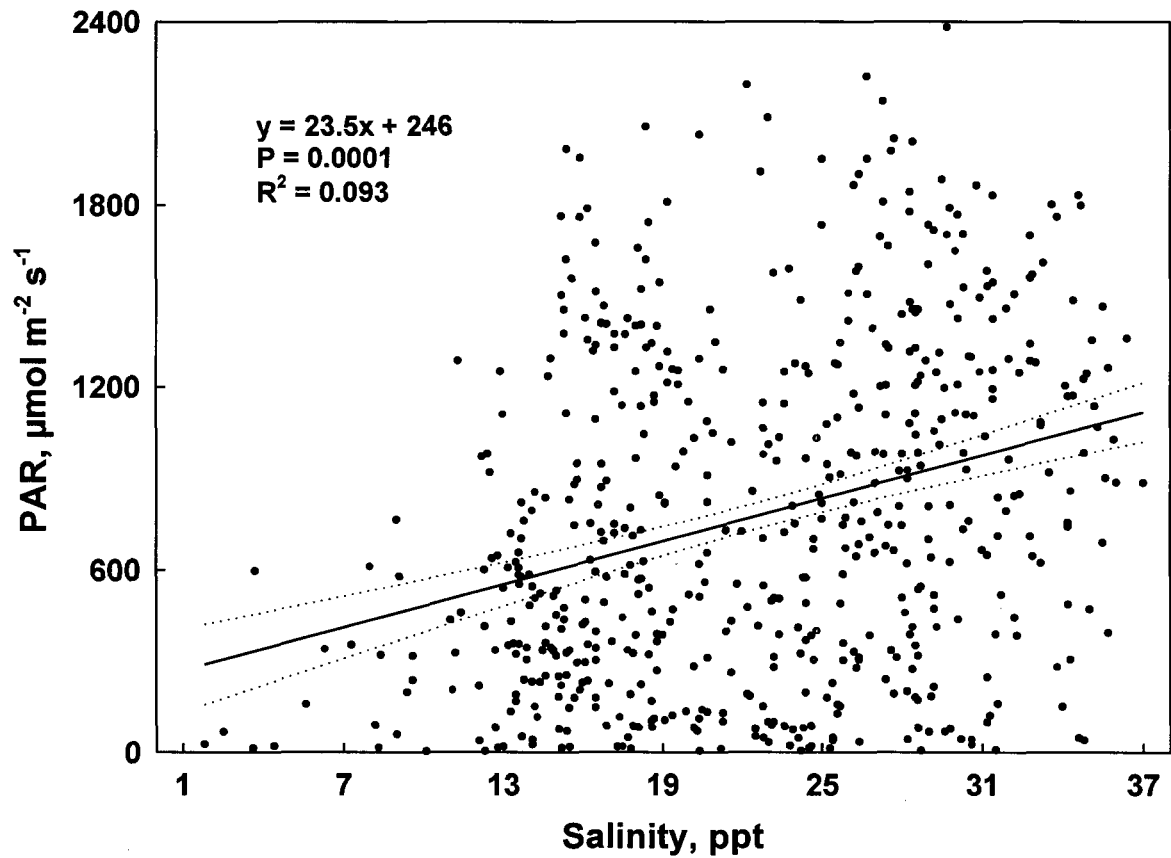


Fig. 7.5 Linear regression analysis of underwater PAR vs. salinity based on weekly water quality sampling at IRL monitoring stations (all stations combined). Dotted lines indicate 95% confidence intervals of the regression line.

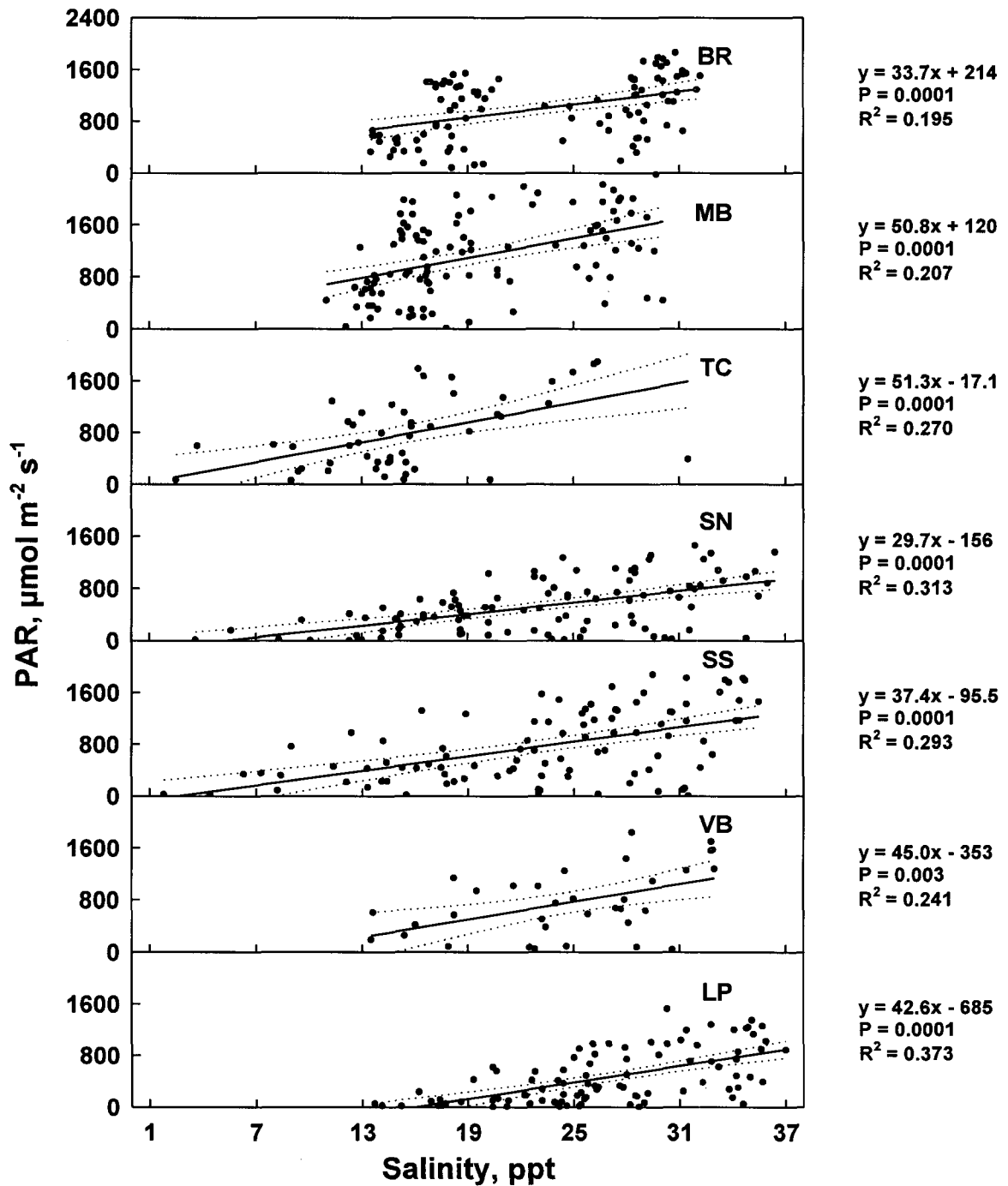


Fig. 7.6 Linear regression analysis of underwater PAR vs. salinity based on weekly water quality sampling at each IRL monitoring station. Dotted lines indicate 95% confidence intervals of the regression line.

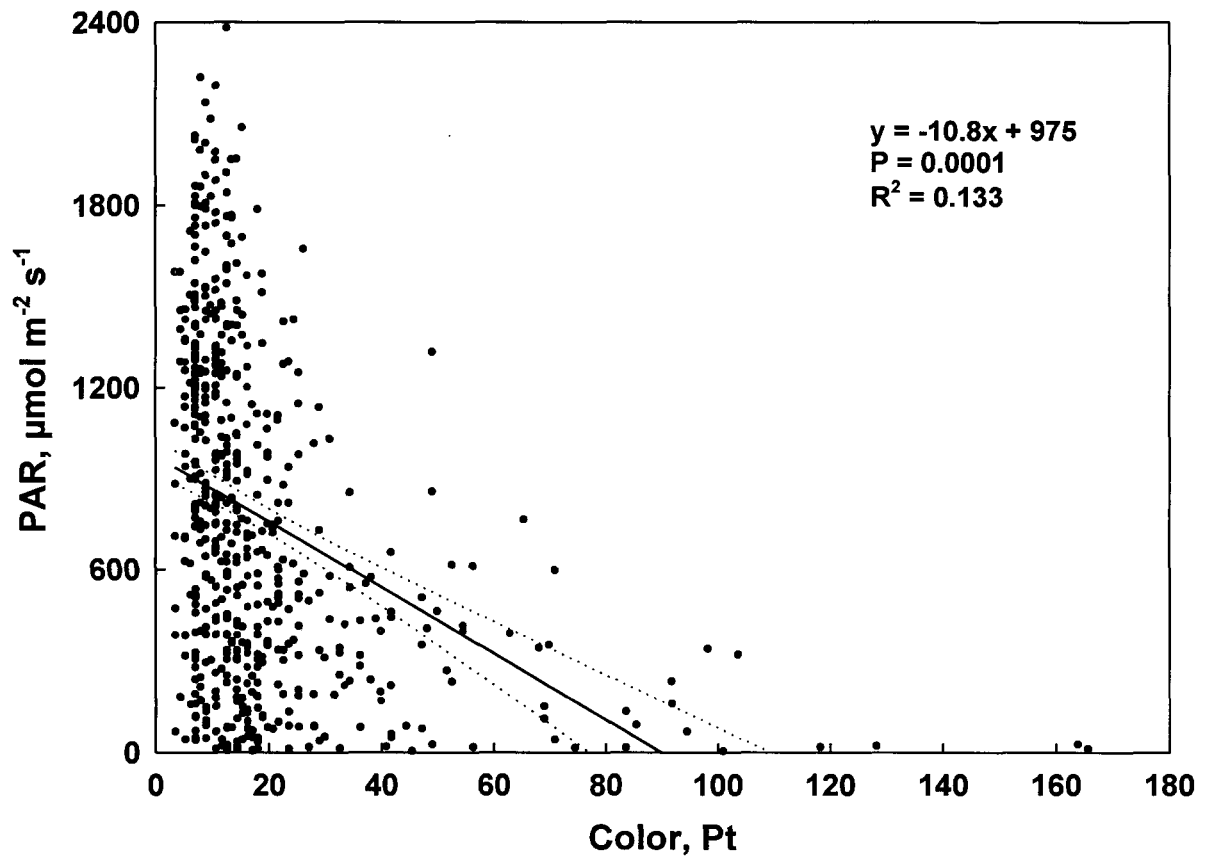


Fig. 7.7 Linear regression analysis of underwater PAR vs. color based on weekly water quality sampling at IRL monitoring stations (all stations combined). Dotted lines indicate 95% confidence intervals of the regression line.

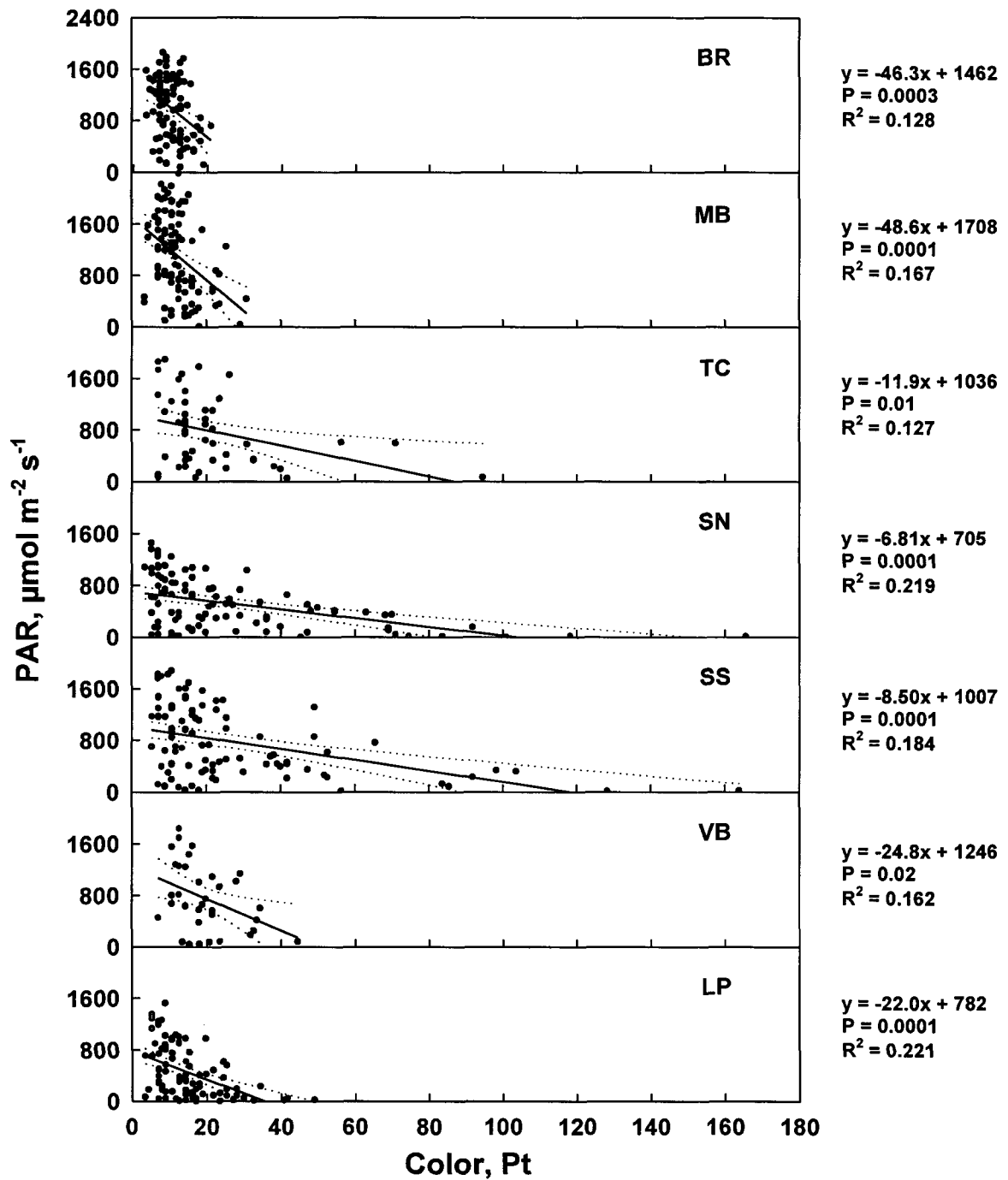


Fig. 7.8 Linear regression analysis of underwater PAR vs. color based on weekly water quality sampling at each IRL monitoring station. Dotted lines indicate 95% confidence intervals of the regression line.

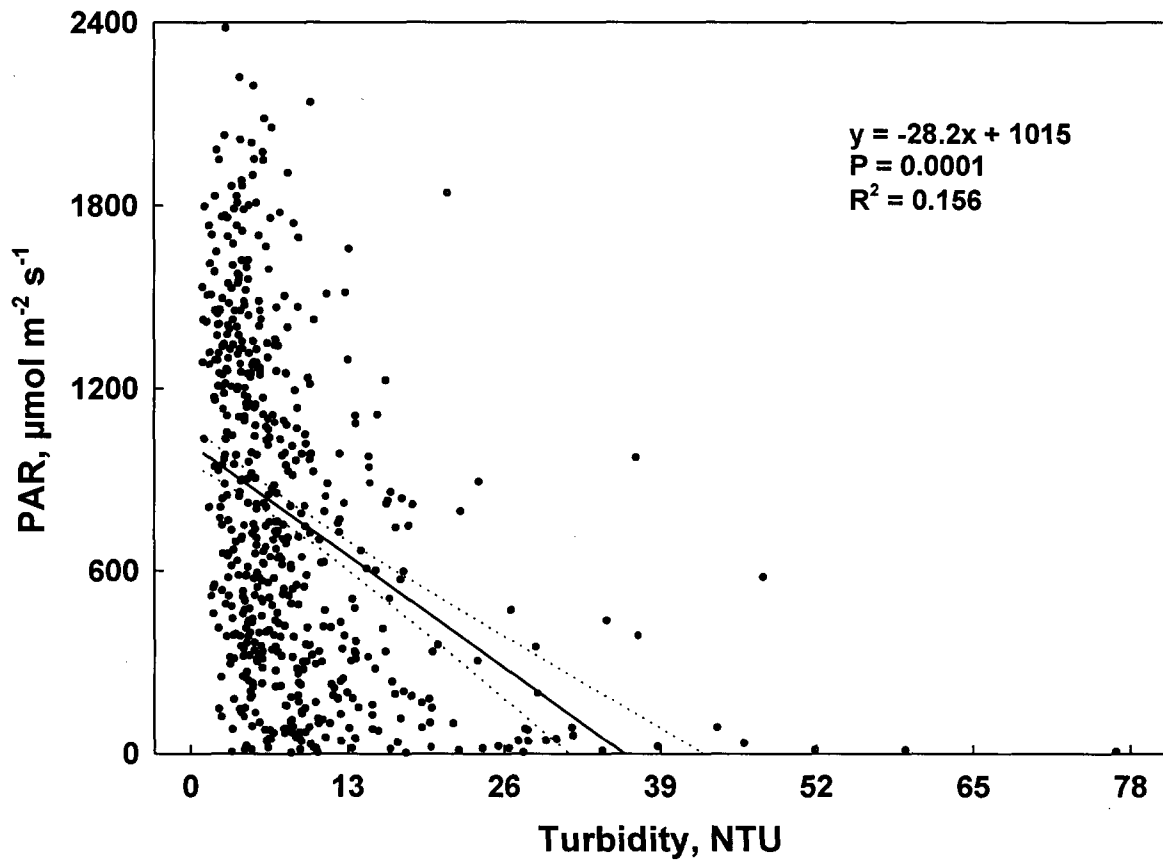


Fig. 7.9 Linear regression analysis of underwater PAR vs. turbidity based on weekly water quality sampling at IRL monitoring stations (all stations combined). Dotted lines indicate 95% confidence intervals of the regression line.

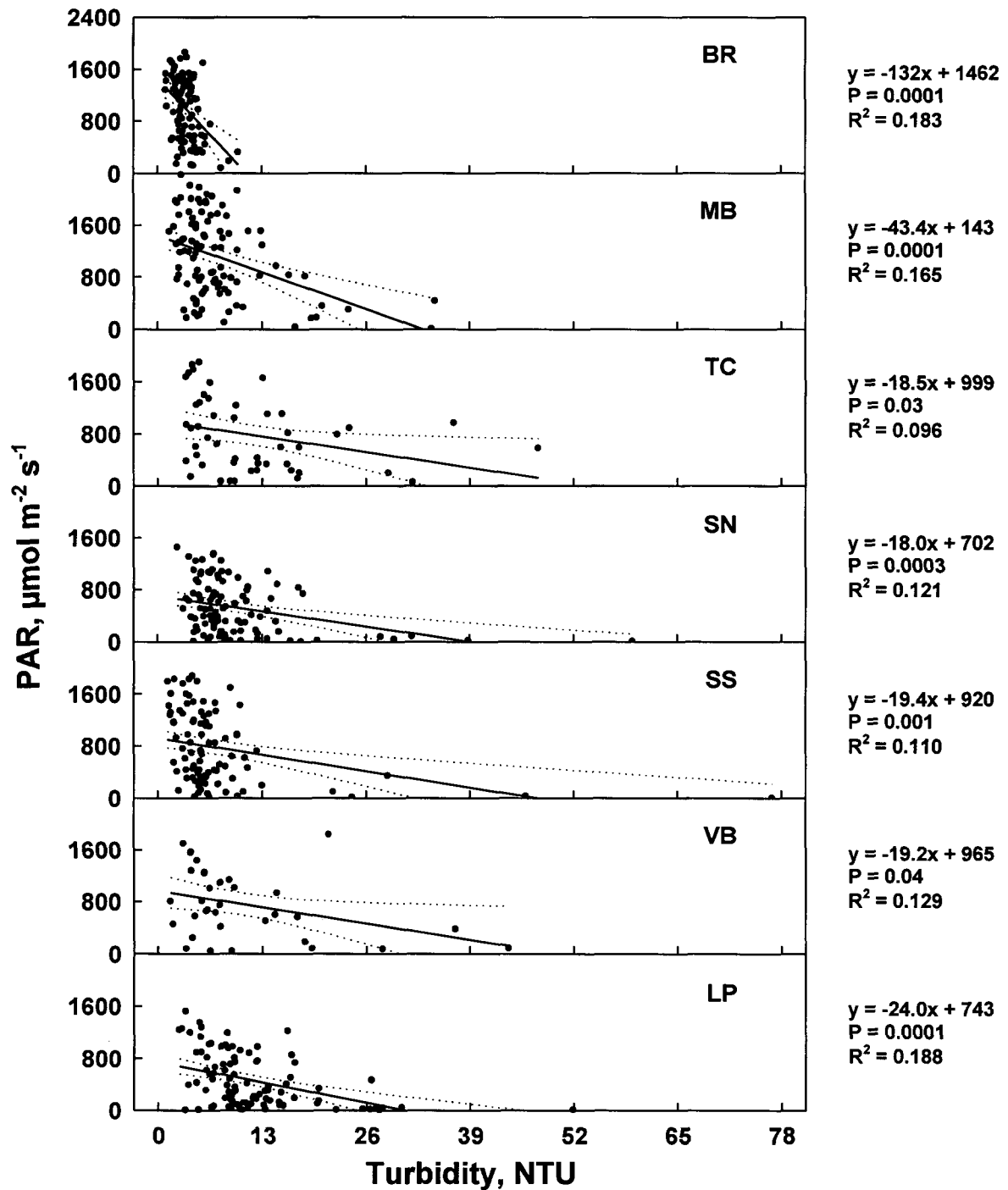


Fig. 7.10 Linear regression analysis of underwater PAR vs. turbidity based on weekly water quality sampling at each IRL monitoring station. Dotted lines indicate 95% confidence intervals of the regression line.

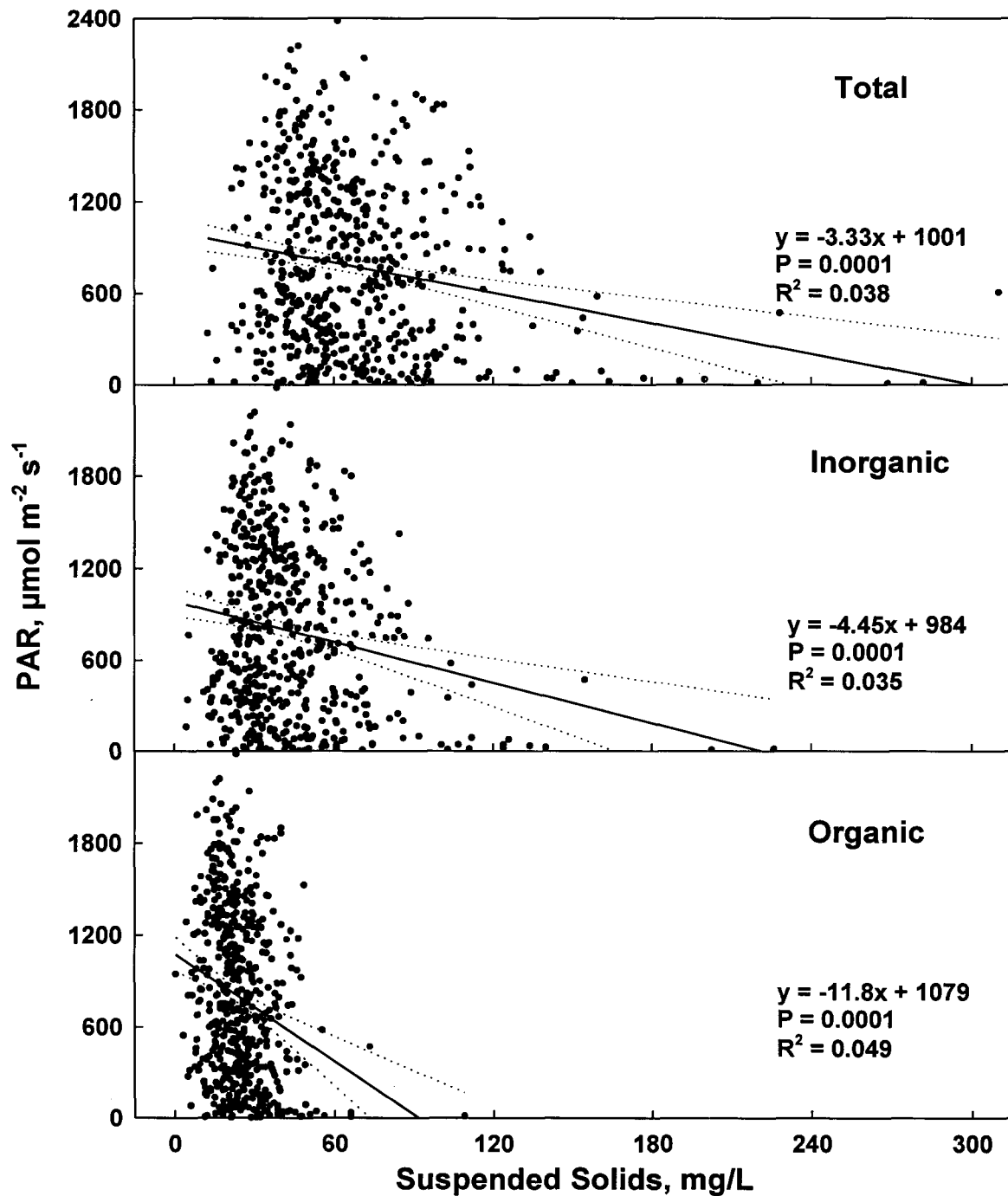


Fig. 7.11 Linear regression analysis of underwater PAR vs. total, inorganic, and organic suspended solids based on weekly water quality sampling at IRL monitoring stations (all stations combined). Dotted lines indicate 95% confidence intervals of the regression line.

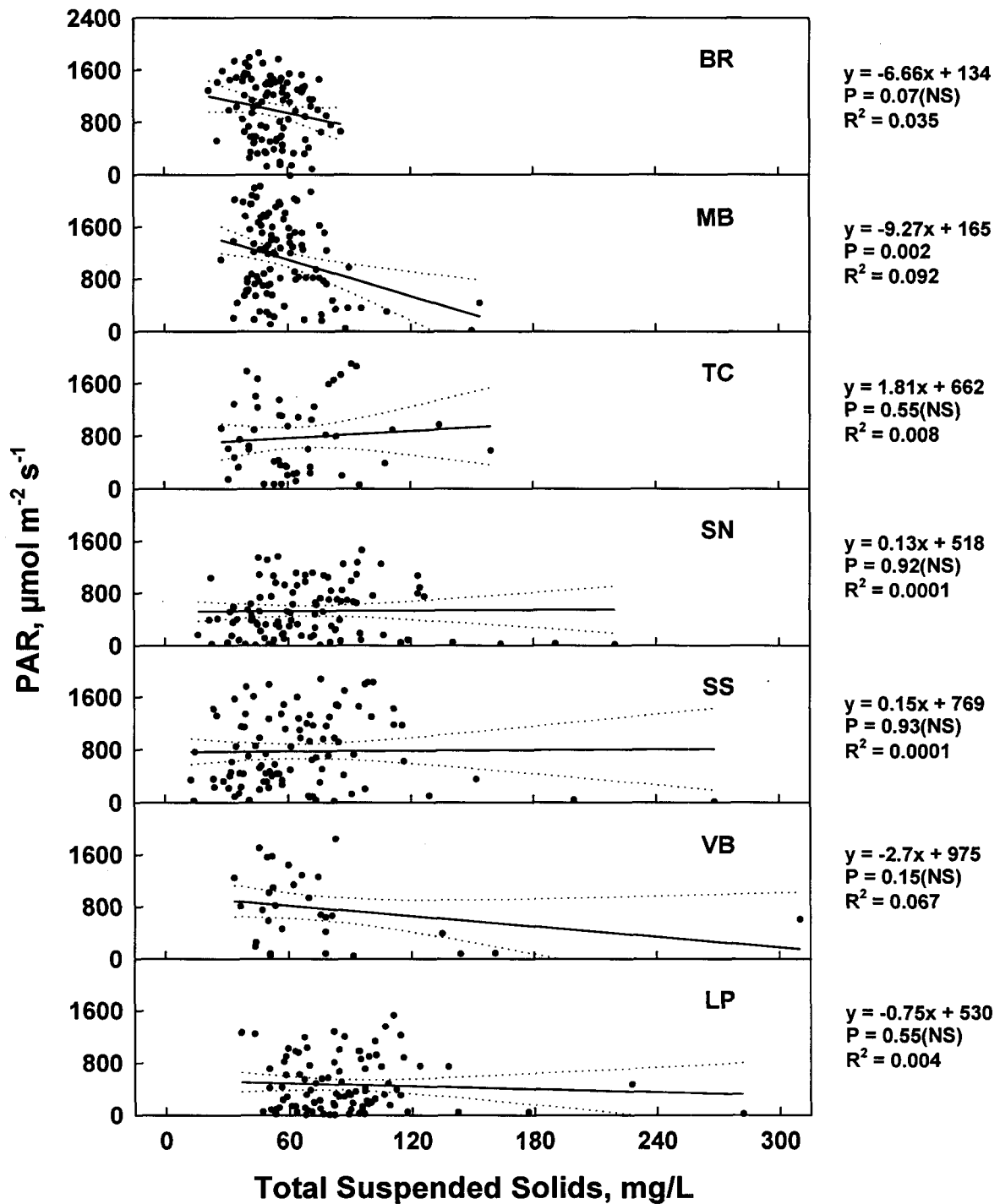


Fig. 7.12 Linear regression analysis of underwater PAR vs. total suspended solids based on weekly water quality sampling at each IRL monitoring station. Dotted lines indicate 95% confidence intervals of the regression line.

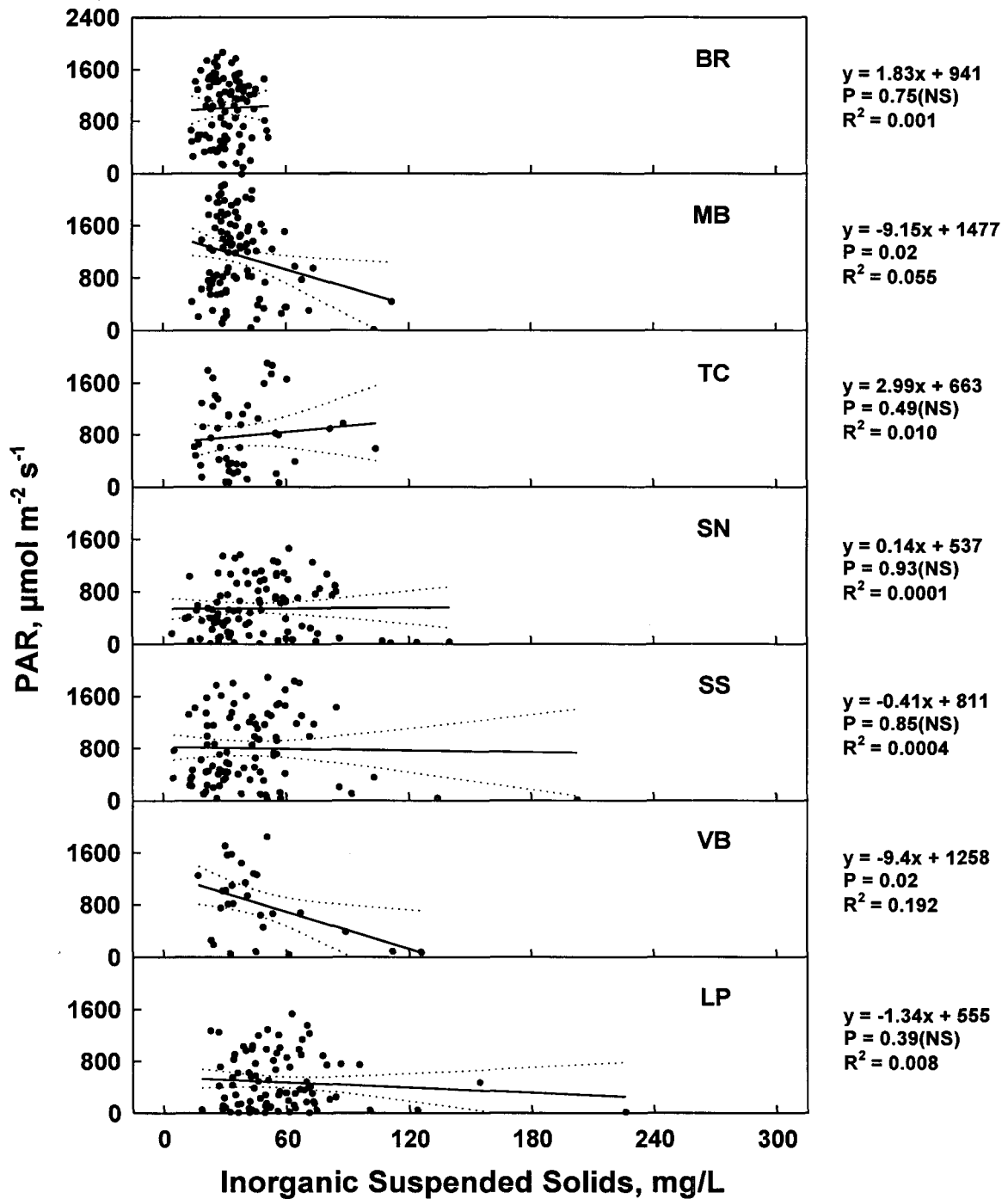


Fig. 7.13 Linear regression analysis of underwater PAR vs. inorganic suspended solids based on weekly water quality sampling at each IRL monitoring station. Dotted lines indicate 95% confidence intervals of the regression line.

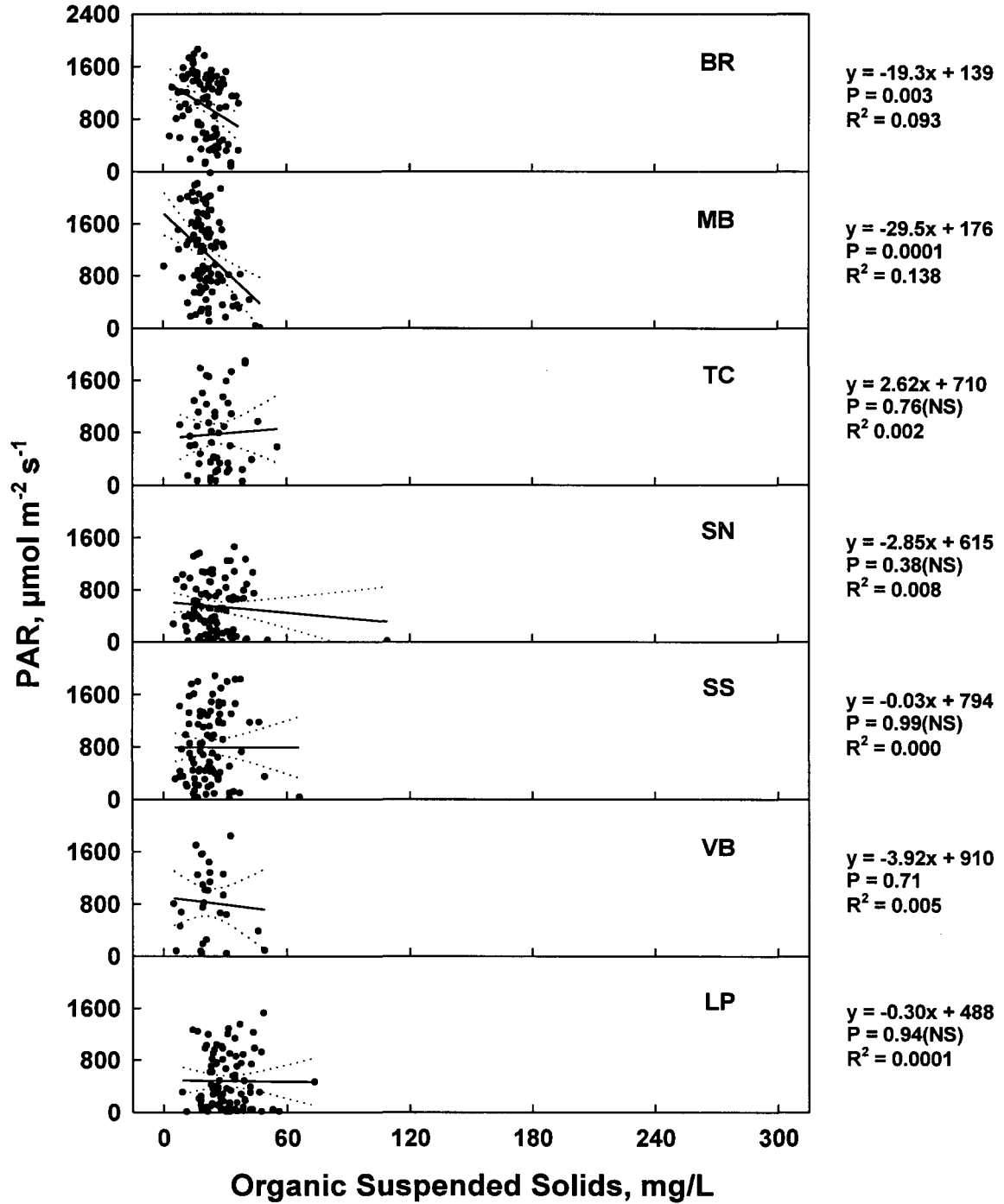


Fig. 7.14 Linear regression analysis of underwater PAR vs. organic suspended solids based on weekly water quality sampling at each IRL monitoring station. Dotted lines indicate 95% confidence intervals of the regression line.

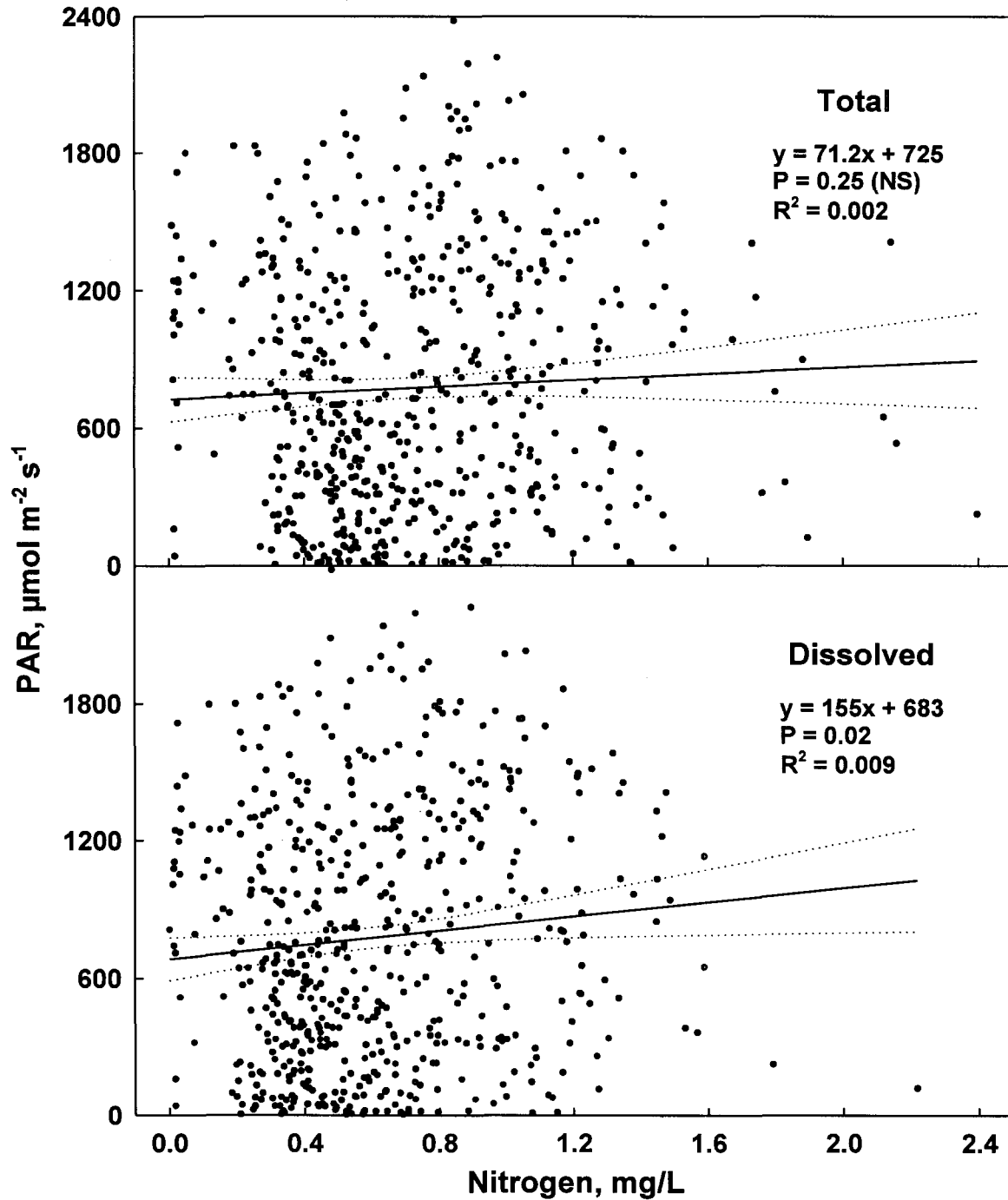


Fig. 7.15 Linear regression analysis of underwater PAR vs. total nitrogen and total dissolved nitrogen based on weekly water quality sampling at IRL monitoring stations (all stations combined). Dotted lines indicate 95% confidence intervals of the regression line.

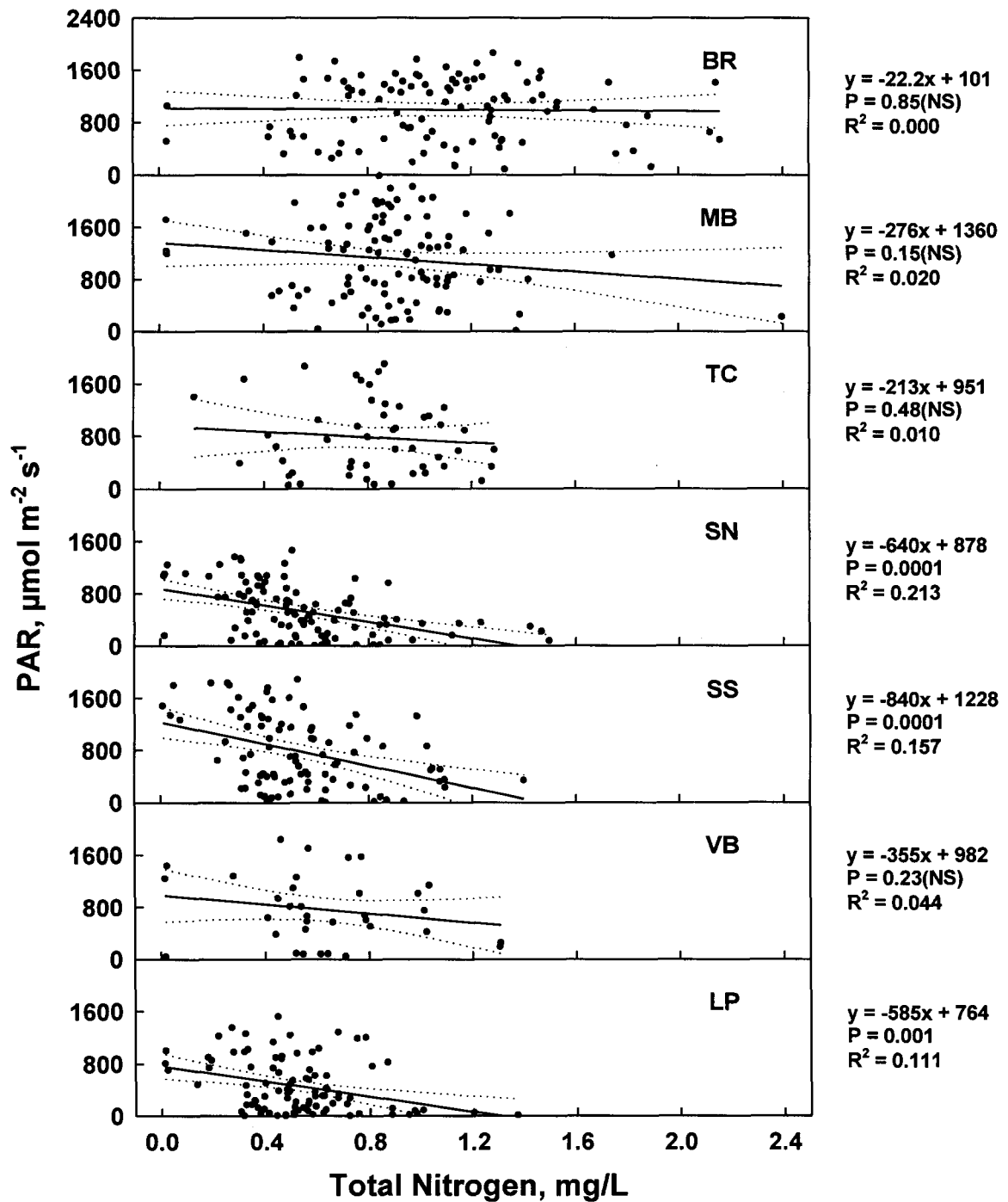


Fig. 7.16 Linear regression analysis of underwater PAR vs. total nitrogen based on weekly water quality sampling at each IRL monitoring station. Dotted lines indicate 95% confidence intervals of the regression line.

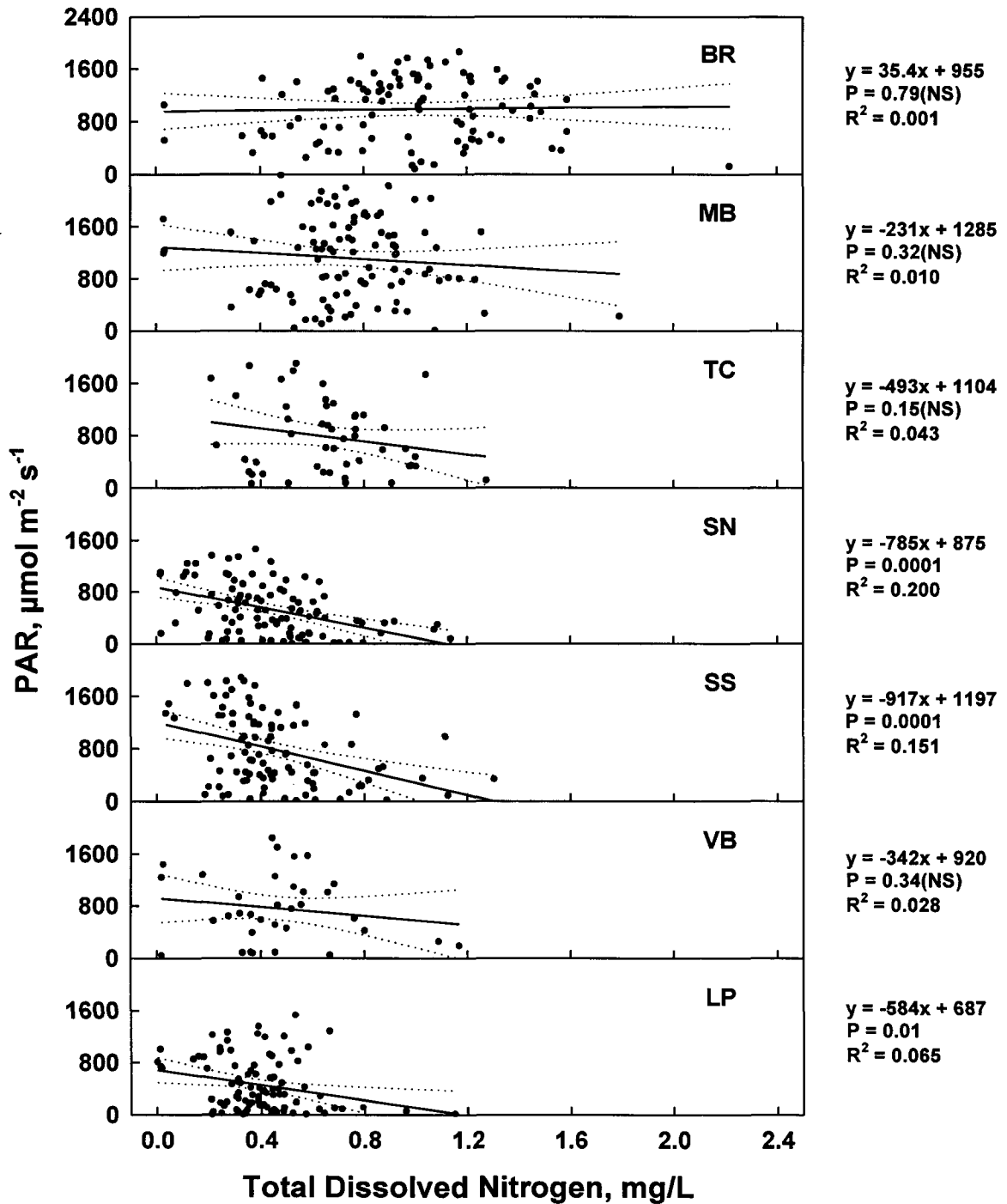


Fig. 7.17 Linear regression analysis of underwater PAR vs. total dissolved nitrogen based on weekly water quality sampling at IRL monitoring stations for each station. Dotted lines indicate 95% confidence intervals of the regression line.

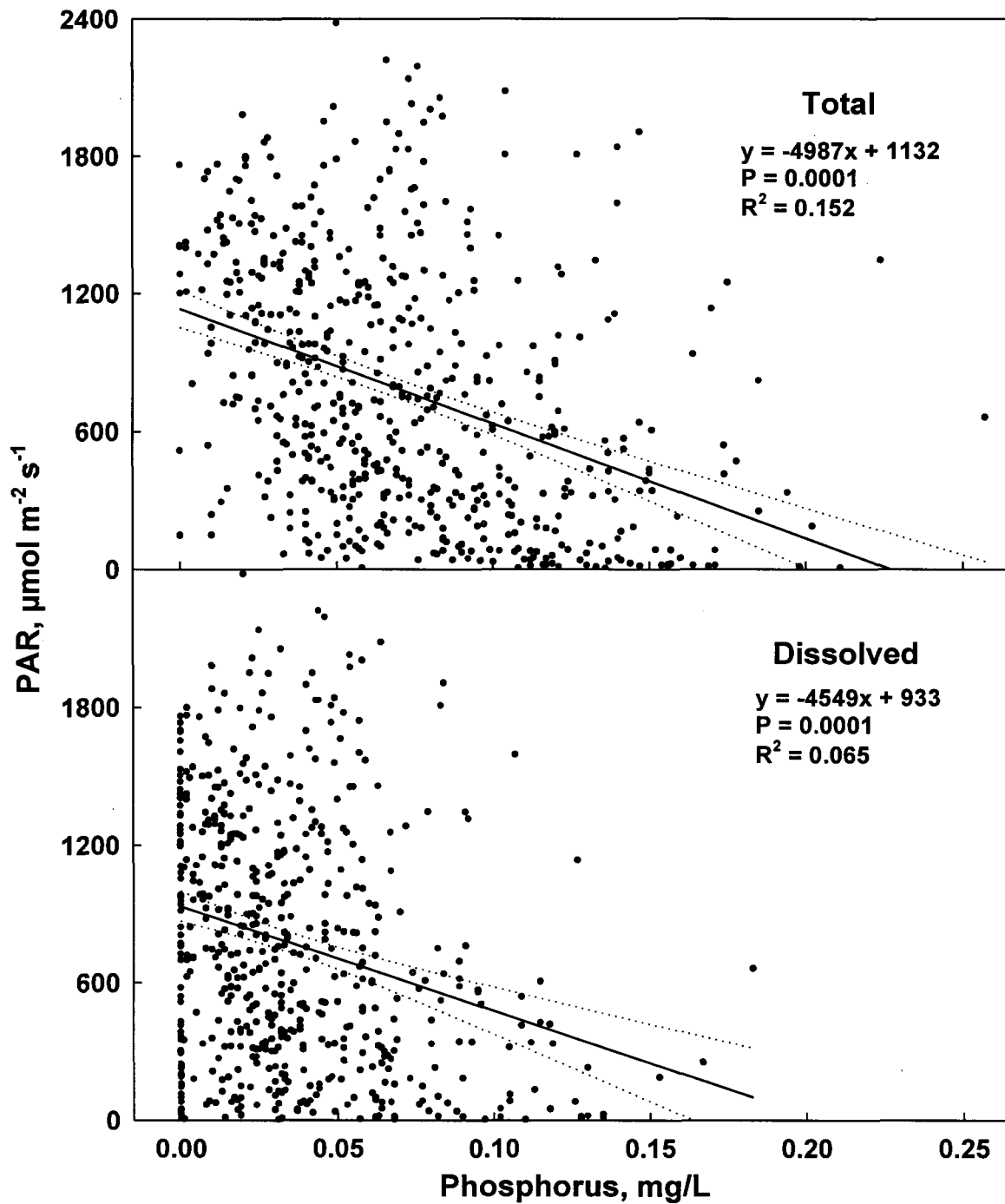


Fig. 7.18 Linear regression analysis of underwater PAR vs. total phosphorus and total dissolved phosphorus based on weekly water quality sampling at IRL monitoring stations (all stations combined). Dotted lines indicate 95% confidence intervals of the regression line.

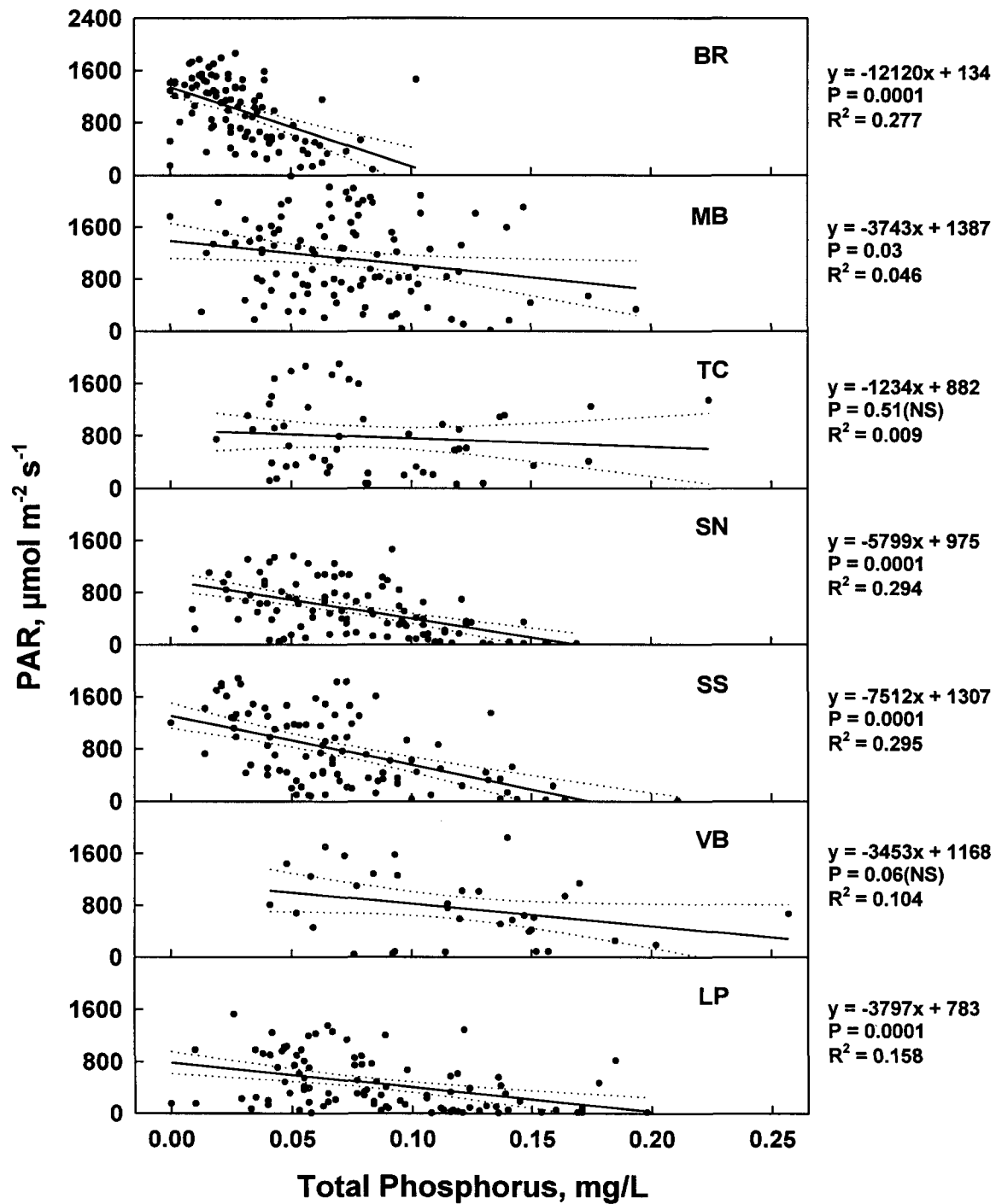


Fig. 7.19 Linear regression analysis of underwater PAR vs. total phosphorus based on weekly water quality sampling at each IRL monitoring station. Dotted lines indicate 95% confidence intervals of the regression line.

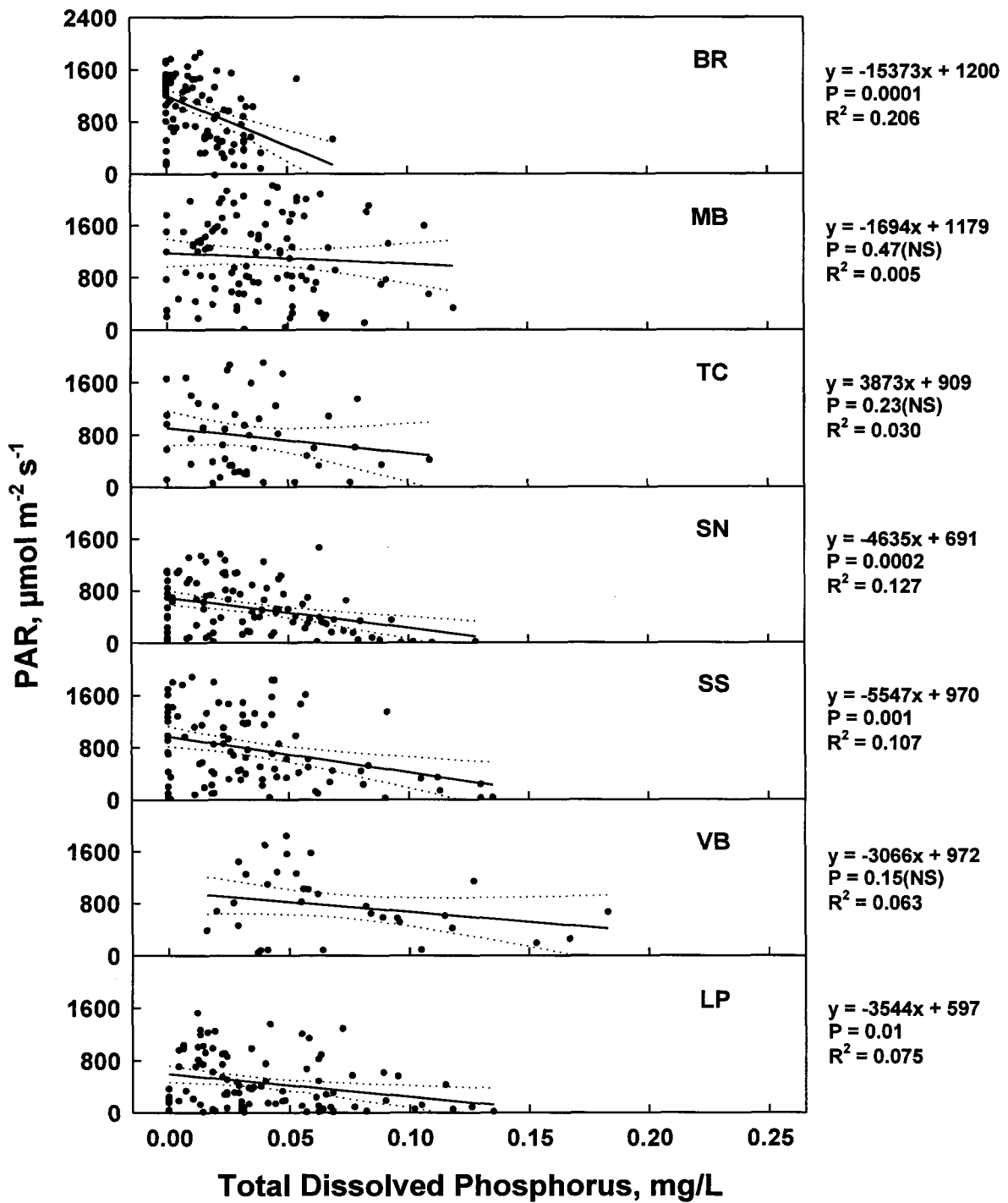


Fig. 7.20 Linear regression analysis of underwater PAR vs. total dissolved phosphorus based on weekly water quality sampling at each IRL monitoring station. Dotted lines indicate 95% confidence intervals of the regression line.

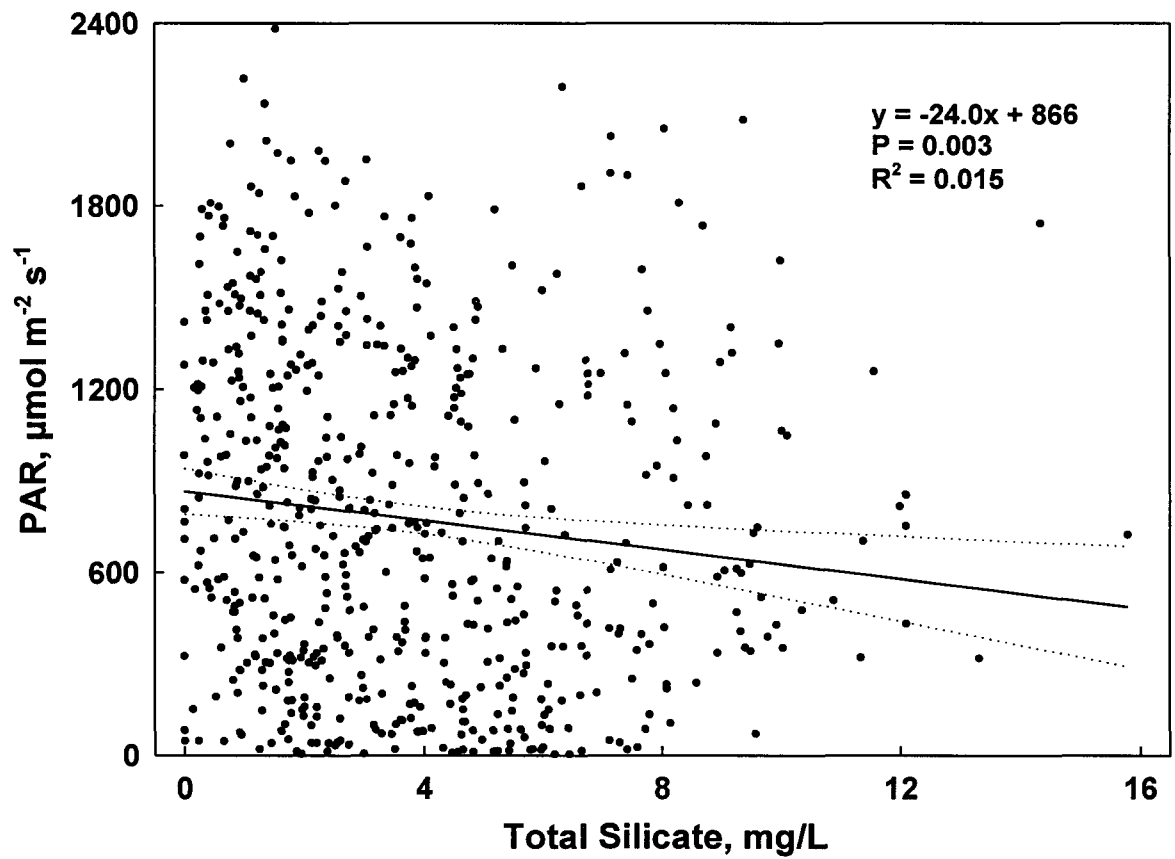


Fig. 7.21 Linear regression analysis of underwater PAR vs. total silicate based on weekly water quality sampling at IRL monitoring stations (all stations combined). Dotted lines indicate 95% confidence intervals of the regression line.

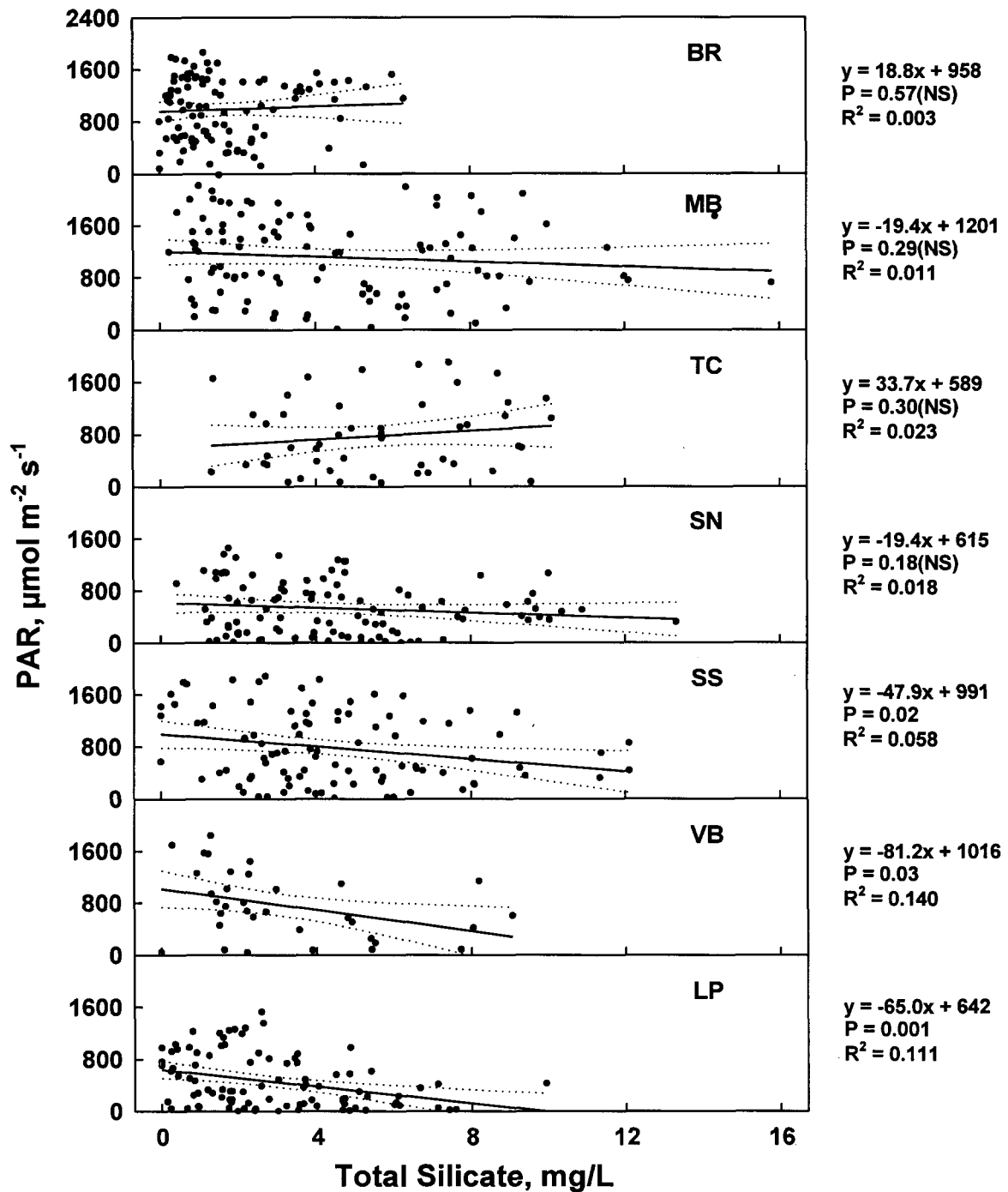


Fig. 7.22 Linear regression analysis of underwater PAR vs. total silicate based on weekly water quality sampling at each IRL monitoring station. Dotted lines indicate 95% confidence intervals of the regression line.

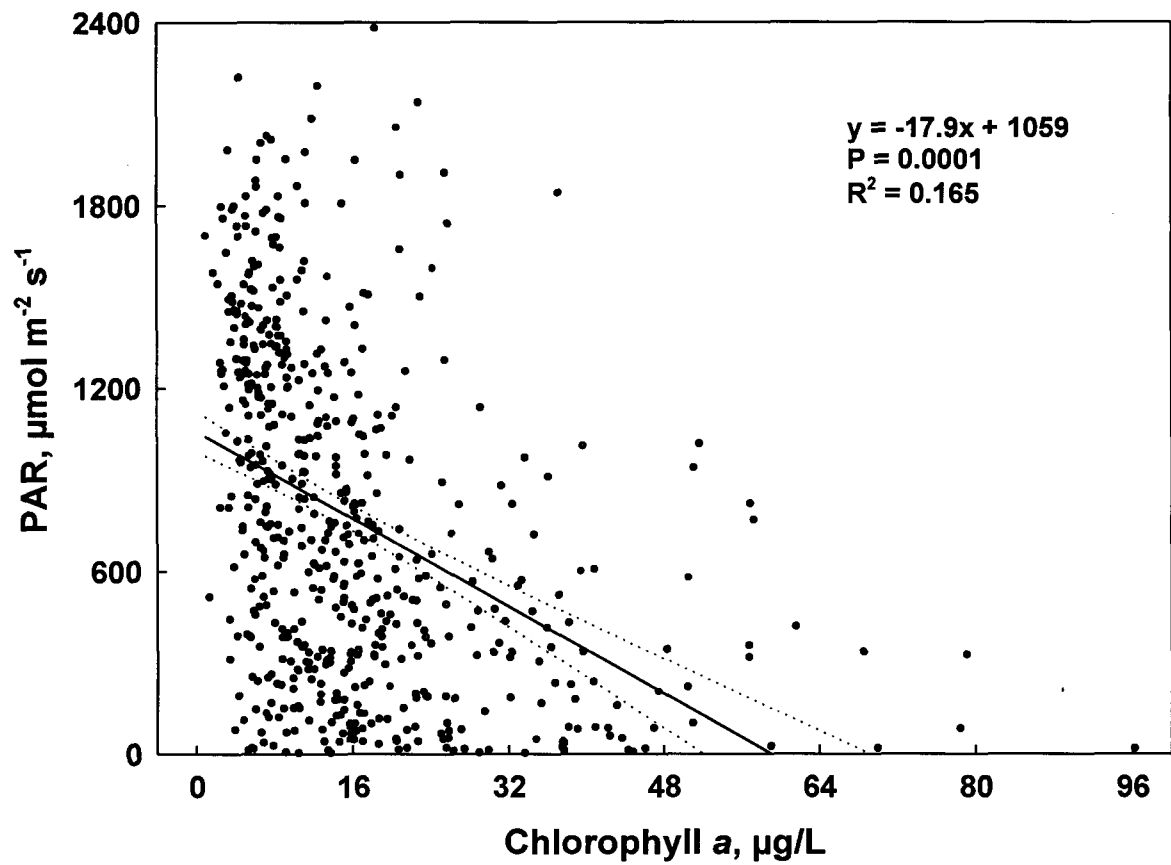


Fig. 7.23 Linear regression analysis of underwater PAR vs. chlorophyll *a* based on weekly water quality sampling at IRL monitoring stations (all stations combined). Dotted lines indicate 95% confidence intervals of the regression line.

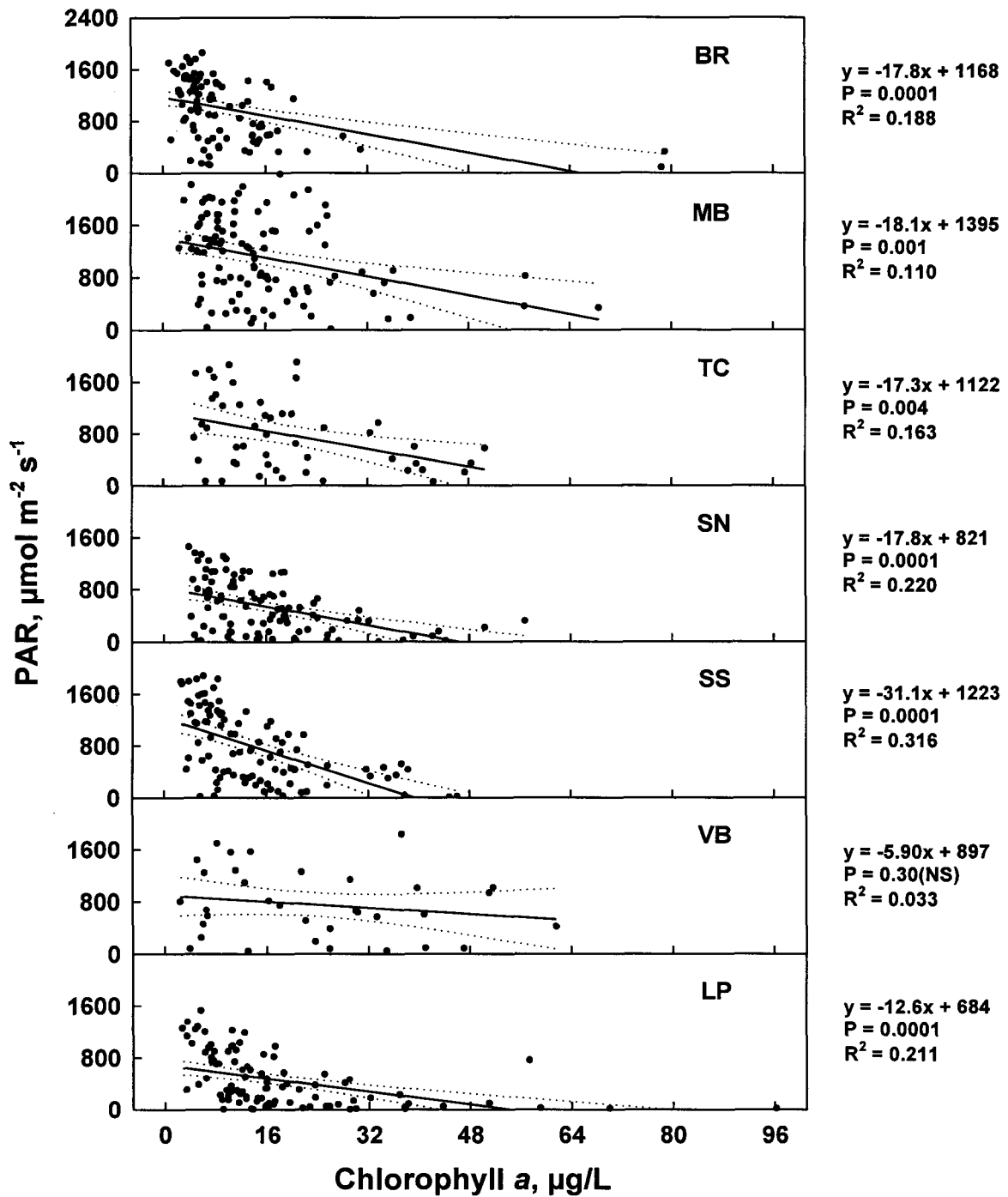


Fig. 7.24 Linear regression analysis of underwater PAR vs. chlorophyll a based on weekly water quality sampling at each IRL monitoring station. Dotted lines indicate 95% confidence intervals of the regression line.

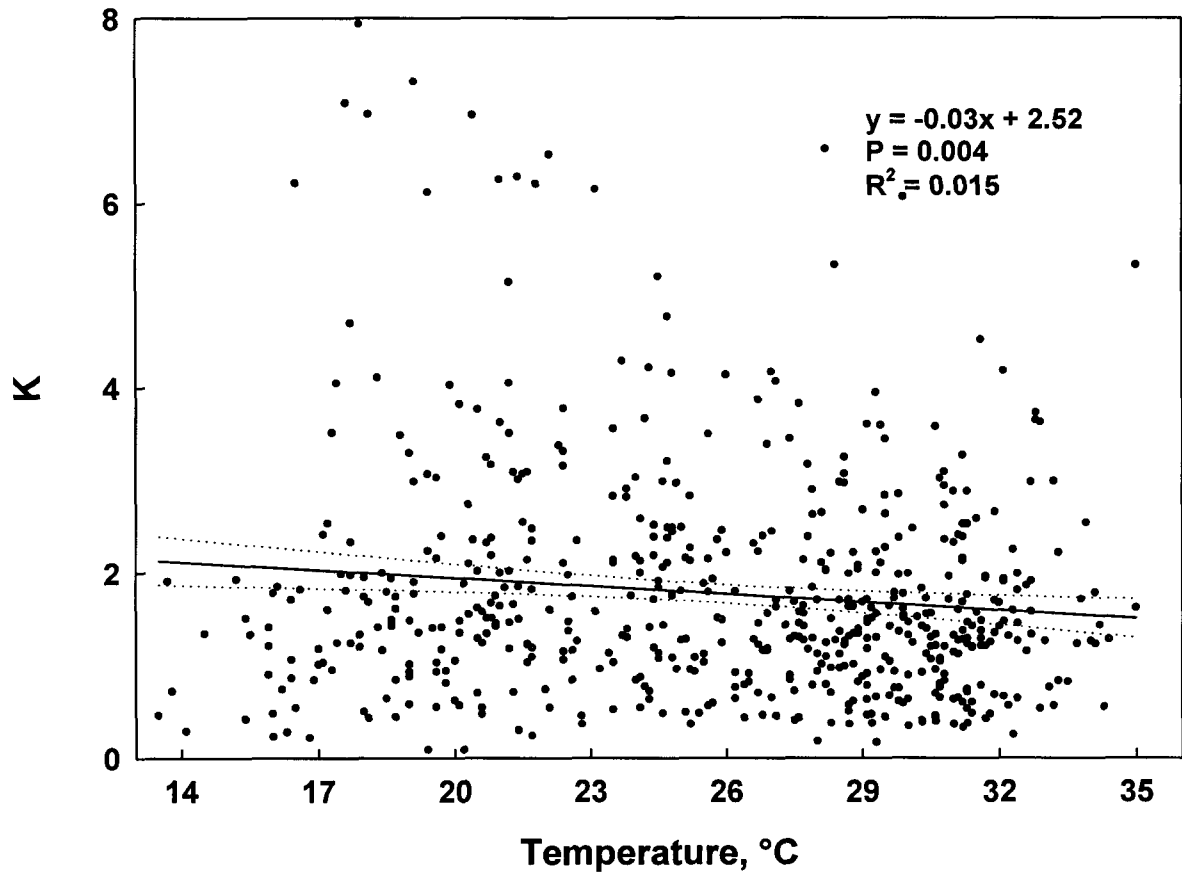


Fig. 7.25 Linear regression analysis of K vs. temperature based on weekly water quality sampling at IRL monitoring stations (all stations combined). Dotted lines indicate 95% confidence intervals of the regression line.

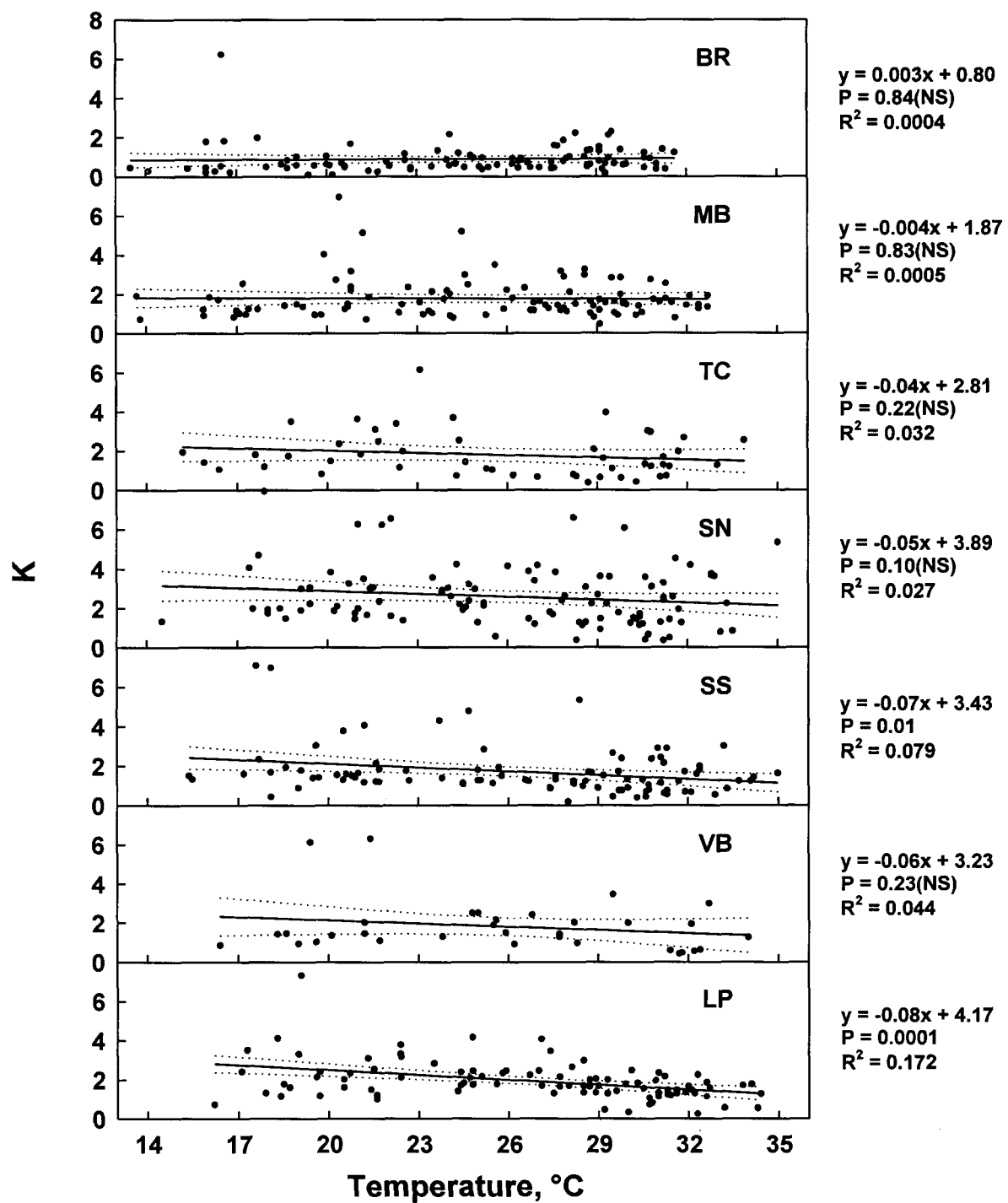


Fig. 7.26 Linear regression analysis of K vs. temperature based on weekly water quality sampling at each IRL monitoring station. Dotted lines indicate 95% confidence intervals of the regression line.

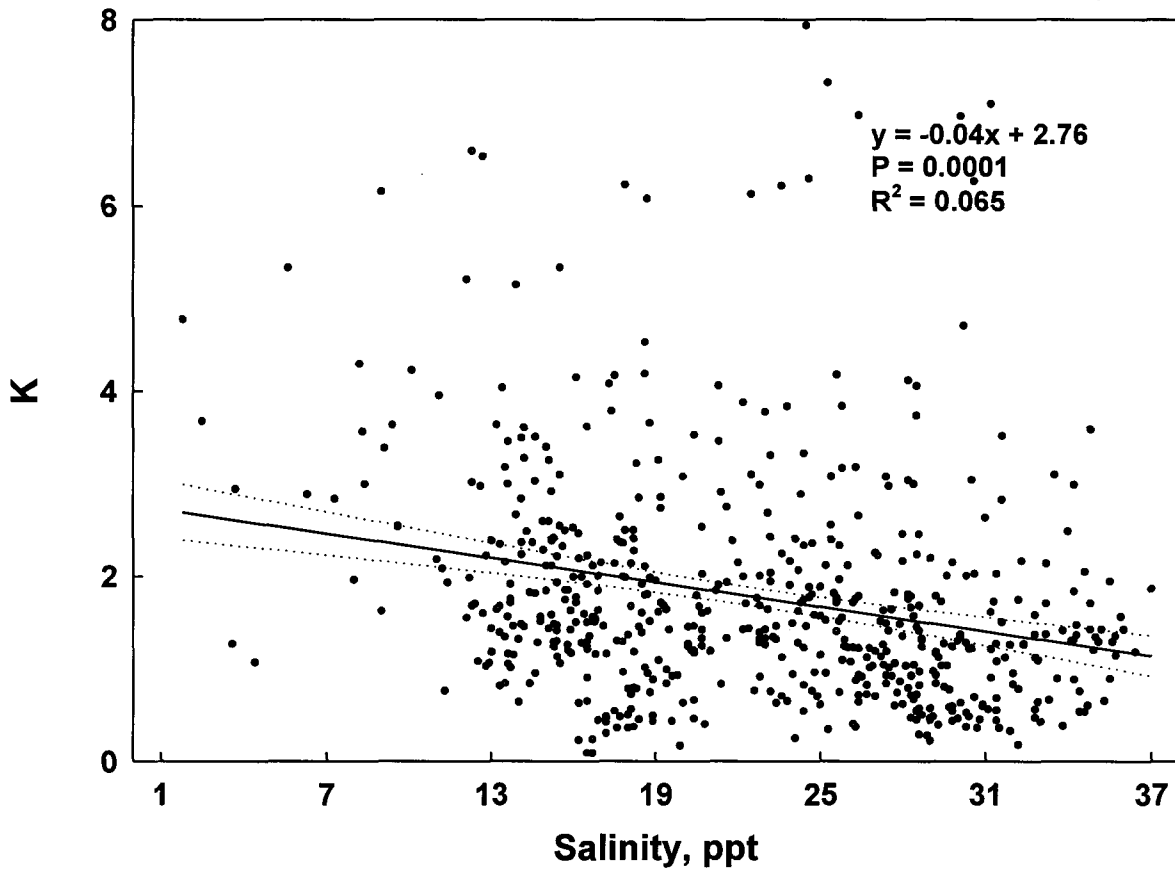


Fig. 7.27 Linear regression analysis of K vs. salinity based on weekly water quality sampling at IRL monitoring stations (all stations combined). Dotted lines indicate 95% confidence intervals of the regression line.

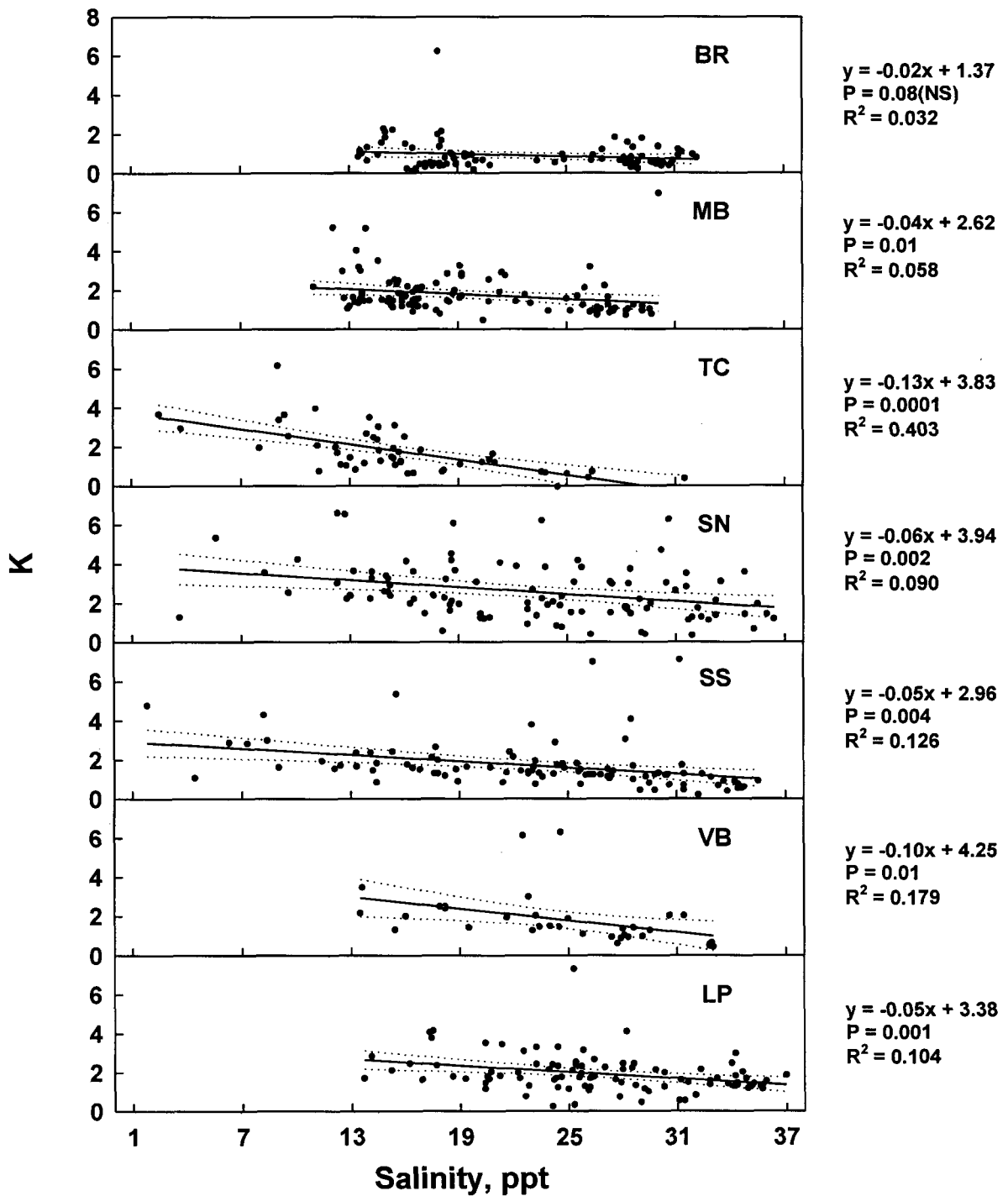


Fig. 7.28 Linear regression analysis of K vs. salinity based on weekly water quality sampling at each IRL monitoring station. Dotted lines indicate 95% confidence intervals of the regression line.

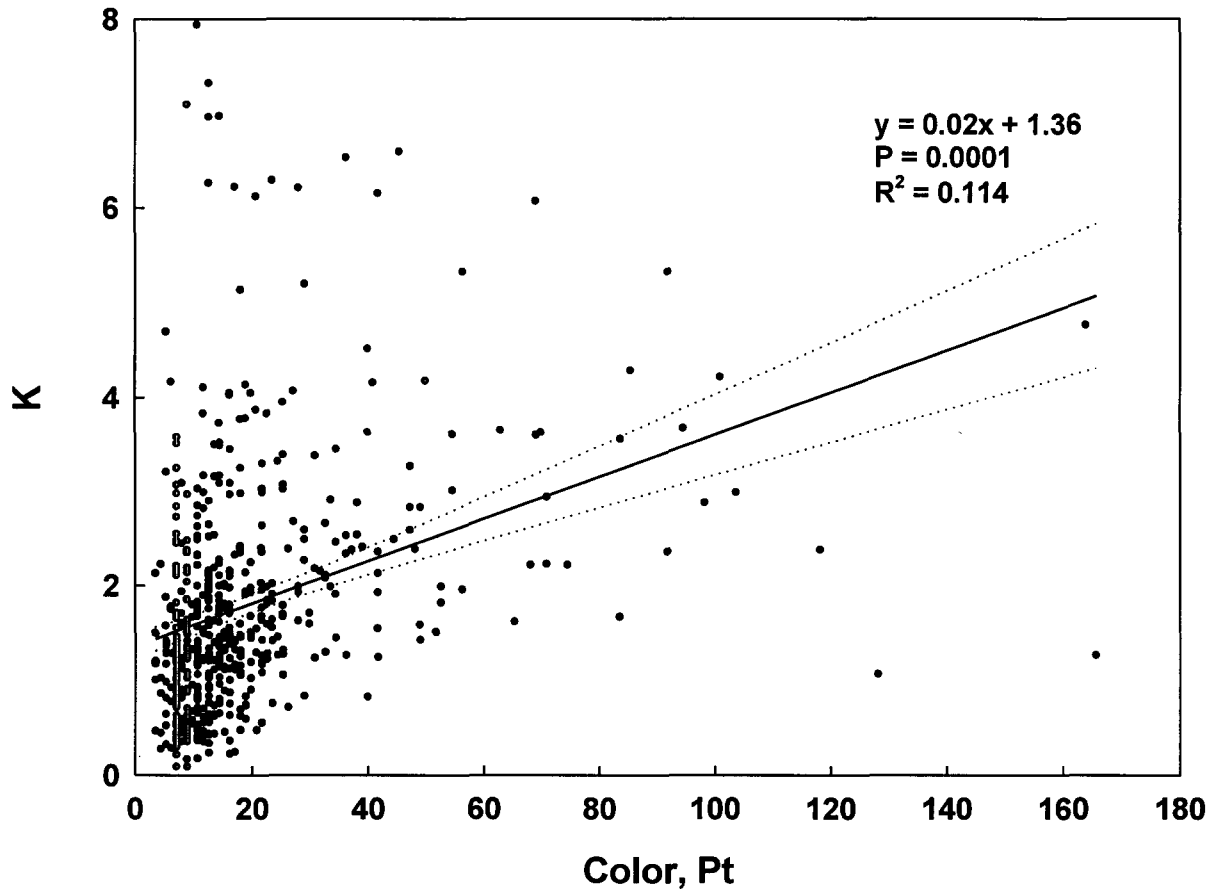


Fig. 7.29 Linear regression analysis of K vs. color based on weekly water quality sampling at IRL monitoring stations (all stations combined). Dotted lines indicate 95% confidence intervals of the regression line.

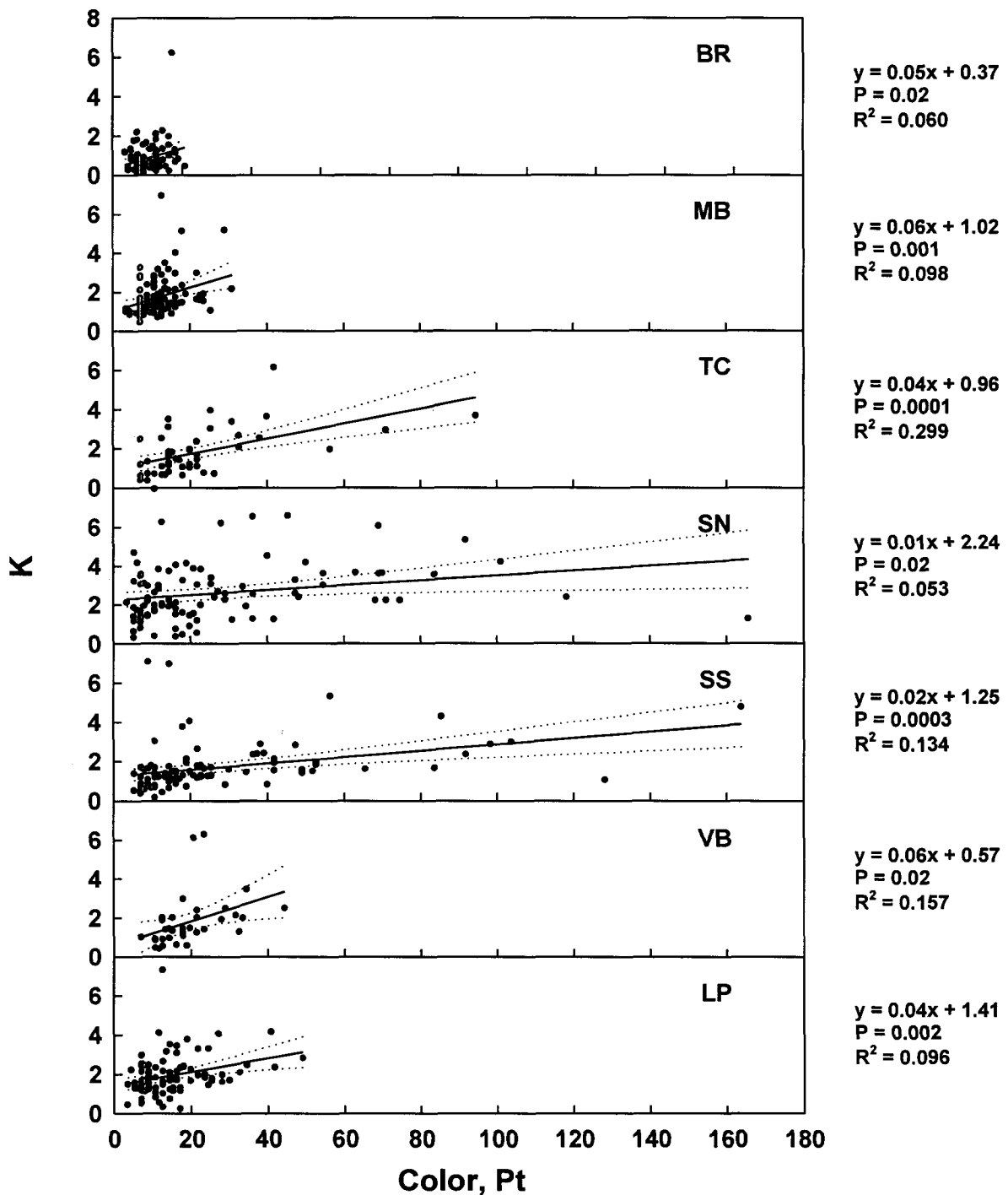


Fig. 7.30 Linear regression analysis of K vs. color based on weekly water quality sampling at each IRL monitoring station. Dotted lines indicate 95% confidence intervals of the regression line.

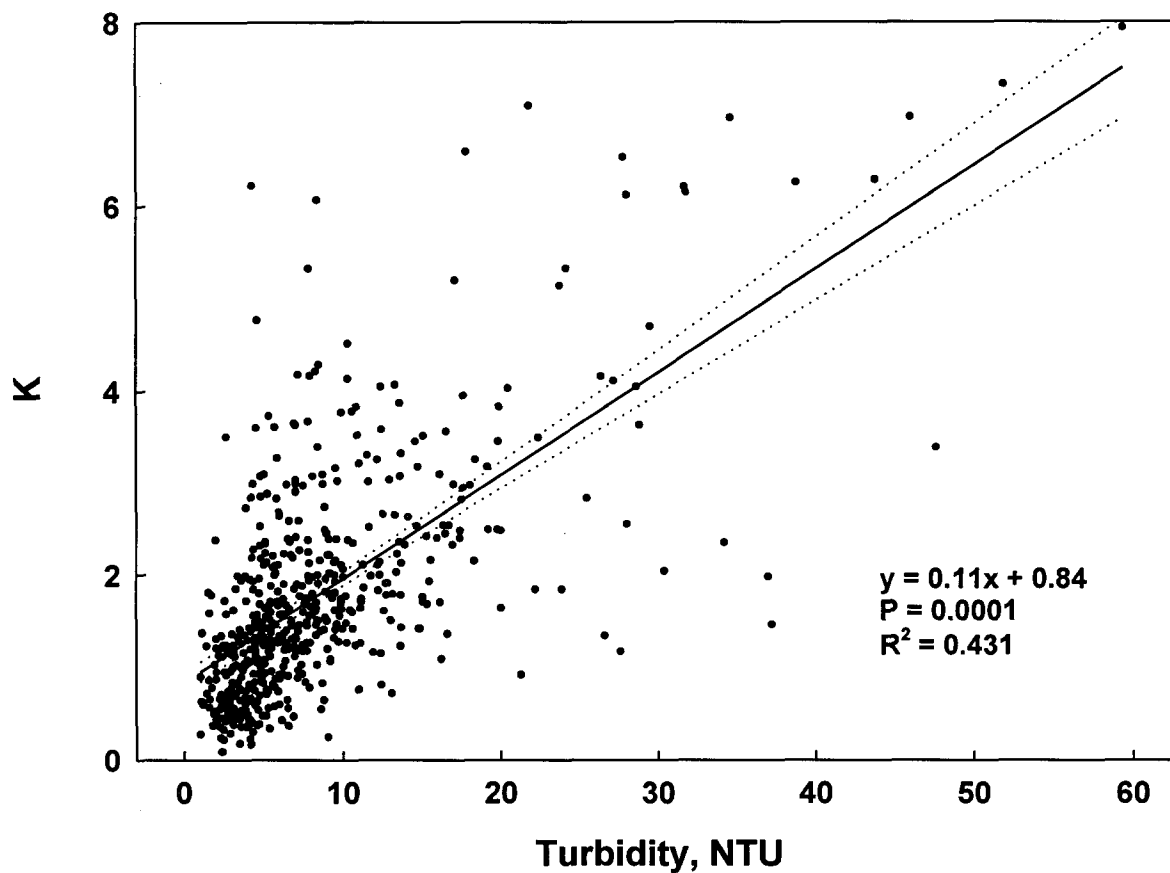


Fig. 7.31 Linear regression analysis of K vs. turbidity based on weekly water quality sampling at IRL monitoring stations (all stations combined). Dotted lines indicate 95% confidence intervals of the regression line.

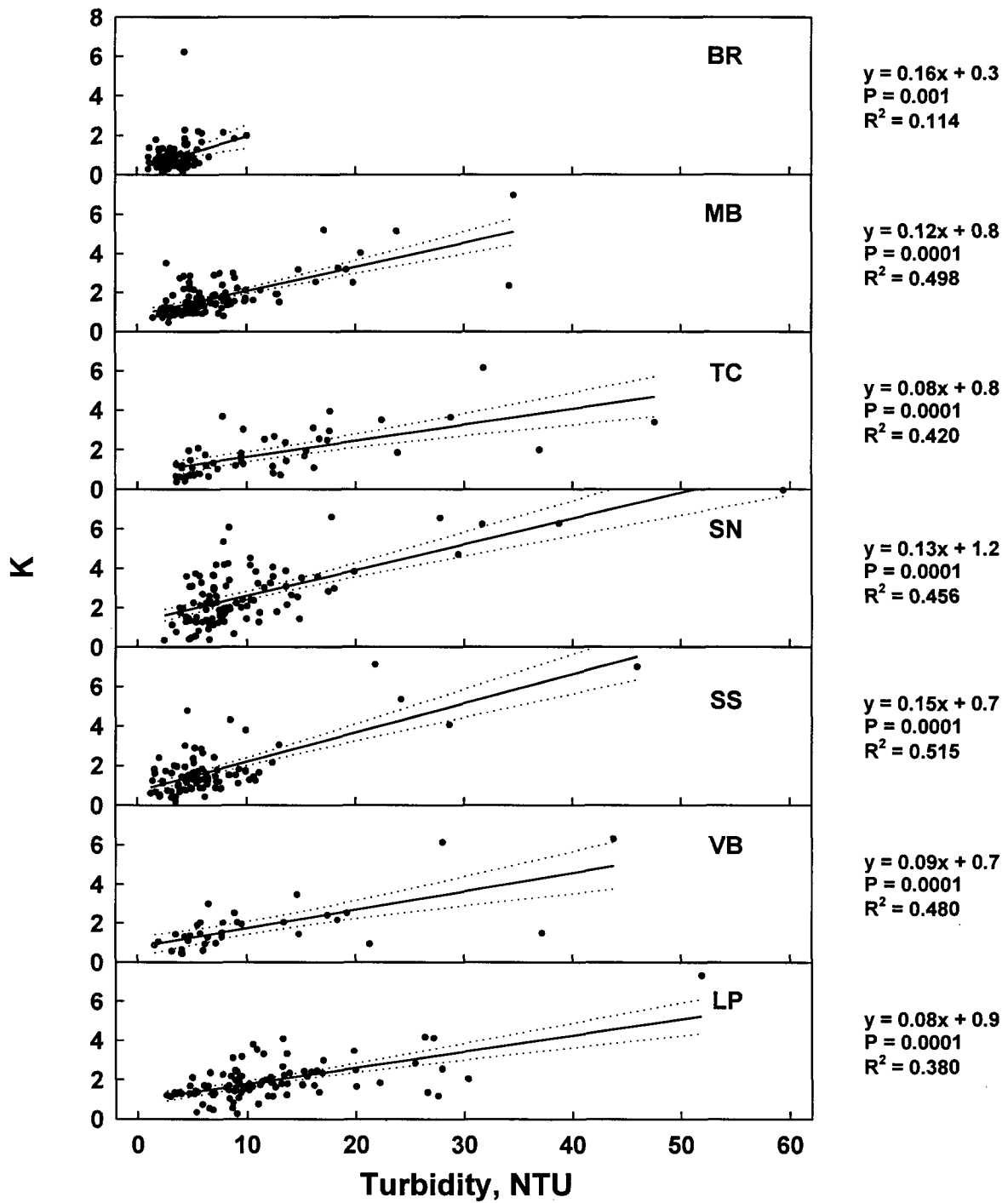


Fig. 7.32 Linear regression analysis of K vs. turbidity based on weekly water quality sampling at each IRL monitoring station. Dotted lines indicate 95% confidence intervals of the regression line.

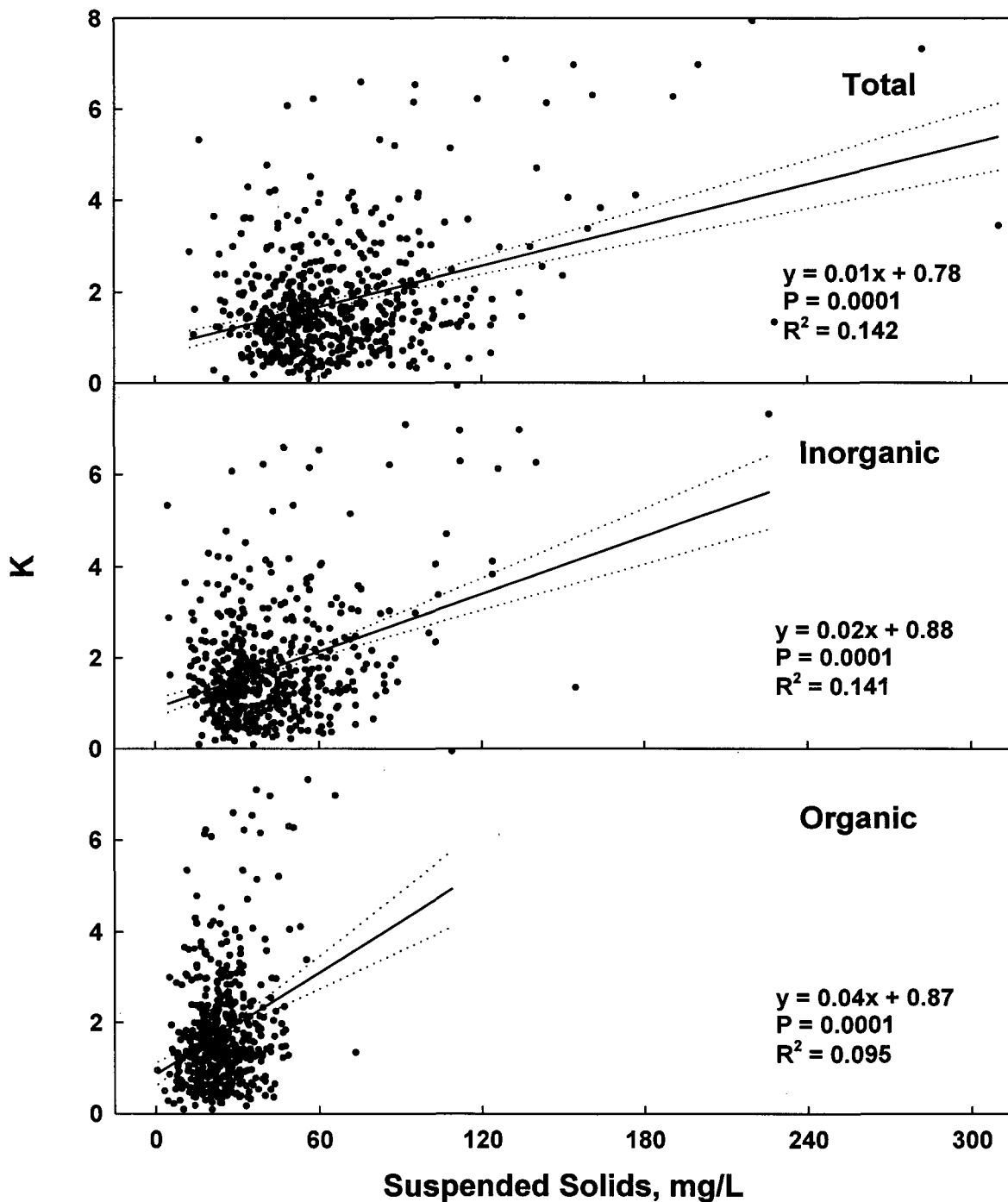


Fig. 7.33 Linear regression analysis of K vs. total, inorganic, and inorganic suspended solids based on weekly water quality sampling at IRL monitoring stations (all stations combined). Dotted lines indicate 95% confidence intervals of the regression line.

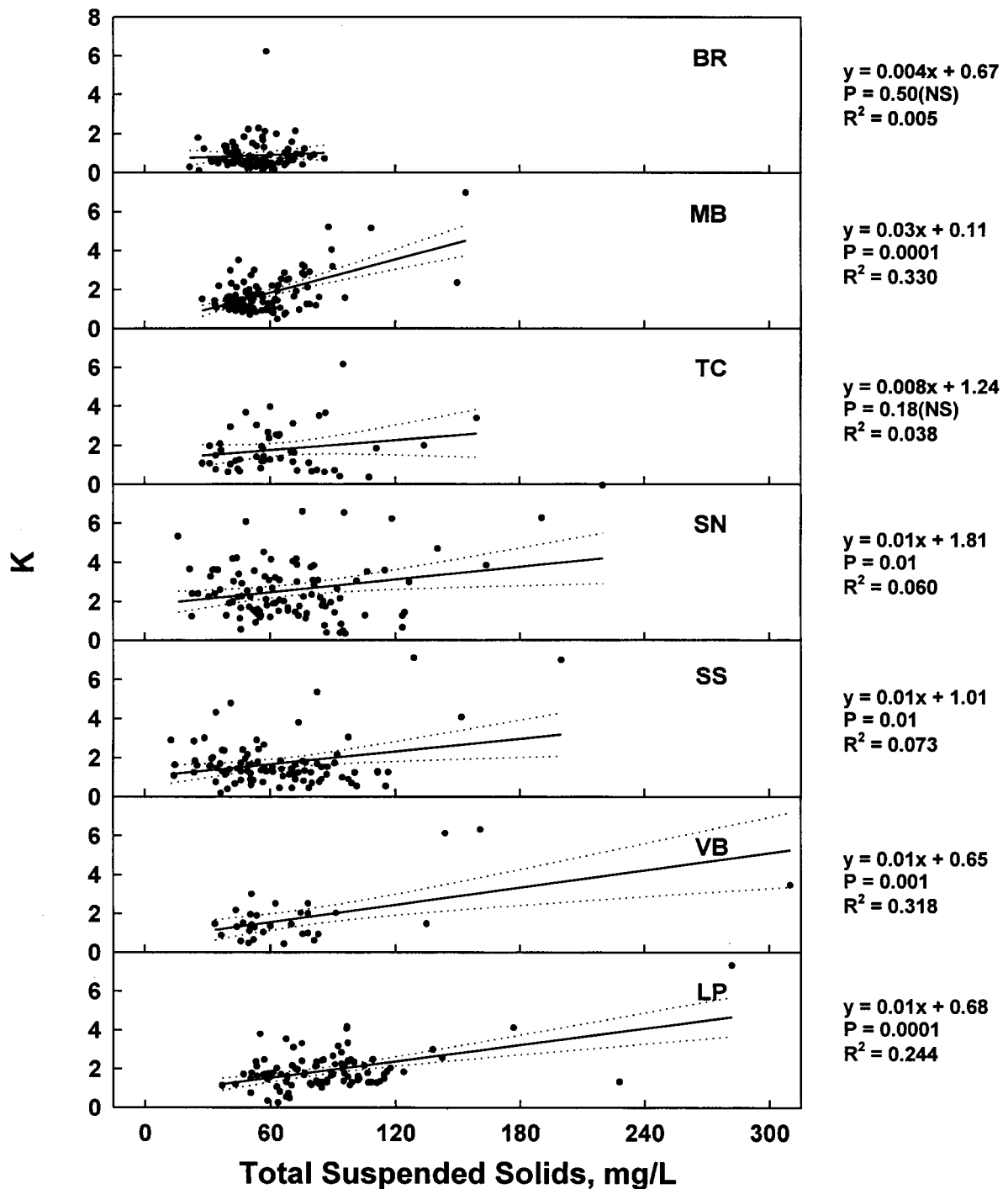


Fig. 7.34 Linear regression analysis of K vs. total suspended solids based on weekly water quality sampling at each IRL monitoring station. Dotted lines indicate 95% confidence intervals of the regression line.

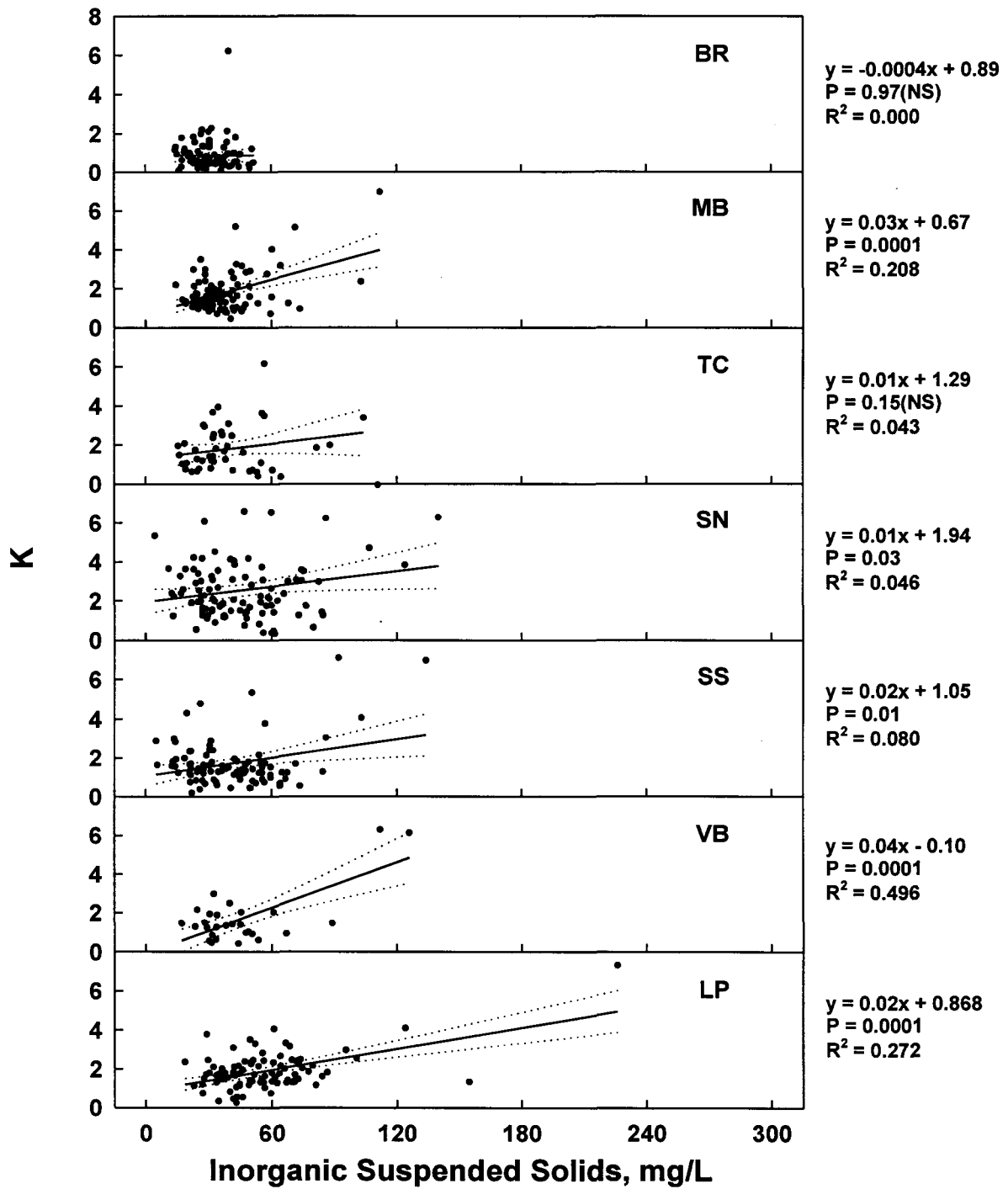


Fig. 7.35 Linear regression analysis of K vs. inorganic suspended solids based on weekly water quality sampling at each IRL monitoring station. Dotted lines indicate 95% confidence intervals of the regression line.

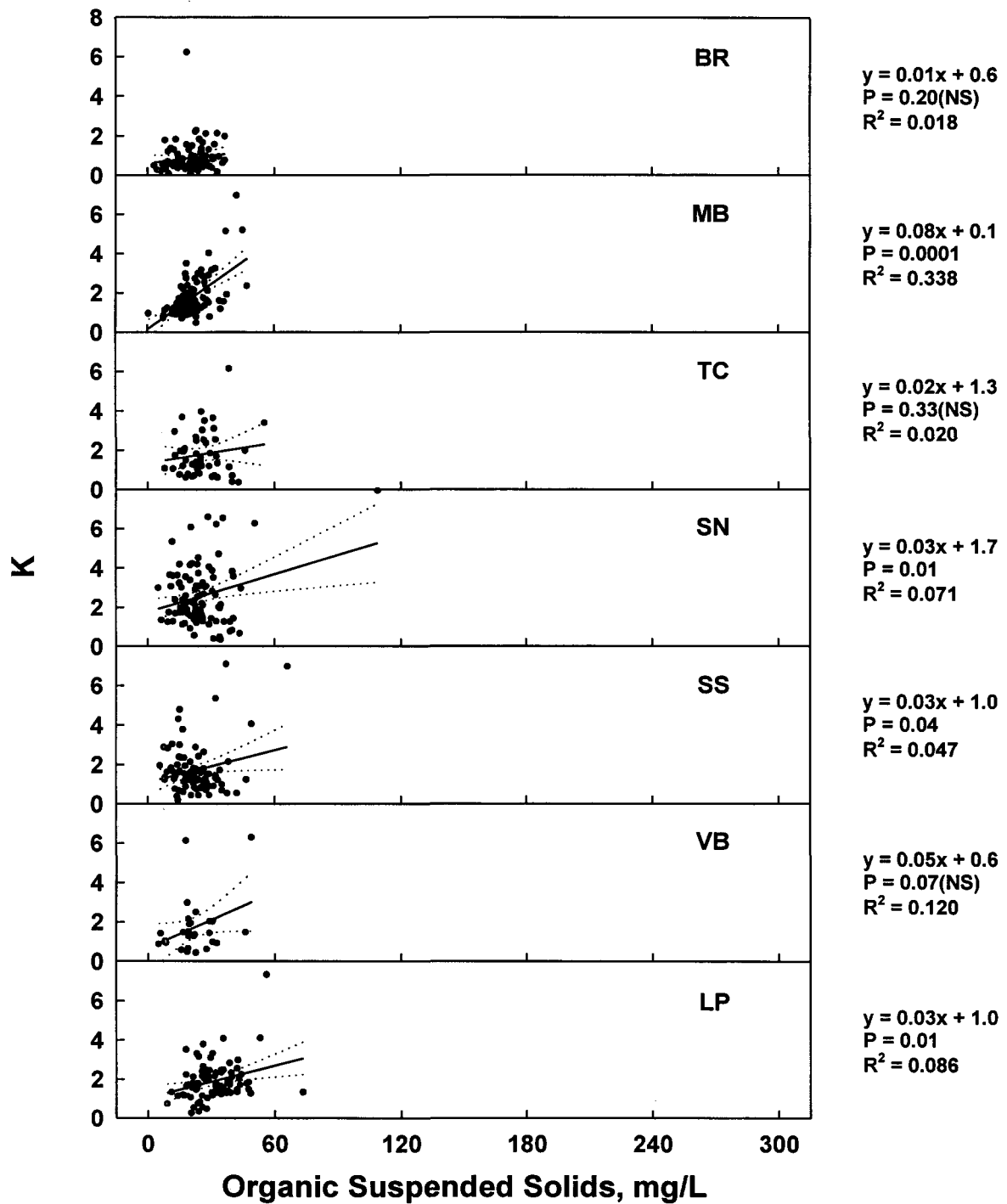


Fig. 7.36 Linear regression analysis of K vs. organic suspended solids based on weekly water quality sampling at each IRL monitoring station. Dotted lines indicate 95% confidence intervals of the regression line.

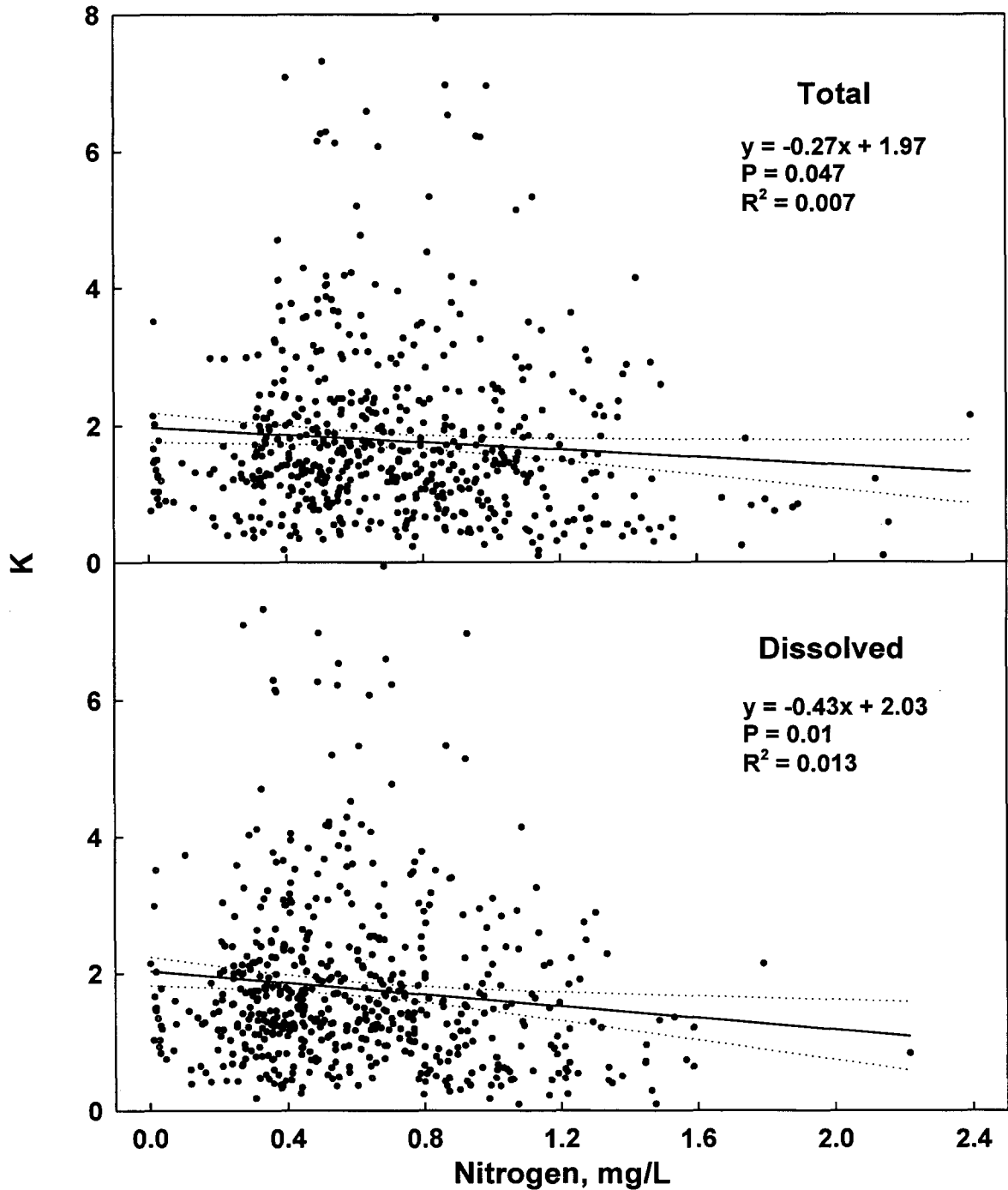


Fig. 7.37 Linear regression analysis of K vs. total nitrogen and total dissolved nitrogen based on weekly water quality sampling at IRL monitoring stations (all stations combined). Dotted lines indicate 95% confidence intervals of the regression line.

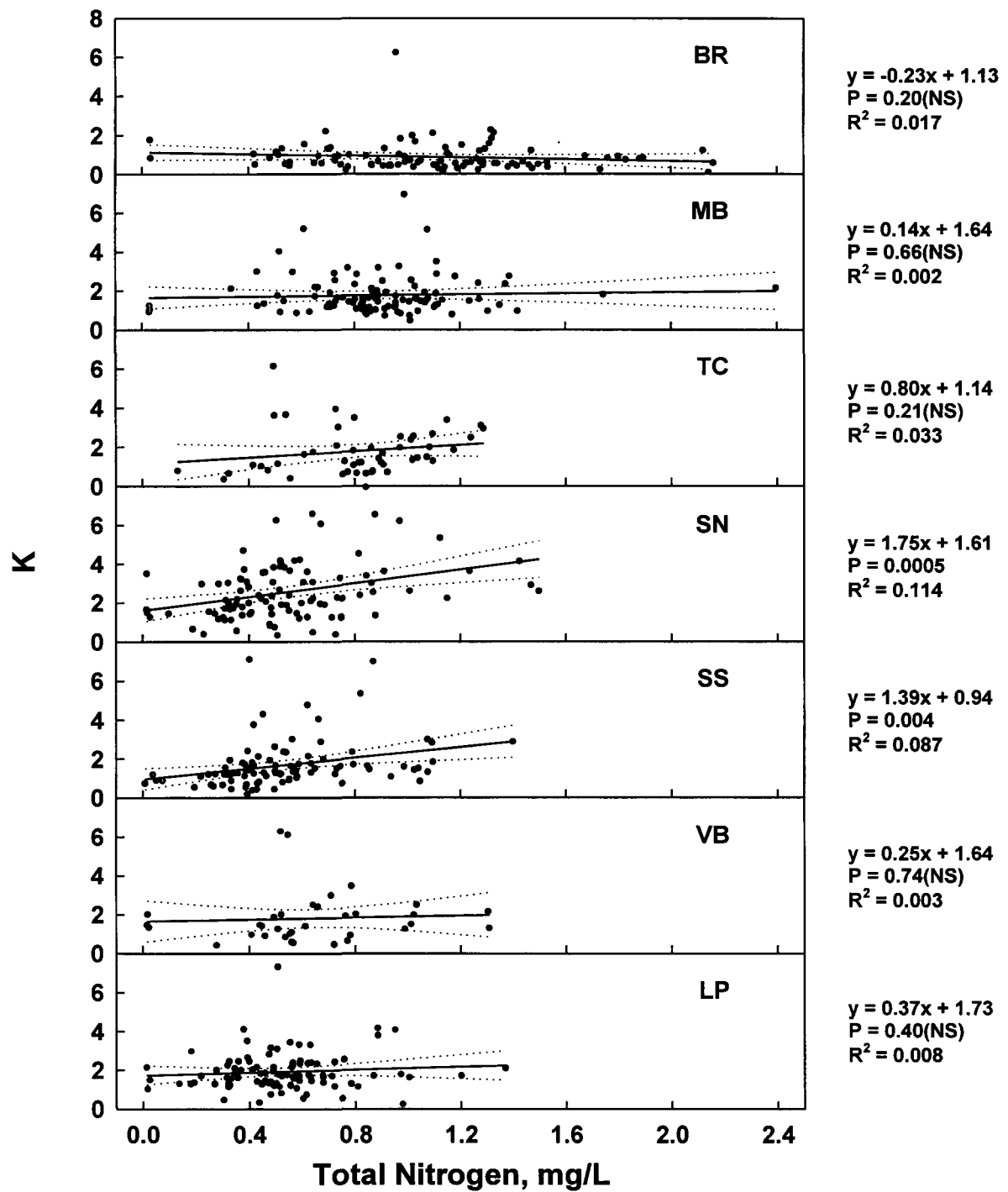


Fig. 7.38 Linear regression analysis of K vs. total nitrogen based on weekly water quality sampling at each IRL monitoring station. Dotted lines indicate 95% confidence intervals of the regression line.

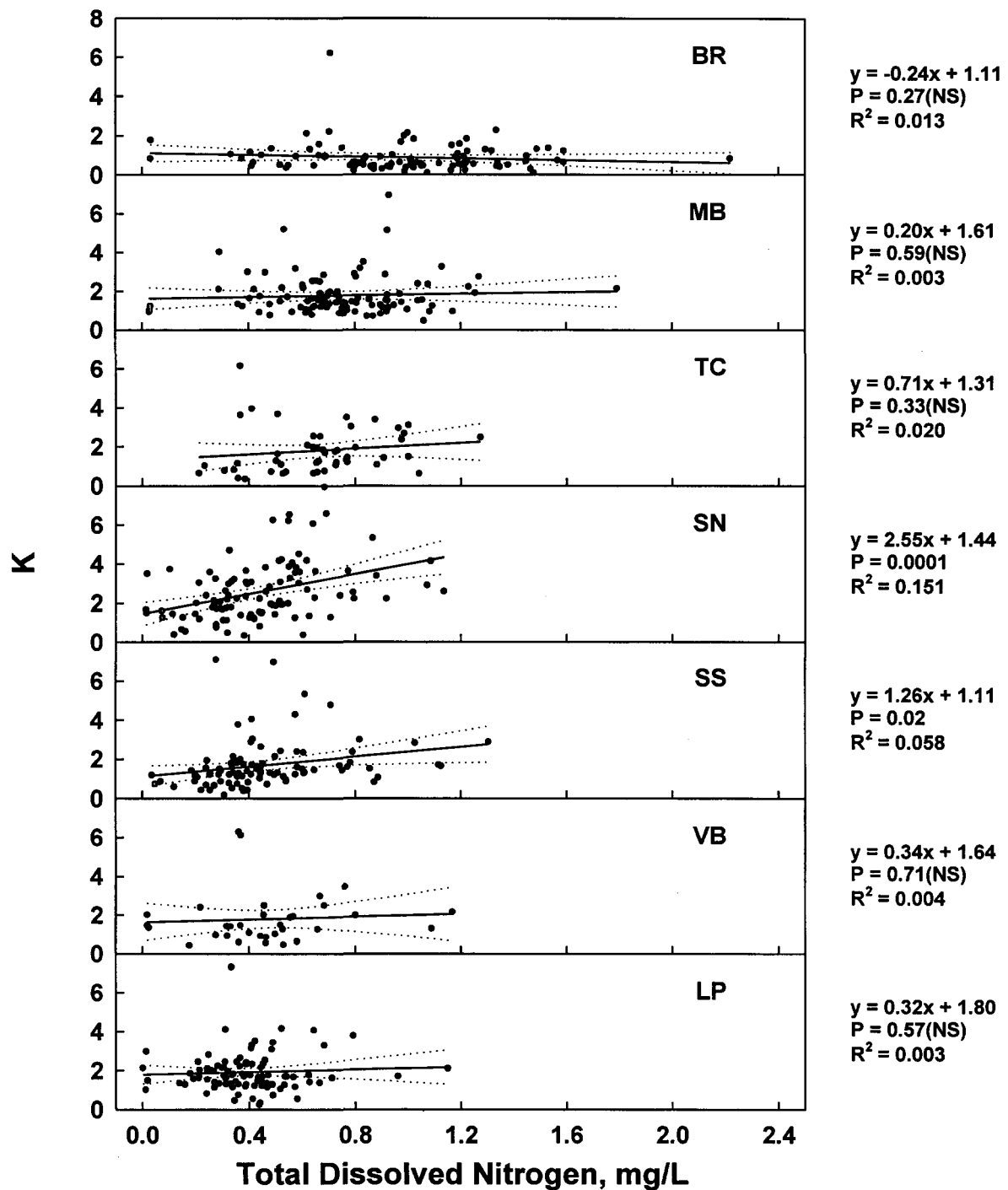


Fig. 7.39 Linear regression analysis of K vs. total dissolved nitrogen based on weekly water quality sampling at each IRL monitoring station. Dotted lines indicate 95% confidence intervals of the regression line.

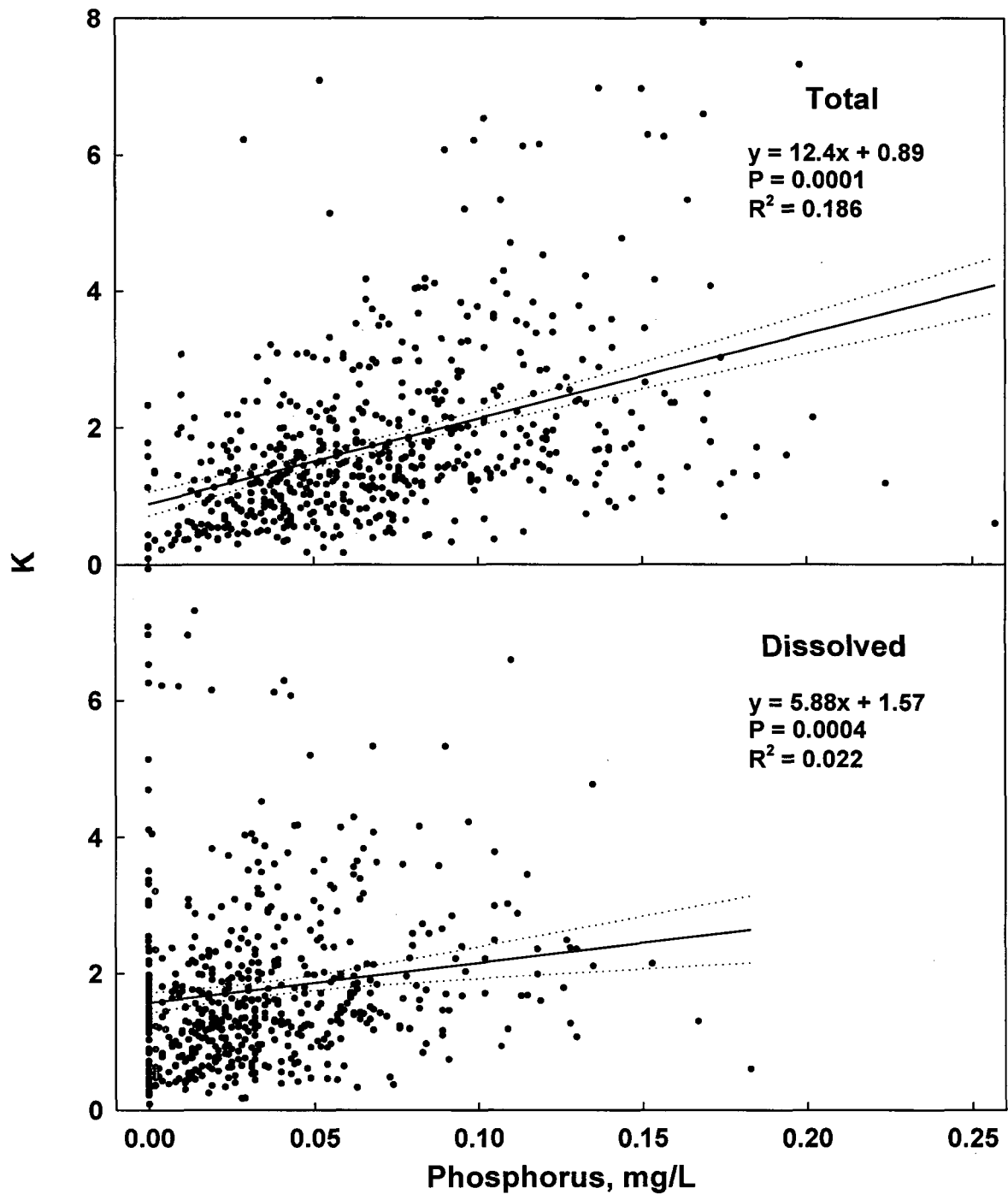


Fig. 7.40 Linear regression analysis of K vs. total phosphorus and total dissolved phosphorus based on weekly water quality sampling at IRL monitoring stations (all stations combined). Dotted lines indicate 95% confidence intervals of the regression line.

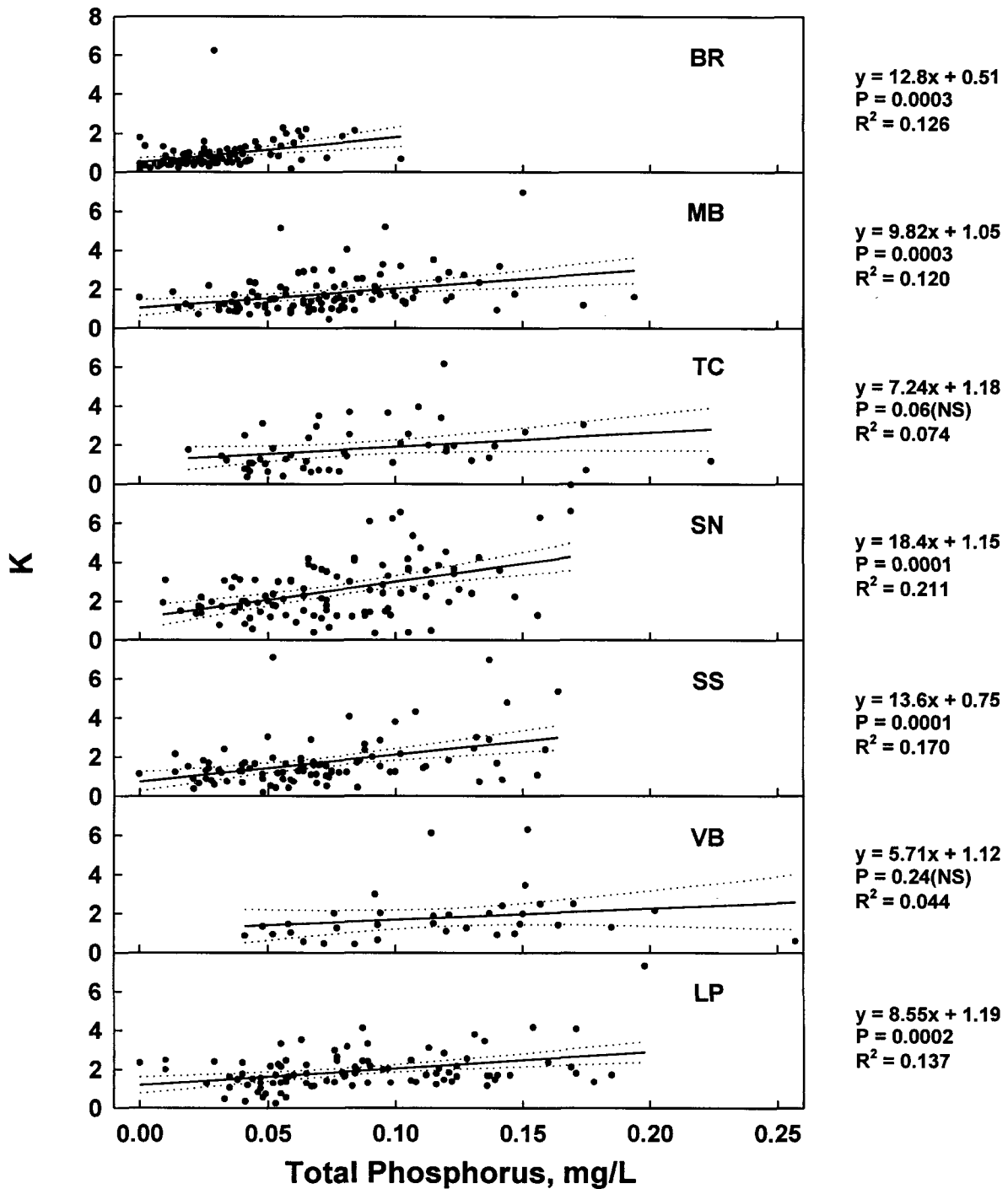


Fig. 7.41 Linear regression analysis of K vs. total phosphorus based on weekly water quality sampling at each IRL monitoring station. Dotted lines indicate 95% confidence intervals of the regression line.

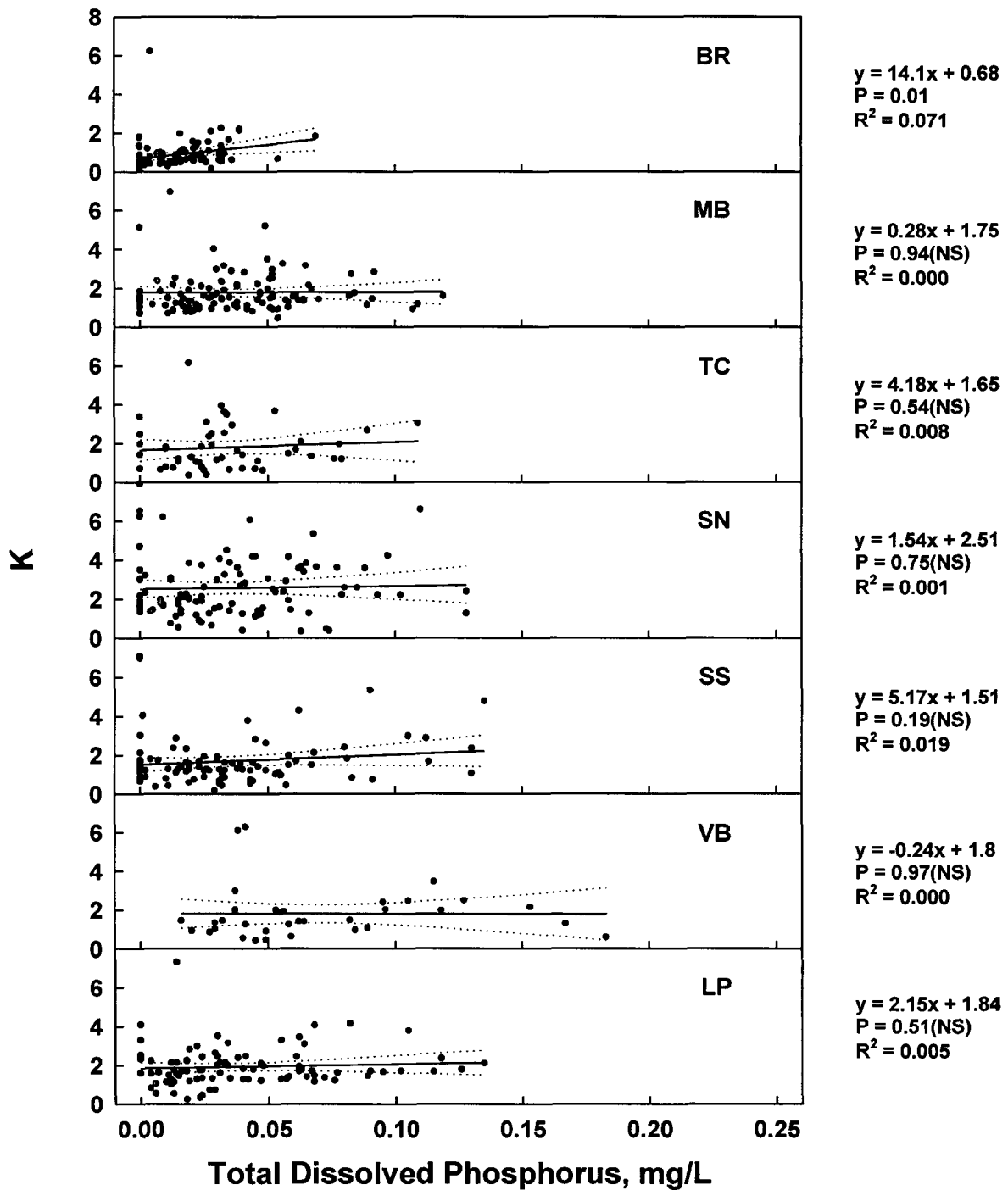


Fig. 7.42 Linear regression analysis of K vs. total dissolved phosphorus based on weekly water quality sampling at each IRL monitoring station. Dotted lines indicate 95% confidence intervals of the regression line.

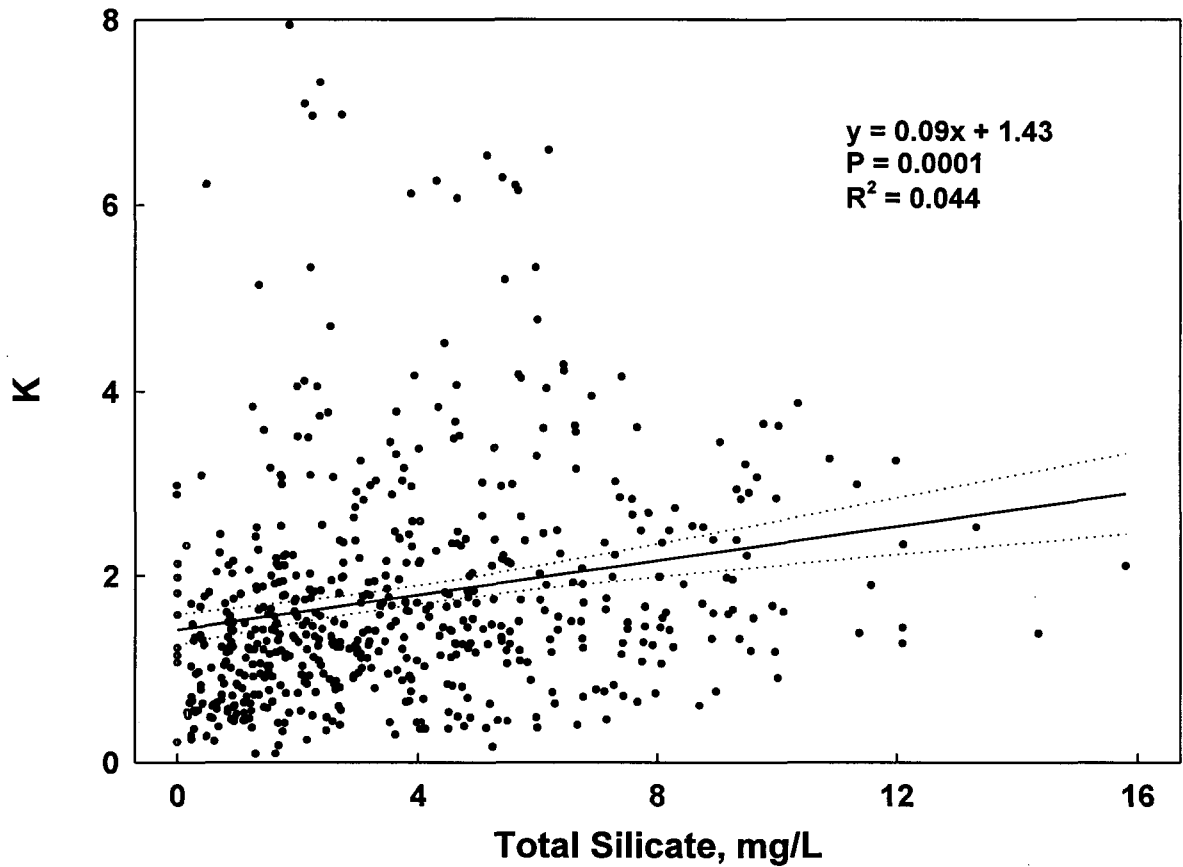


Fig. 7.43 Linear regression analysis of K vs. total silicate based on weekly water quality sampling at IRL monitoring stations (all stations combined). Dotted lines indicate 95% confidence intervals of the regression line.

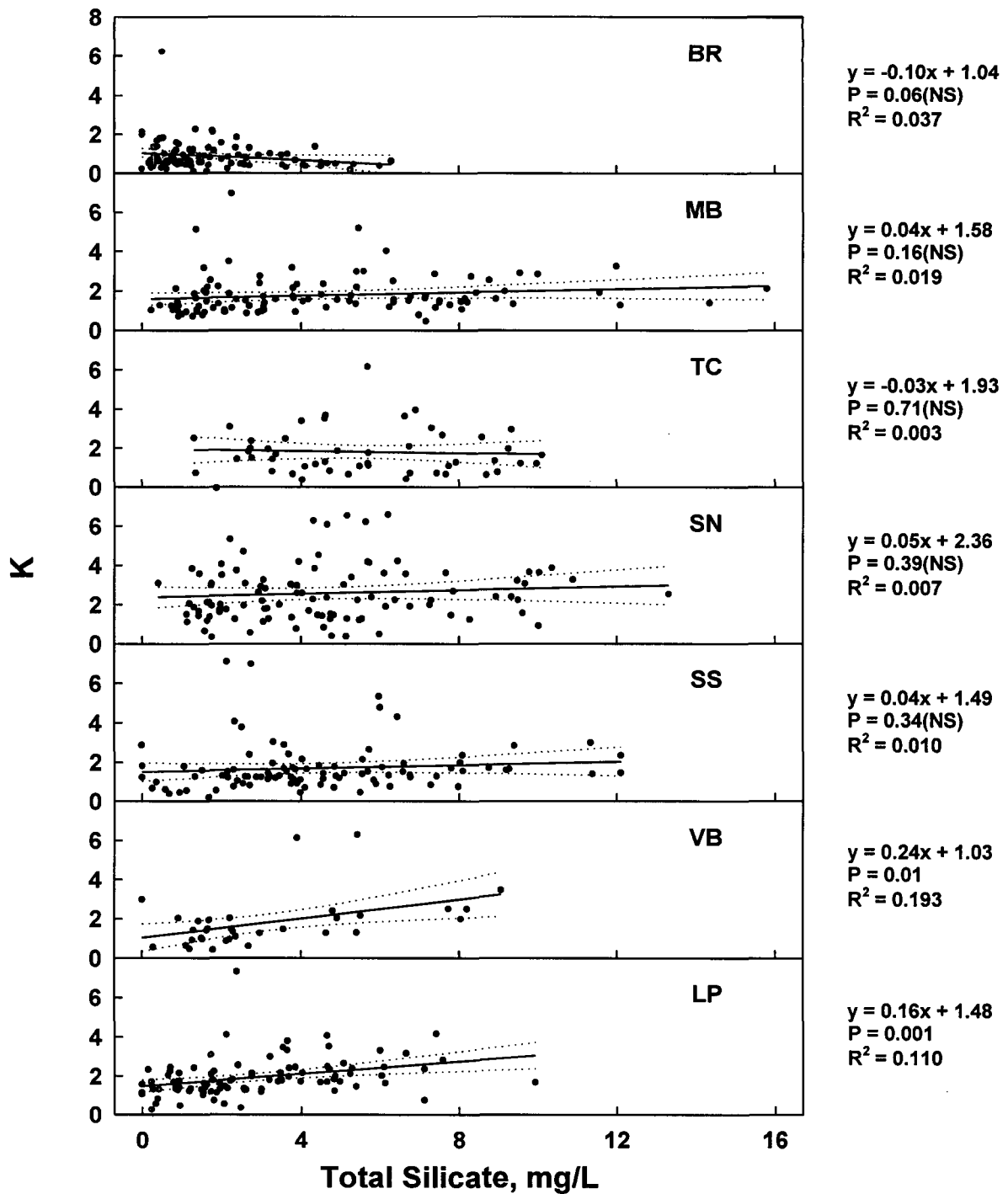


Fig. 7.44 Linear regression analysis of K vs. total silicate based on weekly water quality sampling at each IRL monitoring station. Dotted lines indicate 95% confidence intervals of the regression line.

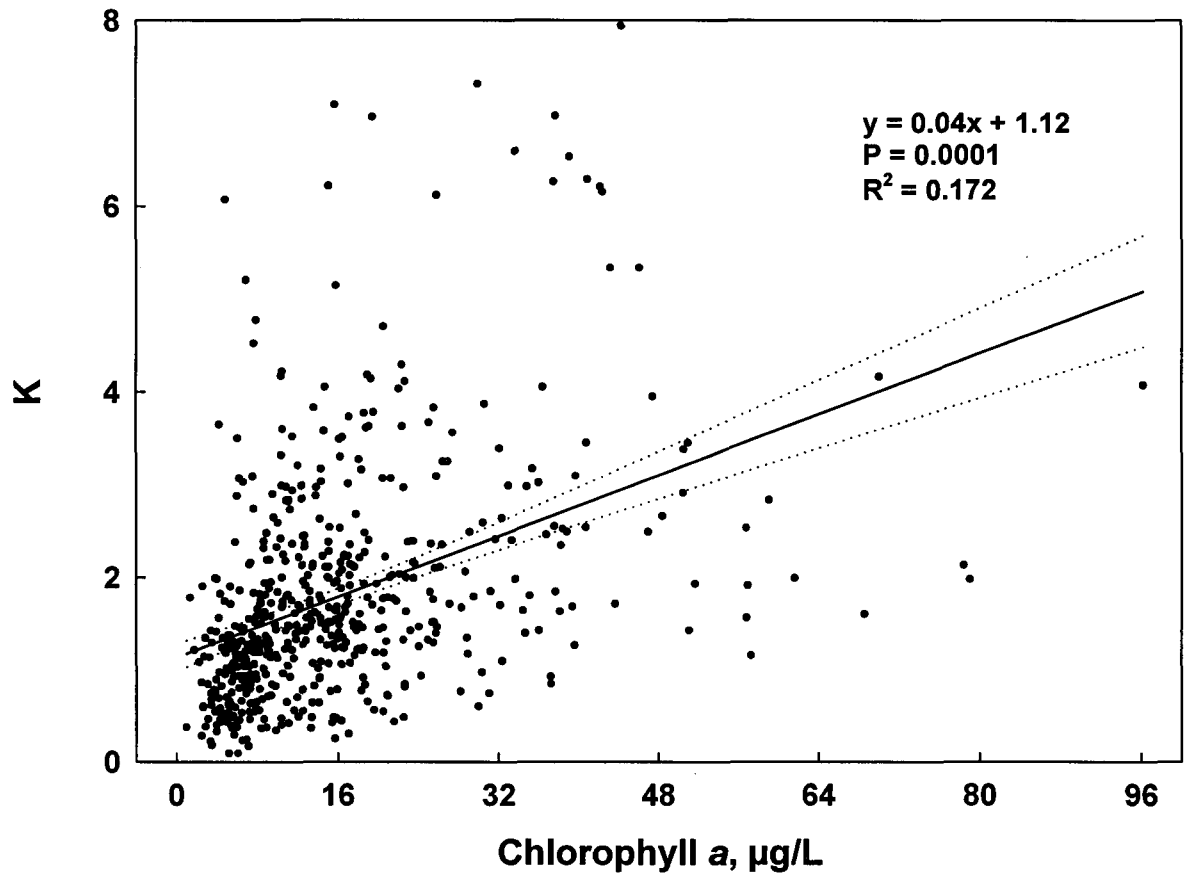


Fig. 7.45 Linear regression analysis of K vs. chlorophyll *a* based on weekly water quality sampling at IRL monitoring stations (all stations combined). Dotted lines indicate 95% confidence intervals of the regression line.

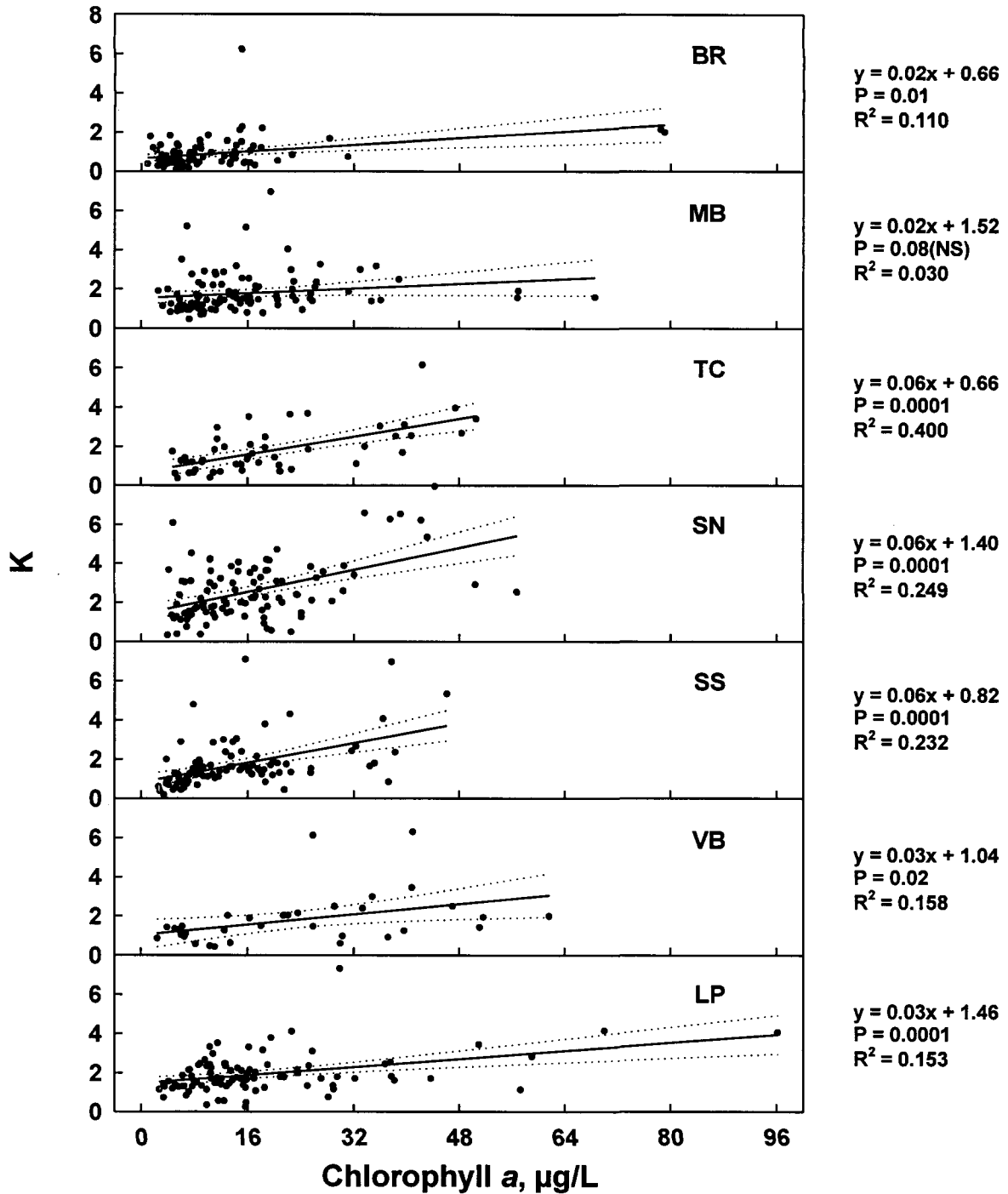


Fig. 7.46 Linear regression analysis of K vs. chlorophyll a based on weekly water quality sampling at each IRL monitoring station. Dotted lines indicate 95% confidence intervals of the regression line.

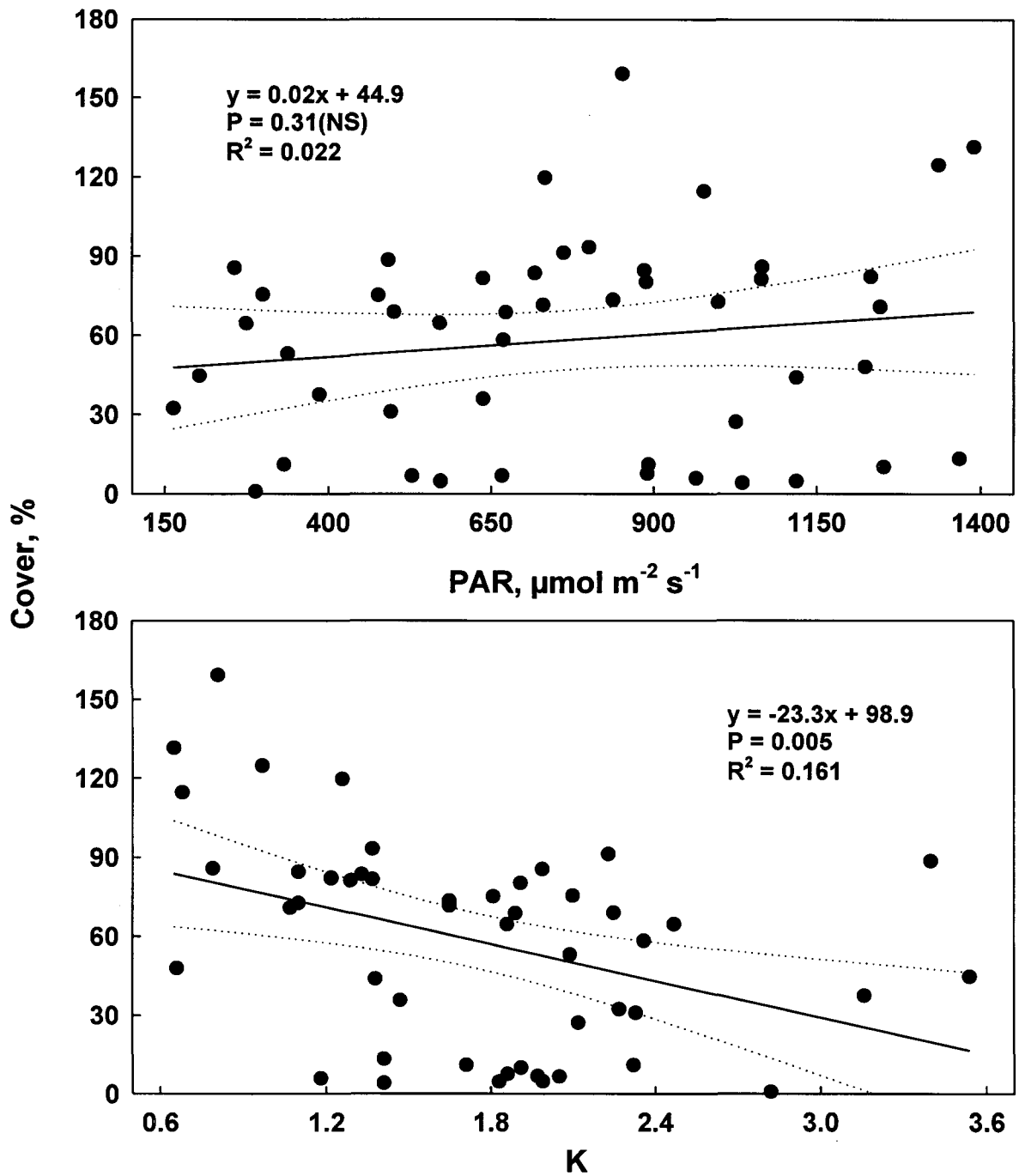


Fig. 7.47 Linear regression analysis of seagrass cover vs. underwater PAR and vertical light attenuation coefficient (K) based on quarterly sampling of seagrass and quarterly means for PAR and K at IRL monitoring stations (all stations combined). Dotted lines indicate 95% confidence intervals of the regression line.

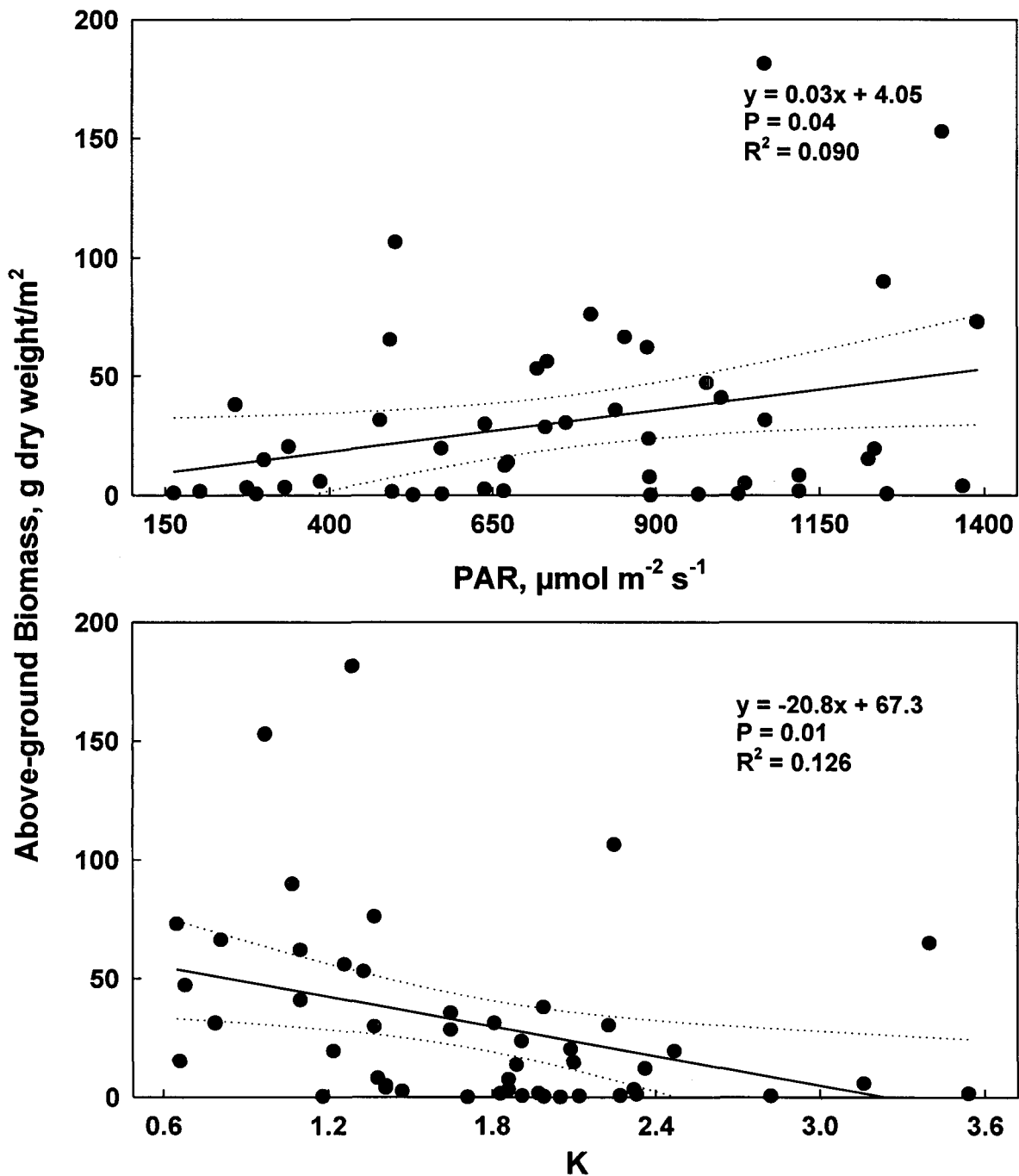


Fig. 7.48 Linear regression analysis of above-ground seagrass biomass vs. underwater PAR and vertical light attenuation coefficient (K) based on quarterly sampling of seagrass and quarterly means for PAR and K at IRL monitoring stations (all stations combined). Dotted lines indicate 95% confidence intervals of the regression line.

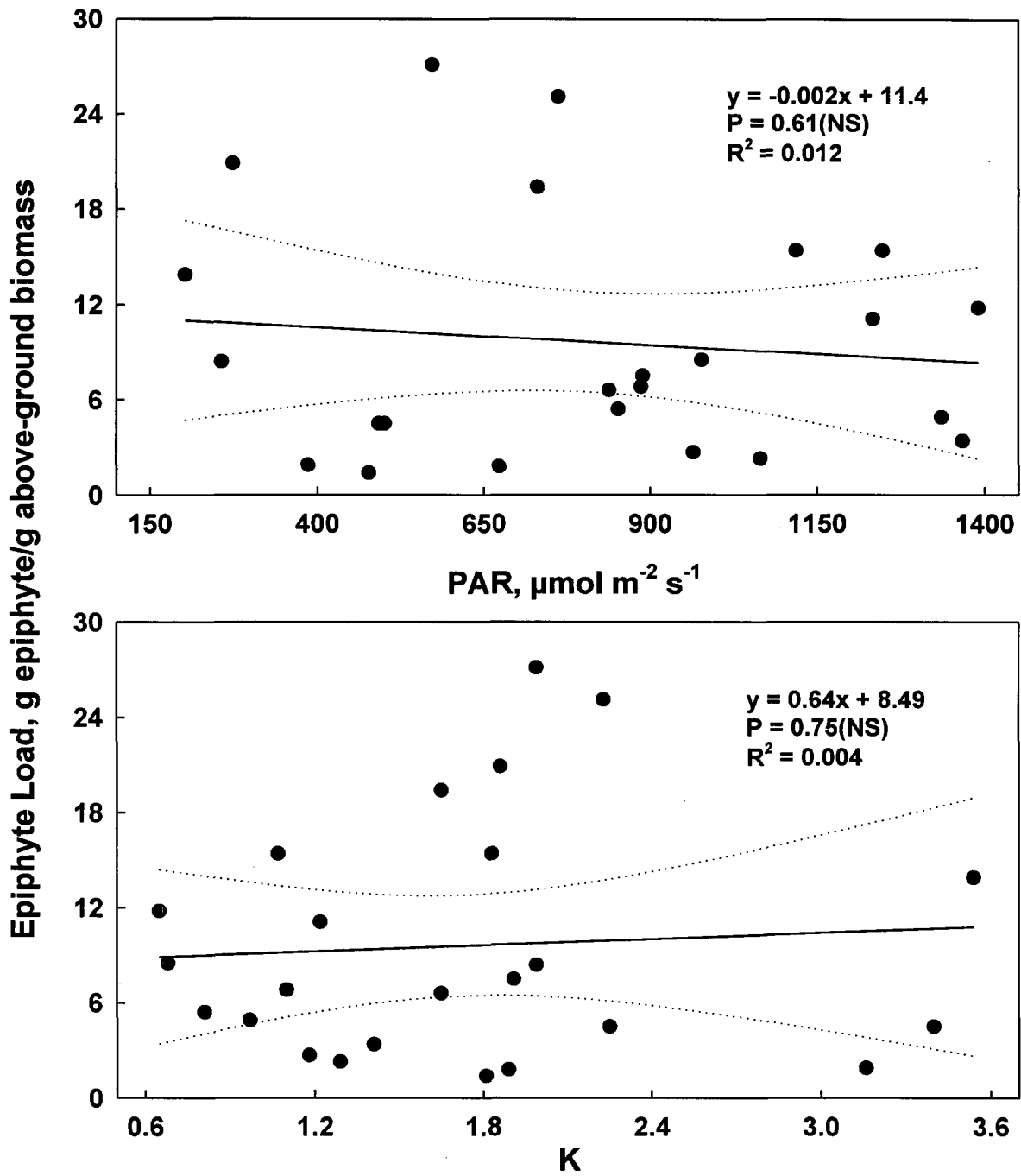


Fig. 7.49 Linear regression analysis of epiphyte load vs. underwater PAR and vertical light attenuation coefficient (K) based on quarterly sampling of epiphyte loads and quarterly means for PAR and K at IRL monitoring stations (all stations combined). Dotted lines indicate 95% confidence intervals of the regression line.

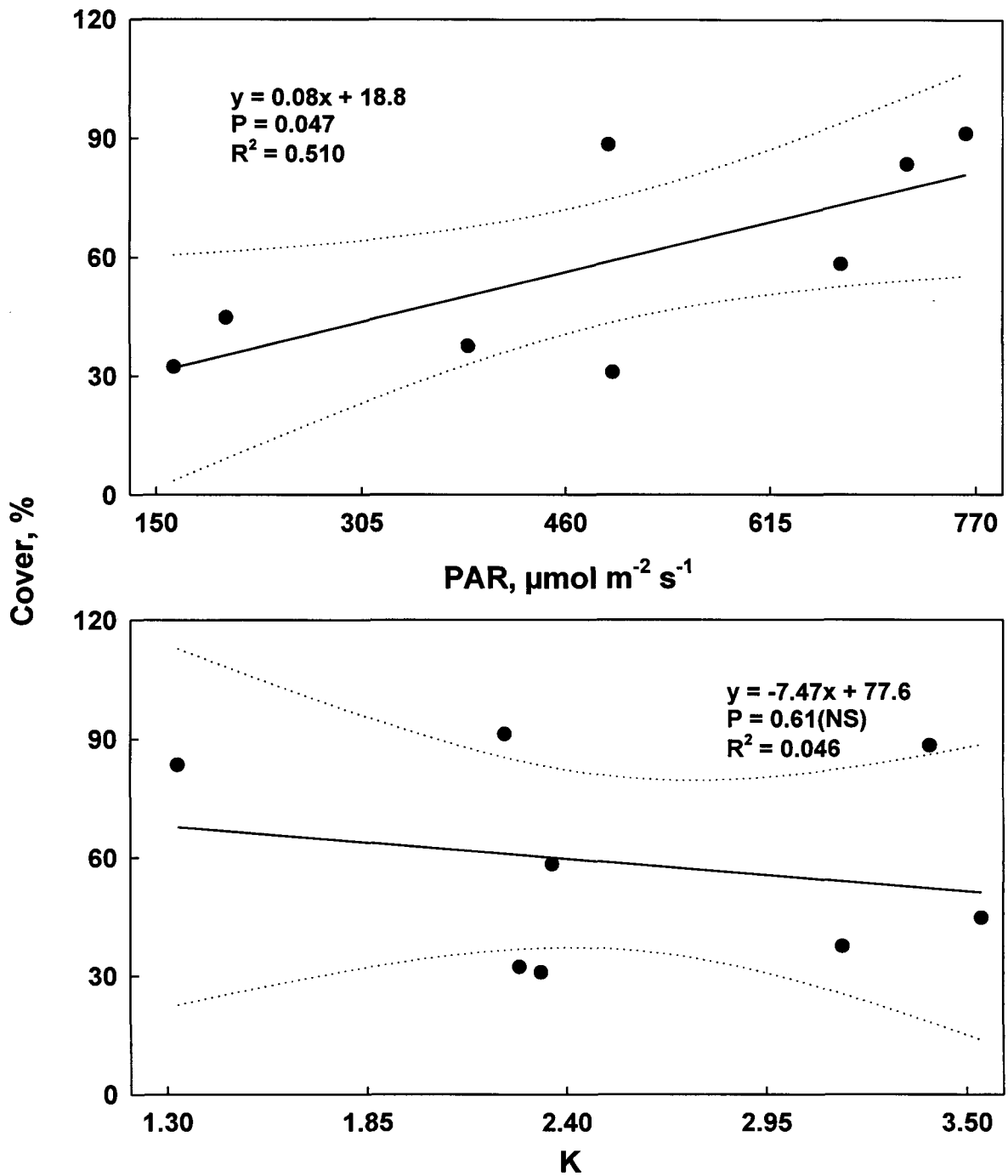


Fig. 7.50 Linear regression analysis of seagrass cover vs. underwater PAR and vertical light attenuation coefficient (K) based on quarterly sampling of seagrass and quarterly means for PAR and K at SS. Dotted lines indicate 95% confidence intervals of the regression line.

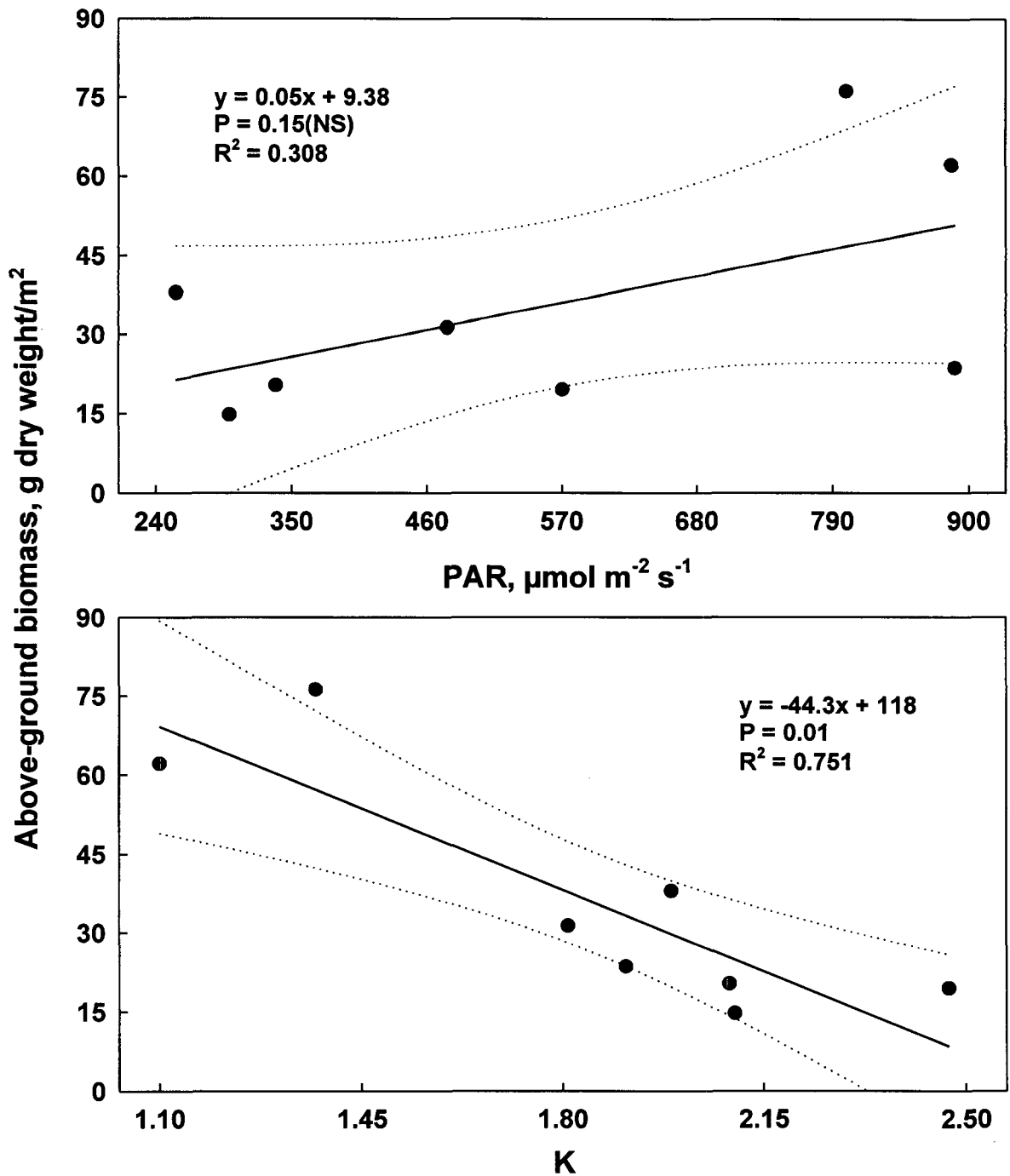


Fig. 7.51 Linear regression analysis of above-ground seagrass biomass vs. underwater PAR and vertical light attenuation coefficient (K) based on quarterly sampling of seagrass and quarterly means for PAR and K at LP. Dotted lines indicate 95% confidence intervals of the regression line.

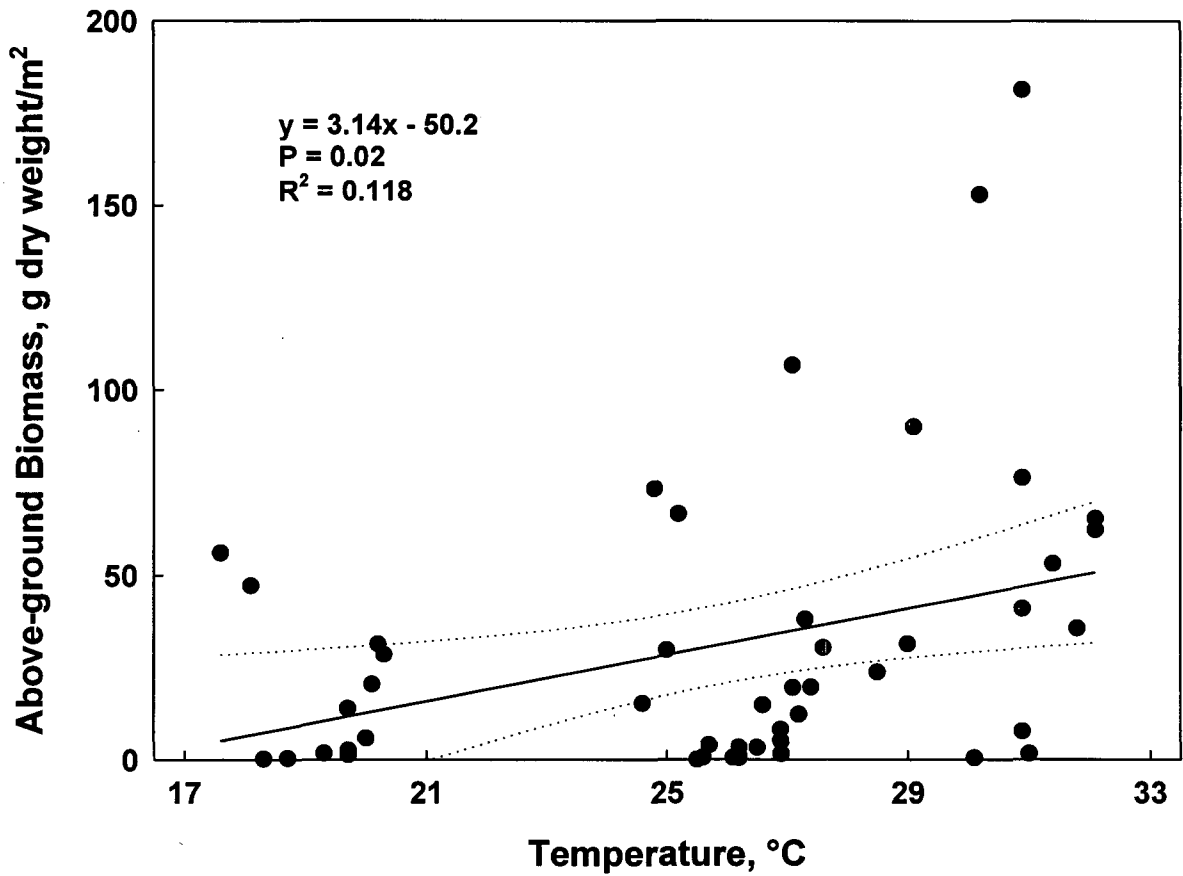


Fig. 7.52 Linear regression analysis of above-ground seagrass biomass vs. temperature based on quarterly sampling of seagrass and quarterly means for temperature at IRL monitoring stations (all stations combined). Dotted lines indicate 95% confidence intervals of the regression line.

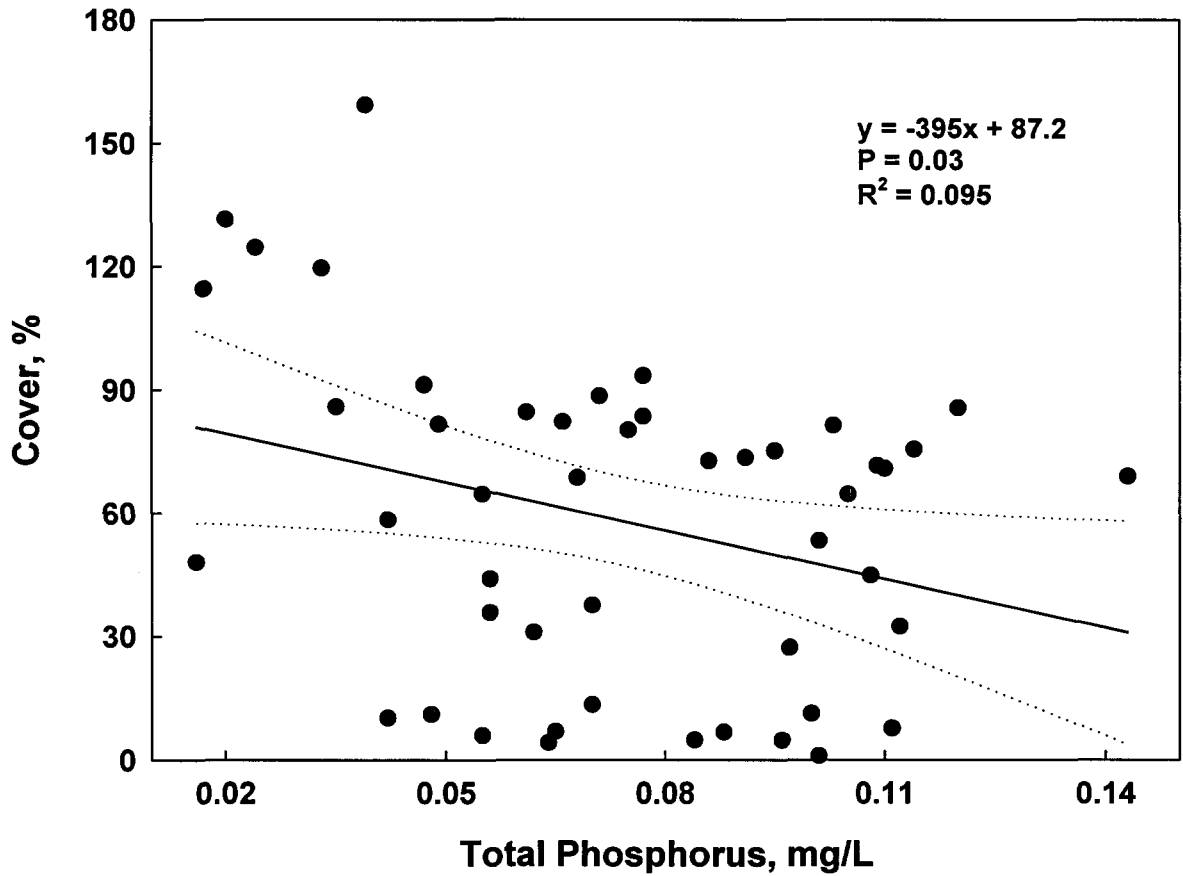


Fig. 7.53 Linear regression analysis of seagrass cover vs. total phosphorus based on quarterly sampling of seagrass and quarterly means for total phosphorus at IRL monitoring stations (all stations combined). Dotted lines indicate 95% confidence intervals of the regression line.

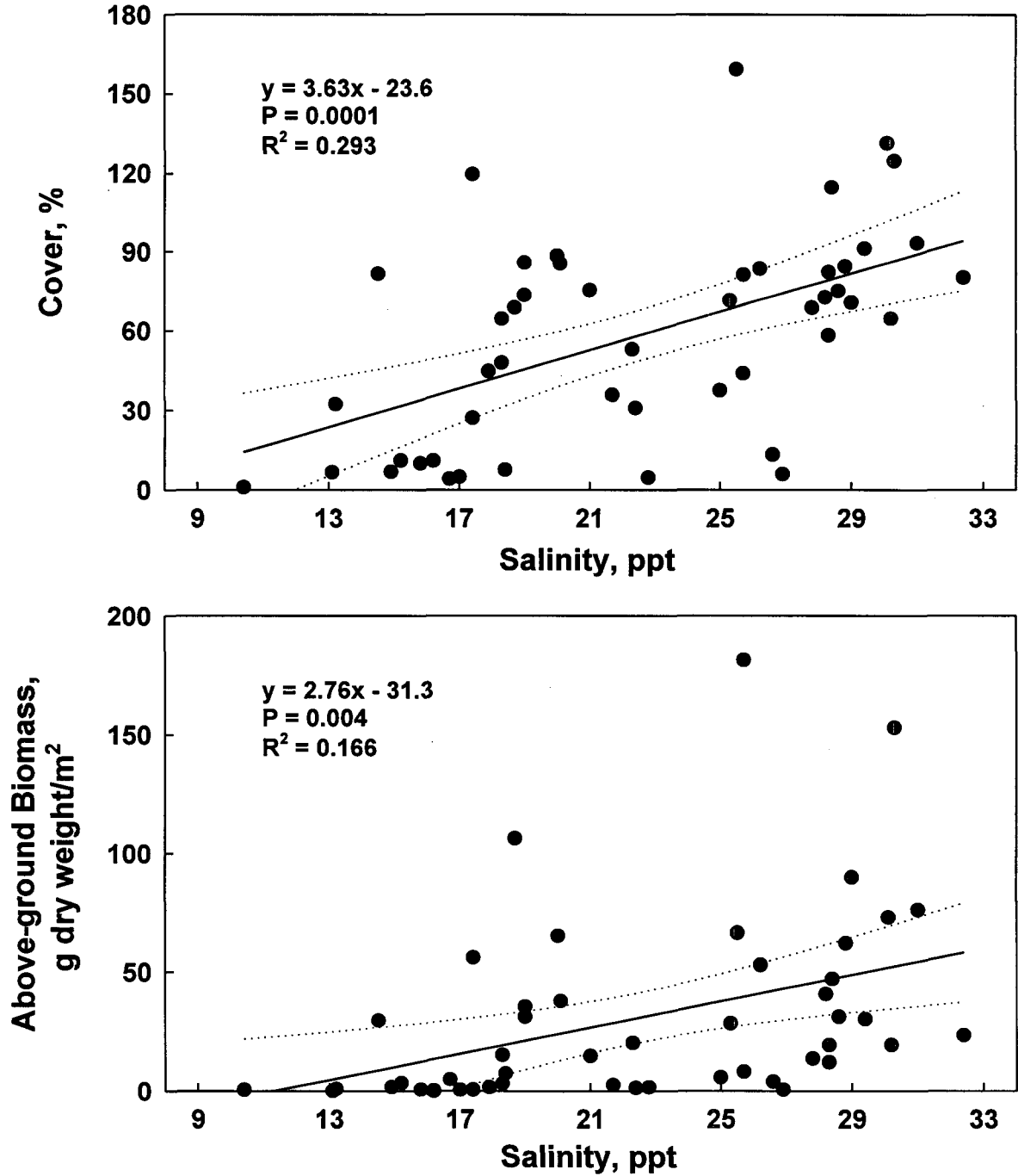


Fig. 7.54 Linear regression analysis of seagrass cover and above-ground seagrass biomass vs. salinity based on quarterly sampling of seagrass and quarterly means for salinity at IRL monitoring stations (all stations combined). Dotted lines indicate 95% confidence intervals of the regression line.

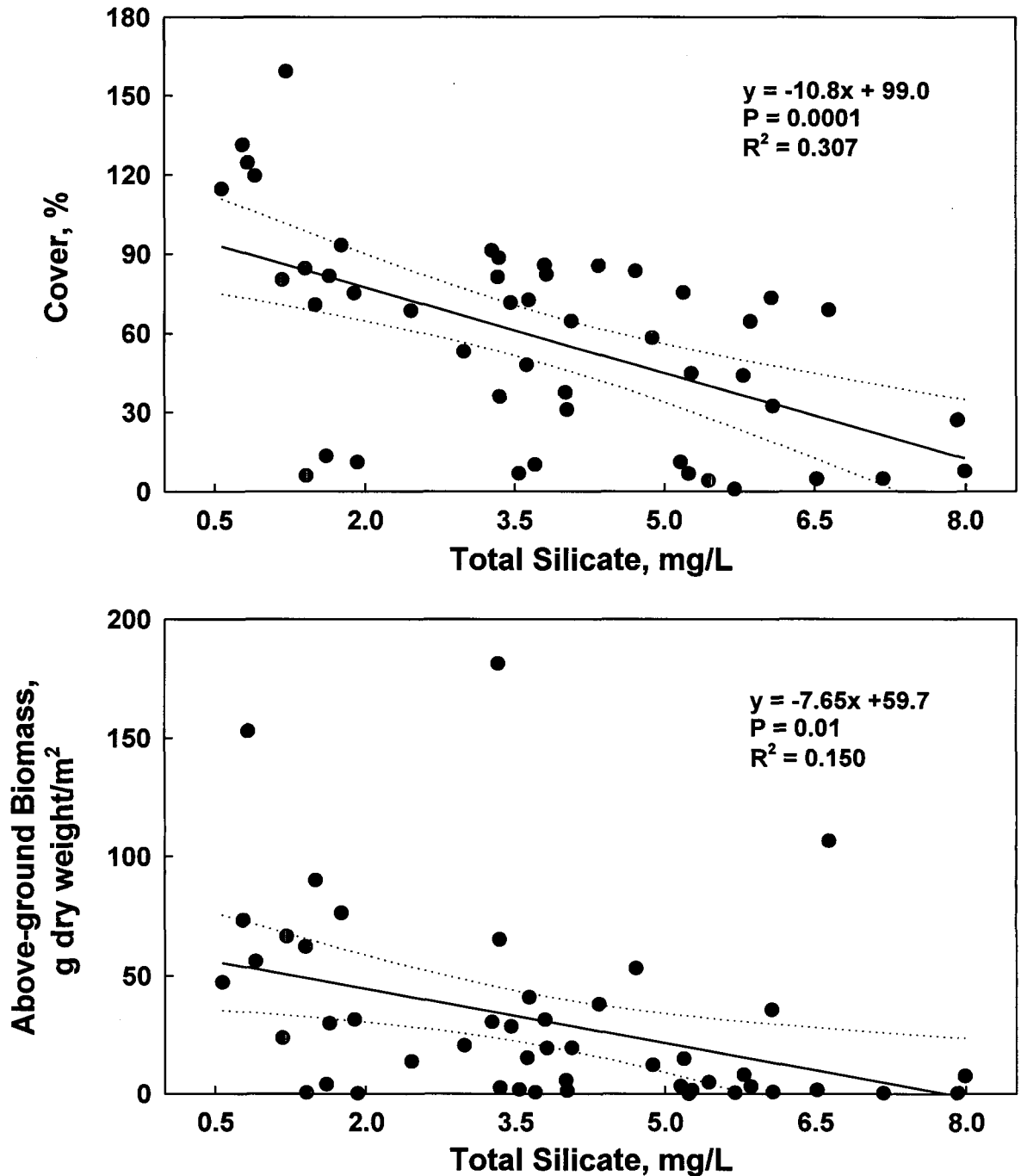


Fig. 7.55 Linear regression analysis of seagrass cover and above-ground seagrass biomass vs. total silicate based on quarterly sampling of seagrass and quarterly means for total silicate at IRL monitoring stations (all stations combined). Dotted lines indicate 95% confidence intervals of the regression line.

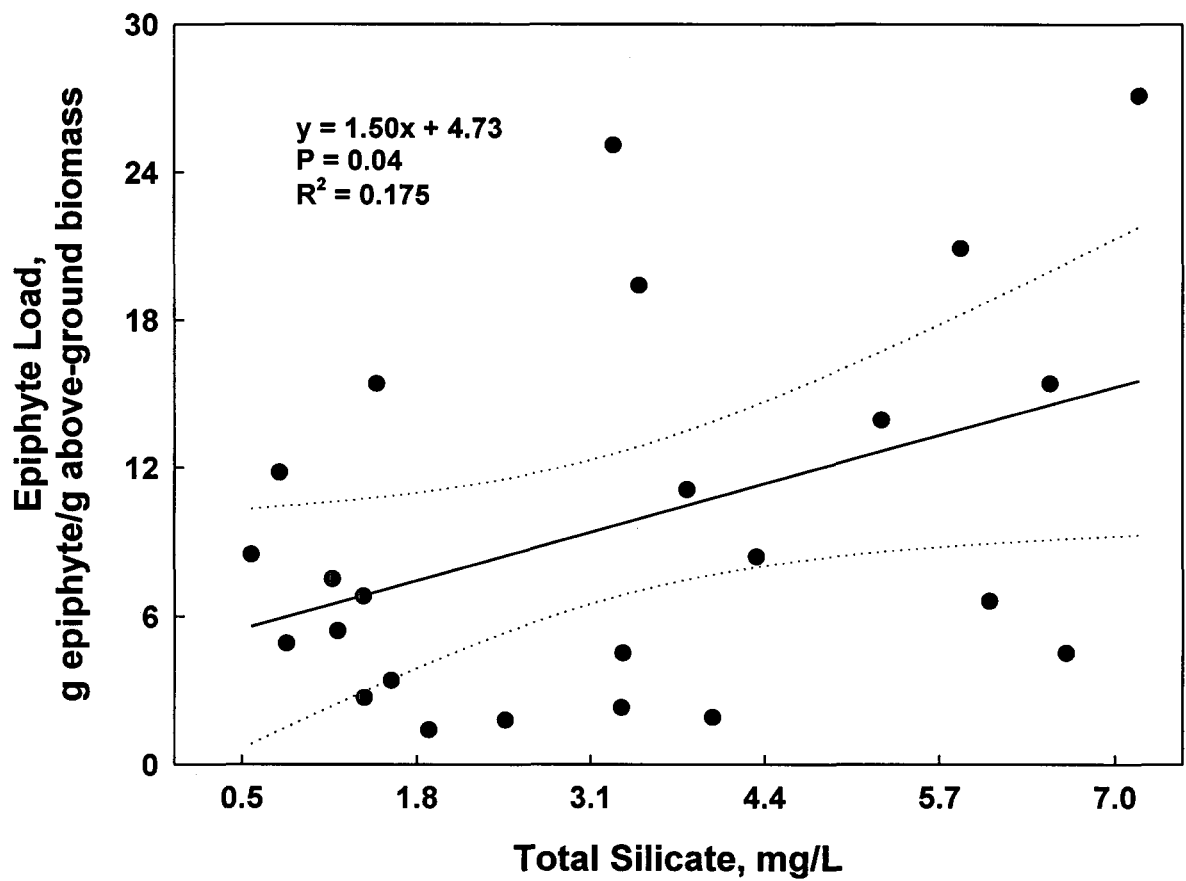


Fig. 7.56 Linear regression analysis of epiphyte load vs. total silicate based on quarterly sampling of epiphyte loads and quarterly means for total silicate at IRL monitoring stations (all stations combined). Dotted lines indicate 95% confidence intervals of the regression line.

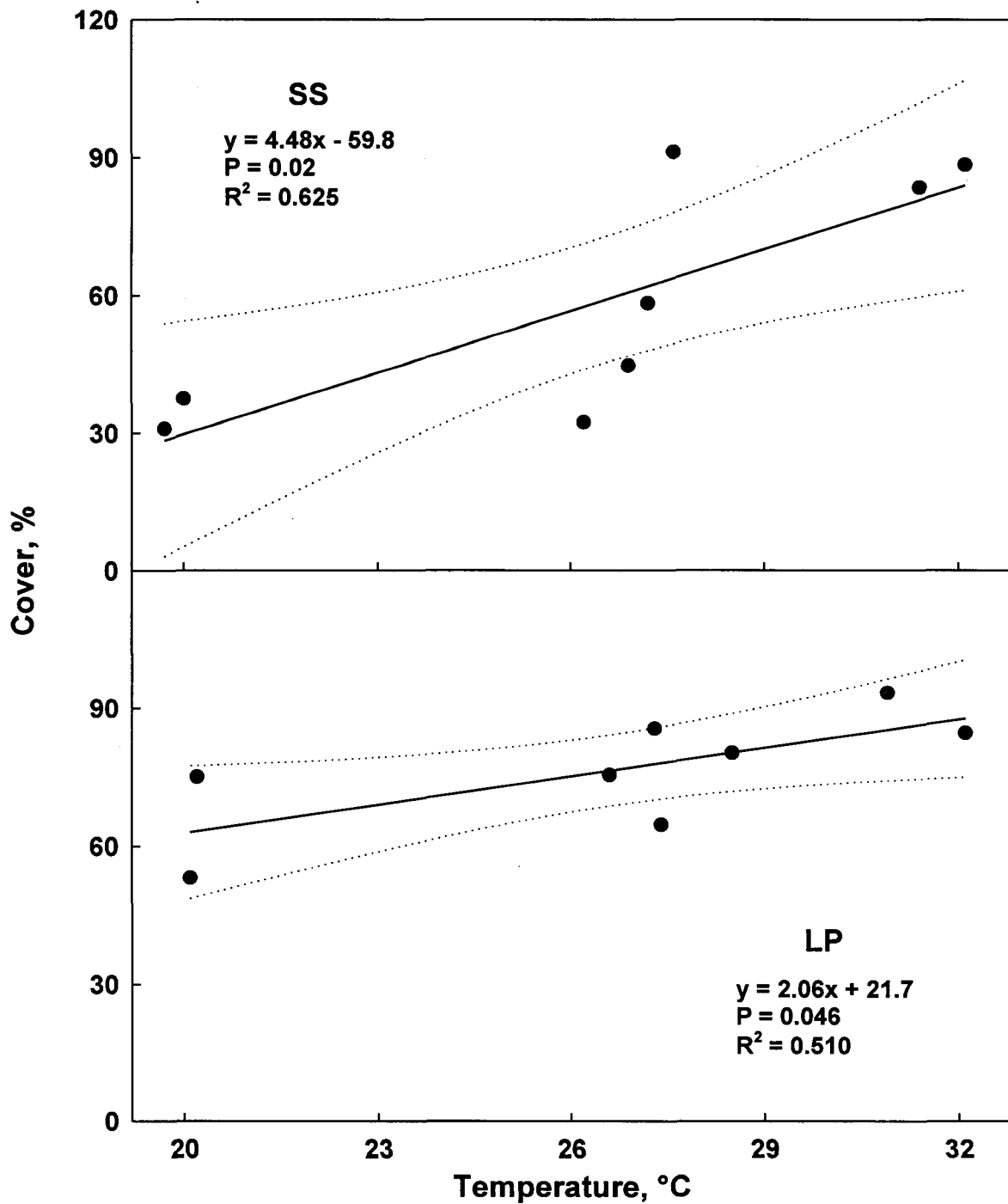


Fig. 7.57 Linear regression analysis of seagrass cover vs. temperature based on quarterly sampling of seagrass and quarterly means for temperature at SS and LP. Dotted lines indicate 95% confidence intervals of the regression line.

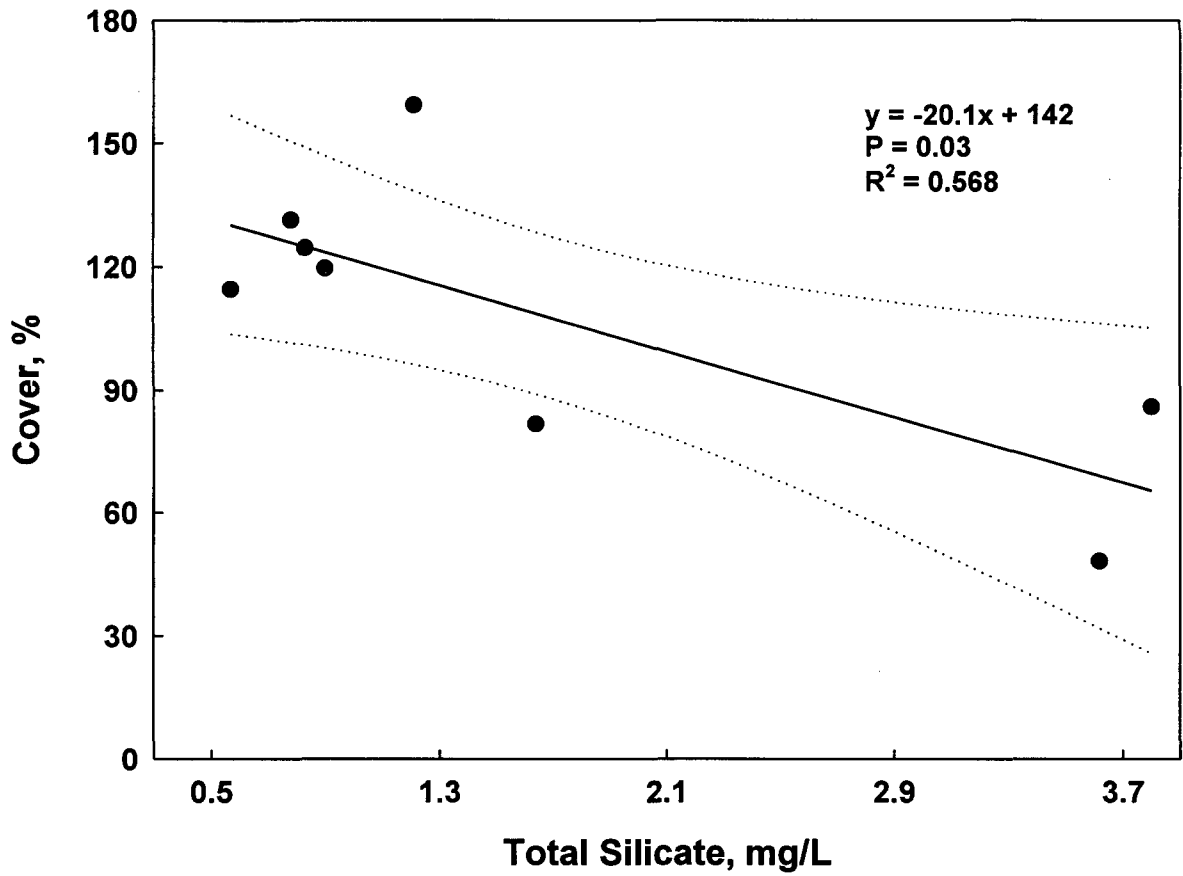


Fig. 7.58 Linear regression analysis of seagrass cover vs. total silicate based on quarterly sampling of seagrass and quarterly means for total silicate at BR. Dotted lines indicate 95% confidence intervals of the regression line.

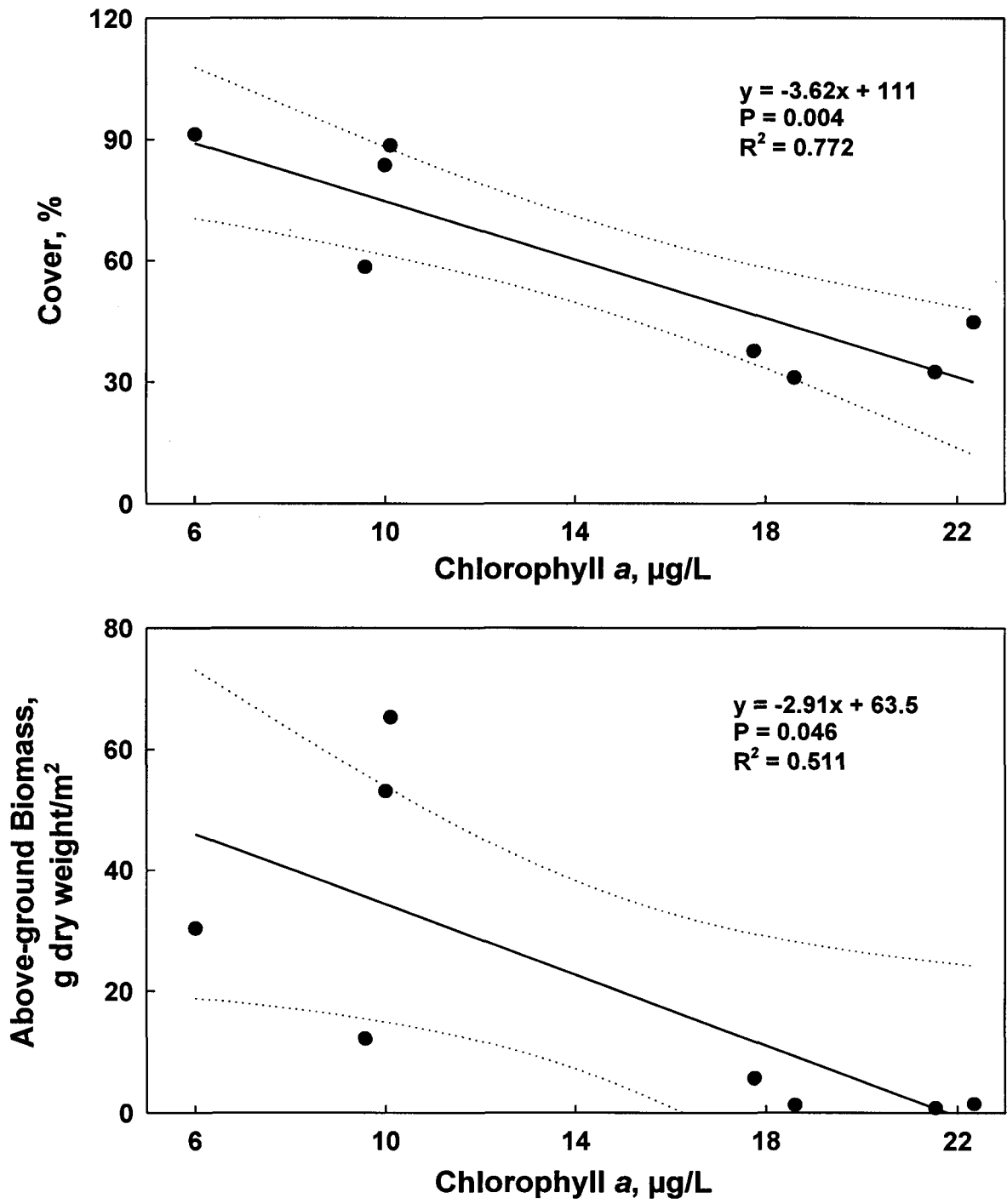


Fig. 7.59 Linear regression analysis of seagrass cover and above-ground seagrass biomass vs. chlorophyll a based on quarterly sampling of seagrass and quarterly means for chlorophyll a at SS. Dotted lines indicate 95% confidence intervals of the regression line.

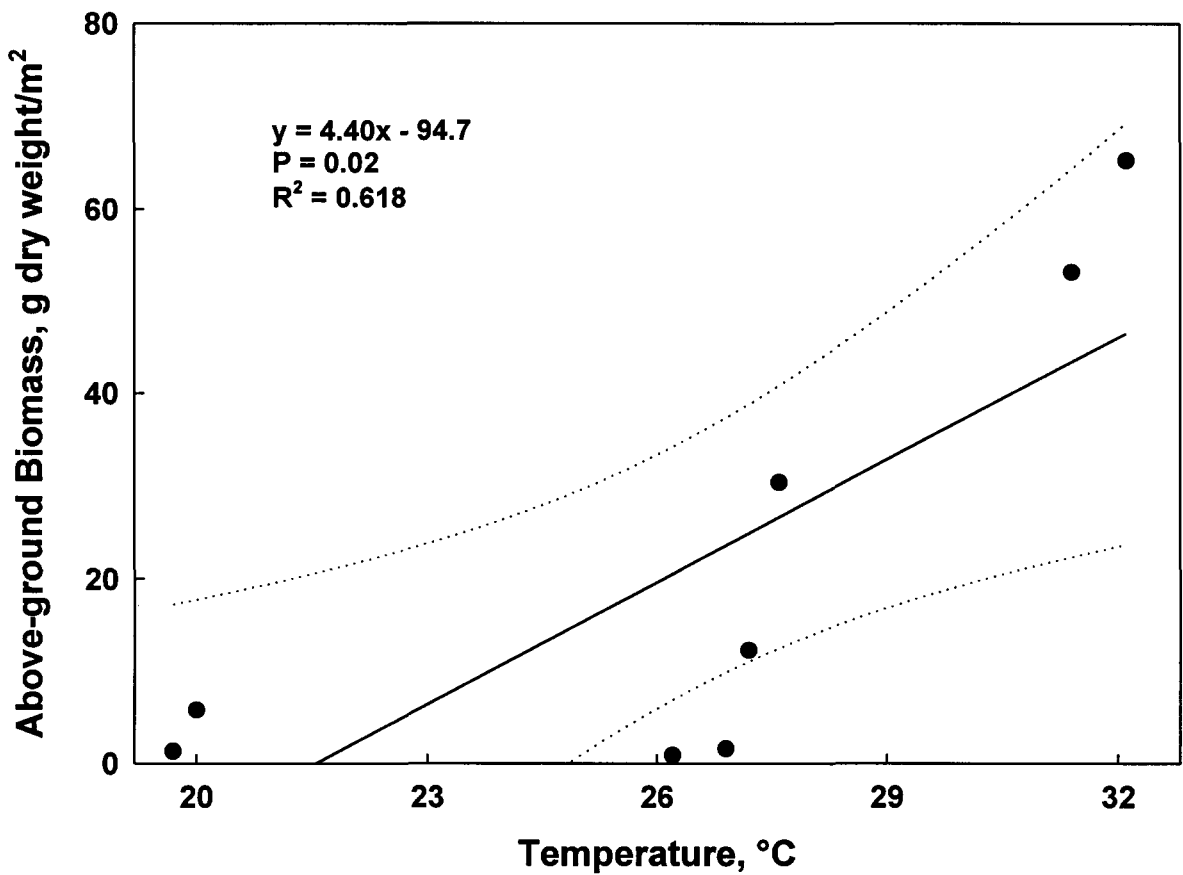


Fig. 7.60 Linear regression analysis of above-ground seagrass biomass vs. temperature based on quarterly sampling of seagrass and quarterly means for temperature at SS. Dotted lines indicate 95% confidence intervals of the regression line.

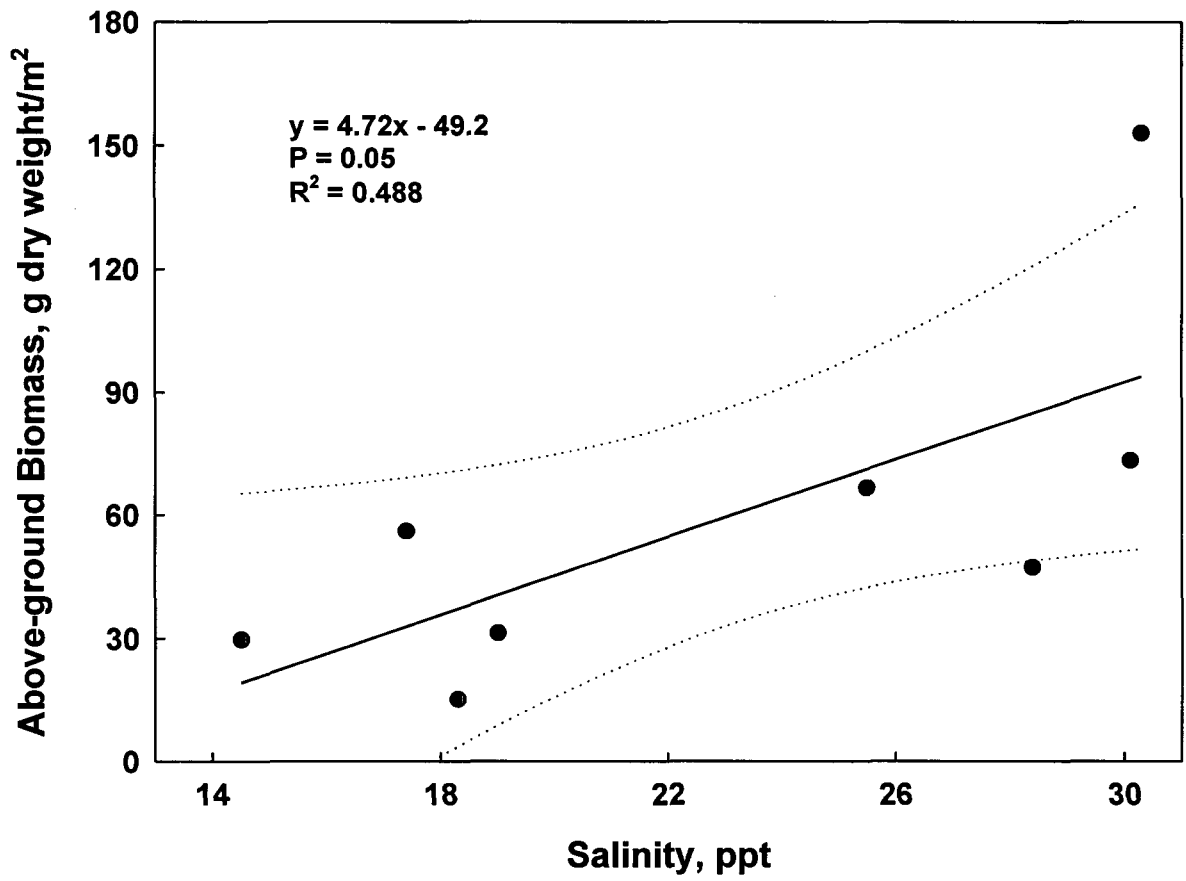


Fig. 7.61 Linear regression analysis of above-ground seagrass biomass vs. salinity based on quarterly sampling of seagrass and quarterly means for salinity at BR. Dotted lines indicate 95% confidence intervals of the regression line.

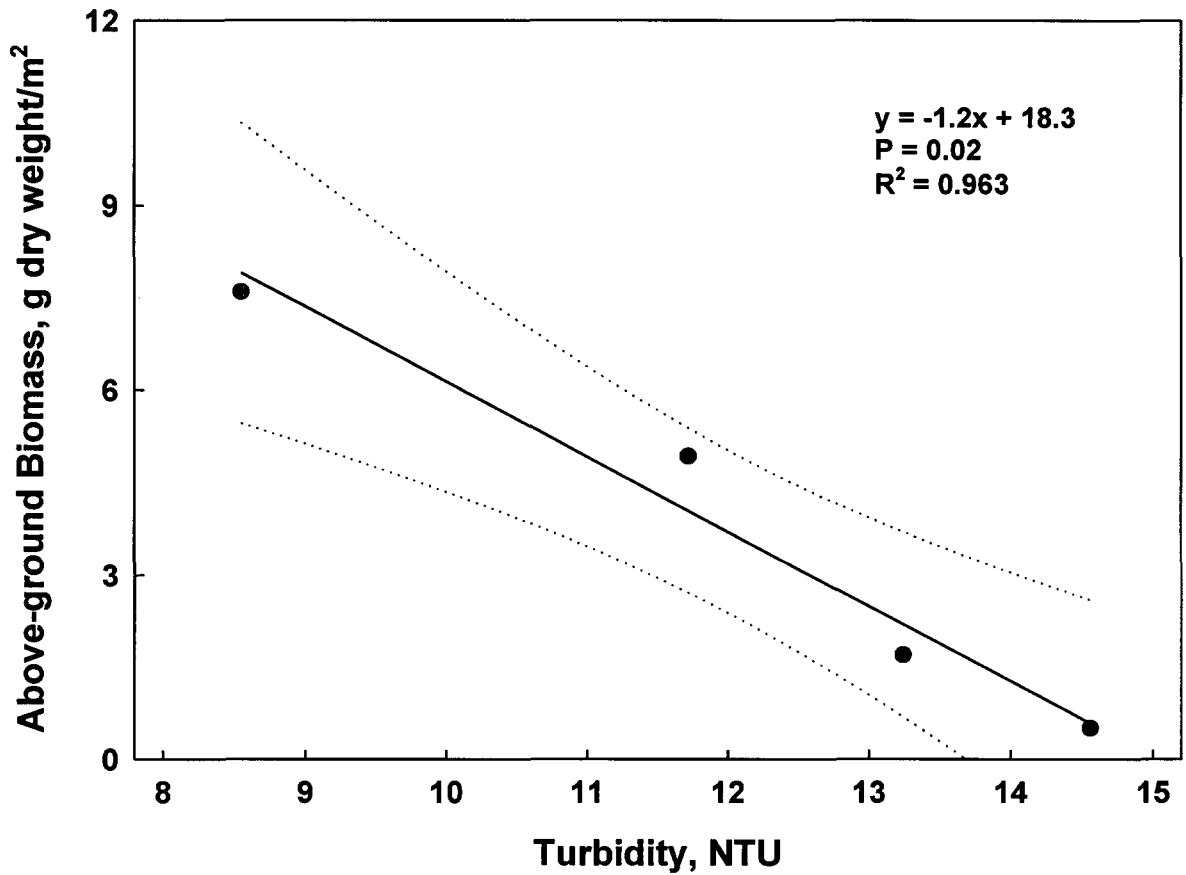


Fig. 7.62 Linear regression analysis of above-ground seagrass biomass vs. turbidity based on quarterly sampling of seagrass and quarterly means for turbidity at TC. Dotted lines indicate 95% confidence intervals of the regression line.

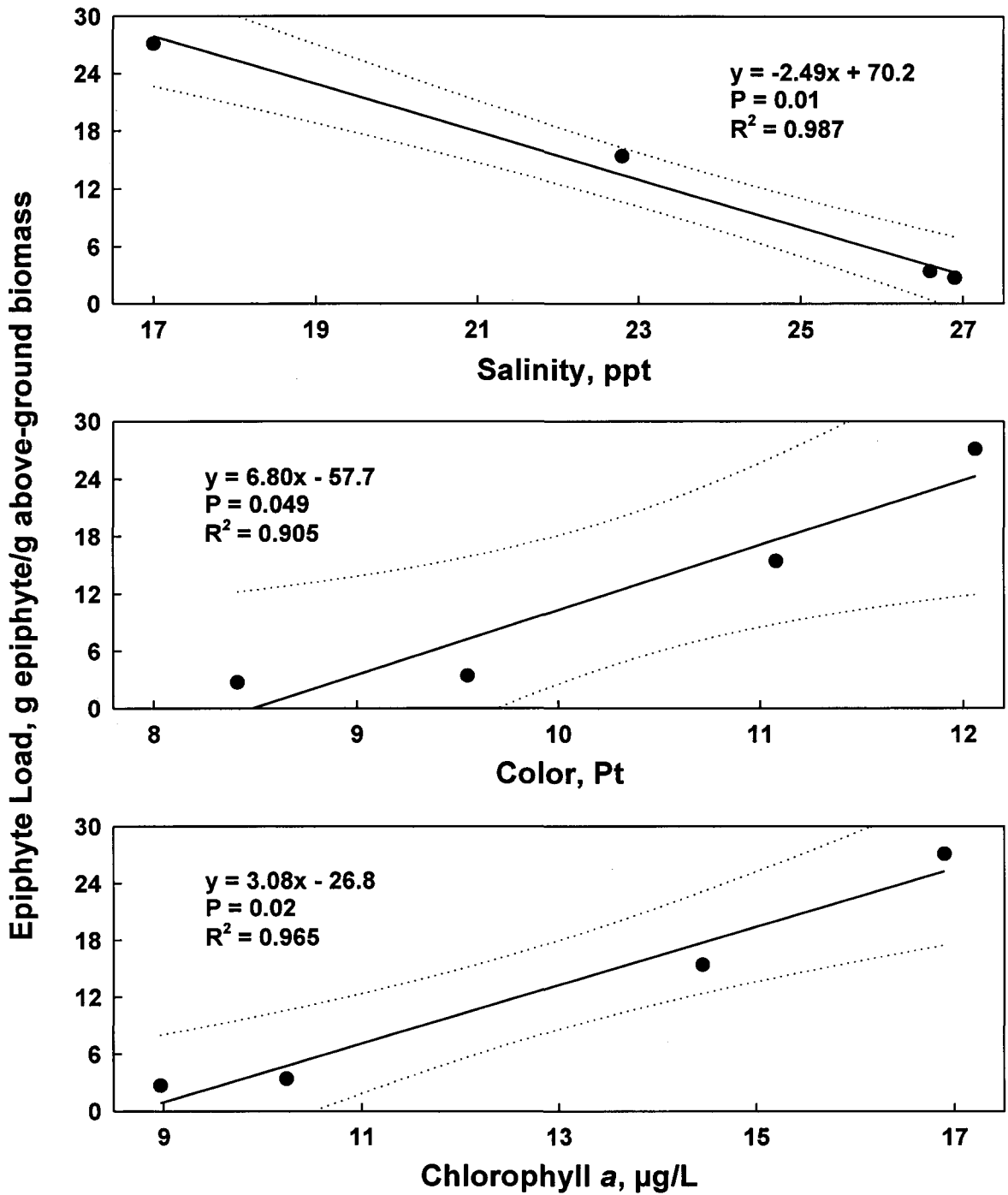


Fig. 7.63 Linear regression analysis of epiphyte load vs. salinity, color, and chlorophyll a based on quarterly sampling of epiphyte loads and quarterly means for salinity, color, and chlorophyll a at MB. Dotted lines indicate 95% confidence intervals of the regression line.

Chapter 8: Ancillary Information on Epiphyte Grazers, Nutrient-Epiphyte Interactions, and Par Attenuation Due to Epiphytes

8.1 Introduction

In addition to the data obtained for the other project tasks, the District was also interested in the importance of grazers on seagrass epiphytes and interactions of epiphytes with nutrients and PAR. Information was gathered or obtained on: (1) the relative abundance of epiphyte grazers at the IRL monitoring stations (collection of new data), (2) nutrient-epiphyte interactions (based on data collected by the Principal Investigator in mesocosm experiments on a Sea Grant-funded project, as well as from previous studies), and (3) estimates of PAR attenuation due to epiphytes in IRL [based on a study conducted by Florida Institute of Technology (F.I.T.)].

8.2 Task Description

Task 8: To provide or obtain data relevant, but ancillary, to the other tasks, specifically on the relative abundance of epiphyte grazers, nutrient-epiphyte interactions, and PAR attenuation due to epiphytes.

8.3 Methods

The relative abundance of grazers was sampled during the quarterly sampling of SAV (Chapter 4) and epiphytes (Chapter 5) with an epifaunal sampler (Virnstein and Howard 1987). The sampling frequency was the same as that for the SAV and epiphyte sampling: for each station except MB and TC, 10 samples were taken along the "whole-bed" Transect 1 and 6 samples each along the "mid-bed" Transect 2 and the "deep-edge" Transect 3. At MB and TC, 10 samples were taken along Transect 2 only. Thus, at 5 stations, a total of 22 samples were taken, and at MB and TC, 10 samples were taken, for a total of 120 samples each quarter in Year 1 and 108 samples each quarter in Year 2.

This sampling effort was much greater than what had been initially proposed. Sampling was conducted for 9 quarters; the contract called for only 5 quarters of sampling. Moreover, each quarterly sampling effort was substantially greater than what was specified in the contract ($n = 6$ per station, 6 stations; total samples = 36 per quarter). So, while the contract called for the analysis of 180 samples (5 sampling events @ 6 stations x 6 samples per station), 1,042 samples (see Table 4.1), nearly 6 times the number of samples contracted, were collected and analyzed.

The epifaunal sampler was designed to sample above-ground seagrass and its epifaunal community (primarily crustaceans and gastropods); this sampler was not designed to sample fish. Sampling locations for grazers along each transect were determined by random numbers. After each sample was collected, the seagrass with its macroscopic grazers was washed onto a 0.5-mm mesh sieve, placed in individual, labeled plastic bags on ice, and frozen until processed.

In the laboratory, grazers were sorted and counted. Sorting was done to major taxonomic groupings (snails, amphipods, shrimp, tanaidaceans, isopods, and other crustaceans); this sorting was beyond the scope of the work plan, which only required a total count of the animals. Seagrass biomass (g dry weight) was dried at 80°C to constant weight, and weighed. Grazer abundance was calculated both on a per sample (number of grazers/sample) and on a per seagrass biomass (number of grazers/g dry weight seagrass) basis.

In this report, data are presented as means±standard error (SE). Statistical analyses were performed with SAS statistical software (SAS Institute 1988). Statistical significance among means was tested with analysis of variance (ANOVA). When ANOVA indicated the existence of significant differences, the Tukey-Kramer test (T-K) determined which means were significantly different ($P \leq 0.05$). Prior to performing ANOVA, counts were transformed with the logarithmic transformation (Sokal and Rohlf 1981).

Relationships among the abundance of grazers, epiphytes (data from Chapter 5), and above-ground seagrass biomass (data from Chapter 4) were determined by linear regression analyses (Sokal and Rohlf 1981). The data used for these analyses were station means for all samples. The minimal level of statistical significance for all regression analyses was $P \leq 0.05$.

8.4 Results

The presentation of results begins with the patterns of abundance of grazing epifauna at the stations (Section 8.4.1). The grazer community is characterized in terms of its major groups, and patterns in total grazer abundance are analyzed for differences among stations, years, seasons, and transects. Regression analyses (Section 8.4.2) relate the grazer data with epiphyte and SAV data previously presented (Chapters 4 and 5) to define the relationships of these parameters. Nutrient-epiphyte interactions are summarized based primarily on mesocosm experiments conducted by the Principal Investigator as part of another project and supplemented with information from other studies (Section 8.4.3). Lastly, estimates of PAR attenuation due to epiphytes (based on the F.I.T. study) are provided (Section 8.4.4).

8.4.1 Abundance of Epiphyte Grazers

The grazing epifaunal community sampled in this study consisted of snails and crustaceans (Fig. 8.1), with snails the most numerous component (69% of the grazers were snails). Although no data are presented herein, the most widespread snail encountered was *Bittolum varium*. Amphipods (11% of all grazers sampled) were the most numerous group of crustaceans, followed by shrimp (9%), miscellaneous crustaceans (8%), tanaidaceans (2%), and isopods (1%).

Differences among stations in total abundance of grazing epifauna (Fig. 8.2) were highly significant (ANOVA; $P = 0.0001$). Over the course of the entire study, the mean number of individual grazers per sample (Fig. 8.2) was greatest at BR and VB, least at MB and SS, and intermediate at the other stations (T-K: $P < 0.05$).

Site-specific comparisons of grazer abundance were confounded by significant interannual variation in grazer abundance at BR and SS. At BR, grazer abundance was much higher (ANOVA: $P = 0.0001$) during 1994 than 1995 (Fig. 8.2). This decline was due primarily to snails (Fig. 8.3). The abundance of amphipods and miscellaneous crustaceans also declined significantly during 1995, but shrimp were more abundant during 1995. At SS, grazer abundance was marginally lower during 1995 (ANOVA: $P = 0.046$). This relatively modest decline at SS was due to significant declines in amphipods, isopods, and miscellaneous crustaceans.

The interannual variation at BR altered the analysis of site-specific differences during the 2 years. In 1994, grazer abundance (Fig. 8.2) was highest at BR and VB, lowest at MB and SS, and intermediate at the other stations (T-K: $P < 0.05$). In 1995, there were considerably less differences among stations; the only significant difference was higher grazer abundance at SN than at MB and SS (T-K: $P < 0.05$).

The major difference in terms of grazer composition among stations (Fig. 8.3) was the much higher abundance of snails at BR and VB; crustaceans were more abundant than snails at the other stations. Thus, the difference in the abundance of grazing epifauna at the stations was primarily due to the differential distribution of snails.

Analysis of the seasonal samples (Fig. 8.4) indicated that grazer abundance was fairly constant at most stations, with occasional sharp peaks in abundance. The major station differences noted previously were primarily a function of large peaks in abundance (due to snails) in the August 1994 samples at BR, VB, and LP. When data were pooled for all stations, grazer abundance was highest in August 1994 and lowest in November 1995 and February 1996 (T-K: $P < 0.05$).

When there was a difference among transects in grazer abundance (numbers/sample), it was usually a decline at the "deep-edge" Transect 3 (Fig. 8.5).

8.4.2 Regression Analyses: Grazers, Epiphytes, and SAV Interactions

The station means for grazing epifauna abundance were used in regression analyses that involved two other parameters previously presented: epiphyte load (Chapter 5) and above-ground seagrass biomass (Chapter 4). These analyses specifically addressed the questions:

- (1) What is the relationship of epiphyte loads and the abundance of epiphyte grazers?
- (2) What is the relationship of the abundance of grazers with the amount of seagrass?
- (3) What is the relationship of seagrass biomass to epiphyte load?

Epiphyte Load and Grazers

Epiphyte load decreased as grazer abundance increased (Fig. 8.6). The regression model for epiphyte load and grazer abundance was significant ($P = 0.03$). The R^2 value for the model indicated that 71% of the variability of epiphyte load among the station means could be explained by the abundance of grazing epifauna.

Grazer Abundance and Above-ground Seagrass Biomass

Grazer abundance increased as above-ground seagrass biomass increased (Fig. 8.7). The regression model for grazer abundance and above-ground seagrass on a per sample basis was not quite significant ($P = 0.06$). The R^2 value for the model indicated that 53% of the variability of grazer abundance among the station means could be explained by the amount of above-ground seagrass biomass.

Above-ground Seagrass Biomass and Epiphyte Load

Above-ground seagrass biomass decreased as a function of increased epiphyte load (Fig. 8.8). The regression model for above-ground seagrass biomass and epiphyte load was significant ($P = 0.04$). The R^2 value for the model indicated that 67% of the variability of above-ground seagrass biomass could be explained by the amount of epiphytes.

8.4.3 Nutrient-Epiphyte-Seagrass Interactions

A low-priority portion of Task 8 was to briefly review the effects of nutrients on seagrasses and their epiphytes, primarily relying on a recent, unpublished study conducted by the Principal Investigator (Hanisak 1996) in mesocosms along IRL. The basis for reviewing this information is the general belief that, in addition to reduced PAR

availability, elevated nutrient levels are a major stressor to seagrass (e.g., Sand-Jensen 1977, Borum 1985, Twilley et al. 1985, Silberstein et al. 1986, Tomasko and Lapointe 1991, Dennison et al. 1993, Neckles et al. 1993). The generally accepted mechanism of nutrient stress on seagrass is the stimulation of the growth of algae, including phytoplankton and epiphytes, that further reduces the PAR available to sustain the growth of the underlying seagrass.

Hanisak (1996) employed a 5 x 3 factorial design (PAR x nutrients) in outdoor mesocosms to determine the synergistic effects of PAR and nutrients on the survival of *Halodule wrightii* and its epiphyte load. The major results of the mesocosm work, as related to this IRL monitoring study were:

- (1) Decreases in PAR or increases in nutrients (nitrate and phosphate) both significantly reduced shoot density and biomass of *H. wrightii*. The effect of decreased PAR was more rapid (significant declines within 2-4 weeks after the stress began) and more significant than the effect of elevated nutrients.
- (2) *H. wrightii* in IRL requires about 20% of incident PAR for long-term survival.
- (3) There were no significant effects of PAR, nutrients, or their interactions on epiphyte load (g dry weight epiphyte/g dry weight shoot). Given the effect that grazers can have on epiphyte loads (e.g., Neckles et al. 1993, Williams and Ruckelshaus 1993; see also section 8.4.2), the mesocosm experiments were conducted with grazers present at ecological relevant levels [pinfish (*Lagodon rhomboides*) and snails (*Bittium varium*) were used in separate experiments]. In the presence of grazers, epiphytes did not reduce the survival of *H. wrightii*.
- (4) Elevated nutrients, even at the relatively low levels of 5 μM $\text{NO}_3\text{-N}$ and 0.31 μM $\text{PO}_4\text{-P}$, were deleterious to the survival of *H. wrightii*. Significant declines first occurred after 8 weeks. This decline was not related to epiphyte load, but appeared to be a direct toxicity, perhaps like that observed by Burkholder et al. (1992) for *Zostera marina*. In that study, the mechanism of toxicity was unclear but the authors attributed it to an overload of nitrogen assimilated through the leaves and associated with increased carbohydrate consumption by roots and rhizomes.
- (5) On an areal basis (g dry weight/m²), both PAR and nutrients were important in determining epiphyte load, but PAR was the more important factor. Areal epiphyte biomass increased with increased PAR; at higher PAR levels, elevated nutrients reduced areal epiphyte biomass. Other studies have found more epiphyte growth at higher irradiance (e.g., Jewett-Smith 1991, Tomasko and Lapointe 1991), but the relative importance of nutrients has varied. Jewett-Smith (1991) found that, while PAR was a very important factor for regulating epiphyte levels on *H. wrightii* in a field study in Texas, there was no significant relationship with nutrient levels. Tomasko

and Lapointe (1991) determined that both PAR and nutrients, as well as their interactions, both significantly increased the epiphyte load of *Thalassia testudinum* in aquarium experiments conducted in the Florida Keys.

- (6) The results of the HBOI study appeared to be a paradox – according to the paradigm, elevated nutrients should result in increased epiphytes, but this did not always occur. The paradox is resolved, however, when grazers and seagrass density are considered. Grazers maintained a relatively constant epiphyte load (on a per seagrass biomass basis) among the various PAR-nutrient combinations. On an areal basis, seagrass density, not PAR or nutrients, directly determined the epiphyte load; the negative impact of increased nutrients on *H. wrightii* reduced areal epiphyte biomass.

8.4.4 Attenuation of PAR by Epiphytes

Another low-priority item assigned to Task 8 was estimating PAR attenuation due to epiphytes in IRL. No new data collection was proposed; rather, this information was derived from a Sea Grant-funded project on this topic to F.I.T. (P.I.'s: W. Nelson and D. Norris). Stations were located from near Fort Pierce Inlet to just north of the Sebastian Inlet. The major product of that study was a M.S. Thesis (Harden 1994). The major results of the F.I.T. study, as related to this IRL monitoring study, were:

- (1) All epiphyte parameters measured (species composition, percent cover, biomass, and percent PAR absorbance) were similar, both spatially (among stations) and temporally (monthly) for the dominant seagrasses of IRL (*H. wrightii*, *Syringodium filiforme*, and *T. testudinum*). No statistical differences for these parameters were found.
- (2) The dominant epiphytes on all seagrass species were diatoms.
- (3) The annual mean percentage epiphyte cover for outside (= older) blades ranged from 77% to 81% for the 3 species. The annual mean percentage epiphyte cover for inside (= younger) blades ranged from 41 to 44% for the 3 species.
- (4) Among species, the percent PAR absorbance by epiphytes was surprisingly constant. The grand means for the 3 species ranged from 59 to 61% for outside blades and 31 to 34% for inside blades.
- (5) Among stations for any given species, the percent PAR absorbance by epiphytes was also relatively constant. Station means for *H. wrightii* ranged from 51 to 66% for outside blades and 28 to 40% for inside blades. Station means for *S. filiforme* ranged from 55 to 68% for outside blades and 25 to 38% for inside blades. Station means

for *T. testudinum* ranged from 54 to 70% for outside blades and 26 to 40% for inside blades.

- (6) Highly significant correlations were found between epiphyte percent cover, epiphyte biomass, and percent of PAR absorbed due to epiphytes for all species. Despite this significance, there was substantial variation in the relationship (i.e., low R^2 values).

8.5 Discussion

Although a complete assessment of the interactions of seagrass, epiphytes, and their grazers in IRL was beyond the scope of this project, a number of important relationships involving these biotic components were determined by this study. Significant differences in the abundance of grazing epifauna among stations was primarily due to the differential distribution of snails. Stations with higher grazer abundances (and more snails) had mixed seagrass communities (Chapter 4); lower grazer abundances (and fewer snails) were found at stations with monospecific communities of *H. wrightii*. Regression analysis indicated that grazer abundance increased as above-ground biomass increased. Those data suggest that grazer abundance was directly related to the amount of habitat provided by seagrass.

The current study did not attempt to segregate out any effects that seagrass species composition may have had on grazing epifauna populations. For example, Virstein and Howard (1987), who worked at the LP station, noted that, while the species composition of epifauna was similar among *H. wrightii*, *S. filiforme*, and *T. testudinum*, these species had significant differences in the abundances of various epifaunal species.

Previous studies, primarily conducted in microcosms or mesocosms, have demonstrated convincingly that grazers can significantly affect epiphyte loads (Howard and Short 1986; Neckles et al. 1993). The present study used regression analysis to determine that, as grazer abundance decreased among stations, epiphyte load increased. Moreover, as epiphyte load increased among stations, above-ground seagrass biomass decreased. This latter result supports the previously stated paradigm involving the negative impact of epiphytes on seagrass. However, it is important to recognize that relationships established in this IRL monitoring study are largely correlative; cause-and-effect relationships require additional experimentation, possibly in mesocosms. Howard and Short (1986) demonstrated in mesocosm tanks at HBOI that the suppression of epiphyte biomass by grazing epifauna may be an important factor in the maintenance of growth, productivity, and depth distribution of seagrasses, particularly in light- and nutrient-stressed conditions.

While the existing data from the IRL monitoring study support the hypothesis that decreased grazing pressure results in increased epiphyte load and reduced seagrass

biomass, the data also support the interpretation that increased seagrass biomass increases the amount of grazing epifauna which leads to reduced epiphytes. In other words, “healthy seagrass” may be either a cause or an effect of the grazer-epiphyte relationship. The two alternatives are not mutually exclusive, but encompass the complex biotic interactions that exist in seagrass beds.

Not all studies on seagrass-epiphyte-nutrient interactions have included grazers. Among the studies that have, some have indicated the important role of grazers in ameliorating algal growth when nutrients are added (e.g., Neckles et al. 1993, Williams and Ruckelshaus 1993, Short et al. 1995), but others have not (e.g., Tomasko and Lapointe 1991). The mesocosm study (Hanisak, unpublished) demonstrated that even at elevated nutrient loading, but under average grazer abundances, epiphyte loads, while substantial, were not deleterious to seagrass survival. Total epiphyte abundance (i.e., on an areal basis) was more related to the amount of seagrass present than to nutrient loading. Given the epiphyte-grazer relationship defined in this chapter and the disparate nutrient patterns among stations (Chapter 3), it appears that grazers may be more important than nutrients in mediating seagrass-epiphyte interactions in IRL. Where sufficient grazing occurs *in situ*, as is likely to be the case in “healthy” seagrass beds, elevated nutrients do not necessarily lead to increased epiphytic growth and seagrass decline. In more extreme cases of eutrophication, or in the absence of grazers, epiphytes may exert a more negative impact on seagrass.

The only study that has measured the effect of epiphytes on light attenuation in IRL (Hardin 1994) concluded that there is a surprisingly constant attenuation of PAR by seagrass epiphytes. While there was a high amount of variability in measurements made in that study (e.g., within the whole data set, there was a 5 to 96% reduction in PAR by epiphytes), the overall conclusion is that, at the community level, PAR attenuation by epiphytes is a relatively constant, and predictable, feature.

While the competitive interactions of epiphytes and seagrass are of continued scientific interest, in terms of elucidating the physiological and ecological bases of the interactions, it appears that PAR attenuation by epiphytes may not be an important factor, in terms of predictive capability, in a PAR-SAV model of IRL. More important would be a clear understanding of the PAR requirements of various seagrass species, derived from field or mesocosm measurements and the impact of key water quality parameters on PAR attenuation (see Chapter 7). The HBOI mesocosm study (Hanisak 1996) and others cited previously have demonstrated that while there may be a critical value (15 to 20% of incident PAR) necessary to sustain seagrass, any reduction in ambient PAR is likely, at least in shallow-water beds, to have a negative impact on the seagrass resource. Given that major water quality factors that attenuate PAR (Chapter 3) vary much more, both spatially and temporally, than do epiphyte loads (Hardin 1994, Chapter 6), greater emphasis in management actions should be placed on water quality than on epiphyte loads.

The paradigm that elevated nutrients are harmful to seagrass only because they stimulate algal growth which reduces PAR availability to seagrass needs to be reconsidered in lieu of the evidence presented for direct toxicity of nitrate (Burkholder et al. 1992, 1994; Hanisak 1996). Moreover, Hanisak (1996) found that elevated nutrients were detrimental to *H. wrightii* only at high PAR levels. This observation suggests the disturbing possibility that nutrients (nitrate) could have a significant impact on the seagrass resource prior to limitations by PAR caused by other impacts of elevated nutrients (e.g., elevated algal chlorophyll attenuating PAR to the seagrass). As the system becomes more eutrophic and PAR attenuation increases due to elevated suspended solids, chlorophyll, or color, direct nutrient toxicity may be less of a concern (i.e., at limiting PAR, nutrients were not toxic to *H. wrightii*). Thus, it is important to examine the synergistic effects of PAR and nutrients on seagrass productivity and survival. Such interactions need to be considered in developing target water quality criteria to ensure the protection of seagrass in estuarine and coastal waters (Kenworthy and Haurert 1991, Dennison et al. 1993).

The relationships between seagrass, epiphytes, and grazing epifauna are more complex than this, or any other, study has yet quantified. Healthy seagrass beds provide more habitat for grazing epifauna than do stressed seagrass beds. Higher seagrass density also supports more epiphyte biomass on an areal basis; these epiphytes are, in turn, trophically important, because they provide the bulk of the food for the grazers in seagrass beds. The high biodiversity of IRL may depend to a large extent on rich, diverse epiphyte communities to buffer direct nutrient impacts on the seagrass community (i.e., reducing water column levels of nitrates) and to provide the bulk of the primary productivity that is incorporated into the food web.

8.6 Summary

Information was gathered or obtained on the relative abundance of epiphyte grazers at the monitoring stations, nutrient-epiphyte interactions, and estimates of PAR attenuation due to epiphytes. The major results of this study are:

- (1) The grazing epifauna community sampled consisted of snails and crustaceans, with snails the most numerous component.
- (2) Differences among stations in total abundance of grazing epifauna were highly significant. Over the course of the entire study, grazers were most abundant at BR and VB, least abundant at MB, and intermediate at the other stations. Stations with higher grazer abundances had mixed seagrass communities (Chapter 4); lower grazer abundances were found at stations with monospecific communities of *H. wrightii*.

- (3) The major difference in terms of grazer composition among stations was the much higher abundance of snails at BR and VB; crustaceans were more abundant than snails at the other stations. Thus, the difference in the abundance of grazing epifauna at the stations was primarily due to the differential distribution of snails.
- (4) Site-specific comparisons of grazer abundance were confounded by significant interannual variation in grazer abundance at two stations, BR and SS. At BR, grazer abundance was much higher during 1994 than 1995. This decline was due primarily to snails. At SS, grazer abundance was marginally lower during 1995. This relatively modest decline at SS was due to significant declines in amphipods, isopods, and miscellaneous crustaceans.
- (5) The interannual variation at BR altered the analysis of site-specific differences during the two years. In 1994, grazer abundance was highest at BR and VB, lowest at MB and SS, and intermediate at the other stations. In 1995, there were considerably less differences among stations, with the only significant difference being that grazer abundance was higher at SN than at MB and SS.
- (6) Analysis of the seasonal samples indicated that grazer abundance was fairly constant at most stations, with occasional sharp peaks in abundance. The major station differences noted previously were primarily a function of large peaks in abundance (due to snails) in the August 1994 samples at BR, VB, and LP. When data were pooled for all stations, grazer abundance was highest in August 1994 and lowest in November 1995 and February 1996.
- (7) Regression analysis of station means for grazer abundance with epiphyte loads (Chapter 6) and above-ground seagrass biomass (Chapter 4) indicated the following significant relationships among stations:
 - Epiphyte load decreased as grazer abundance increased. This observation demonstrates the important potential of grazers regulating epiphyte loads.
 - Grazer abundance increased as above-ground biomass increased. This result suggests that grazer abundance was directly related to the amount of habitat structure provided by seagrass.
 - Above-ground seagrass biomass decreased as epiphyte load increased. This result supports the paradigm of the negative impact of epiphytes on seagrass.
- (8) The major results of the mesocosm study on PAR and nutrient stress on *H. wrightii* (Hanisak 1996), as related to this IRL monitoring study were reviewed. Key points were:

- Decreases in PAR or increases in nutrients (nitrate and phosphate) were significantly associated with reduced shoot density and biomass of *H. wrightii*. The effect of decreased PAR was more rapid and more significant than the effect of elevated nutrients.
 - *H. wrightii* in IRL requires about 20% of incident PAR for long-term survival.
 - There were no significant effects of PAR, nutrients, or their interactions on epiphyte load (g dry weight epiphyte/g dry weight shoot). The experiments were conducted with grazers present at ecologically relevant levels.
 - The decline of *H. wrightii* associated with elevated nutrients was not related to epiphyte load, but appeared to be a direct toxicity, the mechanism of which is unclear.
 - Areal epiphyte biomass increased with increased PAR; at higher PAR levels, elevated nutrients reduced areal epiphyte biomass. On an areal basis, what directly determined the epiphyte load was not the levels of PAR or nutrients, but seagrass density; the direct negative impact of increased nutrients on *H. wrightii* resulted in reduced areal epiphyte biomass.
- (9) The major results of the F.I.T. study (Harden 1994) that estimated PAR attenuation due to epiphytes, as related to this IRL monitoring study, were reviewed. Key points were:
- All epiphyte parameters measured (species composition, percent cover, biomass, and percent PAR absorbance) were similar, both spatially (among stations) and temporally (monthly) for the dominant seagrasses (*H. wrightii*, *S. filiforme*, and *T. testudinum*) of IRL. No statistical differences for these parameters were found.
 - The dominant epiphytes on all seagrass species were diatoms.
 - The annual mean percentage epiphyte cover for outside (= older) blades ranged from 77% to 81% for the 3 species. The annual mean percentage epiphyte cover for inside (= younger) blades ranged from 41 to 44% for the 3 species.
 - Among species, the percent PAR absorbance was surprisingly constant. The grand means for the 3 species ranged from 59 to 61% for outside blades and 31 to 34% for inside blades.
 - Among stations for any given species, the percent PAR absorbance was also relatively constant.

- Highly significant correlations were found between epiphyte percent cover, epiphyte biomass, and percent of PAR absorbed due to epiphytes for all 3 species, but there was substantial variation in the relationships.
- (10) While the data collected on this project support the hypothesis that decreased grazing pressure results in increased epiphytes and reduced seagrass biomass, the data also support the interpretation that increased seagrass biomass increases the amount of grazing epifauna which leads to reduced epiphytes. "Healthy seagrass" may be either a cause or an effect of the grazer-epiphyte relationship. The two alternatives are not mutually exclusive, but encompass the complex biotic interactions that exist in seagrass beds.
 - (11) Given the epiphyte-grazer relationship defined in this chapter and the disparate nutrient patterns among stations (Chapter 3), it appears that grazers may be more important than nutrients in mediating seagrass-epiphyte interactions in IRL. Higher epiphyte loads do not necessarily have a significant negative ecological impact on seagrass. In more extreme cases of eutrophication, or in the absence of grazers, epiphytes may exert a more negative impact on seagrass.
 - (12) The paradigm that elevated nutrients are harmful to seagrass only because they stimulate algal growth which reduces PAR availability to seagrass needs to be reconsidered in lieu of the evidence presented for direct toxicity of nitrate (Burkholder et al. 1992, 1994; Hanisak 1996).
 - (13) Healthy seagrass beds provide more habitat for grazing epifauna than do stressed seagrass beds. Higher seagrass density also supports more epiphyte biomass on an areal basis; these epiphytes are, in turn, trophically important, because they provide the bulk of the food for the grazers in seagrass beds. The high biodiversity of IRL may depend to a large extent on the rich, diverse epiphyte communities to buffer direct nutrient impacts on the seagrass community and to provide the bulk of the primary productivity that is incorporated into the food web.

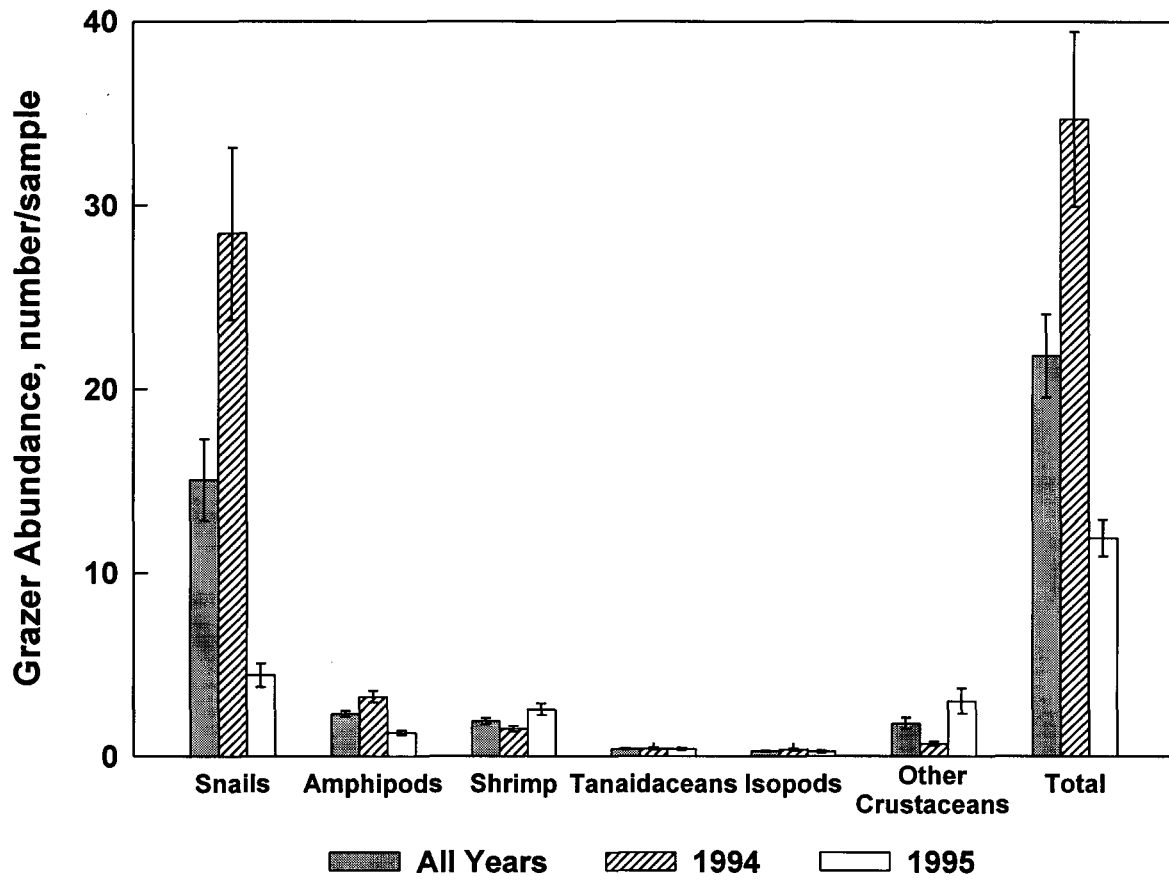


Fig. 8.1 Abundance of grazing epifauna, by taxonomic groups for the entire study and for individual years. Data are means (\pm SE) for all samples collected at all stations. "All Years" includes data from March 1996 as well as from quarterly samples in 1994 and 1995.

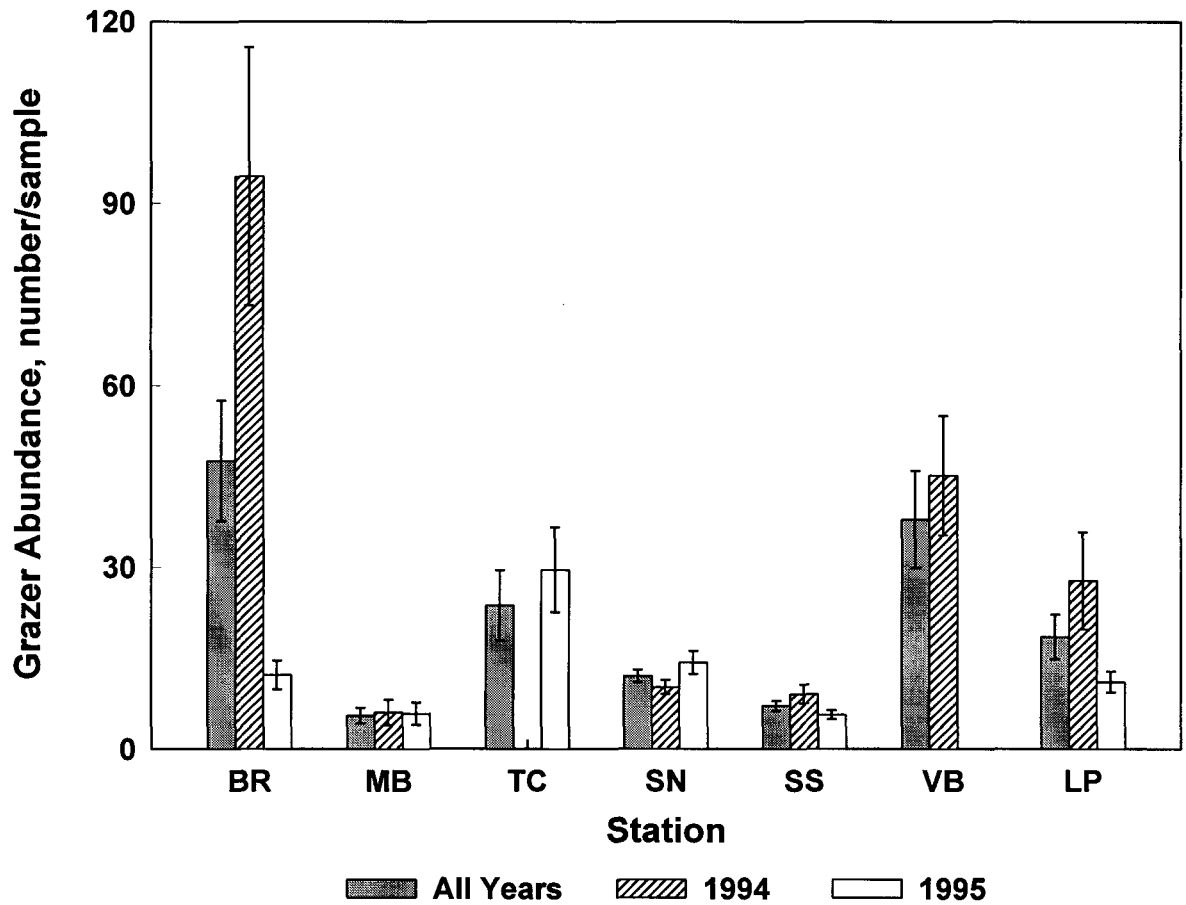


Fig. 8.2 Abundance of grazing epifauna, by station for the entire study and for individual years. Data are means (\pm SE). "All Years" includes data from March 1996 as well as from quarterly samples in 1994 and 1995.

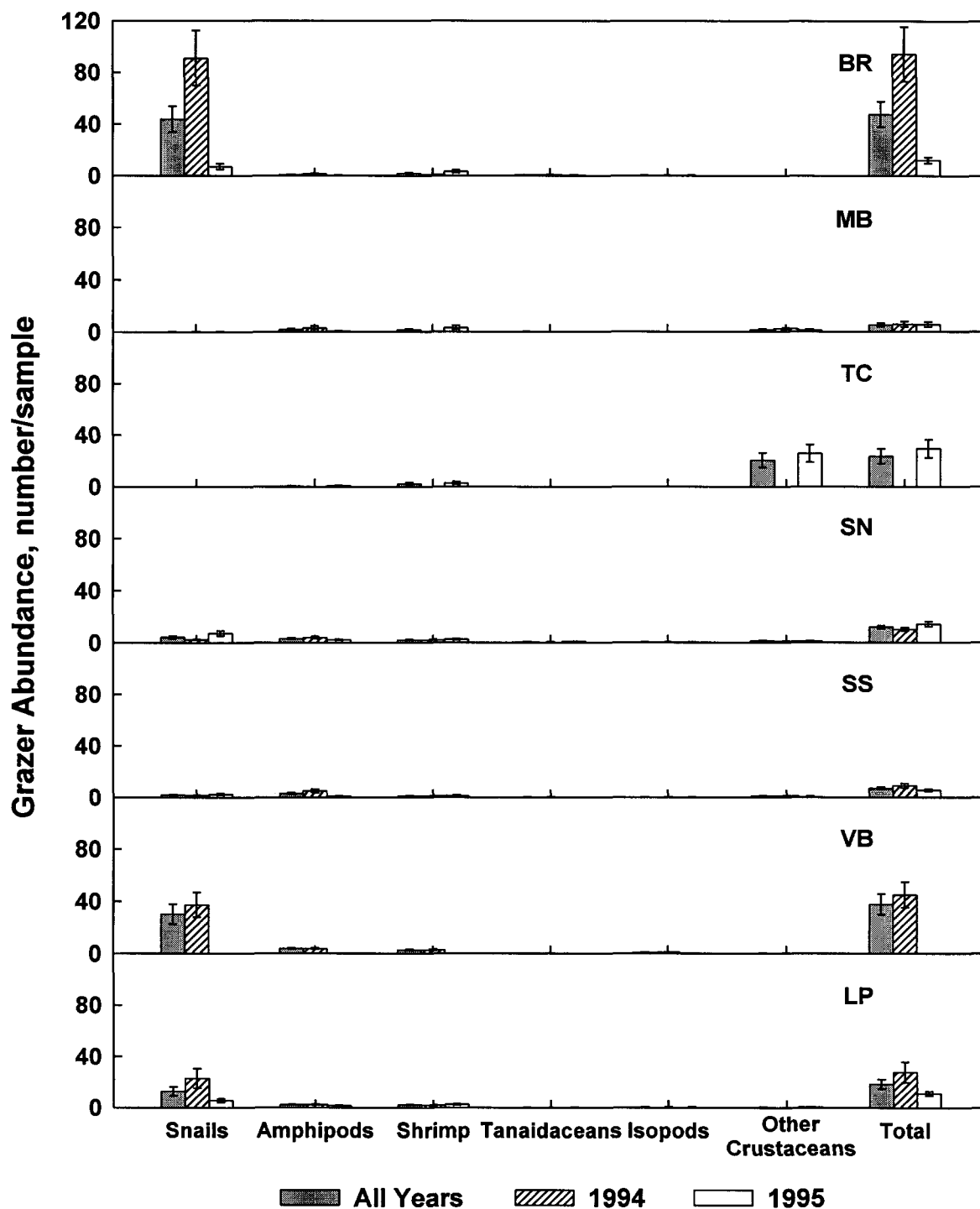


Fig. 8.3 Abundance of grazing epifauna, by station and taxonomic groups for the entire study and for individual years. Data are means (\pm SE). "All Years" includes data from March 1996 as well as from quarterly samples in 1994 and 1995.

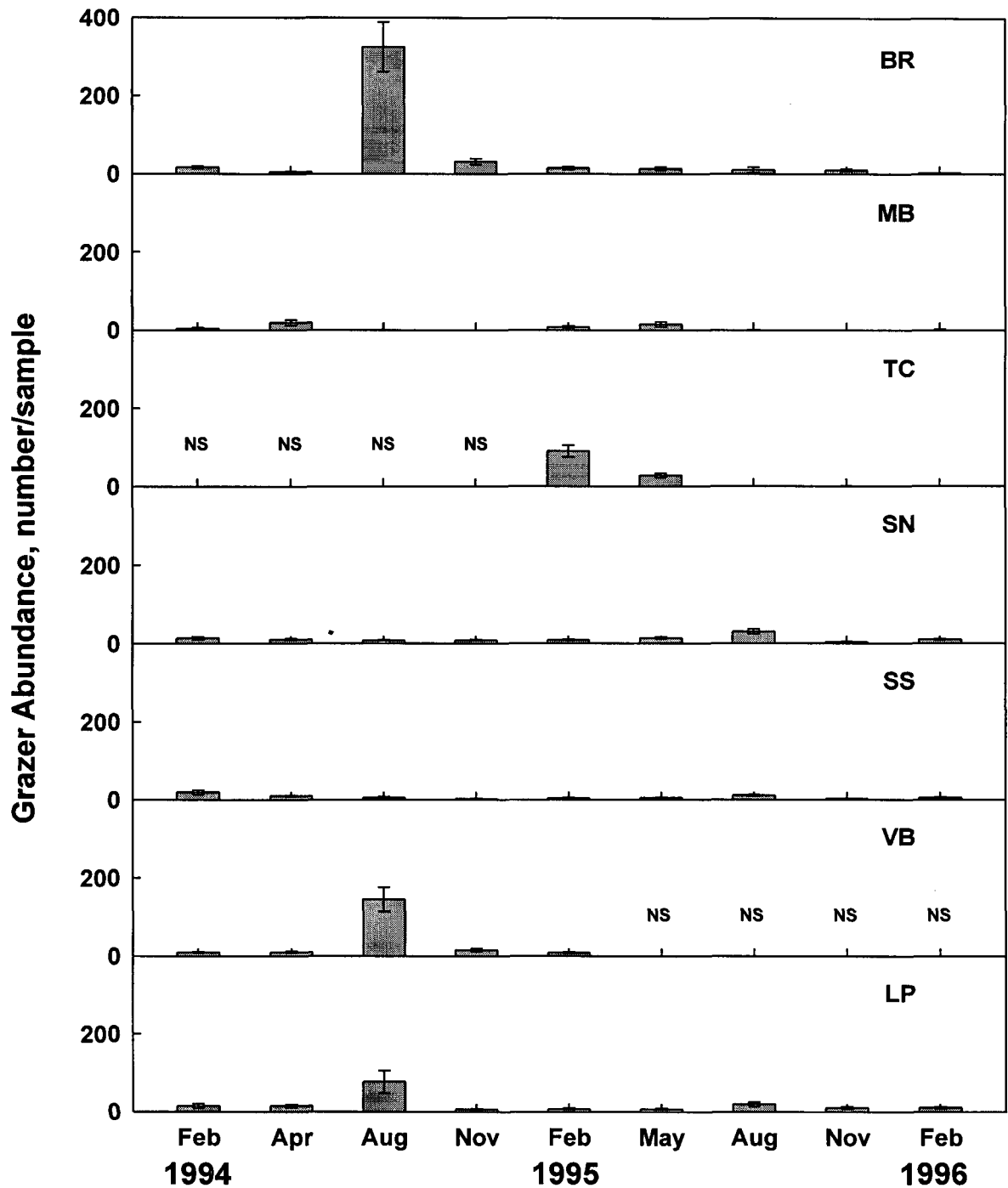


Fig. 8.4 Abundance of grazing epifauna, by station and season for the entire study and for individual years. Data are means (\pm SE) for all station-season combinations. NS = not sampled (TC: Year 1, VB: Year 2).

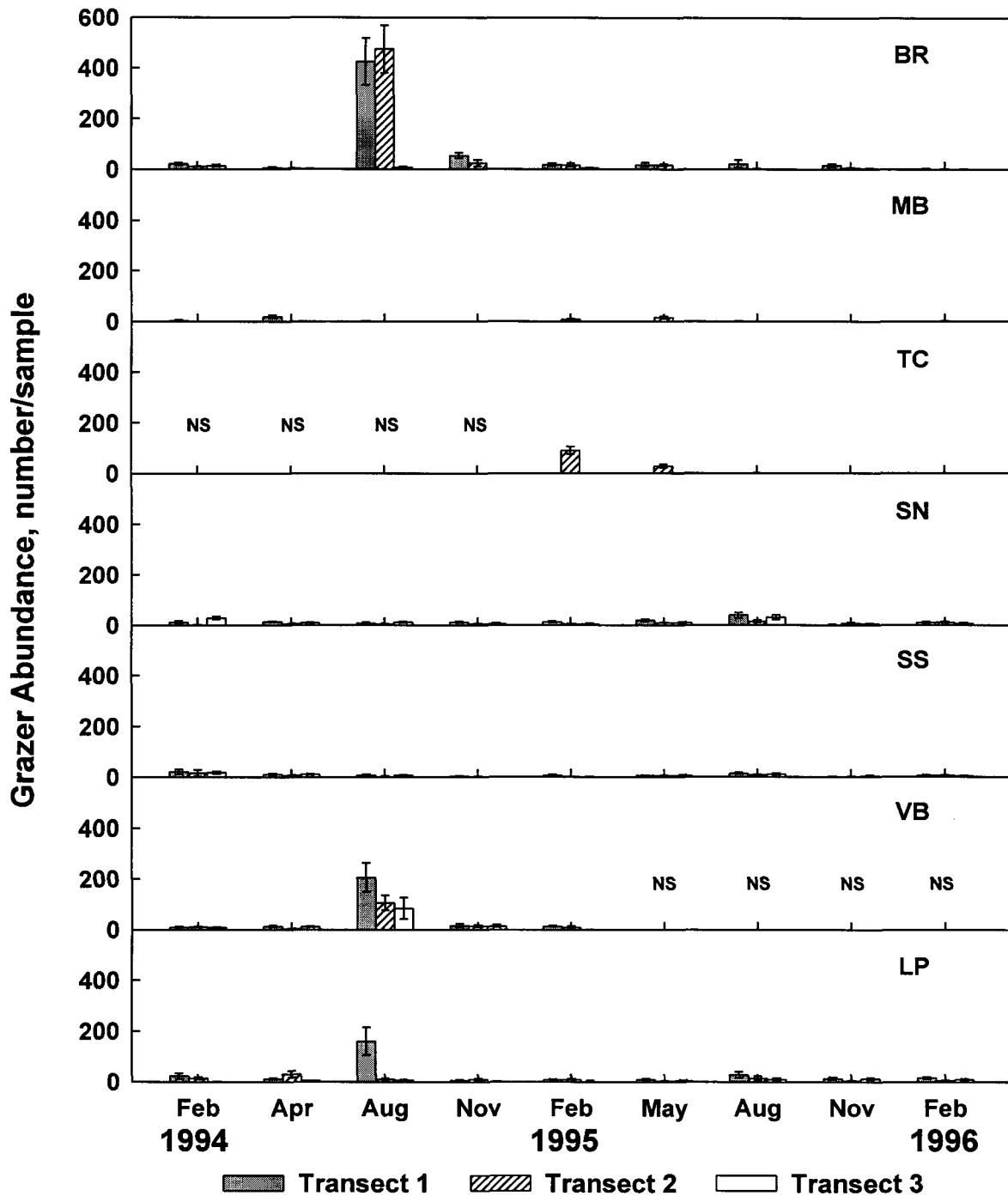


Fig. 8.5 Abundance of grazing epifauna, by station, transect, and season for the entire study and for individual years. Data are means (\pm SE) for all station-transect-season combinations. NS = not sampled (TC: Year 1, VB: Year 2).

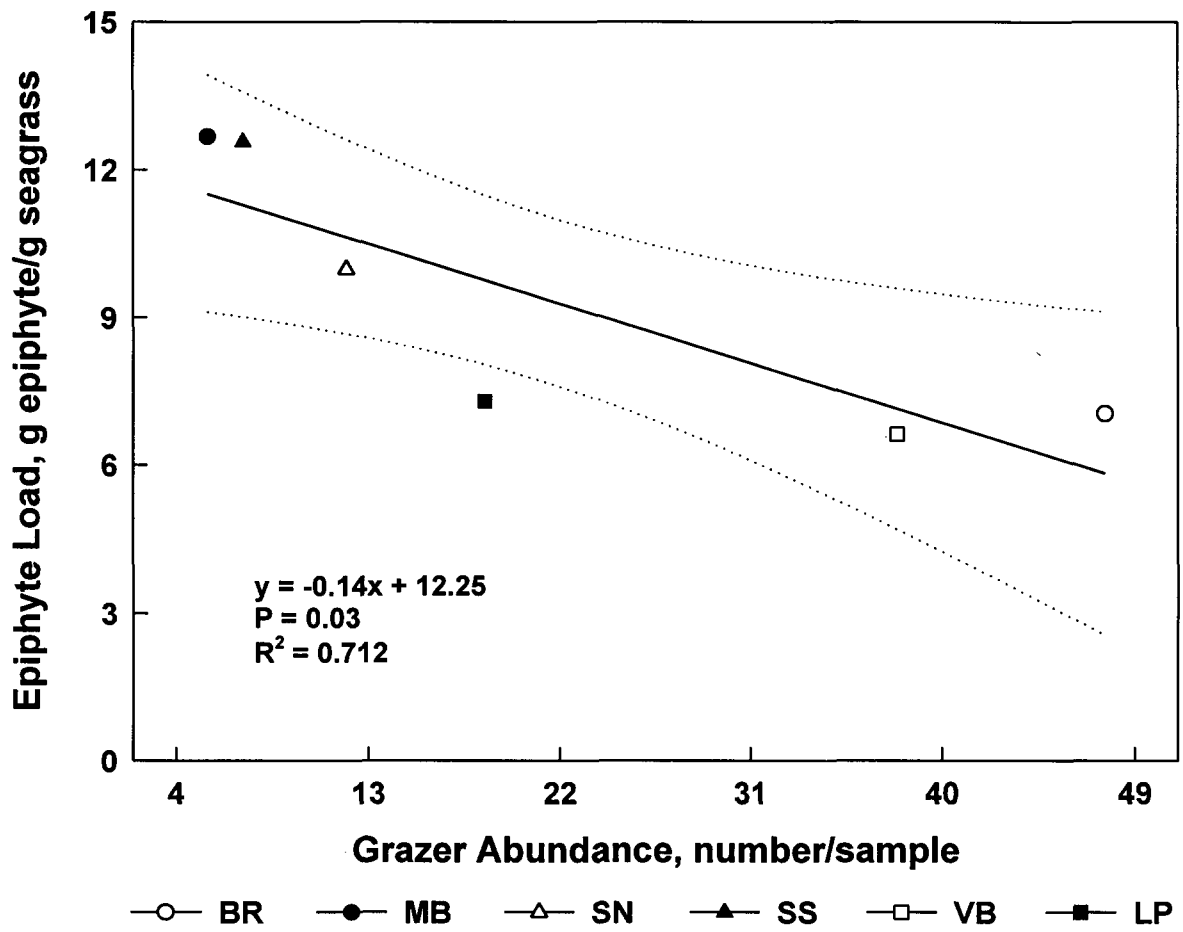


Fig. 8.6 Linear regression analysis of epiphyte load vs. abundance of grazing epifauna, based on station means.

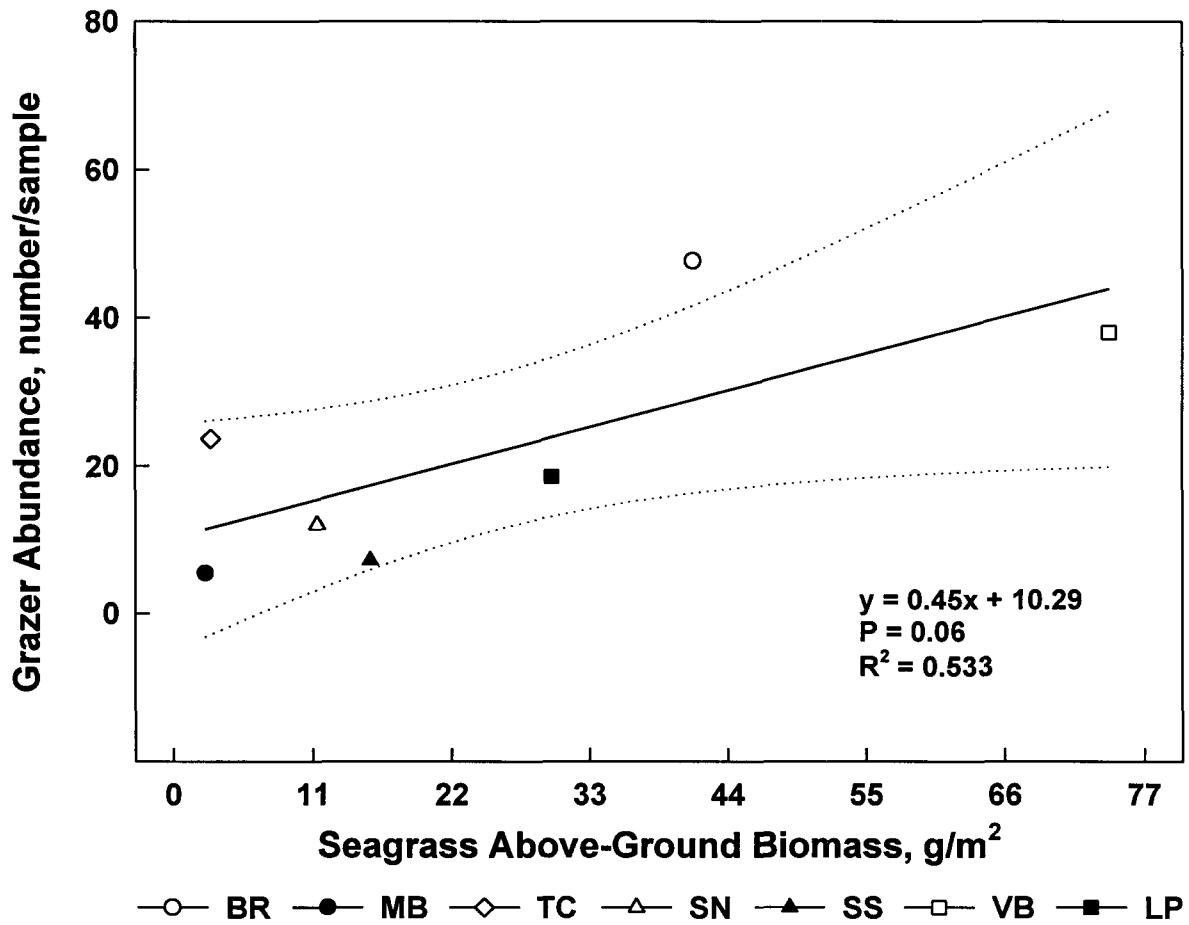


Fig. 8.7 Linear regression analysis of abundance of grazing epifauna vs. above-ground seagrass biomass based on station means.

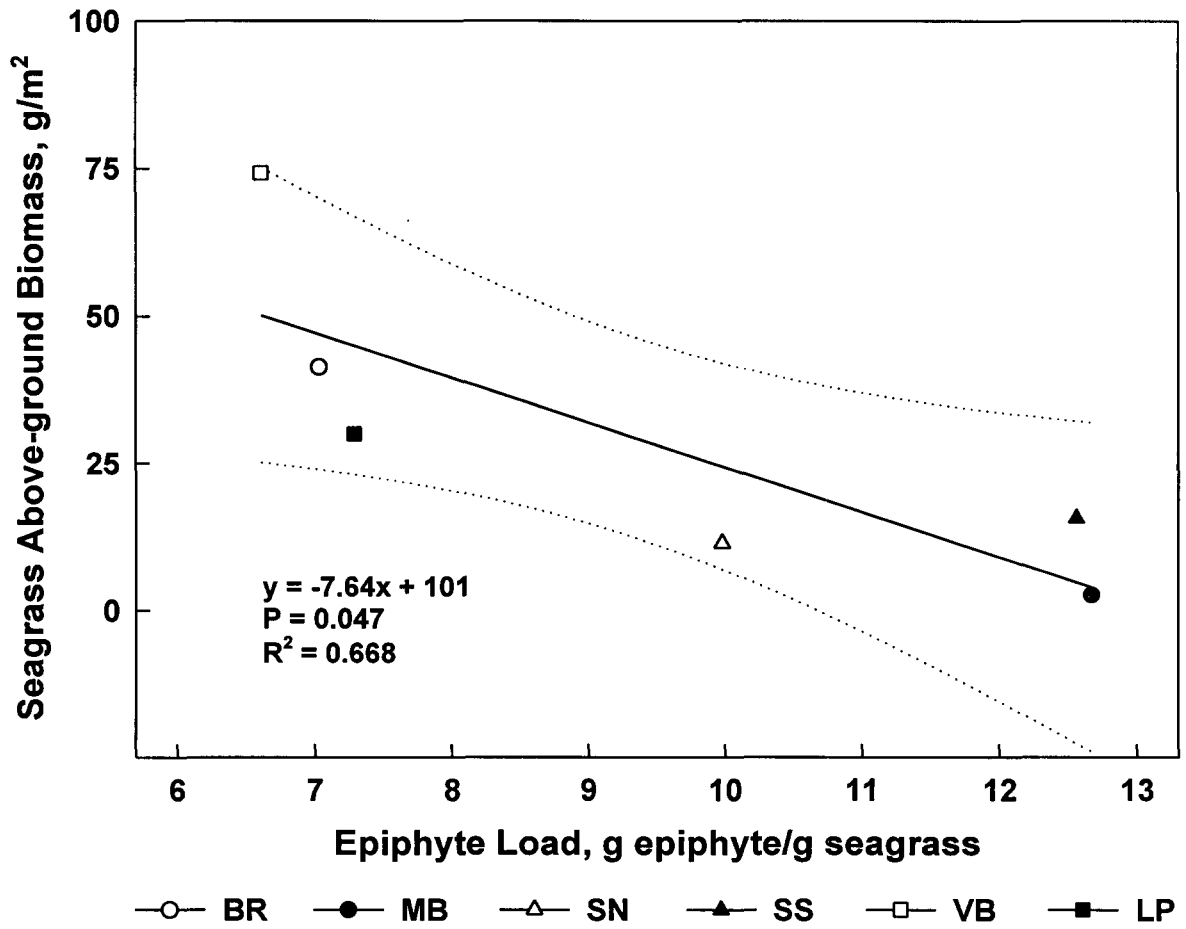


Fig. 8.8 Linear regression analysis of above-ground seagrass biomass vs. epiphyte load based on station means.

Chapter 9: Management Recommendations

9.1 Background

Over the last decade there has been a growing realization that healthy seagrass habitat is required for the ecological functioning and the economical viability of Indian River Lagoon (IRL). This improved appreciation of the importance of seagrass in the lagoon has triggered significant interest in a better understanding and management of this resource. While there is evidence that the health of seagrass within the lagoon has declined because of decreased water quality, there has not been a clear understanding of how this decline is related to differences in manageable water quality parameters.

This study determined the interrelationships of seagrass, epiphytes, water quality, underwater light, and light attenuation in IRL. The approach and design of this project was based on three important relationships: (1) light is the primary factor determining seagrass distribution in IRL; (2) water clarity is the primary factor determining the light availability to seagrass; and (3) water clarity is determined by several physical, chemical, and biological factors.

The results of this study are intended to be a mechanism to assist decision-making in regards to managing seagrass and water quality within IRL. There is encouraging evidence that management action in Tampa Bay, a system rather similar to IRL, has resulted in improved water quality and water clarity and, subsequently, in increased seagrass cover (D. Tomasko, personal communication). The starting point for justifying similar management action in IRL is the analysis of the PAR-water quality relationships in this study and ongoing efforts to develop a water quality model by the District. Data from this study will be used in this predictive simulation model that will link water quality with seagrass health and survival and be a management tool for restoring and protecting seagrasses in IRL.

9.2 Task Description

Task 9: To provide information from this study in a form that will be useful in making decisions relevant to the management of SAV and water quality in Indian River Lagoon.

9.3 Recommendations

Based on information from this study, the following are recommendations relevant to the management of SAV and water quality in IRL.

9.3.1 Seagrass Monitoring

- (1) Seagrass species composition is an important factor influencing the measurement of seagrass parameters due to differences in size and resource allocation among species. Differences in species composition make comparisons of the total seagrass community among sites within IRL difficult. Parameters such as above-ground biomass and cover, which incorporate all species, need to be used for modeling seagrass in the lagoon.
- (2) Among rapid assessment parameters, cover is probably the most ecologically meaningful one, as it is also an estimate of habitat availability. The high degree of correlation among SAV parameters suggests that rapid assessment techniques for assessing SAV status and changes through time, such as the District's current monitoring of permanent transects (over 70 sites in IRL), are appropriate.
- (3) Grazers may be more important than nutrients in mediating seagrass-epiphyte interactions in IRL, under current conditions. Present epiphyte loads do not necessarily have a significant negative ecological impact on seagrass. In more extreme cases of eutrophication, or in the absence of grazers, epiphytes may exert a more negative impact on seagrass. Under current conditions, there seems to be little justification for measuring epiphyte loads as part of a regular monitoring program. Reliable rapid assessment techniques for epiphytes have yet to be developed, and current assessment techniques require large number of samples and tedious processing.
- (4) Healthy seagrass beds provide more habitat for grazing epifauna than do stressed seagrass beds; higher seagrass density supports more epiphyte biomass on an areal basis. These epiphytes are trophically important because they provide the bulk of the food for the grazers in seagrass beds. The high biodiversity of IRL may depend to a large extent on the rich, diverse epiphyte communities to buffer direct nutrient impacts on the seagrass community and to provide the bulk of the primary productivity that is incorporated into the food web. Additional studies on trophic relationships within seagrass beds of IRL are warranted.
- (5) The lack of pattern in carbon fixation among stations suggests that the measurement of primary productivity has limited value as an index of SAV conditions. Other seagrass parameters (percent cover, biomass, or growth rates) are much more likely to be effective biological integrators of environmental conditions in an IRL monitoring program. To be more useful, productivity measurements would have to be performed more frequently than the quarterly measurements made in this study. If incorporating ¹⁴C measurements into a monitoring program is considered in the future, care must be taken to standardize the methodology to effectively make temporal and spatial comparisons within the lagoon.

- (6) The required frequency of seagrass monitoring in IRL depends on the purpose of the monitoring. Given the large amount of spatial and temporal heterogeneity in IRL and the interannual variation in rainfall and related water quality parameters, it seems that seagrass monitoring primarily needs to address long-term changes in the lagoon in response to management actions (time scale: years to decades) and needs to determine substantial, not subtle, changes in seagrass status. Thus, the sampling frequency (twice per year) of the District's current monitoring network of transects is appropriate as, in essence, the transects become replicates, within a stratified sampling design, to assess long-term changes in IRL.

9.3.2 PAR Monitoring

- (7) Cosine sensors do not measure all of the PAR available for seagrass, as do spherical sensors, but do provide similar temporal (diel, monthly, and seasonal) patterns of PAR and K. Spherical sensors are recommended for future monitoring that focuses on seagrass-PAR relationships in IRL because those sensors measure all of the photons available for photosynthesis by seagrass and other primary producers.
- (8) While absolute values of PAR and K change throughout the year, diel patterns in PAR and K are consistent throughout seasons and months of the study. If both measurements of PAR and K are desired, it is recommended that the standard procedure of making measurements between the hours of 1000 to 1400 be followed. If K alone is of interest, there is a broader period of time each day when measurements can be made. This period is somewhat site- and season-specific; without site-specific information, it is recommended that K measurements be made between the hours of 0900 to 1500.
- (9) Continuous monitoring of underwater PAR is not required to adequately characterize underwater PAR or K in IRL. While continuous monitoring of PAR has the advantages of providing a large data set for detailed analysis of underwater PAR and estimates of K, there are significant disadvantages, including the need for frequent cleaning of sensors and maintenance of data loggers. Fouling of the sensors impacts measurement of PAR (within 2 or 3 days after sensors are cleaned) quicker than K (usually no change within the first 3 days). It would be better to put limited financial resources into other management needs (e.g., more intensive water quality monitoring) than into continuous monitoring of PAR.
- (10) Highly significant seasonal differences in PAR and K were found at all stations; future PAR monitoring (assumed to be non-continuous) needs to adequately address this variability. The frequency of measurements required to characterize PAR and K at a site in IRL is dependent upon location and the desired levels of accuracy and precision. While in most cases, differentiation among stations

continues to improve all the way up to continuous monitoring, reasonably good estimates of PAR and K ($\pm 10\%$ accuracy) at any particular site can be made by sampling every 2 weeks.

- (11) Although PAR is the primary factor that determines the productivity and survival of seagrass, PAR is not something that managers can directly manage. Partitioning of water quality factors associated with light attenuation can be used to direct management actions. Relationships between water quality parameters with K are more significant statistically than those with underwater PAR; thus, light attenuation coefficients are more useful than PAR measurements in addressing water quality effects on underwater light availability. The strategy of managing seagrass by addressing water quality problems that elevate K appears sound. Ultimately, protection of seagrass habitat will need to be translated into water quality "standards" or targets.

9.3.3 Water Quality Monitoring

- (12) The most significant attenuator of light in IRL is turbidity. Strong relationships also exist between K and suspended solids, which are highly correlated to turbidity. Measurement of turbidity, which can be made quickly in field monitoring efforts, may serve as a good proxy of suspended solids in IRL. Management actions that reduce the input of suspended solids into IRL may be the single most effective management action to increase water clarity, and, thus, enhance seagrass in the lagoon. It would be desirable to determine the extent to which anthropogenic impacts have contributed to the current levels of suspended solids in the water column, as some fraction of them are a part of the "natural" system, particularly in a shallow, wind-dominated system like IRL.
- (13) Color and chlorophyll have smaller roles than turbidity/suspended solids as attenuators of light in IRL, and their importance is likely to be quite variable throughout IRL because of their large amount of spatial and temporal variability. Elevated color levels are good indicators of freshwater inputs into IRL. While the impact of freshwater may be fairly localized within IRL, it is clear that a return to pre-development flows of freshwater into IRL would be beneficial to water clarity and seagrass beds.
- (14) Enhanced nutrient levels associated with low salinity suggest that freshwater discharges into IRL are a significant source of nutrients to the system, but that the relationships of nutrients with light attenuation are less important than those with turbidity, color, and chlorophyll. In multiple regression models with chlorophyll, phosphorus was the most significant nutrient, with nitrogen secondary. Thus, nitrogen limitation may not be as widespread throughout the lagoon as previously

thought. The relative and absolute roles of nitrogen and phosphorus as factors limiting algal growth in IRL merit study.

- (15) Chlorophyll was not a significant part of the multiple regression model of K and water quality parameters; this observation suggests that management action addressing phytoplankton blooms (e.g., reduction of current nutrient inputs) would not significantly improve water clarity, under the current conditions in IRL. Of course, given the well-known negative impacts of eutrophication, anthropogenic sources of nutrients into IRL should be reduced for reasons other than their relationship with water clarity.
- (16) The good agreement of overall spatial water quality patterns in the current study with those synthesized by Woodward-Clyde (1994b) suggests that relationships among water quality parameters and their relationships with extinction coefficients derived in the current study could be broadly applied to the IRL water quality database and be used in development and verification of water quality models.
- (17) The frequency of water quality sampling required to characterize a site in IRL is dependent upon location, the water quality parameters involved, and the desired levels of accuracy and precision. The amount of sampling required to characterize a station is less than what is needed to detect differences among stations. To the extent that these stations represent the continuum found in IRL, monthly water quality is recommended for routine water quality efforts. More intensive efforts would be required for some efforts (e.g., model development and verification, identification of point-source impacts), but the considerable added expense for most monitoring efforts does not appear to be warranted.
- (18) Major changes in water quality parameters are due primarily to changes in freshwater inputs. Those changes are associated with natural forces, but accelerated by anthropogenic impacts. Storm events may be the most important triggers of changes in water quality; it would be desirable to incorporate an element of "post-storm" sampling into water quality monitoring programs.
- (19) Station-specific differences in water quality, which appear to be driven by gradients associated with IRL's north-south orientation and freshwater inputs, as well as station-specific differences in the multiple regression models of water quality and K, demonstrate the need for management of IRL on a segment-by-segment basis. The development and verification of a lagoon-wide hydrodynamic model by the District needs to consider the enormous range in water quality patterns found throughout IRL, their complex interactions, and their impacts on seagrass.
- (20) This study identified significant relationships between seagrass abundance and water quality parameters. More and stronger relationships might be seen with more

frequent sampling (i.e., monthly) which would provide greater statistical resolution due to a larger sample size, but such a sampling program involving many sites in IRL is financially impractical. Emphasis on water quality-light attenuation relationships should be the focus of near-term management and modeling efforts, with impacts on seagrass simulated by models and verified by *in situ* measurements at selected sites.

- (21) It is clear from this study that considerable differences in water quality and underwater light exist throughout the lagoon. The northern lagoon, as represented by the BR station, may merit additional study as to ecological function in what are relatively pristine conditions in IRL, with limited anthropogenic impacts. Water quality conditions in that portion of the lagoon system may be eventual targets for lagoon managers to achieve for most of IRL.
- (22) Turbidity and color are water quality parameters that are important to light attenuation and that can be quickly measured in field monitoring efforts as rapid assessments of water quality. Now that the initial relationships between water quality and light attenuation have been established for different sites in IRL, it would be desirable to determine those relationships over a broader area. Rapid assessment of PAR, water quality, and SAV, perhaps in relationship to the District's extensive monitoring network of seagrass transects, would provide a fairly simply obtained, yet meaningful, synoptic evaluation of a large area of the lagoon.

Chapter 10: Literature Cited

- APHA. 1985. Standard Methods for Examination of Water and Wastewater. 16th Edition. American Public Health Association. Washington, D.C.
- Benz, M.C., N.J. Eiseman, and E.E. Gallaher. 1979. Seasonal occurrence and variation in standing crop of a drift algal community in the Indian River, Florida. *Bot. Mar.* 22:413-420.
- Borum, J. 1985. Development of epiphytic communities on eelgrass (*Zostera marina*) along a nutrient gradient in a Danish estuary. *Mar. Biol.* 87:211-218.
- Bulletin of Marine Science. 1995. Indian River Lagoon Biodiversity Conference. *Bull. Mar. Sci.* 57:1-300.
- Burkholder, J.M., H.B. Glasgow Jr, and J.E. Cooke. 1994. Comparative effects of water-column nitrate enrichment of eelgrass *Zostera marina*, shoalgrass *Halodule wrightii*, and widgeongrass *Ruppia maritima*. *Mar. Ecol. Prog. Ser.* 105:121-138.
- Burkholder, J.M., K.M. Mason, and H.B. Glasgow Jr. 1992. Water-column nitrate enrichment promotes decline of eelgrass *Zostera marina*: evidence from seasonal mesocosm experiments. *Mar. Ecol. Prog. Ser.* 81:163-178.
- Cahoon, L.B. and J.E. Cooke. 1992. Benthic microalgal production in Onslow Bay, North Carolina, USA. *Mar. Ecol. Prog. Ser.* 84:185-196.
- Caye, G., C. Bulard, A. Meinesz, and F. Loques. 1992. Dominant role of seawater osmotic pressure on germination in *Cymodocea nodosa*. *Aquat. Bot.* 42:187-193.
- Congdon, R.A. and A.J. McComb. 1979. Productivity of *Ruppia*: seasonal changes and dependence on light in an Australian estuary. *Aquat. Bot.* 6:121-32.
- Cuthbert, I.D. and P. del Giorgio. 1992. Toward a standard method of measuring color in freshwater. *Limnol. Oceanogr.* 37:1319-26.
- Dawes, C.J., M.D. Hanisak, and W.J. Kenworthy. Seagrass biodiversity in the Indian River Lagoon. *Bull. Mar. Sci.* 37:59-66.
- Dennison, W.C. 1987. Effects of light on seagrass photosynthesis, growth and depth distribution. *Aquat. Bot.* 27:15-26.

- Dennison, W.C., R.J. Orth, K.A. Moore, J.A. Stevenson, V. Carter, S. Kollar, P.W. Bergstrom, and R.A. Batiuk. 1993. Assessing water quality with submersed aquatic vegetation. *BioScience* 43:86-94.
- Durako, M.J., M.D. Murphy, and K.D. Haddad. 1988. Assessment of Fisheries Habitat: Northeast Florida. Fla. Mar. Res. Publ. No. 45. Fla. Dept. of Nat. Resour. Bur. Mar. Res., St. Petersburg, Florida. 51 pp.
- Environmental Protection Agency. 1979. Methods for chemical analysis of water and wastes. EPA-600/4-79-020.
- Gallegos, C. L. 1994. Refining habitat requirements of submersed aquatic vegetation: role of optical models. *Estuaries* 17:187-199.
- Gilmore, R.G. 1987. Subtropical-tropical seagrass communities of the southeastern United States: fishes and fish communities. Pp. 117-137 in M.J. Durako, R.C. Phillips, and R.R. Lewis (eds.), Proceedings of the Symposium on Subtropical-Tropical Seagrasses of the Southeastern United States. Fla. Mar. Res. Publ. No. 42. Fla. Dept. Nat. Resour. Bur. Mar. Res., St. Petersburg, Florida.
- Gilmore, R.G., P.A. Hastings, and D.J. Herrema. 1983. Ichthyofaunal addition to the Indian River lagoon and adjacent waters, east-central Florida. *Fla. Sci.* 46:22-30.
- Gough, S.B. and W.J. Woelkerling. 1976. On the removal and quantification of algal aufwuchs from macrophyte hosts. *Hydrobiologia* 48:203-207.
- Haddad, K.D. 1985. Habitats of the Indian River Lagoon. Pp. 23-28 in D. Barile (ed.), Proceedings of the Indian River Resources Symposium, Florida Sea Grant Project 84-28, Gainesville, Florida.
- Hall, M.O. and N.J. Eiseman. 1981. The seagrass epiphytes of the Indian River, Florida. I. Species List with Descriptions and Seasonal Occurences. *Bot. Mar.* 24:139-146.
- Hanisak, M.D. 1990. The use of *Gracilaria tikvahiae* as a model system to understand the nitrogen nutrition of cultured seaweeds. *Hydrobiologia* 204/205:79-87.
- Hanisak, M.D. in R.G. Gilmore, and M.D. Hanisak. 1991. Environmental Survey Relative to the Expansion and Development of the Port of Fort Pierce. Final Report submitted to St. Lucie County Port and Airport Authority. 187 pp.
- Hanisak, M.D. 1996. Effects of light and nutrient stress on the seagrass *Halodule wrightii* in mesocosm experiments. Unpublished Manuscript.

- Harden, S.W. 1994. Light Requirements, Epiphyte Load and Light Reduction for Three Seagrass Species in the Indian River Lagoon, Florida. M.S. Thesis, Florida Institute of Technology, Melbourne, Florida. 130 pp.
- Heffernan J.J. and R.A. Gibson. 1983. A comparison of primary production rates in Indian River, Florida seagrass systems. *Florida Sci.* 46:295-306.
- Howard, R.K. and F.T. Short. 1986. Seagrass growth and survivorship under the influence of epiphyte grazers. *Aquat. Bot.* 24:287-302.
- IRLNEP. 1993. The Preliminary Comprehensive Conservation and Management Plan for the Indian River Lagoon. Indian River Lagoon National Estuary Program, Melbourne, FL. 105 pp.
- Jeffrey, S.W. and G.F. Humphrey. 1975. New spectrophotometric equations for determining chlorophylls a, b, c1, and c2 in higher plants, algae, and natural phytoplankton. *Biochem. Physiol. Pflanzen.* 167:223-227.
- Jensen P.R. and R.A. Gibson. 1986. Primary production in three subtropical seagrass communities: a comparison of four autotrophic components. *Florida Sci.* 49:129-141.
- Jewett-Smith, J. 1991. Factors influencing the standing crop of diatom epiphytes of the seagrass *Halodule wrightii* Ascers. in south Texas seagrass beds. *Contrib. Mar. Sci.* 32:27-40.
- Kemp, W.M., M.R. Lewis, and T. W. Jones. 1986. Comparison of methods for measuring production by the submersed macrophyte *Potamogeton perfoliatus* L. *Limnol. Oceanogr.* 31:1322-1334.
- Kenworthy, W.J. 1993. Defining the ecological compensation point of seagrasses in the Indian River Lagoon. Pp. 195-210 in L.J. Morris and D.A. Tomasko (eds.), *Proceedings and Conclusions of Workshops on Submerged Aquatic Vegetation Initiative and Photosynthetically Active Radiation*. Special Publication SJ93-SP13. St. Johns River Water Management District. Palatka, Florida.
- Kenworthy, W.J. and D.E. Haurert. 1991. The Light Requirements of Seagrasses: Proceedings of a Workshop to Examine the Capability of Water Quality Criteria, Standards and Monitoring Programs to Protect Seagrasses. NOAA Tech Memo NMFS-SEFC-287. 187 pp.
- Larkum, A.W. D., A.J. McComb, and S.A. Shepherd. 1989. *Biology of Seagrasses*. Elsevier, New York. 841 pp.

- Livingston, R.J. 1987. Historic trends of human impacts on seagrass meadows in Florida. Pp. 139-152 in M.J. Durako, R.C. Phillips, and R.R. Lewis (eds.), Proceedings of the Symposium on Subtropical-Tropical Seagrasses of the Southeastern United States. Fla. Mar. Res. Publ. No. 42. Fla. Dept. Nat. Resour. Bur. Mar. Res., St. Petersburg, Florida.
- Lubbers, L., W.R. Boynton, and W.M. Kemp. 1990. Variations in structure of estuarine fish communities in relation to abundance of submersed plants. Mar. Ecol. Prog. Ser. 65:1-14.
- Macauley, J.M., J.R. Clark, and W.A. Price. 1988. Seasonal changes in the standing crop and chlorophyll content in *Thalassia testudinum* Banks ex Konig and its epiphytes in the northern Gulf of Mexico. Aquat. Bot. 31:277-297.
- Meulemans, J.T. 1988. Seasonal changes in biomass and production of periphyton growing upon reed in Lake Maarsseveen. Arch. Hydrobiol. 112:21-42.
- Miller, R.R. 1997. Spatial Distribution of Epiphyte Loadings on Seagrass (*Halodule wrightii*) in the Indian River Lagoon, Florida. M.S. Thesis. Florida Institute of Technology, Melbourne. 66 pp.
- Moncreiff, C.A., M.J. Sullivan, and A.E. Daehnick. 1992. Primary production dynamics in seagrass beds of Mississippi Sound: the contributions of seagrass, epiphytic algae, sand microflora, and phytoplankton. Mar. Ecol. Prog. Ser. 87:161-171.
- Moore, K.A. and J.J. Goodman. 1993. Daily variability in the measurement of light attenuation using scalar (spherical) and downwelling quantum sensors. Pp. 159-167 in L.J. Morris and D.A. Tomasko (eds.), Proceedings and Conclusions of Workshops on Submerged Aquatic Vegetation Initiative and Photosynthetically Active Radiation. Special Publication SJ93-SP13. St. Johns River Water Management District. Palatka, Florida.
- Morris, L.J. and D.A. Tomasko (eds.). 1993. Proceedings and Conclusions of Workshops on Submerged Aquatic Vegetation Initiative and Photosynthetically Active Radiation. Special Publication SJ93-SP13. St. Johns River Water Management District. Palatka, Florida. 244 pp. & appendix.
- Neckles, H.A., R.L. Wetzel, and R.J. Orth. 1993. Relative effects of nutrient enrichment and grazing on epiphyte-macrophyte (*Zostera marina* L.) dynamics. Oecologia 93:285-295.

- Orth, R.J., and K.A. Moore. 1983. Chesapeake Bay: an unprecedented decline in submerged aquatic vegetation. *Science* 222:51-53.
- Pohle, D.G., V.M. Bricelj, and Z. Garcia-Esquivel. 1991. The eelgrass canopy: an above-bottom refuge from benthic predators for juvenile bay scallops *Argopecten irradians*. *Mar. Ecol. Prog. Ser.* 74:47-59.
- Powell, G.V.N., and F.C. Schaffner. 1991. Water trapping by seagrasses occupying bank habitats in Florida Bay. *Est. Coast. Shelf Sci.* 32:43-60.
- Rice, J.D., R.P. Trocine, and G.N. Wells. 1983. Factors influencing seagrass ecology in the Indian River Lagoon. *Florida Sci.* 46:276-286.
- Sand-Jensen, K. 1977. Effect of epiphytes on eelgrass photosynthesis. *Aquat. Bot.* 3:55-63.
- SAS Institute. 1988. *SAS/STAT for Personal Computers*. Cary, N.C. 696 pp.
- SCOR/UNESCO. 1966. *Monographs on Oceanographic Methodology*. UNESCO.
- Short, F.T., D.M. Burdick, and J.E. Kaddy. 1995. Mesocosm experiments quantify the effects of eutrophication on eelgrass, *Zostera marina*. *Limnol. Oceanogr.* 40:740-749.
- Silberstein, K. A.W. Chiffings, and A.J. McComb. 1986. The loss of seagrass in Cockburn Sound, Western Australia. II. The effect of epiphytes on productivity of *Posidonia australis* Hook. *Aquat. Bot.* 24:355-371.
- Smith, N.P. 1993. Tidal and nontidal flushing of Florida's Indian River Lagoon. *Estuaries* 16:739-746.
- Sokal, R.R. and F.J. Rohlf. 1981. *Biometry*. W.H. Freeman & Co, San Francisco. 859 pp.
- Steward, J., R. Virmstein, D. Haurert, and F. Lund. 1994. *Surface Water Improvement and Management (SWIM) Plan for the Indian River Lagoon, FL*. St. Johns River Water Management District and South Florida Water Management District, Palatka and West Palm Beach, FL. 120 pp.
- Thayer, G.W., W.J. Kenworthy, and M.S. Fonseca. 1984. *The Ecology of Seagrass Meadows of the Atlantic Coast: A Community Profile*. U.S. Fish Wildl. Serv. FWS/OBS-84/02.

- Thorhaug, A. 1974. The effect of thermal effluent on the marine biology of southeastern Florida. Pp. 518-531 in J.W. Gibbons and R.R. Sharitz (ed.), Thermal Ecology. AEC Symposium Series, United States Atomic Energy Commission Technology Information Center, Oak Ridge, Tennessee.
- Tomasko, D.A. 1992. Variation in growth form of shoal grass (*Halodule wrightii*) due to changes in the spectral composition of light below a canopy of turtle grass (*Thalassia testudinum*). *Estuaries* 15:214-217.
- Tomasko, D.A. and B.E. Lapointe. 1991. Productivity and biomass of *Thalassia testudinum* as related to water column nutrient availability and epiphyte levels: field observations and experimental studies. *Mar. Ecol. Prog. Ser.* 73:9-17.
- Twilley, R.R., W.M. Kemp, K.W. Staver, J.C. Stevenson, and W.R. Boynton. 1985. Nutrient enrichment of estuarine submerged vascular plant communities: 1. Algal growth and effects on production of plants and associated communities. *Mar. Ecol. Prog. Ser.* 23:179-191.
- Vimstein, R.W. 1982. Leaf growth rate of the seagrass *Halodule wrightii* photographically measured in situ. *Aquat. Bot.* 12:209-218.
- Vimstein, R.W. and P.A. Carbonara. 1985. Seasonal abundance and distribution of drift algae and seagrasses in the mid-Indian River Lagoon, Florida. *Aquat. Bot.* 23:67-82.
- Vimstein, R.W. and R.K. Howard. 1987. Motile epifauna of marine macrophytes in the Indian River Lagoon, Florida. I. Comparisons among three species of seagrasses from adjacent beds. *Bull. Mar. Sci.* 41:1-12.
- Vimstein, R.W. and L.J. Morris. 1996. Seagrass Preservation and Restoration: A Diagnostic Plan for Indian River Lagoon. Technical Memo #14. St. Johns River Water Management District, Palatka, FL. 43 pp.
- Whaley, R. 1990. Causes of seagrass decline in the Tampa Bay Area. *The Palmetto* 10:7-10.
- Williams, S.L. and M.H. Ruckelhaus. 1993. Effects of nitrogen availability and herbivory on eelgrass (*Zostera marina*) and epiphytes. *Ecology* 74:904-918.
- Windsor, J.G. and J.S. Steward. 1987. Water and Sediment Quality. Pp. 5-1 - 5-58 in J.S. Steward and J. Van Armen (eds.), Indian River Lagoon Joint Reconnaissance Report, St. Johns River Water Management District, Palatka, and South Florida Water Management District, West Palm Beach.

- Wood, E.J.F., W.E. Odum, and J.C. Zieman. 1969. Influence of seagrasses on the productivity of coastal lagoons. *Lagunas Costeras*. Pp. 495-502 in Proc. UN Symposio Mem. Simp. Intern. UNAM-UNESCO, Mexico, D.F. Nov. 1967.
- Woodward-Clyde Consultants. 1994a. Historical Imagery Inventory and Seagrass Assessment Indian River Lagoon. Final Technical Report prepared for Indian River Lagoon National Estuary Program. Project Number 92F274C.
- Woodward-Clyde Consultants. 1994b. Preliminary Water and Sediment Quality Assessment of the Indian River Lagoon. Final Technical Report prepared for Indian River Lagoon National Estuary Program. Project Number 92F274C.
- Zieman, J.C. 1987. A review of ecological aspects of the growth, distribution, and decomposition of the seagrasses of the southeastern United States. Pp. 53-76 in M.J. Durako, R.C. Phillips, and R.R. Lewis (eds.), *Proceedings of the Symposium on Subtropical-Tropical Seagrasses of the Southeastern United States*. Fla. Mar. Res. Publ. No. 42, Fla. Dept. Nat. Resour. Bur. Mar. Res., St Petersburg, Florida.
- Zimba, P.V. 1995. Epiphytic biomass in the littoral zone of Lake Okeechobee, Florida. *Archiv. Hydrobiol.* 45:233-240.